

Durham E-Theses

Synthetic Retinoids

JONATHAN HAROLD BARNARD

How to cite:

BARNARD, JONATHAN HAROLD (2010) *Synthetic Retinoids*. Doctoral thesis, Durham University.

Use policy

The full-text may be used and/or reproduced, and given to third parties in any format or medium, without prior permission or charge, for personal research or study, educational, or not-for-profit purposes provided that:

- a full bibliographic reference is made to the original source
- a <https://etheses.durham.ac.uk/id/eprint/288/> is made to the metadata record in Durham E-Theses
- the full-text is not changed in any way

The full-text must not be sold in any format or medium without the formal permission of the copyright holders.

Please consult the [full Durham E-Theses policy](#) for further details.

Declaration

The work described in this thesis was carried out in the Department of Chemistry at the Durham University between October 2005 and February 2010, under the supervision of Prof. Todd B. Marder and Prof. Andrew Whiting. All the work is my own work, unless otherwise stated, and has not been submitted previously for a degree at this or any other university.

Jonathan H. Barnard

Statement of copyright

The copyright of this thesis rests with the author. No quotation from it should be published without prior written consent and information derived from it should be acknowledged.

Acknowledgements

I would like to thank my supervisors Prof. Todd Marder and Prof. Andrew Whiting for their guidance, advice and enthusiasm which have made my studies in their research groups so enjoyable, not to mention their endless patience. Special thanks go to my colleagues in the Marder laboratory. To Brian Hall for making sure that the laboratory ran smoothly by his maintenance and repair of vital and temperamental equipment. Thanks to Dr. Jonathan Collings for help on the retinoids project and for over three years of invaluable advice. Thanks to Caroline Bridgens, Ibraheem Mkhalid, Maha Mkhalid, Richard Ward, Vickie Christie, Menguan Tay, Peter Harrisson, Andrew Crawford, Andreas Steffan, Bianca Bitterlich, Christian Kleeburg, Kittya Wongkhan, Nim, Chao Liu, Li Qiang and everyone else who has passed through CY052 for friendship, support and solidarity throughout my studies.

I would also like to thank all of the departmental staff, especially those from the NMR service, Ian Kenwright, Ian McKeag and Catherine Heffernan, and to Dr. Andrei Batsanov of the X-ray crystallography service for getting excellent results from the most unlikely looking of crystals.

Conferences attended

- North-east England Stem Cell Institute (NESCI) Research Day, Newcastle, UK, 18th May 2007
- EuroBoron IV, Bremen, Germany, 2 – 6 September 2007
- North-east England Stem Cell Institute (NESCI) Research Day, Durham, UK, October 2007
- Imeboron XIII, Platja d'Aro, Spain, 22 – 26 September 2008
- North-east England Stem Cell Institute (NESCI) Research Day, Durham, UK, 24th October 2008

Publications

- **Synthesis and evaluation of synthetic retinoid derivatives as inducers of stem cell differentiation**, V. B. Christie, J. H. Barnard, A. S. Batsanov, C. E. Bridgens, E. B. Cartmell, J. C. Collings, D. J. Maltman, C. P. F. Redfern, T. B. Marder, S. A. Przyborski and A. Whiting, *Organic and Biomolecular Chemistry*, 2008, **6**, 3497–3507, DOI: 10.1039/b808574a
- **Proteomic profiling of the stem cell response to retinoic acid and synthetic retinoid analogues: identification of major retinoid-inducible proteins**, D.J. Maltman, V. B. Christie, J. C. Collings, J. H. Barnard, S. Fenyk, T. B. Marder, A. Whiting, S. A. Przyborski, *Molecular Biosystems*, **2009**, *5*, 458–471, DOI: 10.1039/b817912c

- **C-H Activation for the Construction of C-B Bonds**, I. A. I. Mkhaliid, J. M. Murphy, J. H. Barnard, T. B. Marder, J. F. Hartwig, *Chemical Reviews* **2010**, *110*, 890-931, DOI: 10.1021/cr900206p
- **Synthetic Retinoids: Structure-Activity Relationships**, J. H. Barnard, J. C. Collings, A. Whiting, S. A. Przyborski, T. B. Marder, *Chemistry; a European Journal* **2009**, *15*, 11430-11442, DOI: 10.1002/chem20091952
- **Synthesis of biologically active retinoids via sequential C-H borylations and Suzuki-Miyaura cross-couplings**, J. H. Barnard, I. A. I. Mkhaliid, C. E. Bridgens, A. S. Batsanov, J. A. K. Howard, S. A. Przyborski, A. Whiting, T. B. Marder, manuscript in preparation.
- **Mild and selective formation of vinyl boronate esters via rhodium catalyzed borylation of alkene C-H bonds**, J. H. Barnard, A. S. Batsanov, J. A. K. Howard, S. A. Przyborski, A. Whiting, T. B. Marder, manuscript in preparation.

Abstract

Chapter one is split into three sections, providing general overviews of synthetic retinoids and their biology, Pd-catalysed C-C bond forming reactions and transition metal-catalysed borylation of aromatic and vinylic C-H bonds, respectively.

Chapter two details the application of sequential Ir-catalysed aromatic C-H borylations, Pd-catalysed C-C bond forming reactions and Rh-catalysed vinylic C-H borylations for the stereo-controlled synthesis of stilbene-based TTNPB retinoids.

Chapter three details the application of Ir-catalysed aromatic C-H borylations, Sonogashira cross-couplings and Suzuki-Miyaura cross-couplings for the synthesis of tolan-, and biaryl-based retinoids.

Chapter four details the development and applications of new Rh^I catalyst precursors for the dehydrogenative borylation of unactivated olefins. The dehydrogenative borylation reactions were utilised in one-pot, single solvent syntheses of 2-arylindenes from indene and arylhalides through C-H borylation and subsequent Suzuki-Miyaura cross-couplings.

List of abbreviations

Å	Angstrom	L	monodentate ligand
Ar	Aryl	mg	milligrams
Acac	acetoacetyl	mL	millilitre
BBE	bis-boronate ester	m.p.	melting point
bpy	2,2'-bipyridine	Me	methyl
^tBu	<i>tert</i> -butyl	MS	mass spectrometry
cat	catecholato (1,2-O ₂ C ₆ H ₄)	MTBE	methyl- <i>tert</i> -butyl ether
COD	<i>cis</i> -cyclooctadiene	<i>m/z</i>	mass/charge ratio
COE	cyclooctene	neop	neopentane glycolato (OCH ₂ CMe ₂ CH ₂ O)
Cp	cyclopentadienyl	pin	pinacolato (OCMe ₂ CMe ₂)
Cp[*]	pentamethylcyclopentadienyl	Ph	phenyl
Cy	Cyclohexyl	ⁱPr	<i>iso</i> -propyl
dba	dibenzylideneacetone	Pr	propyl
DMF	N,N-dimethylformamide	R	group
dtbpy	4,4 di- <i>tert</i> -butyl-2,2'-dipyridine	rt	room temperature
DMSO	dimethylsulfoxide	Temp	temperature
equiv.	equivalents	TIC	total ion chromatogram
Et	ethyl	THF	tetrahydrofuran
Et₂O	diethyl ether	TMS	trimethylsilyl
EI	electronic ionization	tol	tolyl
ES	electrospray	VBBE	vinyl bis-boronate ester
g	grams	VBE	vinyl boronate ester
h	hours		

1.1.3.1	Modification of the hydrophobic unit	38
1.1.3.2	Modification of the polar terminus	40
1.1.3.3	Modification of the linker unit	42
1.2	Palladium-catalysed cross-couplings	46
1.2.1	Oxidative addition	46
1.2.2	Transmetallation	51
1.2.3	Reductive elimination	51
1.2.4	The Sonogashira reaction	54
1.2.4.1	Mechanism of the Sonogashira reaction	54
1.2.4.2	Transmetallation in the Sonogashira reaction	57
1.2.4.3	Recent developments in the Sonogashira reaction	57
1.2.5	The Suzuki-Miyaura reaction	59
1.2.5.1	Transmetallation in the Suzuki-Miyaura reaction	60
1.2.5.2	Potassium organotrifluoroborates and their reactions	62
1.2.5.3	Suzuki-Miyaura cross-couplings of organoboron reagents with alkyl halides	64
1.2.5.4	Suzuki-Miyaura cross-couplings of organoboron reagents with aryl chlorides	65
1.3	Transition metal-catalysed borylations of C-H bonds	69
1.3.1	Synthesis of organoborons	69
1.3.2	Transition metal-catalysed C-H borylations	70
1.3.3	Transition metal-catalysed benzylic C-H borylation	72
1.3.4	Transition metal-catalysed aromatic C-H borylation	74
1.3.5	Stoichiometric group XII and XIII carbonyl mediated borylations	75
1.3.6	Rhodium-catalysed aromatic C-H borylation	76
1.3.7	Iridium-catalysed aromatic C-H borylation	78
1.3.7.1	Applications of the [Ir(X)COD] ₂ /bpy catalyst system	84
1.3.7.1.1	Borylations of monosubstituted arenes	84
1.3.7.1.2	Borylations of 1,2-disubstituted arenes	85

1.3.7.1.3	Borylations of 1,3-disubstituted arenes	86
1.3.7.1.4	Borylations of 1,4-disubstituted arenes	86
1.3.7.1.5	Borylations of polyaromatic substrates	87
1.3.7.1.6	Borylations of 5-membered heterocycles	92
1.3.7.1.7	Borylations of benzofused 5-membered heterocycles	94
1.3.7.1.8	Borylations of 6-membered heterocycles and benzofused analogues	96
1.3.7.2	Tandem reactions	98
1.3.7.3	Iridium-catalysed borylations of silicon containing substrates	101
1.3.7.4	Novel iridium catalysts for aromatic C-H borylations	103
1.3.7.5	Proposed mechanism for the Ir(OMe)COD/L ₂ -catalysed borylation of arenes	105
1.3.8	Dehydrogenative borylation of olefins	107
1.3.8.1	Dehydrogenative borylation of olefins using borane clusters	108
1.3.8.2	Dehydrogenative borylation of olefins with concomitant hydrogenation and/or hydroboration	108
1.3.8.3	Photochemically induced stoichiometric dehydrogenative olefin borylation	113
1.3.8.4	Dehydrogenative borylation of olefins under hydroboration conditions	114
1.3.8.5	Dehydrogenative borylation of olefins without sacrificial hydrogenation and/or hydroboration	116
1.3.8.6	Boryl transfer reactions and β -boryl elimination	122

List of equations for chapter one

Equation 1.1	Stille couplings of allyl stannanes and allyl halides with catalytic maleic anhydride.	52
Equation 1.2	Suzuki-Miyaura reactions of allyl chloride and sodium tetraphenylborate with catalytic dimethyl fumarate.	53

Equation 1.3 Epoxidation of potassium 1-alkenyl trifluoroborates with dimethyldioxirane.	63
Equation 1.4 Nucleophilic substitution of iodomethyl trifluoroborates.	63
Equation 1.5 Cross-couplings unactivated aryl chlorides with aryl boronic acids by Nolan and coworkers.	66
Equation 1.6 Addition of B ₂ Cl ₄ to ethane by Schlesinger and coworkers.	69
Equation 1.7 Methods for the synthesis of arylboron compounds.	70
Equation 1.8 Benzylic borylation of methylarenes by Marder and coworkers.	71
Equation 1.9 Rhodium-catalysed borylations of arenes by Hartwig and coworkers, and Smith and coworkers.	75
Equation 1.10 Regioselective aromatic borylations in cyclohexane by Smith and coworkers.	76
Equation 1.11 Borylation of benzene with [Rh(Cl)(N ₂)(P ⁱ Pr ₃) ₂] by Marder and coworkers.	76
Equation 1.12 Thermal reactions of [IrCp [*] PMe ₃ (H)(Ph)] with HBcat and HBpin.	77
Equation 1.13 [Cp [*] Ir(PMe ₃)(H)(Bpin)]-catalysed borylation of arenes.	78
Equation 1.14 Iridium-catalysed arene C-H borylations by Smith and coworkers.	79
Equation 1.15 Iridium-catalysed borylation of monosubstituted arenes with B ₂ pin ₂ at 80 °C.	84
Equation 1.16 Iridium catalysed borylation of 1,2-disubstituted arenes with B ₂ pin ₂ at 80 °C.	84
Equation 1.17 [Ir(OMe)COD] ₂ /dtbpy-catalysed borylations of 1,3-disubstituted arenes.	85
Equation 1.18 Iridium-catalysed borylation of 4-substituted benzonitriles by Smith and coworkers.	86
Equation 1.19 Iridium-catalysed borylation of azulene with B ₂ pin ₂ by Sugihara and coworkers.	87
Equation 1.20 Ir-catalysed borylation of polyaromatic hydrocarbons by Marder and coworkers.	88
Equation 1.21 Ir-catalysed borylation of ferrocenes with B ₂ pin ₂	89

by Plenio and coworkers.	
Equation 1.22 Ir-catalysed borylation of crystalline polystyrenes by Bae and coworkers.	89
Equation 1.23 Regioselectivities of the Ir-catalysed borylation of substituted porphyrins with B ₂ pin ₂ .	90
Equation 1.24 Ir-catalysed borylation of 5-membered heterocycles .	92
Equation 1.25 Ir-catalysed borylation of substituted thiophenes by Smith and coworkers.	93
Equation 1.26 Iridium-catalysed borylations of benzofused heterocycles by Miyaura and coworkers.	94
Equation 1.27 Selective borylation of the 7-position in 2-substituted indoles.	95
Equation 1.28 Ir-catalysed borylation of pyridines and related substrates.	97
Equation 1.29 Cu-catalysed couplings of boronic acids and boronate esters with N-, and O-nucleophiles.	99
Equation 1.30 Sequential C-H borylation/Buchwald–Hartwig reactions by Smith and coworkers.	100
Equation 1.31 One-pot synthesis of chiral α,α -diarylmethylsufinylamines by Hartwig and Boebel.	101
Equation 1.32 PdBr ₂ -catalysed dehydrogenative borylation of propene with pentaborane by Sneddon and coworkers. Terminal and bridging hydrogens on the boron cluster are omitted for clarity.	107
Equation 1.33 Rhodium-catalysed dehydrogenative borylations of vinylarenes by Brown <i>et al.</i>	108
Equation 1.34 Rhodium-catalysed dehydrogenative borylation of olefins by Masuda and coworkers.	110
Equation 1.35 Ruthenium-catalysed dehydrogenative borylation of olefins by Masuda and coworkers.	110
Equation 1.36 Iridium-catalysed borylations of cyclic olefins by Szabo and coworkers.	111
Equation 1.37 Iridium-catalysed dehydrogenative borylation of olefins and subsequent cross-coupling by Szabó and coworkers.	112

Equation 1.38 Stoichiometric reactions of $[\text{Cp}^* \text{Ti}(\eta^2\text{-CH}_2\text{=CH}_2)]$ with boranes and ethene by Smith and coworkers.	113
Equation 1.39 Photochemically induced dehydrogenative borylation of olefins by Hartwig and coworkers.	114
Equation 1.40 Borylation of α -methylstyrene with HBcat catalysed by	116
Equation 1.41 Rhodium-catalysed dehydrogenative borylations of olefins by Marder and coworkers.	117
Equation 1.42 Dehydrogenative borylation of 1,2-disubstituted alkenes by Suginome and coworkers.	122

List of schemes for chapter one

Scheme 1.1 Basic catalytic cycle for Pd-catalysed cross-couplings.	46
Scheme 1.2 Oxidative addition pathways from top to bottom: nucleophilic addition, single electron transfer and 3-centred concerted addition.	47
Scheme 1.3 Mono-, and bis-ligated pathways for oxidative addition of aryl halides to Pd^0 .	49
Scheme 1.4 Reversible coordination of dba to Pd^0 centres	50
Scheme 1.5 Classical Sonogashira reaction mechanism. X = Br, I or TfO.	55
Scheme 1.6 Recent proposal for the mechanism of the Sonogashira reaction.	56
Scheme 1.7 Mechanism of the Suzuki–Miyaura reaction.	60
Scheme 1.8 Base assisted transmetalation of organoborons. compounds to Pd^{II}	61
Scheme 1.9 Mechanism of head to tail coupling in Suzuki-Miyaura reactions.	62
Scheme 1.10 Activation of palladacycle 18 in 2-propanol.	66
Scheme 1.11 Catalytic cycle for the borylation of toluene with $[\text{Rh}(\text{Cl})(\text{P}^i\text{Pr}_3)_2]$ and HBpin.	72
Scheme 1.12 Pathways for the formation of Ir^{I} monoboryl complexes from $\text{Ir}(\text{OMe})$ precursors.	82

Scheme 1.13	Current scope of one-pot C-H borylation / transformation of the Bpin group.	97
Scheme 1.14	Proposed catalytic cycle of [Ir(X)COD] ₂ /dtbpy-catalysed borylation of arenes with B ₂ pin ₂ .	105
Scheme 1.15	Rhodium-catalysed dehydrogenative borylations of vinylarenes by Brown et al.	109
Scheme 1.16	Stoichiometric Ru-mediated formation of vinylboranes reported by Marder, Baker and coworkers.	115
Scheme 1.17	Ruthenium-catalysed transfer borylation of vinylarenes by Pietraszuk and coworkers.	123

List of figures for chapter one

Figure 1.1	Natural retinoids	24
Figure 1.2	Retinoid structure.	24
Figure 1.3	ATRA biosynthesis precursors and ATRA.	25
Figure 1.4	Multiple retinoid signaling pathways.	27
Figure 1.5	Levels of transcriptional activation of RARE <i>via</i> RAR binding and activation and repression of transcription from RAREs by RAR antagonism.	28
Figure 1.6	Synthetic RAR α selective retinoids.	30
Figure 1.7	Synthetic retinoids.	30
Figure 1.8	Synthetic retinoid TTNPB.	31
Figure 1.9	Crystal structure of the hRAR β LBP–TTNPB complex. revealing an additional cavity in the LBP.	31
Figure 1.10	Model structure of the docking of RAR β agonist / RAR γ agonist BMS 453 into the RAR β and RAR γ LBP.	31
Figure 1.11	Modelling of the interactions of ATRA, AC 55649 and AC 261066 with the AF-2 domain.	33
Figure 1.12	RAR γ selective retinoids.	33
Figure 1.13	Modelling of the CD 666-hRAR γ complex.	34

Figure 1.14	RXR selective retinoids.	35
Figure 1.15	Retinoid numbering scheme.	36
Figure 1.16	Products of ATRA oxidative metabolism.	36
Figure 1.17	Arotinoids.	37
Figure 1.18	Modification of the hydrophobic unit in TTNPB arotinoids and their activities in the TOC assay.	38
Figure 1.19	Crystal structures of 9cRA-RAR and 9cRA-RXR complexes	40
Figure 1.20	Modifications of the polar terminus.	42
Figure 1.21	Synthetic retinoids possessing varying linker units.	43
Figure 1.22	RXR selective synthetic retinoids possessing varying linker units.	44
Figure 1.23	Pd(dppe)Me ₂ and Pd(transphos)Me ₂ complexes.	50
Figure 1.24	Phosphine-olefins ligands synthesised by Lei and coworkers.	55
Figure 1.25	Palladacyclic catalyst precursors.	58
Figure 1.26	<i>N</i> -heterocyclic carbene (NHC) precursors and a Pd ^{II} complex bearing an NHC ligand.	59
Figure 1.27	Dialkylbiarylphosphines for Suzuki-Miyaura reactions of aryl chlorides.	68
Figure 1.28	Diboron compounds.	70
Figure 1.29	Novel ligands and Ir complexes employed in Ir-catalysed C-H borylations.	103
Figure 1.30	Iridium tris-, and bis-boryl complexes ligated by dtbpy.	105
Figure 1.31	Conformation leading to the formation of (<i>E</i>)-VBE product.	119
Figure 1.32	Bulky rhodium diimine catalysts for dehydrogenative borylation of olefins by Westcott and coworkers.	120

List of tables for chapter one

Table 1.1	Divergent residues in the RAR isotype ligand binding pocket.	29
Table 1.2	Cross-couplings of 9-alkyl-9-BBN derivatives with alkyl bromides by Fu and coworkers.	65

Table 1.3	Pd/C-catalysed benzylic borylations of alkyl arenes with B ₂ pin ₂ and HBpin.	73
Table 1.4	Stoichiometric borylations of PhX with [CpFe(CO) ₂ BCat].	74
Table 1.5	Iridium-catalysed direct borylations of arenes with B ₂ pin ₂ .	80
Table 1.6	Effects of iridium sources on the borylation of benzene with B ₂ pin ₂ at room temperature.	82
Table 1.7	Effects of ligands on the borylation of benzene with B ₂ pin ₂ at room temperature.	83
Table 1.8	Iridium-catalysed dehydrogenative borylation of cyclic vinyl ethers.	121

Chapter two: Synthesis of biologically active retinoids *via* sequential C-H borylations and Suzuki-Miyaura cross-couplings.

2.1	Introduction	142
2.2	Results and discussion	145
2.2.2	Discussion of the relative solid and solution state structures of TTNPB esters and their vinylic precursors	174
2.3	Conclusions	176
2.4	Experimental	177

List of equations for chapter two

Equation 2.1	Synthesis of 6 by Ir-catalysed aromatic C-H borylation of 5 .	146
Equation 2.2	Synthesis of 7	147
Equation 2.3	Synthesis of pentamethylated tetrahydronaphthalene 9 .	141
Equation 2.4	Attempted Ir-catalysed aromatic C-H borylation of 9 .	149
Equation 2.5	Synthesis of 12 <i>via</i> Friedel-Crafts acetylation and	151

	Wittig methylenation.	
Equation 2.6	Iodination of 9 with HIO_4/I_2 to give 13 .	153
Equation 2.7	Palladium-catalysed borylations of 13 with B_2pin_2 and B_2neop_2 .	155
Equation 2.8	Synthesis of 12 <i>via</i> Suzuki-Miyaura cross-coupling of 14 with 2-bromopropene.	159
Equation 2.9	Synthesis of 16 <i>via</i> iodination of 5 and subsequent Miyaura borylation with B_2neop_2 .	160
Equation 2.10	Dehydrogenative borylations of 7 and 12 to give 17, 18, 19 and 20 .	165
Equation 2.11	Suzuki-Miyaura reactions of 17 and 18 with aryl iodides to give 21, 22, 23 and 24 .	169

List of schemes for chapter two

Scheme 2.1	Synthesis of TTNPB by Loeliger and coworkers.	143
Scheme 2.2	Synthesis of disila-TTNPBs by Tacke and coworkers.	144
Scheme 2.3	Retrosynthetic analysis for the synthesis of TTNPBs <i>via</i> a combination of C-H borylations and Suzuki-Miyaura cross-couplings.	115

List of figures for chapter two

Figure 2.1	Natural and synthetic retinoids.	142
Figure 2.2	GC (TIC) of the synthesis of 6 after 4 h.	146
Figure 2.3	MS of 6 .	146
Figure 2.4	GC (TIC) of the reaction of 6 and 2 bromopropene after 2 h.	147
Figure 2.5	MS of 7 .	141
Figure 2.6	GC (TIC) of the attempted synthesis of 10a by aromatic C-H borylation of 9 with B_2pin_2 .	149
Figure 2.7	Ion chromatogram ($m/z = 328$) of the attempted synthesis of 10a by aromatic C-H borylation of 9 with B_2pin_2 .	150

Figure 2.8	MS of 10a .	150
Figure 2.9	GC (TIC) of the acetylation of 9 with acetyl chloride to give 11 after 18 h.	151
Figure 2.10	MS of 11 .	151
Figure 2.11	The molecular structure of ketone 11 .	152
Figure 2.12	GC (TIC) of the reaction of 11 with PPh ₃ CH ₃ I to give 12 after 48 h.	152
Figure 2.13	MS of 12 .	152
Figure 2.14	The molecular structure of olefin 12 .	153
Figure 2.15	GC (TIC) for the iodination of 9 with I ₂ /HIO ₄ to give 13 after 18 h.	154
Figure 2.16	MS of 13 .	154
Figure 2.17	GC (TIC) of the borylation of 13 with B ₂ pin ₂ to give 10a after 96 h.	155
Figure 2.18	MS of 10a .	155
Figure 2.19	GC (TIC) of the borylation of 13 with B ₂ neop ₂ to give 14 after 18 h.	156
Figure 2.20	MS of 14 .	156
Figure 2.21	The molecular structure of 10a showing the non-disordered molecule of 10a in the asymmetric unit. The disordered molecule of 10a is not shown for clarity.	157
Figure 2.22	(a) The molecular structure of 10a with two independent molecules in the asymmetric unit, showing the disorder of one of the two molecules of 10a , (b) disorder in alkyl ring of one of the molecules of 10a . All hydrogen atoms, the C(21) methyl group and the Bpin group are removed for clarity.	158
Figure 2.23	The molecular structure of 14 .	158
Figure 2.24	GC (TIC) of the reaction of 14 with 2-bromopropene to give 12 after 18 h.	160
Figure 2.25	GC (TIC) of the iodination of 5 with I ₂ /HIO ₄ to give 15 after 4 h	161
Figure 2.26	MS of 15 .	161

Figure 2.27	GC (TIC) of the borylation of 15 with B ₂ neop ₂ to give 16 after 18 h.	161
Figure 2.28	MS of 16 .	162
Figure 2.29	The molecular structure of 16 .	162
Figure 2.30	GC (TIC) of the dehydrogenative borylation of 7 with B ₂ pin ₂ to give 17 after 48 h.	135
Figure 2.31	MS of 17 .	165
Figure 2.32	GC (TIC) of the dehydrogenative borylation of 12 with B ₂ pin ₂ to give 18 after 72 h/	166
Figure 2.33	MS of 18 .	166
Figure 2.34	GC (TIC) of the dehydrogenative borylation of 7 with B ₂ neop ₂ to give 19 after 48 h.	166
Figure 2.35	MS of 19 .	167
Figure 2.36	GC (TIC) of the dehydrogenative borylation of 12 with B ₂ neop ₂ to give 20 after 72 h.	167
Figure 2.37	MS of 20 .	167
Figure 2.38	Molecular structure of TTNPB. Shown as one half of its doubly hydrogen bonded dimer.	168
Figure 2.39	GC (TIC) of the Suzuki-Miyaura reaction of 17 and 4-C ₆ H ₄ -CO ₂ Me to give 21 after 48 h.	169
Figure 2.40	MS of 21 .	169
Figure 2.41	GC (TIC) of the Suzuki-Miyaura reaction of 17 and 3-C ₆ H ₄ -CO ₂ Me to give 22 after 48 h.	170
Figure 2.42	MS of 22 .	170
Figure 2.43	GC (TIC) of the Suzuki-Miyaura reaction of 18 and 4-C ₆ H ₄ -CO ₂ Me to give 23 after 48 h.	170
Figure 2.44	MS of 23 .	171
Figure 2.45	GC (TIC) of the Suzuki-Miyaura reaction of 18 and 3-C ₆ H ₄ -CO ₂ Me to give 25 after 48 h.	171
Figure 2.46	MS of 24 .	171
Figure 2.47	Molecular structures of compound 22 in conformations	172

	A and B (a and b , respectively). Superimposition of both conformations of compound 22 (c).	
Figure 2.48	Molecular structure of compound 23 .	173
Figure 2.49	Comparison of the molecular structures of 17 and 18 , showing the increase in the <i>i/ii</i> dihedral angle caused by the <i>ortho</i> -methyl group in 18 . Disorder of the Bpin group is removed for clarity in 17 . Disorder of the C(15)C(16)C(17)C(18) alkyl group is removed for clarity in 18 .	174
Figure 2.50	Comparison of TTNPB and 3-Me TTNPB methyl ester 23 , showing the increase in the <i>i/ii</i> dihedral angle caused by the <i>ortho</i> -methyl group in 23 .	175

List of tables for chapter two

Table 2.1	Effects of base on Suzuki-Miyaura cross-couplings of 6 and 16 with 2-bromopropene to give 7 .	163
Table 2.2	UV-vis spectrometry data of TTNPB esters and vinylic precursors.	176
Table 2.3	Photophysical data for all compounds in CHCl ₃ .	197

Chapter three: Synthesis of tolan-, and biaryl-based retinoids *via* palladium-catalysed cross couplings.

3.1	Introduction	202
3.2	Synthetic retinoids based on the tolan structure	204
3.2.2	Synthesis of 3-methylated retinoids based on the tolan structure	212
3.3	Synthesis of retinoid esters based on the biaryl structure	219
3.4	Conclusions	226
2.5	Experimental for Chapter 3	227

List of equations for chapter three

Equation 3.1	Unsuccessful attempts to synthesise functionalised tetrahydronaphthalenes.	205
Equation 3.2	Bromination of 1 with Br ₂ /BF ₃ ·OEt ₂ to give 2 .	205
Equation 3.3	Sonogashira cross-couplings of 2 to give 3 and 4 .	203
Equation 3.4	Mild Sonogashira cross-coupling to give 4 .	209
Equation 3.5	Desilylation of 4 with KOH to give acetylene 5 .	179
Equation 3.6	Sonogashira cross-coupling of 5 with 4-iodomethylbenzoate to give 6 .	210
Equation 3.7	Hydrolysis of 6 with aqueous hydroxide to give 7 .	212
Equation 3.8	Synthesis of 8 <i>via</i> Sonogashira cross-coupling.	214
Equation 3.9	Desilylation of 8 with NaOH to give 9 .	215
Equation 3.10	Sonogashira cross-couplings of 9 with iodomethylbenzoates to give 10 and 11 .	216
Equation 3.11	Hydrolysis of 10 and 11 with LiOH to give 12 and 13 .	219
Equation 3.12	Synthesis of biaryl retinoid esters 14 , 15 and 16 <i>via</i> Suzuki-Miyaura cross-couplings.	220
Equation 3.13	Synthesis of biaryl retinoid esters 17 , 18 and 19 <i>via</i> Suzuki-Miyaura cross-couplings of <i>d</i> .	223
Equation 3.14	Hydrolysis of biaryl retinoid esters 14 – 19 .	226

List of schemes for chapter three

Scheme 3.1	Retrosynthetic analysis of tolan-based retinoids <i>via</i> Sonogashira cross-couplings.	205
Scheme 3.2	Retrosynthetic analysis for the 3-methylated EC retinoid skeleton <i>via</i> Sonogashira cross-couplings.	213

List of figures for chapter three

Figure 3.1	Natural retinoids.	202
Figure 3.2	Arotinoid analogues (detailed in this work) of ATRA and 9cRA, R = H, Me.	204
Figure 3.3	GC (TIC) for the synthesis of 2 <i>via</i> bromination of 1 with BF ₃ ·OEt ₂ .	206
Figure 3.4	MS of 2 .	206
Figure 3.5	GC (TIC) of the Sonogashira reaction of 2 with 2-methyl-3-butyn-2-ol to give 3 after 72h.	207
Figure 3.6	MS of 3 .	208
Figure 3.7	GC (TIC) of the Sonogashira reaction of 2 with TMSA to give 4 after 18 h.	208
Figure 3.8	MS of 4 .	208
Figure 3.9	GC (TIC) for the desilylation of 4 with KOH to give 5 .	209
Figure 3.10	MS of 5 .	210
Figure 3.11	Molecular structure of alkyne 5	210
Figure 3.12	GC (TIC) for the Sonogashira cross-coupling of 5 with <i>p</i> -iodomethylbenzoate to give 6 .	211
Figure 3.13	MS of 6 .	211
Figure 3.14	Molecular structure of compound 6 .	212
Figure 3.15	GC (TIC) for the synthesis of 8 <i>via</i> Sonogashira cross-coupling.	214
Figure 3.16	MS of 8 .	214
Figure 3.17	GC (TIC) for the desilylation of 8 to give 9 after 2 h.	215
Figure 3.18	MS of 8 .	215
Figure 3.19	GC (TIC) for the synthesis of 10 from 9 and 4-iodomethylbenzoate after 18 h.	216
Figure 3.20	MS of 10 .	216
Figure 3.21	GC (TIC) for the synthesis of 11 from 9 and	217

	3-iodomethylbenzoate after 18 h.	
Figure 3.22	MS of 11 .	217
Figure 3.23	Molecular structure of compound 10 .	218
Figure 3.24	Molecular structure of compound 11 .	218
Figure 3.25	Boronate ester building blocks for retinoid synthesis.	219
Figure 3.26	GC (TIC) for the synthesis of 14 from boronate ester <i>a</i> .	221
Figure 3.27	MS of 14 .	221
Figure 3.28	GC (TIC) for the synthesis of 15 from boronate ester <i>a</i> .	221
Figure 3.29	MS of 15 .	222
Figure 3.30	GC (TIC) for the synthesis of 16 from boronate ester <i>a</i> .	222
Figure 3.31	MS of 16 .	222
Figure 3.32	GC (TIC) for the synthesis of 17 from pinacol boronate ester <i>d</i> .	224
Figure 3.33	MS of 17 .	224
Figure 3.34	GC (TIC) for the synthesis of 18 from pinacol boronate ester <i>d</i> .	224
Figure 3.35	MS of 18 .	225
Figure 3.36	GC (TIC) for the synthesis of 19 from pinacol boronate ester <i>d</i> .	225
Figure 3.37	MS of 19 .	225

Chapter four: Mild and selective formation of vinylboronate esters *via* the borylation of alkene C-H bonds

4.1	Introduction	247
4.2	Results and discussion	248
4.3	Investigations into the mechanism of the dehydrogenative borylation reaction	256
4.4	Conclusions	261
4.5	Experimental for Chapter 4	262

List of equations for chapter four

Equation 4.1	Borylation of indene and synthesis of 2-arylindenes <i>via</i> one-pot, single solvent C-H borylation/Suzuki-Miyaura cross-coupling.	255
---------------------	--	------------

List of schemes for chapter four

Scheme 4.1	Catalytic dehydrogenative borylation of alkenes.	247
Scheme 4.2	Proposed formation of 9 from 4 .	258
Scheme 4.3	Reactions of 9 .	259
Scheme 4.4	Bimetallic oxidative addition of B ₂ cat ₂ to a dimeric Ni ^I complex.	260
Scheme 4.5	Proposed catalytic cycle for the Rh(PPh ₃) _n (CO)X-catalysed dehydrogenative borylation of alkenes with B ₂ pin ₂ .	261

List of figures for chapter four

Figure 4.1	162 MHz ³¹ P{ ¹ H} NMR spectrum of the borylation of 2-phenylpropene with 20 mol % of 6 in 3:1 C ₆ D ₆ /CD ₃ CN after 6 h at 20 °C.	256
Figure 4.1	162 MHz ³¹ P{ ¹ H} NMR spectrum of the borylation of 2-phenylpropene with 20 mol % of 4 in 3:1 C ₆ D ₆ /CD ₃ CN after 6 h at 20 °C.	257
Figure 4.3	162 MHz ³¹ P{ ¹ H} NMR spectrum of the reaction of 4 and B ₂ pin ₂ (10 equiv.) in C ₆ D ₆ after 4 h at 20 °C.	268
Figure 4.4	162 MHz ³¹ P{ ¹ H} NMR spectrum of the reaction of 4 and B ₂ pin ₂ (10 equiv) in C ₆ D ₆ after 18 h at 20 °C.	268
Figure 4.5	128 MHz ¹¹ B NMR spectrum of the reaction of 4 and B ₂ pin ₂ (10 equiv) in C ₆ D ₆ after 18 h at 20 °C.	269

Figure 4.6	162 MHz $^{31}\text{P}\{^1\text{H}\}$ NMR spectrum of the reaction of 6 and B_2pin_2 (10 equiv) in C_6D_6 after 18 h at 20 °C.	270
Figure 4.7	128 MHz ^{11}B NMR spectrum of the reaction of 6 and B_2pin_2 (10 equiv) in C_6D_6 after 18 h at 20 °C.	270
Figure 4.8	162 MHz $^{31}\text{P}\{^1\text{H}\}$ NMR spectrum of the reaction of HBpin with 9 and B_2pin_2 in C_6D_6 after 18 h at 20 °C.	271
Figure 4.9	128 MHz ^{11}B NMR spectrum of the reaction of HBpin with 9 and B_2pin_2 in C_6D_6 after 18 h at 20 °C.	271
Figure 4.10	162 MHz $^{31}\text{P}\{^1\text{H}\}$ NMR spectrum of the reaction of 2-phenylpropene with 9 and B_2pin_2 in C_6D_6 after 18 h at 20 °C.	272
Figure 4.11	128 MHz ^{11}B NMR spectrum of the reaction of 2-phenylpropene with 9 and B_2pin_2 in C_6D_6 after 18 h at 20 °C.	273
Figure 4.12	GC (TIC) of the reaction of 2-phenylpropene with 9 and B_2pin_2 in C_6D_6 after 18 h at 20 °C.	273
Figure 4.13	EI-MS of the peak at 7.3 minutes for the reaction of 2-phenylpropene with 9 and B_2pin_2 in C_6D_6 after 18 h at 20 °C.	274
Figure 4.14	162 MHz $^{31}\text{P}\{^1\text{H}\}$ NMR spectrum of the reaction of 2-phenylpropene with 9 and B_2pin_2 in C_6D_6 after 3 d at 20 °C.	274
Figure 4.15	162 MHz $^{31}\text{P}\{^1\text{H}\}$ NMR spectrum of the reaction of 2-phenylpropene with 6 and B_2pin_2 in C_6D_6 after 18 h at 20 °C.	275
Figure 4.16	128 MHz ^{11}B NMR spectrum of the reaction of 2-phenylpropene with 6 and B_2pin_2 in C_6D_6 after 18 h at 20 °C.	276
Figure 4.17	GC (TIC) of the reaction of 2-phenylpropene with 6 and B_2pin_2 in C_6D_6 after 18 h at 20 °C.	276
Figure 4.18	EI-MS of the peak at 7.3 minutes for the reaction of 2-phenylpropene with 6 and B_2pin_2 in C_6D_6 after 18 h at 20 °C.	277
Figure 4.19	400 MHz ^1H NMR spectrum of compound 5 in C_6D_6 .	278
Figure 4.20	162 MHz $^{31}\text{P}\{^1\text{H}\}$ NMR spectrum of compound 5 in C_6D_6 .	278
Figure 4.21	X-ray molecular structure of <i>trans</i> - $[\text{Rh}(\text{PPh}_3)_2(\text{CO})(\text{O}_2\text{CPh})]\cdot\text{MeOH}$ (5), showing thermal ellipsoids	279

at the 50% probability level and the disorder of the methanol molecule and the PPh₃ phenyl ring.

List of tables for chapter four

Table 4.1	Dehydrogenative borylations of 2-phenylpropene with B ₂ pin ₂ in the presence of bases.	249
Table 4.2	Rh-catalysed dehydrogenative borylation of 2-phenylpropene with B ₂ pin ₂ .	250
Table 4.3	Dehydrogenative borylations of alkenes with B ₂ pin ₂ catalysed by 6 .	252
Table 4.4	Dehydrogenative borylation of 2-phenylpropene in different solvents.	254

Chapter five: Future work	286
---------------------------	------------

1.1 Retinoids

1.1.1 Natural retinoids and their biology

The retinoids are a class of over 4000 natural and synthetic molecules structurally and/or functionally related to all-*trans*-retinoic acid (ATRA), a metabolite of vitamin A (retinol).¹ Endogenous ATRA regulates a range of essential processes during chordate embryogenesis and adult homeostasis including; embryonic development,² vision,³ and cellular differentiation, proliferation and apoptosis.⁴ Retinoids are successfully used to treat certain dermatological conditions⁵ and have the potential to act as chemo-preventative and chemotherapeutic agents, although toxicity issues have prevented their more widespread use.^{6,7} ATRA isomerises under laboratory and physiological conditions to give mixtures of ATRA, 9-*cis*-retinoic acid (9cRA), 13-*cis*-retinoic acid (13cRA) (**Figure 1.1**) and other species.^{8,9,10,11,12}

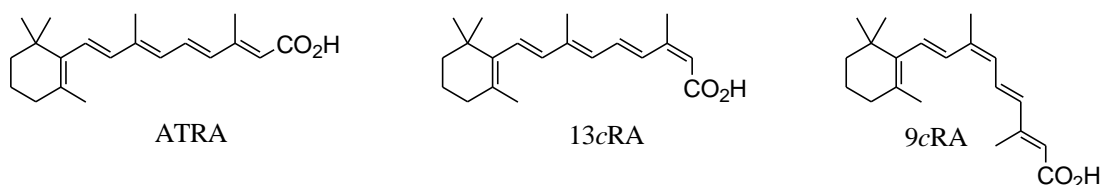


Figure 1.1 Natural retinoids.

The structure of retinoids can be thought of as comprising three units, (as shown in **Figure 1.2** for ATRA) a bulky, hydrophobic region, a linker unit and a polar terminus, which is usually a carboxylic acid group.

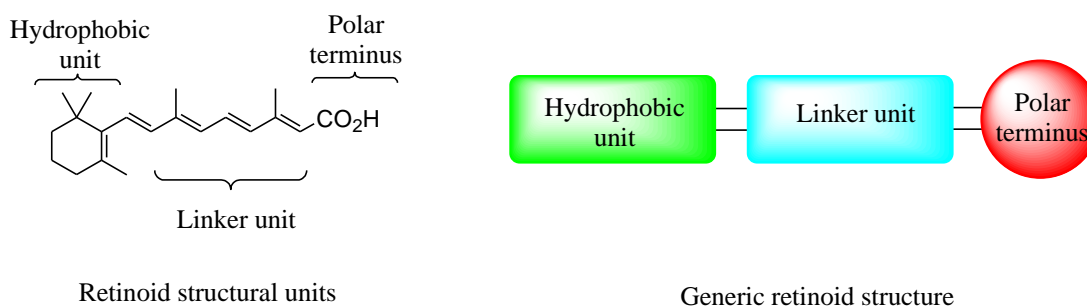


Figure 1.2 Retinoid structure.

Vitamin A (retinol, **Figure 1.3**) cannot be synthesised by any animal species and is obtained through the diet, either from pro-vitamin A carotinoids in plants (such as β -carotenoid) or directly from other animals. Ingested vitamin A is stored as retinyl esters in the liver until needed, at which time it is transported bound to retinol binding protein (RBP).¹³ Retinol is reversibly oxidised by retinol dehydrogenases (ROLDH) to give retinal which may then be irreversibly oxidised to ATRA¹⁴ by retinal dehydrogenases (RALDH), or by cytochrome P450 enzymes in hepatic tissue.¹⁵ ATRA can cross the plasma membrane passively and is translocated by cellular retinoic acid binding proteins (CRABP-I & II) to the nucleus where it binds to nuclear receptors. Otherwise, free ATRA can be stored by binding to retinoic acid binding protein I (CRABP-I), a process which inhibits its biological activity¹⁶ or can be oxidised by cytochrome P450 enzymes in conjunction with CRABP-I to give polar metabolites such as 4-hydroxy-retinoic acid and 18-hydroxy-retinoic acid.¹⁷

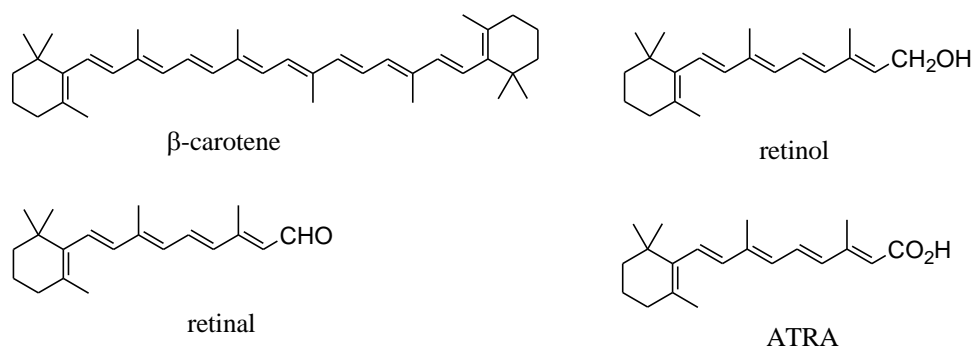


Figure 1.3 ATRA biosynthesis precursors and ATRA.

Retinoid activity results primarily from the transcriptional regulation of specific genes which is regulated by the binding of retinoids to receptors belonging to the steroid/thyroid superfamily of nuclear receptors.¹ There are two classes of retinoid nuclear receptors, retinoic acid receptors (RARs) and retinoid X receptors (RXRs), with each subfamily being structurally and functionally distinct. In both cases the nuclear receptors act as ligand inducible transcriptional regulation factors.¹⁸ Both the RAR and RXR subfamilies are further separated into three isotypes, α , β and γ with the different RAR isotypes possess differing amino acid sequences in their ligand binding domains

(LBDs). In addition, RAR and RXR isotypes are further separated into different isoforms. For each isotype, the LBDs of the different isoforms are identical, but domains that are not involved in ligand binding are not conserved between the differing isoforms.^{19,20} In order to be functional, both RARs and RXRs must dimerise with other nuclear receptors. RARs predominantly heterodimerise with RXRs allowing for the binding of their specific nuclear DNA sequences known as retinoic acid response elements (RAREs), while RXRs form both homodimers and heterodimers^{21,22,23} with RARs and other nuclear receptors including peroxisome-proliferation-activated-receptors (PPARs)²⁴ and vitamin D₃ receptor (VDR).²⁵ The endogenous ligands for retinoid receptors are ATRA and 9cRA, respectively. ATRA binds and activates the three RAR isotypes (α , β and γ) with similar affinities, while 9cRA acts as a pan-agonist for all six retinoid receptor isotypes, binding and activating both the RARs and RXRs.^{26,27} Crystallographic studies of both RAR and RXR ligand binding pockets (LBPs) bound to a variety of ligands have shown that the shape of the LBP differs markedly between RARs and RXRs.^{28,29,30} Crystal structures of the LBPs of RAR γ and RXR α have shown that RAR γ possesses a linear ‘‘I’’ shaped LBP, whereas that of RXR α is a shorter and more restrictive ‘‘L’’ shape. As a result, the linear retinoid ATRA can act as a ligand only for RARs while the flexible 9cRA can adopt both the linear and twisted conformations required for binding to both RARs and RXRs respectively.³¹ The transcriptional activities of RAR agonists are mediated by ligand binding to the RAR LBP of RAR/RXR heterodimers (**Figure 1.4A**). The RXR partner may also bind to ligands, depending on the occupation of the RAR LBP and on the particular DNA-response element to which the heterodimer is bound.^{32,33} Heterodimers of RXRs with RARs, thyroid receptor (TR) and vitamin D₃ receptor (VDR) cannot be activated by the binding of RXR agonists alone and thus are termed ‘non-permissive’ heterodimers. However, RXR agonists can allosterically increase the efficacy of RAR agonists (retinoid synergism), and can activate ‘permissive’ heterodimers³⁴ of RXRs with numerous orphan nuclear receptors (OR) such as PPAR, liver X receptor (LXR), farnesoid X receptor (FXR) and pregnane X receptor (PXR) without the binding of agonists for the partner receptors (**Figure 1.4C**).^{24,35} Thirdly, RXRs can homodimerise on directly repeated sequences which are separated by one nucleotide. These homodimers

are transcriptionally activated by the binding of an RXR agonist such as 9cRA (**Figure 1.4B**).³⁶

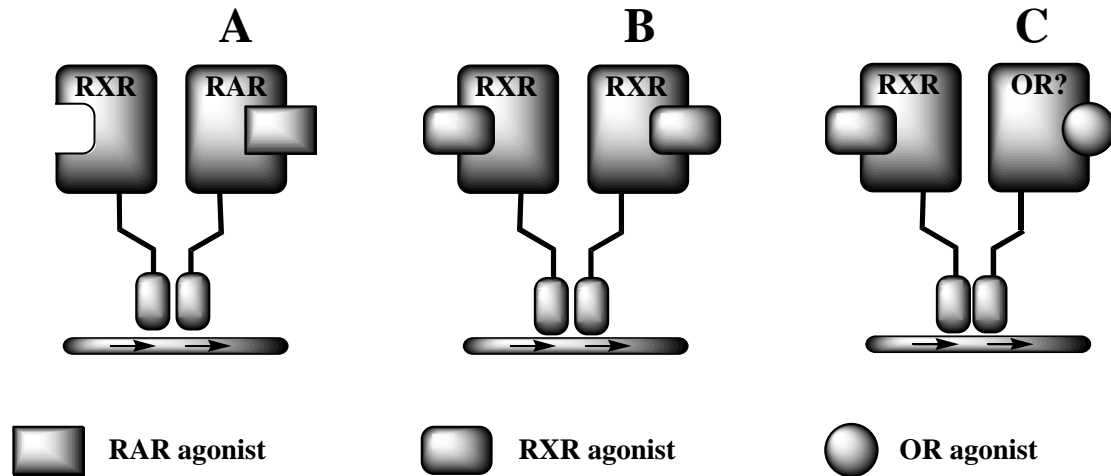


Figure 1.4 Multiple retinoid signalling pathways.

Activation of transcription from RAREs occurs in three stages or levels.³⁶ In the absence of agonists, RARs bind to DNA *via* their DNA binding domains (DBDs) and recruit co-repressors, such as SMRT and NCoRT, leading to suppression of transcription from the response element (**Figure 1.5A**). Binding of RAR agonists, such as ATRA, to the ligand binding domain (LBD) of the RAR causes a conformation change of the RAR. This conformational change dislodges the bound corepressors, resulting in basal transcription levels (**Figure 1.5B**). Recruitment of transcriptional coactivators, such as SRC-1, COACT-X, CBP (steroid receptor coactivator-1, coactivator-X and CREB binding protein, respectively) or P-300, by the RAR-agonist complex results in an activated transcription complex and maximum levels of transcription from the RARE (**Figure 1.5C**). Deactivation of transcription from RAREs may be achieved through the use of RAR antagonists. Binding of RAR antagonists reversibly blocks the LBP without inducing the conformation change in the RAR required to dislodge the bound corepressors (**Figure 1.5D**).³⁶

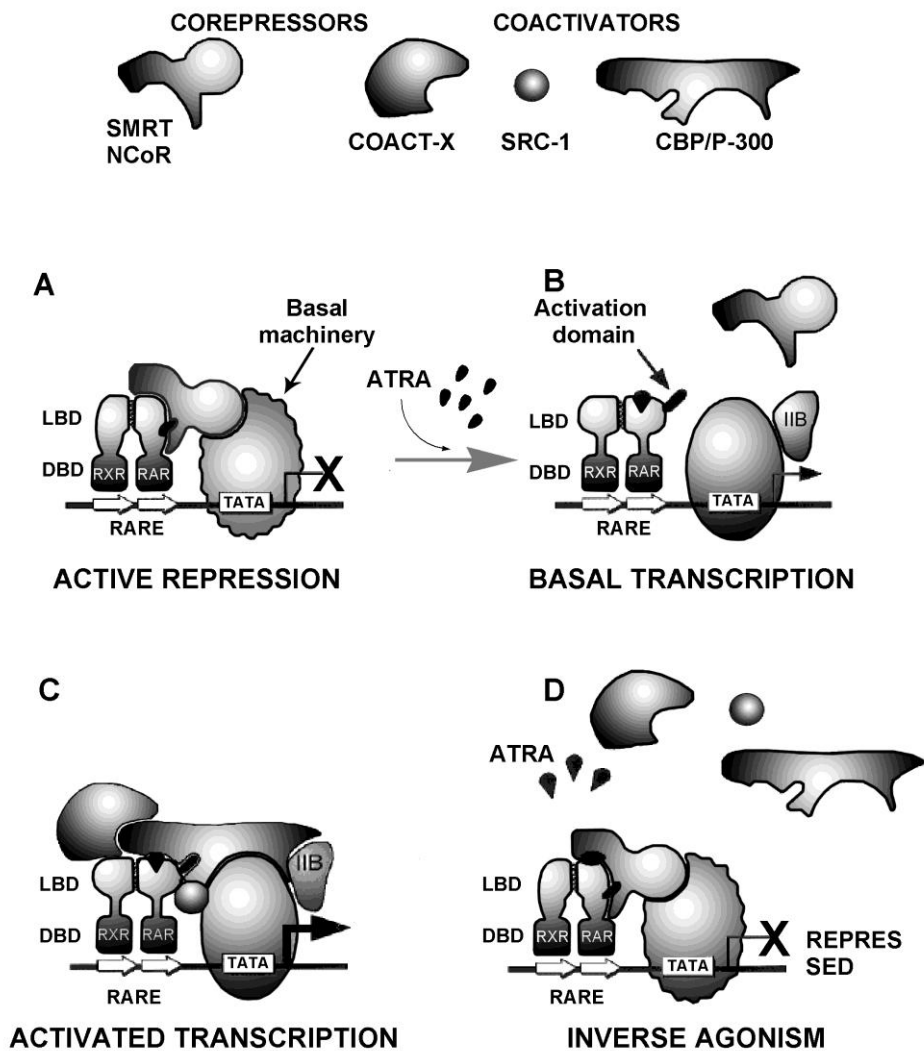


Figure 1.5 Levels of transcriptional activation of RARE *via* RAR binding and activation and repression of transcription from RAREs by RAR antagonism.

1.1.2 Receptor specificity in retinoids.

The RAR/RXR isotypes differ in both their tissue distribution and in the biological processes mediated.³⁷ RAR α is ubiquitous in its distribution, is involved in the differentiation therapy of acute human promyelocytic leukaemia³⁸ and is associated with elevated triglyceride levels.³⁹ RAR β is expressed predominantly in the heart, lungs and spleen³⁷ and RAR β subtypes exhibit suppressive effects on certain cell types⁴⁰ and thus

constitute a possible target for the treatment of breast and other cancers.⁴¹ RAR γ is primarily expressed in the skin and bone^{37,42} and is associated with skin photoaging,⁴³ dermatological diseases⁴⁴ and carcinogenesis.⁴⁵ The wide ranging effects of non-isotype specific retinoids have so far limited their medical use. Thus, the preferential binding to the LBP of specific receptor isotypes is necessary if the high biological activities of the retinoids are to be harnessed for clinical use.

1.1.2.1 RAR Selectivity

Through sequence alignment of the RAR isotypes, it has been shown that the LBPs are highly conserved in the RARs with only 3 LBP residues differing between the 3 isotypes^{28b,31,46} on the 3, 5 and 11 helices. Géhin *et al.* have demonstrated that ligand interaction with these non-conserved residues is crucial for determining RAR isotype selectivity (**Table 1.1**).²⁰

Table 1.1 Divergent residues in the RAR isotype ligand binding pocket.

Receptor	Helices		
	H ₃	H ₅	H ₁₁
RAR α	Ser232	Ile270	Val395
RAR β	Ala225	Ile263	Val388
RAR γ	Ala234	Met272	Ala397

1.1.2.2 RAR α selectivity

The LBP of RAR α differs from that of the β and γ isotypes by the presence on H₃ of a H-bond donor residue Ser232, in contrast to lipophilic Ala225 and Ala234 residues present in the LBPs of RAR β and RAR γ , respectively. The formation of strong H-bonds between synthetic retinoids possessing H-bond acceptors, such as amide groups, in the linker region (i.e. AM 580,⁴⁷ AGN 193836⁴⁸ and AM 555S⁴⁹) and this residue results in RAR α selectivity (**Figure 1.6**).

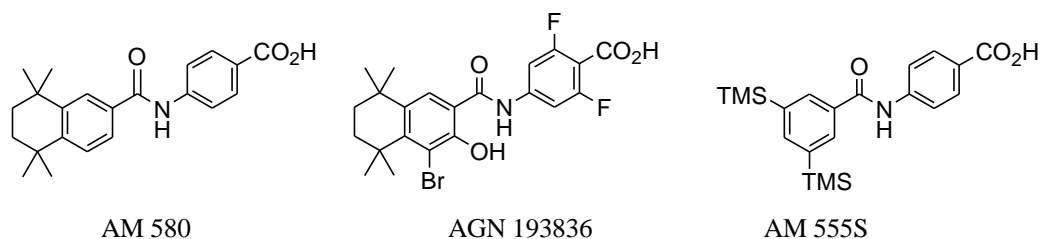


Figure 1.6 Synthetic RAR α selective retinoids.

1.1.2.3 RAR β selectivity

The RAR β LBP lacks the H-bond donor residue Ser232 which is present in the RAR α LBP and thus, cannot interact selectively with ligands *via* H-bonding. Instead, RAR β selectivity is conferred by steric effects, with the smaller Ala225 and Ile263 residues distinguishing the RAR β LBP from that of RAR α and RAR γ , respectively. The less sterically demanding residues in the LBP allow for the binding of larger retinoids, especially those possessing larger lipophilic regions than the widely used 1,1,4,4-tetramethyl-2,2,3,3-tetrahydronaphthalene (**Figure 1.7**).

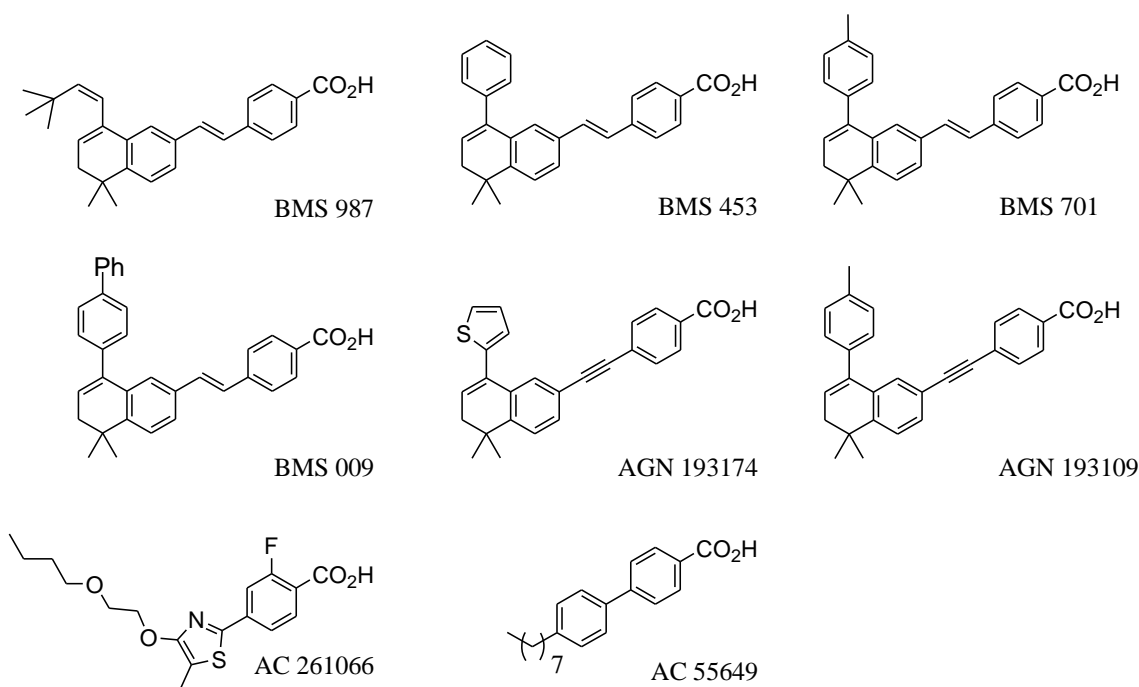


Figure 1.7 Synthetic retinoids.

This can be observed in the crystal structure of the complex of human RAR β (hRAR β) ligand binding domain with the RAR pan-agonist TTNPB⁵⁰ (Figures 1.8 & 1.9),^{28a} in which an additional cavity in the hydrophobic region of the LBP is observed due to the smaller H₃ Ala225 residue.

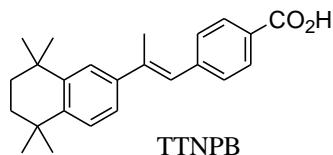


Figure 1.8 Synthetic retinoid TTNPB.

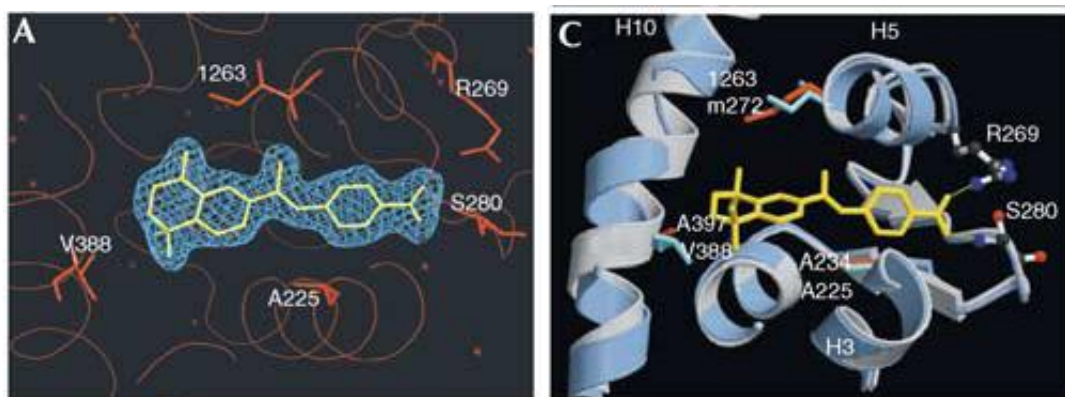


Figure 1.9 Crystal structure of the hRAR β LBP–TTNPB complex revealing an additional cavity in the LBP. Reproduced with permission of the copyright holder.

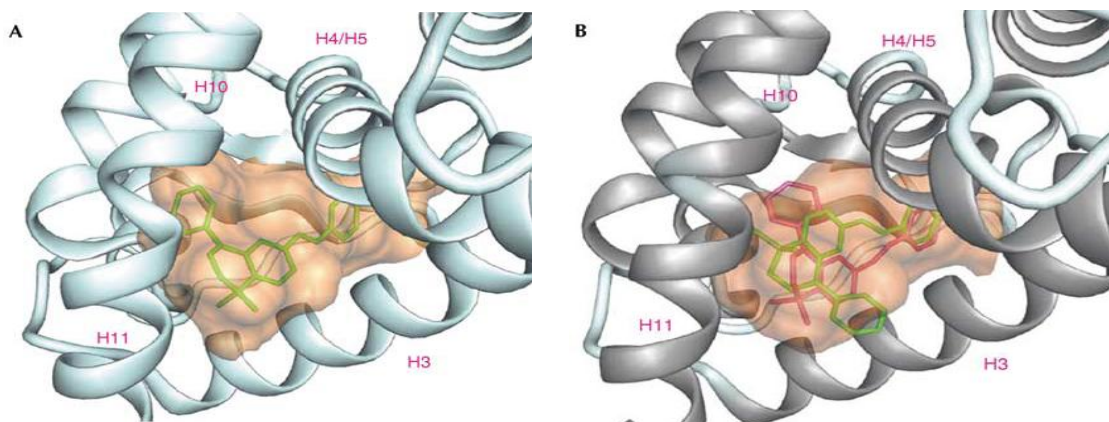


Figure 1.10 Model structure of the docking of RAR β agonist / RAR γ agonist BMS 453 into the RAR β (left) and RAR γ LBP (right). Reproduced with permission of the copyright holder.^{28a}

The mixed agonist/antagonist behaviour of BMS 453^{28a} and AGN 193174⁵¹ results from the inability of BMS 453 and AGN 193174 to effectively induce the conformational change necessary to dislodge bound corepressors when bound into the smaller RAR α and RAR γ LBPs. This can be observed in the structure of the docking of the RAR β agonist BMS453 in the RAR γ LBP, as modelled by VOIDOO and MSMS, which shows steric clashes between the BMS 453 phenyl ring and residues on H₃ and H₅ (**Figure 1.10B**).^{28a} Altering the shape of the retinoid lipophilic unit from (*Z*)-3,3-dimethylbut-2-en-1-yl (BMS 987) to phenyl (BMS 453) reduces RAR β agonist activity suggesting that the phenyl ring may cause some weak interference with H₁₂ positioning and recruitment of coactivator. Further increases in steric bulk lead to further decreased agonist activity for BMS 701 and a high affinity RAR β antagonist in the case of BMS 009.^{28a} Similar effects are observed for the exchange of the thiophenyl moiety of RAR β agonist AGN 193174 with *p*-tolyl to give AGN 193109 which exhibits pan RAR β antagonism.⁵¹ 4'-Octyl-4-biphenylcarboxylic acid⁵² (AC-55649, originally of interest for its liquid crystal phase behaviour^{52b}) and AC-261066 are highly selective agonists for the RAR β 2 receptor isoform. RAR isoform selectivity cannot be achieved *via* interaction with non conserved residues in the LBP (AF-2) as the four RAR β isoform LBPs are identical. Instead, the variation between the isoforms is located in the ligand-independent activation domain (AF-1),⁵³ which cooperates with the ligand binding domain (AF-2) in a promoter context manner.⁵⁴ AF-1 and AF-2 are activating function domains which are responsible for transcriptional activity of nuclear receptors and can interact with coactivators such as p300/CBP.^{53a} Thus, retinoids, such as AC-55649 and AC-261066, which significantly interact with AF-2 (**Figure 1.11**),^{52a} may induce differing interactions between conserved AF-2 and non conserved AF-1 regions in the RAR β isoforms, leading to isoform selectivity.

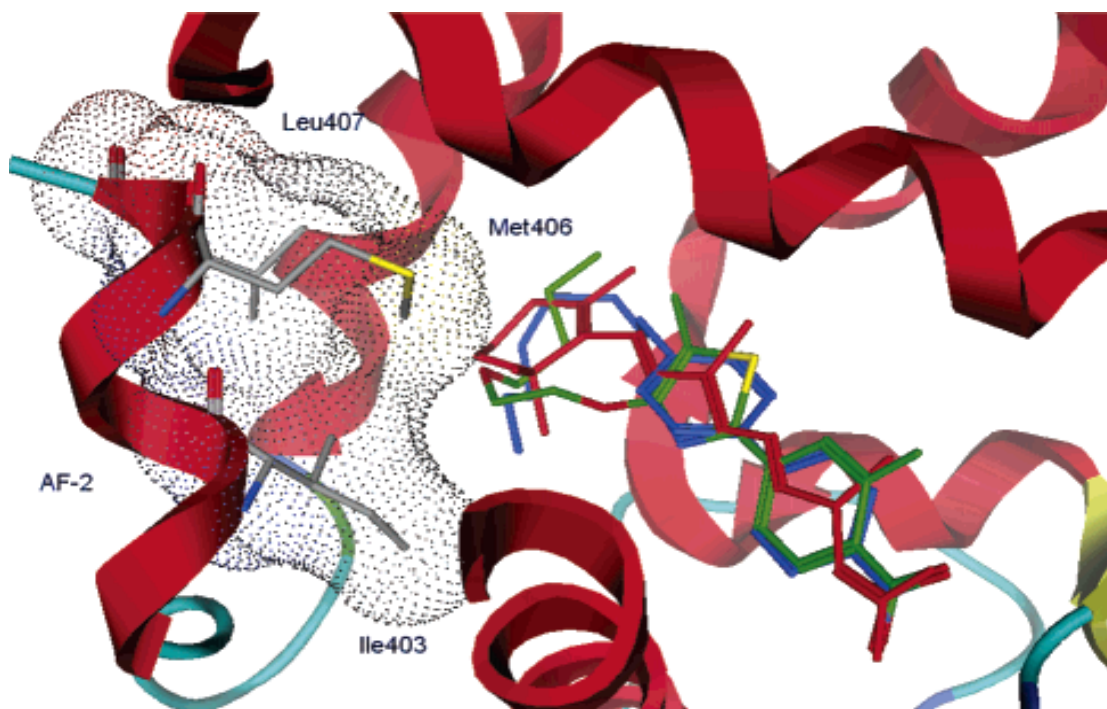


Figure 1.11 Modelling of the interactions of ATRA, AC 55649 and AC 261066 with the AF-2 domain. Reproduced with permission of the copyright holder.^{52a}

1.1.2.4 RAR γ selectivity

The RAR γ LBP differs from that of α and β isotypes by the presence of the weakly polar Met272 residue. The formation of a weak H-bond between this residue and retinoids possessing an H-bond donor on, or adjacent to the hydrophobic region confers RAR γ selectivity.^{31,55} This can be observed in the modelling of the structure of the CD 666-hRAR γ complex (**Figure 1.13**).⁵⁶ In addition, the smaller Ala397 residue allows for the docking of larger hydrophobic moieties, such as the 2-adamantylphenol group of CD 437 (**Figure 1.12**),⁵⁷ against helix 11 of RAR γ , which is not the case for RAR α /RAR β .

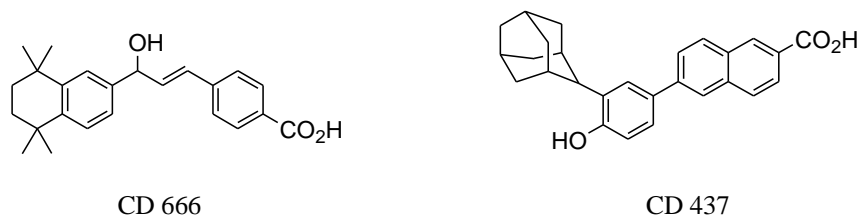


Figure 1.12 RAR γ selective retinoids.

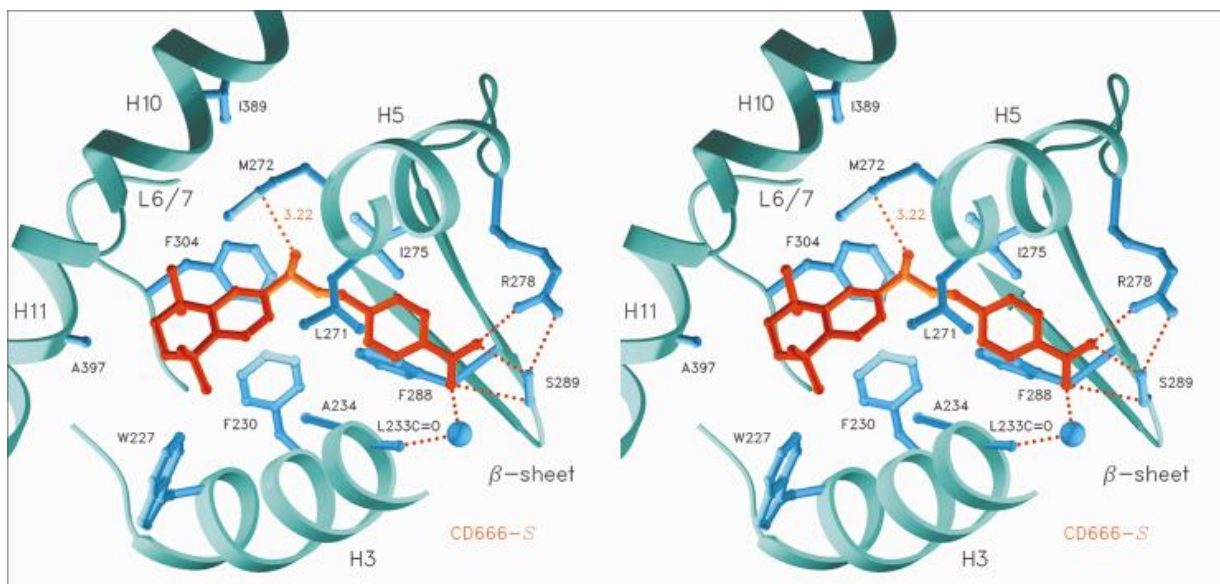


Figure 1.13 Modelling of the CD 666-hRAR γ complex. Reproduced with permission of the copyright holder.⁵⁶

1.1.2.5 RXR selectivity

RXR α is expressed mainly in adult tissue, with RXR β present in nearly all tissue types, while RXR α and RXR γ are expressed mainly in the liver, kidney, spleen and skin and in the brain and muscle, respectively.⁵⁸ The endogenous ligand for RXRs is 9cRA.^{26,27} Crystallographic studies^{29,31} of 9cRA-RXR complexes show distortion of the ligand with the region past C9 twisted perpendicular to the plane of the hydrophobic cyclohexenyl ring. The 9-*cis* double bond in 9cRA allows it to adopt both linear and twisted conformations in comparison to ATRA, which can only adopt linear conformations. This allows 9cRA to act as an agonist for RARs, which possess an elongated LBP with an ‘I’ like shape, and for RXRs with a twisted ‘L’-like LBP. In contrast to the RAR LBPs, the LBP of the RXR isotypes does not differ for each isotype and as yet, no isotype selective retinoids have been reported.⁵⁹ The crystal structures of 9cRA bound to RXR LBPs show that the 9cRA ligand does not completely fill the LBP with 31% of the available LBP volume unfilled, predominantly in two regions.⁶⁰ By synthesising retinoids which favour twisted conformations, and by increasing the size of both the hydrophobic and

hydrophilic regions with respect to 9cRA, the selectivity for RXRs over RARs may be increased. Synthetic retinoids which show high selectivities for RXRs over RARs are usually shorter than RAR agonists, typically with one linker atom between the hydrophobic ring and carboxyl bearing ring. In addition, the presence of *ortho* ring substituents on the hydrophobic ring, which enforce twisted conformations (by steric interactions with the carboxyl bearing ring), is a common feature of many RXR agonists (Figure 1.14).

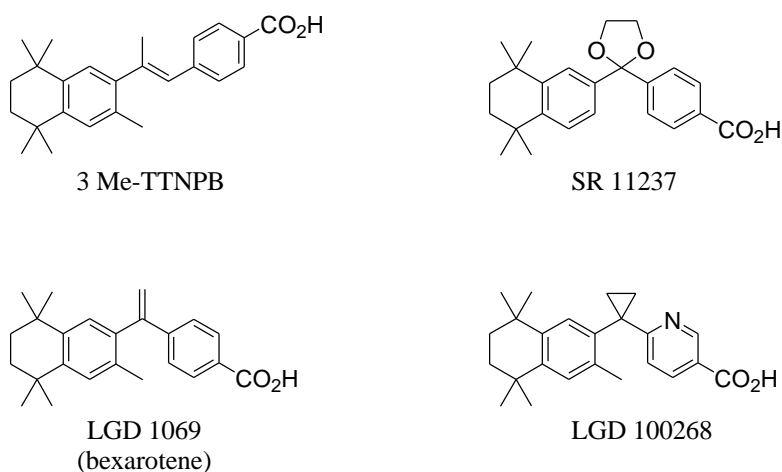


Figure 1.14 RXR selective retinoids.

This is demonstrated by 3-Me TTNPB,^{18,61} which activates both RAR and RXRs, while TTNPB^{18,28,50} shows no RXR activation. SR 11237,⁶² LGD 100268⁶³ and LGD 1069⁶⁴ are all potent RXR agonists with binding affinities in excess of that for 9cRA. The 3-Me groups of LGD 1069 and LGD 100268 both enforce the twisted conformations necessary for RXR selectivity.

1.1.3 Design and structure of synthetic retinoids

The activities of natural retinoids, such as ATRA and 9cRA, are limited by their isomerism into species which possess differing activities and their oxidative metabolism by cytochrome P450 enzymes. These destructive processes proceed *via* reactions of key functionalities in ATRA and 9cRA. By replacing these moieties with more robust pharmacophores, retinoids may be synthesised which exhibit similar efficacies as ligands

for RARs or RXRs, but with improved resistance to metabolism and thus improved activities.

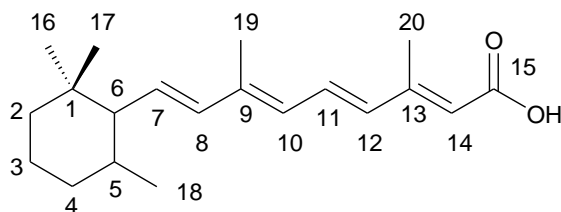


Figure 1.15 Retinoid numbering scheme.

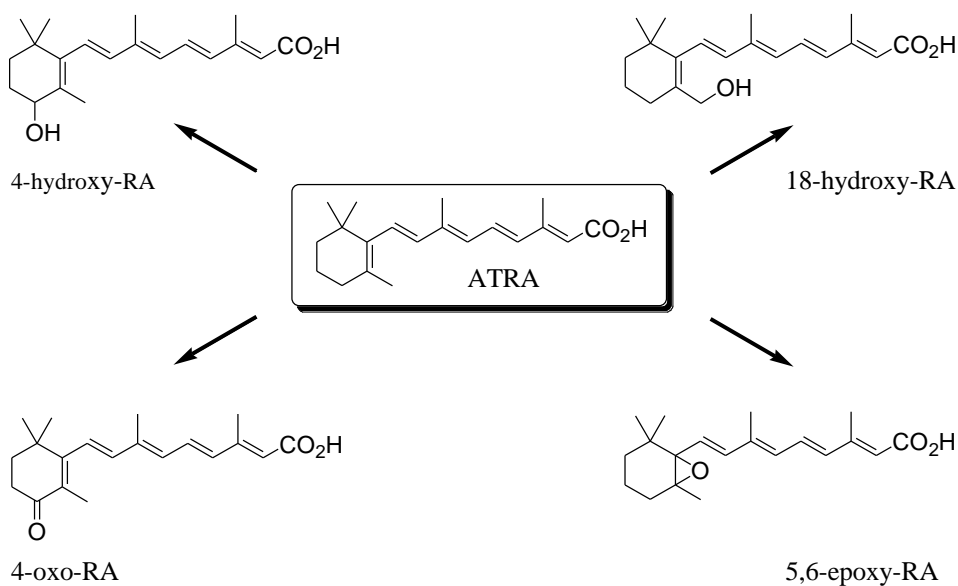


Figure 1.16 Products of ATRA oxidative metabolism.

The oxidative metabolism of ATRA leads to 4-hydroxy-, and 4-oxo-ATRA *via* oxidation at the allylic 4-position and at the 18-position to give 18-hydroxy ATRA. In addition, a 5,6-epoxy derivative is formed from epoxidation of the terminal double bond of the polyene chain (in the cyclohexane ring).⁶⁵ By replacing the trimethylcyclohexenylvinyl unit (C₁-C₈) with a structurally similar 1,1,4,4-tetramethyl-1,2,3,4-tetrahydro-naphthalene moiety, which possesses no allylic protons or alkene double bonds, degradation *via* radical oxidation and epoxidation is reduced. In addition, by replacing two C=C double

bonds in the conjugated polyene by an arene ring, photo-induced isomerism is decreased, leading to greater stability. These synthetic retinoids which contain one or more aromatic rings are termed arotinoids. Further increases in photostability and resistance to oxidative metabolism may be achieved by constraining the flexible polyene chain by incorporating it into one or more aromatic rings. By means of these modifications the trimethylcyclohexenyl ring and the conjugated tetraene of the natural retinoids may be replaced by robust structural units such as stilbene, tolan, biaryl or biaryl amide to give retinoids which exhibit high activity and stability such as TTNPB,⁵⁰ EC23,¹² TTNN (SRI 5898-52)⁶⁶ and Am580,⁴⁷ respectively (**Figure 1.17**).

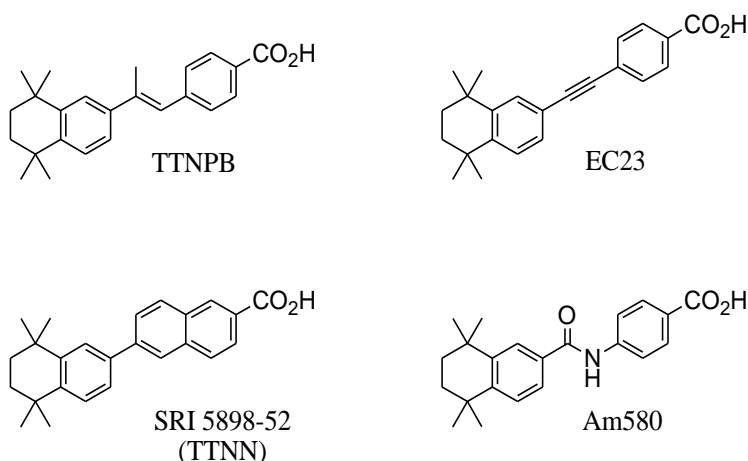


Figure 1.17 Arotinoids.

1.1.3.1 Modification of the hydrophobic unit

The effects of modification of hydrophobic unit on retinoid activity can be observed in the structure-activity relationships for a series of TTNPB analogues on the differentiation of cultured hamster trachea cells (TOC assay).⁶⁷ Replacing the 1,1,4,4-tetramethyl-1,2,3,4-tetrahydro-naphthalene in TTNPB with 1,2,3,4-tetra-methylnaphthalene (SRI 5193-55) led to a decrease in the activity by over 2 orders of magnitude, in comparison to TTNPB, suggesting that it is desirable for the methyl substituents on the hydrophobic unit to lie out of the plane of the aromatic ring. Removal of either of the C₄ methyl groups needed to block oxidation metabolism at that position leads to a drop in activity, with the

S-isomer, SRI 6910-29, showing a reduction in activity of over one order of magnitude, compared to TTNPB. The *R*-isomer, SRI 6910-50, was found to be 4 times less active than the *S*-isomer, SRI 6910-29. Surprisingly a racemic mixture of SRI 6910-29 and SRI 6910-50 displayed a lower activity than either of the isomers on their own. The decreased activity of SRI 6910-29, SRI 6910-50 and racemic mixtures in comparison to TTNPB indicates the need for two methyl groups at the C₄ position for high biological activity.⁶⁸

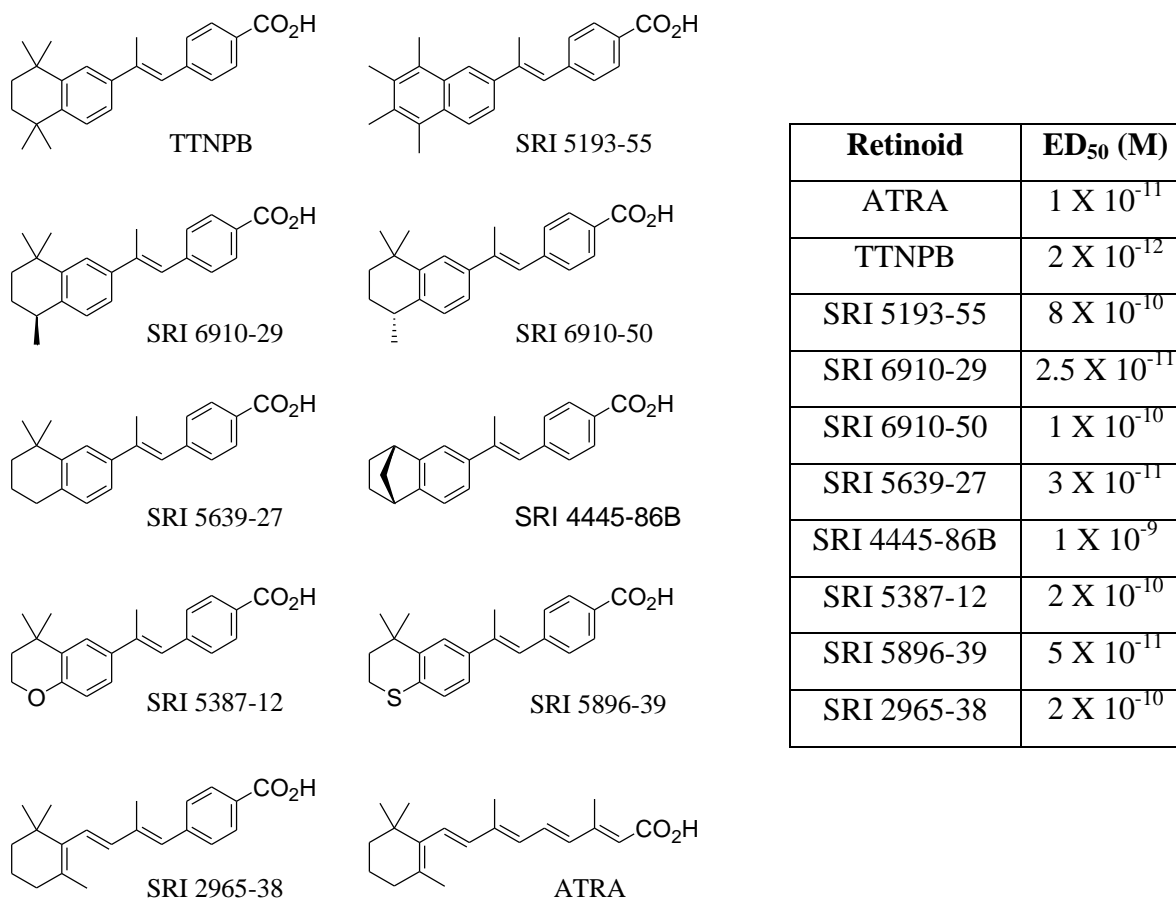


Figure 1.18 Modification of the hydrophobic unit in TTNPB arotinoids and their activities in the TOC assay.

This is reinforced by SRI 5639-27, lacking both C₄ methyl groups, which possesses a similar activity to both SRI 6910-29 and ATRA, and by the dramatic decrease in activity, compared to TTNPB, of nearly 3 orders of magnitude for the benzonorborenyl analogue SRI 4445-86B. SRI 2965-38, a C₁₁-C₁₄ benzofused analogue of ATRA, exhibits a biological activity over one order of magnitude less than SRI 5639-27, which also lacks

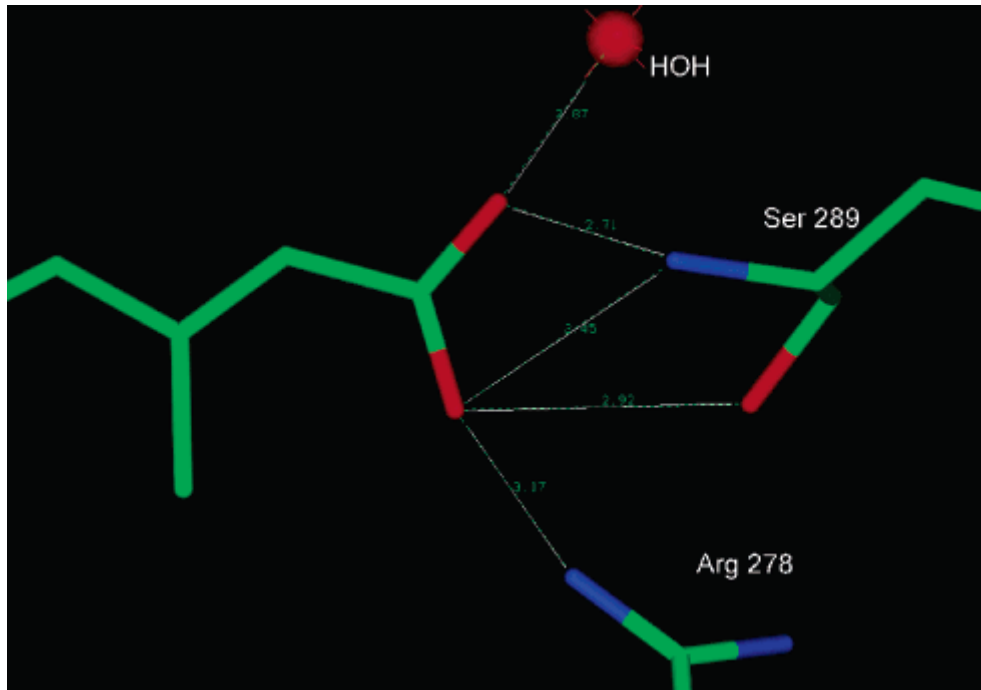
both methyl groups at C₄. This suggests that incorporating the C₅-C₆ and C₇-C₈ double bonds into a benzene ring improves activity in this assay. SRI 2965-38 was also found to possess reduced activity, compared to both TTNPB and ATRA (results are summarised in **Figure 1.18**).⁶⁸

Substitution of the C₄ methylene group of aromatic retinoids with heteroatoms leads to a class of retinoids termed heteroarotinoids, which have demonstrated significant potential as anticancer agents due to their activity as inhibitors of the induction of ornithine decarboxylase (ODC)⁶⁹ and their resultant ability to prevent or inhibit the transformation of healthy cells into cancerous cells.⁷⁰ In addition, several heteroarotinoids exhibit much reduced toxicities,^{69a,70a} in comparison to their carbocyclic analogues, with the reduced toxicity believed to result from the incorporation of the heteroatom.^{70a} Both SRI 5387-12 and its thia-analogue SRI 5896-39 exhibit diminished activity, in TOC assay, compared to the parent retinoid TTNPB, with the loss of activity resulting both from the lack of lipophilic bulk in the 4-position, and the increase in polarity of the hydrophobic unit caused by the substitution with more electronegative atoms. The lower activity of oxy-TTNPB analogue SRI 5387-12, in comparison to SRI 5896-39, results from the increased electronegativity of the oxygen atom, which further reduces hydrophobic interactions with the non-polar residues present around the hydrophobic region of the LBP. Similar trends have been reported by Benbrook *et al.*⁷¹ for other oxygen and sulphur heteroarotinoids. However, it must be noted that dihydrobenzothiapyran based retinoids such as SRI 5896-39 are oxidised to sulfones and sulfoxides which exhibit low activities in the TOC assay.⁶⁸ This ease of oxidation and subsequent deactivation may explain low lower toxicities of sulphur heteroarotinoids in comparison to their carbocyclic analogues.^{70a}

Although oxygen and sulphur are the most prevalent heteroatoms in heteroarotinoids, other elements have also been used, with Tacke *et al.* having reported the synthesis and binding to RARs and RXRs of 1,4-disila-analogues of the arotinoids TTNPB, 3-Me TTNPB⁷² and LGD 1069 (bexarotene).⁷³

1.1.3.2 Modification of the polar terminus

In order to effectively bind to the RAR or RXR LBPs, the polar terminus of the retinoid must be capable of interacting favourably with the residues present in the ‘bottom’ of the LBP. These interactions between the LBP and the ‘anchoring’ group on the polar terminus can be observed in the crystal structures of 9cRA with RAR and RXR (**Figure 1.19**).⁷⁴ In the 9cRA-RAR complex, the carboxylate of 9cRA forms an ion pair with Arg 278 and 3 hydrogen bonds with the main chain amide group, side chain hydroxyl group of Ser 289 and a bound water molecule of RAR. In the 9cRA-RXR complex, an ion pair is formed between the ligand carboxylate and Arg 316, as well as 2 hydrogen bonds between the carboxylate, the amide group of Ala 327 and a bound water molecule of RXR.⁷⁴



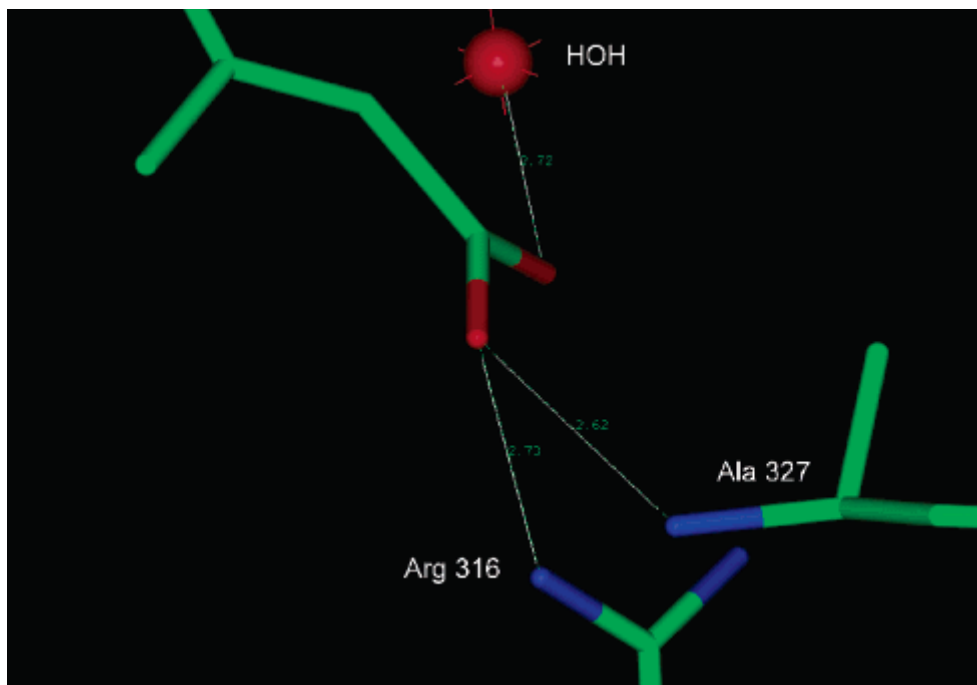


Figure 1.19 Crystal structures of 9cRA-RAR (top) and 9cRA-RXR (bottom) complexes. Reproduced with permission of the copyright holder.⁷⁴

Although not proven, it is believed that the highest oxidation state of vitamin A, ATRA, is responsible for controlling cellular differentiation. Thus, in order to display biological activity of this type, retinol and retinal must be oxidised to ATRA.⁷⁵ As the hamster trachea organ culture (TOC) assay is based on a whole organ culture, it possesses the full complement of enzymes. As a result, retinoid amides, which are inactive in epidermal ODC assay, show high activities in the TOC assay, suggesting that the necessary enzymes for the hydrolysis of retinoid amides prodrugs to the active acid forms are present in the organ culture.^{67,68}

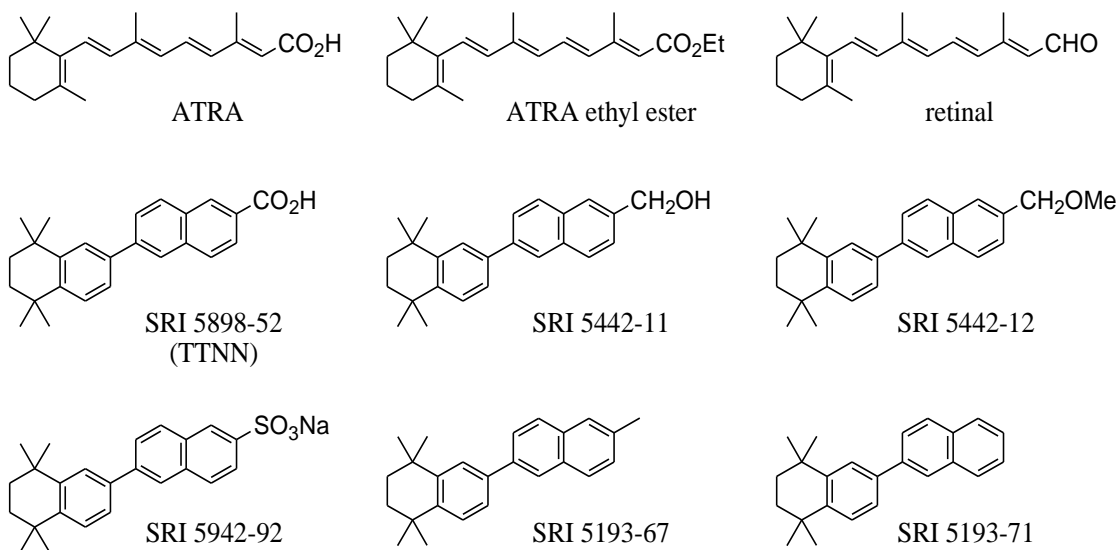


Figure 1.20 Modifications of the polar terminus.

Retinol, which is oxidised *in vivo* to give ATRA, is less active than its acid form in the TOC assay by over 2 orders of magnitude. Similar differences in biological activity were seen between TTNN and both its alcohol form SRI 5442-11 and the methyl ether SRI 5442-12. The sulfonate analogue of TTNN, SRI 5942-92, possessed only a quarter of the activity of TTNN alcohol SRI 5442-11 in the TOC assay, suggesting that the sulfonate moiety does not interact with the receptor residues as effectively as the carboxylate moiety. Due to the full complement of enzymes present in the TOC assay, the methyl naphthalene derivative, SRI 5193-67, may be oxidised *in vivo* to give polar species which exhibit retinoid activity (including TTNN) and showed activity comparable to that of sulfonate SRI 5942-92. The naphthalene derivative, SRI 5193-71, which cannot be oxidised to TTNN, was not active in the TOC assay (**Figure 1.20**).⁶⁸

1.1.3.3 Modification of the linker unit

Most arotinoids feature 1,1,4,4-tetramethyl-1,2,3,4-tetrahydro-naphthalene as the hydrophobic unit and a carboxylate-bearing aromatic ring as the polar terminus, with these two functionalities linked by a short linker unit of 1-3 atoms. Despite the small size of the linker unit, a wide variety of differing functionalities have been employed as

linkers in arotinoid structures, with changes in linker structure allowing for selectivity between RARs and RXRs as well as RAR isotypes to be controlled. The *E*-propenyl linker of TTNPB⁵⁰ closely mimics the skip methylated chain of ATRA. TTNPB is one of the most active synthetic retinoids yet discovered, possessing an activity in the hamster TOC assay 5 times greater than that of ATRA.⁶⁸

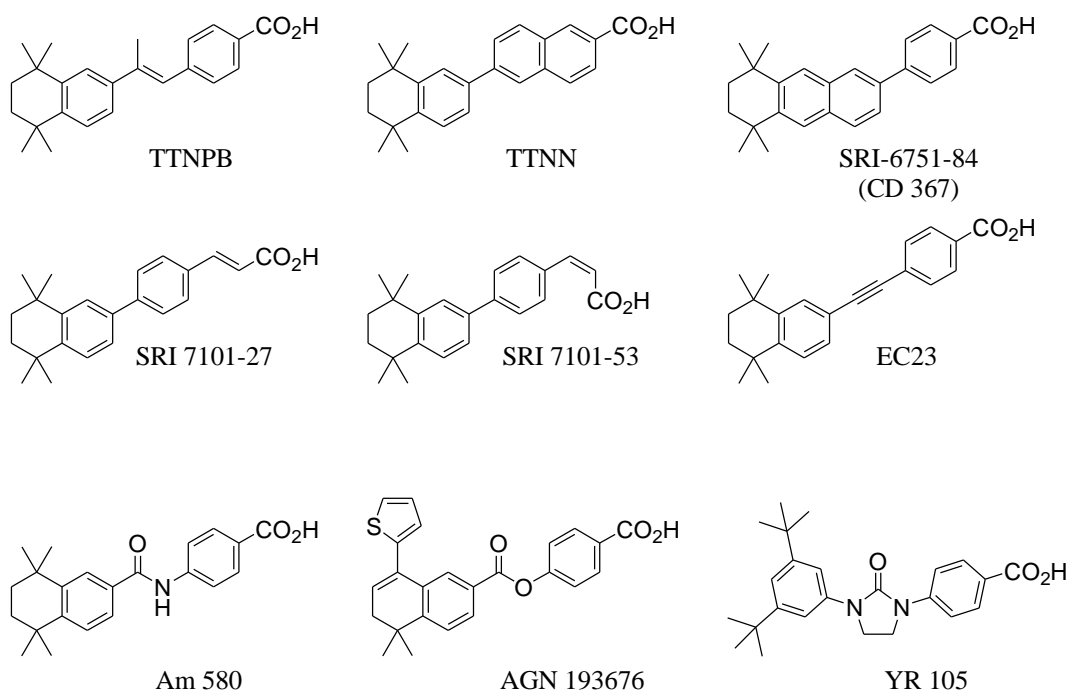


Figure 1.21 Synthetic retinoids possessing varying linker units.

Retinoids TTNN⁶⁶ and SRI-6751-84⁷⁶ can be considered as isomeric, benzo-fused analogues of TTNPB and display high biological activities, with that of TTNN comparable to TTNPB, and that of SRI-6751-84 showing equivalent activity to ATRA. Both TTNN and SRI-6751-84 are RAR selective agonists due to their rigid, linear structures, with TTNN showing a greater affinity for RAR β over RAR α and RAR γ .

Other hydrocarbon linker units include; the biaryl groups of *E*-, and *Z*-cinnamate retinoids SRI 7101-27 and SRI 7101-53, respectively, which show limited biological activities in the TOC assay, and the triple bond of the photostable retinoid EC23, which is highly effective in the induction of neural differentiation in human TERA2.c1.SP12 embryonal carcinoma cells, with activity greater than that of the native ligand ATRA.¹²

Other linker units not based upon hydrocarbons include; the amide linkages of Am 580,⁴⁷ the internal ester linkage of the RAR β agonist AGN 193676⁵¹ and the cyclic urea linkage of YR 105, an inducer of differentiation of HL-60 cells with activity comparable to that of ATRA, (structures are shown in **Figure 1.21**).⁷⁷

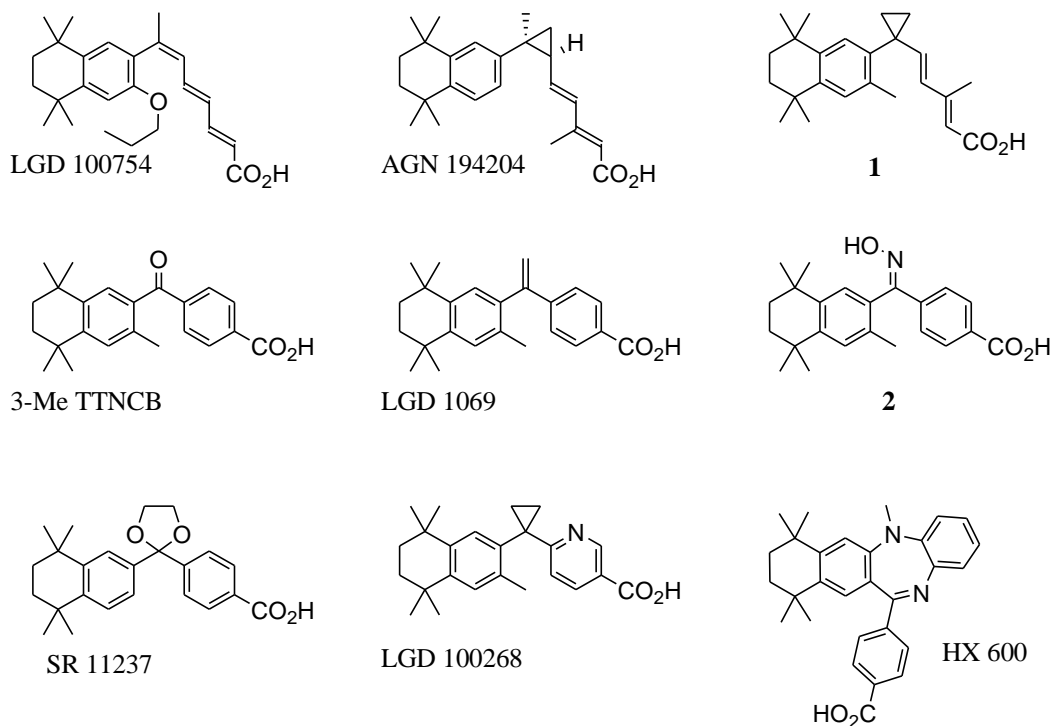


Figure 1.22 RXR selective synthetic retinoids possessing varying linker units.

Due to the differing shapes of the RAR and RXR LBPs, selectivity for RXRs over RARs requires ligands which adopt twisted conformations similar to the natural ligand 9cRA, rather than the linear conformations required for RAR binding. In RXR antagonist LGD 100754,⁷⁸ steric interactions between the 9-*cis* triene linker unit and an *ortho-n*-propyloxy substituent on the hydrophobic aromatic ring result in a twisted conformation. Polyene linker units can be effectively locked in the *cis* conformation by cyclopropanation of the *cis* double bond to give 1,2-*cis*-cyclopropane derivatives such as RXR agonist AGN 194420⁷⁹ or by addition of 1,1 disubstituted cyclopropanyl groups to the linker unit as in **1** (**Figure 1.22**).⁸⁰

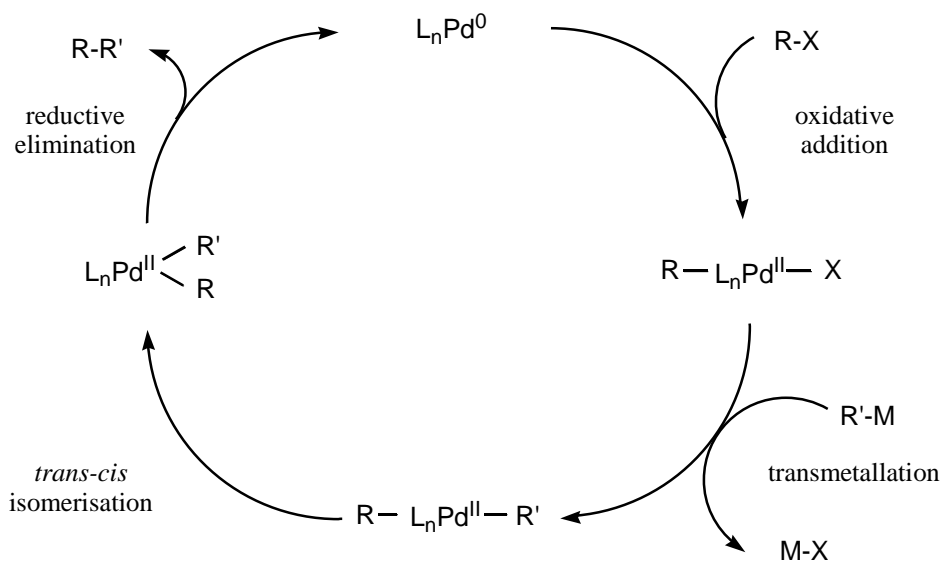
Rigid, one atom linker units, usually in conjunction with *ortho* substituents on the hydrophobic aromatic ring, give RXR selectivity due to minimisation of steric interactions between the aromatic ring of the polar terminus and the *ortho* substituents on the hydrophobic aromatic ring. Examples (**Figure 1.22**) of such rigid linker units include an alkene in LGD 1069 (Targetin[®], bexarotene),⁶⁴ which is currently licensed for the treatment of the treatment of cutaneous manifestations of T-cell lymphoma, a carbonyl group (e.g. 3-Me TTNCB),⁶³ an oxime (e.g. **2**),⁸¹ 2,2-dioxanyl group (SR 11237)⁶² and a 1,1-cyclopropanyl group (LGD 100268).⁶³ Alternatively, the linker unit may be incorporated into a suitably functionalised benzo-fused ring system, as in the RXR agonist HX 600.⁸²

In conclusion, synthetic retinoids can offer many advantages over their endogenous analogues, ATRA and 9cRA, and would appear destined to play a significant role, both as tools for research and in medicine. Not only are synthetic retinoids typically more stable to light and to enzymatic metabolism, which usually leads to greater activity, but RAR isotype selective retinoids can offer a greater degree of control over their effects, which can prove to be beneficial in a clinical context, especially in regards to the reduction of toxicity. In addition, several selective retinoid-based treatments are currently in clinical trials for cancer therapy.

1.2 Palladium-catalysed cross-couplings

Palladium-catalysed cross-coupling reactions play an important role in modern organic synthesis with many syntheses of large molecules featuring at least one Pd-catalysed cross-coupling step.

Mechanistically, the various cross-coupling reactions (Suzuki-Miyaura,⁸³ Stille,⁸⁴ Negishi,⁸⁵ Sonogashira,⁸⁶ Hiyama,⁸⁷ etc.) are all similar, with the basic catalytic cycle (assuming L_n represents two monodentate ligands) consisting of oxidative addition of a C-X (typically halide or triflate) bond to a zero valent metal centre to give a *trans*-Pd^{II} species, transmetalation, and *trans-cis* isomerisation followed by reductive elimination yielding the cross coupled product and the original Pd⁰ species.

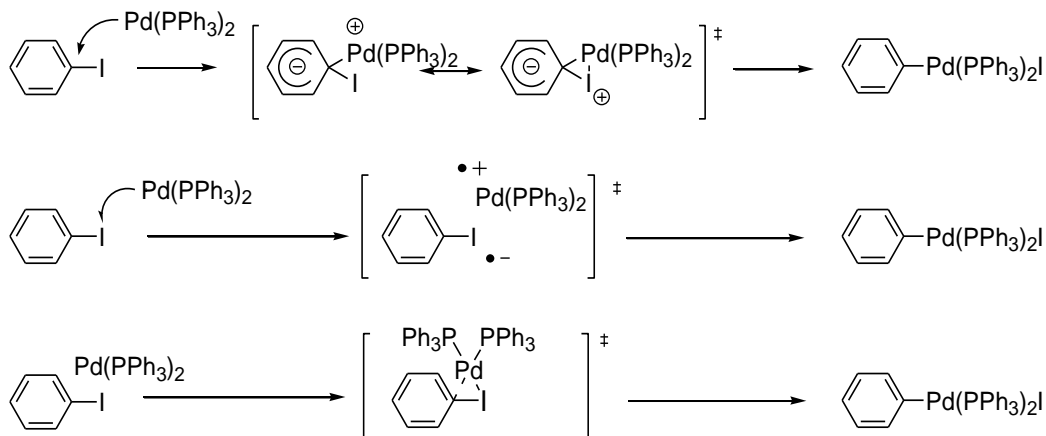


Scheme 1.1 Basic catalytic cycle for Pd-catalysed cross-couplings.

1.2.1 Oxidative addition

The first step of the catalytic cycle in Pd-catalysed cross-couplings is the oxidative addition of the C-X bond to the palladium centre, with reports suggesting that the active species is a coordinatively unsaturated Pd⁰ species bearing one (PdL), or two (PdL₂)

dative ligands.^{88,89,89,90,91,92} For tetrakis(triphenylphosphine)palladium, phosphine dissociation gives rise to $\text{Pd}(\text{PPh}_3)_3$ and $\text{Pd}(\text{PPh}_3)_2$ in solution, with the latter initially considered to be the active species in the oxidative addition step.⁹⁰ A variety of mechanisms have been proposed for oxidative addition, with the exact pathway dependent on metal ion and oxidation state, ligand, substrate and conditions. For aryl halides, the three main pathways are shown in **Scheme 1.2**.^{89b,91}



Scheme 1.2 Oxidative addition pathways from top to bottom: nucleophilic addition, single electron transfer and 3-centred concerted addition.

Work by Fauvarque *et al.*, and later by Amatore *et al.* showed that for the oxidative addition of aryl iodides to $\text{Pd}(\text{PPh}_3)_4$, the mechanisms in THF ^{89a,92} and toluene^{89b} are identical and the slope of the Hammett plots are similar in the two solvents. The similar enthalpies and entropies of activation for the reaction in polar and non polar solvent shows that the transition state for the addition of aryl halides to the coordinatively unsaturated $\text{Pd}^0(\text{PPh}_3)_2$ species has no significant ionic character suggesting that oxidative addition occurs *via* either a concerted three-centre reaction or by a radical mechanism. For oxidative addition of aryl halides, the order of reactivity is found to be $\text{I} > \text{Br} \gg \text{Cl} \gg \text{F}$ with electron deficient aryl halides being more reactive than electron rich ones. This corresponds with a rate limiting step which involves the breaking of the C-X bond.⁹⁰ For a three-centered concerted addition the oxidative addition leads to an initial *cis* adduct which then isomerises to give the thermodynamically more stable *trans* complex.⁹¹ Isomerisation may occur *via* a dissociative pathway with a trigonal

$\text{ArPd}^{\text{II}}\text{PPh}_3\text{X}$ intermediate or by an associative pathway with a trigonal bipyramid $\text{ArPd}^{\text{II}}(\text{PPh}_3)_2\text{XA}$ intermediate formed by the coordination of either solvent or free halide anion (A) to $\text{ArPd}^{\text{II}}(\text{PPh}_3)_2\text{X}$.

Hartwig and coworkers have shown that for the addition of aryl bromides to Pd^0 complexes bearing bulkier phosphine ligands such as $\text{P}(o\text{-tol})_3$ the active species is a $12e^-$ monophosphine complex.⁹³ This was supported by catalytic studies by Fu and coworkers employing $\text{Pd}_2\text{dba}_3/\text{PR}_3$ mixtures in a 1:1 ratio to form the monoligated Pd species *in situ*.⁹⁴ Well defined Pd^0PR_3 complexes were shown to be highly active for the Suzuki-Miyaura cross-coupling of aryl halides with phenylboronic acid by Beller and coworkers.^{87j}

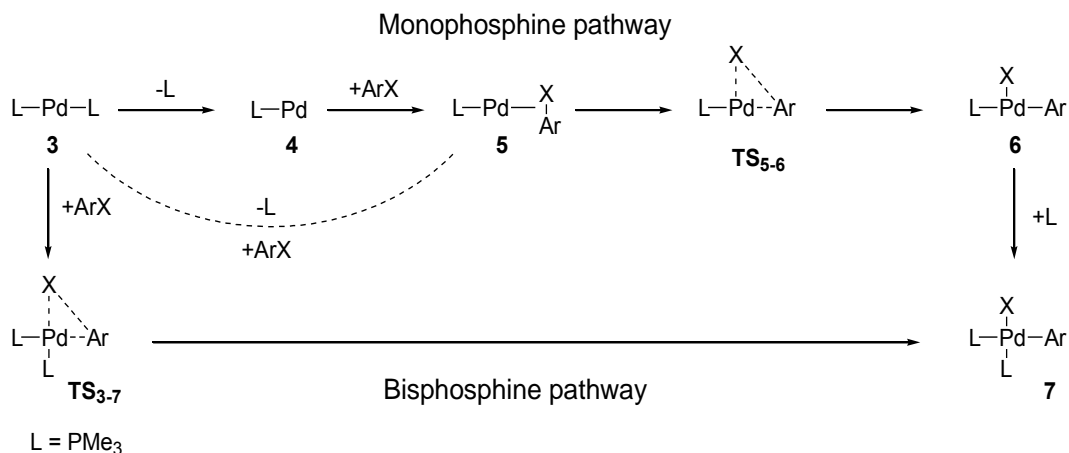
Further evidence for the role of monoligated PdL complexes was provided by the studies of ArX elimination, observed indirectly and directly by Hartwig and coworkers. $\text{P}(o\text{-tol})_3$ ligated arylpalladium halides of the form $[\text{Pd}(\text{Ar})(\mu\text{-X})\text{P}(o\text{-tol})_3]_2$ eliminate ArX upon addition of an excess of $\text{P}'\text{Bu}_3$ to give $\text{Pd}(\text{P}'\text{Bu}_3)_2$. In addition, well defined, three-coordinate $\text{Pd}^{\text{II}}(\text{P}'\text{Bu}_3)(\text{Ar})\text{X}$ complexes were shown to undergo elimination of ArX upon the addition of $\text{P}'\text{Bu}_3$ to give $\text{PR}_3\text{-Pd}^0\text{-P}'\text{Bu}_3$ complexes and ArX in 60–98% yields.⁹⁵

Jutand and co-workers have shown that the nature of the active Pd species for the oxidative addition reaction is sensitive to the bulk of the ligand L, with less bulky or bidentate ligands more likely to promote oxidative addition *via* PdL_2 species while more bulky monodentate ligands such as $\text{P}'\text{Bu}_3$ undergo oxidative addition *via* PdL.⁹⁶

Studies by Hartwig and coworkers on the oxidative additions of chloro-, bromo-, and iodobenzene to $\text{Pd}(\text{Q-phos-tol})_2$ (Q-phos-tol = (di-*tert*-butylphosphino)penta-*p*-tolylferrocene) have shown that the mechanism of oxidative addition is dependent on the identity of the halide. For PhI, associative displacement of ligand by PhI, prior to oxidative addition was found to be rate determining, while for PhBr, ligand dissociation from $\text{Pd}(\text{Q-phos-tol})_2$ is rate determining. In contrast, for PhCl, oxidative addition was

rate determining and is preceded by reversible ligand dissociation. In all cases, the oxidative addition occurred *via* the monoligated Pd(Q-phos-tol) species.⁹⁷

Lin and Marder carried out DFT studies on the oxidative addition of a range of *p*-Y-C₆H₄-X (Y = CN, H, OMe, X = Cl, Br, I) to Pd(PMe₃)₂ with both PdL and PdL₂ pathways investigated (**Scheme 1.3**).⁹⁸



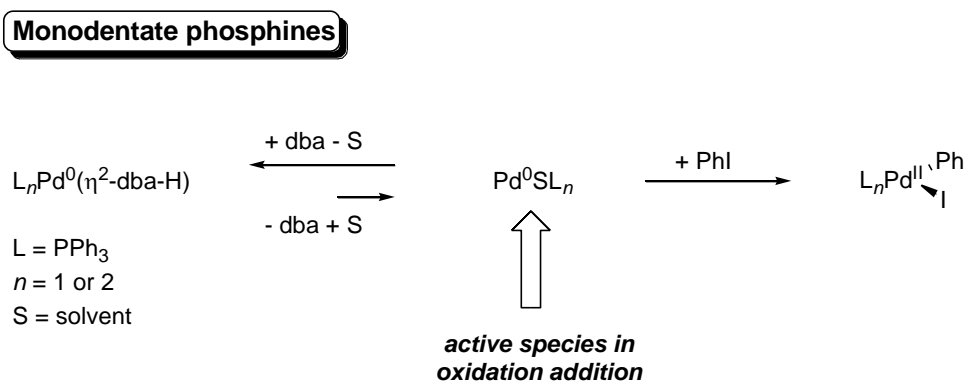
Scheme 1.3 Mono-, and bis-ligated pathways for oxidative addition of aryl halides to Pd⁰.

For aryl chlorides, the monophosphine pathway is favoured with transition state **TS₅₋₆** higher in energy than **4**. Thus oxidation addition is expected to be the rate determining step with the nature of the *para*-substituents on ArX affecting the rate. This is consistent with the results of Hartwig and co-workers for the reaction of PhCl with Pd(Q-phos-tol)₂. For aryl bromides, the monophosphine pathway is also favoured. The energy of monoligated palladium species **4** was found to be similar to **TS₃₋₇** with **TS₃₋₇** being marginally higher in energy than **4** for PhBr and *p*-MeO-C₆H₄-Br, while for *p*-NC-C₆H₄-Br **4** and **TS₃₋₇** are equal in energy.

For aryl iodides PhI and *p*-MeO-C₆H₄-I, the monophosphine pathway is marginally favoured, with the barrier between **5** and **6** being lower than the barrier to phosphine dissociation from **3**. This is consistent with the experimental findings of Hartwig and co-workers for the reaction of PhI and Pd(Q-phos-tol)₂. For *p*-NC-C₆H₄-I, the barrier to

oxidative addition to **3** is lower than the barrier to phosphine dissociation from **3** and thus the bisphosphine pathway is favoured.

Pd^0 complexes of π -acidic olefins such as dba (dibenzylideneacetone) are widely used in conjunction with donor ligands to generate “ Pd^0L_n ” complexes *in situ*. Amatore and Jutand have studied the oxidative addition of “ Pd^0L_2 ” generated from $\text{Pd}_2(\text{dba})_3$ and monodentate ligands to aryl iodides. “ Pd^0L_2 ” exists predominantly as $\text{Pd}^0(\text{dba})\text{L}_2$ which is unreactive for oxidative addition, due to reduction in electron density on the palladium centre due to π -backbonding to dba. The active species, Pd^0L_2 is generated in low concentrations from $\text{Pd}^0(\text{dba})\text{L}_2$, with which it is in an unfavourable equilibrium (**Scheme 1.4**).⁹⁹



Scheme 1.4 Reversible coordination of dba to Pd^0 centres.

Dissociation of dba from $\text{Pd}^0(\text{dba})\text{L}_2$ to give Pd^0L_2 was shown to be the rate determining step. Therefore, the strength of dba binding controls the concentration of the active species for oxidative addition and thus the kinetics of this key step. Fairlamb and coworkers have employed a range of n,n' -disubstituted dba analogues bearing a range of groups (OMe, ^tBu, H, CF₃, NO₂) as ligands in $\text{Pd}_2(\text{dba})_3$ type catalyst precursors in a range of palladium catalysed cross-couplings.¹⁰⁰ As expected, the use of $\text{Pd}_2(\text{dba})_3$ analogues bearing electron donating groups showed higher activity due to weaker π -backbonding between Pd^0 and the dba analogue, which reduces ligation of the active species by the dba analogues.¹⁰¹

1.2.2 Transmetallation

The predominant difference between the various cross-coupling reactions is the nature of the transmetallation step in which the halide or pseudohalide on Pd^{II} is replaced by the nucleophilic carbon centre of the transmetallating species M-R₁. M may be a p-block element such as boron (Suzuki-Miyaura reaction), silicon (Hiyama reaction), tin (Stille reaction) or aluminium, a transition metal such as copper (Sonogashira reaction) or zinc (Negishi reaction) or s-block elements such as magnesium (Kumada-Tamao-Corriu reaction). The transmetallation steps in the Sonogashira and Suzuki-Miyaura reactions will be discussed in more detail in further sections.

1.2.3 Reductive elimination

The increased oxidation state of palladium and the high strength of the C-C bond make the formation of a C-C bond *via* reductive elimination of the two carbon centres on Pd^{II} highly favoured. Due to the lack of polarisation in the bond formed, the elimination step occurs *via* a concerted mechanism. In order for reductive elimination to occur, the two substituents on palladium must be in a *cis* configuration. This is demonstrated by the two dimethyl palladium complexes shown in **Figure 1.23**. The differing bite angles of 1,2-bis-diphenylphosphino-ethane (dppe) and 2,11-bis-[(diphenylphosphanyl)-methyl]-benzo[*c*]phenanthrene enforce *cis* and *trans* conformations, respectively, in their dimethylpalladium complexes. Warming Pd(dppe)Me₂ (**8**) in DMSO produces ethane due to reductive elimination,¹⁰² while no ethane production is observed from Pd(transphos)Me₂ (**9**) under the same conditions.

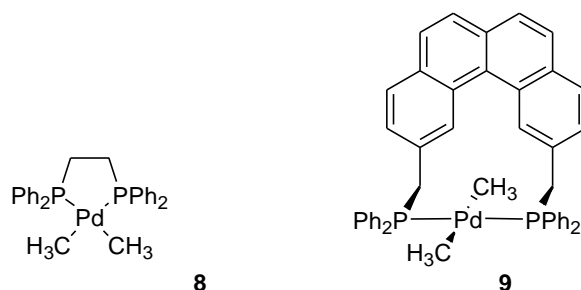
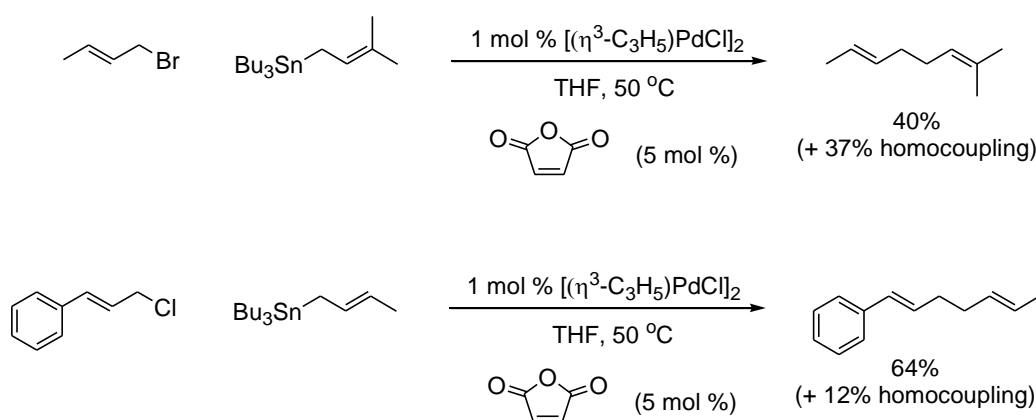


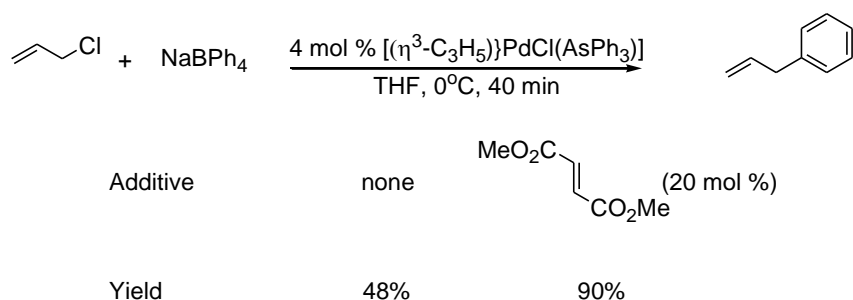
Figure 1.23 Pd(dppe)Me₂ and Pd(transphos)Me₂ complexes.

Facile reductive elimination is important in all cross-coupling reactions but is especially so in the case of the cross-couplings of alkyl nucleophiles and/or electrophiles in which reductive elimination is usually slow and competes with β -hydride elimination. The use of π -acidic olefins either as additives or ligands can enhance reductive elimination rates by removing electron density from Pd^{II} and further favouring the formation of Pd^0 . For example, the coupling of allyl halides with allyl stannanes catalysed by 1 mol % of $(\eta^3\text{-allyl})\text{palladium chloride dimer}$ required maleic anhydride as a co-catalyst (**Equation 1.1**).



Equation 1.1 Stille couplings of allyl stannanes and allyl halides with catalytic maleic anhydride.

On the basis of stoichiometric experiments, the authors suggest that maleic anhydride is required to facilitate reductive elimination from the Pd^{II} bis-allyl intermediate.¹⁰³ The coupling of allyl chloride with NaBPh_4 catalysed by $[\text{Pd}(\eta^3\text{-C}_3\text{H}_5)\text{Cl}(\text{AsPh}_3)]$ gave 48 % of allylbenzene after 40 minutes at 50 °C in the absence of exogenous alkene. Addition of 20 mol % dimethyl fumarate increased the yield to 90% under identical conditions (**Equation 1.2**).¹⁰⁴



Equation 1.2 Suzuki-Miyaura reactions of allyl chloride and sodium tetraphenylborate with catalytic dimethyl fumarate.

Although the use of olefin additives can enhance reductive elimination, when in large excesses, these additives may retard the oxidative addition step similar to the action of dba. To overcome this, Aiwon Lei and coworkers developed novel phosphines bearing an electron deficient olefin (**Figure 1.24**). Palladium complexes of these ligands have proven highly effective in both Negishi couplings involving dialkylzinc reagents possessing β -hydrides¹⁰⁵ and in Cadiot-Chodkiewicz type cross-couplings of bromoalkynes and terminal alkynes.¹⁰⁶ In both cases, undesirable side reactions (β -hydride elimination and alkyne homocoupling, respectively) are minimised, with preliminary kinetic studies into the sp-sp cross-coupling showing that the phosphine-olefin ligand facilitated reductive elimination.



Figure 1.24 Phosphine-olefins ligands synthesised by Lei and co-workers.

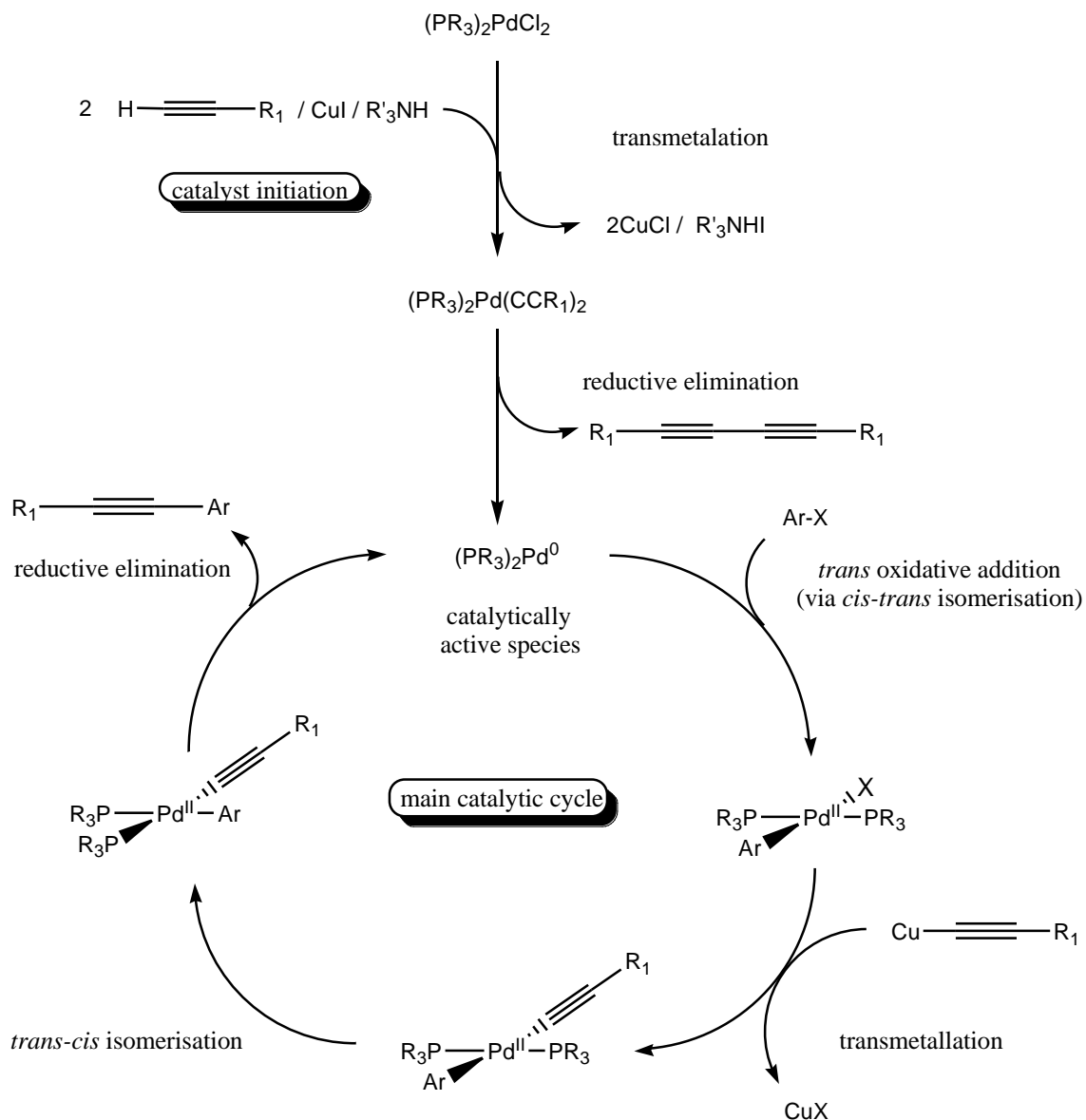
1.2.4 The Sonogashira reaction

The formation of a σ bond between terminal acetylenes and aryl or vinyl halides has been known since the development of the Castro-Stephens reaction over 40 years ago.¹⁰⁷ However, this reaction involves the use of stoichiometric amounts of potentially explosive Cu acetylides in a reaction with aryl halides. In 1975, both Heck¹⁰⁸ and

Cassar¹⁰⁹ reported the coupling of terminal acetylenes with aryl or vinyl bromides and iodides. Heck *et al.* employed catalytic Pd(PPh₃)₂(OAc)₂ in the presence of base at 100 °C, while Cassar showed that Ni(PPh₃)₄ and Pd(PPh₃)₄ in the presence of base mediated similar reactions under milder conditions. Coordination of the alkyne to nickel restricted subsequent oxidative addition steps with Ni⁰(PPh₃)₄, while the use of Pd(PPh₃)₄ allowed the reaction to run catalytically. Sonogashira *et al.* later developed a mild coupling of terminal acetylenes and bromoalkenes, iodoarenes and bromopyridines with catalytic amounts of Pd(PPh₃)₂Cl₂ and CuI in an amine solvent.⁸⁵

1.2.5.1 Mechanism of the Sonogashira reaction

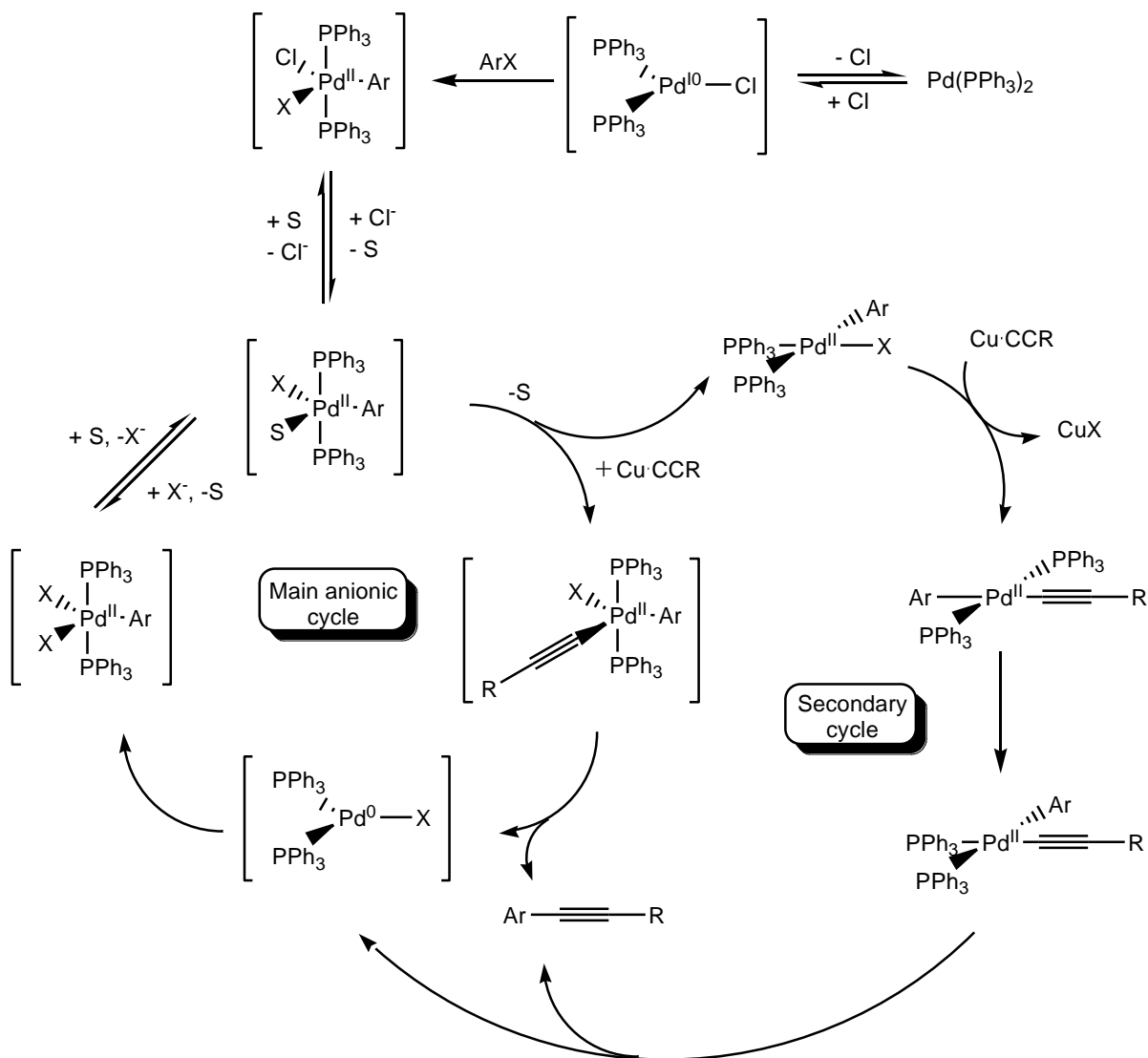
The original catalytic cycle, as proposed by Sonogashira,⁸⁶ features a precatalytic initiation step in which PdL₂X₂ undergoes double transmetallation to give a (bis-alkynyl)palladium complex which reductively eliminates homocoupled diyne and gives rise to the catalytically active Pd⁰L₂ species (**Scheme 1.5**). This initial homocoupling has been quantified by Marder and coworkers.¹¹⁰



Scheme 1.5 Classical Sonogashira reaction mechanism. X = Br, I or TfO.

Recently, detailed mechanistic studies *via* cyclic voltammetry and ^{31}P NMR spectroscopy^{110,111,112} have suggested that the $\text{Pd}^0(\text{PPh}_3)_2$ species generated by electrochemical reduction of $\text{Pd}(\text{PPh}_3)_2\text{Cl}_2$ actually exists as a mixture of three active forms in rapid equilibrium: $[\text{Pd}^0(\text{PPh}_3)_2\text{Cl}]^-$, its dimer $[\text{Pd}^0(\text{PPh}_3)_2\text{Cl}]_2^{2-}$ and $[\text{Pd}^0(\text{PPh}_3)_2\text{Cl}_2]^{2-}$ with the dimeric species being present in trace levels. Two catalytic cycles operate with the dominant cycle dependent on halide and nucleophile concentration as well as the nature of the metal ion, M. When MX exists as ion pairs, or

there is a lack of free halide, anionic palladium complexes are unable to form and the much slower non anionic secondary cycle dominates (**Scheme 1.6**).



Scheme 1.6 Recent proposal for the mechanism of the Sonogashira reaction. S = THF, X = halide.

For conditions in which the halide anion is not bound or is present in large excess (normal reaction conditions), ligation of Pd^0 by halide leads to the formation of $\text{Pd}^0(\text{PPh}_3)_2\text{X}^-$ and $\text{Pd}^0(\text{PPh}_3)_2\text{X}_2^{2-}$ and the dominance of the anionic cycle. The highly transient $\text{Pd}^{\text{II}}(\text{PPh}_3)_2\text{ArX}_2^-$ species can be considered the key catalytic species in both cycles. It is involved in a rapid equilibrium with the neutral penta-coordinated

$\text{Pd}^{\text{II}}(\text{PPh}_3)_2\text{ArXS}$ which may either dissociate solvent to give *trans*- $\text{Pd}^{\text{II}}(\text{PPh}_3)_2\text{ArX}$ or undergo transmetallation to give $\text{Pd}^{\text{II}}(\text{PPh}_3)_2\text{ArX}(\text{CCR})$. $\text{Pd}^{\text{II}}(\text{PPh}_3)_2\text{ArXS}$ interconnects the two cycles and as a result the secondary cycle remains important.^{111,112,113}

1.2.5.2 Transmetallation in the Sonogashira reaction

The transmetallation step involves the transfer of the nucleophilic acetylide moiety from Cu^{I} to Pd^{II} . The transmetallating species is believed to be a Cu-acetylide formed *in situ* by the abstraction of the acidic acetylenic proton by base (typically NR_3 or HNR_2) and coordination of the acetylide anion to Cu^{I} . Subsequent transmetallation yielding Pd acetylide and Cu halide occurs with retention of configuration at Pd suggesting that a concerted mechanism is in operation.

1.2.5.3 Recent developments in the Sonogashira reaction

Recent developments in the Sonogashira reaction have sought to increase both its scope, in relation to potential coupling partners, and its efficiency, in relation to higher turnover numbers (TONs) and the use of milder conditions such as room temperature couplings of aryl bromides. In addition, both Cu and amine free protocols have been developed.

Copper free Sonogashira reactions, also referred to as Heck alkynylation reactions, have been developed to reduce the formation of homocoupled diyne side product in the presence of O_2 by Cu-catalysed Glaser type reactions¹¹⁴ or by Pd/Cu catalysed reactions.^{109,115} Amine free protocols have also been developed, but require the use of stoichiometric amounts of an alternative base to deprotonate the terminal alkyne and to trap the HX byproduct.¹¹⁶

Palladium catalysts featuring bulky, electron rich phosphines have been shown to be highly active for a wide range of cross-coupling reactions. $\text{Pd}(\text{PhCN})_2\text{Cl}_2 / \text{}^t\text{Bu}_3\text{P} / \text{CuI}$ in a 1:2:1.5 ratio was found to promote the room temperature couplings of both activated and deactivated aryl bromides with a range of terminal acetylenes at room temperature.¹¹⁷ A Cu free procedure using 1:1 $\text{Pd}_2(\text{dba})_3 / \text{}^t\text{Bu}_3\text{P}$ was also found to be effective.¹¹⁸

Palladacyclic catalyst precursors such as **10** and **11** (Figure 1.25) possess high thermal stability in comparison to traditional $\text{Pd}(\text{PR}_3)_2\text{X}_2$ catalyst systems. This, and the high TONs often obtained, has led to the use of palladacyclic precursors in a range of cross-couplings, especially for substrates requiring the use of elevated temperatures.

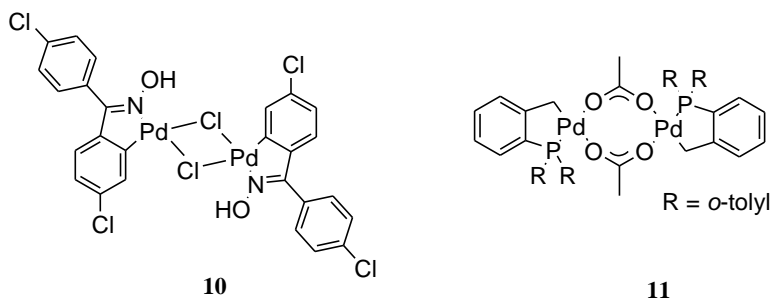


Figure 1.25 Palladacyclic catalyst precursors.

The oxime derived palladacycle **10** was used by Alonso *et al.* for the Cu and amine free Sonogashira reaction of aryl iodides and bromides with a variety of terminal acetylenes. TONs as high as 72000 were observed with tetrabutylammonium acetate as the base in *N*-methylpyrrolidinone at 110 °C.¹¹⁹ Interestingly, the reactions were carried out in air suggesting that an alternative mechanism to the traditional $\text{Pd}^0/\text{Pd}^{\text{II}}$ cycle may be operating. Palladacycle **11**, derived from $\text{P}(\textit{o}\text{-tolyl})_3$ and $\text{Pd}(\text{OAc})_2$, shows high catalytic activity for a range of cross-couplings at elevated temperatures, and has been shown to mediate the Sonogashira reaction in the absence of Cu co-catalyst with very low catalyst loadings. TONs of up to 8000 have been reported in the coupling of 4-bromoacetophenone with phenylacetylene.¹²⁰

N-heterocyclic carbenes (NHCs) have attracted considerable interest as potential ligands for homogeneous catalysis since their isolation by Arduengo *et al.*¹²¹ The strong σ -donor and weak π -acceptor properties of these ligands and their reluctance to dissociate from the metal centre make them attractive alternatives to bulky phosphine ligands.

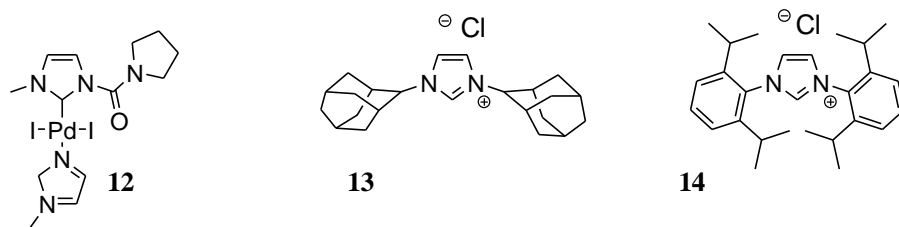


Figure 1.26 *N*-heterocyclic carbene (NHC) precursors and a Pd^{II} complex bearing an NHC ligand.

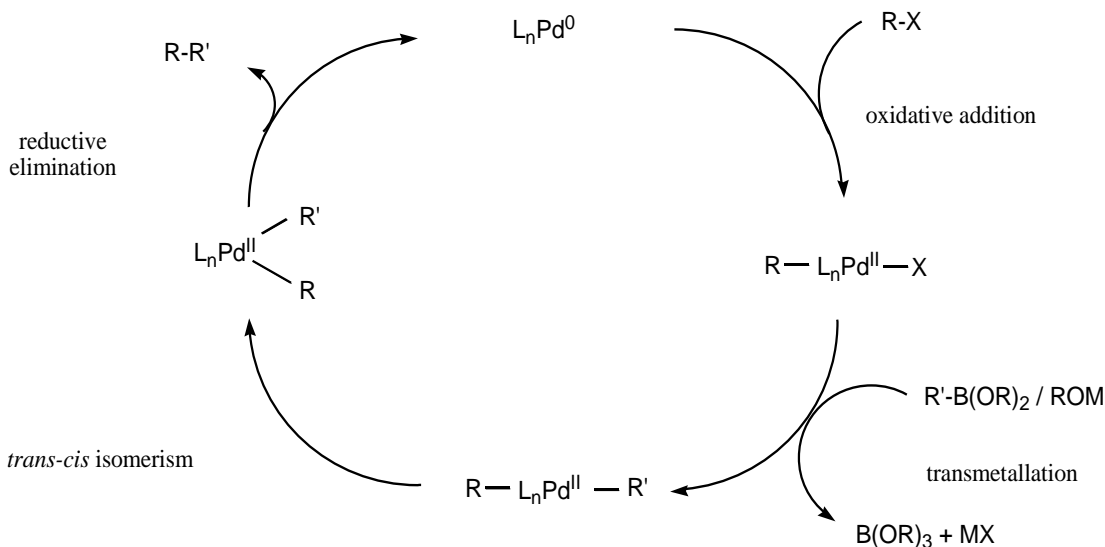
Catalyst precursor **12** (**Figure 1.26**) was shown by Batey *et al.* to promote Sonogashira cross-coupling under mild conditions with PPh₃ and CuI co-catalyst and NEt₃ or Cs₂CO₃ as a base.¹²² Ligand precursor **13** (**Figure 1.26**) was used in conjunction with Pd(OAc)₂ and CuI with base to give highly efficient couplings of *o*-iodohaloarenes in a one-pot synthesis of *N*-substituted indoles. The alkyne product intermediates were not isolated, but overall yields of up to 99% were obtained for the final products.¹²³

In a highly important development, Fu and coworkers employed a range of *N*-heterocyclic carbene precursors, including **14** (**Figure 1.26**), in conjunction with Pd(π -allyl)Cl₂ and CuI for the couplings of a range of unactivated alkyl bromides and iodides possessing β -hydrogens. Yields of up to 81% were reported showing that the catalyst system successfully circumvents the propensity of the oxidative addition products to undergo β -hydride elimination.¹²⁴

1.2.5 The Suzuki-Miyaura reaction

The Suzuki-Miyaura reaction⁸² involves the formation of a σ bond between two carbon atoms *via* the cross-coupling of an organoboron compound and an organic halide or pseudohalide (e.g. TfO). The reaction is tolerant of a wide range of functional groups, and the coupling of aryl or 1-alkenyl boronic acids (or equivalent) proceeds smoothly for aryl, 1-alkenyl, 1-alkynyl, allyl, and benzylic halides. β -Hydride elimination in *trans*-RPdL₂X complexes formed from oxidative addition of RX has limited the use of primary and secondary alkyl halides as coupling partners. The Suzuki-Miyaura reaction follows

an oxidative addition, transmetalation, reductive elimination pathway common to most palladium-catalysed cross-couplings (**Scheme 1.7**).



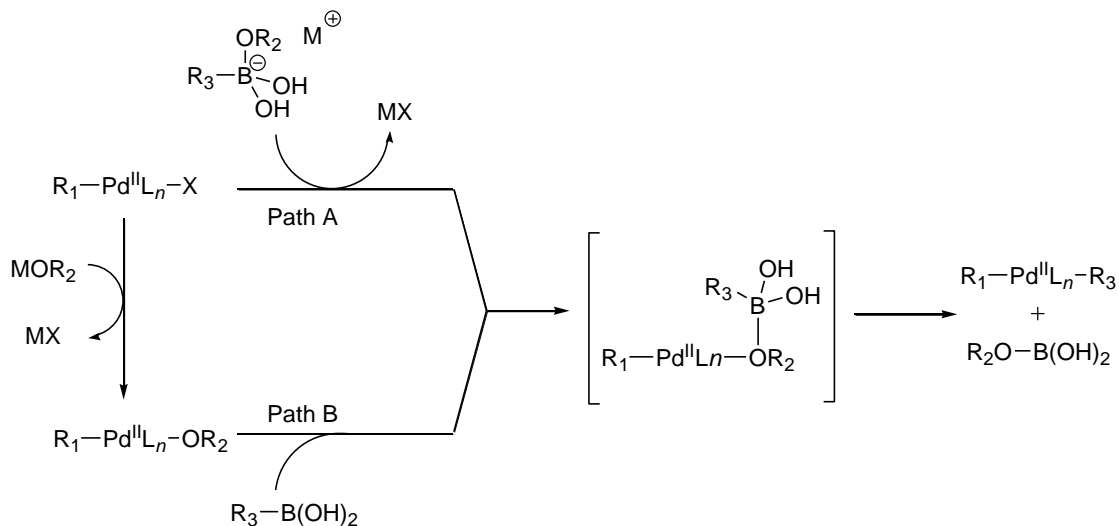
Scheme 1.7 Mechanism of the Suzuki–Miyaura reaction.

Oxidative addition of aryl, 1-alkenyl, 1-alkynyl, allyl, and benzylic halides to a coordinatively unsaturated Pd^0 complex, and subsequent *cis-trans* isomerisation, leads to the formation of a stable *trans*-palladium(II) complex. The reaction proceeds with complete retention of configuration for alkenyl halides and with inversion for allylic and benzylic halides. A variety of Pd^0 complexes such as $Pd^0(PPh_3)_4$ can be used as catalysts, as can mixtures of $Pd_2(dba)_3$ and ligands which form active Pd^0 complexes *in situ*. Air stable Pd^{II} catalyst precursors such as $PdCl_2(PPh_3)_2$ and $Pd(OAc)_2$ /phosphine systems are also highly effective, with *in situ* reduction *via* reaction with phosphines in the presence of water or organometallics generating the active Pd^0 species.¹²⁵ Alternatively, two transmetalations of the organoboronate to Pd^{II} , followed by reductive elimination (i.e. homocoupling) of biaryl gives Pd^0 .

1.2.5.1 Transmetalation in the Suzuki-Miyaura reaction

Organoboronates are inert to transmetalation to palladium^{II} halides in neutral conditions due to the low nucleophilicity of the organic group on boron. Addition of NaOH or other

basic species have been shown to have a dramatic effect on the rate of the transmetallation of organoborons compounds to Au, Ag, Pt and Hg.^{126,127,128} The nucleophilicity of the substituent on boron is enhanced by quaternisation of boron by the coordination of the Lewis base (**Scheme 1.8**). The exact mechanism of the quaternisation of the organoboron species and its subsequent transmetallation to Pd^{II} halides is dependent on the nature of the organoboronate species and occurs *via* either a quaternised boronate species or Pd^{II}OR intermediates.

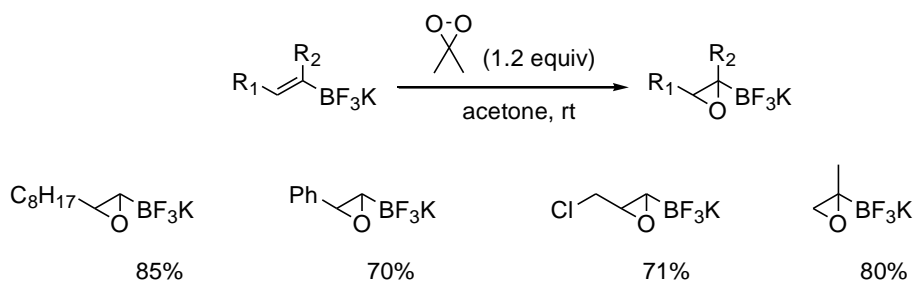


Scheme 1.8 Base assisted transmetallation of organoborons compounds to Pd^{II}(L_n)(R)X.

Evidence for the free boronate pathway in the transmetallation of boronic acids is provided by the observation that the rate of cross-coupling of aryl boronic acids is retarded at pH 7–8.5 relative to that at pH 9.5–11. The pK_a of phenyl boronic acid is 8.8 suggesting the formation of the hydroxyboronate anion R[']-B(OH)₃[−] at pH values in excess of 8.8, and its transmetallation to Pd^{II} halides.¹²⁹ However, although the basicity of the hydroxypalladium species is unknown, the analogous platinum complex Pt^{II}Ph(PPh₃)₂OH is more basic than hydroxide, further complicating the situation.¹³⁰

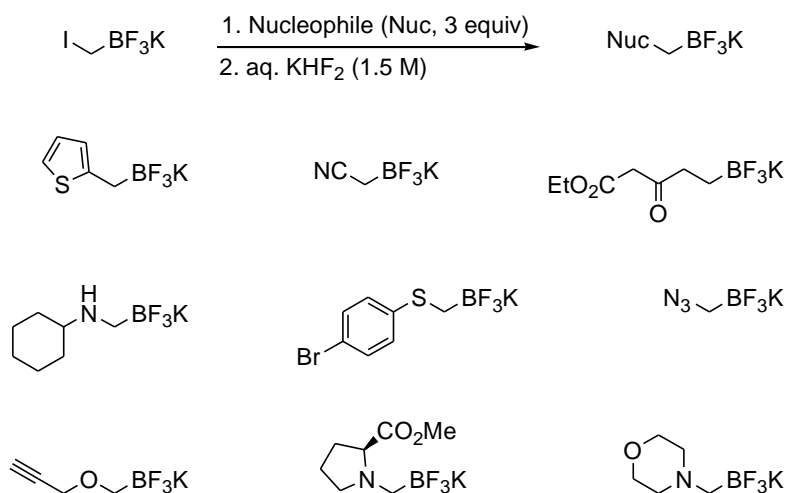
The choice of base has an important effect on the selectivity of the reaction for unsymmetrically substituted alkenyl boronic acids.¹³¹ Strong Lewis bases such as fluoride and hydroxide give a predominantly cross-coupled product. However, in the presence of weakly basic species such as NEt₃, ‘head to tail’ coupling is observed with the coupling

The Lewis acidity and sensitivity of trivalent organoboranes and organoboronates to nucleophiles, bases and oxidants renders selective functional group interconversions of organoboron compounds challenging. In contrast, potassium organotrifluoroborates have been shown to be resistant to a range of nucleophilic, basic and oxidative reaction conditions that destroy organoboronic acids and boronate esters.



Equation 1.3 Epoxidation of potassium 1-alkenyl trifluoroborates with dimethyldioxirane.

Molander and coworkers have shown that 1-alkenyl trifluoroborates could be oxidised with dimethyldioxirane to give their corresponding epoxides. In contrast, 1-alkenyl boronic acids and their corresponding pinacol esters yielded aldehydes, resulting from oxidative B-C cleavage (**Equation 1.3**).¹³⁷ Similarly, aryl and alkyl trifluoroborates bearing alkene moieties underwent *cis*-dihydroxylation in the presence of catalytic OsO₄ and morpholine N-oxide without reaction of the trifluoroborate moiety.¹³⁸



Equation 1.4 Nucleophilic substitution of iodomethyl trifluoroborates.

Potassium organotrifluoroborates have been shown to undergo further functionalisation under basic conditions with retention of the trifluoroborate group. Potassium aryltrifluoroborates were functionalised using Wittig¹³⁹ or Horner-Wadsworth-Emmons¹⁴⁰ reactions, with incorporation of potassium trifluoroborate into both the carbonyl and triphenylphosphonium chloride salt possible. In addition, potassium *p*-bromophenyltrifluoroborate may be functionalised by lithiation and trapping with a variety of electrophiles¹⁴¹ and potassium iodomethyltrifluoroborate can be reacted with a range of nucleophiles, to give a range of functionalised methyltrifluoroborate salts (**Equation 1.4**).¹⁴²

1.2.5.3 Suzuki-Miyaura cross-couplings of organoboron reagents with alkyl halides

In 1992, Suzuki and coworkers showed that 9-alkyl-9-BBN derivatives possessing β -hydrogens as well as 9-aryl/alkenyl-9-BBN derivatives could be cross-coupled with primary alkyl iodides in the presence of catalytic Pd(PPh₃)₄ and excess K₃PO₄.¹⁴³

More recently, work by Fu and coworkers has shown that trialkylphosphine ligands, especially PCy₃, in conjunction with Pd catalyst precursors are effective for the couplings of 9-alkyl-9-BBN derivatives to primary alkyl bromides (**Table 1.2**).¹⁴⁴ Couplings of 9-alkyl-9-BBN derivatives to alkyl tosylates¹⁴⁵ and chlorides¹⁴⁶ were also reported by the same group.

Although easily synthesised by alkene hydroboration, 9-alkyl-9-BBN derivatives are sensitive to air. In comparison, boronic acid derivatives possess high stability with respect to air and water, in addition to being commercially available. A catalyst derived from Pd(OAc)₂/P(*t*Bu)₂Me was found to be highly effective for cross-couplings of arylboronic acids and primary alkyl bromides in the presence of base in *t*-amyl alcohol at room temperature¹⁴⁷ and was shown to oxidatively add bromoalkanes at temperatures as low as 0 °C. Further work with Ni catalysts bearing 2-aminoalcohol ligands showed them to be highly effective for the cross-couplings of arylboronic acids with a variety of

unactivated primary and secondary alkyl halides (including the more challenging alkyl chlorides).¹⁴⁸

Table 1.2 Cross-couplings of 9-alkyl-9-BBN derivatives with alkyl bromides by Fu and co-workers.

entry	Ligand ^a	<i>n</i> -Dec-- <i>n</i> -Hex	<i>n</i> -Dec-- <i>n</i> -Hex
1	PCy ₃	85	<2
2	PPh ₃	<2	<2
3	P(2-furyl) ₃	<2	<2
4	P(<i>o</i> -tol) ₃	<2	14
5	P(2,4,6-methoxyphenyl) ₃	<2	31
6	dppf	<2	12
7	Binap	<2	<2
8	P(OPh) ₃	<2	<2
9	AsPh ₃	<2	<2
10	P ^t Bu ₃	<2	21
11	P ⁿ Bu ₃	9	27
12	dcpe	<2	21
13	P ⁱ Pr ₃	68	6

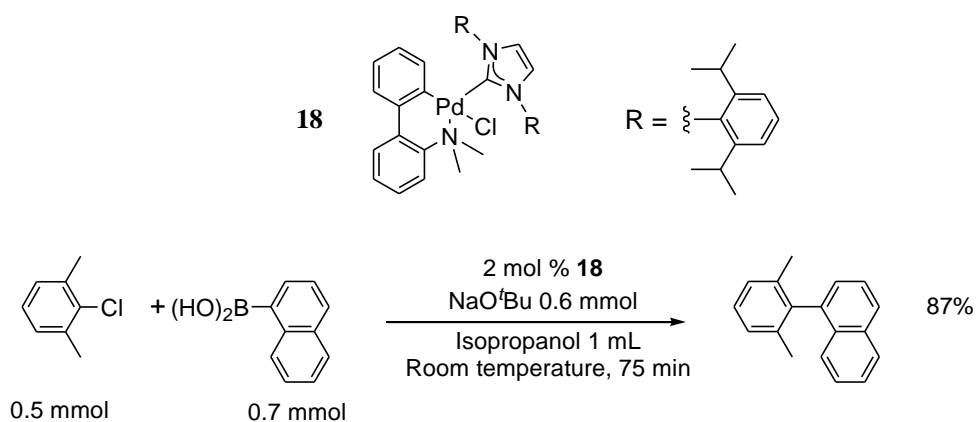
% yield after 16 h (by GC) ^a In the case of bidentate ligands 4% of the ligand was used

1.2.5.4 Suzuki-Miyaura cross-couplings of organoboron reagents with aryl chlorides

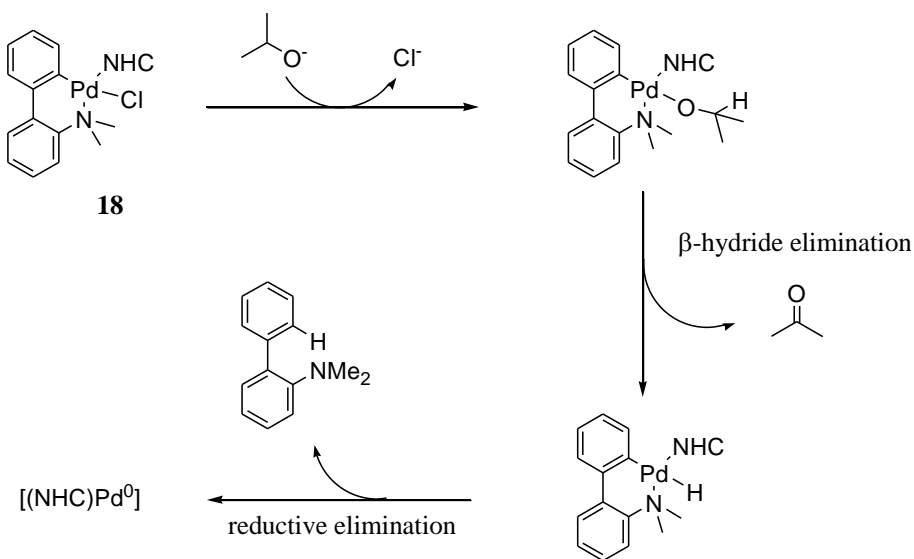
The use of unactivated aryl chlorides as coupling partners in the Suzuki-Miyaura reaction is highly desirable due to the low cost and facile synthesis of aryl chlorides. In the last decade, huge progress has been made in the use of these unreactive substrates in cross-

couplings¹⁴⁹ facilitated by the use of bulky, highly electron rich ligands. In 1995, the Pd(OAc)₂/P(*o*-tolyl)₃ derived palladacycle **11** was shown to mediate the Suzuki-Miyaura reaction of 4-chloroacetophenone and phenylboronic acid with K₂CO₃ base at 130 °C with similar conditions yielding high TONs for the coupling of aryl bromides.^{149d}

Nolan and coworkers have employed the NHC-ligated palladacycle **18** as a precatalyst for the Suzuki-Miyaura coupling of unactivated aryl chlorides bearing *ortho* substituents with boronic acids at room temperature in technical grade *i*PrOH (**Equation 1.5**).



Equation 1.5 Cross-couplings unactivated aryl chlorides with aryl boronic acids by Nolan and co-workers.



Scheme 1.10 Activation of palladacycle **18** in 2-propanol.

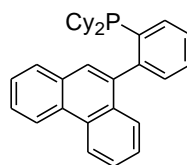
Couplings of aryl chlorides yielded the corresponding biaryl products in high yields with short reaction times with anhydrous *i*-PrOH giving no improvement in activity or yields. It was proposed that the displacement of chloride by *iso*-propoxide in **18** gave a *iso*-propoxy substituted palladacycle which may undergo β -hydride elimination with loss of acetone to give a palladium hydride. Reductive elimination of 2-dimethylaminobiphenyl may then give NHC-Pd⁰ as the active catalytic species (**Equation 1.5** and **Scheme 1.10**).¹⁵⁰

Dialkyl(biaryl)phosphines (**Figure 1.27**) have been shown to be highly active ligands for the cross-coupling of aryl boronic acids and aryl chlorides.^{151,152} A combination of the air stable 2-dimethylamino-2'-dicyclohexylphosphinobiphenyl (davephos) and Pd(OAc)₂ is highly effective for the room temperature couplings of aryl chlorides, even those possessing electron donating groups and *ortho* substituents.¹⁵⁰ In comparison, Pd(PCy₃)₂Cl₂ catalyses the Suzuki-Miyaura reactions of activated aryl halides at 100-120 °C in N-methylpyrrolidone with CsF as base. Electron donating substituents are not tolerated and the presence of *ortho* substituents is found to lower the yield.¹⁵¹ For the synthesis of biphenyls with more than one *ortho* substituent more active systems are required. The dicyclohexyl-(2-phenanthren-9-yl-phenyl)-phosphine ligand **19** gives an extremely active catalyst when used in conjunction with Pd₂(dba)₃. Biaryl products with 4 *ortho*-substituents are produced in high yields from the couplings of aryl chlorides with aryl boronic acids.¹⁵²

The high activities of these ligands are attributed to their electron rich nature and large steric bulk which favours a PdL mediated oxidative addition pathway. Interactions between the π system of the diphenyl moieties and palladium may stabilise highly active monophosphine species and are believed to encourage reductive elimination.¹⁵¹



Davephos



19

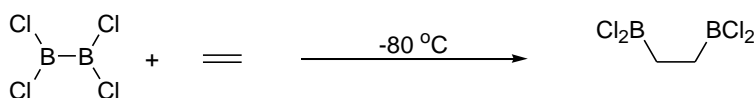
Figure 1.27 Dialkylbiarylphosphines for Suzuki-Miyaura reactions of aryl chlorides developed by Buchwald *et al.*

1.3 Transition metal-catalysed borylations of C-H bonds

Organoboron compounds have received much attention, especially as intermediates in organic synthesis.^{153,154} The B-C bond may be cleaved with or without homologation and organoboranes can be utilised as substrates in a variety of catalytic reactions including Suzuki-Miyaura cross couplings,⁸² copper-catalysed Chan-Lam type couplings with N-, and O-nucleophiles,¹⁵⁵ and rhodium-catalysed additions to a variety of unsaturated compounds.¹⁵⁶

1.3.1 Synthesis of organoborons

The synthesis of organoboranes has traditionally involved the trapping of Grignard or organolithium reagents with trialkylborates¹⁵² or hydroboration of alkenes and alkynes,¹⁵² as developed by H. C. Brown and coworkers, where the addition of the H-B bond proceeds with anti-Markovnikov regioselectivity. Diborylated products may be synthesised by the addition of diboron compounds to unsaturated systems. This was first demonstrated by Schlesinger and coworkers with the addition of B₂Cl₂ to ethene¹⁵⁷ to form Cl₂BC₂H₄BCl₂, (**Equation 1.6**).



Equation 1.6 Addition of B₂Cl₄ to ethene by Schlesinger and co-workers.

However, due to the difficulty of preparation and instability of B₂Cl₄, this reaction has not found general application. However, the use of more stable diboron reagents such as B₂(NMe₂)₄,¹⁵⁸ B₂pin₂¹⁵⁹ (pin = pinacolato = OCMe₂CMe₂O), B₂neop₂¹⁶⁰ (neop = neopentane glycolato = OCH₂CMe₂CH₂O) and B₂cat₂^{159, 161} (cat = catecholato = 1,2-O₂C₆H₄) has allowed for the development of a variety of diborylation reactions, although transition metal catalysts are required to cleave the B-B bond.¹⁶² **Figure 1.28.**

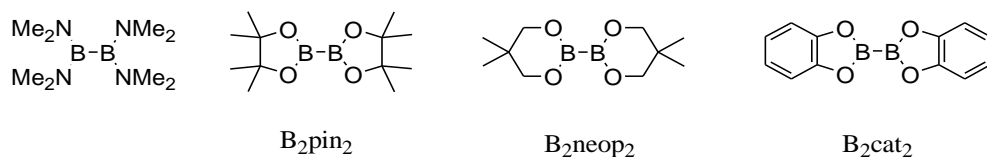
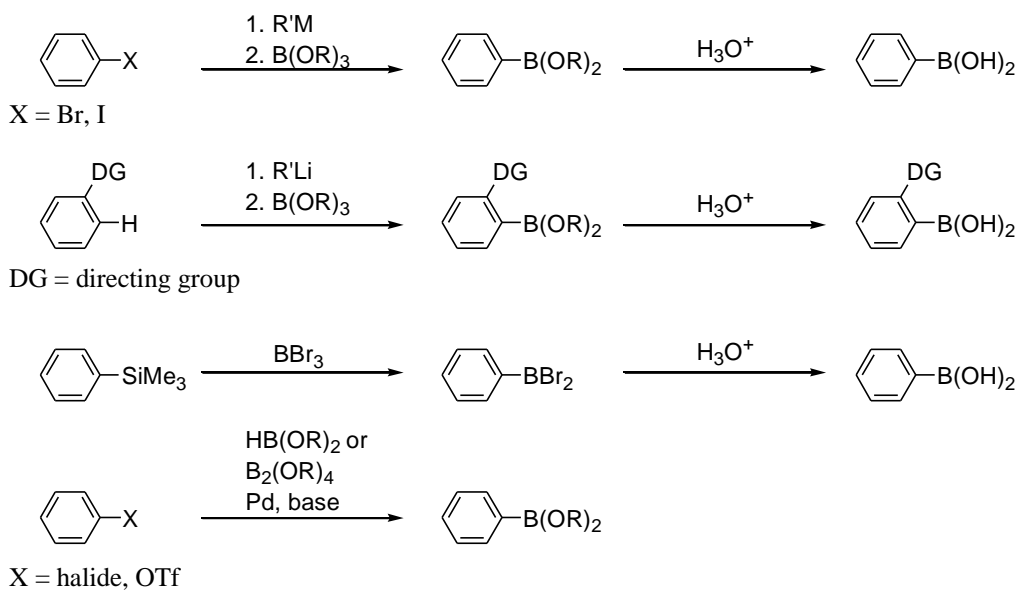


Figure 1.28 Diboron compounds.

Methods for the synthesis of aryl boron compounds have traditionally required preactivation of the aromatic ring or the presence of a directing group.¹⁶³ **Equation 1.7.**



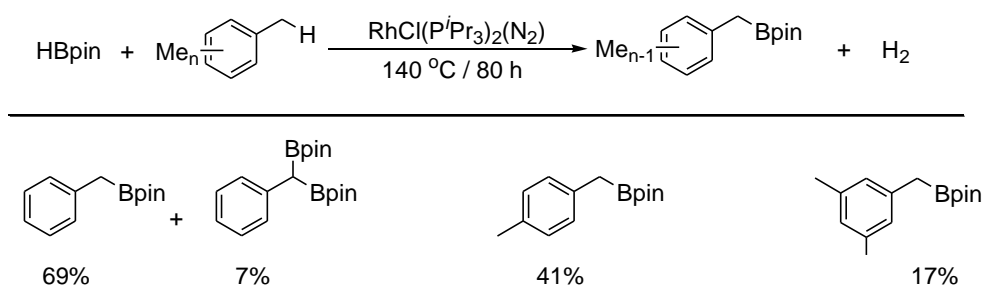
Equation 1.7 Methods for the synthesis of arylboron compounds.

1.3.2 Transition metal-catalysed C-H borylations

The synthesis of aryl and benzylic boron compounds, which cannot be synthesised *via* hydroboration, by the direct functionalisation of C-H bonds is highly attractive as it eliminates the need for preliminary steps associated with the preactivation of arenes. The rest of this section will concentrate on the scope and limitations of methods for the synthesis of aryl-, benzyl-, and vinyl boronate esters *via* transition metal catalysed borylations of aromatic, benzylic and vinylic C-H bonds.

1.3.3 Transition metal-catalysed benzylic C-H borylation

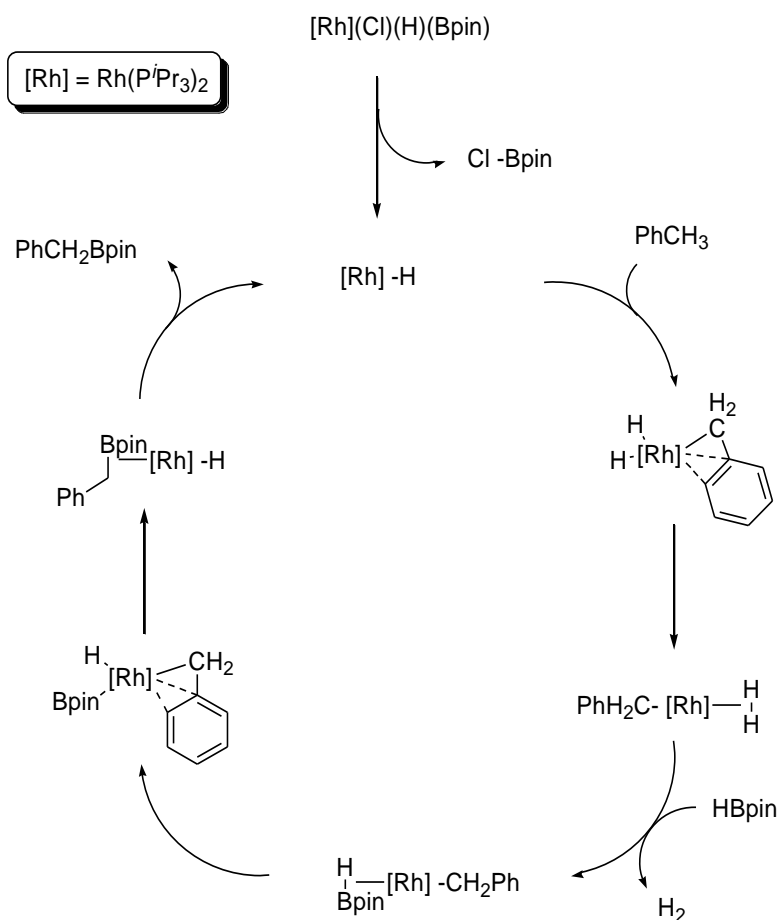
Marder and coworkers reported the use of $[\text{Rh}(\text{Cl})(\text{N}_2)(\text{P}^i\text{Pr}_3)_2]$ with HBpin to generate a catalyst for the benzylic borylation of methylarenes at 140 °C with Rh loadings between 1 and 0.3 mol % (**Equation 1.8**). In addition, the same catalyst system was found to be effective for the aromatic C-H borylation of benzene. The borylation of mesitylene, *p*-xylene and toluene led predominantly to benzylic borylation products with only small amounts of products of arene C-H borylation observed. Toluene was borylated in 76% yield with 81% selectivity for benzylic borylation after 80 h at 140 °C. Reactions of *p*-xylene and mesitylene lead to lower yields (41 and 17% respectively) with 100% selectivity for benzylic functionalisation, which was attributed to increased steric hindrance around the aromatic C-H bonds. In the borylation of toluene, greater than statistical levels of bis-pinacolboryl-methylbenzene were observed, suggesting that the presence of a boryl group further activates adjacent benzylic C-H bonds.¹⁶⁴



Equation 1.8 Benzylic borylation of methylarenes by Marder and co-workers.¹⁶⁴

Subsequent computational studies¹⁶⁵ into the reaction have suggested that oxidative addition of HBpin to the 14 electron species $[\text{Rh}(\text{Cl})(\text{P}^i\text{Pr}_3)_2]$, **19**, followed by elimination of ClBpin generated the active catalytic species $[\text{Rh}(\text{H})(\text{P}^i\text{Pr}_3)_2]$. Coordination of toluene gives a σ C-H complex which undergoes oxidative addition of the bound C-H bond to give $[\text{Rh}(\text{P}^i\text{Pr}_3)_2(\eta^3\text{-benzyl})(\text{H})_2]$. Stabilisation of the benzylic C-H activation product by η^3 coordination accounts for the observed selectivity for benzylic over aromatic C-H borylation. Reductive elimination of H_2 from $[\text{Rh}(\text{P}^i\text{Pr}_3)_2(\eta^3\text{-benzyl})(\text{H})_2]$ gives a $\sigma\text{-H}_2$ complex, from which H_2 is displaced by HBPin to give a $\sigma\text{-HBpin}$ complex. Subsequent

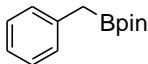
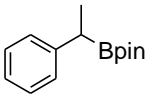
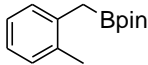
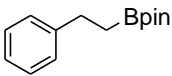
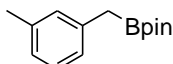
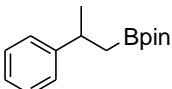
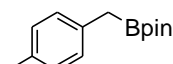
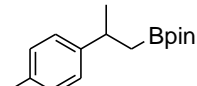
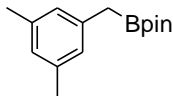
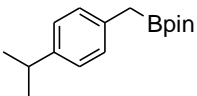
oxidative addition yields $[\text{Rh}(\text{P}^i\text{Pr}_3)_2(\eta^3\text{-benzyl})(\text{H})(\text{Bpin})]$ which reductively eliminates the borylated product to regenerate the Rh(I) hydride catalyst (**Scheme 1.11**).



Scheme 1.11 Catalytic cycle for the borylation of toluene with $[\text{Rh}(\text{Cl})(\text{P}^i\text{Pr}_3)_2]$ and HBpin .

Ishiyama *et al.* reported that the widely available palladium on carbon (10% Pd/C) catalysed the benzylic borylation of alkyl arenes with both HBpin and B_2pin_2 at $100\text{ }^\circ\text{C}$ without aromatic C-H borylation (**Table 1.3**).¹⁶⁶ Reactions of toluene, *o*-, *m*-, and *p*-xylene and mesitylene led to exclusive formation of benzylic borylation products whereas in the reaction of ethylbenzene, a mixture of benzylic and terminal C-H activation was observed. The lower yields and slower reactions observed when HBpin is used instead of B_2pin_2 indicated that reactions involving diboron occur *via* a two step process involving a fast and quantitative reaction with diboron, followed by a slower reaction with the HBpin generated by the earlier process.

Table 1.3 Pd/C-catalysed benzylic borylations of alkyl arenes with B₂pin₂ and HBpin.¹⁶⁶

Product	Yields / %	a	b	Product	Yields / %	a	b
	72		54		72		54
	77				15		6
	79				38		13
	72		51		39		42
	64		45		9		5

a with B₂pin₂, **b** with HBpin. Yields relative to boron

Beller *et al.* have reported that combinations of 2,2'-bipyridine (bpy) and the rhodium complexes [RhCl(COD)]₂, [Rh(acac)COD] and Rh₂(OAc)₄ at 1.5 mol % Rh loadings are effective for the benzylic borylation of *ortho*-xylene at 80 °C with ratios of sp³:sp² borylation of up to 67:3.¹⁶⁷

1.3.4 Transition metal-catalysed aromatic C-H borylation

Direct functionalisation of aromatic C-H bonds is an attractive proposition, due to the elimination of synthetic steps usually associated with the preactivation of arenes. Of these reactions, the direct borylation of arene C-H bonds is of particular interest due to the wide range of transformations which utilize organoboranes. This field has recently been reviewed by Miyaura and Ishiyama.¹⁶⁸

1.3.5 Stoichiometric group XII and XIII carbonyl mediated borylations

One of the first examples of aromatic C-H borylation was reported by Hartwig and coworkers. Under photolytic conditions the stoichiometric borylation of benzene and toluene was achieved with $[\text{Mn}(\text{CO})_5\text{BCat}]$, **20**, $[\text{Re}(\text{CO})_5\text{BCat}]$, **21** and $[\text{CpFe}(\text{CO})_2\text{BCat}]$, **22**. Reactions of toluene with Mn and Fe boryls **20** and **22** showed no formation of *ortho* substituted products and *meta:para* ratios of 1.6:1 and 1.1:1 respectively.¹⁶⁹ Later work by the same group reported the photolysis of **22** in benzene to give PhBcat in 99% yield.¹⁷⁰ Photolysis of **22** in a range of monosubstituted arenes was studied, with the formation of only *meta* and *para* borylation products observed. Only photolysis reactions carried out in anisole yielded any *ortho* substituted products. This suggests that the regioselectivity is typically determined by steric effects, although the significant proportion of *ortho*-borylation observed for the reaction of **22** with anisole may result from the methoxy group acting as a directing group. The results are summarised in **Table 1.4**

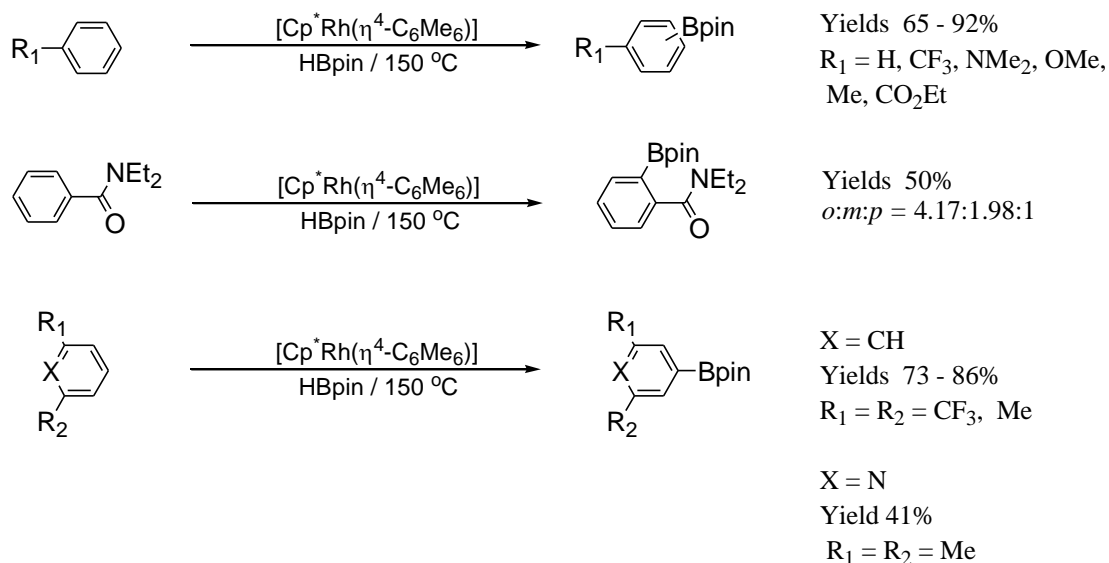
Table 1.4 Stoichiometric borylations of PhX with $[\text{CpFe}(\text{CO})_2\text{BCat}]$, **22**.

X	Product selectivities			Yield / %
	<i>o</i>	<i>m</i>	<i>p</i>	
Me	-	1.1	1.0	70
OMe	1.0	1.6	1.1	52
Cl	-	1.5	1.0	55
CF ₃	-	1.5	1.0	33
NMe ₂	-	1.0	8.0	30

A pathway involving photochemical dissociation of CO to give a 16 electron intermediate followed by C-H bond oxidative addition or metathesis followed by reductive elimination of the B-C bond was proposed.

1.3.6 Rhodium-catalysed aromatic C-H borylation

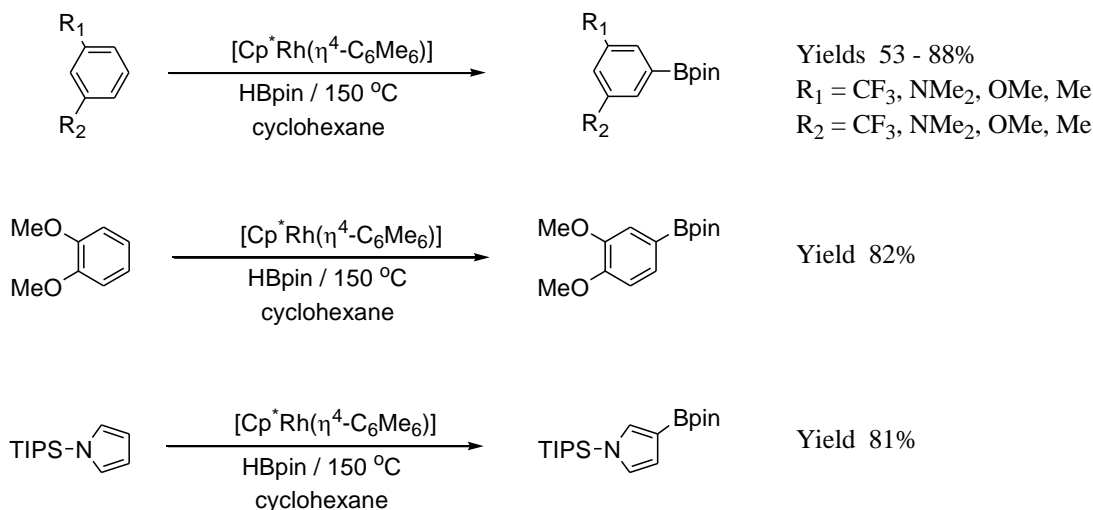
Hartwig and coworkers reported the use of $[\text{Cp}^*\text{Rh}(\eta^4\text{-C}_6\text{Me}_6)]$, **23**, in the borylation of benzene with HBpin. Catalyst loadings of 5 and 0.5 mol % were employed and the reactions were carried out at 150 °C in mixtures of arene substrate and HBpin.¹⁷¹ Further work by Smith and coworkers detailed the borylation of a range of functionalised arenes with the same catalyst.¹⁷² Monosubstituted arenes gave statistical distributions of *meta:para* borylation products, the exception being that of diethylbenzamide, the borylation of which gave a ratio of *o:m:p* products of 4.17:1.98:1. The statistical ratio of *meta* and *para* isomers suggest that a chelation directed *ortho* metallation and non directed pathways are in direct competition. 1,3-disubstituted arenes and 2,6-lutidine were borylated selectively in the *meta* position (**Equation 1.9**).



Equation 1.9 Rhodium-catalysed borylations of arenes by Hartwig and coworkers, and Smith and coworkers.

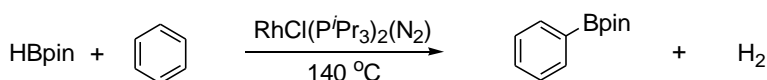
Smith and coworkers demonstrated the use of cyclohexane as an inert solvent in the borylation of arenes with HBpin and **23**. This is highly desirable for the borylation of expensive or non volatile substrates, for which the use of the substrate as the solvent presents issues with cost and work up.¹⁷³ Although **23** is able to catalyse the borylation of alkanes, secondary and tertiary C-H positions are not readily borylated. A range of 1,3-

disubstituted arenes were borylated to give 1,3,5-substituted products, while veratrole (1,2-dimethoxybenzene) was borylated in the 4-position. N-protected 1-triisopropylsilylpyrrole was selectively borylated in the least hindered 3-position (**Equation 1.10**).



Equation 1.10 Regioselective aromatic borylations in cyclohexane by Smith and coworkers.

Catalyst precursor $[\text{Rh}(\text{Cl})(\text{N}_2)(\text{P}^i\text{Pr}_3)_2]$, **19**, previously discussed in relation to benzylic C-H borylation of methylarenes, is also effective for the aromatic C-H borylation of arenes (**Equation 1.11**).¹⁶³ In the borylation of toluene, although benzylic C-H activation predominates, the ratio of $\text{sp}^3:\text{sp}^2$ products of 4:1 shows that the aromatic C-H borylation pathway is in competition with benzylic borylation and gives *meta*- $\text{MeC}_6\text{H}_4\text{Bpin}$ as the main aromatic borylation product. Computational studies¹⁶⁴ also show that the aromatic borylation pathway is similar in energetics to that for benzylic borylation. The borylation of benzene with HBpin in the presence of 1 mol % **19** gave 62% of PhBpin after 14 hours, increasing to 86% after 58 hours.

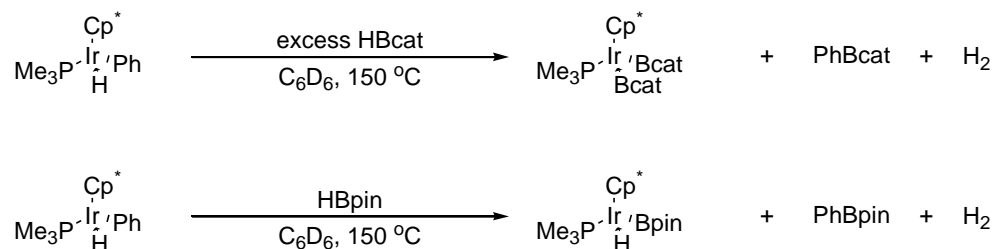


Equation 1.11 Borylation of benzene with $[\text{Rh}(\text{Cl})(\text{N}_2)(\text{P}^i\text{Pr}_3)_2]$ by Marder and co-workers.

1.3.7 Iridium-catalysed aromatic C-H borylation

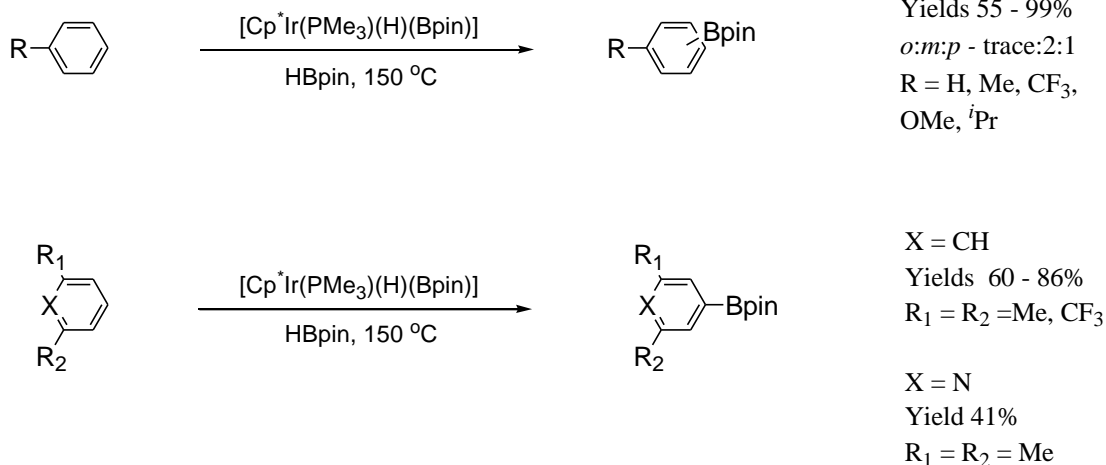
In 1993, during the preparation of $\text{Ir}(\eta^6\text{-MeC}_6\text{H}_5)(\text{Bcat})_3$ from $\text{Ir}(\eta^5\text{-C}_9\text{H}_7)(\text{COD})$, **24**, and excess HBcat in toluene, Marder and coworkers observed substoichiometric borylation of the arene solvent. Reactions employing benzene and C_6D_6 gave similar results leading to the production of phenyl-Bcat and $\text{C}_6\text{D}_5\text{-Bcat}$ as side products. When toluene was used as the solvent, 2 isomers of tolyl-Bcat were observed in a 2:1 ratio.¹⁷⁴

Later work by Smith and coworkers,¹⁷⁵ in the light of earlier work by Bergman¹⁷⁶ and Jones¹⁷⁷ on alkyl C-H activation by group VII $\text{M}(\text{Cp}^*)\text{PMe}_3$ complexes, detailed the thermal C-H activation of benzene using a $\text{Cp}^*(\text{PMe}_3)\text{Ir}^{\text{I}}$ complex to give $[\text{Cp}^*\text{Ir}(\text{PMe}_3)(\text{H})(\text{Ph})]$, **25**. Reactions of **25** with HBpin and HBcat gave Ph-Bpin and Ph-Bcat as the major products respectively (**Equation 1.12**).



Equation 1.12 Thermal reactions of $[\text{IrCp}^*\text{PMe}_3(\text{H})(\text{Ph})]$ with HBcat and HBpin.

The major product from the reaction of $[\text{Cp}^*\text{Ir}(\text{PMe}_3)(\text{H})(\text{Ph})]$ with HBpin, $[\text{Cp}^*\text{Ir}(\text{PMe}_3)(\text{H})(\text{Bpin})]$, **26**, was found to be a precatalyst for the borylation of arenes with HBpin. The borylation of benzene was carried out with a catalyst loading of 17 mol %, at 150 °C for 120 hours, with three turnovers occurring in that time. Complex **26** was also employed as a catalyst in the borylation of a range of substituted arenes. Borylation was found to occur selectively in the *meta* and *para* positions, with many of the monosubstituted substrates giving statistical mixtures (in the range of 2:1) of *meta* and *para* isomers, **Equation 1.13**.

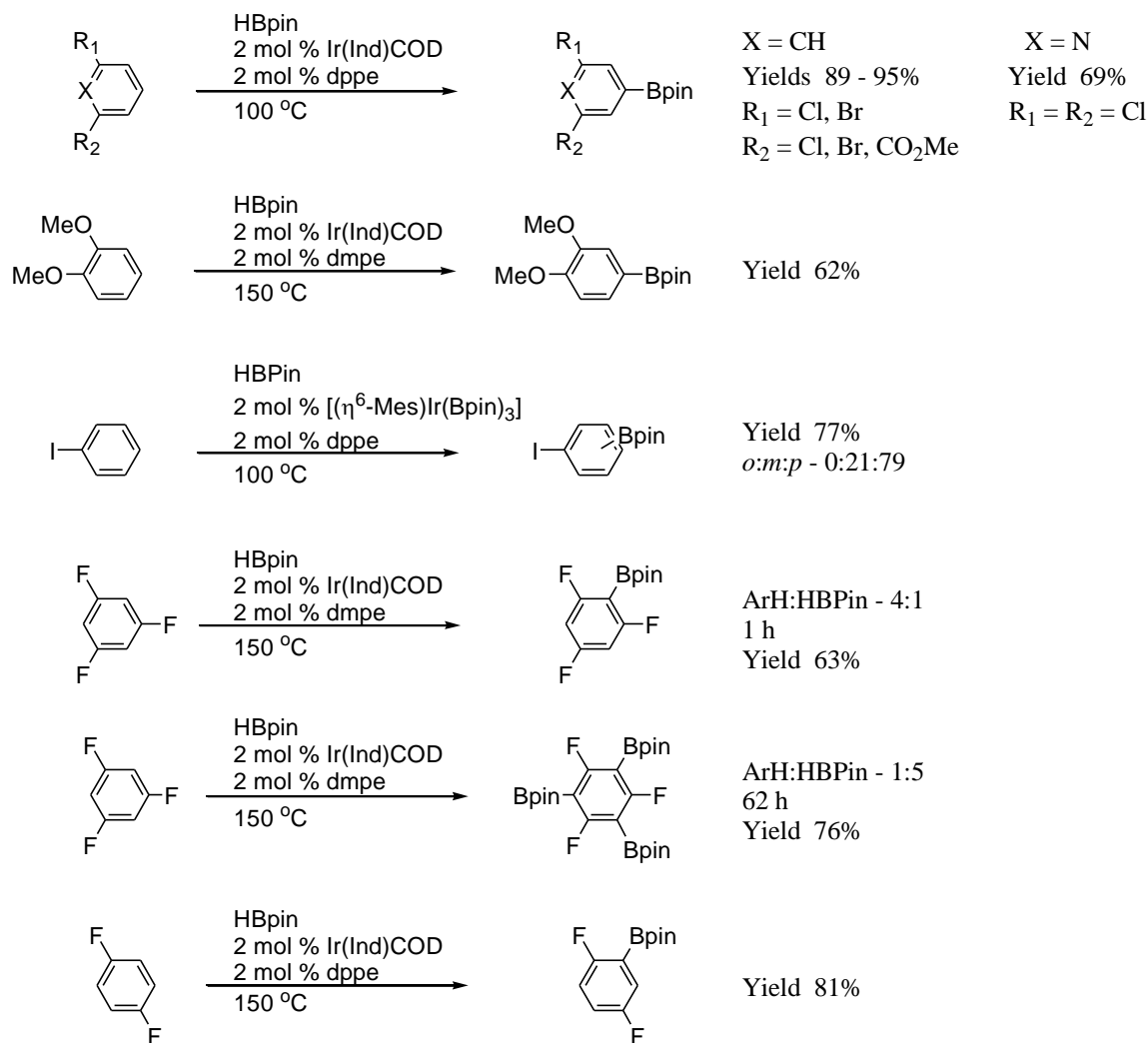


Equation 1.13 [Cp*Ir(PMe₃)(H)(Bpin)]-catalysed borylation of arenes.

In 2002, building on the result of Marder,¹⁷³ Smith and coworkers synthesised (η^6 -1,3,5-Me₃C₆H₃)Ir(Bpin)₃ by an analogous route from [Ir(η^5 -C₉H₇)(COD)], **24**. This complex was used in conjunction with PMe₃ to generate an active catalyst for the borylation of benzene with HBpin.¹⁷⁸ The rate of borylation was found to decrease dramatically when the [P]:[Ir] ratio was 3:1 or higher, while [P]:[Ir] ratios of less than 3:1 gave appreciable rates of borylation, suggesting that the active species possesses two dative ligands. In addition, catalysts were prepared *in situ* from a combination of **24**, ligand and HBpin. Chelating phosphines such as 1,2-bis(diphenylphosphino)ethane (dppe) and 1,2-bis(dimethylphosphino)ethane (dmpe) led to substantial increases in activity and TONs, as demonstrated by dmpe, where the effective TON of 4500 represents an improvement of 1500 fold over precatalyst (η^6 -1,3,5-Me₃C₆H₃)Ir(Bpin)₃. In addition, it was demonstrated that a combination of the commercially available [Ir(Cl)COD]₂ dimer, **27**, and dmpe led to an active catalyst for the borylation of benzene with HBpin.

Catalyst precursor [Ir(η^5 -C₉H₇)(COD)], **24**, in conjunction with dmpe and dppe, was utilised for the borylation of a range of mono-, and disubstituted arenes. As in borylations employing [Cp*Ir(PMe₃)(H)(Bpin)], monosubstituted substrates gave statistical mixtures of *meta* and *para* isomers, while borylation of 1,3-disubstituted substrates occurred selectively at the mutually *meta* position. Borylation *ortho* to fluorine was demonstrated

for 1,4-difluorobenzene, demonstrating that the fluorine group has similar steric demands to that of a proton. In addition, 1,2-dimethoxybenzene was borylated at the 4-position. The results of these reactions are summarised in **Equation 1.14**.

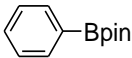
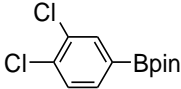
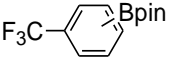
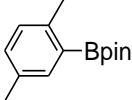
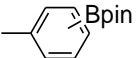
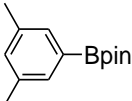
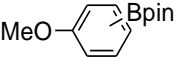
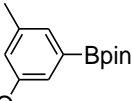
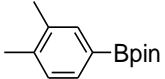
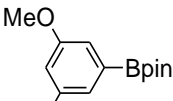
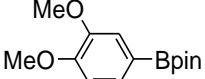


Equation 1.14 Iridium-catalysed arene C-H borylations by Smith and coworkers.

Hartwig, Miyaura and coworkers demonstrated that a combination of [Ir(Cl)COD]₂, **27**, and 2,2'-bipyridine (bpy) ligand was effective for the borylation of arenes with B₂pin₂ at 80 °C in neat arene solvent.¹⁷⁹ Both electron rich and electron poor arenes were borylated in high yields. Reactions were carried out over 16 hours using a 3 mol % Ir loading. Monosubstituted arenes gave statistical mixtures of *meta* and *para* borylation products, with steric effects preventing the formation of the *ortho* products for all substrates other

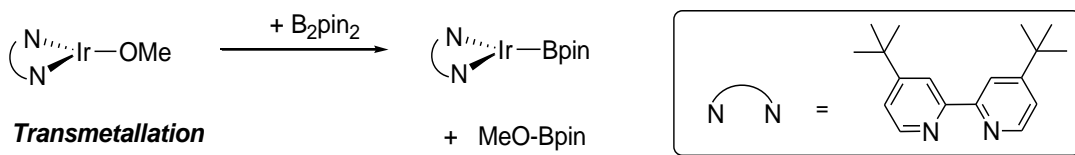
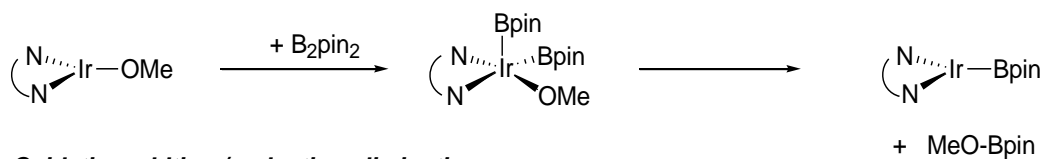
than anisole. Borylation of 1,2-disubstituted arenes, where $R_1 = R_2$, gave single products resulting from borylation in the *para* position, while 1,3-disubstituted arenes yielded 1,3,5-substituted products resulting from borylation of the C-H bond *meta* to both substituents. Overall, the regioselectivity for the borylation of these arenes was characterized by the lack of borylation *ortho* to groups on the arene and statistical ratios of the *meta* and *para* borylation products, suggesting that it is the steric environment around the C-H bond, rather than electronic effects that determines the regioselectivity of Ir-catalysed borylations of substituted arenes. Borylations of benzene in the presence of either *o*-, *m*-, or *p*-borylanisole did not result in the formation of anisole, nor isomerisation of the boryl anisoles, showing that isomer ratios are kinetically rather than thermodynamically determined. The borylation of *p*-xylene, in which all aromatic C-H bonds are *ortho* to a methyl group, gives a single product although yields are lower than for *o*- and *m*-xylene due to steric hindrance (**Table 1.5**).

Table 1.5 Iridium-catalysed direct borylations of arenes with B_2pin_2 .

Product	Yield / % (<i>o:m:p</i>)	Product	Yield / % (<i>o:m:p</i>)
	95		83
	95 (1:74:25)		58
	82 (0:69:31)		86
	82 (0:70:30)		72
	83		73
	86		

Competition reactions carried out in equimolar mixtures of trifluoromethylbenzene and toluene, trifluoromethylbenzene and anisole, and toluene and anisole gave product ratios of 90:10, 85:15 and 40:60, respectively, indicating that electron poor arenes are more reactive than electron rich ones. The higher reactivity of anisole, in comparison to toluene, suggests that coordination of substituent groups or inductive effects may also influence the reactivity of arenes.

Later work by the same group sought to optimise this catalyst system *via* systematic studies into the effect of the nature of the 2,2'-bipyridine ligand and the iridium source on the catalytic activity in room temperature reactions.¹⁸⁰ Combinations of bpy and [IrX(COD)]₂ complexes containing strongly basic and nucleophilic anions such as methoxide and hydroxide were found to be highly effective for the borylation of benzene with B₂pin₂ at room temperature in neat arene with 3 mol % Ir loadings, as was the use of [IrCl(COD)]₂, **27**, in conjunction with excess NaOH to generate [Ir(OH)COD]₂ *in situ*. In contrast, the use of Ir(I)COD complexes of less basic and nucleophilic anions such as acetate, chloride and tetrafluoroborate as iridium sources showed little if any catalytic activity under identical conditions (**Table 1.6**). The high catalytic activity of (hydroxyl)-, and (alkoxy)-iridium complexes can be explained by faster formation of iridium monoboryl complexes. These species are formed by either; oxidative addition of B₂pin₂ to (hydroxyl)-, or (alkoxy)-iridium species followed by reductive elimination of ROBpin or *via* transmetallation between B₂pin₂ and (hydroxyl)-, or (alkoxy)-iridium species (**Scheme 1.12**). In both cases the enhanced ability of hydroxyl and alkoxy ligands to interact with the vacant boron π -orbital and the formation of a strong B-O bond makes reactions more facile than for those of chloride, acetate and tetrafluoroborate complexes.



Scheme 1.12 Pathways for the formation of Ir^I monoboryl complexes from Ir(OMe) precursors.

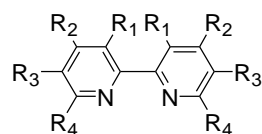
Table 1.6 Effects of differing iridium sources on the borylation of benzene with B₂pin₂ at room temperature.

Entry	Ir ^I precursor	Time / h	Conversion / %	Yield / %
1	[IrCl(COD)] ₂	24	0	0
2	[Ir(COD) ₂]BF ₄	24	3	0
3	[Ir(OH)COD] ₂	4	100	88
4	[Ir(OPh)COD] ₂	4	100	84
5	[Ir(OMe)COD] ₂	4	100	90
6	[{IrCl(COD)} ₂] / 4NaOH	4	100	73
7	[Ir(OAc)COD] ₂	24	19	1

To examine steric and electronic effects of substituents in 2,2'-bipyridine ligands a range of substituted 2,2'-bipyridines were used in conjunction with [Ir(OMe)COD]₂, **28**, (3 mol % Ir loading) for the room temperature of benzene with B₂pin₂ (**Table 1.7**). No large differences in activity was observed in catalysts featuring bpy (**29a**), 4,4'- and 5,5'-dimethyl-2,2'-bipyridine (**29b** and **29c**, respectively) as ligands. The 3,3'-dimethyl derivative **29d** lead to reduced activity, suggesting that a planar ligand is desirable for high activity. The use 6,6'-dimethyl substituted ligand **29e** was ineffective due to steric crowding around the iridium centre. The use of ligands with electron donating substituents in the 4 and 4'-positions (**29f-29h**) gave rise to higher activities than those

with no group or electron withdrawing groups in the 4 and 4'-positions (**29i** and **29j**, respectively).

Table 1.7 Effects of ligands on the borylation of benzene with B₂pin₂ at room temperature.



29a: R₁, R₂, R₃, R₄ = H **29f:** R₂ = NMe₂, R₁, R₃, R₄ = H
29b: R₂ = Me, R₁, R₃, R₄ = H **29g:** R₂ = OMe, R₁, R₃, R₄ = H
29c: R₃ = Me, R₁, R₂, R₄ = H **29h:** R₂ = ^tBu, R₁, R₃, R₄ = H
29d: R₁ = Me, R₂, R₃, R₄ = H **29i:** R₂ = , R₁, R₃, R₄ = H
29e: R₄ = Me, R₁, R₂, R₃ = H **29j:** R₂ = NO₂, R₁, R₃, R₄ = H

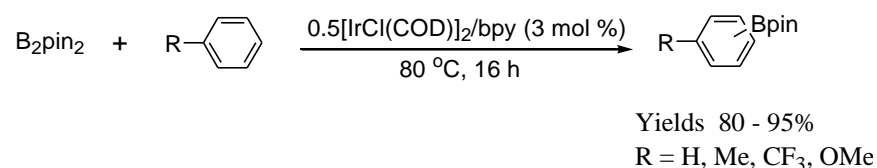
Entry	Ir ^I precursor	Ligand	Time / h	Conversion / %	Yield / %
1	[Ir(OMe)COD] ₂	29a	4	100	90
2	[Ir(OMe)COD] ₂	29b	4	100	89
3	[Ir(OMe)COD] ₂	29c	2	100	82
4	[Ir(OMe)COD] ₂	29d	8	100	60
5	[Ir(OMe)COD] ₂	29e	24	27	0
6	[Ir(OMe)COD] ₂	29f	2	100	89
7	[Ir(OMe)COD] ₂	29g	4	100	90
8	[Ir(OMe)COD] ₂	29h	4	100	83
9	[Ir(OMe)COD] ₂	29i	24	16	0
10	[Ir(OMe)COD] ₂	29j	24	46	0

1.3.7.1 Applications of the [Ir(X)COD]₂/bpy catalyst system

Since its initial publication, the use of [Ir(X)COD]₂ (X = Cl, OMe) with 2,2'-bipyridine ligands has become the predominant catalyst system for C-H borylation of arenes due to the stability of the catalyst precursors and its high activity under mild conditions in comparison to other reported systems. In the following pages the applications of this catalyst system will be reviewed.

1.3.7.1.1 Borylation of monosubstituted arenes

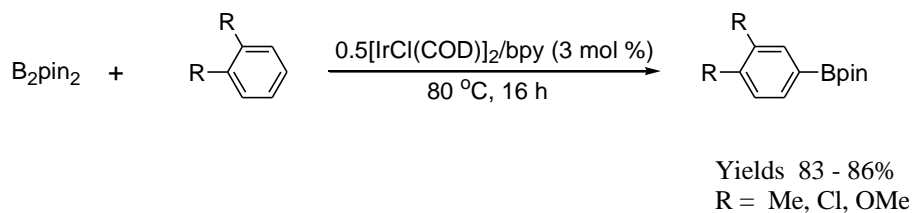
Using a mixture of **27**/bpy a range of monosubstituted arenes have been borylated with B_2pin_2 at 80 °C using neat substrate as the solvent.¹⁷⁸ Borylation occurred in the *meta* and *para* positions giving a statistical ratio of products. Borylation *ortho* to the substituent is typically avoided due to steric factors (**Equation 1.15**).



Equation 1.15 Iridium-catalysed borylation of monosubstituted arenes with B_2pin_2 at 80 °C.

1.3.7.1.2 Borylation of 1,2-disubstituted arenes

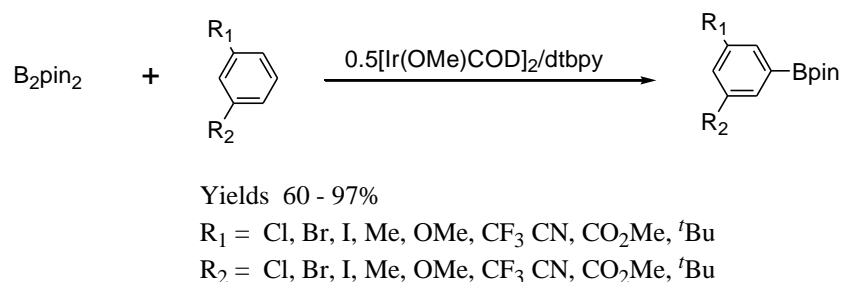
Borylation of 1,2-disubstituted arenes has been demonstrated with both the **27**/bpy and **28**/dtbpy catalyst systems.^{178,179} For symmetrical 1,2-disubstituted arenes, borylation *para* to the substituents yields a single regioisomer, with borylation of the C-H bonds *ortho* to substituents not observed (**Equation 1.16**). Borylation of unsymmetrical 1,2-disubstituted arenes, which would yield two regioisomers, has, as yet, not been reported.



Equation 1.16 Iridium catalysed borylation of 1,2-disubstituted arenes with B_2pin_2 at 80 °C.

1.3.7.1.3 Borylation of 1,3-disubstituted arenes

Borylation of 1,3-disubstituted arenes has been widely explored with both **27**/bpy and **28**/dtbpy catalyst systems.^{178,179,181} For the latter, reactions may be carried out in a range of solvents at both ambient and elevated temperatures. Borylation typically occurs at the mutually *meta* position to yield 1,3,5-trisubstituted arenes with 100% regioselectivity. Due to the wide range of functional groups (Cl, Br, I, Me, OMe, CF₃, CN, CO₂Me, *t*-Bu) tolerated by Ir-catalysed borylation, this method offers an effective method for the functionalisation at the 5-position in 1,3-disubstituted benzenes which is often difficult to access with *ortho/para* directing substituents. Borylations of 1,3-disubstituted arenes catalysed by the **28**/dtbpy catalyst systems are summarised in **Equation 1.17**.

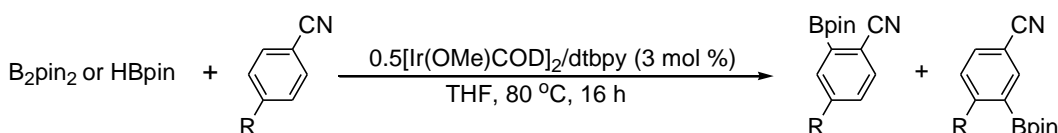


Equation 1.17 [Ir(OMe)COD]₂/dtbpy-catalysed borylations of 1,3-disubstituted arenes.

1.3.7.1.4 Borylation of 1,4-disubstituted arenes

Although aromatic C-H bonds *ortho* to substituents are typically not borylated in the presence of less hindered aromatic C-H bonds, in substrates such as 1,4-disubstituted and 1,3,5-trisubstituted benzenes borylation *ortho* to substituents can occur, albeit more slowly than with less hindered substrates. Borylation of *p*-xylene and 1,4-dichlorobenzene was reported by Miyaura and coworkers using **27**/bpy and **28**/dtbpy respectively in 53–58% yields.^{178,179}

Further work by Smith and coworkers detailed the borylation of a range of 4-substituted benzonitriles, for which borylation *ortho* to the two substituents may yield two isomeric products (**Equation 1.18**).¹⁸² Borylation *ortho* to the cyano group dominated when the 4-substituent was larger than the cyano group, while for 4-fluorobenzonitrile, borylation *ortho* to the smaller fluoro group was favoured. The observed selectivity complements existing directed *ortho* metallation (DoM)¹⁸³ and electrophilic aromatic substitution (EAS)¹⁸⁴ chemistry allowing for selective functionalisation of 1,4-disubstituted arenes *ortho* to the cyano group in the presence of stronger *ortho* directing metallation groups (OMe, SMe, NMe₂, CO₂Me, NHAc) and *ortho/para* directors in the 4-position.



R = F, Cl, Br, I, Me, OMe, SMe
NMe₂, CO₂Me, NHAc, CF₃

Yields 55 - 70%

R = CF₃, NHAc, CO₂Me, NMe₂, Br, I

R = Cl, SMe₂, Me,

R = OMe

R = F

Ratio

99:1

90:10

67:33

8:92

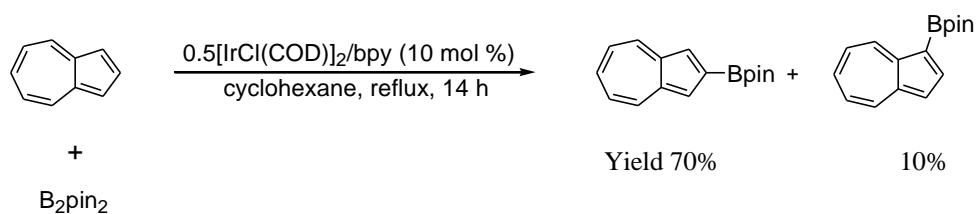
Equation 1.18 Iridium-catalysed borylation of 4-substituted benzonitriles by Smith and coworkers.

1.3.7.1.5 Borylation of polyaromatic substrates

The high degree of regioselectivity displayed in Ir-catalysed arene borylations, and the steric basis of this selectivity allows for the functionalisation of a wide range of aromatic substrates with selectivity complementary to that of other methodologies.

Sugihara and coworkers used a combination of **27** and bpy at 10 mol % Ir loading for the borylation of azulenes with B₂pin₂ in cyclohexane at reflux (**Equation 1.19**).¹⁸⁵ Borylation occurred predominantly at the 2-position with a minor isomer resulting from borylation of the more hindered 1-position adjacent to the ring junction. Interestingly, although the 7-membered ring possesses acidic and sterically unencumbered hydrogens,

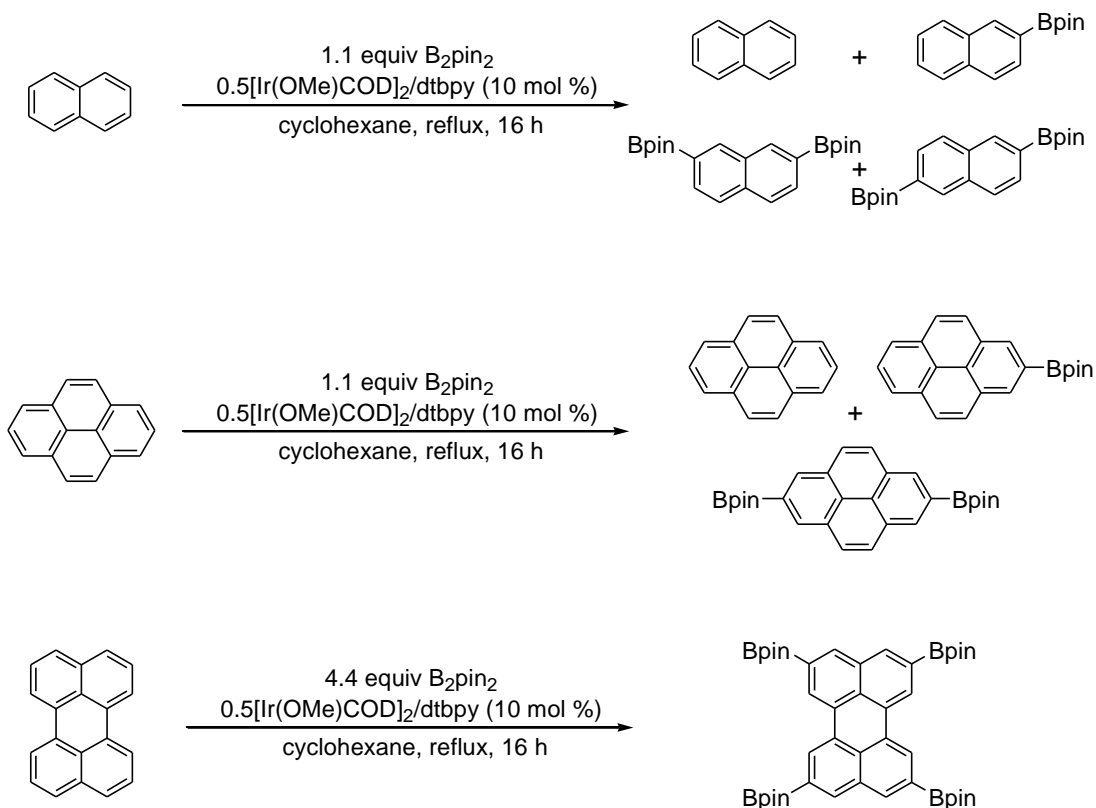
borylation of these C-H bonds is not observed. The authors attributed this selectivity to the more favourable formation of π -coordinated precursors to C-H cleavage with the five membered ring. Borylation of both 4,6,8-trimethylazulene and 1,4-dimethyl-7-isopropylazulene required longer reaction times and gave lower yields. In both cases, selective functionalisation of the 2-position was observed due to increased steric hindrance at the 1-, and 3-positions and blocking of the 2-position respectively.



Equation 1.19 Iridium-catalysed borylation of azulene with B_2pin_2 by Sugihara and coworkers.

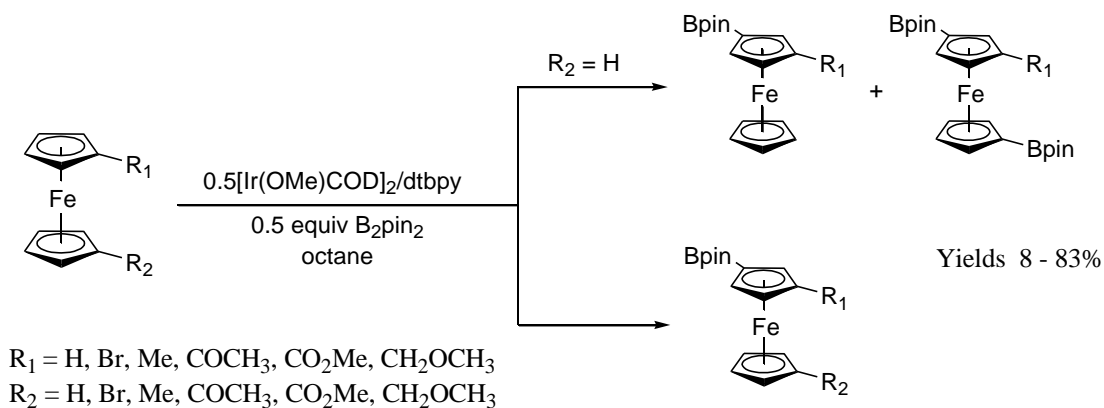
Marder and coworkers utilised **28**/dtbpy for the borylation of a range of polycyclic aromatic hydrocarbons with B_2pin_2 .¹⁸⁶ Borylation of naphthalene with 1.1 equivalents of B_2pin_2 and 10 mol % Ir loading in cyclohexane at 80 °C led to the formation of monoborylated product along with 2 isomeric bisborylated products and unreacted starting material in a ratio of 29:49:10:12. The combined yield of the bisborylated products could be increased to 93% by the use of 2.2 molar equivalents of B_2pin_2 . The borylation of pyrene under identical conditions with 1.1 equivalents of B_2pin_2 led to mono and bisborylated products in 68% and 6% yields respectively, with selective functionalisation at the 2-, and 7-positions. The use of 2.2 equivalents of B_2pin_2 yielded 2,7-bisborylated pyrene as the sole product in 97% yield. Perylene was borylated with 4.4 equivalents of B_2pin_2 to give a 2,5,8,11-tetraborylated product in 83% yield. The results are summarised in **Equation 1.20**. Hartwig and coworkers also reported the borylation of phenanthrene with B_2pin_2 and 1 mol % **28**/dtbpy in cyclohexane to give 2 isomeric products.¹⁸⁷ Although not fully analysed, by comparison with an authentic sample, it was shown that neither of the isomers were the 9-borylated product and were tentatively assigned as 2-, and 3-Bpin-phenanthrene.

In all cases, borylation occurred at the least hindered C-H bonds, while positions *ortho* to ring junctions were not borylated. For pyrene and perylene selective functionalisation of these positions is not possible by electrophilic aromatic substitution, which occurs at the 1-, and 4-positions of pyrene and may occur at the 1-, 3-, 4-, 9-, and 10-positions of perylene. Thus selectivity of iridium-catalysed borylation for reaction of the less hindered C-H bonds complements that of electrophilic aromatic substitution which leads to reaction at the most electron rich positions.



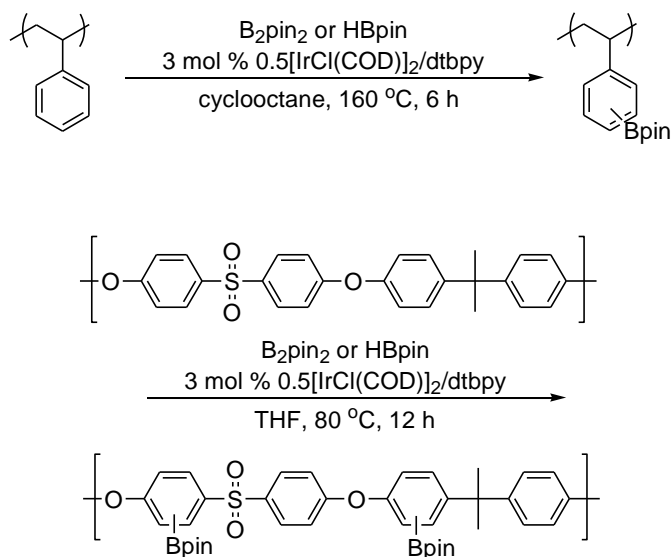
Equation 1.20 Ir-catalysed borylation of polyaromatic hydrocarbons by Marder and coworkers.

Plenio and coworkers reported the borylation of monosubstituted and 1,1'-disubstituted ferrocenes (**Equation 1.21**), along with the half sandwich complexes CpMn(CO)₃ and CpMo(CO)₃Me in octane at 126 °C.¹⁸⁸



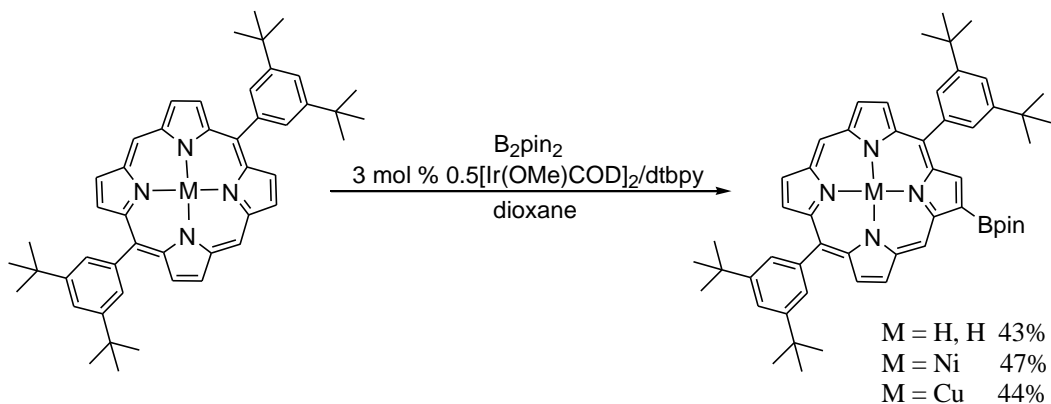
Equation 1.21 Ir-catalysed borylation of ferrocenes with B_2pin_2 by Plenio and coworkers.

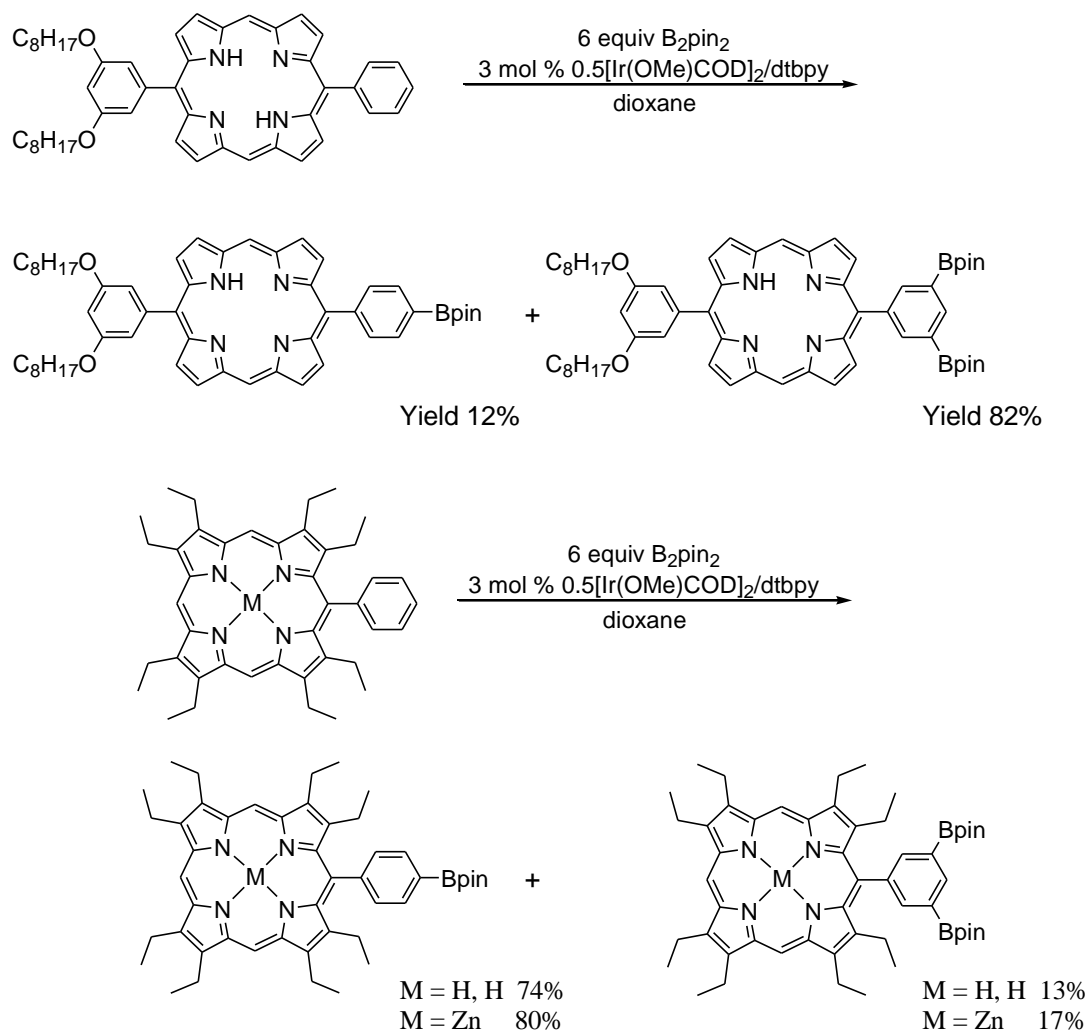
Bae and coworkers reported the borylation of crystalline polystyrenes with **27**/dtbpy in cyclooctane at 150 °C, with introduction of Bpin of up to 42% (**Figure 58**).¹⁸⁹ Further work by the same group detailed the borylation of aromatic main-chain polymer to give borylated polysulfones (**Equation 1.22**).¹⁹⁰ In both cases, subsequent transformations of the borylated polymer *via* Suzuki-Miyaura cross coupling or oxidation to give hydroxyl groups was demonstrated.



Equation 1.22 Ir-catalysed borylation of polymers by Bae and coworkers.

Osuka and coworkers have demonstrated that iridium-catalysed borylation is effective for the regioselective functionalisation of a range of porphyrins and aromatic substituents on porphyrins (**Equation 1.23**). Borylation of 1,15-disubstituted porphyrins, bearing groups which are unable to undergo borylation themselves, underwent borylation selectively at the β -position, with borylation of both free and metalloporphyrins being demonstrated.¹⁹¹ Exhaustive borylation of 5,15-di(1,5-di-*tert*-butylphenyl)porphyrin with an excess of B_2pin_2 led to a tetraborylated product resulting from the reaction of all 4 β C-H bonds. For 1-aryl-10-phenyl-porphyrins bearing no β -substituents, no borylation occurs at the β -positions due to steric effects of the 1,10-substituents. Instead, when an excess of B_2pin_2 is employed, borylation occurs on the substituents phenyl group leading to the formation of products resulting from *para* borylation and diborylation of the *meta* isomer. In contrast to most borylations of monosubstituted arenes, borylation of 1-phenyl- β -substituted porphyrins showed a high level of selectivity for the formation of the *para* product. This can be attributed to the extreme steric demands of the substituted porphyrin group which inhibits borylation of the *meta* C-H bonds on the phenyl ring.¹⁹²



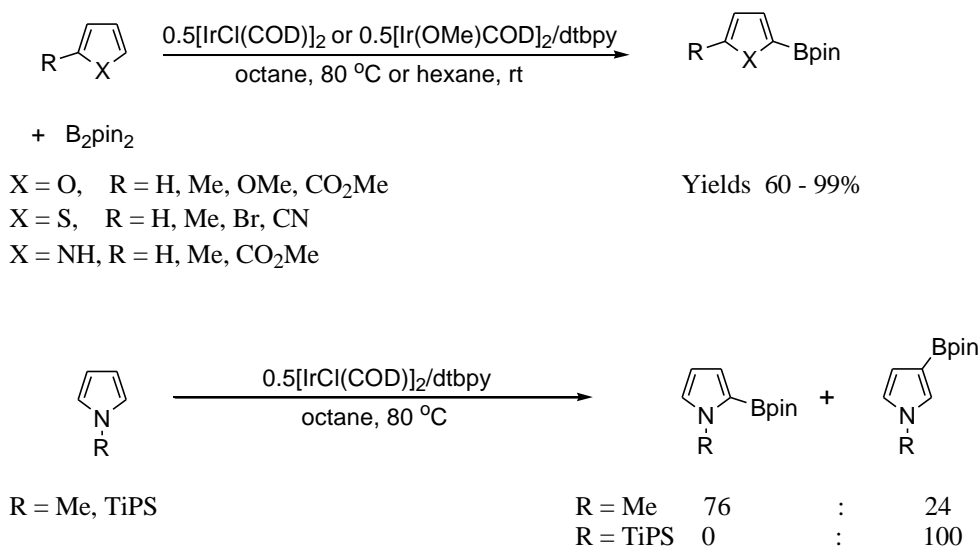


Equation 1.23 Regioselectivities of the Ir-catalysed borylation of substituted porphyrins with B_2pin_2 .

1.3.7.1.6 Borylation of 5-membered heterocycles

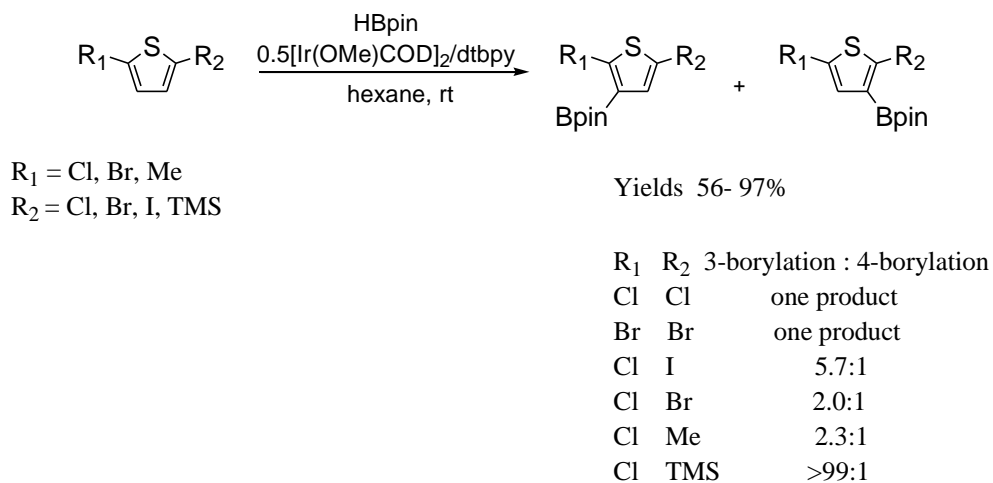
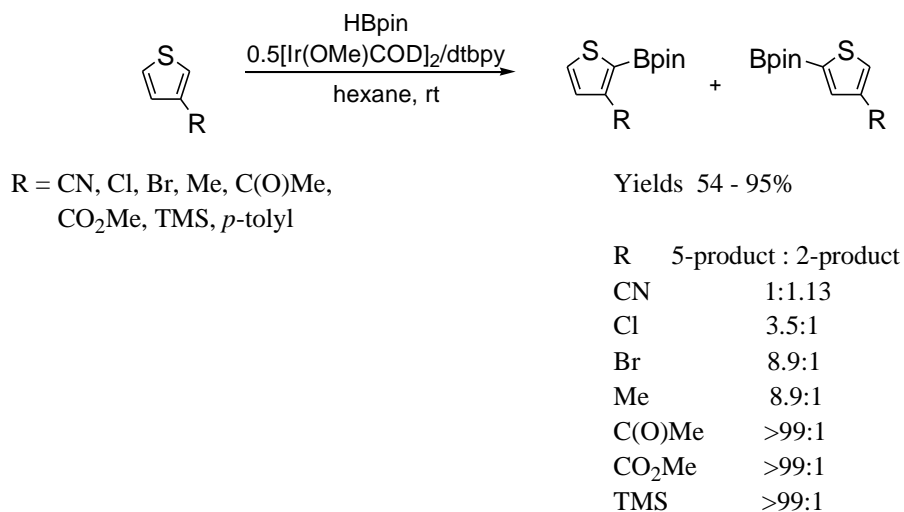
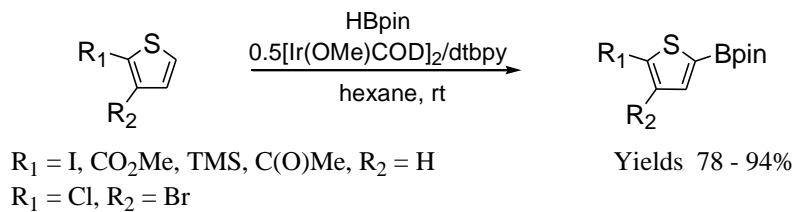
Miyaura and coworkers have reported the iridium-catalysed borylation of a range of thiophenes, free and N-protected pyrroles and furans with B_2pin_2 using **27**/*dtbpy* in octane at 80 °C, and with **28**/*dtbpy* in hexane at room temperature.^{193,194} The borylation of thiophene, pyrrole and N-methylpyrrole was also reported by Beller *et al.* using the **27**/*bpy* catalyst system.¹⁶⁶ For thiophenes, free pyrroles and furans, borylation was found to occur at the 2-position. However, for pyrroles bearing N-substituents, borylation at the 2-position is less favourable due to steric hindrance. Borylation of N-methylpyrrole

yielded a mixture of 2-, and 3-borylated products in a 76:24: ratio, while borylation of 1-triisopropylsilylpyrrole, previously reported by Smith¹⁷² using $[\text{Cp}^*\text{Rh}(\eta^4\text{-C}_6\text{Me}_6)]$, gave exclusive formation of the 3-borylated product. The results are summarised in **Equation 1.24**.



Equation 1.24 Ir-catalysed borylation of 5-membered heterocycles.

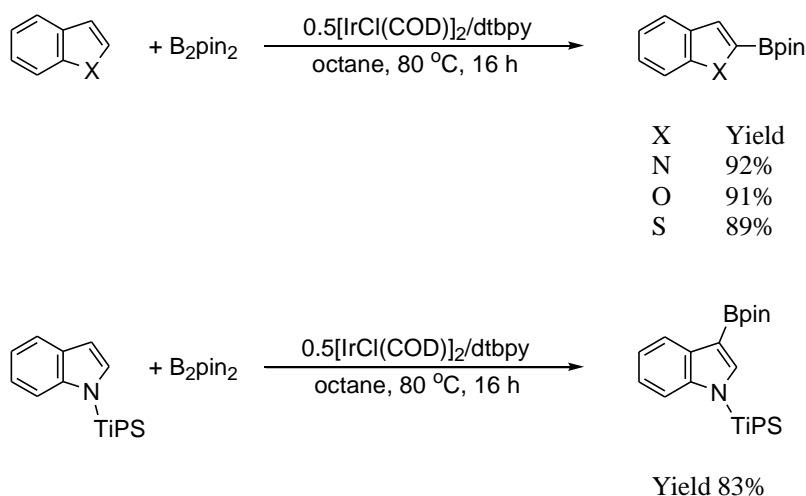
Smith and coworkers have carried out an extensive study into the borylation of 2-, 3-, 2,3- and 2,5-substituted thiophenes¹⁹⁵ using **28**/dtbpy (**Equation 1.25**). Borylation of 2-, and 2,3-substituted thiophenes gave single products resulting from selective borylation at the 5-position. In 3-substituted thiophenes borylation occurred in both the 2-, and 5-positions with borylation at the 5-position favoured. The degree of selectivity was reported to be determined by the size of the 3-substituent, although how the relative size of the substituents were determined was not mentioned. For 2,5-substituted thiophenes borylation *ortho* to the smaller substituent was favoured, similar to the borylation of unsymmetrical 1,4-disubstituted benzenes. Borylations were carried out using **28**/dtbpy with HBPin at room temperature in hexane, except for 2,5-dimethylthiophene, which required the use of 2 mol % $[(\text{Ind})\text{Ir}(\text{COD})]/\text{dmpe}$ in neat HBpin at 150 °C.



Equation 1.25 Ir-catalysed borylation of substituted thiophenes by Smith and coworkers.

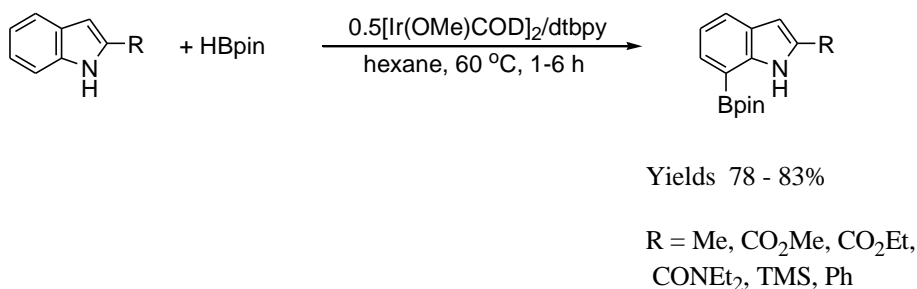
1.3.7.1.7 Borylation of benzofused 5-membered heterocycles

Miyaura and coworkers have reported the borylation of benzofused heterocycles with **27**/dtbpy at 80 °C. Borylation was found to occur at the 2-position, due to activation of this position by the adjacent heteroatom. Borylation of N-protected substrates was also demonstrated, with N-methyl indole giving 2-, and 3-borylated products in an 89:11 ratio, while N-TiPS indole was selectively borylated at the 3-position.¹⁹² Boron:arene ratios of less than 1:1 were used in order to prevent the formation of diborylated products. Similar work was also reported by Beller *et al.*¹⁶⁶ using **27**/bpy at 80 °C, and by Miyaura using with **28**/dtbpy at room temperature with B₂pin₂ or HBpin.¹⁹³ Borylations of benzofused 5-membered heterocycles are summarised in **Equation 1.26**.



Equation 1.26 Iridium-catalysed borylations of benzofused heterocycles by Miyaura and coworkers.

Smith and coworkers observed that the borylation of indole, with an excess of boron, led to the formation of small amounts of 2,7-diborylated indole as the sole bisborylated product. Further work on 2-substituted indoles showed that borylation occurred selectively at the 7-position, with coordination of the indole nitrogen to either iridium or boron directing the borylation (**Equation 1.27**).¹⁹⁶ Similar results were reported by Beller and coworkers.¹⁹⁷



Equation 1.27 Selective borylation of the 7-position in 2-substituted indoles.

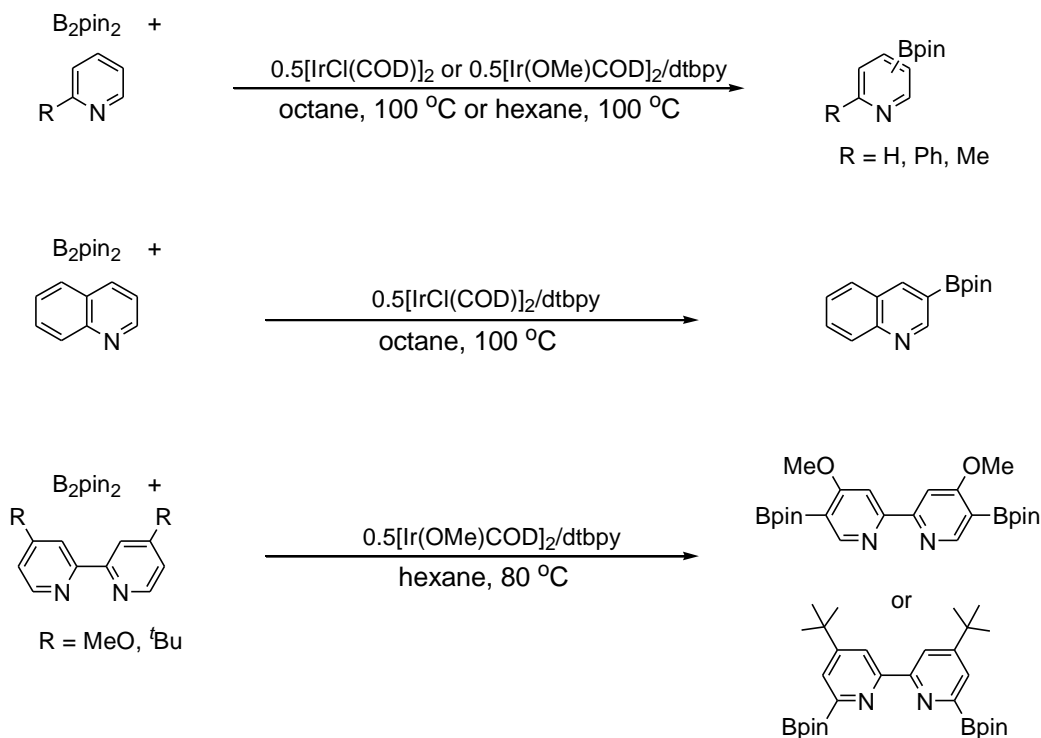
1.3.7.1.8 Borylation of 6-membered N-heterocycles and benzofused analogues

Since the initial report of the borylation of 2,6-lutidine with HBpin and [Cp*Ir(PMe₃)(H)(Bpin)] by Smith and coworkers in 2000,¹⁷⁴ Ir-catalysed borylation of a range of 6-membered heterocycles has been reported. Borylation of pyridine gave statistical mixtures of 3-, and 4-borylated products, with borylation at the 2-position not observed. However pyridine was found to be a poor substrate, giving a combined yield for the 2 isomers of 42% after 16 h at 100 °C. Similarly, borylations of 3-substituted pyridines by Hartwig and coworkers gave moderate conversions, with borylation occurring solely at the 5-position. This is in contrast to the borylations of 2,6-dichloropyridine and 2,6-lutidine which are readily borylated.¹⁹³

It was proposed by Marder and coworkers that the coordination of pyridines to iridium inhibits their borylation, with the strongly donating 4-*tert*-butylpyridine showing no borylation after heating at 80 °C for 2 days with a 2.5 mol % loading of [IrCl(COE)₂]₂ and dtbpy. Further work by the same group has shown that the incorporation of substituents at the 2-position prevents coordination of the pyridine substrate to the sterically hindered iridium centre and allows borylation to occur smoothly at the 4-, and 5-positions.¹⁹⁸ Similarly, quinoline, which may be considered a 2,3-disubstituted pyridine, borylates smoothly at the 3-position, with steric effects preventing borylation at the 4-position *ortho* to the ring junction.¹⁹³

It has been suggested by Hartwig and Miyaura that coordination of pyridine to either iridium or boron sterically hinders the 2-position, thus preventing its borylation.¹⁹² However, in light of the work Smith and coworkers on borylation of indoles,¹⁹⁵ coordination to iridium seems unlikely to be the origin of the observed regioselectivity. In addition, Marder and coworkers have reported that adducts of pyridines and B₂pin₂ do not form, even in highly concentrated solutions. Adducts of this type are known for the more Lewis acidic B₂cat₂ and readily identified by an upfield shift of the ¹¹B NMR resonance for the 4 coordinate boron.¹⁹⁹

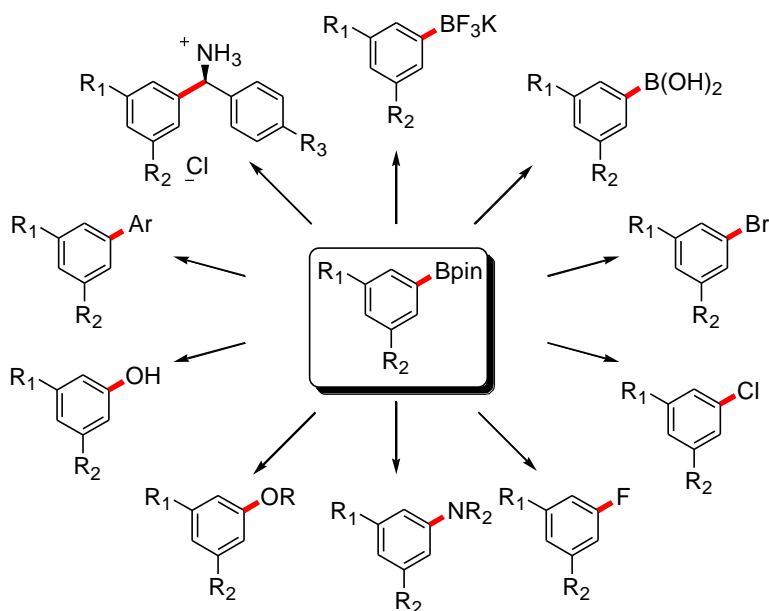
For 4,4'-dimethoxy-2,2'-bipyridine, effectively a 2,4 disubstituted pyridine, borylation occurred in the 5-, and 5'-positions suggesting that borylation will occur at sites other than the 2/6-position even in the presence of a small *ortho* group. Borylation of the more bulky dtbpy lead to reaction at the 6/6'-positions. The results for the borylations of pyridines and quinolines are summarised in **Equation 1.28**.



Equation 1.28 Ir-catalysed borylation of pyridines and related substrates.

1.3.7.2 Tandem reactions

Iridium-catalysed borylation of arenes has been shown to be compatible with a large range of transformations of boronic acids and boronate esters, and a variety of one-pot tandem reactions have been reported which feature aromatic C-H borylation as their initial step. The majority of the one-pot reactions have concentrated on the use of 1,3-disubstituted substrates as their borylation results in a single product. The current scope of transformations of the Bpin group that have been utilised in tandem reactions is shown in **Scheme 1.13**.



Scheme 1.13 Current scope of one-pot C-H borylation / transformation of the Bpin group.

Hartwig and coworkers have reported one-pot syntheses of aryl and heteroaryl boronic acids and potassium trifluoroborates from the corresponding 1,3-disubstituted arenes and benzofused heterocycles.²⁰⁰ Borylations were carried out in THF at 80 °C and the boronate esters were transformed into either boronic acids, *via* oxidative hydrolysis with NaIO₄ in THF/H₂O, or potassium trifluoroborate salts *via* displacement of pinacol with KHF₂ in THF/H₂O.

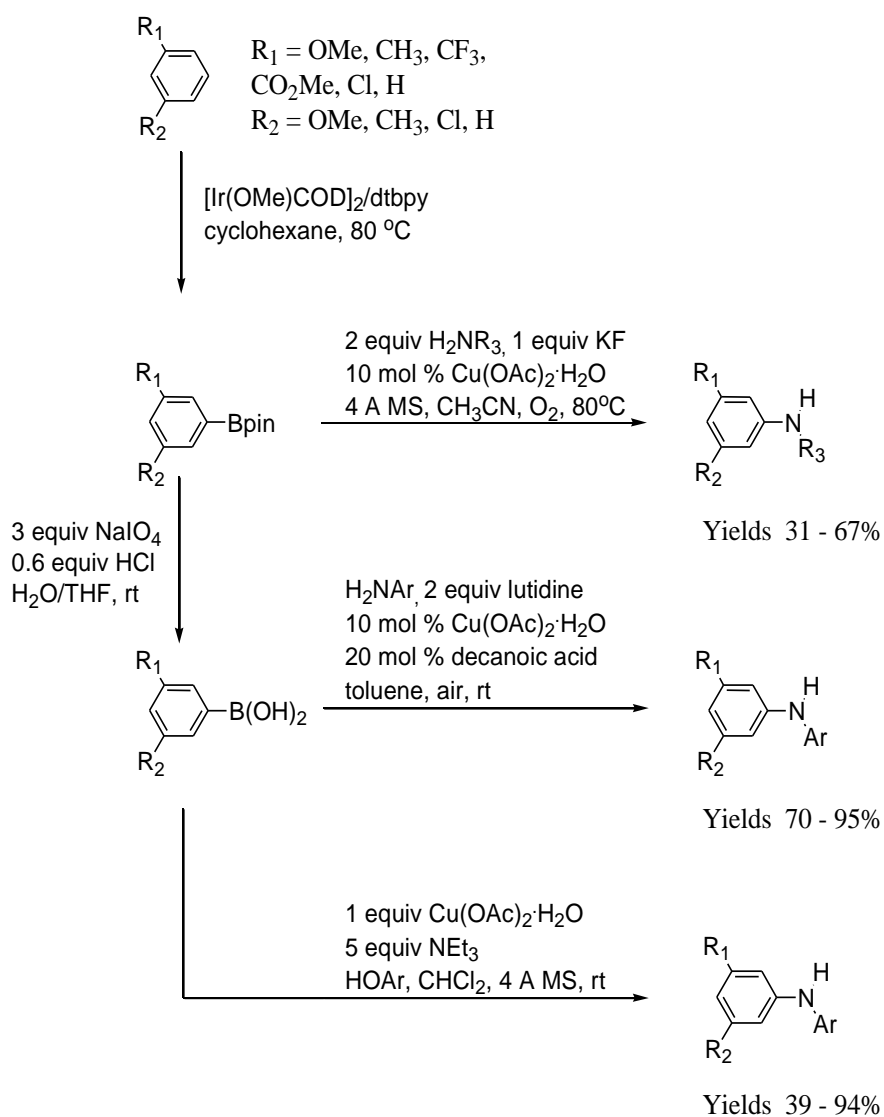
Smith and coworkers have shown that iridium-catalysed C-H borylation/oxidation is an effective, one-pot route for the synthesis of *meta* substituted phenols from 1,3-disubstituted arenes.²⁰¹ Synthesis of these products is notoriously difficult when the 1,3-substituents are *ortho/para* directing groups. Borylations were carried out in substrate/HBpin mixtures using (Ind)Ir(COD)/dmpe as the catalyst, and the subsequent oxidations were performed using aqueous Oxone[®] in acetone at 25 °C giving the products in high yields.

Hartwig and coworkers have demonstrated one-pot *meta* chlorination and bromination of 1,3-disubstituted arenes and 3-substituted pyridines *via* C-H borylations and oxidative halogenation with CuCl₂ and CuBr₂ respectively. Borylations were carried out in THF using 0.2 mol % Ir loadings of **28**/dtbpy, while the subsequent halogenations were carried out in MeOH giving the products in 46–81% yields.²⁰² Although conversions of aryl-, and vinyl-boronic acids and trifluoroborates to the corresponding iodides have been reported by Kabalka,²⁰³ as yet, no one-pot C-H borylation/iodination protocol has been reported.

In addition to simple transformations of the pinacolboronate ester group, Ir-catalysed C-H borylation has been shown to be compatible with transition metal-catalysed couplings of arylboronate esters with a range of electrophiles and nucleophiles.

One-pot C-H borylation/Suzuki-Miyaura cross couplings have been widely reported as demonstrations of the synthetic utility of C-H borylations. Miyaura and coworkers have reported a one-pot C-H borylation/Suzuki-Miyaura reaction synthesis of unsymmetrical biaryls. Borylations were carried out using HBpin in hexane with **28**/dtbpy at 25 °C, while addition of Pd(dppf)Cl₂, K₃PO₄·*n*H₂O, arylbromide and DMF gave the biaryl products.¹⁸⁰ This method is an improvement on previous reports in which the solvent used for borylation was evaporated, prior to carrying out the cross coupling in a secondary solvent. In a further improvement, Marder and coworkers demonstrated a one-pot C-H borylation/Suzuki-Miyaura cross coupling sequence in a single solvent. Both C-H borylation and Suzuki-Miyaura cross couplings were found to proceed smoothly and

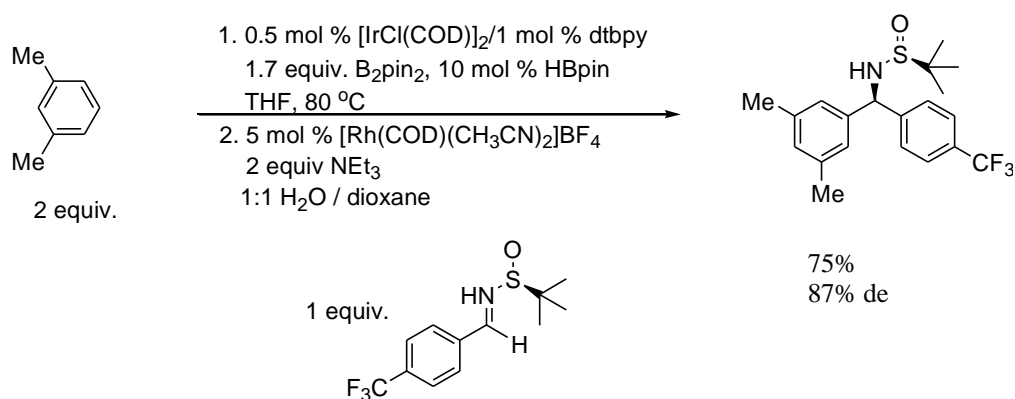
with high yields in methyl-*tert*-butyl ether (MTBE). Other polar solvents typically used for Suzuki-Miyaura reactions, such as DMF and DMSO, have been previously shown to be poor solvents for Ir-catalysed borylations.²⁰⁴ Hartwig and coworkers have reported the combination of C-H borylations and Chan-Lam couplings as a one-pot route to anilines and aryl ethers from arene starting materials (**Equation 1.29**).²⁰⁵ Alkylamines could be coupled directly with the boronate ester products, while the use of phenols and anilines as coupling partners required the boronate ester to be oxidised to the more reactive boronic acid.



Equation 1.29 Cu-catalysed couplings of boronic acids and boronate esters with N-, and O-nucleophiles.

amidoarylboronate ester solution. In both cases the use of anhydrous conditions was found to be essential for preventing unwanted side reactions of the boronate ester group.

Rhodium-catalysed additions of organoboronates to a range of electrophiles are widely known.¹⁵⁵ Hartwig and Boebel have reported that arenes may be converted to chiral α,α -diarylmethylsufinylamines *via* a sequence of C-H borylation and Rh-catalysed addition of aryl boronate esters to chiral sulfinimines.²⁰⁸ Both stepwise and one-pot syntheses were demonstrated, **Equation 1.31**.



Equation 1.31 One-pot synthesis of chiral α,α -diarylmethylsufinylamines by Hartwig and Boebel.

1.3.7.3 Iridium-catalysed borylations of silicon containing substrates

Hartwig and Boebel have utilised the ability of iridium complexes to cleave and functionalise Si-H bonds in two studies into the borylation of silane substrates. Borylation of benzyldimethylsilane led to *ortho*-substituted products with no reaction at the *meta* or *para* positions observed. Phenols and anilines were silylated *via* $[\text{IrCl}(\text{COD})]_2$ catalysed coupling with SiMe_2H_2 to give functionalised dimethylsilanes, followed by silane directed C-H borylation with **27**/dtbpy and B_2pin_2 . The reversal of selectivity observed in the borylation to silane functionalised arenes was attributed to oxidative addition of the Si-H bond to the Ir centre followed by elimination of HBpin to give a new iridium complex in which the arene is coordinated *via* the silane moiety. The

reaction may then occur at the *ortho* C-H bonds of the bound arene, followed by Si-H reductive elimination from Ir(III) which releases the *ortho* borylated product.²⁰⁹

Later work by the same authors reported the catalytic borylation of a range of trialkylsilanes at 80 °C with B₂pin₂ and **28**/dtbpy as the catalyst to give borylsilane products in moderate to high yields.²¹⁰ The borylsilane products were then employed as boron sources in the **28**/dtbpy catalysed borylation of a range of methylarenes. Notably only borylation occurred with no silylation products observed. In contrast to typical **28**/dtbpy catalysed borylation of methylarenes both sp² and sp³ borylation products were observed, with hindered substrates such as mesitylene borylated selectively at the benzylic positions.

1.3.7.4 Novel iridium catalysts for aromatic C-H borylations

Although the catalyst systems developed by Miyaura and Hartwig, and Smith have been the most widely studied and applied, other groups have reported the use of other ligands for iridium alternative catalyst systems (**Figure 1.29**).

Masuda and coworkers have shown that Ir(Tp)COD or combinations of **27** and trispyrazolylborate (Tp) salts are effective catalysts for aromatic C-H borylations. Borylations of mono-, and 1,2-, 1,3- and 1,4-disubstituted arenes showed the same selectivities as for the use of [Ir(X)COD]₂/dtbpy.²¹¹ Nishida and coworkers have shown that combinations of **27** and 2,6-diisopropyl-N-(pyridylmethylene)-aniline, **29**, and related ligands are effective for the borylation of arenes and heteroarenes at 80 °C.²¹² Borylations of 1,3-disubstituted benzenes and 2,6-disubstituted pyridines reacted selectively at the least hindered C-H bond, while benzofuran, benzothiophene and indole underwent selective borylation at the 2-position.

Maguire and coworkers have shown that Ir(I)-salicylaldiminato(COD) complexes such as **30** are effective for the borylation of arenes when used in conjunction with the ionic liquid tributyltetradecylphosphonium dodecylbenzenesulfonate (TBPB), CH₂Cl₂ and

tetra-2-pyridinylpyrazine, giving a catalyst system that can be reused up to 3 times without loss of activity.²¹³ Borylations of monosubstituted benzenes (R = CF₃, OMe and Me) led to the formation of *meta* and *para* substituted products in of 1.3:1, 1.1:1 and 1.5:1 for trifluoromethylbenzene, anisole and toluene, respectively.

Hermann and coworkers synthesised a range of iridium complexes of mono-, and bidentate NHC ligands (**31** and **32**) which were evaluated as catalysts for the borylation of arenes with HBpin at 40–45 °C. Mono-, 1,2-, and 1,3-disubstituted arenes were all effectively borylated although the regioselectivity of the reactions was not confirmed.²¹⁴

Maguire and coworkers have demonstrated that Ir(0) nanoparticles, prepared by the reduction of hydrido-iridiumcarborane (PPh₃)Ir(H)(7,8-*nido*-C₂B₉H₁₁), are active catalysts for the borylation of benzene with HBpin in mixtures of CH₂Cl₂ and ionic liquids when used in conjunction with tetra-2-pyridinylpyrazine and microwave heating. The catalyst systems could be recycled up to 6 times with less than 0.5% loss in activity.²¹⁵

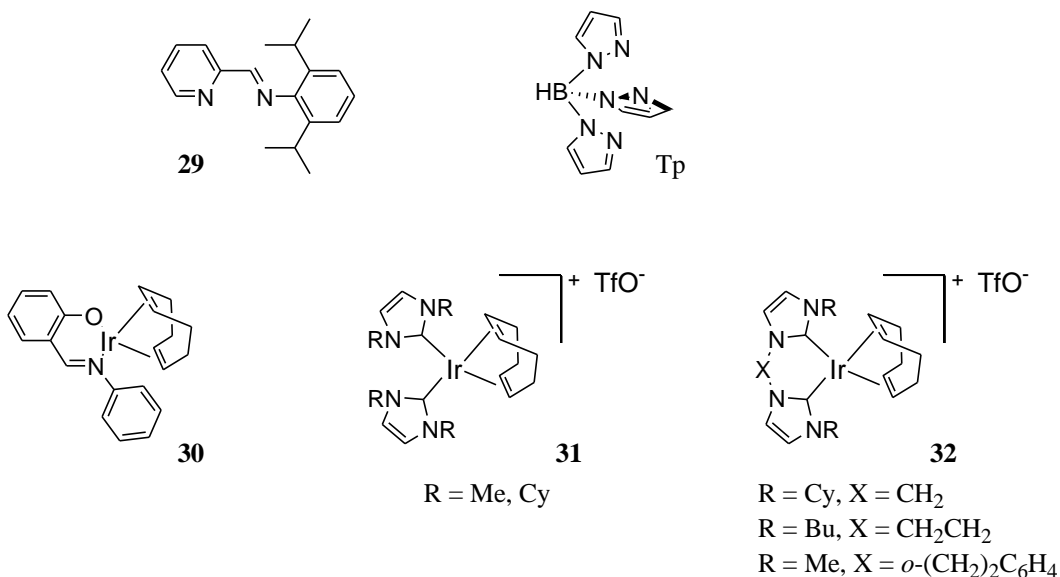
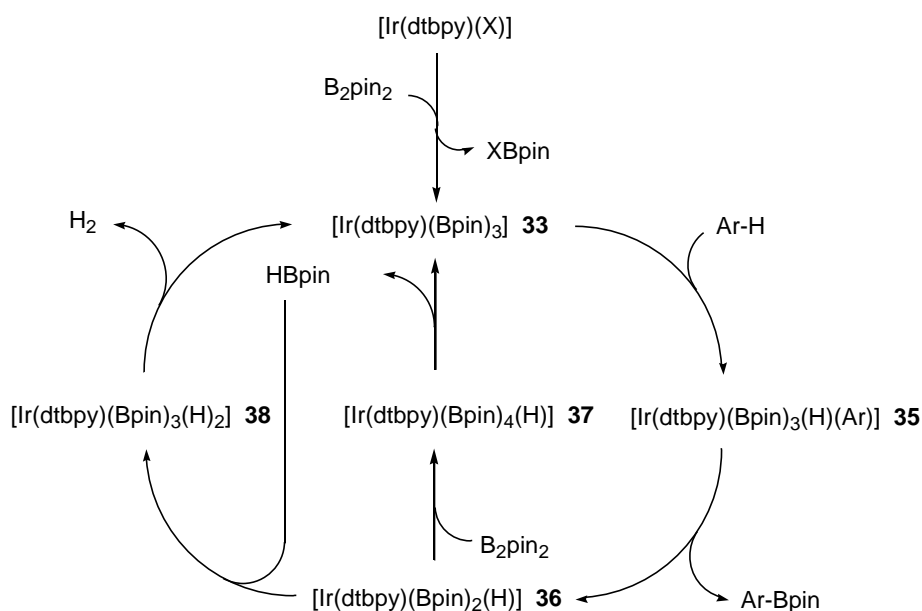


Figure 1.29 Novel ligands and Ir complexes employed in Ir-catalysed C-H borylations.

1.3.7.5 Proposed mechanism for the Ir(OMe)COD/L₂-catalysed borylation of arenes

Miyaura and coworkers have proposed that [Ir(dtbpv)(Bpin)₃], **33**, is the resting catalyst state in the [IrCl(COD)]₂/dtbpv. Analysis of catalytic reactions containing high catalyst loadings by ¹H NMR spectroscopy showed the main species to be a dtbpv-ligated Ir complex. This species was shown to be [Ir(dtbpv)(Bpin)₃] by comparison to be the *fac*-Ir^{III} trisboryl complex [Ir(dtbpv)(Bpin)₃(COE)], **34**, which was independently synthesised from [IrCl(COE)₂]₂, 2 equivalents of dtbpv and 10 equivalents of B₂pin₂ in mesitylene at 50 °C (**Figure 1.30**). Dissolution of **34** in C₆D₆ rapidly generated 3 equivalents of C₆D₅Bpin at room temperature, showing that the complex is chemically and kinetically competent to be an intermediate in the catalytic cycle.¹⁷⁸

The proposed mechanism starts with the coordinatively unsaturated **33** which cleaves and functionalises the arene C-H bonds by either oxidative addition of the arene C-H bond to give the Ir(V) complex [Ir(dtbpv)(Bpin)₃(Ar)(H)], **35**, and subsequent reductive elimination of Ar-Bpin to give [Ir(dtbpv)(Bpin)₂(H)], **36**, or *via* a concerted σ-bond metathesis pathway to give the same products. Reaction of B₂pin₂ with **36** is proposed to give [Ir(dtbpv)(Bpin)₄(H)], **37**, which may reductively eliminate HBpin to reform **33**, completing the catalytic cycle. The HBpin byproduct is utilised in a second catalytic cycle in which HBpin reacts with **36** to give [Ir(dtbpv)(Bpin)₃(H)₂], **38**, which eliminates H₂ to give **33**. This complex then reacts with arene substrate to give Ar-Bpin and to reform **36**. The proposed catalytic cycle featuring an oxidative addition/reductive elimination pathway for C-H borylation is detailed in **Scheme 1.14**.



Scheme 1.14 Proposed catalytic cycle of $[\text{Ir}(\text{X})\text{COD}]_2 / \text{dtbpy}$ catalysed borylation of arenes with B_2pin_2 .

Catalytic borylations carried out with $[\text{Ir}(\text{X})\text{COD}]_2/\text{dtbpy}$ catalyst precursors were found to show an induction period, in which COD is reduced or hydroborated to give COE or related species. Reactions carried out with $[\text{Ir}(\text{X})(\text{COE})_2]_2/\text{dtbpy}$ or $[\text{Ir}(\text{dtbpy})(\text{Bpin})_3(\text{COE})]$ showed no such induction period. In addition, the species formed in the stoichiometric reaction of $[\text{Ir}(\text{TfO})(\text{COD})]$, dtbpy and B_2pin_2 , namely $[\text{Ir}(\text{dtbpy})(\text{Bpin})_2(\text{COD})]\text{TfO}$, **39**, (**Figure 1.30**) did not borylate C_6D_6 in the absence of added B_2pin_2 .¹⁷⁸

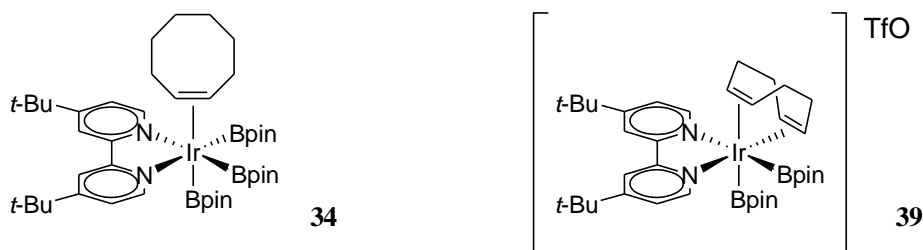


Figure 1.30 Iridium tris-, and bis-boryl complexes ligated by dtbpy.

Sakaki and coworkers have reported a theoretical study of the borylation of benzene using B_2eg_2 (eg = ethylene glycolato) as a model for B_2pin_2 and ethane-1,2-diylidenediamine (diim) or bpy as models of the dtbpy ligand.²¹⁶ The results suggest that $[Ir(bpy)(Bpin)_3]$ is the active species for C-H bond activation, with oxidative addition of Ph-H to $[Ir(bpy)(Bpin)_3]$ to give $[Ir(bpy)(Bpin)_3(H)(Ph)]$ occurring, rather than the reaction with $[Ir(bpy)(Bpin)]$. Reductive elimination of Ph-Bpin was proposed to occur from $[Ir(bpy)(Bpin)_3(H)(Ph)]$ to give $[Ir(bpy)(Bpin)_2(H)]$. Oxidative addition of both B_2pin_2 and HBpin to $[Ir(bpy)(Bpin)_2(H)]$, giving $[Ir(bpy)(Bpin)_4(H)]$ and $[Ir(bpy)(Bpin)_3(H)_2]$ respectively, are feasible, with the reaction of B_2pin_2 more favourable than that of HBpin. This supports the suggestion of Smith *et al.* that the catalytic borylation of benzene with B_2pin_2 at 80 °C is a two step process, with rapid reaction with B_2pin_2 , followed by a slower reaction with HBpin once B_2pin_2 has been consumed. Sakaki and coworkers suggested that the formation of the unusual iridium(V) intermediates is made more favourable by the strongly electron donating Bpin and bpy ligands which stabilise the high oxidation state of iridium. In addition, the use of planar bpy ligands makes the formation of seven coordinate iridium(V) complexes more favourable by reducing steric hindrance in this highly congested intermediate.

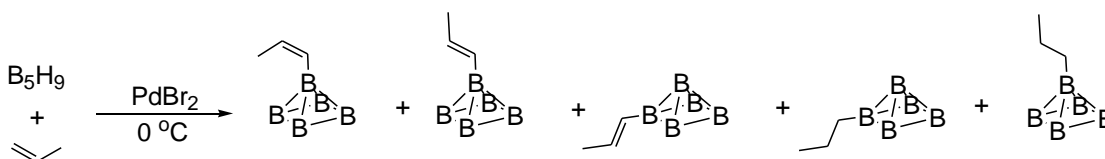
Hartwig and coworkers reported experimental mechanistic studies on the $[Ir(X)COD]/dtbpy$ catalysed borylation of arenes with B_2pin_2 , with the conclusions in consensus with those of Sakaki *et al.* COE was found to dissociate reversibly from **34** to give the active species **33**. As suggested by Sakaki *et al.*, C-H activation *via* $[Ir(dtbp)(Bpin)]$, although energetically feasible, does not occur as the equilibrium for the reversible oxidative addition of B_2pin_2 to $[Ir(dtbp)(Bpin)]$ lies far towards the iridium(III) trisboryl species **33**.¹⁸⁶

1.3.8 Dehydrogenative borylation of olefins

Vinyl boronate esters (VBEs) are useful intermediates in organic chemistry. They have been employed as precursors to aldehydes and vinyl halides, and can undergo a range of metal-catalysed reactions. Vinyl boron reagents can be synthesised by a variety of methods including hydroboration of alkynes,²¹⁷ palladium-catalysed borylation of vinyl halides,²¹⁸ lithiation of vinyl halides and subsequent trapping with trialkylborates,²¹⁹ hydrogenation of 1-borylalkynes,²²⁰ hydrozirconation of 1-borylalkynes,²²¹ cross-metathesis of terminal olefins with pinacolvinylboronate,²²² transmetallation of vinyl metal reagents,²²³ and transition metal-catalysed diboration of alkynes with diboron reagents.²²⁴ However, the majority of these methods involve the preactivation of the vinyl group or are unsuitable for the synthesis of β,β -disubstituted vinylboronates. Thus, the dehydrogenative borylation of olefins, in which a vinylic C-H bond is replaced with a C-B bond, is an attractive alternative to these methods. It does not require the preactivation of the olefin substrates, and it can be used to form VBEs from β,β -disubstituted olefins.

1.3.8.1 Dehydrogenative borylation of olefins using borane clusters

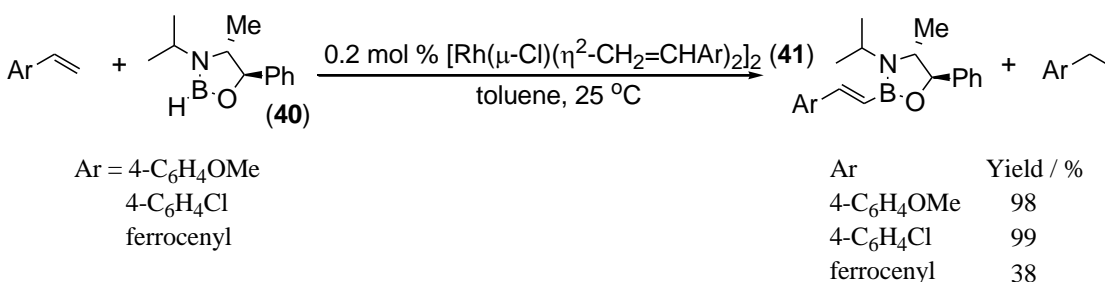
Sneddon and coworkers reported the first dehydrogenative borylations of olefins. The borylation of ethene, but-1-ene and propene was reported to occur with pentaborane in the presence of PdBr_2 as a catalyst (**Equation 1.31**).²²⁵ However, the borylation of propene led to the formation of 3 isomeric vinylboranes, along with 2 hydroboration products. In addition, 50% of the olefin was hydrogenated using the hydrogen which is formed in the dehydrogenative borylation process.



Equation 1.31 PdBr_2 -catalysed dehydrogenative borylation of propene with pentaborane by Sneddon and coworkers. Terminal and bridging hydrogens on the boron cluster are omitted for clarity.

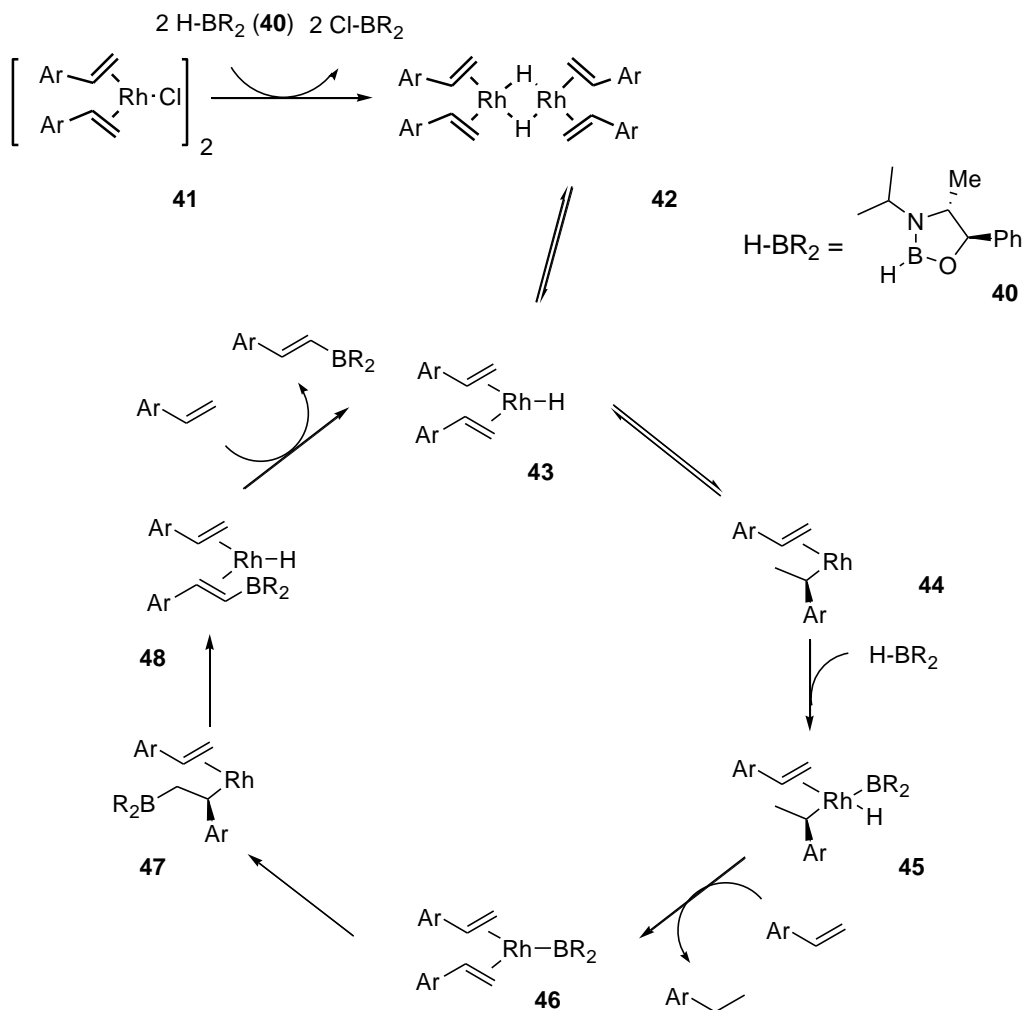
1.3.8.2 Dehydrogenative borylation of olefins with concomitant hydrogenation and/or hydroboration

In 1992, Brown *et al.* reported the dehydrogenative borylation of 4-vinylanisole with oxazaborolidene **40** in the presence of $[\text{Rh}(\mu\text{-Cl})(\eta^2\text{-CH}_2\text{=CHAr})_2]_2$, **41**, (Ar = 4-MeOC₆H₄) as catalyst.²²⁶ Reactions were conducted in toluene at room temperature giving a 1:1 mixture of VBE and hydrogenation products. In a subsequent publication by the same group, borylations of 4-vinylanisole, 4-vinylchlorobenzene and vinylferrocene with oxazaborolidene **40** and 0.2 mol % **41** gave a 1:1 ratio of VBE and hydrogenation products.²²⁷ No products from hydroboration were observed (**Equation 1.33**).



Equation 1.33 Rhodium-catalysed dehydrogenative borylations of vinylarenes by Brown *et al.*

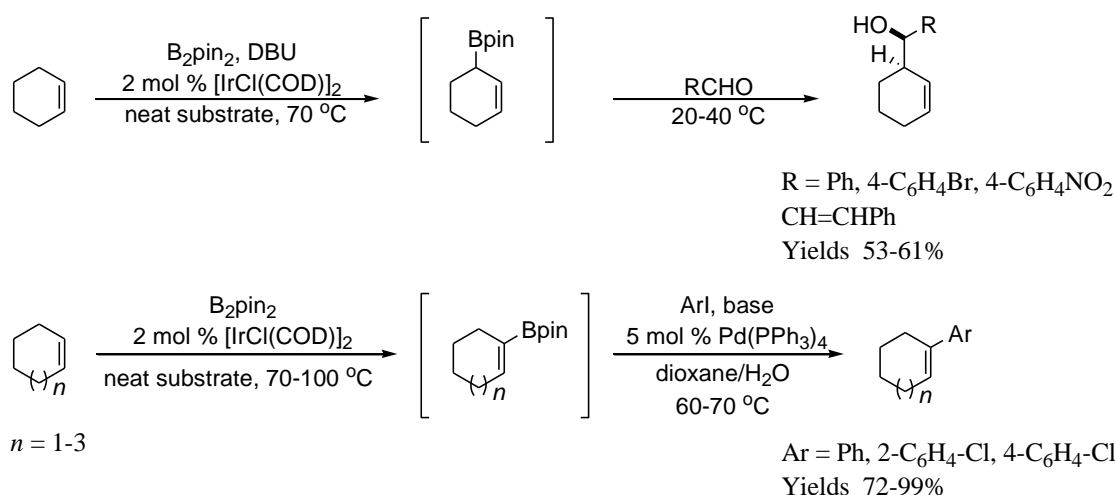
The proposed mechanism of Brown's rhodium-catalysed dehydrogenative borylation of vinylarenes is detailed in **Scheme 1.15**. Initial reaction of the borane species with $[\text{Rh}(\mu\text{-Cl})(\eta^2\text{-CH}_2\text{=CHAr})_2]_2$, **41**, is proposed to lead to the formation of **42**, which acts as a source of the active monomeric rhodium hydride **43**. Reversible 1,2-insertion of one of the bound olefin ligands into the Rh-H bond then gives the 12 electron species **44** which oxidatively adds the oxazaborolidene B-H bond to give **45**. Reductive elimination of alkane and coordination of additional olefin would then give rhodium boryl complex **46** which may insert one of the olefin ligands into the Rh-B bond to give the rhodium β -borylalkyl species **47**. Subsequent β -hydride elimination gives the rhodium hydride complex **48** from which the bound VBE product is displaced by unreacted olefin to regenerate **43** and complete the catalytic cycle.



Scheme 1.15 Rhodium-catalysed dehydrogenative borylations of vinylarenes by Brown *et al.*

Masuda and coworkers have reported the dehydrogenative borylation of olefins with HBpin catalysed by $[\text{RhCl}(\text{COD})]_2$ at room temperature in toluene (**Scheme 1.34**).²²⁸ This reaction is clearly reminiscent of the $[\text{Rh}(\mu\text{-Cl})(\eta^2\text{-olefin})_2]_2$ -catalysed reaction reported by Brown and Lloyd-Jones. VBE products were obtained in high yields with respect to HBpin and with selectivities as high as 96%; however, in all cases, the formation of an equal quantity of the ethylarene byproduct resulting from the sacrificial hydrogenation of the substrate was observed. In addition, the synthesis of an unsymmetrical stilbene by a one-pot sequence of dehydrogenative borylation, followed by Suzuki-Miyaura cross-coupling, was reported.

Sabo-Etienne and coworkers have demonstrated that $[\text{Ru}(\text{H})_2(\text{H}_2)_2(\text{PCy}_3)_2]$ and $[\text{RuH}\{(\mu\text{-H})_2\text{Bpin}\}(\sigma\text{-HBpin})(\text{PCy}_3)_2]$ are catalyst precursors for the dehydrogenative borylation of linear and cyclic olefins with HBpin.²³⁰ The reaction of HBpin with $[\text{Ru}(\text{H})_2(\text{H}_2)_2(\text{PCy}_3)_2]$ formed H_2 and $[\text{RuH}\{(\mu\text{-H})_2\text{Bpin}\}(\sigma\text{-HBpin})(\text{PCy}_3)_2]$. The reaction of this complex with ethene formed $[\text{RuH}(\text{Bpin})(\text{C}_2\text{H}_4)(\text{PCy}_3)_2]$, and this complex was proposed to be the catalyst resting state. A range of linear and cyclic olefins underwent dehydrogenative borylation at room temperature leading to mixtures of VBEs, hydroboration products, and alkanes from sacrificial hydrogenation of the substrates.

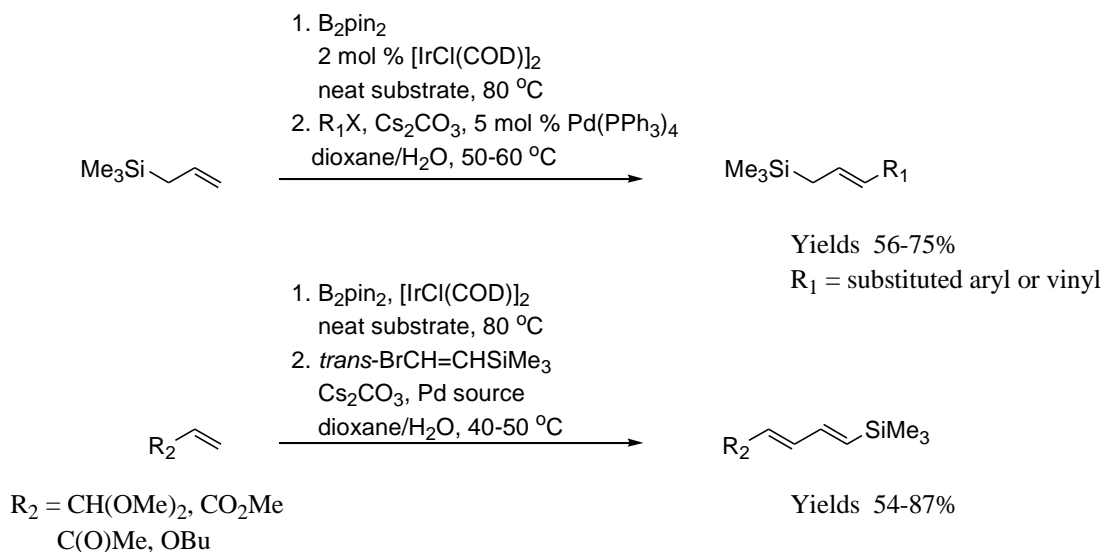


Equation 1.36 Iridium-catalyzed borylations of cyclic olefins by Szabó and coworkers.

Szabó and coworkers reported the dehydrogenative borylation of cyclic olefins using B_2pin_2 catalysed by $[\text{IrCl}(\text{COD})]_2$ (**Equation 1.36**).²³¹ For cyclohexene, a 1:1 ratio of allylic and vinylic borylation products was obtained after 3 h at $70\text{ }^\circ\text{C}$, while only the vinylic borylation product was observed after 16 h. Addition of 0.5 equivalents of 1,8-diazabicyclo[5.4.0]undecane (DBU) led to an increase in the ratio of allylic to vinylic products (5:1 after 3 h at $70\text{ }^\circ\text{C}$), although the proportion of the vinylic product increased with prolonged heating. At $90\text{-}100\text{ }^\circ\text{C}$, the borylation reactions gave equimolar amounts of vinylboronate esters and their saturated counterparts, the latter resulting from sacrificial hydrogenation of the substrate. The vinylboronate products were coupled *in*

situ with aryl iodides to give cyclic trisubstituted olefins, whereas the allylic boronates were allowed to react with aldehydes *in situ* to give stereo-defined homoallyl alcohols.

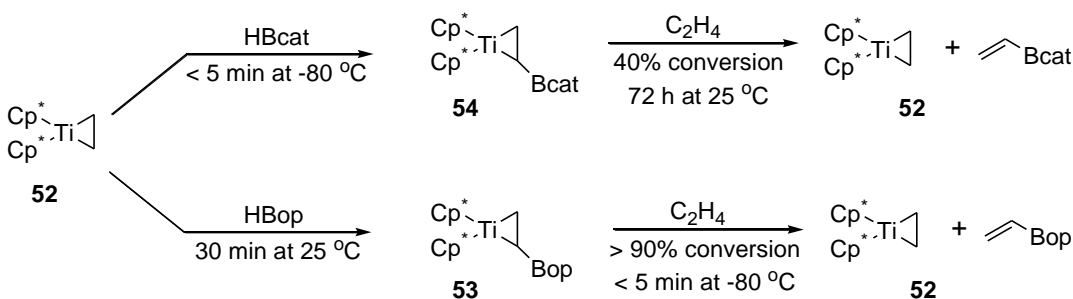
Szabó also reported the dehydrogenative borylation of certain linear, terminal olefins with $[\text{IrCl}(\text{COD})]_2$ and B_2pin_2 at $80\text{ }^\circ\text{C}$ to give vinylboronate esters which were then coupled with a range of aryl and vinyl halides in a one-pot process (**Equation 1.37**).²³² Allylsilanes and carbonyl, acetal and ether substituted olefins underwent dehydrogenative borylation to give 1:1 ratios of vinyl-, and alkylboronate ester products, the latter resulting from hydroboration by the HBpin generated by the dehydrogenative borylation with B_2pin_2 . Of particular interest was the selective formation of VBEs over allylboronates from the reaction of B_2pin_2 with allyltrimethylsilane. This selectivity was attributed to a greater thermodynamic stability of the VBE product and a more favorable β -hydride elimination step.



Equation 1.37 Iridium-catalysed dehydrogenative borylation of olefins and subsequent cross-coupling by Szabó and coworkers.

Smith and coworkers reported the reactions of ethene with monoboranes catalysed by 3 mol % $[\text{Cp}^*\text{Ti}(\eta^2-\text{CH}_2=\text{CH}_2)]$, **52**.^{233,234} The catalytic reaction using HBop (op = benzo-1,2,3-diazaborolene) gave VBE (58% yield) plus ethane. In contrast catalytic reactions

using HBcat gave the hydroboration product, ethylBcat, instead. Stoichiometric addition of HBcat or HBop to **52** led to the formation of boryl-substituted titanacycles, which underwent ligand exchange with additional ethene to regenerate **52** and give the VBE products. Borylation of **52** with HBop to give **53** was much slower than that with HBcat; however, subsequent displacement of the VBE by ethene was much faster for the Bop analog **14** than for the Bcat compound **54** (**Equation 1.38**).

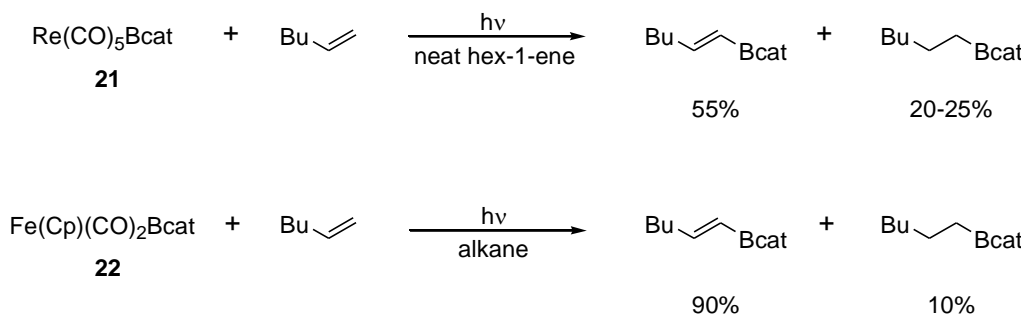


Equation 1.38 Stoichiometric reactions of $[\text{Cp}^*_2\text{Ti}(\eta^2\text{-CH}_2\text{=CH}_2)]$ with boranes and ethene by Smith and coworkers.

1.3.8.3 Photochemically induced stoichiometric dehydrogenative olefin borylation

During the course of initial studies on stoichiometric C-H activation reactions, Hartwig and coworkers reported the photolysis of $[\text{CpFe}(\text{CO})_2(\text{Bcat})]$, **22**, and $[\text{Re}(\text{CO})_5(\text{Bcat})]$, **21**, in the presence of terminal and internal olefins (**Equation 1.39**).^{169,170} The reaction of **22** with hex-1-ene led to the formation of the terminal hexenylboronate ester in 90% yield, along with 10% of hexyl-Bcat. The reaction of rhenium boryl **21** with hex-1-ene gave 55% of the terminal, *trans*-VBE product by NMR spectroscopy, with the majority of the remaining material (20–25%) consisting of the alkylboronate, presumably formed by metal-catalysed hydroboration. Reactions of **21** with internal olefins were less selective; the reaction of 4-octene gave the VBE product, along with at least 3 isomeric vinylboronates and octyl-Bcat from hydroboration. Photolysis of **21** in the presence of norbornene gave a single VBE product, along with two isomeric hydroboration products,

whereas the reaction with cyclohexene formed products other than vinylboronate esters. The formation of the VBE products was proposed to occur *via* photochemically induced dissociation of CO, followed by coordination of the olefin and either direct C-H bond cleavage or migratory insertion of the olefin into the M-B bond, followed by β -hydride elimination.



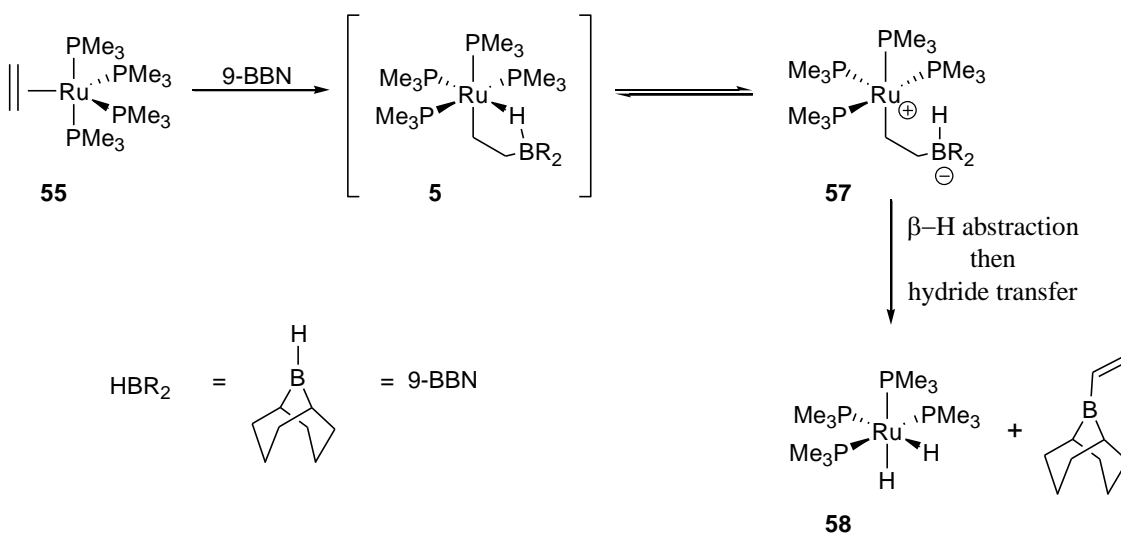
Equation 1.39 Photochemically induced dehydrogenative borylation of olefins by Hartwig and coworkers.

1.3.8.4 Dehydrogenative borylation of olefins under hydroboration conditions

Marder, Baker and coworkers observed the formation of vinylboranes in the stoichiometric reactions of $[\text{Ru}(\eta^2\text{-C}_2\text{H}_4)(\text{PMe}_3)_4]$, **55**, with 9-borabicyclo[3.3.1]nonane (9-BBN).²³⁵ Addition of the boryl group to the bound olefin formed the cyclic species **56** which is in equilibrium with the ruthenium β -borylalkyl complex **57**, from which β -hydride elimination and hydride transfer gave the vinylborane product and $[\text{Ru}(\text{H})_2(\text{PMe}_3)_4]$, **58** (Scheme 1.16).

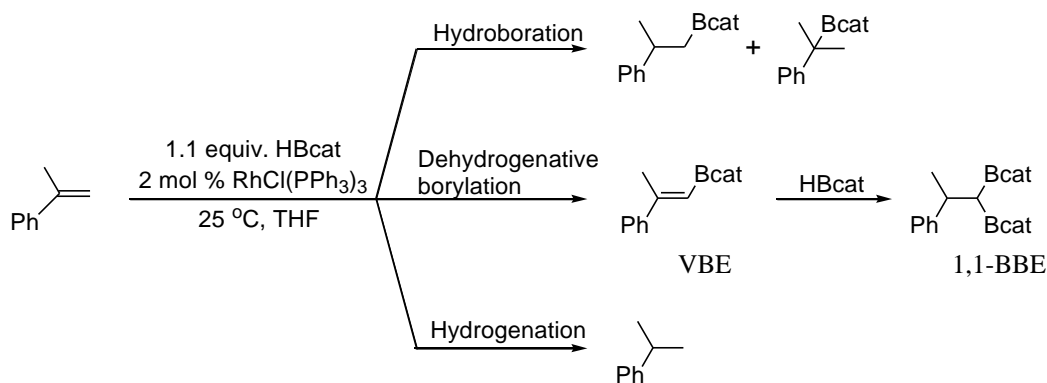
The same group observed the formation of VBE products in their study of the stoichiometric insertion of olefins into Rh-B bonds.²³⁶ Analysis of the reaction of $[\text{RhCl}(\text{Bcat})_2(\text{PPh}_3)_2]$ with 2 equivalents of 4-vinylanisole in CD_2Cl_2 by ^1H NMR spectroscopy showed the formation of VBE, 1,2-bis(boronate ester) (1,2-BBE) and internal hydroboration products in a 2:3:2 ratio, and trace amounts of the terminal hydroboration product.

VBEs were observed as side products in the catalytic diborations of olefins with B_2cat_2 and 1 mol % of $[RhCl(PPh_3)_3]$ as catalyst precursor at room temperature²³⁷ and in the catalytic hydroborations of certain allyl silyl ethers with HBcat in the presence of $[RhCl(PPh_3)_3]$ as catalyst.²³⁸



Scheme 1.16 Stoichiometric Ru-mediated formation of vinylboranes reported by Marder, Baker and coworkers.

Marder, Baker and coworkers reported the first example of catalytic dehydrogenative olefin borylation without significant hydrogenation of the substrate.²³⁹ In addition, they reported the dehydrogenative borylation of 1,1-disubstituted olefins. The reaction of α -methylstyrene with 1.1 equivalents of HBcat in the presence of 2 mol % of $[RhCl(PPh_3)_3]$ as a catalyst precursor in THF at room temperature gave VBE and 1,1-BBE (derived from the hydroboration of the VBE product) with a combined selectivity of 80% (53% for VBE and 27% for 1,1-BBE), along with 17% hydroboration and 3% hydrogenation. The pathways are summarised in **Equation 1.40**.



Equation 1.40 Borylation of α -methylstyrene with HBcat catalysed by $[\text{RhCl}(\text{PPh}_3)_3]$ (Wilkinson's catalyst).

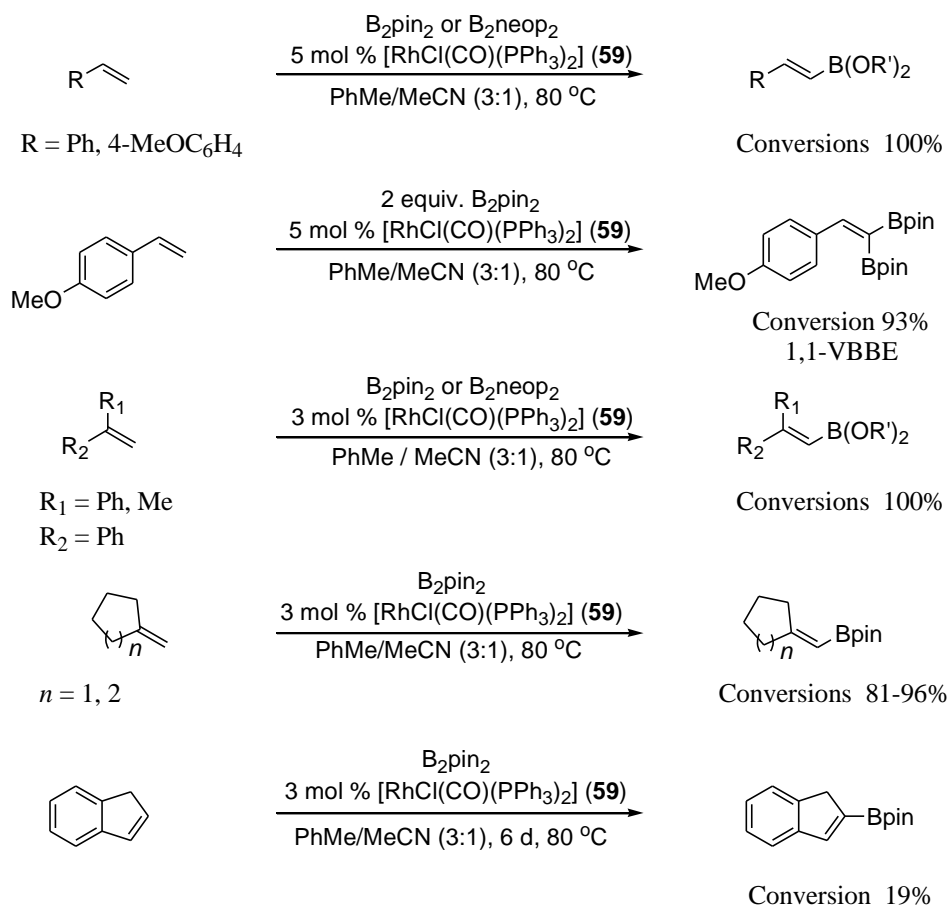
Westcott and coworkers reported several systems for the dehydrogenative borylation of olefins. They showed that the dehydrogenative borylation of aminopropyl vinyl ethers in the presence of $[\text{RhCl}(\text{PPh}_3)_3]$ as a catalyst precursor formed exclusively VBE as the sole boron containing product,²⁴⁰ although the issue of whether sacrificial hydrogenation of the substrate occurred was not explicitly addressed.

1.3.8.5 Dehydrogenative borylation of olefins without sacrificial hydrogenation and/or hydroboration

In 2003, Marder and coworkers reported the dehydrogenative borylation of olefins with B_2pin_2 or B_2neop_2 (neop = neopentane glycolate = $\text{OCH}_2\text{CMe}_2\text{CH}_2\text{O}$) in the presence of 3 mol % of the catalyst precursor *trans*- $[\text{RhCl}(\text{CO})(\text{PPh}_3)_2]$, **59**, at 80 °C without sacrificial hydrogenation of an equivalent of the substrate.²⁴¹ Vinylarenes, such as 4-vinylanisole, along with 1,1-disubstituted olefins, such as α -methylstyrene, diphenylethylene, methylenecyclopentane and methylenecyclohexane, underwent dehydrogenative borylation in the presence of **59** as the catalyst precursor. The selectivity depended on the solvent. Reactions conducted in THF, toluene and 1,4-dioxane yielded complex mixtures of VBEs, hydroboration products, hydrogenation, vinyl-bis(boronate) esters (VBBEs) and saturated bis-boronate esters (BBEs) with 4-vinylanisole as substrate. In contrast,

reactions conducted in neat CH₃CN selectively formed VBEs, but these reactions were slow. Reactions performed in a 3:1 mixture of toluene to CH₃CN selectively formed VBEs with acceptable rates. Reactions conducted with substoichiometric amounts of B₂pin₂ (0.67 equivalents) occurred in up to 100% conversion, showing that both boron moieties of B₂pin₂ can be incorporated into the VBE products with some substrates.

In subsequent work, Marder and coworkers extended the scope of the dehydrogenative borylations catalysed by **59** (Equation 1.41).²⁴² In addition to the diboron reagents B₂pin₂ and B₂neop₂, they found that HBpin was an effective borylating agent; however, reactions with HBpin are slower than reactions conducted with B₂pin₂ or B₂neop₂.



Equation 1.41 Rhodium-catalysed dehydrogenative borylations of olefins by Marder and coworkers.

The relative reactivity of B_2neop_2 vs. B_2pin_2 was found to vary somewhat with substrate, but it appears that 1 equivalent of the former diboron compound is required to effect complete conversions as only one of the two boron moieties can be readily incorporated. This is presumably due to the instability of $HBneop$ formed under the reaction conditions. Using 2 equivalents of B_2pin_2 , and increasing the catalyst loading from 3 to 5 mol % with 4-vinylanisole as substrate, led to the formation of the 1,1-vinyl bis(boronate ester) (1,1-VBBE), i.e., the replacement of both geminal hydrogen atoms on the $=CH_2$ group with boronate moieties in a single catalytic reaction (up to 93% selectivity for VBBE formation). The range of substrates was expanded from the vinyl arenes and 1,1-disubstituted olefins previously studied to include 1-octene and indene. The reaction of 1-octene was rapid, but led to mixtures of the VBBE and VBE in a 2:1 ratio with the VBBE product consisting of several isomers, presumably resulting from double bond isomerization. Of the VBBEs formed, the major component is the 1,1-VBBE isomer (66%), indicating that both geminal olefin hydrogens were replaced. In contrast, the borylation of indene with B_2pin_2 led to selective formation of the VBE, with borylation occurring at the 2-position, but was slow giving only 19% conversion after 6 days at 80 °C. The slow reaction of indene was attributed to an unfavorable β -hydride elimination step due to the difficulty of achieving coplanarity of the Rh and β -hydride moieties, although it is possible that this substrate is borylated *via* a different mechanism from other olefins. No reaction was observed with 2-methyl-2-butene or 3,4,4-trimethyl-2-pentene, suggesting that the system is not effective for dehydrogenative borylation of 1,1,2-trisubstituted olefins.

The reactions could also be conducted at 150 °C in sealed tubes in a microwave reactor giving, in general, fairly similar product distributions to those obtained by conventional heating at 80 °C, but with much shorter reaction periods (minutes vs. days). For 1,1-disubstituted styrenes, conversions were improved when the amount of B_2pin_2 was increased from 0.67 equivalents to 1.0 or 2.0 equivalents. In general, the rate enhancements observed in the microwave reactions were consistent with that expected from the higher temperature employed, and thus do not appear to reflect any special

microwave enhancement, although catalyst lifetimes were somewhat reduced at the higher temperatures.

The origin of the selectivity for VBE formation over diboration/hydroboration and the origins of the beneficial role of MeCN solvent in achieving the highest selectivities remain unclear. Certainly, the system promotes rapid β -hydride elimination following olefin insertion into a Rh-B bond, which must be faster than competing processes that would result in saturated products.

The observed selectivity for the formation of (*E*)-vinyl boronate products was proposed to result from diastereoselective β -hydride elimination from a rhodium β -borylalkyl intermediate. For α -methylstyrene, highly selective borylation of the C-H bond *cis* to the Me group gives rise to a 1,1-disubstituted product that cannot be prepared by alkyne hydroboration. Following a *syn* addition of Rh and boryl groups to the olefin, either of the 2 diastereotopic β -hydrogens may be transferred to Rh. As β -hydride elimination requires a *syn* disposition of rhodium and hydride moieties, rotation around the C-C bond is required. Elimination from the least hindered rotamer (as illustrated for the α -methylstyrene case in **Figure 1.31**) would therefore lead to the observed (*E*)-product. The direction of the insertion of the styrenic substrates into the Rh-B bond generates the more hindered insertion product, placing the large groups α to the metal center. This is presumably a direct consequence of the nucleophilicity of the boryl ligands,²⁴³ which prefer to attack the terminal carbon of the styrenes during the olefin insertion step.

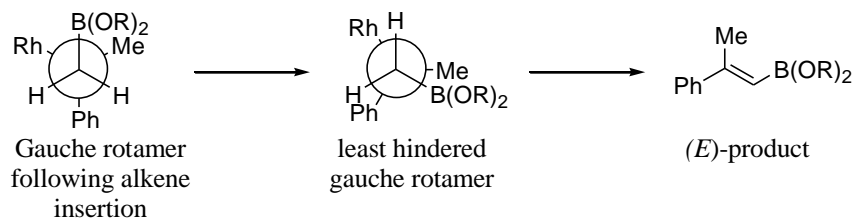


Figure 1.31 Conformation leading to the formation of (*E*)-VBE product.

Westcott and coworkers reported dehydrogenative borylations of a range of vinylarenes in the presence of bulky rhodium diimine complexes as catalysts.²⁴⁴ The reactions of

HBcat, B₂cat₂ and HBpin with vinylarenes catalysed by **60**, **61** and **62** (**Figure 85**) gave complex mixtures of products, but reactions with B₂pin₂ gave predominantly *trans*-VBE products. The borylation of 4-fluorostyrene with B₂pin₂ and an unspecified catalytic amount of **61** in toluene at 80 °C gave a 98% yield of the VBE product along with trace hydrogenation products.

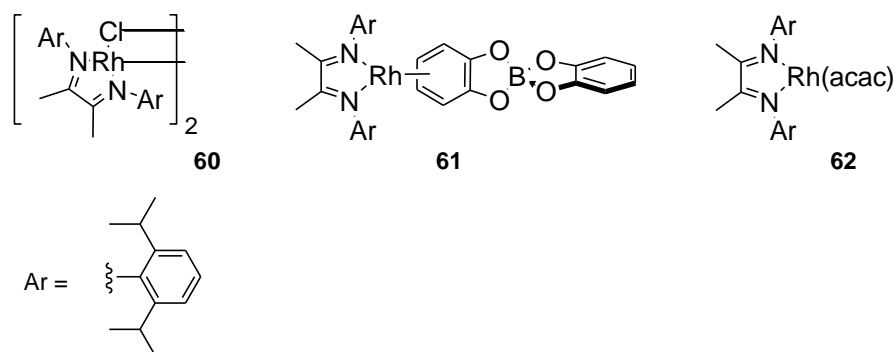
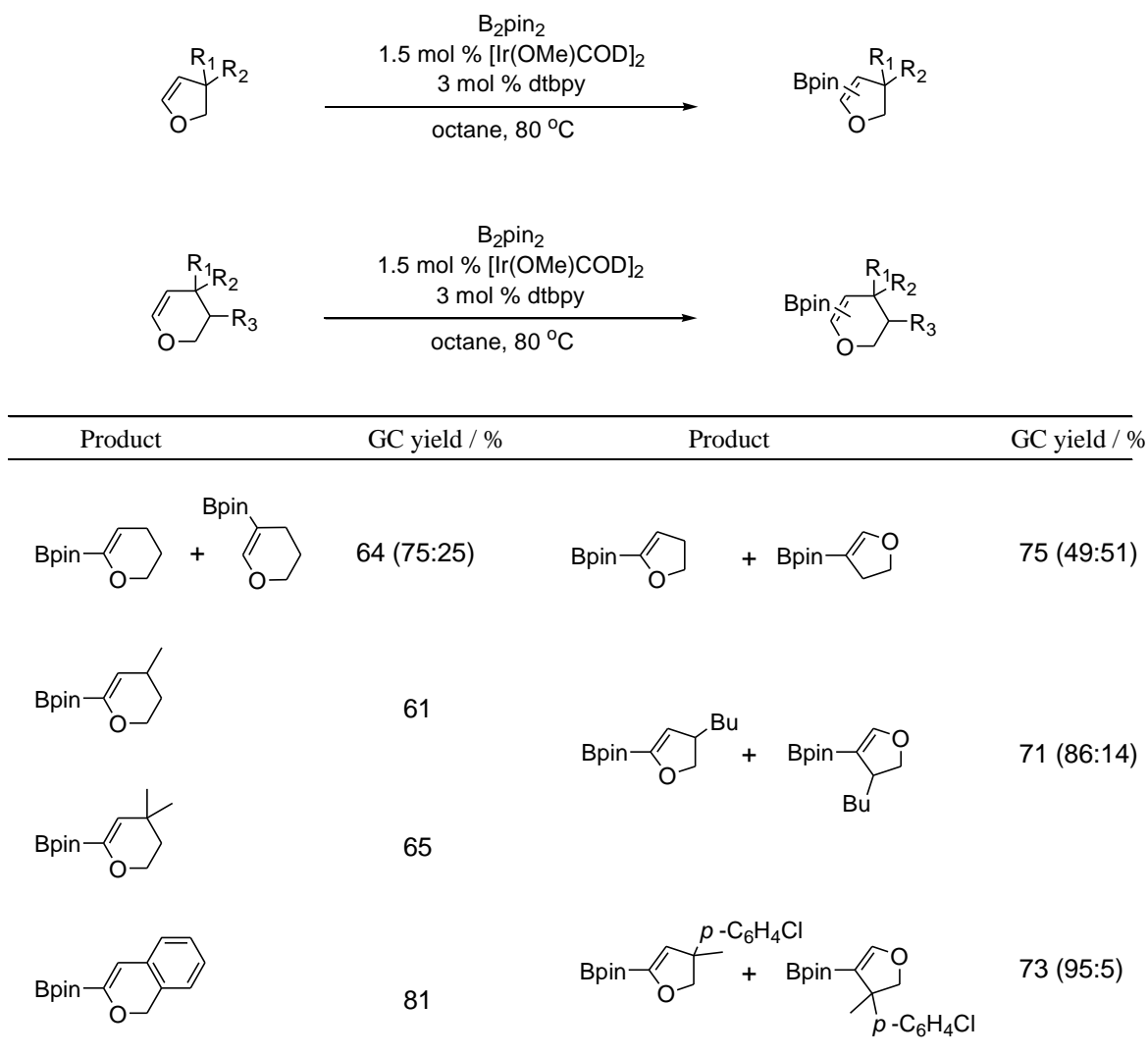


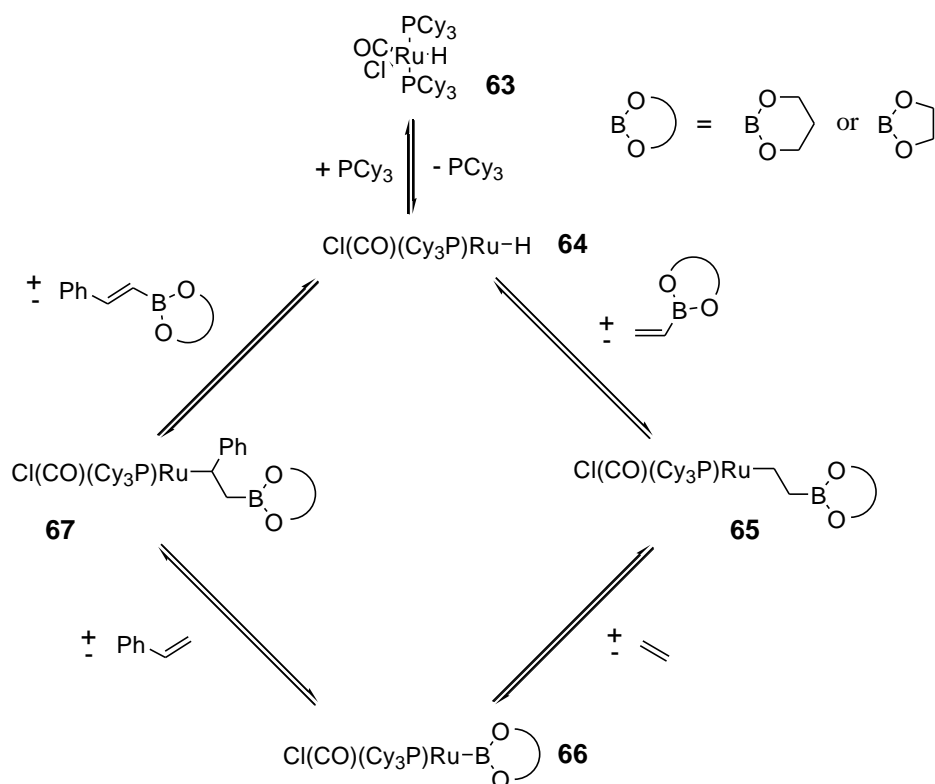
Figure 1.32 Bulky rhodium diimine catalysts for dehydrogenative borylation of olefins by Westcott and coworkers

Miyaura and coworkers reported the borylation of vinyl C-H bonds in cyclic vinyl ethers by B₂pin₂ catalysed by [Ir(OMe)COD]₂ and dtbpy (**Table 1.8**).²⁴⁵ This catalyst has been used widely for the borylation of aromatic C-H bonds, *vide supra*. Borylation of 1,4-dioxene with 0.5 equivalents of B₂pin₂ at room temperature in hexane gave the VBE product in 81% yield. Borylations of dihydropyran and dihydrofuran gave regioisomeric mixtures of α -, and β -borylated products in ratios of 75:25 and 49:51, respectively. The introduction of substituents at the γ -position in dihydropyrans increased the regioselectivity, with borylation occurring solely at the α -position. Borylation of dihydrofurans was less selective; even γ,γ -disubstituted substrates gave products resulting from both α -, and β -borylation. In addition, the borylation of 1*H*-isochromene occurred solely α to oxygen, even in the presence of unhindered aromatic C-H bonds.

Table 1.8 Iridium-catalysed dehydrogenative borylation of cyclic vinyl ethers.

All reactions were carried out at 80 °C for 8 h using B_2pin_2 (1.0 mmol), substrate (3.0 mmol), $[Ir(OMe)COD]_2$ (0.015 mmol), dtbpy (0.03 mmol) in octane in a sealed tube. GC yields based on boron moieties in B_2pin_2 .

Suginome and coworkers have reported a platinum-catalysed dehydrogenative borylation of 1,2-disubstituted olefins tethered to silylboronate groups to give (*E*)-VBEs, in which Si-B and olefinic C-H bonds are transformed into Si-H and C-B bonds, respectively (**Equation 1.42**).²⁴⁶ Silylboronates were synthesised from their corresponding alcohols²⁴⁷ by reaction with $ClPh_2SiBpin$, and were stirred in toluene at 80–100 °C in the presence of 5 mol % $Pt(dba)_3$ and 11 mol % PAR_3 , to give the VBE products in moderate to high yields, with no products arising from intramolecular alkene silylboration²⁴⁸ observed. A mechanism was proposed in which oxidative addition of the Si-B bond to the Pt^0 center



Scheme 1.17 Ruthenium-catalysed transfer borylation of vinylarenes by Pietraszuk and coworkers.

The mechanism of the above process was also examined via DFT calculations.²⁵⁰

The energetics of the reversibility of the boryl ligand migration (olefin insertion into a metal-boryl bond) was explored, and the β -boryl elimination process was calculated to have a low barrier. It was concluded that the “empty” p orbital on boron of the boryl ligand was not important in either the boryl migration or β -boryl elimination processes, but that the high nucleophilicity of the Ru-boryl σ -bond promotes the boryl migration.

References for 1.1 Retinoids

¹ Sporn, M. B.; Roberts, A. B.; Goodman, D. S. *The Retinoids*. 2 ed.; Academic press: Orlando, **1984**.

² Ross, S. A.; McCaffery, P. J.; Drager, U. C.; De Luca, L. M. *Physiol. Rev.* **2000**, *80*, 1021-1054.

³ Wald, G., *Nature* **1968**, *219*, 800-807.

- ⁴ Napoli, J. L. *Clin. Immunol. Immunopathol.* **1996**, *80*, S52-62.
- ⁵ Lowe, N.; Marks, R. *Retinoids: a Clinicians Guide*. 2 ed.; Informa Healthcare: London, **1997**.
- ⁶ Soprano, D. R.; Qin, P.; Soprano, K. J. *Annu. Rev. Nutr.* **2004**, *24*, 201-221.
- ⁷ Freemantle, S. J.; Dragnev, K. H.; Dmitrovsky, E. *J. Natl. Cancer Inst.* **2006**, *98*, 426-427.
- ⁸ Murayama, A.; Suzuki, T.; Matsui, M. *J. Nutr. Sci. Vitaminol.* **1997**, *43*, 167-176..
- ⁹ Bempong, D. K.; Honigberg, I. L.; Meltzer, M. N. *J. Pharm. Biomed. Anal.* **1995**, *13*, 285-291
- ¹⁰ Suzuki, T.; Rao Kunchala, S.; Matsui, M.; Murayama, A. *J. Nutr. Sci. Vitaminol.* **1998**, *43*, 729-736.
- ¹¹ Kunchala, S. R.; Suzuki T.; Murayama, A. *Ind. J. Biochem. Biophys.* **2000**, *37*, 71-76.
- ¹² Christie, V. B.; Barnard, J. H.; Batsanov, A. S.; Bridgens, C. E.; Cartmell, E. B.; Collings, J. C.; Maltman, D. J.; Redfern, C. P. F.; Marder, T. B.; Przyborski, S. A.; Whiting, A. *Org. Bio. Chem.* **2008**, *6*, 3497-3507
- ¹³ Quadro, L.; Hamberger, L.; Colantuoni, V.; Gottesman, M. E.; Blaner W. S. *Mol. Aspects Med.* **2003**, *24*, 421-430.
- ¹⁴ Blaner, W. S.; Olson, J. A. Retinol and retinoic acid metabolism. In *The Retinoids, Biology, Chemistry and Medicine*, Sporn, M. B.; Roberts, A. B.; Goodman, D. S., Eds. Raven Press: New York, **1994**; pp 229-256.
- ¹⁵ Chen, H.; Howald, W. N.; Juchau, M. R. *Drug Metab. Dispos.* **2000**, *28*, 315-322.
- ¹⁶ Dong, D.; Ruuska, S. E.; Levinthal, D. J.; Noy, N. *J. Biol. Chem.* **1999**, *274*, 23695-23698.
- ¹⁷ Marill, J.;_Capron, C. C.; Idres, N.; Chabo, G. G. *Biochem. Pharmacol.* **2002**, *63*, 933-943.
- ¹⁸ Mangelsdorf, D. J.; Thummel, C.; Beato, M.; Herrlich, P.; Schütz, G.; Umesono, K.; Blumberg, B.; Kastner, P.; Mark, M.; Chambon, P.; Evans, R. M. *Cell*, **1995**, *83*, 835-839.
- ¹⁹ Chung, A. C.-K.; Cooney, A. J. Retinoid Receptors. In *The Nuclear Receptors and Genetic Disease*, Academic Press: San Diego, **2001**; pp 245-295.

- ²⁰ Géhin, M.; Vivat, V.; Wurtz, J.-M.; Losson, R.; Chambon, P.; Moras, D.; Gronemeyer, H. *Chem. Biol.* **1999**, *6*, 519-529.
- ²¹ Ostrowski, J.; Roalsvig, T.; Hammer, L.; Marinier, A.; Starrett Jr., J. E.; Yu, K.-L.; Reczek, P. R. *J. Biol. Chem.* **1998**, *273*, 3490-3495.
- ²² Yu, V. C.; Delsert, C.; Anderson, B.; Holloway, J. M.; Devary, O. V.; Näär, A. M.; Kim, S. Y.; Boutin, J.-M.; Glass, C. K.; Rosenfeld, M. G. *Cell* **1991**, *67*, 1251-1266.
- ²³ Mangelsdorf, D. J.; Evans, R. M. *Cell*, **1995**, *83*, 841-850.
- ²⁴ Kliewer, S. A.; Umeseno, K.; Noonan, D. J.; Heymann, R. A.; Evans, R. *Nature*, **1992**, *358*, 771-774.
- ²⁵ Wang, K.; Chen, S.; Xie, W.; Yvonne Wan, Y.-J. *Biochem. Pharmacol.* **2008**, *75*, 2204-2213.
- ²⁶ (a) Allegretto, E. A.; McClurg, M. R.; Lazarchik, S. B.; Clemm, D. L.; Kerner, S. A.; Elgort, M. G.; Boehm, M. F.; White, S. K.; Pike, J. W.; Heyman, R. A. *J. Biol. Chem.* **1993**, *268*, 26625-26633; (b) Allenby, G.; Bocquel, M. T.; Saunders, M.; Kazmer, S.; Speck, J.; Rosenberger, M.; Lovey, A.; Kastner, P.; Grippo, J. F.; Chambon, P.; Levin, A. A. *Proc. Natl. Acad. Sci. U.S.A.* **1993**, *90*, 30-34.
- ²⁷ (a) Zhang, X.-K.; Lehmann, J.; Hoffmann, B.; Dawson, M. I.; Cameron, J.; Graupner, G.; Hermann, T.; Tran, P.; Pfahl, M. *Nature* **1992**, *358*, 587-591; (b) Egea, P. F.; Mitschler, A.; Moras, D. *Mol. Endocrinol.* **2002**, *16*, 987-997.
- ²⁸ (a) Germain, P.; Kammerer, S.; Perez, E.; Peluso-Iltis, C.; Tortolani, D.; Zusi, F. C.; Starrett, J.; Lapointe, P.; Daris, J.-P.; Marinier, A.; de Lera, A. R.; Rochel, N.; Gronemeyer, H. *EMBO Rep.* **2004**, *5*, 877-882; (b) Renaud, J.-P.; Rochel, N.; Ruff, M.; Vivat, V.; Chambon, P.; Gronemeyer, H.; Moras, D. *Nature* **1995**, *378*, 681-689.
- ²⁹ Bourguet, W.; Ruff, M.; Chambon, P.; Gronemeyer, H.; Moras, D. *Nature* **1995**, *375*, 377-382.
- ³⁰ Bourguet, W.; Vivat, V.; Wurtz, J.-M.; Chambon, P.; Gronemeyer, H.; Moras, D. *Mol. Cell* **2000**, *5*, 289-298.
- ³¹ Klaholz, B. P.; Renaud, J.-P.; Mitschler, A.; Zusi, C.; Chambon, P.; Gronemeyer, H.; Moras, D. *Nat. Struct. Biol.* **1998**, *5*, 199-202.
- ³² Forman, B. M.; Umesono, K.; Chen, J.; Evans, R. M., *Cell* **1995**, *81*, 541-550.

- ³³ La Vista-Picard, N.; Hobbs, P. D. P., M.; Dawson, M. I.; Pfahl, M. *Mol. Cell Biol.* **1996**, *16*, 4137-4146.
- ³⁴ Leblanc, B. P.; Stunnenberg, H. G. *Genes Dev.* **1995**, *9*, 1811-1816.
- ³⁵ Schulman, I. G.; Shao, G.; Heyman, R. A. *Mol. Cell Biol.* **1998**, *18*, 3483-3494.
- ³⁶ Blumberg, B. *Semin. Cell Dev. Biol.* **1997**, *8*, 417-428.
- ³⁷ Rees, J. *Br. J. Dermatol.* **1992**, *126*, 97-104.
- ³⁸ (a) Raelson, J. V.; Nervi, C.; Rosenauer, A.; Benedetti, L.; Monczak, Y.; Pearson, M.; Pelicci, P. G.; Miller, W. H. Jr. *Blood* **1996**, *88*, 2826-2832; (b) Mandelli, F.; Diverio, D.; Avvisati, G.; Luciano, A.; Barbui, T.; Bernasconi, C.; Broccia, G.; Cerri, R.; Falda, M.; Fioritoni, G.; Leoni, F.; Liso, V.; Petti, M. C.; Rodeghiero, F.; Saglio, G. Vegna, M. L.; Visani, G.; Jehn, U.; Willemze, R.; Muus, P.; Pelicci, P. G.; Biondi, A.; Lo Coco, F. *Blood* **1997**, *90*, 1014-1021.
- ³⁹ Standeven, A. M.; Beard, R. L.; Johnson, A. T.; Boehm, M. F.; Escobar, M.; Heyman, R. A.; Chandraratna, R. A. S. *Fund. Appl. Toxicol.* **1996**, *33*, 264-271.
- ⁴⁰ (a) Seewaldt, V. L.; Johnson, B. S.; Parker, M. B.; Collins, S. J.; Swisshelm, K. *Cell Growth Differ.* **1995**, *6*, 1077-1088; (b) Si, S. P.; Lee, X.; Tsou, H. C.; Buchsbaum, R.; Tibaduiza, E.; Peacocke, M. *Exp. Cell Res.* **1996**, *223*, 102-111; (c) Xu, X. C.; Sneige, N.; Liu, X.; Nandagiri, R.; Lee, J. J.; Lukmanji, F.; Hortobagyi, G.; Lippman, S. M.; Dhingra, K.; Lotan, R. *Cancer Res.* **1997**, *57*, 4992-4996.
- ⁴¹ Nagpal, S.; Chandraratna, R. A. S. *Curr. Pharm. Design* **1996**, *2*, 295-316.
- ⁴² Elder, J. T.; Fischer, G. J.; Zhang, Q.-Y.; Eisen, D.; Krust, A.; Kastner, P.; Chambon, P.; Voorhees, J. J. *J. Invest. Dermatol.* **1991**, *96*, 425-433.
- ⁴³ Wang, Z.; Boudjelal, M.; Kang, S.; Voorhees, J. J.; Fisher, G. J. *Nat. Med.* **1999**, *5*, 418-422.
- ⁴⁴ (a) Nagpal, S.; Thacher, S. M.; Patel, S.; Friant, S.; Malhotra, M.; Shafer, J.; Krasinski, G.; Asano, A. T.; Teng, M.; Duvic, M.; Chandraratna, R. A. S. *Cell Growth Differ.* **1996**, *7*, 1783-1791; (b) Fisher, G. J.; Voorhees, J. J., *FASEB J.* **1996**, *10*, 1002-1013.
- ⁴⁵ Spanjaard, R. A.; Ikeda, M.; Lee, P. J.; Charpentier, B.; Chin, W. W.; Eberlein, T. J. *J. Biol. Chem.* **1997**, *272*, 18990-18999.
- ⁴⁶ Wurtz, J.-M.; Bourguet, W.; Renaud, J.-P.; Vivat, V.; Chambon, P.; Moras, D.; Gronemeyer, H. *Nature Struct. Biol.* **1996**, *3*, 87-94.

- ⁴⁷ Kagechika, H.; Kawachi, E.; Hashimoto, Y.; Shudo, K.; Himi, T. *J. Med. Chem.* **1988**, *31*, 2182-2192.
- ⁴⁸ Teng, M.; Duong, T. T.; Klein, E. S.; Pino, M. E.; Chandraratna, R. A. S. *J. Med. Chem.* **1996**, *39*, 3035-3038.
- ⁴⁹ Yamakawa, a, T.; Kagechika, H.; Kawachi, E.; Hashimoto, Y.; Shudo, K. *J. Med. Chem.* **1990**, *33*, 1430-1437.
- ⁵⁰ (a) P. Loeliger (Inventor), Hoffmann-La Roche & Co AG, Basel, Switzerland, Ger. Offen. DE 2854354 A1, July 5, **1979**; (b) Loeliger, P.; Loeliger, P.; Bollag, W.; Mayer, H. *Eur. J. Med. Chem. Chim. Ther.* **1980**, *15*, 9-15; (c) Lotan, R.; Stolarsky, T.; Lotan, D. *J. Nutr. Growth Cancer* **1983**, *1*, 71-76; (d) Dawson, M. I.; Hobbs, P. D.; Derdzinski, K.; Chan, R. L. S.; Gruber, J.; Chao, W.; Smith, S.; Thies, R. W.; Schiff, L. J. *J. Med. Chem.* **1984**, *27*, 1516-1531; (e) Minucci, S.; Saint-Jeannet, J.-P.; Toyama, R.; Scita, G.; DeLuca, L. M.; Taira, M.; Levin, A. A.; Ozato, K.; Dawid, I. B. *Proc. Natl. Acad. Sci. USA* **1996**, *93*, 1803-1807; (f) Standeven, A. M.; Johnson, A. T.; Escobar, M.; Chandraratna, R. A. S. *Toxicol. Appl. Pharmacol.* **1996**, *138*, 169-175; (g) Standeven, A. M.; Teng, M.; Chandraratna, R. A. S. *Toxicol. Lett.* **1997**, *92*, 231-240; (h) Wu, K.; Kim, H.-T.; Rodriguez, J. L.; Hilsenbeck, S. G.; Mohsin, S. K.; Xu, X.-C.; Lamph, W. W.; Kuhn, J. G.; Green, J. E.; Brown, P. H. *Cancer Epidemiol. Biomarkers Prev.* **2002**, *11*, 467-474; (i) Pignatello, M. A.; Kauffman, F. C.; Levin, A. A. *Toxicol. Appl. Pharmacol.* **2002**, *178*, 186-194; (j) Gardiner, D.; Ndayibagira, A.; Grün, F.; Blumberg, B. *Pure Appl. Chem.* **2003**, *75*, 2263-2273; (k) Pogenberg, V.; Guichou, J.-F.; Vivat-Hannah, V.; Kammerer, S.; Pérez, E.; Germain, P.; de Lera, A. R.; Gronemeyer, H.; Royer, C. A.; Bourguet, W. *J. Biol. Chem.* **2005**, *280*, 1625-1633; (l) Simoni, D.; Roberti, M.; Invidiata, F. P.; Rondanin, R.; Baruchello, R.; Malagutti, C.; Mazzali, A.; Rossi, M.; Grimaudo, S.; Dusonchet, L.; Meli, M.; Raimondi, M. V.; D'Alessandro, N.; Tolomeo, M. *Bioorg. Med. Chem. Lett.* **2000**, *10*, 2669-2673.
- ⁵¹ Johnson, A. T.; Klein, E. S.; Wang, L.; Pino, M. E.; Chandraratna, R. A. S. *J. Med. Chem.* **1996**, *39*, 5027-5130.
- ⁵² (a) Lund, B. W.; Piu, F.; Gauthier, N. K.; Eeg, A.; Currier, E.; Sherbukhin, V.; Brann, M. R.; Hacksell, U.; Olsson, R. *J. Med. Chem.* **2005**, *48*, 7517-7519; (b) Amaranatha Reddy, R.; Sadashiva, B. K. *J. Mater. Chem.* **2004**, *14*, 310-319.

- ⁵³ (a) Gelman, L.; Zhou, G.; Fajas, L.; Raspé, E.; Fruchart, J.-C.; Auwerx, J. *J. Biol. Chem.* **1999**, *274*, 7681-7688; (b) Benecke, A.; Champon, P.; Gronemeyer, H. *EMBO Rep.* **2000**, *1*, 151-157.
- ⁵⁴ (a) Nagpal, S.; Saunders, M.; Kastner, P.; Durand, B.; Nakshatri, H.; Champon, P. *Cell* **1992**, *70*, 1007; (b) Nagpal, S.; Friant, S.; Nakshatri, H.; Chambon, P. *EMBO J.* **1993**, *12*, 2349-2360.
- ⁵⁵ Klaholz, B. P.; Mitschler, A.; Belema, M.; Zusi, C.; Moras, D. *Proc. Natl. Acad. Sci. USA*, **2000**, *97*, 6322-6327.
- ⁵⁶ Klaholz, B. P.; Mitschler, A.; Moras, D. *J. Mol. Biol.* **2000**, *302*, 155-170.
- ⁵⁷ Bernard, B. A.; Bernardon, J. M.; Delescluse, C.; Martin, B.; Lenoir, M.-C.; Maignan, J.; Charpentier, B.; Pilgrim, W.R.; Reichert, U.; Shroot, B. *Biochem. Biophys. Res. Comm.*, **1992**, *186*, 977-983.
- ⁵⁷ (a) Mangelsdorf, D. J.; Ong, E. S.; Dyck, J. A.; Evans, R. M. *Nature* **1990**, *345*, 224-229; (b) Mangelsdorf, D. J.; Borgmeyer, U.; Heyman, R. A.; Zhou, J. Y.; Ong, E. S.; Oro, A. E.; Kakizuka, A.; Evans, R. M. *Genes Dev.* **1992**, *6*, 329-344; (c) Dollé, P.; Fraulob, V.; Kastner, P.; Chambon, P. *Mech. Dev.* **1994**, *45*, 91-104. (d) Hamada, K.; Gleason, S. L.; Levi, B. Z.; Hirschfeld, S.; Appella, E.; Ozato, K. *Proc. Natl. Acad. Sci. USA*, **1989**, *86*, 8289-8293; (e) Haugen, B. R.; Brown, N. S.; Wood, W. M.; Gordon, D. F.; Ridgway, E. C. *Mol. Endocrinol.* **1997**, *11*, 481-489; (f) Chiang, M. Y.; Misner, D.; Kempermann, G.; Schikorski, T.; Giguère, V.; Sucov, H. M.; Gage, F. H.; Stevens, C. F.; Evans, R. M. *Neuron* **1998**, *21*, 1353-1361.
- ⁵⁹ Germain, P.; Chambon, P.; Eichele, G.; Evans, R. M.; Lazar, M. A.; Leid, M.; de Lera, A. R.; Lotan, R.; Mangelsdorf, D. J.; Gronemeyer, H. *Pharmacol. Rev.* **2006**, *58*, 760-772.
- ⁶⁰ Love, J. D.; Gooch, J. T.; Benko, S.; Li, C.; Nagy, L.; Chatterjee, V. K. K.; Evans, R. M.; Schwabe, J. W. R. *J. Biol. Chem.* **2002**, *277*, 11385-11391.
- ⁶¹ (a) Beard, R. L.; Gil, D. W.; Marler, D. K.; Henry, E.; Colon, D. F.; Gillett, S. J.; Arefieg, T.; Breen, T. S.; Krauss, H.; Davies, P. J. A.; Chandraratna, R. A. S. *Bioorg. Med. Chem. Lett.* **1994**, *4*, 1447-1452; (b) Gambone, C. J.; Hutcheson, J. M.; Gabriel, J. L.; Beard, R. L.; Chandraratna, R. A. S.; Soprano, K. J.; Soprano, D. R. *Mol. Pharmacol.* **2002**, *61*, 334-342; (c) Strickland, S.; Breitman, T. R.; Frickel, F.; Nürrenbach, A.;

Hädicke, E.; Sporn, M. B. *Cancer Res.* **1983**, *43*, 5268-5272; (d) Boehm, M. F.; McClurg, M. R.; Pathirana, C.; Mangelsdorf, D.; White, S. K.; Hebert, J.; Winn, D.; Goldman, M. E.; Heyman, R. *J. Med. Chem.* **1994**, *37*, 408-414; (e) Beard, R. L.; Chandraratna, R. A. S.; Colon, D. F.; Gillett, S. J.; Henry, E.; Marler, D. K.; Song, T.; Denys, L.; Garst, M. E.; Arefieg, T.; Klein, E.; Gil, D. W.; Wheeler, L.; Kochhar, D. M.; Davies, P. J. A. *J. Med. Chem.* **1995**, *38*, 2820-2829; (f) Beard, R. L.; Colon, D. F.; Klein, E. S.; Vorse, K. A.; Chandraratna, R. A. S. *Bioorg. Med. Chem. Lett.* **1995**, *5*, 2729-2734; (g) Totpal, K.; Chaturvedi, M. M.; LaPushin, R.; Aggarwal, B. B. *Blood* **1995**, *85*, 3547-3555; (h) Islam, T. C.; Skarin, T.; Sumitran, S.; Toftgård, R. *Br. J. Dermatol.* **2000**, *143*, 709-719.

⁶² Lehmann, J. M.; Jong, L.; Fanjul, A.; Cameron, J. F.; Lu, X. P.; Haefner, P.; Dawson, M. I.; Pfahl, M. *Science* **1992**, *258*, 1944-1946.

⁶³ Boehm, M. F.; Zhang, L.; Zhi, L.; McClurg, M. R.; Berger, E.; Wagoner, M.; Mais, D. E.; Suto, C. M.; Davies, P., J. A.; Heyman, R. A.; Nadzan, A. M. *J. Med. Chem.* **1995**, *38*, 3146-3155.

⁶⁴ Boehm, M. F.; Zhang, L.; Badea, B. A.; White, S. K.; Mais, D. E.; Berger, E.; Suto, C. M.; Goldman, M. E.; Heyman, R. A. *J. Med. Chem.* **1994**, *37*, 2930-2941.

⁶⁵ (a) Roberts, A. B.; Nichols, M. D.; Newton, D. L.; Sporn, M. B. *J. Biol. Chem.* **1979**, *254*, 6296-6302; (b) Frolik, C. A. Metabolism of retinoids, in *The Retinoids*, Vol. 2, Sporn, M. B. and Goodman, D. S. Eds., Academic Press: New York, **1984**, 177. (c) McCormick, A. M.; Napoli, J. L.; Schnoes, H. K.; de Luca, H. F. *Biochemistry* **1978**, *17*, 4085-4090.

⁶⁶ Dawson, M. I.; Chan, R. L.; Derdzinski, K.; Hobbs, P. D.; Chao, W. R.; Schiff, L. J. *J. Med. Chem.* **1983**, *26*, 1653-1656.

⁶⁷ (a) Clamon, G. H.; Sporn, M. B.; Smith, J. M.; Saffioti, U. *Nature* **1974**, *250*, 64; (b) Sporn, M. B.; Clamon, G. H.; Dunlop, N. M.; Newton, D. L.; Smith, J. M.; Saffioti, U. *Nature* **1975**, *253*, 47-50; (c) Sporn, M. B.; Dunlop, N. M.; Newton, D. L.; Henderson, W. R. *Nature* **1976**, *263*, 110-113.

⁶⁸ Schiff, L. J.; Okamura, W. H.; Dawson, M. I.; Hobbs, P. D. Structure-Biological Activity Relationships of New Synthetic Retinoids on Epithelial Differentiation of

Cultured Hamster Trachea, in *Chemistry and Biology of Synthetic Retinoids*. CRC Press: Boca Raton, FL, **1990**, 307–363.

⁶⁹ Spruce, L. W.; Gale, J. B.; Berlin, K. D.; Verma, A. K.; Breitman, T. R.; Ji, X.; van der Helm, D. *J. Med. Chem.* **1991**, *34*, 430-439.

⁷⁰ (a) Benbrook, D. M.; Madler, M. M.; Spruce, L. W.; Birckbichler, P. J.; Nelson, E. C.; Subramanian, S.; Weerasekare, G. M.; Gale, J. B.; Patterson Jr., M. K.; Wang, B.; Wang, W.; Lu, S.; Rowland, T. C.; DiSilvestro, P.; Lindamood III, C.; Hill, D. L.; Berlin, K. D. *J. Med. Chem.* **1997**, *40*, 3567-3583; (b) Spruce, L. W.; Rajadhyaksha, S. N.; Berlin, K. D.; Gale, J. B.; Miranda, E. T.; Ford, W. T.; Blosssey, E. C.; Verma, A. K.; Hossain, M. B.; van der Helm, D.; Breitman, T. R. *J. Med. Chem.* **1987**, *30*, 1474-1482; (c) Waugh, K. M.; Berlin, K. D.; Ford, W. T.; Holt, E. M.; Carrol, J. P.; Schomber, P. R.; Thompson, M. D.; Schiff, L. J. *J. Med. Chem.* **1985**, *28*, 116-124.

⁷¹ Benbrook, D. M.; Subramanian, S.; Gale, J. B.; Liu, S.; Brown, C. W.; Boehm, M. F.; Berlin, K. D. *J. Med. Chem.* **1998**, *41*, 3753-3757.

⁷² Büttner, M. W.; Burschka, C.; Daiss, J. O.; Ivanova, D.; Rochel, N.; Kammerer, S.; Peluso-Iltis, C.; Bindler, A.; Gaudon, C.; Germain, P.; Moras, D.; Gronemeyer, H.; Tacke, R. *ChemBioChem.* **2007**, *8*, 1688-1699.

⁷³ Daiss, J. O.; Burschka, C.; Mills, J. S.; Montana, J. G.; Showell, G. A.; Fleming, I.; Gaudon, C.; Ivanova, D.; Gronemeyer, H.; Tacke, R. *Organometallics*, **2005**, *24*, 3192-3199.

⁷⁴ Sussman, F.; de Lera, A. R. *J. Med. Chem.* **2005**, *48*, 6212-6219.

⁷⁵ Williams, J. B.; Napoli, J. L. *Proc. Natl. Acad. Sci. USA*, **1985**, *82*, 4658-4662.

⁷⁶ Dawson, M. I.; Hobbs, P. D.; Derdzinski, K. A.; Chao, W.-R.; Frenking, G.; Loew, G. H.; Jetten, A. M.; Napoli, J. L.; Williams, J. B.; Sani, B. P.; Wille Jr. J. J.; Schiff, L. J. *J. Med. Chem.* **1989**, *32*, 1504-1517.

⁷⁷ Kurihara, M.; Rouf, A. S. S.; Kansui, H.; Kagechika, H.; Okuda, H.; Miyata, N. *Bioorg. Med. Chem. Lett.* **2004**, *14*, 4131-4134.

⁷⁸ Canan Koch, S. S.; Dardashti, L. J.; Hebert, J. J.; White, S. K.; Croston, G. E.; Flatten, K. S.; Heyman, R. A.; Nadzan, A. M. *J. Med. Chem.* **1996**, *39*, 3229-3234.

⁷⁹ Vuligonda, V.; Thacher, S. M.; Chandraratna, R. A. S. *J. Med. Chem.* **2001**, *44*, 2298-2303.

- ⁸⁰ Farmer, L. J.; Lin, Z.; Jeong, S.; Kallel, E. A.; Croston, G.; Flatten, K. S.; Heyman, R. A.; Nadzan, A. M. *Bioorg. Med. Chem. Lett.* **1997**, *7*, 2747-2752.
- ⁸¹ Canan Koch, S. S.; Dardashti, L. J.; Cesario, R. M.; Croston, G. E.; Boehm, M. F.; Heyman, R. A.; Nadzan, A. M. *J. Med. Chem.* **1999**, *42*, 742-750.
- ⁸² Takahashi, B.; Ohta, K.; Kawachi, E.; Fukusawa, H.; Hashimoto, Y.; Kagechika, H. *J. Med. Chem.* **2002**, *45*, 3327-3330.

References for 1.2 Palladium-catalysed cross-couplings

- ⁸³ Miyaura, N.; Suzuki, A. *Chem. Rev.* **1995**, *95*, 2457-2483.
- ⁸⁴ Stille, J. K. *Angew. Chem. Int. Ed.* **1986**, *25*, 508-524.
- ⁸⁵ King, A. O.; Okukado, N.; Negeshi, E. *Chem. Commun.* **1977**, 683-684.
- ⁸⁶ Sonogashira, K.; Tohda, Y.; Hagihara, N. *Tetrahedron Lett.* **1975**, *50*, 4467-4470.
- ⁸⁷ Hatanaka, Y.; Hiyama, T. *J. Org. Chem.* **1988**, *53*, 918-920.
- ⁸⁸ (a) Christmann, U.; Vilar, R. *Angew. Chem. Int. Ed.* **2005**, *44*, 366-374; (b) Lewis, A. K. D.; Caddick, S.; Cloke, F. G. N.; Billingham, N. C.; Hitchcock, P. B.; Leonard, J. *J. Am. Chem. Soc.* **2003**, *125*, 10066-10073; (c) Caddick, S.; Geoffrey, F.; Cloke, N.; Hitchcock, P. B.; Leonard, J.; Lewis, A. K. D.; McKerrecher, D.; Titcomb, L. R. *Organometallics* **2002**, *21*, 4318-4319; (d) Stauffer, S. R.; Lee, S. W.; Stambuli, J. P.; Hauck, S. I.; Hartwig, J. F. *Org. Lett.* **2000**, *2*, 1423-1426; (e) Alcazar-Roman, L. M.; Hartwig, J. F. *J. Am. Chem. Soc.* **2001**, *123*, 12905-12906; (f) Jutand, A.; Mosleh, A. *Organometallics* **1995**, *14*, 1810-1817; (g) Strieter, E. R.; Blackmond, D. G.; Buchwald, S. L. *J. Am. Chem. Soc.* **2003**, *125*, 13978-13980; (h) Shen, Q.; Shekhar, S.; Stambuli, J. P.; Hartwig, J. F. *Angew. Chem. Int. Ed.* **2005**, *44*, 1371-1375; (i) Andreu, M. G.; Zapf, A.; Beller, M. *Chem. Commun.* **2000**, 2475-2476.
- ⁸⁹ (a) Amatore, C.; Azzabi, M.; Jutand, A. *J. Am. Chem. Soc.* **1991**, *113*, 1670-1677; (b) Amatore, C.; Jutand, A.; Suarez, A. *J. Am. Chem. Soc.* **1993**, *115*, 9531-9541.
- ⁹⁰ (a) Fauvarque, J.-F.; Pflüger, F.; Troupel, M. *J. Organomet. Chem.* **1981**, *208*, 419-427; (b) Amatore, C.; Pflüger, F. *Organometallics* **1990**, *9*, 2276-2282.
- ⁹¹ Fitton, P.; Rick, E. A. *J. Organomet. Chem.* **1971**, *28*, 287-291.
- ⁹² Cassado, A. L.; Espinet, P. *Organometallics* **1998**, *17*, 954-959.

- ⁹³ (a) Paul, F.; Patt, J.; Hartwig, J. F. *J. Am. Chem. Soc.* **1994**, *116*, 5969-5970; (b) Hartwig, J. F.; Paul, F. *J. Am. Chem. Soc.* **1995**, *117*, 5373-5374; (c) Stambuli, J. P.; Bühl, M.; Hartwig, J. F. *J. Am. Chem. Soc.* **2002**, *124*, 9346-9347;
- ⁹⁴ Littke, A. F.; Dai, C.; Fu, G. C. *J. Am. Chem. Soc.* **2000**, *122*, 4020-4028.
- ⁹⁵ (a) Roy, A. H.; Hartwig, J. F. *J. Am. Chem. Soc.* **2001**, *123*, 1232-1233; (b) Roy, A. H.; Hartwig, J. F. *J. Am. Chem. Soc.* **2003**, *125*, 13944-133945; (c) Roy, A. H.; Hartwig, J. F. *Organometallics* **2004**, *23*, 1533-1542.
- ⁹⁶ Galardon, E.; Ramdeehul, S.; Brown, J. M.; Cowley, A.; Hii, K. K.; Jutand, A. *Angew. Chem. Int. Ed.* **2002**, *41*, 1760-1763.
- ⁹⁷ Hartwig, J. F.; Barrios-Landeros, F. *J. Am. Chem. Soc.* **2005**, *127*, 6944-6945.
- ⁹⁸ Lam, K. C.; Marder, T. B.; Lin, Z. *Organometallics* **2007**, *26*, 758-760.
- ⁹⁹ Amatore, C.; Jutand, A.; Khalil, F.; M'Barki, M. A.; Mottier, L. *Organometallics* **1993**, *12*, 3168-3178.
- ¹⁰⁰ (a) Fairlamb, I. J. S.; Kapdi, A. R.; Lee, A. F. *Org. Lett.* **2004**, *6*, 4435-4438; (b) Fairlamb, I. J. S.; Kapdi, A. R.; Lee, A. F.; McGlacken, G. P.; Weissburger, F.; de Vries, A. H. M.; de Vondervoort, L. S.-V. *Chem. Eur. J.* **2006**, *12*, 8750-8761.
- ¹⁰¹ Mac, Y.; Kapdi, A. R.; Fairlamb, I. J. S.; Jutand, A. *Organometallics* **2006**, *25*, 1795-1800.
- ¹⁰² Gillie, J.; Stille, J. K. *J. Am. Chem. Soc.* **1980**, *102*, 4933-4941.
- ¹⁰³ Gollaszewski, A.; Schwartz, J. *Organometallics* **1985**, *4*, 415-417.
- ¹⁰⁴ Kurosawa, H.; Kajimaru, H.; Miyoshi, M.-A.; Ohnishi, H.; Ikeda, I. *J. Mol. Catal.* **1992**, *74*, 481-488.
- ¹⁰⁵ (a) Luo, X.; Zhang, H.; Duan, H.; Liu, Q.; Zhu, L.; Zhang, T.; Lei, A. *Org. Lett.* **2007**, *9*, 4571-4574; (b) Zhang, H.; Luo, X.; Wongkhan, K.; Duan, H.; Li, Q.; Zhu, L.; Wang, J.; Batsanov, A. S.; Howard, J. A. K.; Marder, T. B.; Lei, A. *Chem. Eur. J.* **2009**, *15*, 3823-3829.
- ¹⁰⁶ Shi, W.; Luo, Y.; Luo, X.; Chao, L.; Zhang, H.; Wang, J.; Lei, A. *J. Am. Chem. Soc.* **2008**, *130*, 14713-14720.
- ¹⁰⁷ Castro, C. E.; Stephens, R. D. *J. Org. Chem.* **1963**, *28*, 3313.
- ¹⁰⁸ Dieck, H. A.; Heck, F. R. *J. Organomet. Chem.* **1975**, *93*, 259-263.
- ¹⁰⁹ Cassar, L. *J. Organomet. Chem.* **1975**, *93*, 253-257.

- ¹¹⁰ Nguyen, P.; Yuan, Z.; Agocs, L.; Lesley, G.; Marder, T. B. *Inorg. Chim. Acta.* **1994**, *220*, 289-296
- ¹¹¹ Amatore, C.; Azzambì, M.; Jutand, A. *J. Am. Chem. Soc.* **1991**, *113*, 8375-8384.
- ¹¹² Amatore, C.; Jutand, A. *Acc. Chem. Res.* **2000**, *33*, 314-321 and references therein.
- ¹¹³ Amatore, C.; Azzambì, M.; Jutand, A. *J. Organomet. Chem.* **1989**, *363*, C41-C45.
- ¹¹⁴ Siemsen, P.; Livingston, R. C.; Diederich, F. *Angew. Chem. Int. Ed.* **2000**, *39*, 2632-2657.
- ¹¹⁵ Batsanov, A. S.; Collings, J. C.; Fairlamb, I. J. S.; Holland, J. P.; Howard, J. A. K.; Lin, Z.; Marder, T. B.; Parsons, A. C.; Ward, R. M.; Zhu, J. *J. Org. Chem.* **2005**, *70*, 703-706.
- ¹¹⁶ Alami, M.; Ferri, F.; Linstumelle, G. *Tetrahedron Lett.* **1993**, *34*, 6403-6406.
- ¹¹⁷ Hundertmark, T.; Littke, A. L.; Buchwald, S. L.; Fu, G. C. *Org. Lett.* **2000**, *2*, 1729-1731.
- ¹¹⁸ Mori, A.; Kawashima, J.; Suguro, M.; Hirabayashi, K.; Nishihara, Y. *Org. Lett.* **2000**, *2*, 2935-2937.
- ¹¹⁹ Alonso, D. A.; Najera, C.; Pacheco, M. C. *Tetrahedron Lett.* **2002**, *43*, 9365-9368.
- ¹²⁰ Herrmann, W. A.; Reisenger, C.-P.; Öfele, K.; Broßmer, C.; Beller, M.; Fischer, H. *J. Mol. Catal. A* **1996**, *108*, 51-56..
- ¹²¹ Arduengo, A. J. III; Harlow, R. L.; Kline, M. J. *J. Am. Chem. Soc.* **1991**, *113*, 361-363.
- ¹²² Batey, R. A.; Shen, M.; Lough, A. J. *Org. Lett.* **2002**, *2*, 1411-1414.
- ¹²³ Ackermann, L. *Org. Lett.* **2005**, *7*, 439-442.
- ¹²⁴ Eckhardt, M.; Fu, G. C. *J. Am. Chem. Soc.* **2003**, *125*, 13642-13643.
- ¹ Amatore, C.; Jutand, A.; M'Barki, M. A. *Organometallics* **1992**, *11*, 3009-3013.
- ¹²⁵ Brown, H. C.; Hébert, N. C.; Snyder, C. H. J. *J. Am. Chem. Soc.* **1961**, *83*, 1001-1002.
- ¹²⁶ Brown, H. C.; Verbrugge, C.; Snyder, C. H. J. *J. Am. Chem. Soc.* **1961**, *83*, 1001.
- ¹²⁷ Larock, R. C.; Brown, H. C. *J. Am. Chem. Soc.* **1970**, *92*, 2467-2471.
- ¹²⁸ Wallow, T. I.; Novak, B. M. *J. Org. Chem.* **1994**, *59*, 5034-5037
- ¹²⁹ Miyaura, N.; Yamada, K.; Suzuki, A. *Tetrahedron Lett.* **1979**, *20*, 3437-3440.
- ¹³⁰ Miyaura, N.; Yamada, K.; Surrinome, H.; Suzuki, A. *J. Am. Chem. Soc.* **1985**, *107*, 972-980.

- ¹³¹ Miyaura, N.; Suzuki, A. *J. Organomet. Chem.* **1981**, *213*, C53-C56.
- ¹³² Darses, S.; Genet, J.-P. *Chem. Rev.* **2008**, *108*, 288-325.
- ¹³³ Vedejs, E.; Chapman, R. W.; Fields, S. C.; Lin, S.; Schrimpf, M. R. *J. Org. Chem.* **1995**, *60*, 3020-3027.
- ¹³⁴ (a) Molander, G. A.; Bernardi, C. R. *J. Org. Chem.* **2002**, *67*, 8424-8429; (b) Molander, G. A.; Ito, T. *Org. Lett.* **2001**, *3*, 393-396; (c) Molander, G. A.; Biolatto, B. *Org. Lett.* **2002**, *4*, 1867-1870. (d) Molander, G. A.; Machrouhi, F.; Katona, B. *J. Org. Chem.* **2002**, *67*, 8416-8123.
- ¹³⁵ Matos, K.; Soderquist, J. A. *J. Org. Chem.* **1998**, *63*, 461-470.
- ¹³⁶ Molander, G. A.; Ribagorda, M. *J. Am. Chem. Soc.* **2003**, *125*, 11148-11149.
- ¹³⁷ Molander, G. A.; Figueroa, R. *Org. Lett.* **2006**, *8*, 75-78.
- ¹³⁸ Molander, G. A.; Ham, J.; Canturk, B. *Org. Lett.* **2007**, *9*, 821-824.
- ¹³⁹ Molander, G. A.; Figueroa, R. *J. Org. Chem.* **2006**, *71*, 6135-6140.
- ¹⁴⁰ Molander, G. A.; Ellis, N. M. *J. Org. Chem.* **2006**, *71*, 7491-7493.
- ¹⁴² (a) Molander, G. A.; Sandrock, D. L. *Org. Lett.* **2007**, *9*, 1597-1600; (b) Molander, G. A.; Ham, J. *Org. Lett.* **2006**, *8*, 2767-2770; (c) Molander, G. A.; Ham, J. *Org. Lett.* **2006**, *8*, 2031-2134.
- ¹⁴³ Ishiyama, T.; Abe, S.; Miyaura, N.; Suzuki, A. *Chem. Lett.* **1992**, 691-694.
- ¹⁴⁴ Netherton, M. R.; Dai, C.; Neuschütz, K.; Fu, G. C. *J. Am. Chem. Soc.* **2001**, *123*, 10099-10100.
- ¹⁴⁵ Netherton, M. R.; Fu, G. C. *Angew. Chem., Int. Ed.* **2002**, *41*, 3910-3912.
- ¹⁴⁶ Kirchhoff, J. H.; Dai, C.; Fu, G. C. *Angew. Chem. Int. Ed.* **2002**, *41*, 1945-1947.
- ¹⁴⁷ Kirchhoff, J. H.; Netherton, M. R.; Hills, I. D.; Fu, G. C. *J. Am. Chem. Soc.* **2002**, *124*, 13662-13663.
- ¹⁴⁸ González-Bobes, F.; Fu, G. C. *J. Am. Chem. Soc.* **2006**, *128*, 5360-5361.
- ¹⁴⁹ Heck reaction: (a) Littke, A. F.; Fu, G. C. *J. Org. Chem.* **1999**, *64*, 10-11; (b) Shaughnessy, K. H.; Kim, P.; Hartwig, J. F. *J. Am. Chem. Soc.* **1999**, *121*, 2123-2132; (c) Herrmann, W. A.; Böhm, V. P. W.; Reisinger, C. P. *J. Organomet. Chem.* **1999**, *576*, 23-41; (d) Herrmann, W. A.; Broßmer, C.; Ofele, K.; Reisinger, C. P.; Priermeier, T.; Beller, M.; Fischer, H. *Angew. Chem., Int. Ed.* **1995**, *34*, 1844-1848.
- Stille reaction: Littke, A. F.; Fu, G. C. *Angew. Chem. Int. Ed.* **1999**, *38*, 2411-2413.

Kumada reaction: Huang, J.; Nolan, S. P. *J. Am. Chem. Soc.* **1999**, *121*, 9889-9890.

Buchwald-Hartwig reaction: (a) Wolfe, J. P.; Buchwald, S. L. *Angew. Chem, Int. Ed.* **1999**, *38*, 2413-2415; (b) Mann, G.; Incarvito, C.; Rheingold, A. L.; Hartwig, J. F. *J. Am. Chem. Soc.* **1999**, *121*, 3224-3225.

¹⁵⁰ Navarro, O.; Marion, N.; Oonishi, Y.; Kelly, R. A.; Nolan, S. P. *J. Org. Chem.* **2006**, *71*, 685-682.

¹⁵¹ (a) Old, D. W.; Wolfe, J. P.; Buchwald, S. L. *J. Am. Chem. Soc.* **1998**, *120*, 9722-9723; (b) Buchwald, S. L.; Fox, J. M. *The Strem Chemiker* **2000**, *28*, No. 1.

¹⁵² Yin, J.; Rainka, M. P.; Zhang, X.-X.; Buchwald, S. L. *J. Am. Chem. Soc.* **2002**, *124*, 1162-1163.

References for 1.3 Transition metal-catalysed borylations of C-H bonds

¹⁵³ Muetterties, E. L. *The Chemistry of Boron and its Compounds*, John Wiley & Sons, Inc.: New York, **1976**.

¹⁵⁴ Brown, H. C. *Boranes in Organic Chemistry*, Cornell University Press: Ithaca, **1972**.

¹⁵⁵ Chan, D. M. T.; Lam, P. Y. S. Recent Advances in Copper-promoted C-Heteroatom Bond Cross-coupling Reactions with Boronic Acids and Derivatives. In *Boronic Acids*, Hall, D. G. Ed. Wiley-VCH: Weinheim, **2005**; pp 205-241.

¹⁵⁶ Yoshida, K.; Hayashi, T. Rhodium-catalysed Additions of Boronic Acids to Alkenes and Carbonyl Compounds. In *Boronic Acids*, Hall, D. G. Ed. Wiley-VCH: Weinheim, **2005**; pp 171-241.

¹⁵⁷ Urry, G.; Kerrigan, J.; Parsons, T. D.; Schlesinger, H. I. *J. Am. Chem. Soc.* **1954**, *76*, 5299-5301.

¹⁵⁸ (a) Brotherton, R. J.; McCloskey, A. L.; Petterson, L. L.; Steinberg, H. *J. Am. Chem. Soc.* **1960**, *82*, 6242-6245; (b) Brotherton, R. J.; McCloskey, A. L.; Boone, J. L.; Manasevit, H. M. *J. Am. Chem. Soc.* **1960**, *82*, 6245-6248.

¹⁵⁹ (a) Brotherton, R. J.; Woods, G. W. *US Patent*, **1961**, 3 009 941; (b) Ishiyama, T.; Murata, M.; Ahiko, T.; Miyaura, N. *Org. Synth.* **1999**, *77*, 176-182; (c) Nöth, H. *Naturforsch.* **1984**, *39b*, 1463-1466; (d) Lesley, M. J. G.; Norman, N. C.; Rice, C. R. *Inorg. Synth.* **2004**, *34*, 1-5.

- ¹⁶⁰ (a) Nguyen, P.; Lesley, G.; Taylor, N. J.; Marder, T. B.; Pickett, N. L.; Clegg, W.; Elsegood, M. R. J.; Norman, N. C. *Inorg. Chem.* **1994**, *33*, 4623-4624; (b) Clegg, W.; Elsegood, M. R. J.; Lawlor, F. J.; Norman, N. C.; Pickett, N. L.; Robins, E. G.; Scott, A. J.; Nguyen, P.; Taylor, N. J.; Marder, T. B. *Inorg. Chem.* **1998**, *37*, 5289-5293; (c) Lawlor, F. J.; Norman, N. C.; Pickett, N. L.; Robins, E. G.; Nguyen, P.; Lesley, G.; Marder, T. B.; Ashmore, J. A.; Green, J. C. *Inorg. Chem.* **1998**, *37*, 5282-5288.
- ¹⁶¹ Welch, C. N.; Shore, S. G. *Inorg. Chem.* **1968**, *7*, 225-230.
- ¹⁶² Marder, T. B.; Norman, N. C. *Topics in Catalysis* **1998**, *5*, 63-73.
- ¹⁶³ Hall, D. G. Structure, Properties, and Preparation of Boronic Acid Derivatives. Overview of Their Reactions and Applications. In *Boronic Acids*, Hall, D. G. Ed. Wiley-VCH: Weinheim, **2005**; pp 1-101.
- ¹⁶⁴ Shimada, S.; Batsanov, A. S.; Howard, J. A. K.; Marder, T. B. *Angew. Chem. Int. Ed.* **2001**, *40*, 2168-2871.
- ¹⁶⁵ Lam, W. H.; Lam, K. C.; Lin, Z.; Shimada, S.; Perutz, R. N.; Marder, T. B. *Dalton Trans.* **2004**, 1556-1562.
- ¹⁶⁶ Ishiyama, T.; Ishida, K.; Takagi, J.; Miyaura, N. *Chem. Lett.* **2001**, *30*, 1082-1083.
- ¹⁶⁷ Mertins, K.; Zapf, A.; Beller, M. *J. Mol. Catal. A* **2004**, *207*, 21-25.
- ¹⁶⁸ (a) Ishiyama, T.; Miyaura, N. *J. Organomet. Chem.* **2003**, *680*, 3-11; (b) Ishiyama, T.; Miyaura, N. Metal-catalyzed Borylation of Alkenes and Arenes via C-H Activation for Synthesis of Boronic Esters. In *Boronic Acids*, Hall, D. G. Ed. Wiley-VCH: Weinheim, **2005**; pp 101-123.
- ¹⁶⁹ Waltz, K. M.; He, X.; Muhoro, C.; Hartwig, J. F. *J. Am. Chem. Soc.* **1995**, *117*, 11357-11358.
- ¹⁷⁰ Waltz, K. M.; Muhoro, C.; Hartwig, J. F. *Organometallics* **1999**, *18*, 3383-2293.
- ¹⁷¹ Chen, H.; Schlecht, S.; Semple, T. C.; Hartwig, J. F. *Science* **2000**, *287*, 1995-1997.
- ¹⁷² Cho, J. Y.; Iverson, C. N.; Smith, M. R. III *J. Am. Chem. Soc.* **2000**, *122*, 12868-12869.
- ¹⁷³ Tse, M. K.; Cho, J. Y.; Smith, M. R. III *Org. Lett.* **2001**, *3*, 2831-2833.
- ¹⁷⁴ Nguyen, P.; Blom, H. P.; Wescott, S. A.; Taylor, N. J.; Marder, T. B. *J. Am. Chem. Soc.* **1993**, *115*, 9329-9330.
- ¹⁷⁵ Iverson, C. N.; Smith, M. R. III *J. Am. Chem. Soc.* **1999**, *121*, 7696-7697.

- ¹⁷⁶ Bergmann, R. G. *Science* **1984**, *223*, 902-908.
- ¹⁷⁷ Jones, W. D.; Feher, F. J. *Acc. Chem. Res.* **1989**, *22*, 91-100.
- ¹⁷⁸ Cho, J. Y.; Tse, M. K.; Holmes, D.; Maleczka, R. E.; Smith, M. R. III *Science* **2002**, *295*, 305-308.
- ¹⁷⁹ Ishiyama, T.; Takagi, J.; Ishida, K.; Miyaura, N.; Anastasi, N. R.; Hartwig, J. F. *J. Am. Chem. Soc.* **2002**, *124*, 390-391.
- ¹⁸⁰ Ishiyama, T.; Takagi, J.; Hartwig, J. F.; Miyaura, N. *Angew. Chem. Int. Ed.* **2002**, *41*, 3056-3058.
- ¹⁸¹ Kukuchi, T.; Nobuta, Y.; Umeda, J.; Yamamoto, Y.; Ishiyama, T.; Miyaura, N. *Tetrahedron* **2008**, *64*, 4967-4971.
- ¹⁸² Chotana, G. A.; Rak, M. A.; Smith, M. R. III *J. Am. Chem. Soc.* **2005**, *127*, 10539-10544.
- ¹⁸³ Snieckus, V. *Chem. Rev.* **1990**, *90*, 879-933.
- ¹⁸⁴ Price, C. C. *Chem. Rev.* **1941**, *29*, 37-67.
- ¹⁸⁵ Kurotobi, K.; Miyauchi, M.; Takahura, K.; Murafuji, T.; Sugihara, Y. *Eur. J. Org. Chem.* **2003**, 3663-3365.
- ¹⁸⁶ Coventry, D. N.; Batsanov, A. S.; Goeta, A. E.; Howard, J. A. K.; Marder, T. B.; Perutz, R. N. *Chem. Commun.* **2005**, 2172-2174.
- ¹⁸⁷ Boller, T. M.; Murphy, J. M.; Hapke, M.; Ishiyama, T.; Miyaura, N.; Hartwig, J. F. *J. Am. Chem. Soc.* **2005**, *127*, 14263-14278.
- ¹⁸⁸ Datta, A.; Köllehofer, A.; Plenio, H. *Chem. Commun.* **2004**, 1508-1509.
- ¹⁸⁹ Shin, J.; Jensen, S. M.; Ju, J.; Lee, S.; Xue, Z.; Noh, S. K.; Bae, C. *Macromolecules* **2007**, *40*, 8600-8608.
- ¹⁹⁰ Jo, T. S.; Kim, S. H.; Shin, J.; Bae, C. *J. Am. Chem. Soc.* **2009**, *131*, 1656-1657.
- ¹⁹¹ Hata, H.; Shinokubo, H.; Osuka, A. *J. Am. Chem. Soc.* **2005**, *127*, 8264-8265.
- ¹⁹² Hata, H.; Yamaguchi, S.; Mori, G.; Nakazono, S.; Katoh, T.; Takatsu, K.; Hiroto, S.; Shinokubo, H.; Osuka, A. *Chem. Asian J.* **2007**, *2*, 849-859.
- ¹⁹³ Takagi, J.; Sato, K.; Hartwig, J. F.; Ishiyama, T.; Miyaura, N. *Tetrahedron Lett.* **2002**, *43*, 5649-5651.
- ¹⁹⁴ Ishiyama, T.; Takagi, J.; Yonekawa, Y.; Hartwig, J. F.; Miyaura, N. *Adv. Synth. Catal.* **2003**, *345*, 1103-1106.

- ¹⁹⁵ Chotana, G. A.; Kallepalli, V. A.; Maleczka, R. E.; Smith, M. R. III *Tetrahedron* **2008**, *64*, 6103-6114.
- ¹⁹⁶ Paul, S.; Chotana, G. A.; Holmes, D.; Reichle, R. C.; Maleczka, R. E.; Smith, M. R. III *J. Am. Chem. Soc.* **2006**, *128*, 15552-15553.
- ¹⁹⁷ Lo, W. F.; Kaiser, H. M.; Spannenberg, A.; Beller, M.; Tse, M. K. *Tetrahedron Lett.* **2007**, *48*, 371-375.
- ¹⁹⁸ Mkhaliid, I. A. I.; Coventry, D. N.; Albesa-Jove, D.; Batsanov, A. S.; Howard, J. A. K.; Perutz, R. N.; Marder, T. B. *Angew. Chem. Int. Ed.* **2006**, *45*, 489-491.
- ¹⁹⁹ (a) Nguyen, P.; Dai, C.; Taylor, N. J.; Power, W. P.; Pickett, N. L.; Norman, N. C.; Marder, T. B. *Inorg. Chem.* **1995**, *34*, 4290-4291; (b) Clegg, W.; Dai, C.; Lawlor, F. J.; Nguyen, P.; Norman, N. C.; Pickett, N. L.; Power, W. P.; Scott, A. J.; Marder, T. B. *Dalton Trans.* **1997**, 839-846.
- ²⁰⁰ Murphy, J. M.; Tzschucke, C. C.; Hartwig, J. F. *Org. Lett.* **2007**, *9*, 757-760.
- ²⁰¹ Maleczka, R. E.; Shi, F.; Holmes, D.; Smith, M. R. III *J. Am. Chem. Soc.* **2003**, *125*, 7792-7793.
- ²⁰² Murphy, J. M.; Liao, X.; Hartwig, J. F. *J. Am. Chem. Soc.* **2007**, *129*, 15434-15435.
- ²⁰³ Kabalka, G. W.; Mereddy, A. R. *Nuclear Medicine and Biology* **2004**, *31*, 935-938.
- ²⁰⁴ Harrisson, P.; Morris, J.; Steel, P. G.; Marder, T. B. *Synlett.* **2009**, 147-150.
- ²⁰⁵ Tzschucke, C. C.; Murphy, J. M.; Hartwig, J. F. *Org. Lett.* **2007**, *9*, 761-764.
- ²⁰⁶ Holmes, D.; Chotana, G. A.; Maleczka, R. E.; Smith, M. R. III *Org. Lett.* **2006**, *8*, 1407-1410.
- ²⁰⁷ Shi, F.; Maleczka, R. E.; Smith, M. R. III *Org. Lett.* **2006**, *8*, 1411-1414.
- ²⁰⁸ Boebel, T. A.; Hartwig, J. F. *Tetrahedron* **2008**, *64*, 6824-6830.
- ²⁰⁹ Boebel, T. A.; Hartwig, J. F. *J. Am. Chem. Soc.* **2008**, *130*, 7534-7535.
- ²¹⁰ Boebel, T. A.; Hartwig, J. F. *Organometallics* **2008**, *27*, 6013-6019.
- ²¹¹ Murata, M.; Odajima, H.; Watanabe, S.; Masuda, Y. *Bull. Chem. Soc. Jpn.* **2006**, *79*, 1980-1982.
- ²¹² Tagata, T.; Nishida, M. *Adv. Synth. Catal.* **2004**, *346*, 1655-1660.
- ²¹³ Yinghuai, Z.; Yan, K. C.; Jizhong, L.; Hwei, C. S.; Hon, Y. C.; Emi, A.; Zhenshun, S.; Winata, M.; Hosmane, N. S.; Maguire, J. A. *J. Organomet. Chem.* **2007**, *692*, 4244-4250.

- ²¹⁴ Frey, G. D.; Rentzsch, C. F.; Presyng, D.; Scherg, T.; Mühlhofer, m.; Herdtweck, E.; Herrmann, W. A. *J. Organomet. Chem.* **2006**, *691*, 5725-5738.
- ²¹⁵ Yinghuai, Z.; Chenyan, K.; Peng, A. T.; Emi, A.; Monalisa, W.; Louis, L. K.-J.; Hosmane, N. S.; Maguire, J. A. *Inorg. Chem.* **2008**, *47*, 5756-5761.
- ²¹⁶ Tamura, H.; Yamzaki, H.; Sato, H.; Sakaki, S. *J. Am. Chem. Soc.* **2003**, *125*, 16114-16126.
- ²¹⁷ Brown, H. C.; Gupta, S. K. *J. Am. Chem. Soc.* **1975**, *97*, 5249-5255.
- ²¹⁸ Takagi, J.; Takahashi, K.; Ishiyama, T.; Miyaura, N. *J. Am. Chem. Soc.* **2002**, *124*, 8001-8006.
- ²¹⁹ Brown, H. C.; Bhat, N. G. *Tetrahedron Lett.* **1988**, *29*, 21-24.
- ²²⁰ Srebnik, M.; Bhat, N. G.; Brown, H. C. *Tetrahedron Lett.* **1988**, *29*, 2635-2638.
- ²²¹ Deloux, L.; Skrzypczak-Jankun, E.; Cheesman, B. V.; Srebnik, M.; Sabat, M., *J. Am. Chem. Soc.* **1994**, *116*, 10302-10303.
- ²²² (a) Blackwell, H. E.; O'Leary, D. J.; Chatterjee, A. K.; Washenfelder, R. A.; Bussmann, D. A.; Grubbs, R. H. *J. Am. Chem. Soc.* **2000**, *122*, 58-71; (b) Morrill, C.; Grubbs, R. H. *J. Org. Chem.* **2003**, *68*, 6031-6034; (c) Morrill, C.; Funk, T. W.; Grubbs, R. H. *Tetrahedron Lett.* **2004**, *45*, 7733-7736.
- ²²³ Cole, T. E.; Quintanilla, R.; Rodewald, S. *Organometallics* **1991**, *10*, 3777-3781.
- ²²⁴ (a) Ishiyama, T.; Matsuda, N.; Miyaura, N.; Suzuki, A. *J. Am. Chem. Soc.* **1993**, *115*, 11018-11019; (b) Ishiyama, T.; Matsuda, N.; Murata, M.; Ozawa, F.; Suzuki, A.; Miyaura, N. *Organometallics* **1996**, *15*, 713-720; (c) Lesley, G.; Nguyen, P.; Taylor, N. J.; Marder, T. B.; Scott, A. J.; Clegg, W.; Norman, N. C. *Organometallics* **1996**, *15*, 5137-5154; (d) Iverson, C. N.; Smith, M. R. III *Organometallics* **1996**, *15*, 5155-5165; (e) Thomas, R. Ll.; Souza, F. E. S.; Marder, T. B., *Dalton Trans.* **2001**, 1650-1656.
- ²²⁵ Davan, T.; Corcoran, E. W. Jr.; Sneddon, L. G. *Organometallics* **1983**, *2*, 1693-1694.
- ²²⁶ Brown, J. M.; Lloyd-Jones, G. C. *J. Chem. Soc. Chem. Commun.* **1992**, 710-712.
- ²²⁷ Brown, J. M.; Lloyd-Jones, G. C. *J. Am. Chem. Soc.* **1994**, *116*, 866-878.
- ²²⁸ Murata, M.; Watanabe, S.; Masuda, Y. *Tetrahedron Lett.* **1999**, *40*, 2585-2588.
- ²²⁹ Murata, M.; Kawakita, K.; Asana, T.; Watanabe, S.; Masuda, Y. *Bull. Chem. Soc. Jpn.* **2002**, *75*, 825-829.
- ²³⁰ Caballero, A.; Sabo-Etienne, S. *Organometallics* **2007**, *26*, 1191-1195.

- ²³¹ Olsson, V. J.; Szabó, K. J. *Angew. Chem. Int. Ed.* **2007**, *46*, 6891-6893.
- ²³² Olsson, V. J.; Szabó, K. J. *Org. Lett.* **2008**, *10*, 3129-3131.
- ²³³ Motry, D. H.; Smith, M. R. III *J. Am. Chem. Soc.* **1995**, *117*, 6615-6616.
- ²³⁴ Motry, D. H.; Brazil, A. G.; Smith, M. R. III *J. Am. Chem. Soc.* **1997**, *119*, 2743-2744.
- ²³⁵ Baker, R. T.; Calabrese, J. C.; Westcott, S. A.; Marder, T. B. *J. Am. Chem. Soc.* **1995**, *117*, 8777-8784.
- ²³⁶ Baker, R. T.; Calabrese, J. C.; Westcott, S. A.; Nguyen, P.; Marder, T. B. *J. Am. Chem. Soc.* **1993**, *115*, 4367-4368.
- ²³⁷ Baker, R. T.; Nguyen, P.; Marder, T. B.; Westcott, S. A. *Angew. Chem. Int. Ed.* **1995**, *34*, 1336-1338.
- ²³⁸ Burgess, K.; van der Donk, W. A.; Westcott, S. A.; Marder, T. B.; Baker, R. T.; Calabrese, J. C. *J. Am. Chem. Soc.* **1992**, *114*, 9350-9359.
- ²³⁹ Westcott, S. A.; Marder, T. B.; Baker, R. T. *Organometallics* **1993**, *12*, 975-979.
- ²⁴⁰ Vogels, C. M.; Hayes, P. G.; Shaver, M. P.; Westcott, S. A. *Chem. Commun.* **2000**, 51-52.
- ²⁴¹ Coapes, R. B.; Souza, F. E. S.; Thomas, R. Ll.; Hall, J. J.; Marder, T. B. *Chem. Commun.* **2003**, 614-615.
- ²⁴² Mkhaldid, I. A. I.; Coapes, R. B.; Edes, S. N.; Coventry, D. N.; Souza, F. E. S.; Thomas, R. Ll.; Hall, J. J.; Bi, S.-W.; Lin, Z.; Marder, T. B. *Dalton Trans.* **2008**, 1055-1064.
- ²⁴³ (a) Zhao, H.; Lin, Z.; Marder, T. B. *J. Am. Chem. Soc.* **2006**, *128*, 15637-15643; (b) Dang, L.; Zhao, H.; Lin, Z.; Marder, T. B. *Organometallics* **2007**, *26*, 2824-2832; (c) Zhao, H.; Dang, L.; Marder, T. B.; Lin, Z. *J. Am. Chem. Soc.* **2008**, *130*, 5586-5594; (d) Dang, L.; Lin, Z.; Marder, T. B. *Organometallics* **2008**, *27*, 4443-4454; (e) Dang, L.; Lin, Z.; Marder, T. B. *Chem. Commun.*, **2009**, 27, 3987-399
- ²⁴⁴ Geier, S. J.; Chapman, E. E.; McIsaac, D. I.; Vogels, C. M.; Decken, A.; Westcott, S. A. *Inorg. Chem. Commun.* **2006**, *9*, 788.
- ²⁴⁵ Kikuchi, T.; Takagi, J.; Ishiyama, T.; Miyaura, N. *Chem. Lett.* **2008**, *37*, 664-665.
- ²⁴⁶ Ohmura, T.; Takasaki, Y.; Furukawa, H.; Suginome, M. *Angew. Chem. Int. Ed.* **2009**, *48*, 2372-2375.

- ²⁴⁷ Ohmura, T.; Masuda, K.; Furukawa, H.; Suginome, M. *Organometallics* **2007**, *26*, 1291-1294.
- ²⁴⁸ Ohmura, T.; Furukawa, H.; Suginome, M. *J. Am. Chem. Soc.* **2006**, *128*, 13366-13367.
- ²⁴⁹ Marciniak, B.; Jankowska, M.; Pietraszuk, C. *Chem. Commun.* **2005**, 663-665.
- ²⁵⁰ Lam, K. C.; Lin, Z.; Marder, T. B. *Organometallics* **2007**, *26*, 3149-3156.

Synthesis of retinoids *via* sequential catalytic C-H borylations and Suzuki-Miyaura cross-couplings

2.1 Introduction

Retinoids are a group of more than 4000 natural and synthetic molecules that are structurally and/or functionally analogous to all-*trans*-retinoic acid (ATRA, **1**) (**Figure 2.1**), the major active metabolite of vitamin A. Endogenous retinoids regulate a range of essential processes during chordate embryogenesis and adult homeostasis, including embryonic development,²⁵¹ vision,²⁵² and cellular differentiation, proliferation and apoptosis.²⁵³

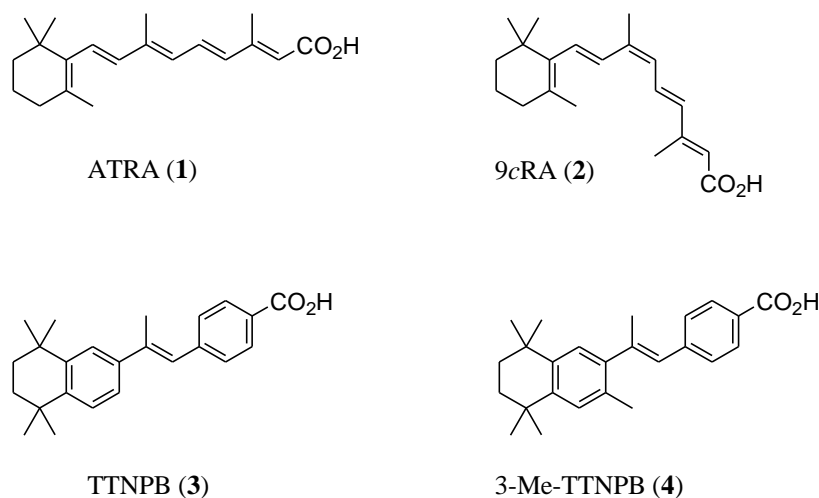
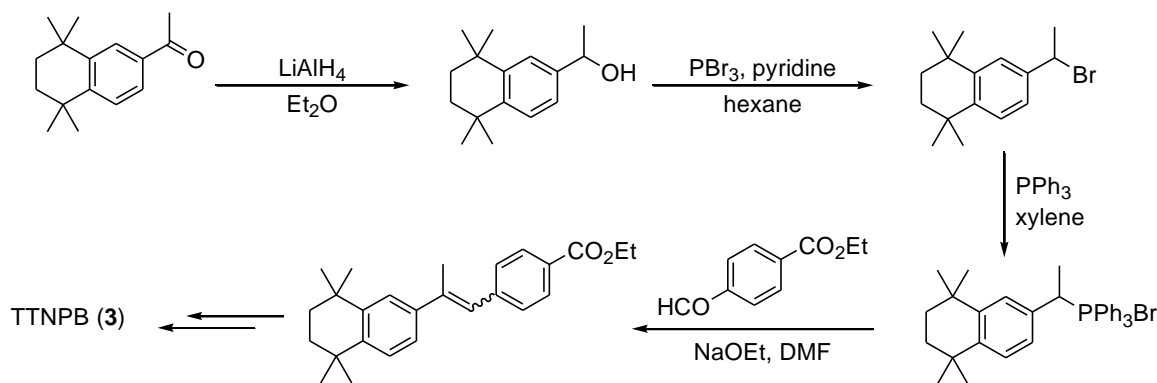


Figure 2.1 Natural and synthetic retinoids.

Retinoids are successfully used to treat dermatological conditions²⁵⁴ and have the potential to act as chemopreventative and chemotherapeutic agents.^{255,256} However, for many retinoids, administration at efficacious concentrations is associated with side effects ranging from skin irritation to toxicity and teratogenicity.²⁵⁷ The pleiotropic (multiple) effects of retinoids are mediated *via* the retinoid nuclear receptors (RARs and RXRs).^{258,259} ATRA binds strongly with all three isotypes of RAR (α , β and γ) but has no

affinity for the RXRs, whereas 9-*cis*-retinoic acid (9cRA, **2**), another physiological retinoid, binds and transactivates both the RARs and RXRs.²⁶⁰

A common approach to designing new retinoids is to modify the structure of ATRA, for example, by replacing the tetraene chain with one or more aromatic rings in order to constrain the geometric conformation. These compounds are often referred to as arotinoids. One of the first retinoids of this type to be prepared was 4-(*E*)-[2-(5,6,7,8-tetrahydro-5,5,8,8-tetramethyl-2-naphthalenyl)-1-propenyl]-benzoic acid (TTNPB, **3**) (**Scheme 2.1**),^{261,262} a highly teratogenic pan-RAR agonist which is cytotoxic and a strong inducer of apoptosis, with a potency 500 times greater than that of ATRA. TTNPB **3** was initially prepared from 2-(5,6,7,8-tetrahydro-5,5,8,8-tetramethyl-2-naphthalenyl)-ethan-1-one, *via* a reduction-bromination-phosphorylation-Wittig sequence to derive the methyl-diphenyl tri-substituted alkene. The Wittig reaction gave a mixture of *Z*-, and *E*-isomers, the *E*-isomer being separated by crystallization, and subsequent hydrolysis of the ethyl ester gave **3**.

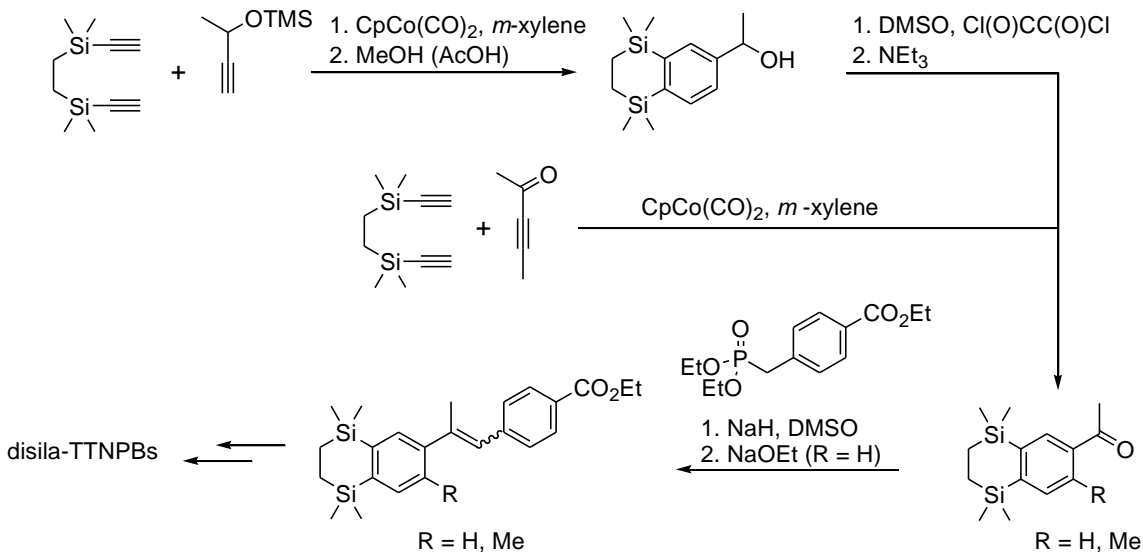


Scheme 2.1 Synthesis of TTNPB by Loeliger and coworkers.

The replacement of a proton in the 3-position in **3** by a methyl group generates 4-(*E*)-[2-(3,5,5,8,8-pentamethyl-5,6,7,8-tetrahydro-2-naphthalenyl)-1-propenyl]-benzoic acid, (3-Me-TTNPB, **4**),²⁶² (**Figure 2.1**). RAR- β and RAR- γ isotypes are activated by **4**, as is RXR- α . The RAR binding affinity of **4**, and consequently its toxicity, is decreased by 100-fold compared to **3**. The differences in the observed receptor selectivities between **3** and **4** result from unfavorable steric interactions between the C-3 methyl substituent

and the vinylic proton in **4**, which are not present in **3**. This causes a conformational change that alters the dihedral angle about the arene-olefin bond, giving **4** a twisted conformation that interacts more favorably with the RXRs and less favorably with the RARs.

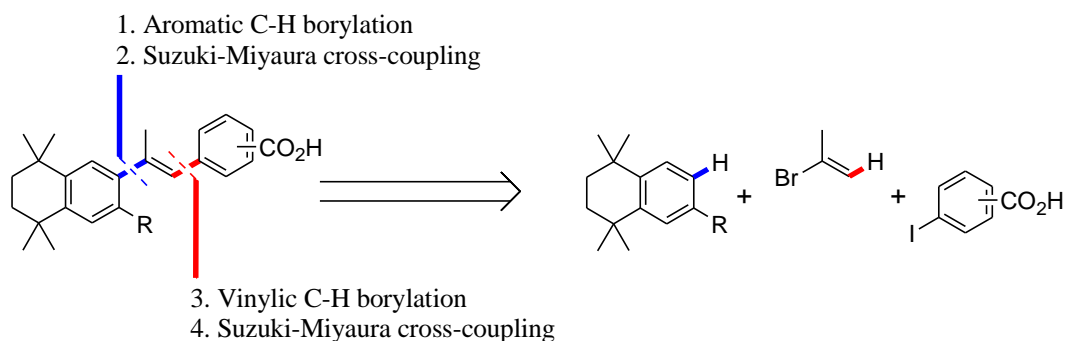
Heteroarotinoid analogues of TTNPB **3** and 3-Me TTNPB **4** are also known with 5-oxo,²⁶³ 5-thia^{263,264} and 5,8-disila-TTNPB²⁶⁵ (accessed by a [2+2+2]-cobalt-mediated phenyl ring construction, **Scheme 2.2**)²⁶⁶ previously synthesised as well as analogues bearing heterocycles such as thiophene,²⁶⁷ thiazole,²⁶⁸ imidazole,²⁶⁸ isoxazole²⁶⁹ and pyridine²⁶⁷ in place of the phenyl ring in the benzoic acid polar terminus.



Scheme 2.2 Synthesis of disila-TTNPBs by Tacke and coworkers.

A rapid synthesis of TTNPB **3** and its analogues from simple hydrocarbon starting materials *via* a sequence of C-H borylations and subsequent Suzuki-Miyaura cross-couplings was envisaged (**Scheme 2.3**). Iridium-catalysed aromatic C-H borylation of tetrahydronaphthalenes would give arylboronate esters which would be cross coupled with 2-bromopropene to give the desired α -methylstyrenes. Rhodium-catalysed dehydrogenative alkene borylation would yield (*E*)-vinylboronate esters that could

undergo Suzuki-Miyaura cross-coupling with iodobenzoic acids to give the desired products.

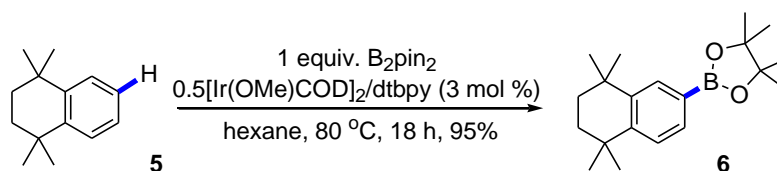


Scheme 2.3 Retrosynthetic analysis for the synthesis of TTNPBs *via* a combination of C-H borylations and Suzuki-Miyaura cross-couplings.

Iridium-catalysed aromatic C-H borylation has attracted much attention since its original development due to the atom efficiency that results from the direct functionalisation of C-H bonds and the high levels of largely sterically induced selectivity observed, which complement traditional methods such as EAS (electrophilic aromatic substitution)²⁷⁰ and DoM (directed *ortho* metalation)²⁷¹ chemistry. However, despite its inherent advantages and the large amount of methodological work published, its application in synthesis is extremely limited, with examples being the works of Hartwig,²⁷² Moore,²⁷³ Gaunt,²⁷⁴ and Odom.²⁷⁵

2.2 Results and discussion

Borylation of 1,1,4,4-tetramethyl-1,2,3,4-tetrahydronaphthalene **5** was performed in hexane with 1 equivalent of B₂pin₂ and [Ir(OMe)COD]₂/dtbpy (3 mol % Ir) as catalyst precursors. The reaction was monitored by *in situ* GC-MS analysis, with heating for 18 hours at 80 °C required to give full conversion to **6**,²⁷⁶ (95% isolated yield) with 100% regioselectivity for borylation of the least hindered aromatic C-H bonds (**Equation 2.1**).



Equation 2.1 Synthesis of **6** by Ir-catalysed aromatic C-H borylation of **5**.

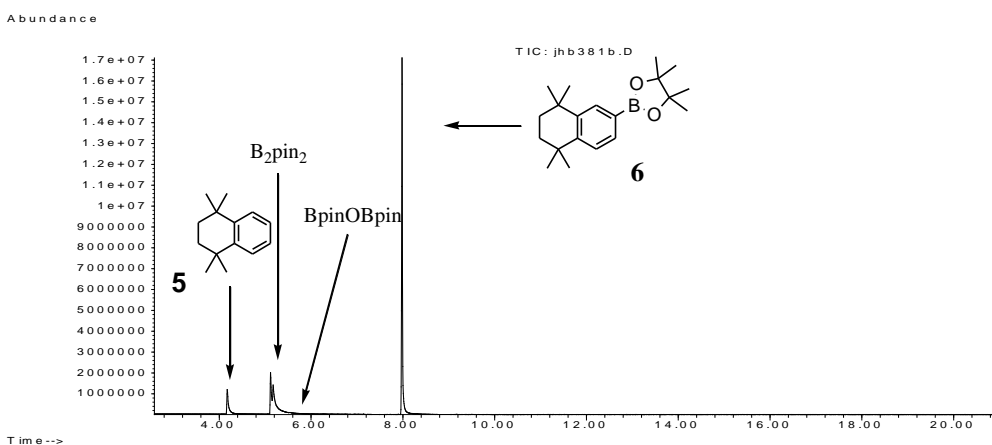


Figure 2.2 GC (TIC) of the synthesis of **6** after 4 h.

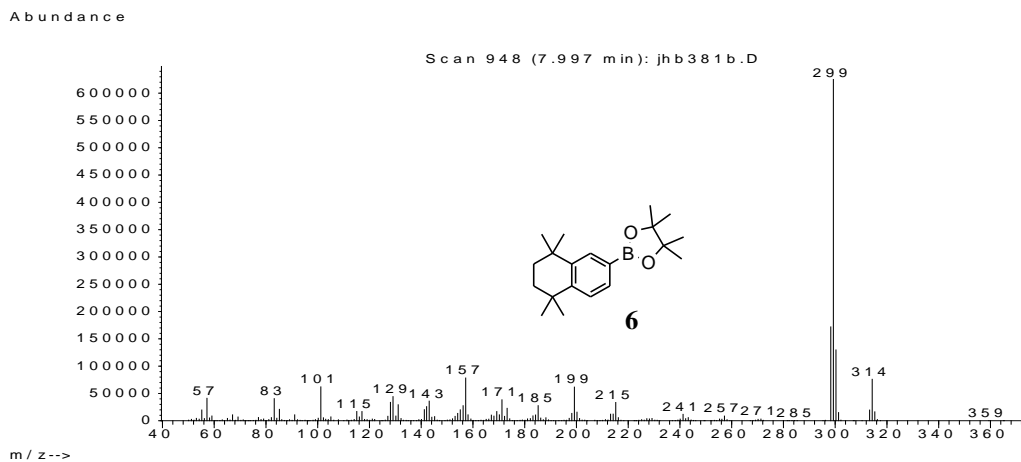
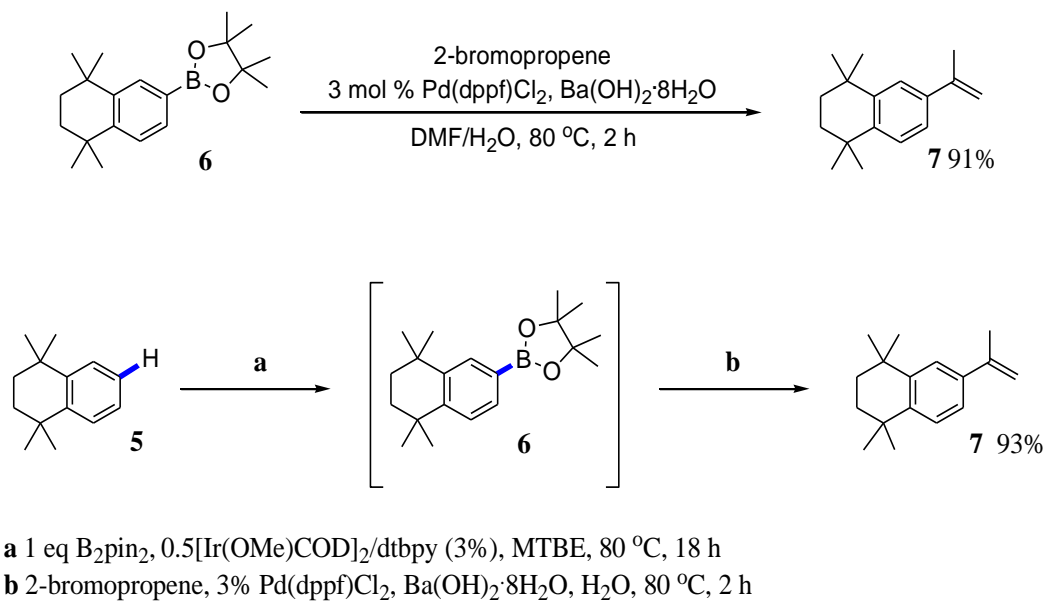


Figure 2.3 MS of **6**.

The Suzuki-Miyaura coupling of **6** with 2-bromopropene was carried out with 3 mol % $Pd(dppf)Cl_2$ and 2 equivalents of $Ba(OH)_2 \cdot 8H_2O$ base to give the α -methylstyrene product **7** in high yields.²⁷⁷ Reactions were heated thermally at 80 °C in a 5:1 mixture of DMF/ H_2O . In addition, **7** could be synthesised from 1,1,4,4-tetramethyl-1,2,3,4-tetrahydronaphthalene in a one-pot C-H, single solvent²⁷⁸ borylation/Suzuki-Miyaura

reaction process in which both reactions were performed in MTBE, with thermal heating at 80 °C (**Equation 2.2**).



Equation 2.2 Synthesis of **7**.

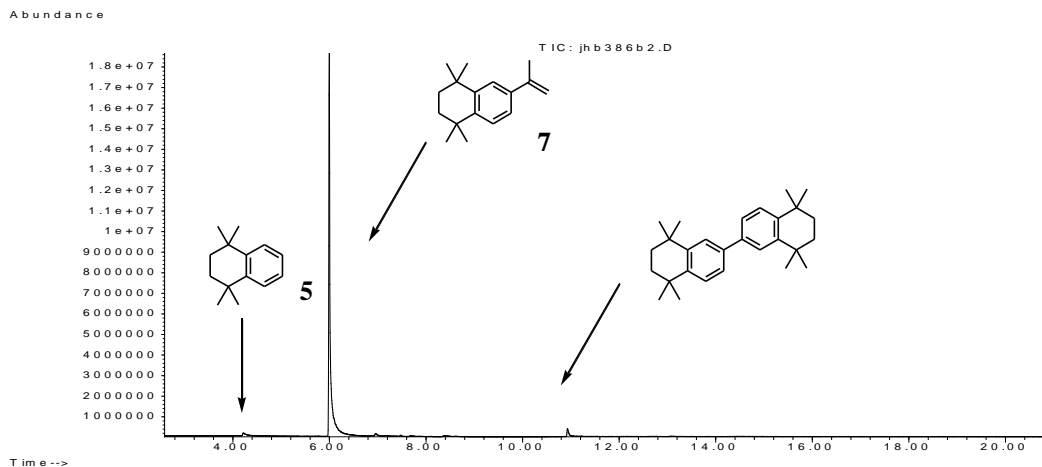


Figure 2.4 GC (TIC) of the reaction of **6** and 2-bromopropene after 2 h.

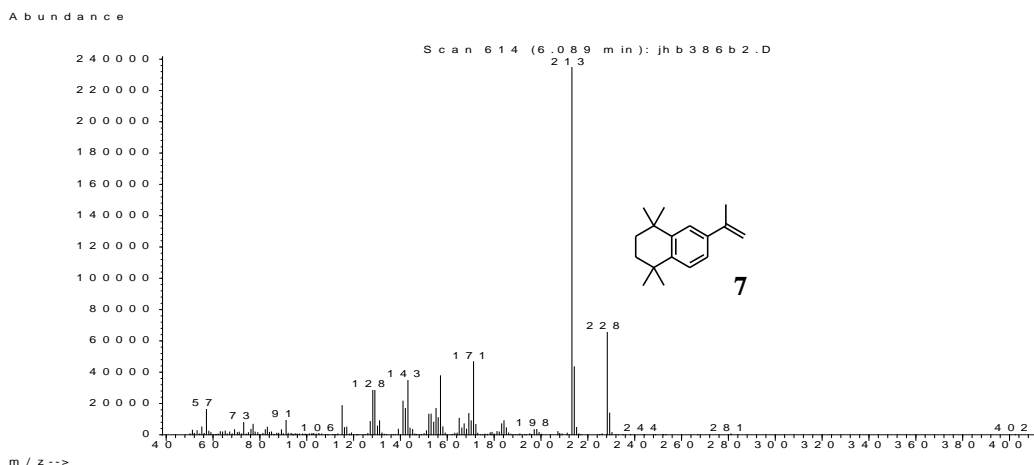
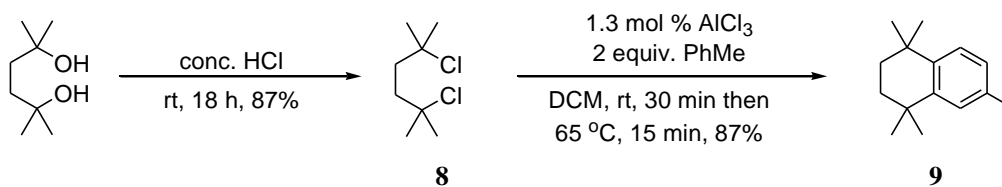


Figure 2.5 MS of **7**.

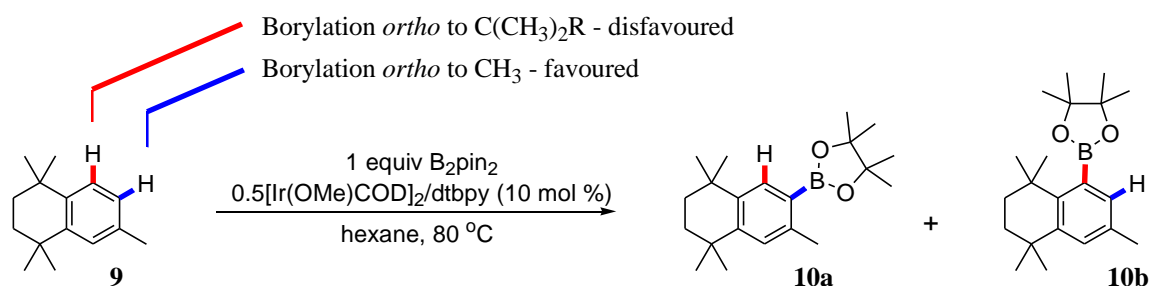
Synthesis of pentamethylated tetrahydronaphthalene **9**^{262c} was achieved *via* AlCl_3 -catalysed Friedel-Crafts dialkylation of toluene with 2,3-dichloro-2,3-dimethylbutane, **8**,²⁷⁹ which was synthesised from 2,3-dimethylbutane-2,3-diol *via* chlorination in neat HCl (**Equation 2.3**). The use of high purity toluene was found to be necessary as reactions carried out with GPR (general purpose reagent) grade toluene led to a competing reaction between toluene and traces of *ortho*-xylene which were clearly present. Clearly the activating effect of the additional methyl group in *ortho*-xylene is significant, with even small quantities of xylene reacting preferentially over toluene. Similarly, attempts to synthesise 1,1,4,4-tetramethyl-1,2,3,4-tetrahydronaphthalene *via* AlCl_3 catalysed Friedel-Crafts dialkylation of benzene with 2,3-dichloro-2,3-dimethylbutane resulted in the formation of the doubly reacted product even when reactions were carried out in neat benzene.



Equation 2.3 Synthesis of pentamethylated tetrahydronaphthalene **9**.

Borylations of 1,4-disubstituted benzenes typically give low conversions due to steric hindrance, with the exceptions being fluoro-, or cyano-substituted substrates.²⁸⁰

Borylation of **9**, in which all aromatic C-H bonds are adjacent to methyl or bulky $\text{CMe}_2\text{CH}_2\text{R}$ substituents, proceeded slowly with 10% iridium loadings and prolonged reaction times giving only 45% conversion. In contrast to the reaction of 1,1,4,4-tetramethyl-1,2,3,4-tetrahydronaphthalene, two isomeric borylation products were observed by GC-MS in an 85:15 ratio, resulting from competing borylation of the two least hindered C-H bonds (**Equation 2.4**).



Equation 2.4 Attempted Ir-catalysed aromatic C-H borylation of **9**.

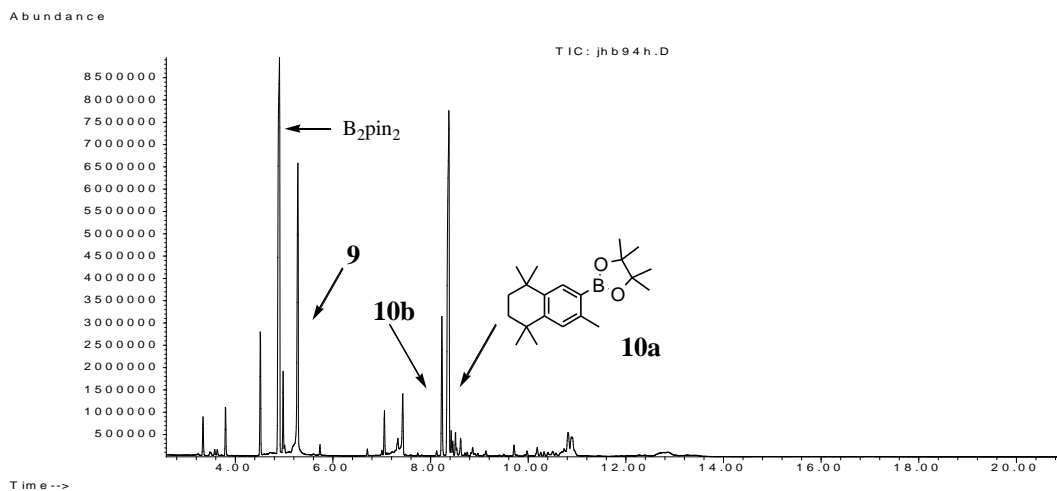


Figure 2.6 GC (TIC) of the attempted synthesis of **10a** by aromatic C-H borylation of **9** with B_2pin_2 .

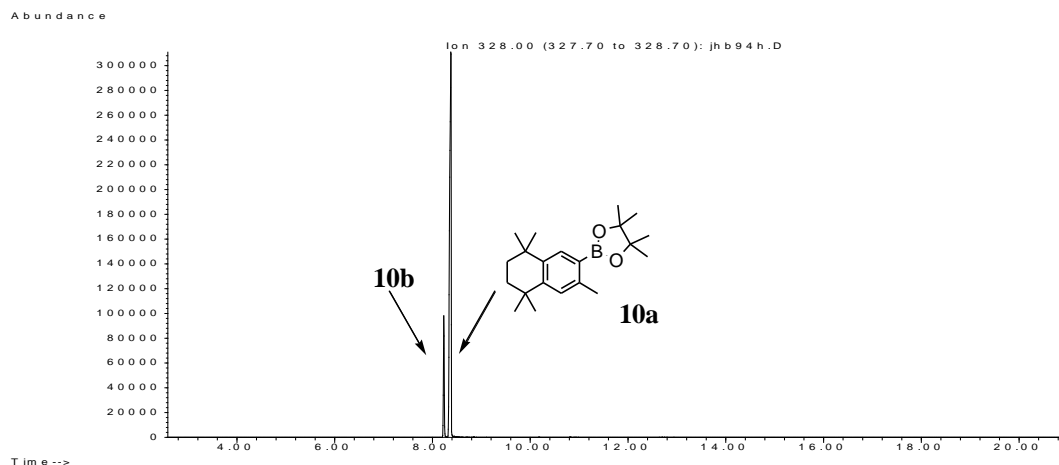


Figure 2.7 Ion chromatogram ($m/z = 328$) of the attempted synthesis of **10a** by aromatic C-H borylation of **9** with B_2pin_2 .

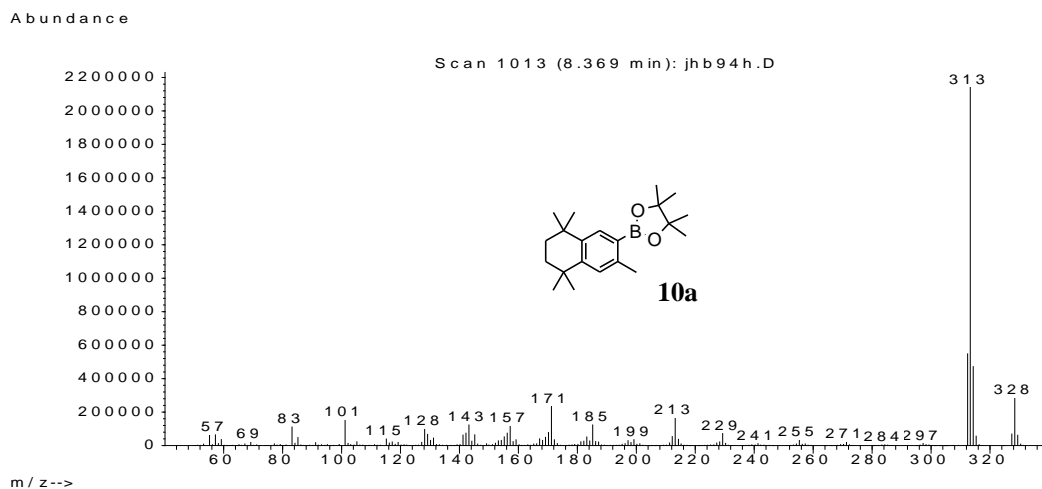
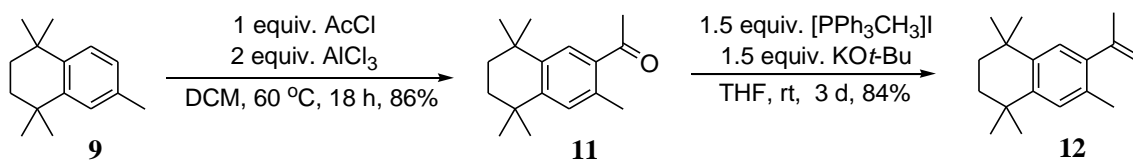


Figure 2.8 MS of **10a**.

In light of the poor selectivity and low reactivity exhibited in the Ir-catalysed C-H borylation of **9**, alternative routes to the methylated analogue of **2** were sought. Friedel-Crafts acylation of **9** with acetylchloride and $AlCl_3$ gave ketone **11**²⁸¹ The combination of 3 *ortho/para* directing groups on benzene in a 1,2,5 substitution pattern favoured acylation *para* to the strongest activating group $C(Me)_2R$ and *ortho* to the methyl substituent with a regioselectivity of >99% observed by GC-MS. Ketone **11** was purified by Kugelrohr distillation to give pure product in high yields. Wittig methylenation of **11** with PPh_3CH_3I and potassium *tert*-butoxide in THF gave olefin **12** which was purified by Kugelrohr distillation.



Equation 2.5 Synthesis of **12** via Friedel-Crafts acetylation and Wittig methylenation.

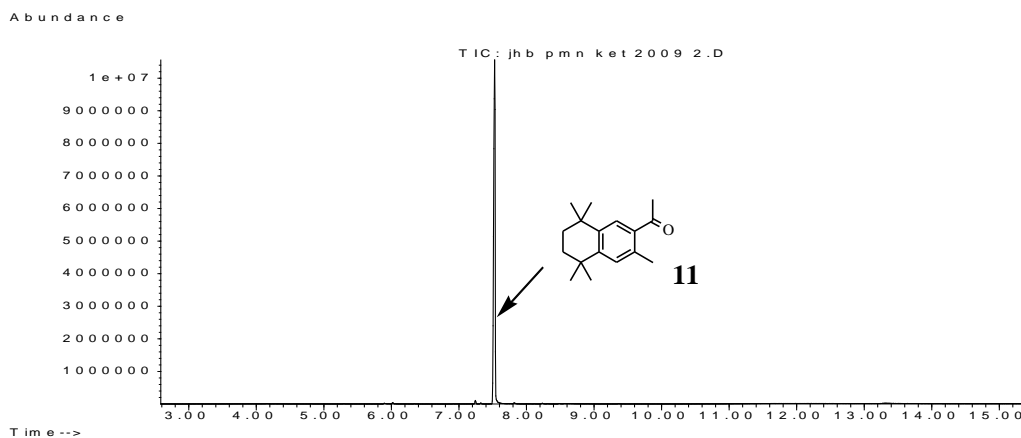


Figure 2.9 GC (TIC) of the acetylation of **9** with acetyl chloride to give **11** after 18 h.

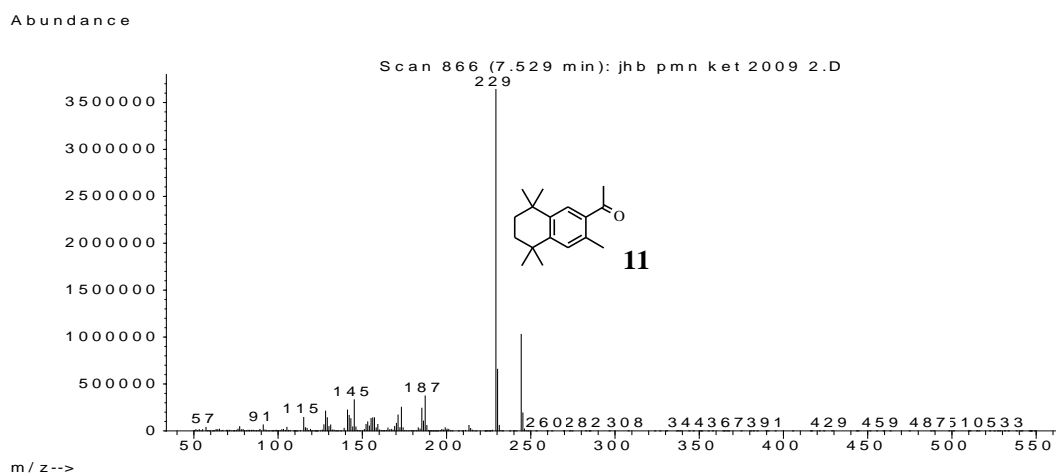


Figure 2.10 MS of **11**.

Monoclinic single crystals ($P2_1/c$) of compound **11** grew from liquid **11** upon standing. The C(O)Me group is inclined by 24.6° to the arene plane. The C(15) and O atoms are tilted out of this plane by 0.14 \AA and 0.63 \AA , while the methyl atom C(17) is displaced to the opposite side by -0.02 \AA (**Figure 2.11**).

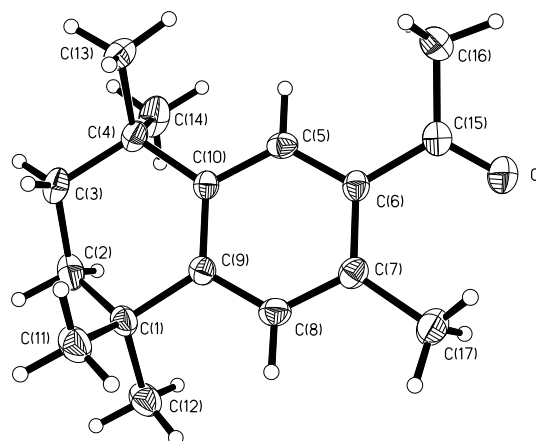


Figure 2.11 The molecular structure of ketone **11**. Thermal ellipsoids are drawn at 50% probability.

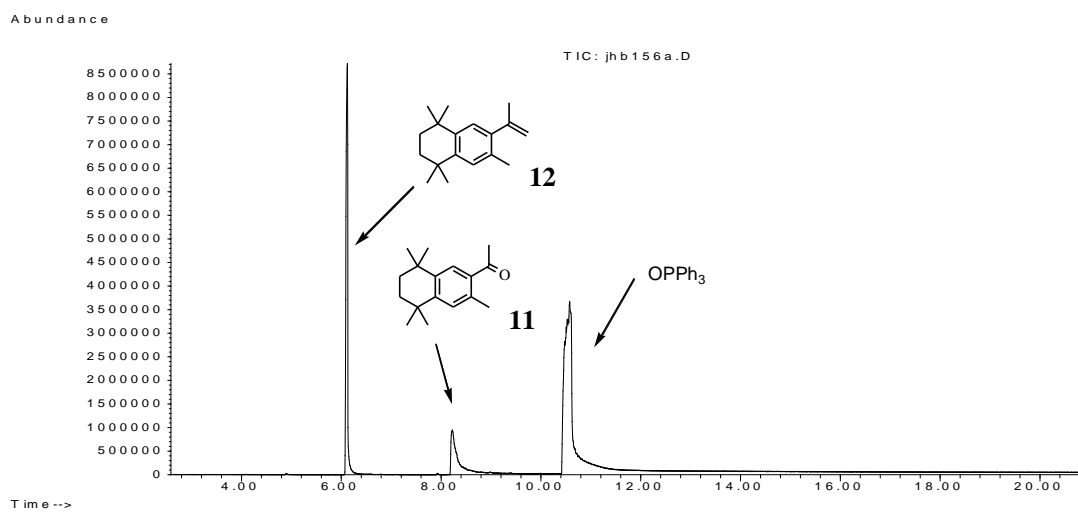


Figure 2.12 GC (TIC) of the reaction of **11** with $\text{PPh}_3\text{CH}_3\text{I}$ to give **12** after 48 h

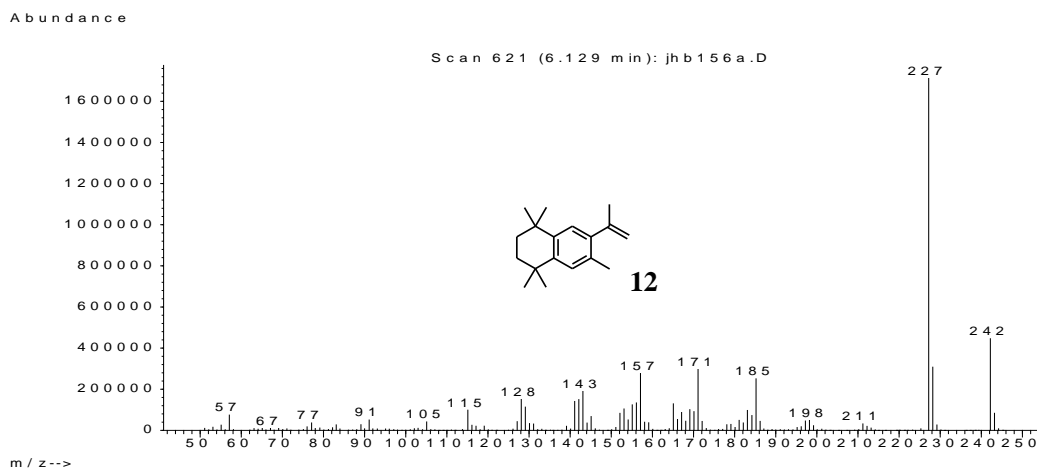


Figure 2.13 MS of **12**.

Monoclinic single crystals ($P2_1/c$) of olefin **12** were obtained by the slow evaporation of a diethyl ether/hexafluorobenzene solution. In **12** the olefinic moiety forms a dihedral angle of 80° with the benzene ring, due to steric interactions with the C(18) *ortho*-methyl group on the arene ring (**Figure 2.14**).

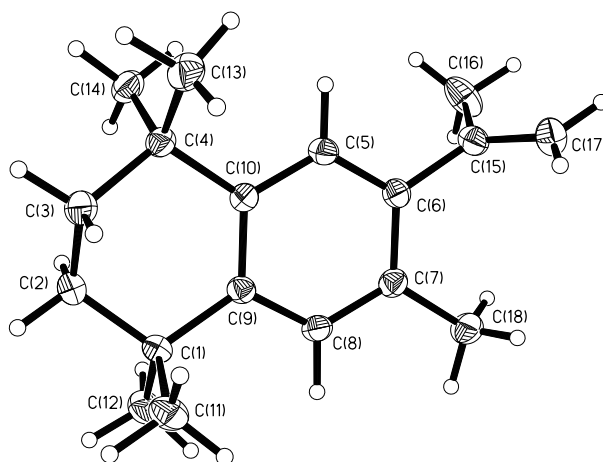
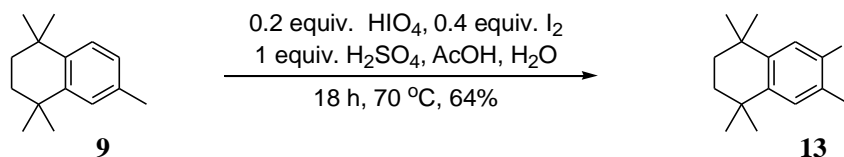


Figure 2.14 The molecular structure of olefin **12**. Thermal ellipsoids are drawn at 50% probability.

Alternatively, olefin **12** could be synthesised *via* a borylation/Suzuki-Miyaura cross-coupling route, analogous to the synthesis of **7**. Due to the poor results obtained in the direct borylation of **9** alternative routes to the *ortho*-methylated boronate ester **10a** were sought. Iodination of **9** with I_2/HIO_4 in $AcOH/H_2O/H_2SO_4$ gave iodide **13**. Although substoichiometric amounts of I_2 were employed, *in situ* GC-MS analysis showed that full consumption of **9** occurred, with **13** being the sole species observed (**Equation 2.6**).



Equation 2.6 Iodination of **9** with HIO_4/I_2 to give **13**.

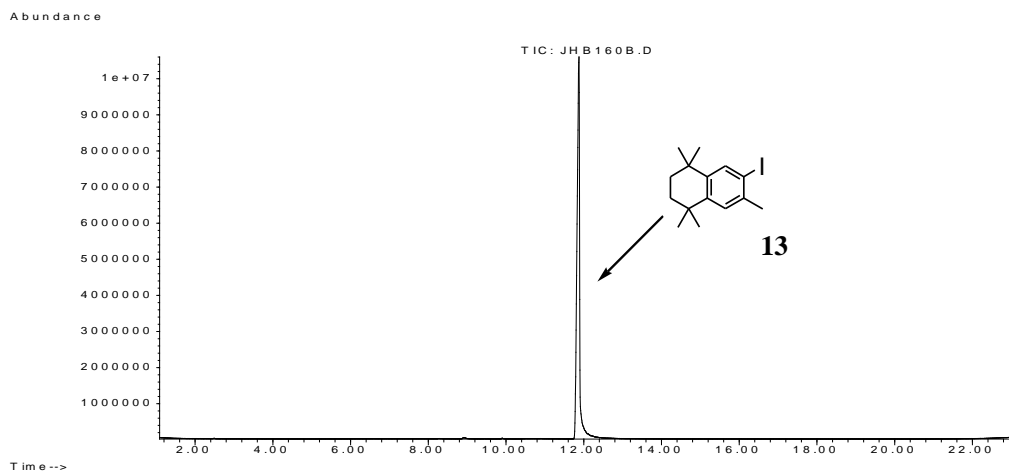


Figure 2.15 GC (TIC) for the iodination of **9** with I_2/HIO_4 to give **13** after 18 h.

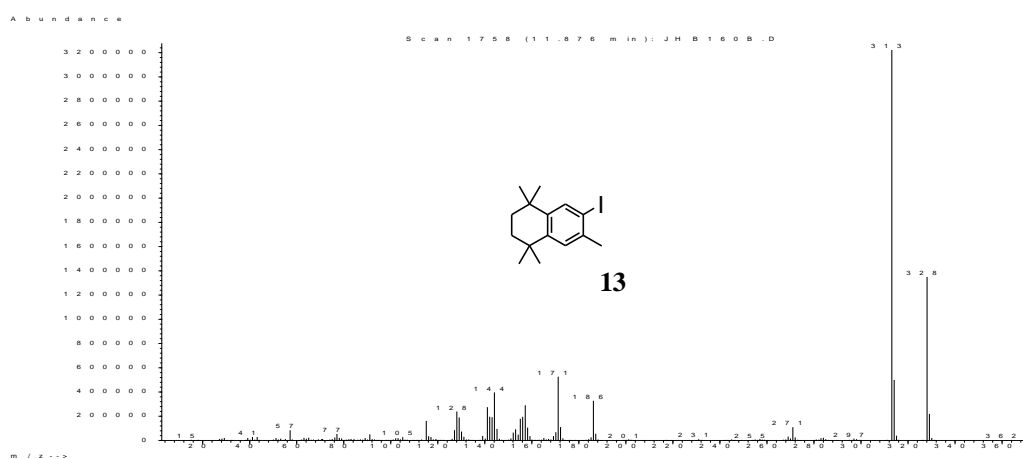
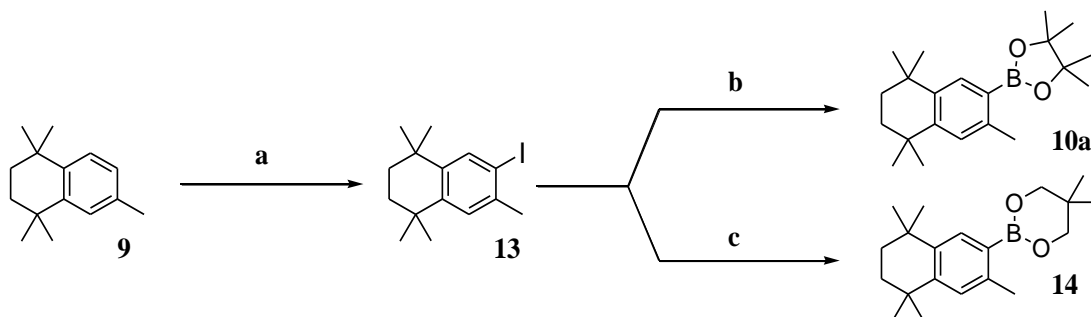


Figure 2.16 MS of **13**.

Miyaura borylation²⁸² of **13** with B_2pin_2 and KOAc in the presence of 5 mol % $Pd(dppf)Cl_2$ required heating at 80 °C for a full week in DMF for the reaction to be complete. The use of DMSO as solvent reduced the reaction time to 4 days under the same conditions. Gratifyingly, exchanging B_2neop_2 for B_2pin_2 gave a marked improvement, with reactions in both DMF and DMSO giving full conversion after 18 hours of heating (**Equation 2.7**). Similar results have been reported in the literature, with Wang and coworkers suggesting that the lesser steric demand of B_2neop_2 , compared to B_2pin_2 , led to the increase in reactivity, although a detailed explanation was not given.^{283, 284} Although a variety of approaches have been taken to the Pd-catalysed borylation of reluctant substrates,²⁸⁵ the use of B_2neop_2 as a more active borylating agent has not been widely explored.



a 0.2 equiv. HIO_4 , 0.4 equiv. I_2 , 1 equiv. H_2SO_4 , AcOH, H_2O , 70°C , 18 h, 64%

b 1 equiv. B_2pin_2 , 5 mol % $\text{Pd}(\text{dppf})\text{Cl}_2$, 2 equiv. KOAc, DMSO, 80°C , 4 d, 60%

c 1 equiv. B_2neop_2 , 5 mol % $\text{Pd}(\text{dppf})\text{Cl}_2$, 2 equiv. KOAc, DMSO, 80°C , 18 h, 67%

Equation 2.7 Palladium-catalysed borylations of **13** with B_2pin_2 and B_2neop_2 .

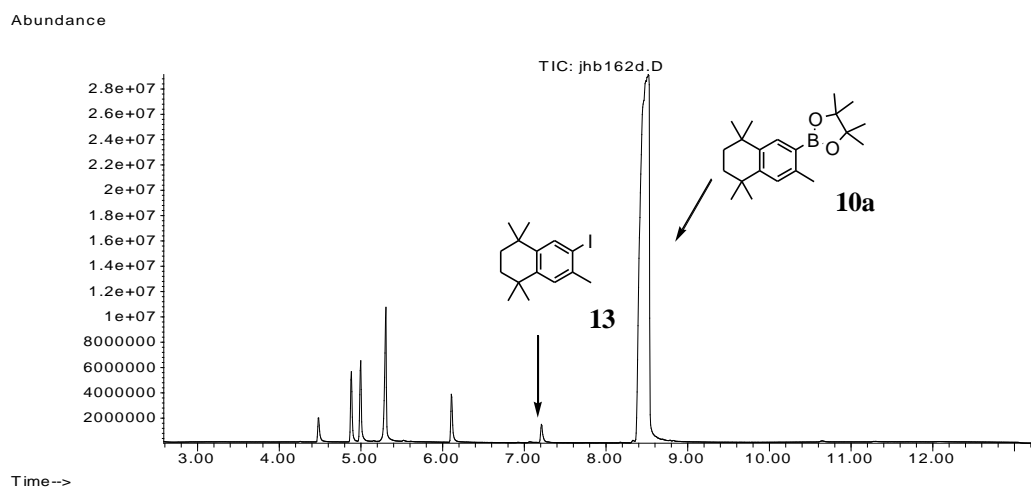


Figure 2.17 GC (TIC) of the borylation of **13** with B_2pin_2 to give **10a** after 96 h.

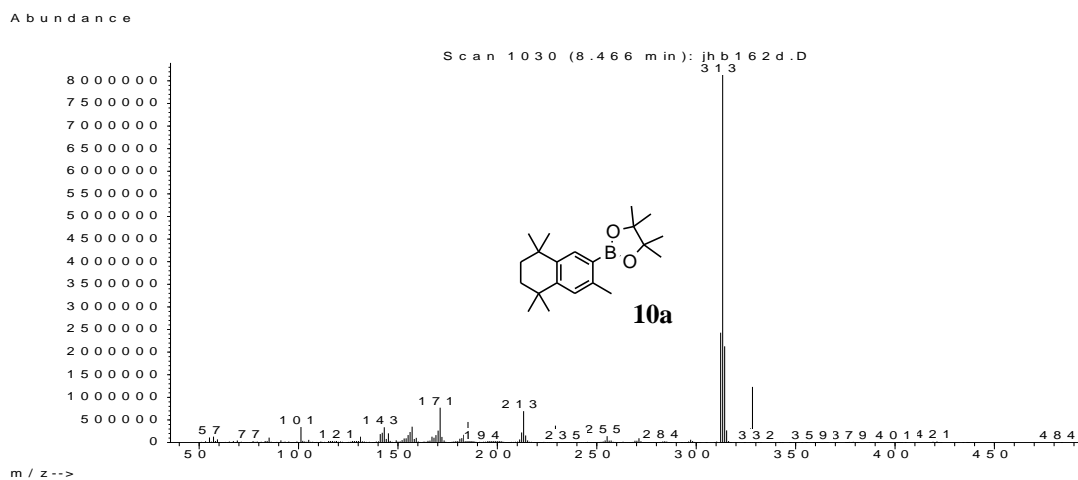


Figure 2.18 MS of **10a**.

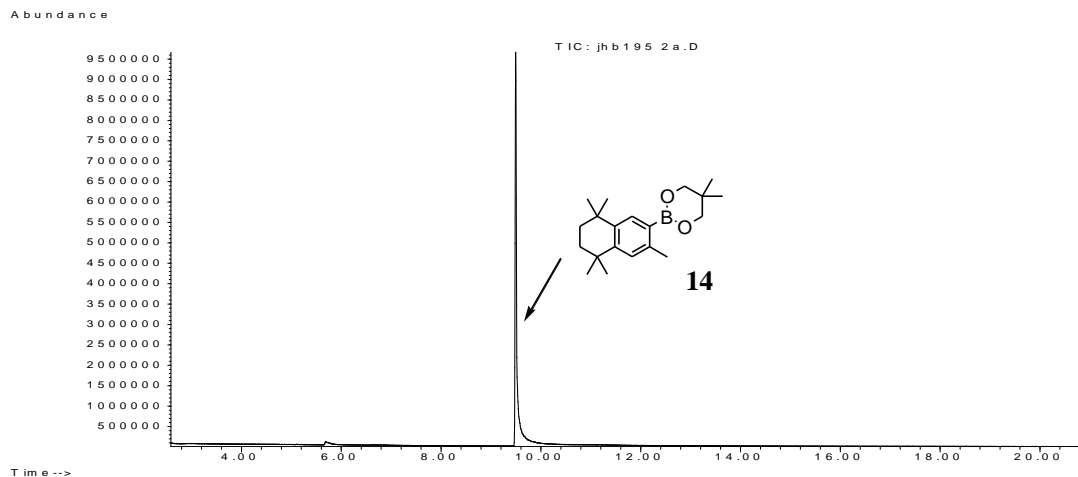


Figure 2.19 GC (TIC) of the borylation of **13** with B_2neop_2 to give **14** after 18 h.

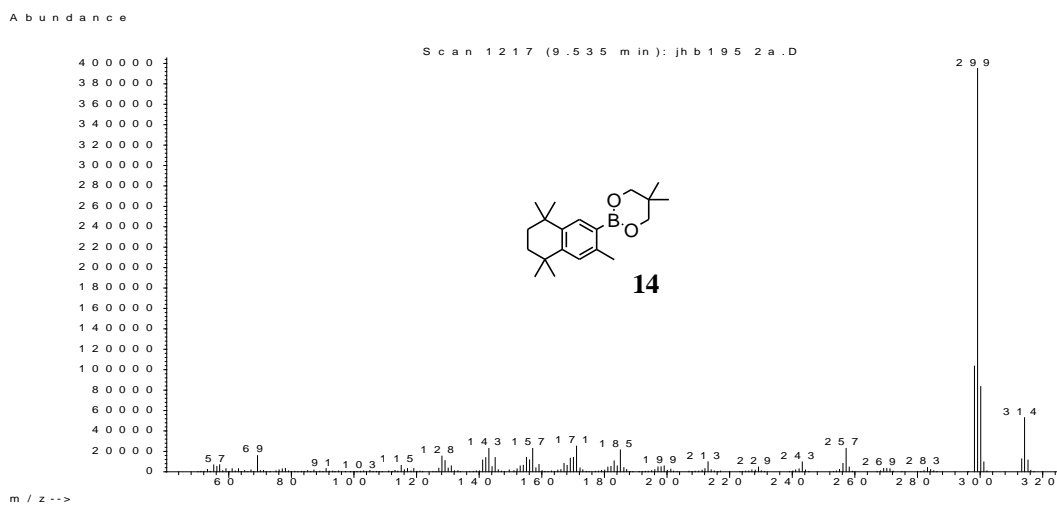


Figure 2.20 MS of **14**.

Monoclinic single crystals (*Pc*) of **10a** were grown from a MeOH / DCM solution at -20 °C (**Figure 2.21**).

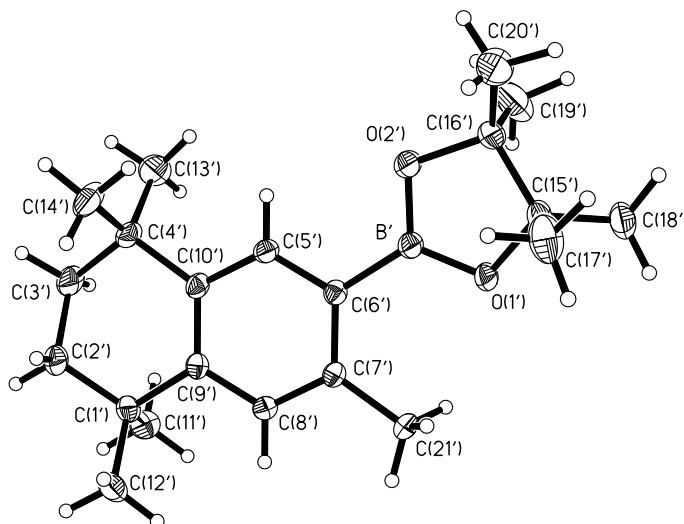


Figure 2.21 The molecular structure of **10a** showing the non-disordered molecule of **10a** in the asymmetric unit. The disordered molecule of **10a** is not shown for clarity. Thermal ellipsoids are drawn at 50% probability.

For **10a**, the asymmetric unit comprises of two molecules, one of which has the alkyl ring and its methyl substituents disordered between two conformations with occupancies 0.626(4) and 0.374(4) (**Figure 2.22**). The methyl C(21) and the B atom deviate slightly from the arene plane in opposite directions, by 0.03 and -0.03 Å in the disordered molecule, and by 0.05 and -0.01 Å in the ordered molecule. The angles between the arene and C(6)BO₂ planes are 2.5° and 6.7° , respectively. (**Figure 2.22**).

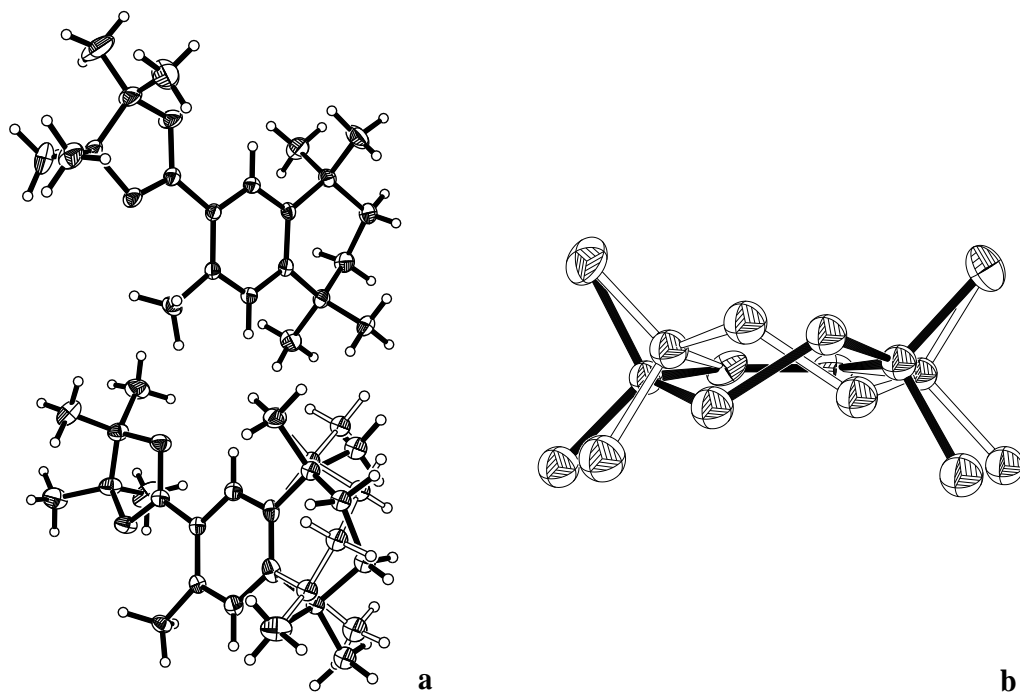


Figure 2.22 (a) The molecular structure of **10a** with two independent molecules in the asymmetric unit, showing the disorder of one of the two molecules of **10a**, (b) disorder in alkyl ring of one of the molecules of **10a**. All hydrogen atoms, the C(21) methyl group and the Bpin group are removed for clarity. Thermal ellipsoids are drawn at 50% probability.

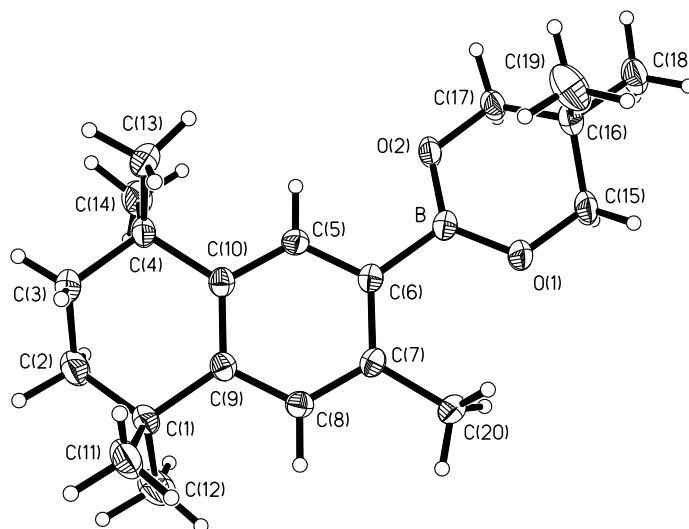
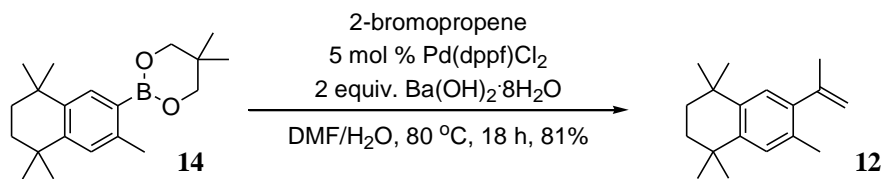


Figure 2.23 The molecular structure of **14**. Thermal ellipsoids are drawn at 50% probability.

Tetragonal crystals ($I4_1/a$) of compound **14** (the neopentane glycolate analogue of **10a**) were grown from a MeOH solution at $-20\text{ }^\circ\text{C}$ (**Figure 2.23**).

In comparison to **10a**, the molecular structure is more strained for **14**, where the arene ring undergoes a small but significant twist of 4.7° between the C(6)–C(7) and C(9)–C(10) bonds. The boron and methyl C(20) atoms are displaced from the mean plane of the ring in opposite directions, by 0.13 and -0.14 \AA , i.e. substantially more than in **10a**. Even so, the intramolecular non-bonding contact O(1)...C(20) of $2.863(2)\text{ \AA}$ in **10** is shorter than the corresponding contacts in **10a**, O(1)...C(21) $2.923(2)$ and O(1')...C(21') $2.942(2)\text{ \AA}$. The angle between the arene and C(6)BO₂ planes is 8.6° , and the 6-membered boryl ring adopts an envelope conformation with the C(16) atom out-of-plane by 0.67 \AA (**Figure 2.13**). Thermal ellipsoids are drawn at 50% probability.

Due to its more rapid synthesis, in comparison to compound **10a**, compound **14** was utilized as the coupling partner in the Suzuki-Miyaura cross coupling to give **12**. The reaction with 2-bromopropene, in the presence of 5 mol % Pd(dppf)Cl₂ catalyst and 2 equivalents of Ba(OH)₂·8H₂O base was carried out in a 5:1 mixture of DMF/H₂O at $80\text{ }^\circ\text{C}$ to give **12** in a high yield (**Equation 2.8**).



Equation 2.8 Synthesis of **12** via Suzuki-Miyaura cross-coupling of **14** with 2-bromopropene.

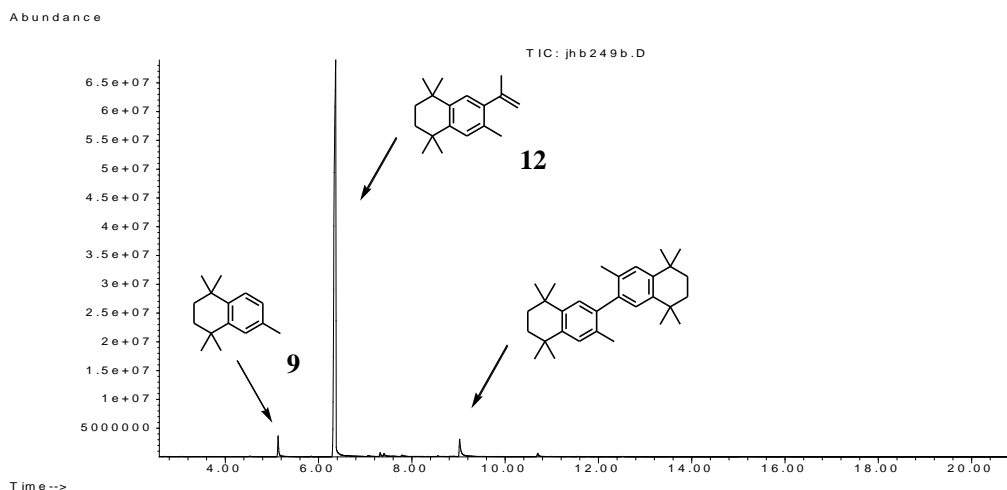
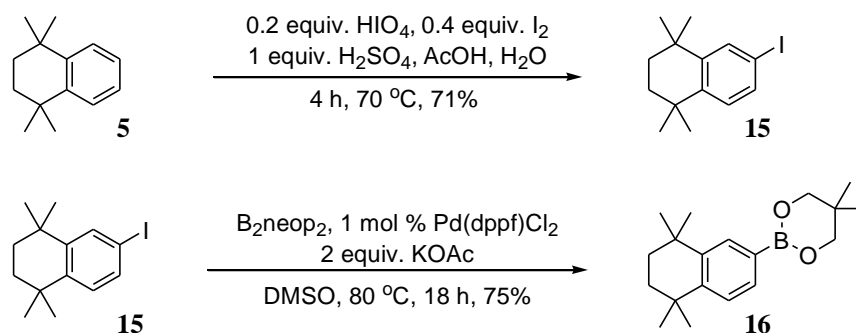


Figure 2.24 GC (TIC) of the reaction of **14** with 2-bromopropene to give **12** after 18 h.

Although compound **6** could be synthesised *via* Pd-catalysed borylation,²⁶ direct C-H borylation is a more efficient route. However, for reasons not yet understood, Ir-catalysed aromatic C-H borylation is currently not effective with B_2neop_2 , making this attractive route to the $Bneop$ analogue of **6** unavailable. Iodination of **5** with I_2/HIO_4 , under the same conditions utilized for the synthesis of **13**, gave iodide **15**.²⁸⁶ Although substoichiometric amounts of I_2 were employed, *in situ* GC-MS analysis showed that full consumption of **5** had occurred after 4 hours, with **15** being the sole species. The borylation of iodide **15** with B_2neop_2 was performed with 1 mol % $Pd(dppf)Cl_2$ catalyst and 2 equivalents of KOAc base in anhydrous DMSO and resulted in the full conversion, after 18 hours at 80 °C, of iodide **15** to the boronate ester **16** (**Equation 2.8**).



Equation 2.9 Synthesis of **16** *via* iodination of **5** and subsequent Miyaura borylation with B_2neop_2 .

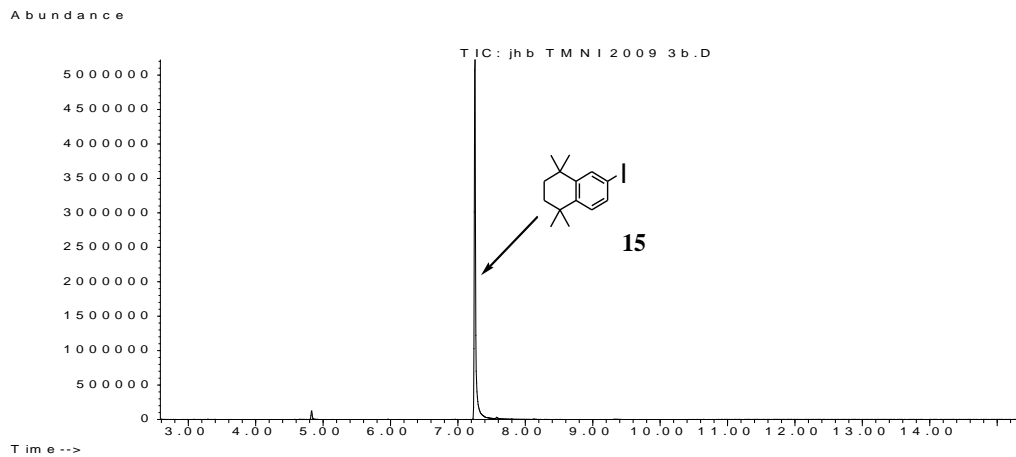


Figure 2.25 GC (TIC) of the iodination of **5** with I_2/HIO_4 to give **15** after 4 h

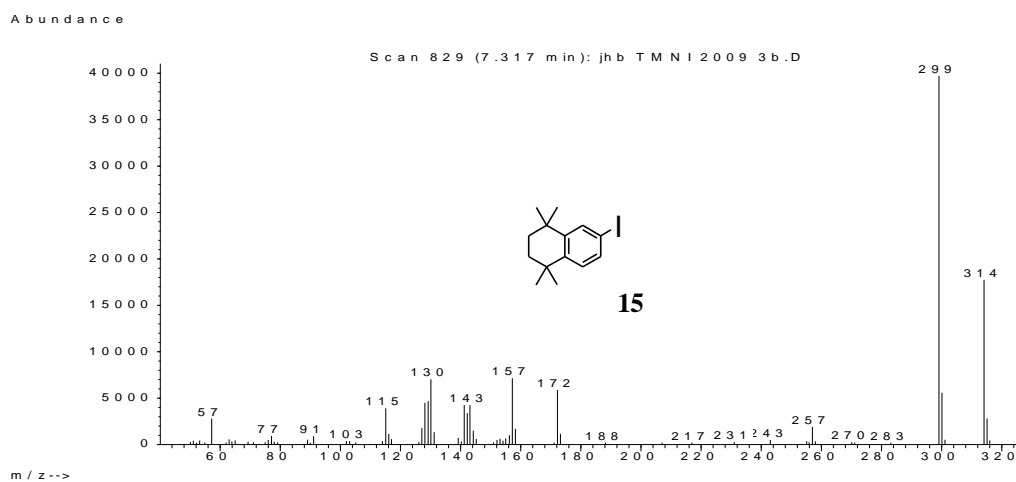


Figure 2.26 MS of **15**.

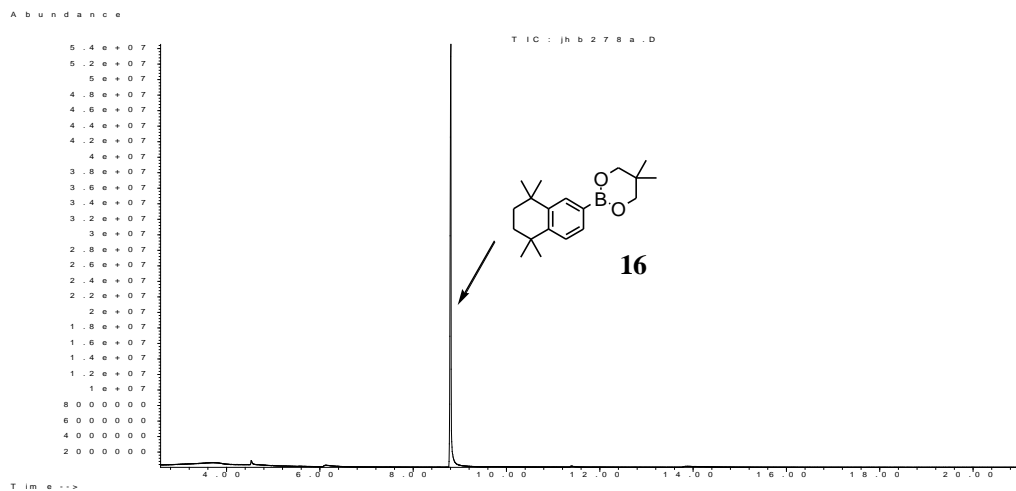


Figure 2.27 GC (TIC) of the borylation of **15** with B_2neop_2 to give **16** after 18 h.

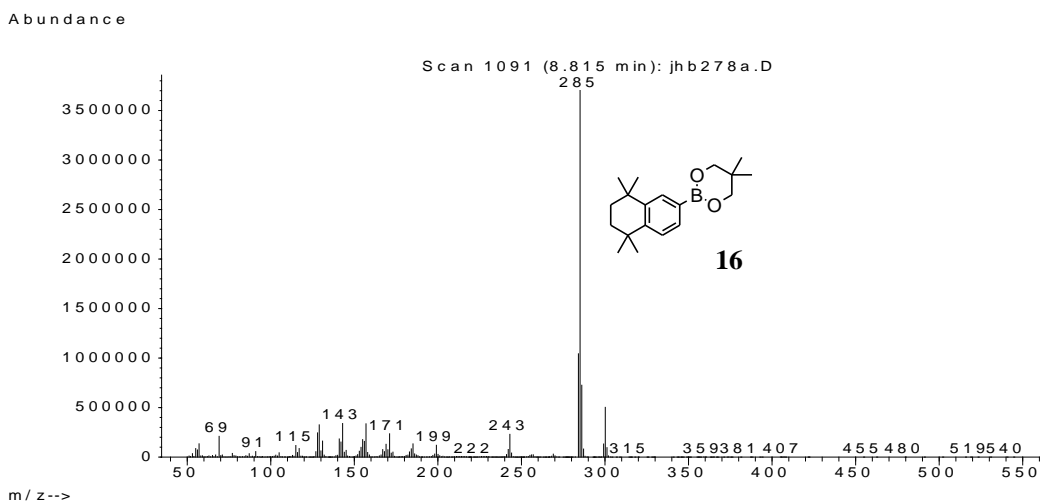


Figure 2.28 MS of **16**.

Orthorhombic single crystals (*Pbca*) of **16** were grown from a concentrated MeOH solution at $-20\text{ }^{\circ}\text{C}$ (**Figure 2.29**).

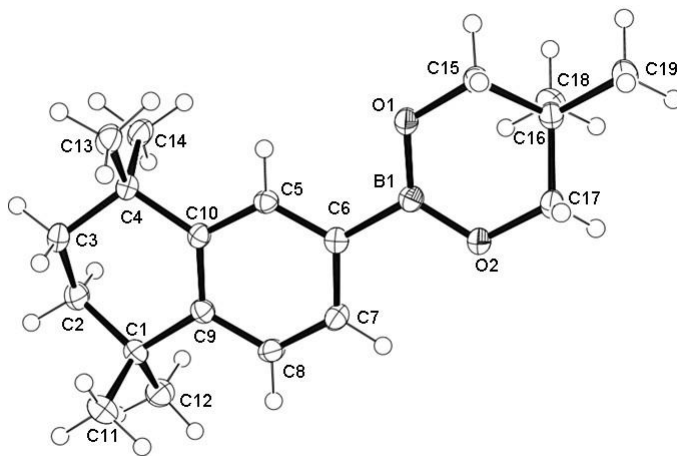
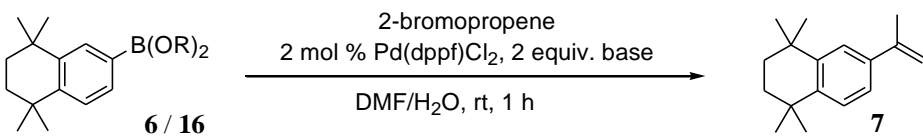


Figure 2.29 The molecular structure of **16**. Thermal ellipsoids are drawn at 50% probability.

The six-membered boryl ring adopts an envelope conformation with the dimethylated atom C(16) is tilted by 0.68 \AA from the mean plane of the remaining five atoms, which is inclined to the benzene ring plane by only 2.2° (**Figure 2.29**). Interestingly, the differences in relative rates of formation of **10a** and **14** were not observed in their subsequent Suzuki-Miyaura cross-couplings with 2-bromopropene to give the product **12**. Thus, reactions of **10a** and **14** at both 80 and $40\text{ }^{\circ}\text{C}$ gave similar results, as did analogous

reactions of the non-*ortho*-methylated aryl boronate esters **6** and **16**. In an attempt to ascertain whether the nature of the base affected the relative activities of Ar-Bpin and Ar-Bneop substrates in Suzuki-Miyaura cross-couplings, aryl boronates **6** and **16** were coupled to 2-bromopropene in the presence of 2 mol % Pd(dppf)Cl₂ with a range of bases at room temperature in a 5:1 mixture of DMF/H₂O to give the product **7** (**Table 2.1**). The reactions were examined by *in situ* GC-MS after 1 hour (i.e. at partial conversion).

Table 2.1 Effects of base on Suzuki-Miyaura cross-couplings of **6** and **16** with 2-bromopropene to give **7**

		
Base	With 6 (Bpin) Protodeborylation / 6 / 7	With 16 (Bneop) Protodeborylation / 16 / 7
Ba(OH) ₂	3 / 48 / 49	6 / 63 / 31
K ₃ PO ₄	9 / 39 / 52	8 / 51 / 41
K ₂ CO ₃	20 / 58 / 19	20 / 54 / 26
KOAc	47 / 52 / 1	31 / 67 / 2

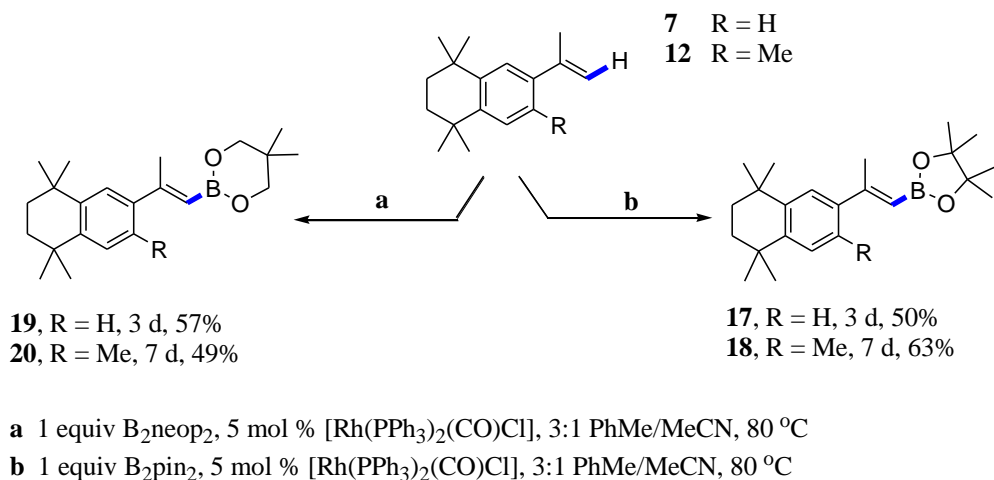
Results for the Suzuki-Miyaura cross-coupling of aryl boronates **6** and **16** with 2-bromopropene in the presence of 2 mol % Pd(dppf)Cl₂ after 1 h at 20 °C. Product ratios were determined by GC-MS.

It is proposed that under the mild conditions required to prevent unwanted Suzuki-Miyaura cross-coupling in the borylation of **13** with B₂pin₂ or B₂neop₂, the use of the more Lewis acidic B₂neop₂ leads to more favorable coordination of the weakly basic Pd(II)(dppf)Ar(OAc) intermediate and thus more facile transmetallation. Under the Suzuki-Miyaura conditions used for the biaryl coupling, with strong bases such as hydroxide and phosphate, transmetallation is rapid, leading to the negligible differences observed in the reactivities of the aryl and vinyl boronates. It was also noted that for the strong bases KOH and K₃PO₄, the Suzuki-Miyaura reaction of **6** is marginally faster than that of **16**, whereas for K₂CO₃ the reverse is observed. Thus, it may be suggested that, under mild conditions, B₂neop₂ and neopentane glycolate boronate esters may be more effective coupling partners than B₂pin₂ and pinacolboronate esters, though this effect is nullified by the use of more forcing conditions. In addition, it must be noted that although in Suzuki-Miyaura cross-couplings with 2-bromopropene, the Bneop aryl boronate ester

16 is a marginally poorer coupling partner, full conversion of **16** to **7** (and of Bneop ester **14** to **12**) can be achieved after heating at 80 °C for 1 h in the presence of 2 mol % Pd(dppf)Cl₂ and 2 equivalents of Ba(OH)₂·8H₂O. This, in conjunction with the more rapid synthesis of the Bneop ester **14** from **13**, makes the use of Bneop aryl boronate esters attractive intermediates for Pd-catalysed borylation/Suzuki-Miyaura reaction sequences.

As noted above, dehydrogenative borylation of 1,1-disubstituted alkenes, using *trans*-[Rh(PPh₃)₂(CO)Cl] as catalyst precursor, offers an attractive method for the synthesis of 1,1-disubstituted vinylboronate esters (VBEs) which cannot be accessed *via* alkyne hydroboration, and yields air and moisture stable products (in contrast to Zr-catalysed carboalumination of alkynes²⁸⁷) which may be coupled with organic halides to give trisubstituted alkenes in high yields and stereoselectivities.²⁸⁸ In contrast, Heck-Mizoroki reactions of α -methylstyrenes are characterised by low conversions and poor selectivities arising from β -hydride elimination pathways giving vinylic and allylic products.²⁸⁹

Alkenes **7** and **12** underwent dehydrogenative borylation with either B₂pin₂ or B₂neop₂ in the presence of *trans*-[Rh(PPh₃)(Cl)CO] at 80 °C, with a 3:1 mixture of toluene and MeCN being the optimal solvent system. *E*-vinyl boronate products were obtained with high stereoselectivities, with no sacrificial hydrogenation of the substrate alkene observed (**Equation 2.10**). Borylations of **12** were noticeably slower than those of **7** and did not proceed past 70% conversion, although the precise origin of this effect is not known. It is possible that either increased steric hindrance or partial loss of conjugation between the alkene and arene π -systems, *vide infra*, are responsible. In addition, no improvement in reaction rate was observed for borylations carried out with B₂neop₂.



Equation 2.10 Dehydrogenative borylations of **7** and **12** to give **17**, **18**, **19** and **20**.

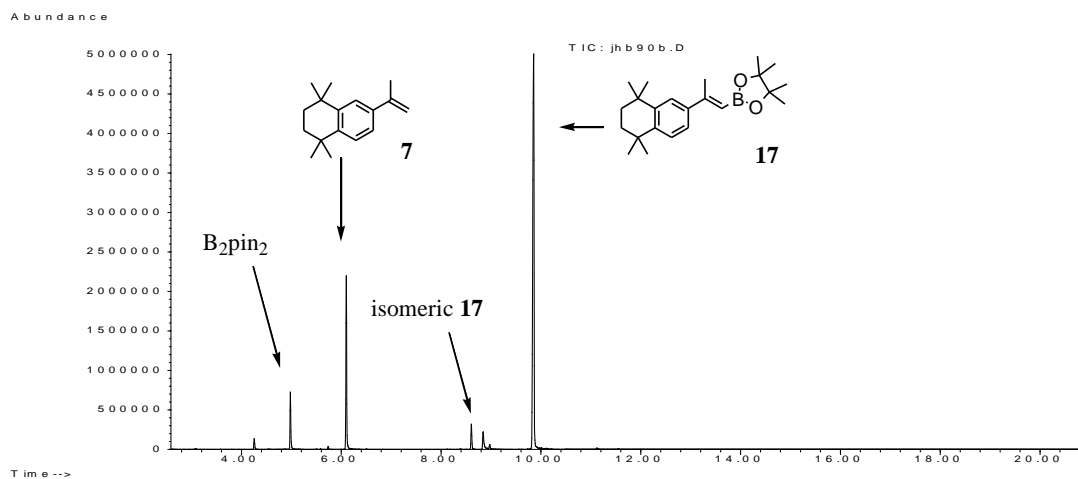


Figure 2.30 GC (TIC) of the dehydrogenative borylation of **7** with B₂pin₂ to give **17** after 48 h.

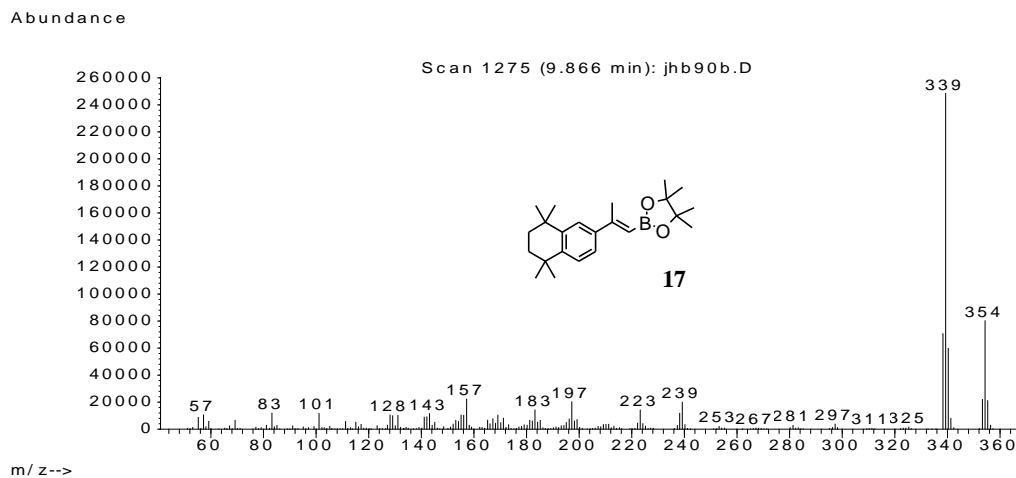


Figure 2.31 MS of **17**.

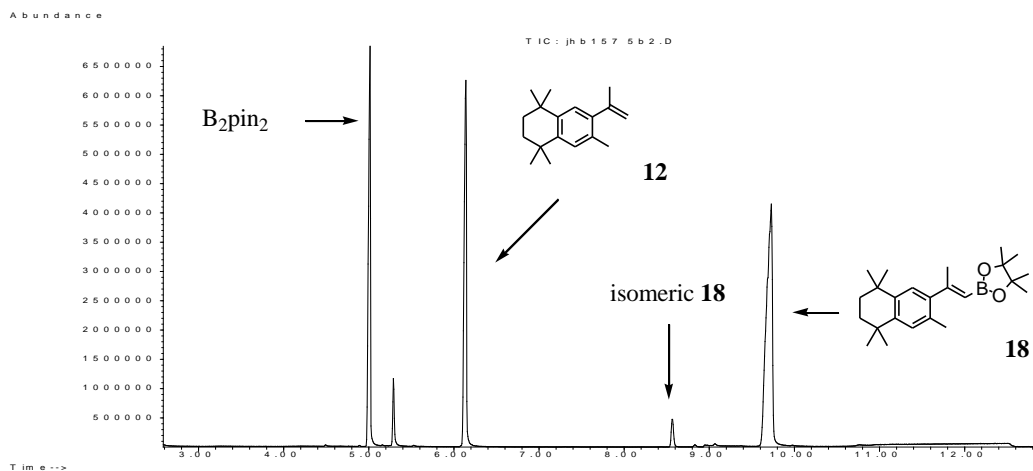


Figure 2.32 GC (TIC) of the dehydrogenative borylation of **12** with B_2pin_2 to give **18** after 72 h.

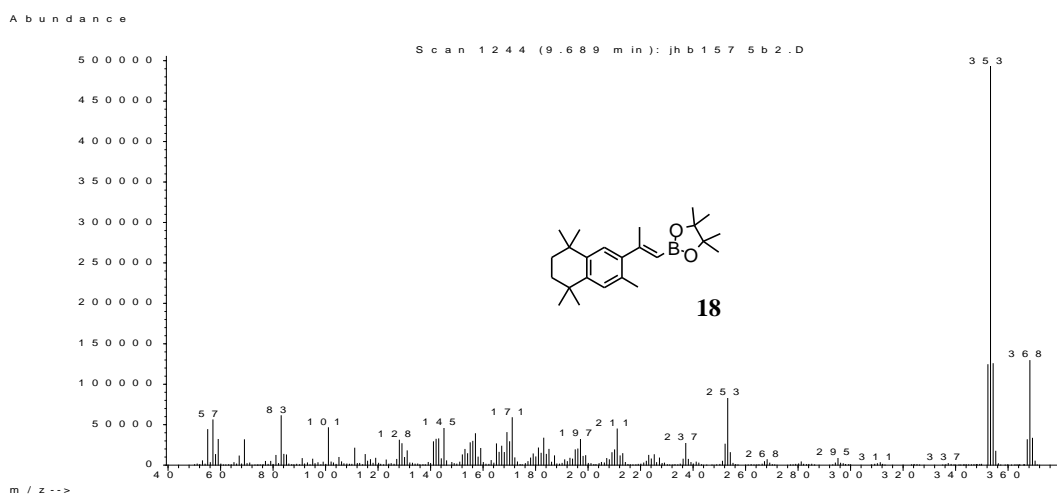


Figure 2.33 MS of **18**.

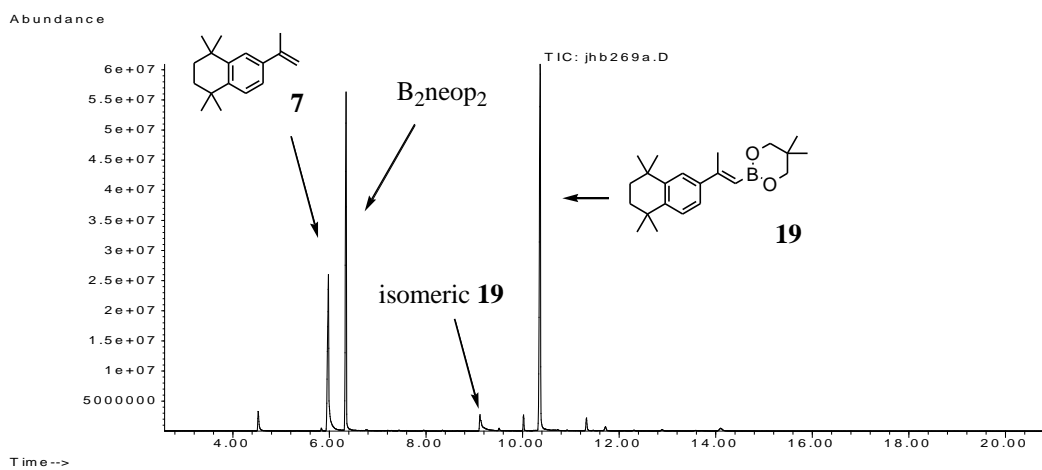


Figure 2.34 GC (TIC) of the dehydrogenative borylation of **7** with B_2neop_2 to give **19** after 48 h.

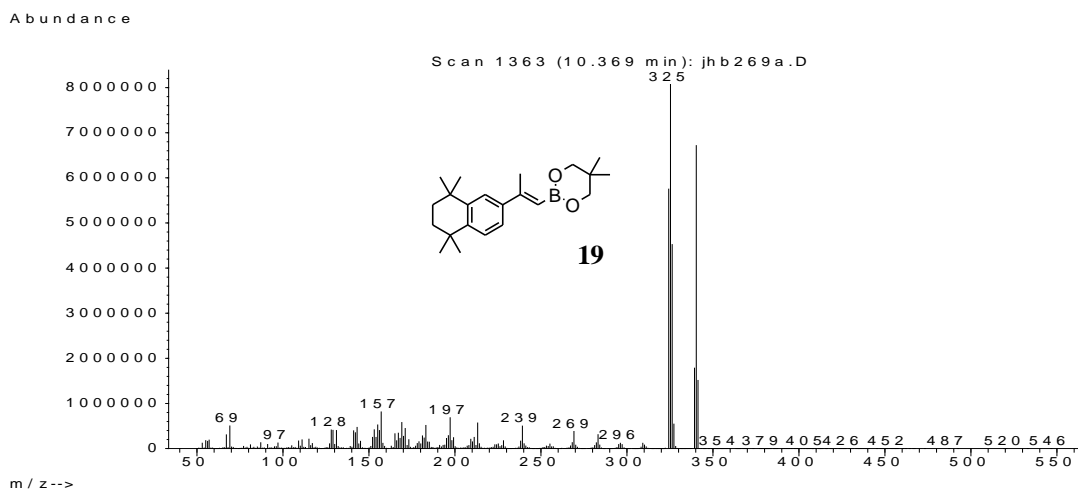


Figure 2.35 MS of 19.

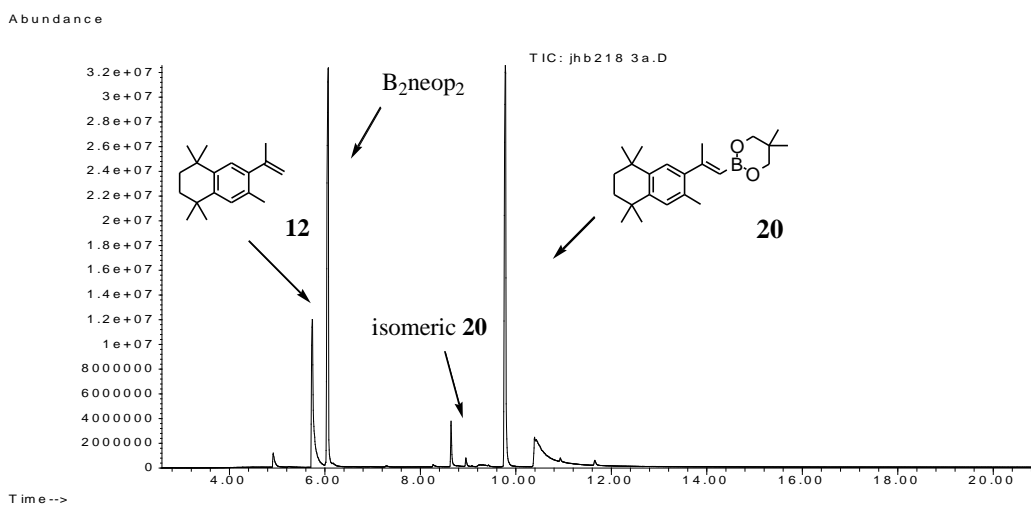


Figure 2.36 GC (TIC) of the dehydrogenative borylation of 12 with B₂neop₂ to give 20 after 72 h.

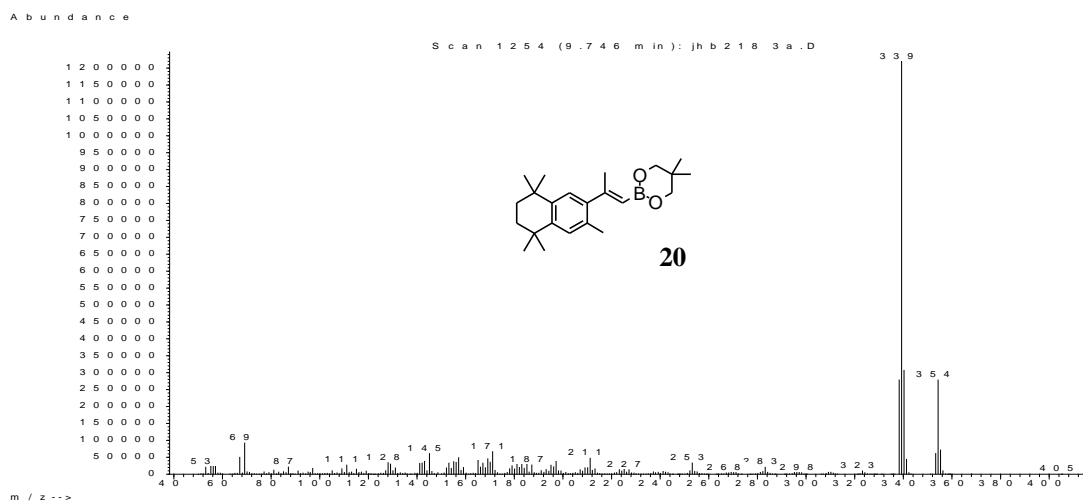


Figure 2.37 MS of 20.

The Suzuki-Miyaura cross-coupling of vinyl boronate ester **17** directly with 4-iodobenzoic acid led to TTNPB **3**. However, analysis of the reaction mixture and subsequent purification of the product was extremely troublesome, making this route inefficient. Despite these drawbacks, monoclinic single crystals ($P2_1/c$) of TTNPB (the acid form of **21**) were grown *via* slow evaporation of a $CDCl_3$ solution of TTNPB derived from the coupling described above. TTNPB crystallised as doubly hydrogen bonded dimers with its inversion equivalent. The carboxylic C-O bond distances C(24)-O(1) 1.278(4) and C(24)-O(2) 1.257(4) Å are nearly symmetrical, suggesting a double-minimum hydrogen bond O(1)...O(2'), in agreement with the electron density distribution along this vector. Two hydrogen atom positions, H(01) and H(02), were included in the final refinement with occupancies of 0.6 and 0.4, respectively. The planes of the arene ring (*i*), olefinic moiety (*ii*), the benzene ring (*iii*) and the carboxylic group (*iv*) were found to form dihedral angles: *i/ii* 41.2, *ii/iii* 31.9, *i/iii* 73.3 and *iii/iv* 3.9° (**Figure 2.38**).

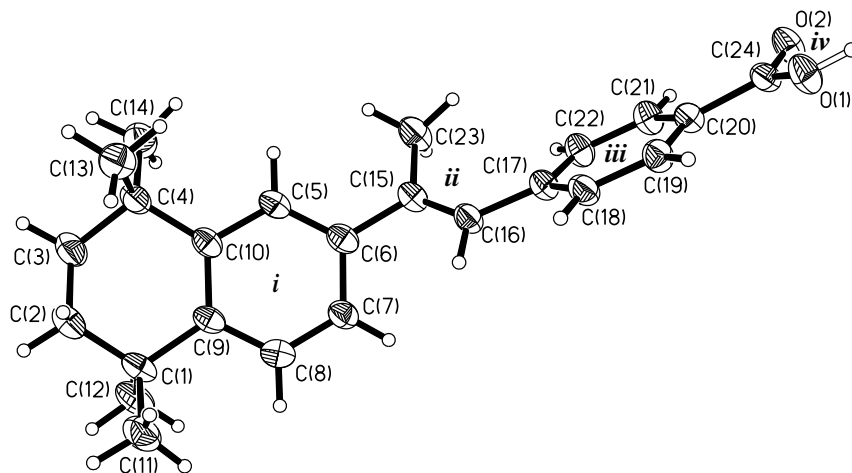
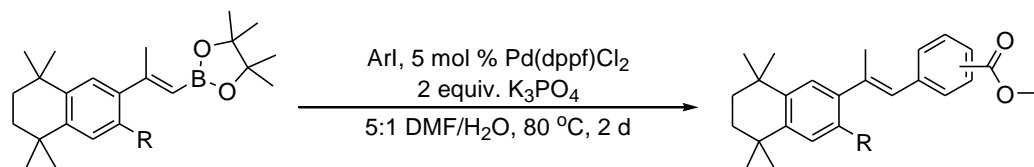


Figure 2.38 Molecular structure of TTNPB. Shown as one half of its doubly hydrogen bonded dimer. Thermal ellipsoids are drawn at 50% probability.

In contrast to the cross-couplings with iodobenzoic acids, the use of 3-, and 4-iodobenzoic acid methyl esters as coupling partners, allowed for easy analysis and purification of products **21**, **22**, **23** and **24** in high yields (**Equation 2.11**).



21, R = H, Ar = 4-C₆H₄CO₂Me, 84%; **22**, R = H, Ar = 3-C₆H₄CO₂Me, 75%;
23, R = Me, Ar = 4-C₆H₄CO₂Me, 86%; **24**, R = Me, Ar = 3-C₆H₄CO₂Me, 86%

Equation 2.11 Suzuki-Miyaura reactions of **17** and **18** with aryl iodides to give **21**, **22**, **23** and **24**.

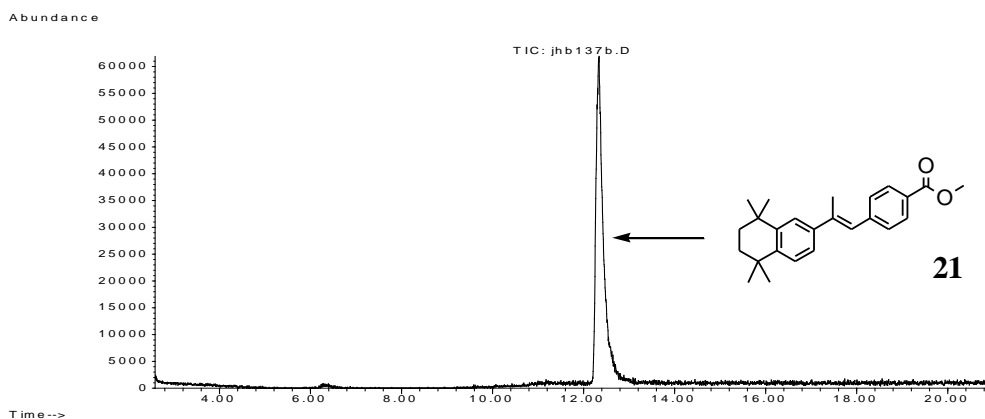


Figure 2.39 GC (TIC) of the Suzuki-Miyaura reaction of **17** and 4-C₆H₄-CO₂Me to give **21** after 48 h.

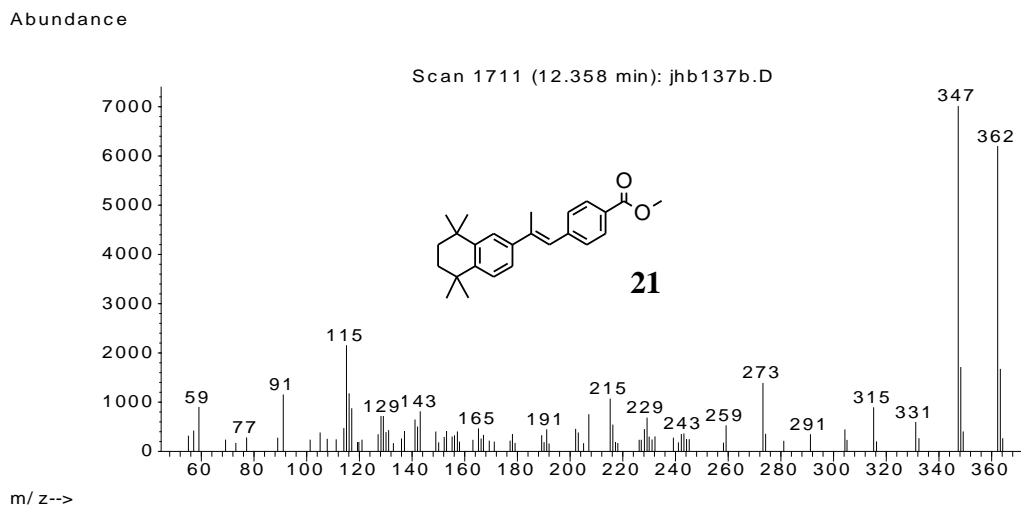


Figure 2.40 MS of **21**.

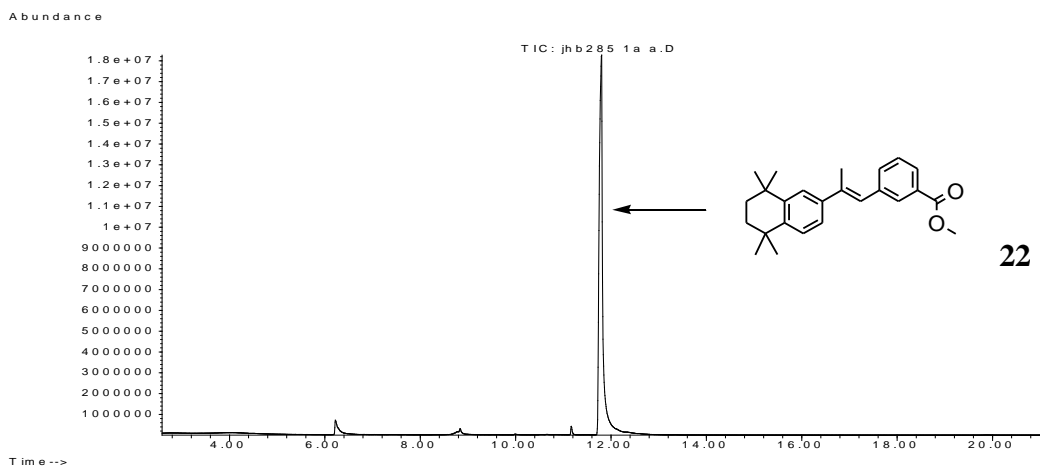


Figure 2.41 GC (TIC) of the Suzuki-Miyaura reaction of **17** and 3-C₆H₄-CO₂Me to give **22** after 48 h.

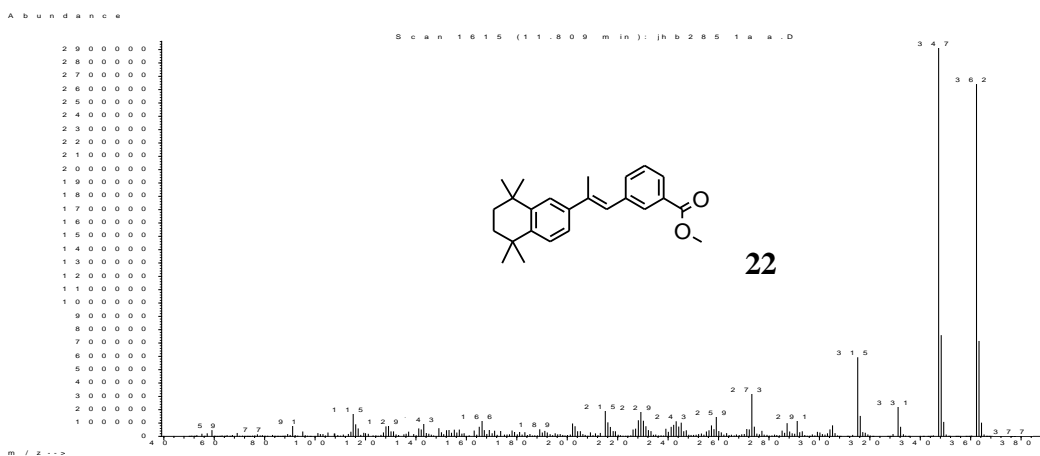


Figure 2.42 MS of **22**.

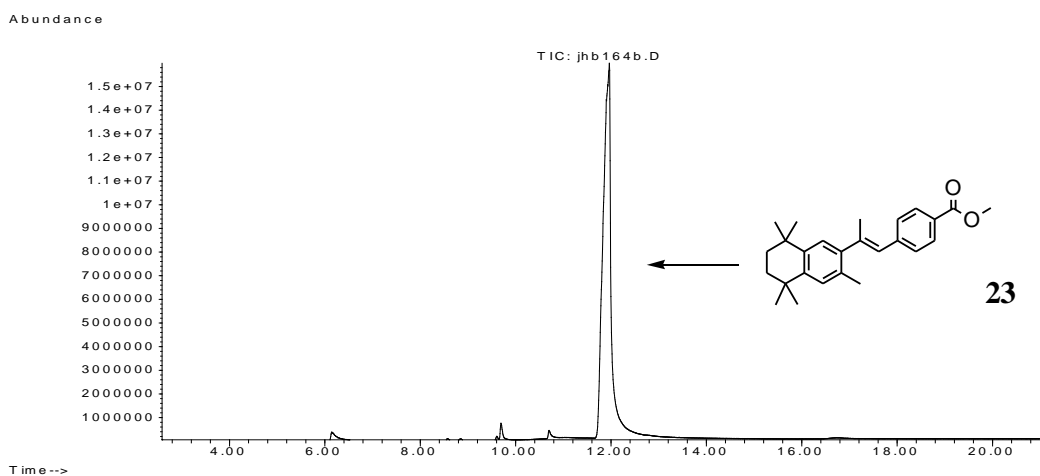


Figure 2.43 GC (TIC) of the Suzuki-Miyaura reaction of **18** and 4-C₆H₄-CO₂Me to give **23** after 48 h.

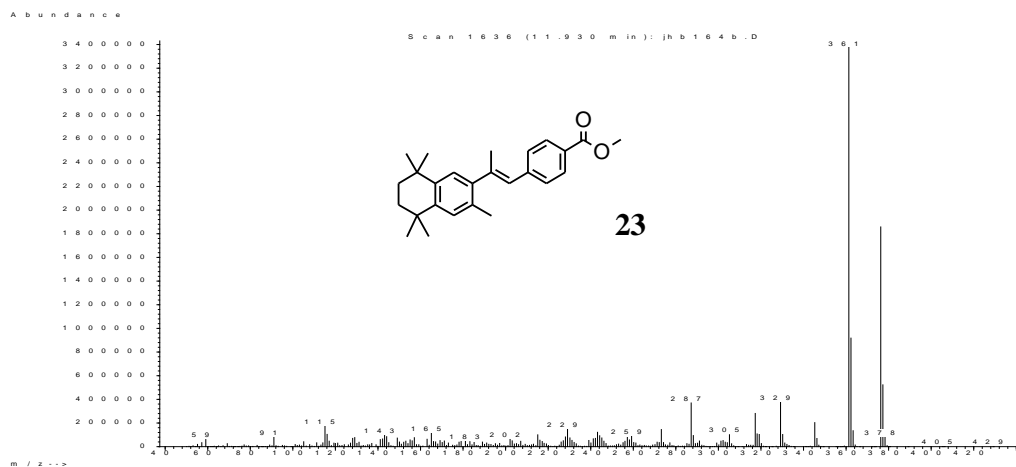


Figure 2.44 MS of 23.

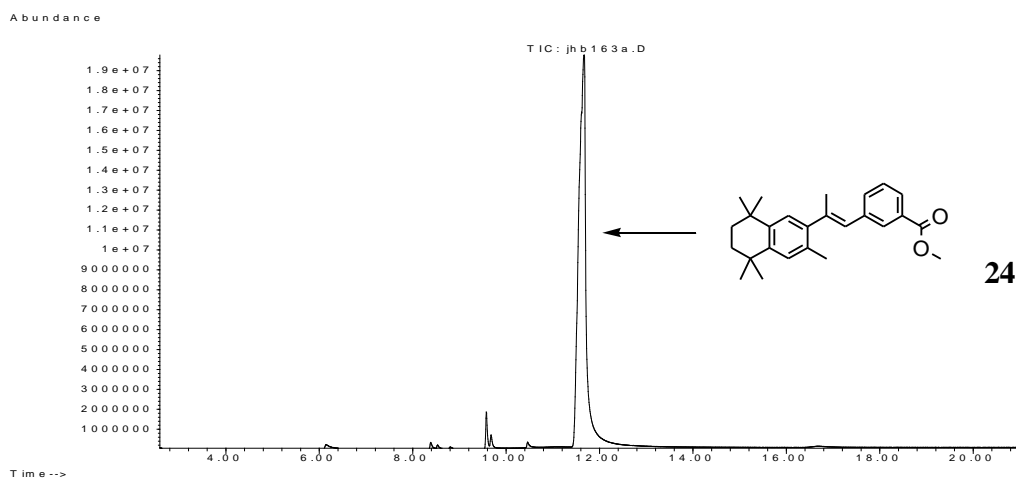


Figure 2.45 GC (TIC) of the Suzuki-Miyaura reaction of 18 and 3-C₆H₄-CO₂Me to give 25 after 48 h.

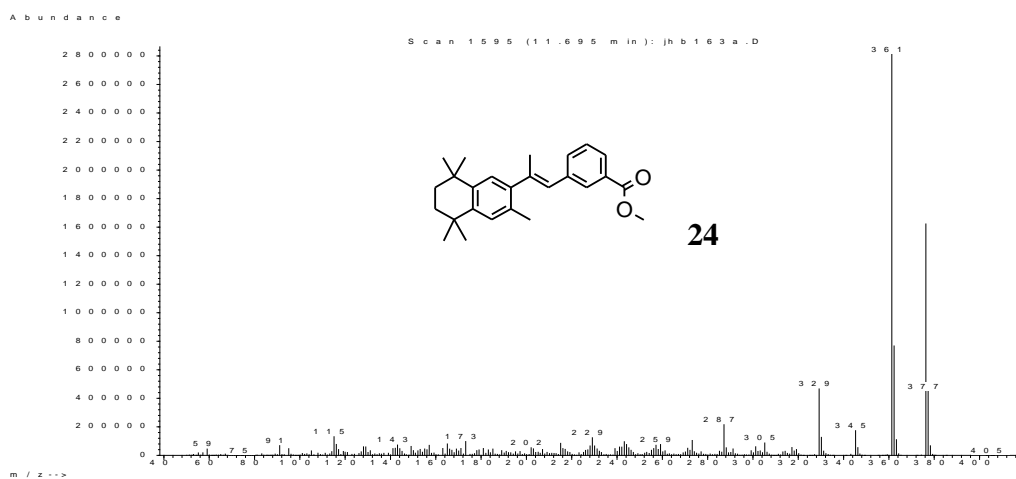


Figure 2.46 MS of 24.

Monoclinic single crystals ($P2_1/c$) of TTNPB methyl esters **22** were grown *via* slow evaporation from a hexane solution.

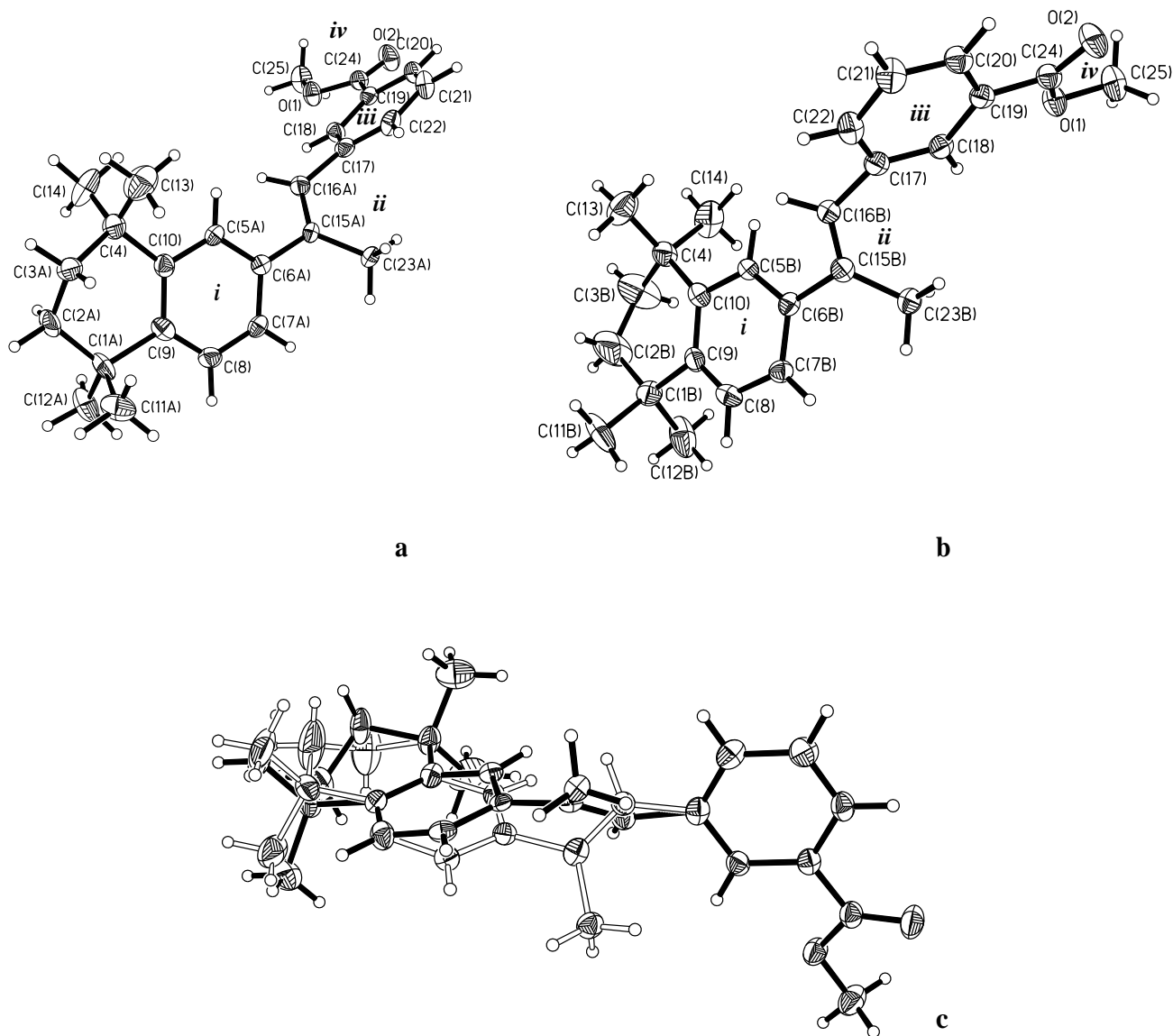


Figure 2.47 Molecular structures of compound **22** in conformations A and B (**a** and **b**, respectively). Superimposition of both conformations of compound **22** (**c**). Thermal ellipsoids are drawn at 50% probability for all figures.

For **22**, the crystal is disordered with equal probability between two conformations (*A* and *B*) with the exceptions being the C(4), C(8), C(9), C(10), C(11), C(12) atoms (with their attached hydrogens) and the benzoate methyl ester moiety which are ordered. The dihedral angles between the planes of the arene ring (*i*), olefinic moiety (*ii*), the benzene ring (*iii*) and the carboxylate group (*iv*) were found to be *i/ii* 41.4, *ii/iii* 51.4, and *i/iii* 88.2° for conformation *A* and 42.0, 42.2 and 83.8° for conformation *B*, respectively. The *iii/iv* angle equals 14.9° in both *A* and *B*.

Monoclinic single crystals ($P2_1/c$) of compound **23** were grown *via* the slow evaporation of a MeOH solution.

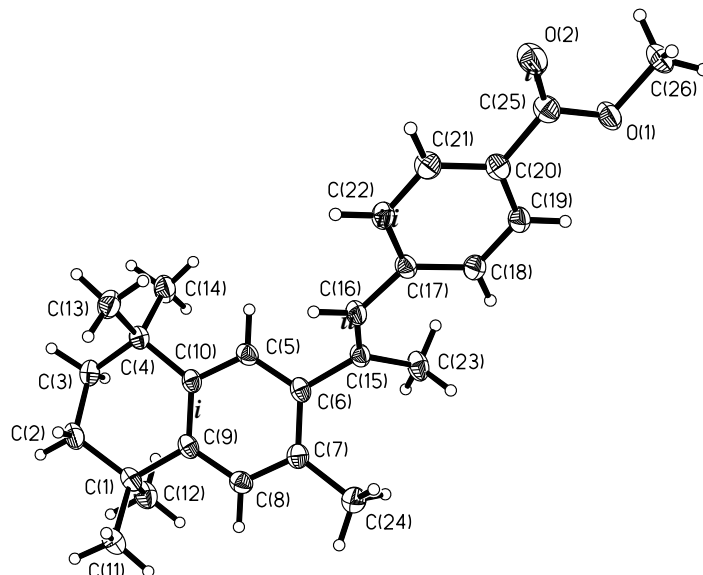


Figure 2.48 Molecular structure of compound **23**. Thermal ellipsoids are drawn at 50% probability.

For **23**, the dihedral angles between the planes of the arene ring (*i*), olefinic moiety (*ii*), the benzene ring (*iii*) and the carboxylic group (*iv*) were found to be *i/ii* 56.1°, *ii/iii* 11.1, *i/iii* 45.0° and *iii/iv* 5.5°.

2.2.2 Discussion of the relative solid and solution state structures of TTNPB esters and their vinylic precursors

The effects of addition of a methyl group (or larger substituents) to the *ortho* position of TTNPB on the biological activity have been widely documented and may result from steric interactions between the 3-substituent and the vinylic proton which induces an increase in the dihedral angle between the aryl ring of the hydrophobic terminus and the alkene moiety, giving a bent a conformation similar to that of 9cRA.

Comparison of the molecular structures of **12**, **17** and **23** with those of **18**, **1** and **22** shows that for *ortho* methylated species, the presence of the 3-substituent makes planar conformations unfavourable. In alkene **12**, the olefinic moiety forms a dihedral angle of 80° with the benzene ring, however crystallographic comparison with **7** was not possible as **7** is a liquid at both room temperature and -20 °C.

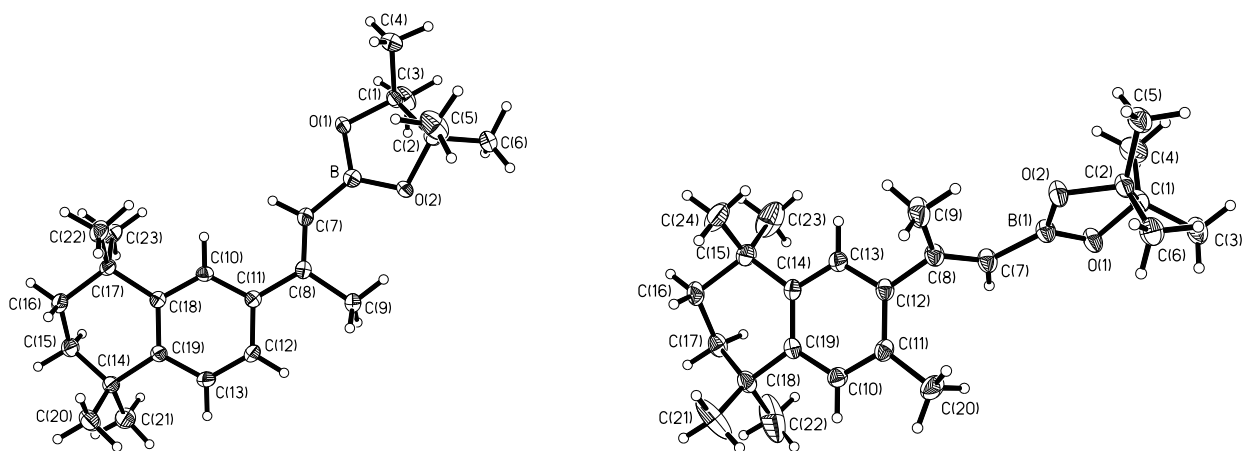


Figure 2.49 Comparison of the molecular structures of **17** and **18**, showing the increase in the dihedral angle between the arene and olefin planes caused by the *ortho*-methyl group in **18** over **17**. Disorder of the Bpin group is removed for clarity in **17**. Disorder of the C(15)C(16)C(17)C(18) alkyl group is removed for clarity in **18**. Thermal ellipsoids are drawn at 50% probability.

In vinylboronate ester **17**, the olefinic fragment C(9)C(8)C(7)B(1) is planar within experimental error, and is inclined by 6.2° to the arene plane. In the *ortho*-methylated

vinylboronate ester **18** the conformation is altered drastically. Due to steric crowding, the olefinic moiety is twisted by 3.4° around the double bond, while its *mean* plane is inclined by 60.3° to the arene plane (**Figures 2.49**)

For TTNPB the dihedral angle between the planes of the benzene ring of the hydrophobic unit and the olefinic moiety is 41.2° . For **23**, the ester of the *ortho*-methylated analogue 3-Me TTNPB, steric interactions between the *ortho*-methyl group and the olefinic moiety lead to an increased dihedral angle of 56.1° (**Figure 2.50**). In the case of **22** direct crystallographic comparison with its *ortho*-methylated analogue **24** was not achieved, but the dihedral angle between the planes of the benzene ring of the hydrophobic unit *i* and the olefinic moiety *ii* was found to be either 41.4 or 42.0° (for the two conformations of **22** present in the unit cell), values similar to that of TTNPB.

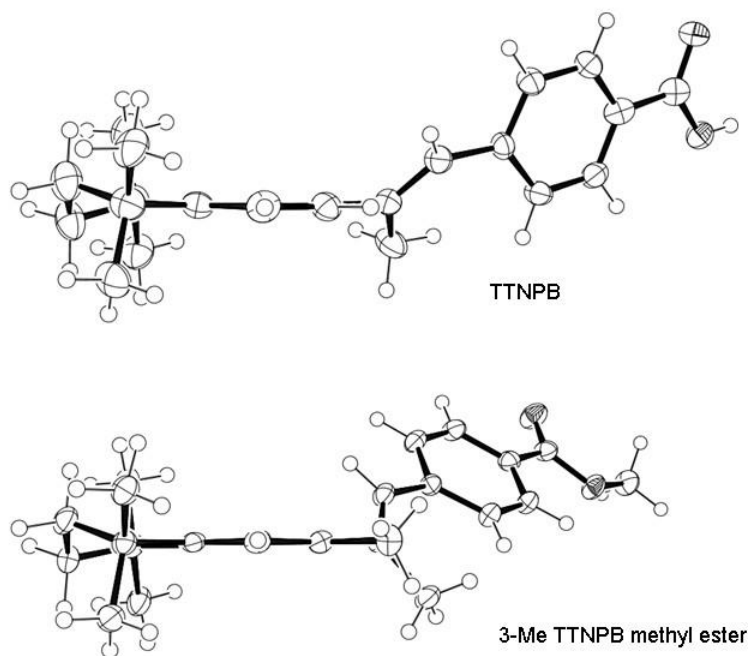


Figure 2.50 Comparison of TTNPB and 3-Me TTNPB methyl ester **23**, showing the increase in the *i/ii* dihedral angle caused by the *ortho*-methyl group in **23**. Thermal ellipsoids are drawn at 50% probability.

Although comparisons of solid state structures are useful, information about the relative solution conformations of the methylated and non-methylated compounds detailed above is necessary as the solid state structures might be influenced by intermolecular interactions (i.e. packing effects). In this case, the use of UV-vis spectrometry is highly

beneficial. Comparisons of λ_{\max} values give information on the relative degrees of conjugation, and therefore twist, in compounds which differ only by the presence of an *ortho*-methyl group (**Table 2.2**). This is especially useful for pairs of compounds for which suitable single crystals could not be obtained for one or both members (i.e. **7** and **12**, where **7** is a liquid at room temperature and at -20 °C).

Table 2.2 UV-vis spectrometry data of TTNPB esters and vinylic precursors

Compound	λ_{\max} (nm) / CHCl ₃	ϵ (L mol ⁻¹ cm ⁻¹) / CHCl ₃
7	246	10900
12	252	4540
17	270	18600
18	253	9500
19	268	10500
20	255	9100
21	309	29500
22	284	22800
23	288	17500
24	241, 268	24800, 16200

Comparison of λ_{\max} values showed that for related pairs of vinylboronate esters and TTNPB methyl esters, the incorporation of an *ortho*-methyl group led to a blue shift in λ_{\max} of between 21 and 13 nm. For Bpin and Bneop vinylboronates **17**, **18**, and **19**, **20**, respectively, the nature of the boronate ester moiety did not greatly affect λ_{\max} . In **21**, **22**, **23**, and **24** conjugation extends throughout the stilbene moiety to the electron withdrawing ester group, with λ_{\max} values for *para*-retinoid esters **21** and **23** being red shifted by 25 and 20 nm compared with their *meta*-substituted analogues, **22** and **24**, respectively. The addition of *ortho*-methyl groups led to blue shifts in the λ_{\max} values of 21 and 16 nm for the *para*-, and *meta*-TTNPB esters, respectively.

2.3 Conclusions

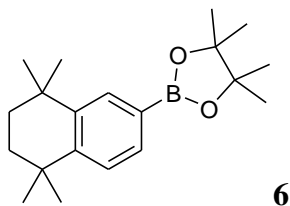
In conclusion, concise and stereoselective syntheses of the methyl esters of the highly active TTNPB series of synthetic retinoids has been achieved. The approach, based upon combinations of Ir-, and Rh-catalysed C-H borylations of unactivated arenes and alkenes to give aryl-, and vinyl-boronate esters, and subsequent Suzuki-Miyaura cross-couplings gave the products in good yields, with excellent regio-, and stereoselectivities, exemplifying the synthetic utility of these transformations. The effect of adding an *ortho*-methyl group, well documented in biological studies, has been studied both crystallographically and spectroscopically, and shown to induce an increase in dihedral angle between the arene and olefin planes, giving twisted conformations which may be proposed to be more like those adopted by the endogenous retinoid 9cRA than for ATRA, hence resulting in the increase in RXR selectivity often shown for *ortho*-methylated retinoids.

2.4 Experimental

General Experimental

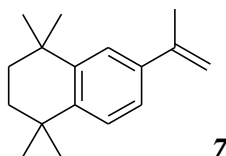
All reactions were carried out under a dry nitrogen atmosphere using standard Schlenk techniques or in an Innovative Technology Inc. System 1 double-length glove box. Glassware was oven dried before transfer into the glove box. Hexane and THF were dried over sodium / benzophenone and acetonitrile was dried over CaH₂ and all were distilled under nitrogen. The solvents 1,4-dioxane, DMF, MTBE, THF and DMSO and H₂O were degassed by 3 freeze-pump-thaw-cycles. Toluene was dried and deoxygenated by passage through columns of activated alumina and BASF-R311 catalyst under Ar pressure using a locally modified version of the Innovative Technology Inc. SPS-400 solvent purification system. The compound 1,1,4,4-tetramethyl-1,2,3,4-tetrahydronaphthalene, **5**, was purchased from Avocado Chemical Company or from Maybridge and was dried over CaH₂ and distilled. [Ir(μ-Cl)(COE)₂]₂,²⁹⁰ [Ir(μ-OMe)COD]₂,²⁹¹

trans-[Rh(PPh₃)₂(CO)Cl]^{292,293} and the Wittig reagent [Ph₃PMe]I²⁹⁴ were synthesised by literature procedures. B₂pin₂ was supplied as a gift by Frontier Scientific Inc., NetChem Inc. and AllyChem Co. Ltd. Hydrochloric acid was obtained from Fisher Scientific and all other compounds were obtained from Aldrich Chemical Company, tested for purity by GC-MS and used without further purification. NMR spectra were recorded at ambient temperature on Varian Inova 500 (¹H, ¹³C{¹H}, HSQC), Varian C500 (¹H, ¹³C{¹H}, HSQC, HMBC Bruker 400 Ultrashield (¹H, ¹³C{¹H}, ¹¹B and ¹¹B{¹H}), Varian Unity 300 (¹¹B and ¹¹B{¹H}) and Bruker AC200 (¹³C{¹H}) instruments. Proton and carbon spectra were referenced to external SiMe₄ *via* residual protons in the deuterated solvents or solvent resonance respectively. ¹¹B NMR spectra were referenced to external BF₃·OEt₂. UV-vis and fluorescence measurements were recorded in CHCl₃. UV-vis absorption spectra and extinction coefficients were obtained on a Hewlett-Packard 8453 diode array spectrophotometer using standard 1 cm quartz cells. Fluorescence spectra were recorded on a Horiba Jobin-Yvon Fluoromax-3 spectrophotometer. The spectra of dilute solutions with absorbance maxima of less than 0.1 were recorded using conventional 90 degree geometry. The emission spectra were fully corrected using the manufacturer's correction curves for the spectral response of emission optical components. Elemental analyses were conducted in the Department of Chemistry at Durham University using an Exeter Analytical Inc. CE-440 Elemental Analyser. GC-MS analyses were performed on a Hewlett-Packard 5890 Series II gas chromatograph equipped with a 5971 mass selective detector and a 7673 autosampler or on an Agilent 6890 Plus GC equipped with a 5973N MSD and an Anatune Focus robotic liquid handling system / autosampler. A fused silica capillary column (10 m or 12 m, cross-linked 5% phenylmethylsilicone) was used, and the oven temperature was ramped from 50 °C to 280 °C at a rate of 20 °C/min. UHP grade helium was used as the carrier gas. The screw-cap autosampler vials used were supplied by Thermoquest Inc. and were fitted with Teflon / silicone / Teflon septa and 0.2 mL micro inserts. HRMS spectra were recorded in the Department of Chemistry at Durham University using a Thermo Finnigan LTQ FT Ultra Hybrid mass spectrometer.



6

4,4,5,5-Tetramethyl-2-(5,5,8,8-tetramethyl-5,6,7,8-tetrahydronaphthalen-2-yl)-[1,3,2]-dioxaborolane (6).²⁷⁶ In a dry, N₂ filled glove box, a solution of [Ir(OMe)COD]₂ (0.16 g, 0.24 mmol) and 4,4'-di-*tert*-butyl-2,2'-bipyridine (0.13 g, 0.48 mmol) in hexane (3 mL) was shaken vigorously and added to a solution of 1,1,4,4-tetramethyl-1,2,3,4-tetrahydronaphthalene, **5**, (3.0 g, 15.9 mmol) and B₂pin₂ (4.45 g, 17.5 mmol) in hexane (12 mL) in a thick walled glass tube fitted with a Young's tap. The mixture was heated at 80 °C until GC-MS analysis showed the reaction to be complete (18 h). The reaction mixture was passed through a short silica gel column (hexane as eluent). The hexane was evaporated and the residue was recrystallised from MeOH giving **6** as a white powder (4.71 g, 95%); mp 115-117 °C; IR (KBr disc, cm⁻¹) 2966, 2857, 1607, 1553, 1466, 1408, 1358, 1314, 1294, 1267, 1210, 1144, 1117, 1099; UV-vis (CHCl₃) λ_{max} (ε) 243 nm (2730 L mol⁻¹ cm⁻¹); λ_{em} (CHCl₃) 298 nm; m/z (EI-MS) 314 (15%, M⁺), 299 (100%, M⁺ - Me); ¹H NMR (400.13 MHz, C₆D₆) δ 8.23 (1H, s), 8.01 (1H, d, *J* = 8.0 Hz), 7.26 (1H, d, *J* = 8.0 Hz), 1.52 (4H, s), 1.19 (6H, s), 1.15 (6H, s) 1.06 (12H, s); ¹³C{¹H} NMR (100.13 MHz, C₆D₆) δ 148.35, 144.22, 133.97, 132.70, 126.39, 88.55, 35.55, 35.40, 34.54, 34.40, 31.94, 31.82, 24.95, the resonance of the carbon attached to boron was not observed; ¹¹B{¹H} NMR (128.37 MHz, C₆D₆) δ 31.30; elemental analysis calcd. (%) for C₂₀H₃₁BO₂: C 76.44, H 9.94; found: C 76.15, H 9.93.

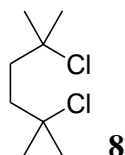


7

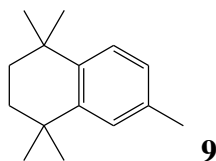
6-Isopropenyl-1,1,4,4-tetramethyl-1,2,3,4-tetrahydronaphthalene (7).²⁷⁷ In a dry, N₂ filled glovebox, Pd(dppf)Cl₂ (64 mg, 0.08 mmol), compound **6** (0.80 g, 2.6 mmol), 2-

bromopropene (0.73 g, 3.3 mmol), and Ba(OH)₂·8H₂O (1.77 g, 5.2 mmol) were added to a thick walled glass tube fitted with a Young's tap along with degassed DMF (10 mL) and degassed H₂O (2 mL). The mixture was heated at 80 °C until GC-MS analysis showed the reaction to be complete (2 h). Dilute HCl_(aq.) (2 mL) was added and the mixture was extracted with DCM (3 x 10 mL). The organic phase was washed with dilute HCl_(aq.) (3 x 10 mL) then H₂O (3 x 10 mL), dried over MgSO₄ and concentrated *in vacuo*. Purification by silica gel chromatography, eluting with 40:60 DCM/hexane gave **7** as a clear oil (0.53 g, 91%); IR (KBr disc, cm⁻¹) 2966, 2857, 1607, 1553, 1466, 1408, 1358, 1314, 1294, 1267, 1210, 1144, 1117, 1099; UV-vis (CHCl₃) λ_{max} (ε) 246 nm (10900 L mol⁻¹ cm⁻¹); λ_{em} (CHCl₃) 315 nm; m/z (EI-MS) 228 (20%, M⁺), 213 (100%, M⁺ - Me); ¹H NMR (400.13 MHz, CDCl₃) δ 7.44 (1H, s), 7.27 (2H, s), 5.35 (1H, s), 5.04 (1H, s), 2.16 (3H, s), 1.70 (4H, s), 1.32 (6H, s) 1.30 (6H, s); ¹³C{¹H} NMR (100.61 MHz, CDCl₃) δ 144.76, 144.44, 143.63, 138.57, 126.58, 123.74, 123.10, 111.69, 35.46, 35.32, 34.43, 34.32, 32.11, 32.04, 22.27.

One-pot synthesis of 7. In a dry, N₂ filled glove box, a solution of [Ir(OMe)COD]₂ (26 mg, 0.04 mmol) and 4,4'-di-*tert*-butyl-2,2'-bipyridine (21 mg, 0.08 mmol) in MTBE (2 mL) was shaken vigorously and added to a solution of **5** (0.50 g, 2.65 mmol) and B₂pin₂ (0.675 g, 2.65 mmol) in MTBE (8 mL) in a thick walled glass tube fitted with a Young's tap. The mixture was heated at 80 °C until GC-MS analysis showed the reaction to be complete (18 h). After transfer of the reaction vessel to a glove box, degassed H₂O (2 mL) was added and the mixture was stirred for 5 minutes. Pd(dppf)Cl₂ (64 mg, 0.079 mmol), Ba(OH)₂·8H₂O (1.67 g, 5.30 mmol) and 2-bromopropene (0.42 g, 3.44 mmol) were added and the reaction mixture was heated at 80 °C until GC-MS analysis showed the reaction to be complete (2 h). Dilute HCl_(aq.) (2 mL) was added and the mixture was extracted with DCM (3 x 10 mL). The organic phase was washed with dilute HCl_(aq.) (3 x 10 mL) then H₂O (3 x 10 mL), dried over MgSO₄ and concentrated *in vacuo*. Purification *via* silica gel chromatography, eluting with 40:60 DCM/hexane and removal of the solvent *in vacuo* gave **7** as a clear oil (0.56 g, 93%). All other analytical data are identical to those obtained when using the above methods.

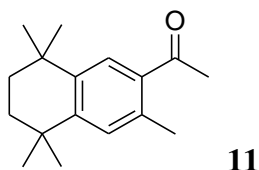


2,5-Dichloro-2,5-dimethyl-hexane (8).^{262c,279} 2,5-Dimethyl-hexane-2,5-diol (20.0 g, 137 mmol) was added to a 1 L conical flask and 250 mL HCl conc. (37% v/v, d = 1.18) was added. The solution was stirred overnight, filtered and the filtrate was washed with H₂O (2 x 100 mL) and then dissolved in Et₂O (200 mL). The organic layer was dried over MgSO₄, filtered and the solvent removed *in vacuo* to give a crude product. Purification *via* a short silica gel column (eluting with hexane) and removal of solvent *in vacuo* gave **8** as white needles (21.8 g, 87%), mp 67-68 °C (lit.^{262c} mp 63-65 °C), m/z (EI-MS) 133 (100% M⁺ - MeCl); ¹H NMR (400.13 MHz, CDCl₃) δ 1.95 (4H, s), 1.59 (12H, s), ¹³C{¹H} NMR (100.61 MHz, CDCl₃) δ 70.57, 41.45, 32.79; elemental analysis calcd. (%) for C₈H₁₆Cl₂: C 52.47, H 8.81; found: C 52.55, H 8.97.

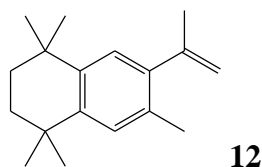


1,1,4,4,6-Pentamethyl-1,2,3,4-tetrahydronaphthalene (9).^{262c} This compound was synthesised as previously described.^{12c} To a stirred solution of toluene (10.0 g, 110 mmol) and compound **8** (10.0 g, 54.5 mmol) in DCM (75 mL) under N₂ was added anhydrous AlCl₃ (0.10 g, 0.75 mmol). The mixture was stirred for 30 min then refluxed for 15 min and then quenched with 10 mL of 10% HCl_(aq.). The mixture was extracted with hexane (2 x 60 mL). The organic layers were combined, washed with H₂O (2 x 100 mL), dried over MgSO₄ and the solvent was removed *in vacuo* to give a brown/orange oil. Kugelrohr distillation (131 °C, 3.3 x 10⁻² mbar) gave **9** as white crystals (9.43 g, 85%); mp 30-32 °C (lit.^{262c} 31-32 °C); IR (KBr disc, cm⁻¹) 2956, 2917, 2868, 1614, 1499, 1456, 1385, 1362, 1274, 1188, 1106, 1068, 1047; UV-vis (CHCl₃) λ_{max} (ε) 289 nm (405 L mol⁻¹ cm⁻¹); λ_{em} (CHCl₃) 357 nm; m/z (EI-MS) 202 (10% M⁺), 187 (100% M⁺ - Me); ¹H NMR (400.13

MHz, CDCl₃) δ 7.25 (1H, d, *J* = 8.0 Hz), 7.14 (1H, s), 6.99 (1H, d, *J* = 8.0 Hz), 2.33 (3H, s), 1.70 (4H, s), 1.30 (6H, s), 1.29 (6H, s); ¹³C{¹H} NMR (100.61 MHz, CDCl₃) δ 144.88, 142.05, 134.95, 127.22, 126.76, 126.64, 35.48, 35.42, 34.35, 34.12, 32.15, 32.09, 21.34; elemental analysis calcd. (%) for C₁₅H₂₂: C 89.04, H 10.96; found: C 89.02, H 11.13.



1-(3,5,5,8,8-Pentamethyl-5,6,7,8-tetrahydronaphthalen-2-yl)ethanone (11).²⁸⁰ To a solution of acetyl chloride (0.7 mL, 9.9 mmol) and compound **9** (2.0 g, 9.9 mmol) in DCM (40 mL) was added anhydrous AlCl₃ (2.63 g, 19.8 mmol) in 0.5 g aliquots. The mixture was refluxed under N₂ for 15 min then stirred overnight at room temperature. 20% HCl_(aq.) (5 mL) was added and the mixture was extracted with hexane (2 x 30 mL). The organic layers were combined, washed with H₂O (2 x 30 mL), dried over MgSO₄ and the solvent was removed *in vacuo* to give a crude product. Purification by Kugelrohr distillation (170 °C, 9 x 10⁻³ mbar) yielded **11** as white crystals (1.94 g, 86%); mp 31-32 °C; IR (KBr disc, cm⁻¹) 2958, 2923, 1673 (C=O), 1609, 1545, 1499, 1460, 1362, 1254, 1117, 1086, 1037; UV-vis (CHCl₃) λ_{max} (ε) 296 nm (1570 L mol⁻¹ cm⁻¹); λ_{em} (CHCl₃) 349 nm; m/z (EI-MS) 244 (35%, M⁺), 229 (100%, M⁺ - Me); ¹H NMR (400.13 MHz, C₆D₆) δ 7.58 (1H, s), 7.08 (1H, s), 2.61 (3H, s), 2.22 (3H, s), 1.55 (4H, s), 1.19 (6H, s), 1.17 (6H, s); ¹³C{¹H} NMR (100.13 MHz, C₆D₆) δ 199.70, 148.53, 142.18, 136.02, 135.75, 130.28, 127.13, 35.26, 35.24, 34.32, 33.93, 31.86, 31.58, 28.88, 21.68; elemental analysis calcd. (%) for C₁₇H₂₄O: C 83.55, H 9.90; found: C 83.73, H 10.03.



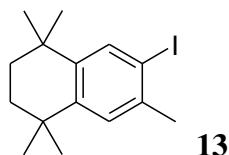
12

6-Isopropenyl-1,1,4,4,7-pentamethyl-1,2,3,4-tetrahydronaphthalene (12).²⁷⁷ To a flask containing a solution of compound **11** (4.0 g, 16.4 mmol) and $[\text{CH}_3\text{PPh}_3]\text{I}$ (9.90 g, 24.6 mmol) in THF (100 mL), under N_2 , was added $\text{KO}(\text{t-Bu})$ (2.75 g, 24.6 mmol). A rapid color change from white to dark orange was observed. The mixture was stirred until GC-MS analysis showed the reaction to be complete (3 d). The solution was filtered through celite with hexane as the eluent and the solvent was removed *in vacuo*. Purification by Kugelrohr distillation (100 °C, 1.5×10^{-1} mbar) yielded **12** as white crystals (3.30 g, 84%); mp 46-47 °C; IR (KBr disc, cm^{-1}) 2956, 2912, 2857, 1637, 1497, 1454, 1387, 1362, 1264, 1189, 1115, 1045; UV-vis (CHCl_3) λ_{max} (ϵ) 252 nm ($4540 \text{ L mol}^{-1} \text{ cm}^{-1}$); λ_{em} (CHCl_3) 328 nm; m/z (EI-MS) 242 (35%, M^+), 227 (100%, $\text{M}^+ - \text{Me}$); ^1H NMR (400.13 MHz, C_6D_6) δ 7.37 (1H, s), 7.27 (1H, s), 5.25 (1H, d, $J = 2.5$ Hz), 5.04 (1H, d, $J = 2.5$ Hz), 2.38 (3H, s), 2.06 (3H, s), 1.71 (4H, s), 1.38 (6H, s), 1.37 (6H, s); $^{13}\text{C}\{^1\text{H}\}$ NMR (100.13 MHz, C_6D_6) δ 146.67, 143.42, 142.17, 141.64, 131.66, 127.34, 126.08, 114.54, 35.63, 35.61, 34.01, 33.98, 32.05, 32.01, 24.56, 19.71; elemental analysis calcd. (%) for $\text{C}_{18}\text{H}_{26}$: C 89.19, H 10.81; found: C 89.30, H 10.86.

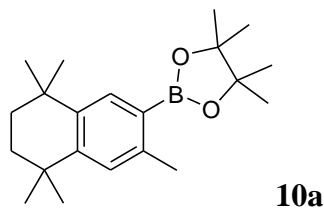
Alternative synthesis of **12** by Suzuki-Miyaura cross-coupling.

In a dry, N_2 filled glovebox, $\text{Pd}(\text{dppf})\text{Cl}_2$ (0.15 g, 0.18 mmol), compound **14** (1.0 g, 3.7 mmol), $\text{Ba}(\text{OH})_2 \cdot 8\text{H}_2\text{O}$ (2.33 g, 7.4 mmol) and 2-bromopropene (0.49 mL, 5.5 mmol) were placed in a thick walled glass tube fitted with a Young's tap along with DMF (10 mL) and H_2O (2 mL). The mixture was heated at 80 °C for 18 h at which time GC-MS analysis showed the reaction to be complete. Dilute $\text{HCl}_{(\text{aq.})}$ (2 mL) was added and the mixture was extracted with Et_2O (3 x 10 mL); the organic phase was washed with dilute $\text{HCl}_{(\text{aq.})}$ (3 x 10 mL), dried over MgSO_4 and concentrated *in vacuo*. The mixture was passed through a short silica gel column (eluting with hexane) and the solvent was removed *in vacuo* to give a clear oil which solidified upon standing to give **12** as a white

solid (0.73 g, 81%). All other analytical data are identical to those obtained when using the above method.

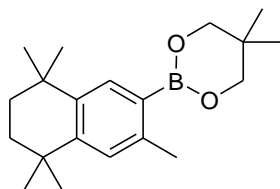


6-Iodo-1,1,4,4,7-pentamethyl-1,2,3,4-tetrahydronaphthalene (13). A solution of compound **9** (10.1 g, 50 mmol), iodine (5.1 g, 20 mmol) and HIO₄ (2.30 g, 10 mmol) in glacial acetic acid (50 mL), H₂O (10 mL) and 98% H₂SO₄ (1.5 mL) was heated at 70 °C for 24 h. The mixture was extracted into Et₂O (200 mL), washed with H₂O (200 mL) and aqueous Na₂S₂O₃ solution (200 mL). The organic layer was dried over MgSO₄ and the solvent was removed *in vacuo*. The crude product was passed through a short silica gel column (eluting with hexane) and the solvent was removed *in vacuo* to give a solid which was recrystallised from hot MeOH to give **13** as white crystals (10.45 g, 64%); mp 65-67 °C; IR (KBr disc, cm⁻¹) 2956, 2917, 2868, 1478, 1385, 1361, 1298, 1264, 1190, 1111, 1071; UV-vis (CHCl₃) λ_{max} (ε) 241 nm (6620 L mol⁻¹ cm⁻¹); λ_{em} (CHCl₃) does not fluoresce; m/z (EI-MS) 328 (40%, M⁺), 315 (100%, M⁺ - Me); ¹H NMR (499.80 MHz, CDCl₃) δ 7.69 (1H, s), 7.15 (1H, s), 2.37 (3H, s), 1.65 (4H, s), 1.25 (12H, s); ¹³C{¹H} NMR (125.67 MHz, CDCl₃) δ 145.57, 145.17, 138.50, 137.34, 128.28, 98.56, 35.25 (two peaks), 34.38, 34.20, 32.11, 32.01, 27.99; elemental analysis calcd. for C₁₅H₂₁I: C 54.89, H 6.45, found: C 54.82, H 6.31.



4,4,5,5-Tetramethyl-2-(3,5,5,8,8-pentamethyl-5,6,7,8-tetrahydronaphthalen-2-yl)-[1,3,2]dioxaborolane (10a). In a dry, N₂ filled glovebox, Pd(dppf)Cl₂ (0.124 g, 0.15 mmol), compound **13** (1.0 g, 3.05 mmol), B₂pin₂ (0.77 g, 3.05 mmol) and KOAc (0.59 g,

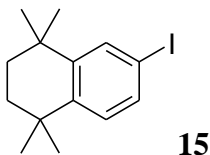
6.1 mmol) were placed in a thick walled glass tube fitted with a Young's tap along with dry, degassed DMSO (8 mL). The mixture was heated at 80 °C until GC-MS analysis showed the reaction to be complete (4 d). The mixture was extracted with DCM (30 mL) and washed with dilute HCl_(aq.) (30 mL) and H₂O (30 mL). The organic layer was dried over MgSO₄, filtered and the solvent removed *in vacuo*. The crude product was passed through a short silica gel column, eluting with hexane, and then 50:50 DCM/hexane. Removal of the solvent *in vacuo* gave a white powder which was recrystallised from hot MeOH to give pure **10a** (0.60 g, 60%); mp 131-133 °C; IR (KBr disc, cm⁻¹) 2963, 2917, 2862, 1606, 1541, 1492, 1409, 1393, 1295, 1266, 1215, 1143, 1112, 1095; UV-vis (CHCl₃) λ_{max} (ε) 241 nm (8240 L mol⁻¹ cm⁻¹); λ_{em} (CHCl₃) 304 nm; m/z (EI-MS) 328 (20%, M⁺), 313 (100%, M⁺ - Me); ¹H NMR (499.80 MHz, CDCl₃) δ 7.73 (1H, s), 7.01 (1H, s), 2.49 (3H, s), 1.67 (4H, s), 1.31 (6H, s), 1.30 (6H, s), 1.27 (12H, s); ¹³C{¹H} NMR (125.67 MHz, CDCl₃) δ 147.91, 141.90, 141.27, 134.69, 128.09, 83.31, 35.48, 35.30, 34.46, 33.99, 32.08, 31.88, 25.09, 22.25; the resonance for the carbon attached to boron was not observed; ¹¹B{¹H} NMR (128.37 MHz, C₆D₆) δ 31.28; elemental analysis calcd. for C₂₁H₃₃BO₂; C 76.83, H 10.13, found: C 76.75, H 10.18.



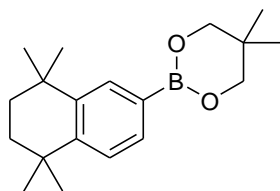
14

5,5-Dimethyl-2-(3,5,5,8,8-pentamethyl-5,6,7,8-tetrahydronaphthalen-2-yl)-[1,3,2]dioxaborinane (14). In a dry, N₂ filled glovebox, Pd(dppf)Cl₂ (0.124 g, 0.15 mmol), compound **13** (1.0 g, 3.05 mmol), B₂neop₂ (0.69 g, 3.05 mmol) and KOAc (0.59 g, 6.1 mmol) were placed in a thick walled glass tube fitted with a Young's tap along with dry, degassed DMSO (8 mL). The mixture was heated at 80 °C for 18 h, at which time analysis by GC-MS showed the reaction to be complete. The mixture was extracted with DCM (30 mL) and washed with dilute HCl (30 mL) and H₂O (30 mL). The organic layer was dried over MgSO₄, filtered and the solvent was removed *in vacuo*. The crude

product was filtered through a SiO₂ plug eluting with hexane and then 50:50 DCM/hexane. Removal of the solvent *in vacuo* gave a white powder which was recrystallised from hot MeOH to give pure **14** (0.64 g, 67%); mp 115-117 °C; IR (KBr disc, cm⁻¹) 2958, 2923, 2865, 1604, 1477, 1417, 1377, 1339, 1308, 1267, 1248, 1124; UV-vis (CHCl₃) λ_{max} (ε) 242 nm (9450 L mol⁻¹ cm⁻¹); λ_{em} (CHCl₃) 305 nm; m/z (EI-MS) 314 (20%, M⁺), 299 (100%, M⁺ - Me); ¹H NMR (499.80 MHz, CDCl₃) δ 7.71 (1H, s), 7.07 (1H, s), 3.75 (4H, s) 2.47 (3H, s), 1.66 (4H, s) 1.29 (6H, s), 1.27 (6H, s), 1.02 (6H, s); ¹³C{¹H} NMR (125.67 MHz, CDCl₃) δ 147.14, 141.22, 141.14, 133.76, 128.34, 72.51, 35.65, 35.50, 34.47, 34.09, 32.23, 32.02, 31.96, 22.53, 22.27; the resonance for the carbon attached to boron was not observed; ¹¹B{¹H} NMR (128.37 MHz, C₆D₆) δ 27.71; elemental analysis calcd. for C₂₀H₃₀BO₂: C 76.44, H 10.18; found: C 76.17, H 10.00.



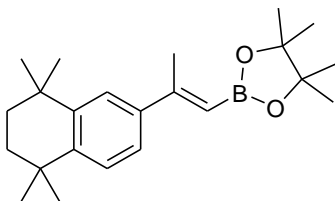
6-Iodo-1,1,4,4-tetramethyl-1,2,3,4-tetrahydronaphthalene (15).²⁸⁶ To a mixture of compound **5** (3.76 g, 20 mmol), iodine (2.04 g, 8.0 mmol) and HIO₄ (0.92 g, 4.0 mmol) was added glacial acetic acid (20 mL), H₂O (4 mL) and concentrated H₂SO₄ (98%, 1 mL). The reaction mixture was heated to 70 °C for 4 h. A precipitate formed upon cooling, which was collected by filtration, dissolved in hexane and passed through a short silica gel column (eluting with hexane). The hexane was evaporated and the residue was recrystallised from EtOH to give **15** as a white crystalline solid (4.45 g, 71%); mp 69-70 °C; IR (KBr disc, cm⁻¹) 2961, 2924, 2856, 1577, 1478, 1457, 1384, 1363, 1295, 1264, 1191, 1107, 1066, 1039; UV-vis (CHCl₃) λ_{max} (ε) 241 nm (4800 L mol⁻¹ cm⁻¹); the compound did not fluoresce; m/z (EI-MS) 314 (25%, M⁺), 299 (100%, M⁺ - Me); ¹H NMR (200 MHz, CDCl₃) δ 7.61 (1H, d, J = 2.0 Hz), 7.44 (1H, dd, J = 8.0, 2.0 Hz), 7.04 (1H, d, J = 8.0 Hz), 1.66 (4H, s), 1.28 (6H, s), 1.26 (6H, s); ¹³C{¹H} NMR (100 MHz, CDCl₃) δ 147.7, 144.6, 135.6, 134.6, 128.7, 91.1, 34.9, 34.8, 34.3, 34.1, 31.8, 31.7; elemental analysis calcd for C₁₄H₁₉I: C, 53.52; H, 6.10. Found: C, 53.66; H, 6.13.



16

5,5-Dimethyl-2-(5,5,8,8-tetramethyl-5,6,7,8-tetrahydronaphthalen-2-yl)-

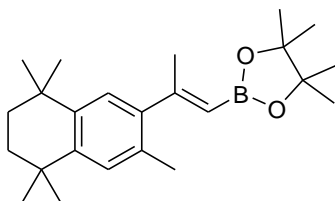
[1,3,2]dioxaborinane (16). In a dry, N₂ filled glovebox, Pd(dppf)Cl₂ (26 mg, 0.032 mmol), compound **15** (1.0 g, 3.18 mmol), B₂neop₂ (790 mg, 3.18 mmol) and KOAc (0.64 g, 6.36 mmol) were placed in a thick walled glass tube fitted with a Young's tap along with dry, degassed DMSO (10 mL). The mixture was heated at 80 °C overnight, at which time analysis by GC-MS showed the reaction to be complete. The mixture was extracted with Et₂O (30 mL) and washed with H₂O (30 mL). The organic layer was dried over MgSO₄, filtered and the solvent was removed *in vacuo*. The crude product was filtered through a SiO₂ plug eluting with hexane, and then 50:50 DCM/hexane. Removal of the solvent *in vacuo* gave white powder which was recrystallised from hot MeOH to give pure **16** (0.71 g, 75%); mp 116-119 °C; IR (KBr disc, cm⁻¹) 2961, 2932, 2888, 1605, 1473, 1417, 1345, 1323, 1296, 1268, 1246, 1135, 1069; UV-vis (CHCl₃) λ_{max} (ε) 241 nm (8700 L mol⁻¹ cm⁻¹); λ_{em} (CHCl₃) 297 nm; m/z (EI-MS) 300 (15%, M⁺), 285 (100%, M⁺ - Me); ¹H NMR (400.13 MHz, C₆D₆) δ 7.78 (1H, s), 7.57 (1H, dd, *J* = 8.0, 1.0 Hz), 7.31 (1H, d, *J* = 8.0 Hz), 3.76 (4H, s), 1.69 (4H, s), 1.32 (6H, s), 1.30 (6H, s), 1.03 (6H, s); ¹³C{¹H} NMR (100.13 MHz, C₆D₆) δ 147.69, 143.41, 132.41, 131.13, 125.93, 72.42, 35.44, 35.25, 34.56, 34.30, 32.03, 32.02, 31.92, 22.09, the resonance of the carbon attached to boron was not observed; ¹¹B{¹H} NMR (128.37 MHz, C₆D₆) δ 26.67; elemental analysis calcd. (%) for C₁₉H₂₈BO₂: C 76.01, H 9.74; found: C 75.88, H 9.51.



17

4,4,5,5-Tetramethyl-2-[2-(5,5,8,8-tetramethyl-5,6,7,8-tetrahydronaphthalen-2-yl)-propenyl]-[1,3,2]-dioxaborolane (17). In a dry, N₂ filled, glovebox, B₂pin₂ (0.33 g, 1.3 mmol), compound **7** (0.30 g, 1.3 mmol), and *trans*-[Rh(PPh₃)₂(CO)Cl] (45 mg, 0.07 mmol) were dissolved in 6 mL of 3:1 toluene/MeCN and added to a thick walled glass tube fitted with a Young's tap. The reaction was heated at 80 °C until GC-MS analysis showed the reaction to be complete (3 d). H₂O (5 mL) was added, and the aqueous layer was washed with ethyl acetate (3 x 5 mL). The combined organic phases were dried over MgSO₄ and concentrated *in vacuo* to give a dark green oil. Recrystallization from hot MeOH gave **17** as a white, fluffy powder (0.23 g, 50%); mp 125-127 °C; IR (KBr disc, cm⁻¹) 2958, 2857, 1618, 1555, 1497, 1453, 1410, 1345, 1263, 1209, 1144, 1108, 1078; UV-vis (CHCl₃) λ_{max} (ε) 270 nm (18600 L mol⁻¹ cm⁻¹); λ_{em} (CHCl₃) 344 nm; m/z (EI-MS) 354 (30%, M⁺), 339 (100%, M⁺ - Me); ¹H NMR (400.13 MHz, C₆D₆) δ 7.64 (1H, d, *J* = 2.0 Hz), 7.31 (1H, dd, *J* = 8.5, 2.0 Hz), 7.10 (1H, d, *J* = 8.0 Hz), 6.28 (1H, s), 2.68 (3H, s), 1.55 (4H, s), 1.19 (6H, s), 1.17 (6H, s), 1.14 (12H, s); ¹³C{¹H} NMR (100.13 MHz, C₆D₆) δ 159.03, 144.85, 144.63, 141.89, 126.72, 124.36, 123.83, 115.43, 82.77, 35.55, 35.41, 34.39, 34.21, 31.92, 31.89, 24.99, 20.48; ¹¹B{¹H} NMR (128.37 MHz, C₆D₆) δ 29.58; elemental analysis calcd. (%) for C₂₃H₃₅BO₂: C 77.96, H 9.96; found: C 78.18, H 10.18.

Alternative synthesis and purification of 17. In a dry, N₂ filled, glove box, B₂pin₂ (89 mg, 0.35 mmol), compound **7** (80 mg, 0.35 mmol) and *trans*-[Rh(PPh₃)₂(CO)Cl] (12 mg, 17 x 10⁻³ mmol) were dissolved in 4 mL of 3:1 toluene/MeCN in a thick walled glass tube fitted with a Young's tap and then heated to 80 °C. The reaction was monitored by GC-MS. After 3 d, the solvent was removed *in vacuo* and the crude solid redissolved in a mixture of hexane/DCM (60:40), and then purified *via* silica gel chromatography (hexane/DCM, 60:40) to yield **17** as an analytically pure white powder (98 mg, 80%); elemental analysis calcd. for C₂₃H₃₅BO₂: C 77.96, H 9.96; found: C 77.84, H 9.77. All other analytical data are identical to those obtained when using the above synthesis and purification.

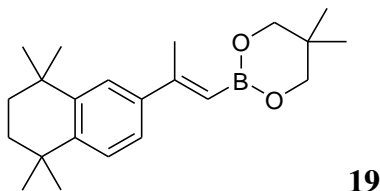


18

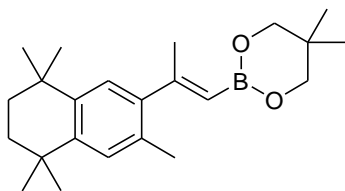
4,4,5,5-Tetramethyl-2-[2-(3,5,5,8,8-pentamethyl-5,6,7,8-tetrahydronaphthalen-2-yl)propenyl]-[1,3,2]-dioxaborolane (18). In a dry, N₂ filled glovebox, B₂pin₂ (0.31 g, 1.2 mmol), compound **12** (0.30 g, 1.2 mmol), and *trans*-[Rh(PPh₃)₂(CO)Cl] (43 mg, 0.07 mmol) were dissolved in 6 mL of 3:1 toluene/MeCN and added to a thick walled glass tube fitted with a Young's tap. The reaction was heated at 80 °C until GC-MS analysis showed no further progress (7 d). H₂O (5 mL) was added, and the aqueous layer was washed with ethyl acetate (3 x 5 mL). The combined organic phases were dried over MgSO₄ and concentrated *in vacuo* to give a dark green oil. Purification by silica gel chromatography, eluting with 1:1 DCM/hexane, and recrystallization from hot MeOH gave **18** as white needles (0.29 g, 63%); mp 69-71 °C; IR (KBr disc, cm⁻¹) 2954, 2857, 1633, 1498, 1435, 1389, 1318, 1287, 1273, 1226, 1213, 1189, 1163, 1146, 1111, 1077; UV-vis (CHCl₃) λ_{max} (ε) 253 nm (9500 L mol⁻¹ cm⁻¹); λ_{em} (CHCl₃) 324 nm; m/z (EI-MS) 368 (35%, M⁺), 353 (100%, M⁺ - Me); ¹H NMR (399.96 MHz, CDCl₃) δ 7.05 (1H, s), 7.02 (1H, s), 5.26 (1H, s), 2.27 (3H, s), 2.24 (3H, s), 1.66 (4H, s), 1.32 (12H, s), 1.27 (6H, s), 1.24 (6H, s); ¹³C{¹H} NMR (100.57 MHz, CDCl₃) δ 161.71, 144.19, 143.44, 142.10, 130.80, 128.17, 125.47, 83.04, 35.41, 35.39, 34.09, 34.08, 32.08, 32.06, 25.13, 23.31, 20.01; the resonance for the carbon attached to boron was not observed; ¹¹B{¹H} NMR (128.37 MHz, C₆D₆) δ 29.70; elemental analysis calcd. (%) for C₂₄H₃₇BO₂: C 78.25, H 10.12; found: C 77.97, H 10.14.

Alternative synthesis and purification of 18. In a dry, N₂ filled glovebox, B₂pin₂ (201 mg, 0.79 mmol), compound **12** (200 mg, 0.83 mmol) and *trans*-[Rh(PPh₃)₂(CO)Cl] (28.5 mg, 41.3 x 10⁻³ mmol) were dissolved in 4 mL of 3:1 toluene/MeCN in a thick walled glass tube fitted with a Young's tap. The reaction was heated to 80 °C and monitored by *in situ* GC-MS. After 3 d, the solvent was removed *in vacuo* and the resulting solid was

redissolved in 40:60 DCM/hexane and then purified *via* silica gel chromatography, eluting with 40:60 DCM/hexane, to yield **18** as an analytically pure white solid (151 mg, 50%); elemental analysis calcd. (%) for C₂₄H₃₇BO₂: C 78.25, H 10.12; found: C 78.12, H 9.98. All other analytical data are identical to those obtained when using the above synthesis and purification.

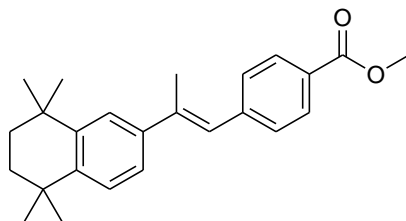


5-Dimethyl-2-[2-(5,5,8,8-tetramethyl-5,6,7,8-tetrahydronaphthalen-2-yl)propenyl]-[1,3,2]dioxaborinane (19). In a dry, N₂ filled, glovebox, B₂neop₂ (0.50 g, 2.20 mmol), compound **7** (0.50 g, 2.20 mmol), and *trans*-[Rh(PPh₃)₂(CO)Cl] (70 mg, 0.1 mmol) were dissolved in 4 mL of 3:1 toluene/MeCN and added to a thick walled glass tube fitted with a Young's tap. The reaction was heated at 80 °C until GC-MS analysis showed the reaction to be complete (3 d). H₂O (5 mL) was added, and the aqueous layer was washed with ethyl acetate (3 x 5 mL). The combined organic phases were dried over MgSO₄ and concentrated *in vacuo* to give a dark green oil. Recrystallization from hot MeOH gave **19** as a white, fluffy powder (0.40 g, 57%); mp 71-72 °C; IR (KBr disc, cm⁻¹) 2960, 2922, 2870, 1615, 1467, 1408, 1341, 1270, 1183; UV-vis (CHCl₃) λ_{max} (ε) 268 nm (10500 L mol⁻¹ cm⁻¹); the compound does not fluoresce; m/z (EI-MS) 340 (25%, M⁺), 325 (100%, M⁺ - Me); ¹H NMR (499.80 MHz, CDCl₃) δ 7.45 (1H, s), 7.26 (2H, s), 5.65 (1H, s), 3.72 (4H, s) 2.37 (3H, s), 1.69 (4H, s) 1.28 (6H, s), 1.27 (6H, s), 1.02 (6H, s); ¹³C{¹H} NMR (125.67 MHz, CDCl₃) δ 156.17, 144.83, 144.74, 141.79, 126.53, 124.28, 123.48, 72.43, 35.53, 35.37, 34.67, 34.45, 32.19, 32.14, 22.27, 19.81; the resonance for the carbon attached to boron was not observed; ¹¹B{¹H} NMR (128.37 MHz, C₆D₆) δ 26.85, elemental analysis calcd. (%) for C₂₂H₃₃BO₂: C 77.62, H 9.77; found: C 77.39, H 9.88.



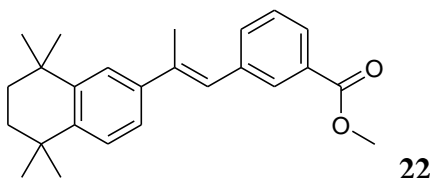
20

5,5-Dimethyl-2-[2-(3,5,5,8,8-pentamethyl-5,6,7,8-tetrahydronaphthalen-2-yl)-propenyl]-[1,3,2]dioxaborinane (20). In a dry, N₂ filled glovebox, B₂neop₂ (0.47 g, 2.1 mmol), compound **12** (0.50 g, 2.1 mmol), and *trans*-[Rh(PPh₃)₂(CO)Cl] (70 mg, 0.1 mmol) were dissolved in 4 mL of 3:1 toluene/MeCN and added to a thick walled glass tube fitted with a Young's tap. The reaction was heated at 80 °C until GC-MS analysis showed no further progress (7 d). H₂O (5 mL) was added, and the aqueous layer was washed with ethyl acetate (3 x 5 mL). The combined organic phases were dried over MgSO₄ and concentrated *in vacuo* to give a dark green oil. Recrystallization from hot MeOH gave **20** as a white, fluffy powder (0.36 g, 49%); mp 67-69 °C; IR (KBr disc, cm⁻¹) 2961, 2926, 1634, 1496, 179, 1335, 1276, 1187, 1085; UV-vis (CHCl₃) λ_{max} (ε) 255 nm (9100 L mol⁻¹ cm⁻¹); λ_{em} (CHCl₃) 368 nm; m/z (EI-MS) 354 (25%, M⁺), 339 (100%, M⁺ - Me); ¹H NMR (499.80 MHz, CDCl₃) δ 7.05 (1H, s), 7.03 (1H, s), 5.18 (1H, s), 3.70 (4H, s), 2.25 (6H, s), 1.66 (4H, s), 1.28 (6H, s), 1.27 (6H, s), 1.02 (6H, s); ¹³C{¹H} NMR (125.67 MHz, CDCl₃) δ 159.28, 144.85, 143.33, 142.19, 130.95, 128.22, 125.64, 72.39, 35.57, 35.55, 34.23, 34.20, 32.22, 32.21, 22.88, 22.32, 20.09; the resonance for the carbon attached to boron was not observed; ¹¹B{¹H} NMR (128.37 MHz, C₆D₆) δ 26.81, elemental analysis calcd. (%) for C₂₃H₃₅BO₂: C 77.96, H 9.96; found: C 77.88, H 9.85.



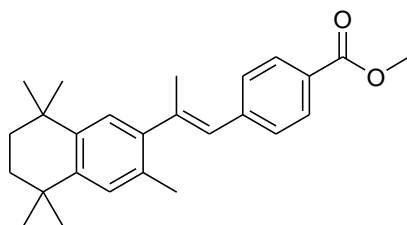
21

4-[2-(5,5,8,8-Tetramethyl-5,6,7,8-tetrahydronaphthalen-2-yl)-propenyl]-benzoic acid methyl ester (21). In a dry, N₂ filled glovebox, Pd(dppf)Cl₂ (33 mg, 0.04 mmol), compound **17** (0.40 g, 1.1 mmol), 4-iodobenzoic acid methyl ester (0.24 g, 0.9 mmol), K₃PO₄·2H₂O (0.57 g, 2.3 mmol) and degassed DMF (15 mL) were added to a thick walled glass tube fitted with a Young's tap. The tube was attached to a Schlenk line and degassed H₂O (3 mL) was added *via* cannula. The mixture was heated at 80 °C for 2 d, at which time GC-MS analysis showed complete consumption of the starting materials. Dilute HCl_(aq.) (2 mL) was added and the mixture was extracted with DCM (3 x 10 mL). The organic phase was washed with dilute HCl_(aq.) (3 x 10 mL), dried over MgSO₄ and concentrated *in vacuo*. The mixture was passed through a short silica gel column eluting with hexane and then 10% DCM/hexane and the solvent was removed *in vacuo*. Recrystallization from hot EtOH gave **21** as a white fluffy powder (280 mg, 84%); mp 137-139 °C; IR (KBr disc, cm⁻¹) 2951, 2920, 2857, 1706 (C=O), 1600, 1560, 1492, 1438, 1388, 1361, 1275, 1182, 1110, 1046, 1016; UV-vis (CHCl₃) λ_{max} (ε) 309 nm (29500 L mol⁻¹ cm⁻¹); λ_{em} (CHCl₃) 388 nm; m/z (EI-MS) 362 (90%, M⁺), 347 (100%, M⁺ - Me); ¹H NMR (499.80 MHz, CDCl₃) δ 8.04 (2H, d, *J* = 8.5 Hz), 7.46 (1H, d, *J* = 2.0 Hz), 7.43 (2H, d, *J* = 8.5 Hz), 7.32 (1H, s), 7.31 (1H, d, *J* = 2.0 Hz), 6.82 (1H, s), 3.94 (3H, s), 2.30 (3H, s), 1.72 (4H, s), 1.34 (6H, s), 1.31 (6H, s); ¹³C{¹H} NMR (125.67 MHz, CDCl₃) δ 167.28, 145.06, 144.76, 143.54, 140.82, 140.08, 129.68, 129.28, 127.96, 126.79, 126.27, 124.31, 123.57, 52.28, 35.74, 35.22, 34.60, 34.37, 32.12, 32.03, 17.91; HRMS calc for C₂₅H₃₁O₂ ([M + H]⁺) 363.23186, found 363.23180.



3-[2-(5,5,8,8-Tetramethyl-5,6,7,8-tetrahydronaphthalen-2-yl)-propenyl]-benzoic acid methyl ester (22). In a dry, N₂ filled glovebox, Pd(dppf)Cl₂ (33 mg, 0.04 mmol), compound **17** (0.40 g, 1.1 mmol), 3-iodobenzoic acid methyl ester (0.24 g, 0.9 mmol),

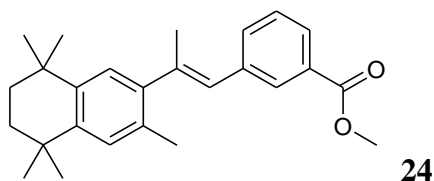
$K_3PO_4 \cdot 2H_2O$ (0.57 g, 2.3 mmol) and degassed DMF (15 mL) were added to a thick walled glass tube fitted with a Young's tap. The tube was attached to a Schlenk line and degassed H_2O (3 mL) was added *via* cannula. The mixture was heated at 80 °C for 2 d, at which time GC-MS analysis showed complete consumption of the starting materials. Dilute $HCl_{(aq)}$ (2 mL) was added and the mixture was extracted with DCM (3 x 10 mL). The organic phase was washed with dilute $HCl_{(aq)}$ (3 x 10 mL), dried over $MgSO_4$ and concentrated *in vacuo*. The mixture was passed through a short silica gel column eluting with hexane and then 10% DCM/hexane and the solvent removed *in vacuo*. Recrystallization from hot EtOH gave **22** as a white fluffy powder (0.25 g, 75%); mp 86–88 °C; IR (KBr disc, cm^{-1}) 2952, 2920, 2856, 1717 (C=O), 1581, 1492, 1440, 1359, 1306, 1287, 1250, 1201, 1106, 1085; UV-vis ($CHCl_3$) λ_{max} (ϵ) 284 nm (22800 $L \text{ mol}^{-1} \text{ cm}^{-1}$); λ_{em} ($CHCl_3$) 386 nm; m/z (EI-MS) 362 (90%, M^+), 347 (100%, $M^+ - Me$); 1H NMR (499.80 MHz, $CDCl_3$) δ 8.05 (1H, s), 7.92 (1H, d, $J = 7.5$ Hz), 7.55 (1H, d, $J = 7.5$ Hz), 7.46 (1H, s), 7.44 (1H, t, $J = 7.5$ Hz), 7.32 (1H, s), 7.31 (1H, t, $J = 7.5$ Hz), 6.82 (1H, s) 3.95 (3H, s), 2.28 (3H, s) 1.72 (4H, s), 1.35 (6H, s), 1.32 (6H, s); $^{13}C\{^1H\}$ NMR (125.67 MHz, $CDCl_3$) δ 167.59, 145.14, 144.67, 140.99, 139.17, 133.92, 130.57, 130.39, 128.56, 127.73, 126.88, 126.17, 124.39, 123.66, 52.52, 35.51, 35.36, 34.72, 34.49, 32.25, 32.17, 17.82; HRMS calc for $C_{50}H_{60}O_4Na$ ($[M_2Na]^+$) 747.43838, found 747.44029.



23

4-[2-(3,5,5,8,8-Pentamethyl-5,6,7,8-tetrahydronaphthalen-2-yl)propenyl]-benzoic acid methyl ester (23). In a dry, N_2 filled glovebox, $Pd(dppf)Cl_2$ (28 mg, 0.03 mmol), compound **18** (0.30 g, 0.82 mmol), 4-iodobenzoic acid methyl ester (0.18 g, 0.68 mmol), $K_3PO_4 \cdot 2H_2O$ (0.42 g, 1.7 mmol) and degassed DMF (15 mL) were added to a thick walled glass tube fitted with a Young's tap. The tube was attached to a Schlenk line and degassed H_2O (3 mL) was added *via* cannula. The mixture was heated at 80 °C for 2 d, at which time GC-MS analysis showed complete consumption of the starting materials.

Dilute HCl_(aq.) (2 mL) was added and the mixture was extracted with DCM (3 x 10 mL). The organic phase was washed with dilute HCl_(aq.) (3 x 10 mL), dried over MgSO₄ and concentrated *in vacuo*. The mixture was passed through a short silica gel column eluting with hexane and then 10% DCM/hexane and the solvent was removed *in vacuo*. Recrystallization from hot EtOH gave **23** as a white fluffy powder (0.22 g, 86 %); mp 137-139 °C; IR (KBr disc, cm⁻¹) 2957, 2918, 2851, 1714 (C=O), 1605, 1562, 1492, 1437, 1411, 1361, 1278, 1182, 1111, 1016; UV-vis (CHCl₃) λ_{max} (ε) 288 nm (17500 L mol⁻¹ cm⁻¹); λ_{em} (CHCl₃) 380 nm; m/z (EI-MS) 376 (90%, M⁺), 361 (100%, M⁺ - Me); ¹H NMR (499.80 MHz, CDCl₃) δ 8.05 (2H, d, *J* = 8 Hz), 7.45 (2H, d, *J* = 8 Hz), 7.13 (1H, s), 7.12 (1H, s), 6.42 (1H, s), 3.94 (3H, s), 3.31 (3H, s), 1.70 (4H, s), 1.31 (6H, s), 1.30 (6H, s); ¹³C{¹H} NMR (125.67 MHz, CDCl₃) δ 167.40, 143.98, 143.31, 143.00, 142.59, 142.19, 131.87, 129.85, 129.18, 128.63, 128.53, 128.11, 126.26, 52.41, 35.54, 35.39, 34.30, 34.39, 32.27, 32.21, 20.69, 20.06; HRMS calc for C₂₆H₃₃O₂ ([M + H]⁺) 377.24695, found 377.24685.



3-[2-(3,5,5,8,8-Pentamethyl-5,6,7,8-tetrahydronaphthalen-2-yl)propenyl]benzoic acid methyl ester (24). In a dry, N₂ filled glovebox, Pd(dppf)Cl₂ (285 mg, 0.03 mmol), compound **18** (0.30 g, 0.82 mmol), 3-iodobenzoic acid methyl ester (0.18 g, 0.68 mmol), K₃PO₄·2H₂O (0.42 g, 1.7 mmol) and degassed DMF (15 mL) were added to a thick walled glass tube fitted with a Young's tap. The tube was attached to a Schlenk line and degassed H₂O (3 mL) was added *via* cannula. The mixture was heated at 80 °C for 2 d, at which time GC-MS analysis showed complete consumption of the starting materials. Dilute HCl_(aq.) (2 mL) was added and the mixture was extracted with DCM (3 x 10 mL). The organic phase was washed with dilute HCl_(aq.) (3 x 10 mL), dried over MgSO₄ and concentrated *in vacuo*. The mixture was filtered through a short silica gel column eluting

with hexane and then 10% DCM/hexane and the solvent was removed *in vacuo*. Recrystallization from hot EtOH gave **24** as a white fluffy powder (0.22 g, 86%); mp 91-92 °C; IR (KBr disc cm^{-1}) 2952, 2919, 2858, 1722 (C=O), 1582, 1496, 1440, 1360, 1292, 1254, 1198, 1108, 1086; UV-vis (CHCl_3) λ_{max} (ϵ) 241 nm (24800 $\text{L mol}^{-1} \text{cm}^{-1}$); λ_{em} (CHCl_3) 383 nm; m/z (EI-MS) 376 (90%, M^+), 361 (100%, $\text{M}^+ - \text{Me}$); ^1H NMR (499.80 MHz, CDCl_3) δ 8.06 (1H, s), 7.92 (1H, d, $J = 7.5$ Hz), 7.56 (1H, d, $J = 7.5$ Hz), 7.46 (1H, t, $J = 7.5$ Hz), 7.13 (1H, s), 7.12 (1H, s), 6.42 (1H, s), 3.95 (3H, s), 2.32 (3H, s), 2.20 (3H, s), 1.70 (4H, s), 1.32 (6H, s), 1.31 (6H, s); $^{13}\text{C}\{^1\text{H}\}$ NMR (125.67 MHz, CDCl_3) δ 167.60, 143.85, 142.98, 142.55, 141.05, 138.86, 133.76, 131.95, 130.41, 130.29, 128.59, 128.48, 128.36, 127.76, 126.35, 52.53, 35.55, 35.52, 34.28, 34.27, 32.27, 32.22, 20.42, 20.08; HRMS calcd for $\text{C}_{26}\text{H}_{33}\text{O}_2$ ($[\text{M} + \text{H}]^+$) 377.24751, found 377.24852.

General experimental for Suzuki-Miyaura cross-couplings of aryl boronic esters at 40 °C.

In a dry, N_2 filled glovebox, aryl boronate (0.32 mmol), $\text{Pd}(\text{dppf})\text{Cl}_2$ (5.2 mg, 0.007 mmol), and base (0.64 mmol) were added to a thick wall glass tube fitted with a Young's tap. Degassed DMF (5 mL) and degassed H_2O (1 mL) were added along with 2-bromopropene (0.043 mL, 0.42 mmol). The tube was sealed and heated at 40 °C and the reaction was monitored by GC-MS.

General experimental for Suzuki-Miyaura cross-couplings of aryl boronic esters at room temperature.

In a dry, N_2 filled glovebox, aryl boronate (0.32 mmol), $\text{Pd}(\text{dppf})\text{Cl}_2$ (5.2 mg, 0.007 mmol), and base (0.64 mmol) were added to a screw top vial. Degassed DMF (5 mL) and degassed H_2O (1 mL) were added along with 2-bromopropene (0.043 mL, 0.42 mmol). The vial was stirred at room temperature inside the glovebox and the reaction was monitored by GC-MS.

General experimental for Suzuki-Miyaura cross-couplings of vinyl boronic esters at 40 °C.

In a dry, N₂ filled glovebox, vinyl boronate (0.28 mmol), 3-iodobenzoic acid methyl ester (0.065g, 0.25 mmol) Pd(dppf)Cl₂ (4.5 mg, 0.006 mmol), and base (0.56 mmol) were added to a thick wall glass tube fitted with a Young's tap. Degassed DMF (5 mL) and degassed H₂O (1 mL) were added. The tube was sealed and heated at 40 °C and the reaction was monitored by GC-MS

General experimental for Suzuki-Miyaura cross-couplings of vinyl boronic esters at room temperature.

In a dry, N₂ filled glovebox, vinyl boronate (0.28 mmol), 3-iodobenzoic acid methyl ester (0.065g, 0.25 mmol) Pd(dppf)Cl₂ (4.5 mg, 0.006 mmol), and base (0.56 mmol) were added to a screw top vial. Degassed DMF (5 mL), and degassed H₂O (1 mL) were added. The vial was stirred at room temperature inside the glovebox and the reaction was monitored by GC-MS.

Table 2.3 Photophysical data for all compounds in CHCl₃

Compound	λ_{\max} (nm)	ϵ (L mol ⁻¹ cm ⁻¹)	λ_{em} (nm) ($\lambda_{\text{ex}} = \lambda_{\max}$ (abs))
TMN-Bpin (6)	243	2730	298
TMN-Bneop (16)	241	8700	297
TMN-isopropene (7)	246	10900	328
PMN-isopropene (12)	252	4540	315
PMN (9)	289	405	357
TMN-I (15)	241	4800	does not fluoresce
PMN-I (13)	241	6620	does not fluoresce
PMN ketone (11)	296	1570	349
PMN-Bpin (10a)	241	8240	304
PMN-Bneop (14)	242	9450	305
TMN Bpin VBE (17)	270	18600	344
PMN Bpin VBE (18)	253	9500	324
TMN Bneop VBE (19)	268	10500	does not fluoresce
PMN Bneop VBE (20)	255	9100	368
TTNPB-Me ester (21)	309	29500	388
<i>m</i> -TTNPB-Me ester (22)	284	22800	386
3-Me-TTNPB-Me ester (23)	288	17500	380
3-Me- <i>m</i> -TTNPB-Me ester (24)	241, 268	24800, 16200	383 (λ_{ex} 241nm), 383 (λ_{ex} 268 nm)

References for chapter 2

²⁵¹ Ross, S. A.; McCaffery, P. J.; Drager, U. C.; De Luca, L. M. *Physiol. Rev.* **2000**, *80*, 1021-1054.

²⁵² Wald, G. *Nature* **1968**, *219*, 800-807.

²⁵³ Napoli, J. L. *Clin. Immunol. Immunopathol.* **1996**, *80*, S52-62.

²⁵⁴ Lowe, N.; Marks, R. *Retinoids: a Clinicians Guide*. 2 ed.; Informa Healthcare: London, **1997**.

²⁵⁵ Soprano, D. R.; Qin, P.; Soprano, K. J. *Annu. Rev. Nutr.* **2004**, *24*, 201-221.

²⁵⁶ Freemantle, S. J.; Dragnev, K. H.; Dmitrovsky, E. *J. Natl. Cancer Inst.* **2006**, *98*, 426-427.

²⁵⁷ Collins, M. D.; Mao, G. E. *Annu. Rev. Pharmacol. Toxicol.* **1999**, *39*, 399-430.

²⁵⁸ Leid, M.; Kastner, P.; Lyons, R.; Nakshatri, H.; Saunders, M.; Zacharewski, T.; Chen, J.-Y.; Staub, A.; Garnier, J.-M.; Mader, S.; Chambon, P. *Cell* **1992**, *68*, 377-395.

²⁵⁹ Mangelsdorf, D. J.; Thummel, C.; Beato, M.; Herrlich, P.; Schütz, G.; Umesono, K.; Blumberg, B.; Kastner, P.; Mark, M.; Chambon, P.; Evans, R. M. *Cell* **1995**, *83*, 835-839.

²⁶⁰ Chambon, P. *FASEB J.* **1996**, *10*, 940-954.

²⁶¹ **TTNPB synthesis and biological studies**

(a) P. Loeliger (Inventor), Hoffmann-La Roche & Co AG, Basel, Switzerland, Ger. Offen. DE 2854354 A1, July 5, 1979; (b) Loeliger, P.; Bollag, W.; Mayer, H. *Eur. J. Med. Chem. Chim. Ther.* **1980**, *15*, 9-15; (c) Lotan, R.; Stolarsky, T.; Lotan, D. *J. Nutr. Growth Cancer* **1983**, *1*, 71-76; (c) Dawson, M. I.; Hobbs, P. D.; Derdzinski, K.; Chan, R. L. S.; Gruber, J.; Chao, W.; Smith, S.; Thies, R. W.; Schiff, L. J. *J. Med. Chem.* **1984**, *27*, 1516-1531; (d) Minucci, S.; Saint-Jeannet, J.-P.; Toyama, R.; Scita, G.; DeLuca, L. M.; Taira, M.; Levin, A. A.; Ozato, K.; Dawid, I. B. *Proc. Natl. Acad. Sci. USA* **1996**, *93*, 1803-1807; (e) Standeven, A. M.; Johnson, A. T.; Escobar, M.; Chandraratna, R. A. S. *Toxicol. Appl. Pharmacol.* **1996**, *138*, 169-175; (f) Standeven, A. M.; Teng, M.; Chandraratna, R. A. S. *Toxicol. Lett.* **1997**, *92*, 231-240; (g) Wu, K.; Kim, H.-T.; Rodriguez, J. L.; Hilsenbeck, S. G.; Mohsin, S. K.; Xu, X.-C.; Lamph, W. W.; Kuhn, J. G.; Green, J. E.; Brown, P. H. *Cancer Epidemiol. Biomarkers Prev.* **2002**, *11*, 467-474. Pignatello, M. A.; Kauffman, F. C.; Levin, A. A. *Toxicol. Appl. Pharmacol.* **2002**, *178*, 186-194; (h) Gardiner, D.; Ndayibagira, A.; Grün, F.; Blumberg, B. *Pure Appl. Chem.* **2003**, *75*, 2263-2273; (i) Germain, P.; Kammerer, S.; Pérez, E.; Peluso-Iltis, C.; Tortolani, D.; Zusi, F. C.; Starrett, J.; Lapointe, P.; Daris, J.-P.; Marinier, A.; de Lera, A. R.; Rochel, N.; Gronemeyer, H. *EMBO Rep.* **2004**, *5*, 877-882; (j) Pogenberg, V.; Guichou, J.-F.; Vivat-Hannah, V.; Kammerer, S.; Pérez, E.; Germain, P.; de Lera, A. R.; Gronemeyer, H.; Royer, C. A.; Bourguet, W. *J. Biol. Chem.* **2005**, *280*, 1625-1633; (k) Jiang, H.; Penner, J. D.; Beard, R. L.; Chandraratna, R. A. S.; Kochhar, D. M. *Biochem. Pharmacol.* **1995**, *50*, 669-676; (l) Simoni, D.; Roberti, M.; Invidiata, F. P.; Rondanin, R.; Baruchello, R.; Malagutti, C.; Mazzali, A.; Rossi, M.; Grimaudo, S.; Dusonchet, L.;

Meli, M.; Raimondi, M. V.; D'Alessandro, N.; Tolomeo, M. *Bioorg. Med. Chem. Lett.* **2000**, *10*, 2669-2673.

²⁶² **3-Me-TTNPB and TTNPB synthesis and biological studies**

(a) Strickland, S.; Breitman, T. R.; Frickel, F.; Nürrenbach, A.; Hädicke, E.; Sporn, M. B. *Cancer Res.* **1983**, *43*, 5268-5272; (b) Boehm, M. F.; McClurg, M. R.; Pathirana, C.; Mangelsdorf, D.; White, S. K.; Hebert, J.; Winn, D.; Goldman, M. E.; Heyman, R. A. *J. Med. Chem.* **1994**, *37*, 408-414 (c) Boehm, M. F.; Zhang, L.; Badea, B. A.; White, S. K.; Mais, D. E.; Berger, E.; Suto, C. M.; Goldman, M. E.; Heyman, R. A. *J. Med. Chem.* **1994**, *37*, 2930-2941; (d) Beard, R. L.; Gil, D. W.; Marler, D. K.; Henry, E.; Colon, D. F.; Gillett, S. J.; Arefieg, T.; Breen, T. S.; Krauss, H.; Davies, P. J. A.; Chandraratna, R. A. S. *Bioorg. Med. Chem. Lett.* **1994**, *4*, 1447-1452 (e) Totpal, K.; Chaturvedi, M. M.; LaPushin, R.; Aggarwal, B. B. *Blood* **1995**, *85*, 3547-3555 (f) Islam, T. C.; Skarin, T.; Sumitran, S.; Toftgård, R. *Br. J. Dermatol.* **2000**, *143*, 709-719; (g) Gambone, C. J.; Hutcheson, J. M.; Gabriel, J. L.; Beard, R. L.; Chandraratna, R. A. S.; Soprano, K. J.; Soprano, D. R. *Mol. Pharmacol.* **2002**, *61*, 334-342.

²⁶³ Benbrook, D. M.; Subramanian, S.; Gale, J. B.; Liu, S.; Brown, C. W.; Boehm, M. F.; Berlin, K. D. *J. Med. Chem.* **1998**, *41*, 3753-3757.

²⁶⁴ Waugh, K. M.; Berlin, K. D.; Ford, W. T.; Holt, E. M.; Carrol, J. P.; Schomber, P. R.; Thompson, M. D.; Schiff, L. J. *J. Med. Chem.* **1985**, *28*, 116-124.

²⁶⁵ Büttner, M. W.; Burschka, C.; Daiss, J. O.; Ivanova, D.; Rochel, N.; Kammerer, S.; Peluso-Iltis, C.; Bindler, A.; Gaudon, C.; Germain, P.; Moras, D.; Gronemeyer, H.; Tacke, R. *ChemBioChem.* **2007**, *8*, 1688-1699.

²⁶⁶ Büttner, M. W.; Penka, M.; Doszczak, L.; Kraft, P.; Tacke, R. *Organometallics* **2007**, *26*, 1295-1298.

²⁶⁷ Beard, R. L.; Chandraratna, R. A. S.; Colon, D. F.; Gillett, S. J.; Henry, E.; Marler, D. K.; Song, T.; Denys, L.; Garst, M. E.; Arefieg, T.; Klein, E.; Gil, D. W.; Wheeler, L.; Kochhar, D. M.; Davies, P. J. A. *J. Med. Chem.* **1995**, *38*, 2820-2829.

²⁶⁸ Beard, R. L.; Colon, D. F.; Klein, E. S.; Vorse, K. A.; Chandraratna, R. A. S. *Bioorg. Med. Chem. Lett.* **1995**, *5*, 2729-2734.

²⁶⁹ Simoni, D.; Invidiata, F. P.; Rondanin, R.; Grimaudo, S.; Cannizzo, G.; Barbusca, E.; Porretto, F.; D'Alessandro, N.; Tolomeo, M. *J. Med. Chem.* **1999**, *42*, 4961-4969.

- ²⁷⁰ Price, C. C. *Chem. Rev.*, **1941**, 29, 37-67.
- ²⁷¹ Snieckus, V. *Chem. Rev.*, **1990**, 90, 879-933.
- ²⁷² Murphy, J. M.; Liao, X.; Hartwig, J. F. *J. Am. Chem. Soc.* **2007**, 129, 15434-15435.
- ²⁷³ Finke, A. D.; Moore, J. S. *Org. Lett.* **2008**, 10, 4851-4854.
- ²⁷⁴ Beck, E. M.; Hatley, R.; Gaunt, M. J. *Angew. Chem. Int. Ed.*, **2008**, 47, 3004-3007.
- ²⁷⁵ Lokare, K. S.; Staples, R. J.; Odom, A. L., *Organometallics* **2008**, 27, 5130-5138.
- ²⁷⁶ Garipova, G.; Gautier, A.; Piettre, S. R., *Tetrahedron* **2005**, 61, 4755-4759.
- ²⁷⁷ Farmer, L. J.; Zhi, L.; Jeong, S.; Kallel, E. A.; Croston, G.; Flatten, K. S.; Heyman, R. A.; Nadzan, A. M.; *Bioorg. Med. Chem. Lett.* **1997**, 7, 2747-2752.
- ²⁷⁸ (a) Harrisson, P.; Morris, J.; Steel, P. G.; Marder, T. B., *Synlett.* **2009**, 147-150; (b) Harrisson, P.; Morris, J.; Steel, P. G.; Marder, T. B. *Org. Lett.* **2009**, 11, 3586-3589.
- ²⁷⁹ Miller, S. A.; Bercaw, J. E. *Organometallics*, **2006**, 25, 3576-3592.
- ²⁸⁰ Chotana, G. A.; Rak, M. A.; Smith, M. R. III *J. Am. Chem. Soc.* **2005**, 127, 10539-10544.
- ²⁸¹ Although ketone **11** is known, its synthesis is not described in the open literature. Instead it is referenced to several patents with the most relevant being; Chandraratna, R. A. S. Method of treatment with compounds having retinoid-like activity and reduced skin toxicity and lacking teratogenic effects US patent 5,324, 840, June 28, 1994.
- ²⁸² Ishiyama, T.; Murata, M.; Miyaura, N. *J. Org. Chem.* **1995**, 60, 7508-7510.
- ²⁸³ Ni, W.; Fang, H.; Springsteen, G.; Wang, B. *J. Org. Chem.* **2004**, 69, 1999-2007.
- ²⁸⁴ Fang, H.; Kaur, G.; Yan, J.; Wang, B. *Tetrahedron Lett.* **2005**, 46, 1671-1674.
- ²⁸⁵ **Miyaura borylations of reluctant substrates**
- (a) Billingsley, K. L.; Barder, T. E.; Buchwald, S. L. *Angew. Chem. Int. Ed.* **2007**, 46, 5359-5363; (b) Ishiyama, T.; Ishida, K.; Miyaura, N. *Tetrahedron Lett.* **2001**, 57, 9813-9816. (c) Ma, Y.; Song, C.; Jiang, W.; Xue, G.; Cannon, J. F.; Wang, X.; Andrus, M. B. *Org. Lett.* **2003**, 5, 4635-4638.
- ²⁸⁶ Christie, V. B.; Barnard, J. H.; Batsanov, A. S.; Bridgens, C. E.; Cartmell, E. B.; Collings, J. C.; Maltman, D. J.; Redfern, C. P. F.; Marder, T. B.; Przyborski, S. A.; Whiting, A. *Org. Biomol. Chem.* **2008**, 6, 3497-3507.
- ²⁸⁷ Van Horn, D. E.; Negishi, E. *J. Am. Chem. Soc.* **1978**, 100, 2252-2254.
- ²⁸⁸ **Dehydrogenative alkene borylations with *trans*-[Rh(PPh₃)₂(CO)Cl]**

(a) Coapes, R. B.; Souza, F. E. S.; Thomas, R. L.; Hall, J. J.; Marder, T. B. *Chem. Commun.* **2003**, 614-615; (b) Mkhaliid, I. A. I.; Coapes, R. B.; Edes, S. N.; Coventry, D. N.; Souza, F. E. S.; Thomas, R. L.; Hall, J. J.; S.-W., B.; Lin, Z.; Marder, T. B. *Dalton Trans.* **2008**, 1055-1064.

²⁸⁹ Beller, M.; Riermeier, T. H. *Eur. J. Inorg. Chem.* **1998**, 29-35.

²⁹⁰ Ent, A. V.; Onderdelinden, A. L. *Inorg. Synth.* **1990**, 28, 90-92.

²⁹¹ Uson, R.; Oro, L. A.; Cabeza, J. A. *Inorg. Synth.* **1985**, 23, 126-130.

²⁹² Evans, D.; Osborn, J. A.; Wilkinson, G. *Inorg. Synth.* **1966**, 8, 215.

²⁹³ McLverty, J. A.; Wilkinson, G. *Inorg. Synth.* **1968**, 11, 99.

²⁹⁴ McCortney, B. A.; Jacobson, B. M.; Vreeke, M.; Lewis, E. S. *J. Am. Chem. Soc.* **1990**, 112, 3554-3559.

Synthesis of tolan-, and biaryl-based retinoids *via* palladium-catalysed cross-couplings

3.1 Introduction

All-*trans* retinoic acid (ATRA), and its two naturally occurring isomers, 9-*cis*-retinoic acid (9cRA) and 13-*cis*-retinoic acid (13cRA) (**Figure 3.1**), are involved in the mediation of many biological processes, in both embryonic development and in adult life, particularly in the nervous system.²⁹⁵ Endogenous retinoids are essential for the mediation of cell proliferation, differentiation and apoptosis, and maintain these processes in both normal and tumour cells both *in vivo* and *in vitro*.

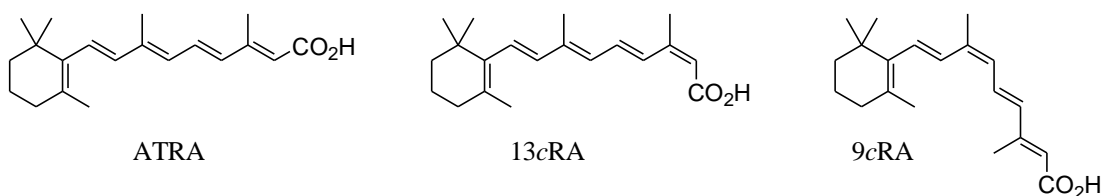


Figure 3.1 Natural retinoids.

The polyene chains of natural retinoids are excellent chromophores, which efficiently absorb light in the region of 300-400 nm (depending on the solvent). This makes these molecules particularly susceptible to photoisomerisation, leading to degradation into a mixture of retinoic acid isomers.²⁹⁶ The isomerisation of ATRA plays an important part in its metabolic pathways within cells, giving rise to 9cRA and 13cRA which possess different mechanisms of action,^{297,298} with Murayama *et al.* reporting that the different retinoic acid isomers differentially affected the ability of mammalian stem cells to differentiate along alternative lineages.²⁹⁶

In addition, cellular responses may be determined by the concentrations of the different retinoic acid isomers present in solution. For example, the induction of the differentiation of pluripotent stem cells using retinoids is variable, resulting in the differential activation of key molecular pathways involved in tissue development in a concentration dependent manner.²⁹⁹ In turn, this variation has the potential to result in mixed proportions of

alternative differentiating cell types leading to increased culture heterogeneity. To reduce such variability in differentiation responses and improve experimental reproducibility, it is essential that compounds used for the induction of cellular differentiation exist in the same form and concentration every time. For compounds such as ATRA and its stereoisomers, this cannot be currently guaranteed, due to the high degree of susceptibility of these compounds to undergo isomerisation under the conditions used for sample preparation, storage of stock solution and in cell culture.

Due to the diverse effects of RA isomers on cells, attempts have been made to limit the isomerisation and degradation of ATRA. A number of additives have been found to inhibit either the *cis-trans* interconversion or oxidation of natural retinoids, including bovine serum albumin (BSA), fibrogen, lysozyme, phosphatidylcholine, *N*-ethylmaleimide and vitamin C.³⁰⁰ However, the addition of such molecules to cell culture media is often not viable as such additives may themselves affect cell behaviour. In addition, none of these additives can completely prevent isomerisation and, for example, the use of BSA is not possible in serum-free culture media.

An alternative is the synthesis of analogues of ATRA in which the unstable polyene chain of the linker unit is incorporated into one or more aromatic rings (arotinoids). As detailed in chapter 1 (section **1.1.3.4**), a wide variety of different functionalities have been employed as linker units in arotinoids, with changes in linker structure allowing for selectivity between RAR and RXR as well as RAR isotypes to be controlled.

Arotinoids possessing linker units based on disubstituted alkynes or biaryl units were chosen because it was envisaged that the use of these moieties as linker units would give retinoids with high degrees of resistance to both thermal and photochemical degradation.

Comparison of ATRA and 9cRA with tolan-, and biaryl-based arotinoids (**Figure 3.2**) shows that *para*-substituted arotinoids appear similar to the natural retinoid ATRA, while their *meta*-substituted analogues may be considered to be potential 9cRA analogues.

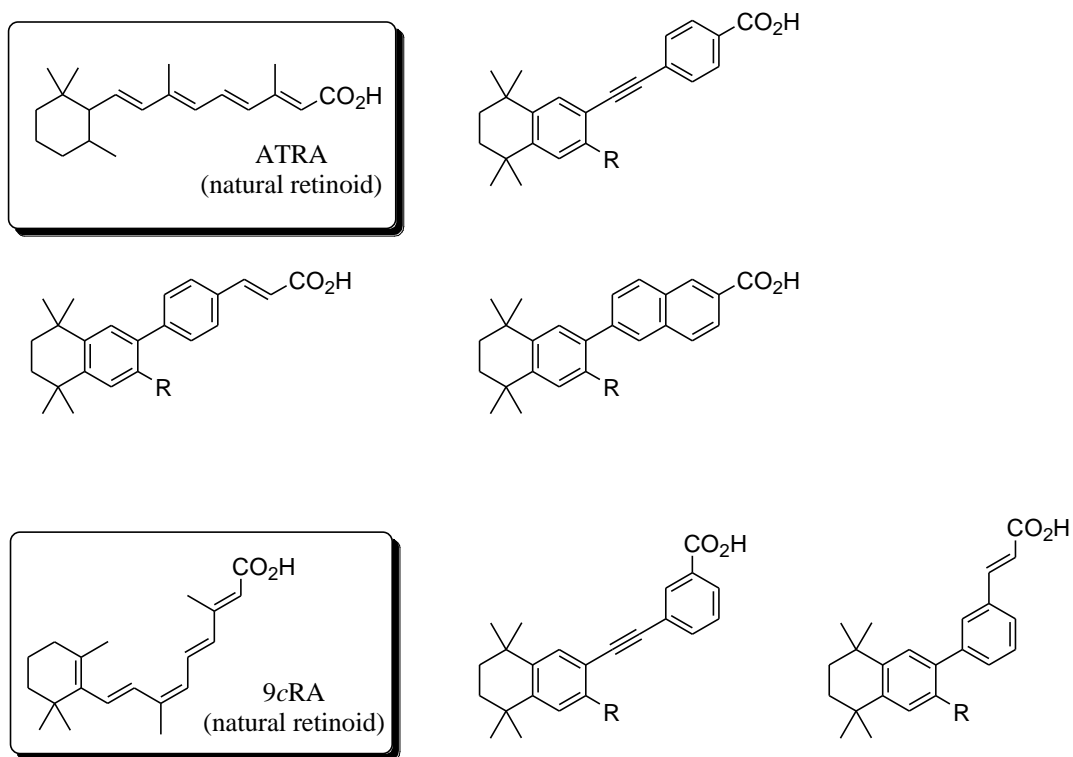
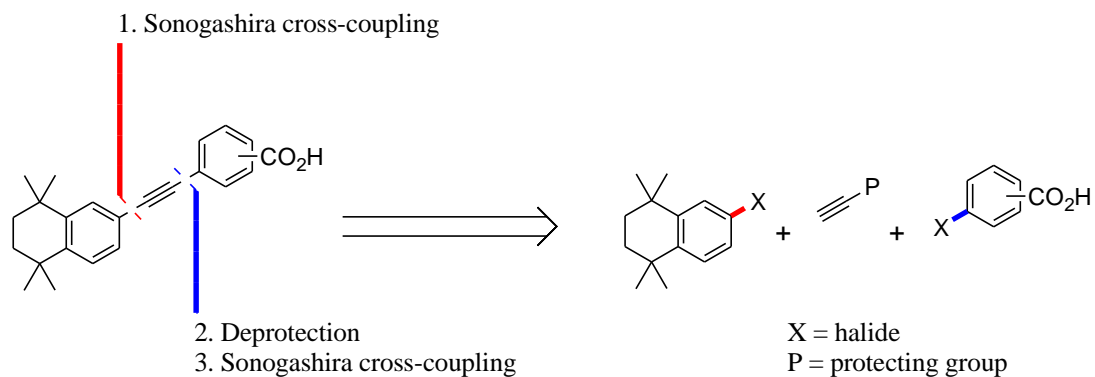


Figure 3.2 Arotinoid analogues (detailed in this work) of ATRA and 9cRA, R = H, Me.

3.2 Synthetic retinoids based on the tolan structure

Although substituted alkynes can be synthesised *via* a variety of methods, the Sonogashira reaction³⁰¹ is one of the most effective methods due to the mild conditions employed and the high degree of functional group tolerance displayed. Thus, a short synthesis of tolan-based arotinoids was devised based upon Sonogashira cross-coupling of an aryl halide with a monoprotected alkyne, removal of the alkyne protecting group and subsequent Sonogashira reaction of the monosubstituted alkyne with a second aryl halide to give the tolan products (**Scheme 3.1**).



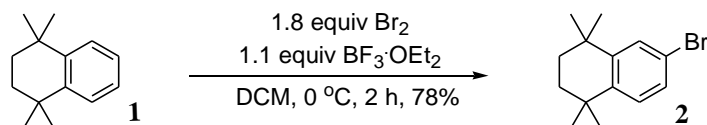
Scheme 3.1 Retrosynthetic analysis of tolan-based retinoids *via* Sonogashira cross-couplings.

Attempts to synthesise the desired aryl bromide *via* AlCl_3 -catalysed Friedel-Crafts dialkylation of bromobenzene with 2,5-dichloro-2,5-dimethylhexane, as described in the literature,³⁰² were unsuccessful, as were reactions of 2,5-dichloro-2,5-dimethyl-hexane with iodobenzene or phenylethylnyltrimethylsilane under the same conditions (**Equation 3.1**).



Equation 3.1 Unsuccessful attempts to synthesise functionalised tetrahydronaphthalenes.

Instead, bromination of the commercially available 1,1,4,4-tetramethyl-1,2,3,4-tetrahydronaphthalene **1** was achieved using $\text{BF}_3 \cdot \text{OEt}_2$ and 1.8 equivalents of bromine in DCM at 0°C to give 6-bromo-1,1,4,4-tetramethyl-1,2,3,4-tetrahydronaphthalene **2** in good yield (**Equation 3.2**).



Equation 3.2 Bromination of **1** with $\text{Br}_2/\text{BF}_3 \cdot \text{OEt}_2$ to give **2**.

Attempts to further increase yields by the use of more forcing conditions led to the formation of a dibrominated product, as evidenced by GC-MS (**Figure 3.3**).

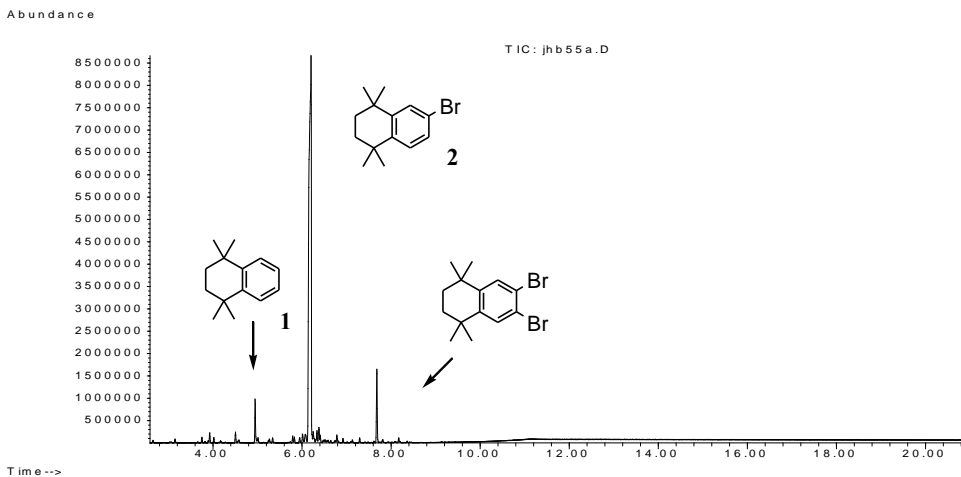


Figure 3.3 GC (TIC) for the synthesis of **2** via bromination of **1** with $\text{BF}_3 \cdot \text{OEt}_2$.

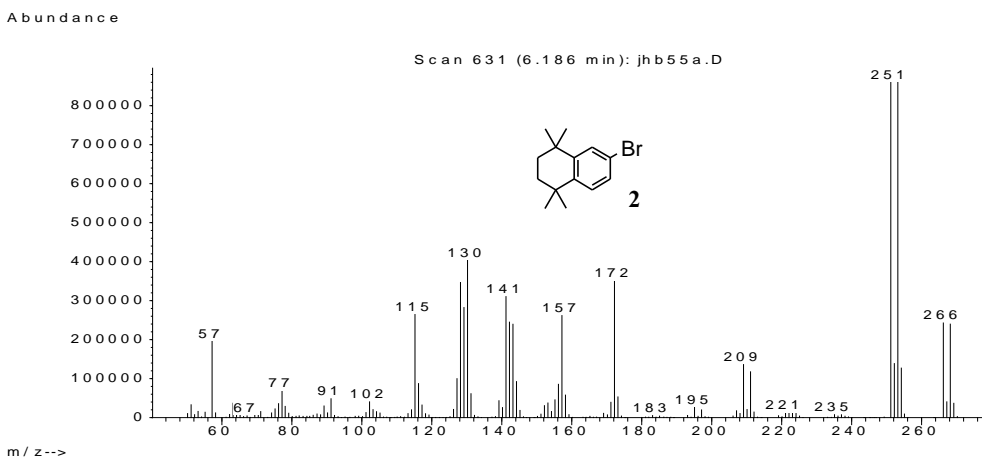
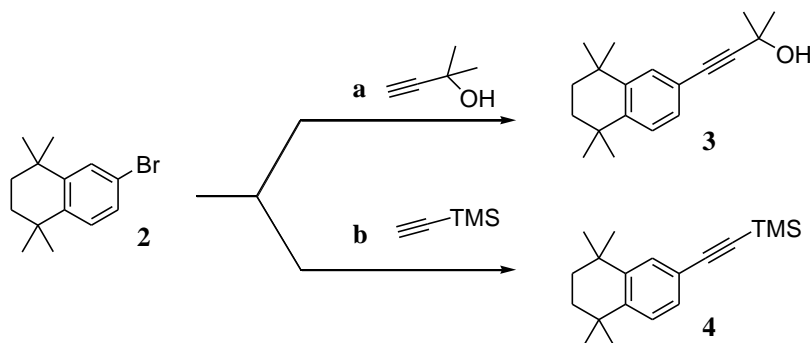


Figure 3.4 MS of **2**.

The subsequent Sonogashira cross-coupling of **2** with 2-methyl-3-butyn-2-ol or ethynyltrimethylsilane (TMSA) (**Equation 3.3**), carried out according to the literature procedure (2 mol % $\text{Pd}(\text{PPh}_3)_2\text{Cl}_2$ and 2 mol % CuI in triethylamine at 78 °C for 18 h),³⁰³ initially gave low conversions of <5%. Increased catalyst loadings (up to 10 mol %), under the same conditions, did not lead to improved conversions, and large amounts of black palladium precipitates were observed. The low activity of **2** in Sonogashira couplings, even under forcing conditions, suggests that the tetramethylated aliphatic ring of **2** is strongly σ -donating and thus deactivating. However, a combination of PdCl_2 , PPh_3

and $\text{Cu}(\text{OAc})_2$, in a 1:5:1 ratio, which generates the active catalyst *in situ*, was found to be effective for the Sonogashira couplings of **2**.

The use of this catalyst system with 10 mol % Pd loadings in the couplings of **2** with both TMSA and 2-methyl-3-butyn-2-ol gave 100% conversions in both cases giving **3**, and **4**, respectively, with no formation of black palladium precipitates observed. The reaction with TMSA was more rapid than that of 2-methyl-3-butyn-2-ol with full conversion to the alkyne products requiring 18 hours and 3 days of heating, respectively (**Equation 3.3**).



a 10 mol % PdCl_2 , 0.5 equiv PPh_3 , 10 mol % $\text{Cu}(\text{OAc})_2$, NEt_3 , 78 °C, 3 d, 45%

b 10 mol % PdCl_2 , 0.5 equiv PPh_3 , 10 mol % $\text{Cu}(\text{OAc})_2$, NEt_3 , 78 °C, 18 h, 81%

Equation 3.3 Sonogashira cross-couplings of **2** to give **3** and **4**.

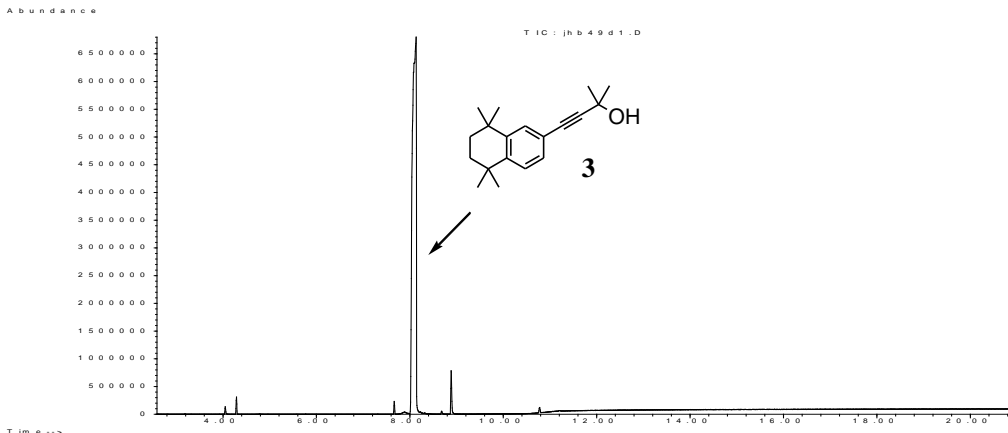
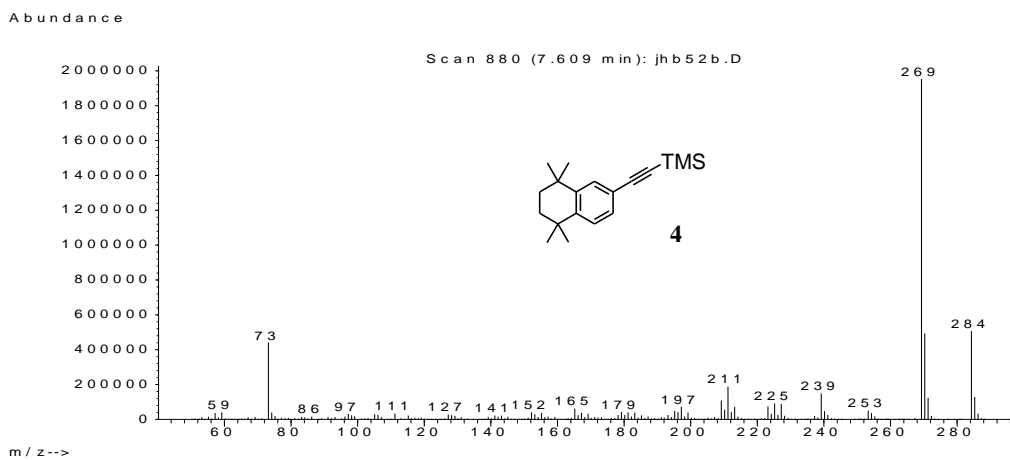
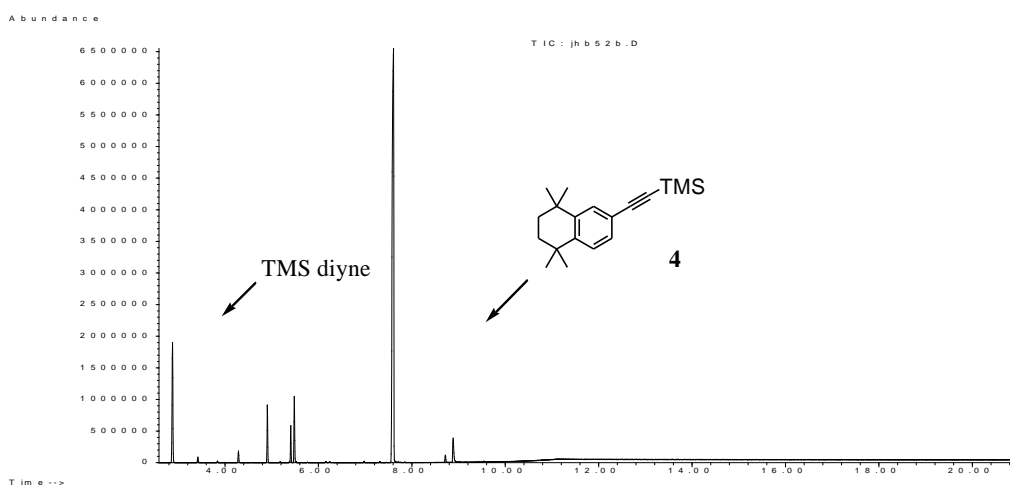
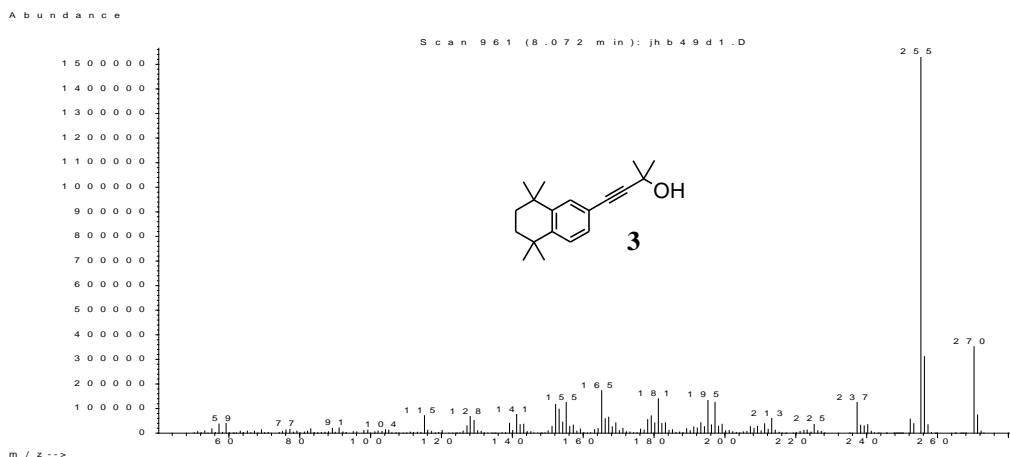
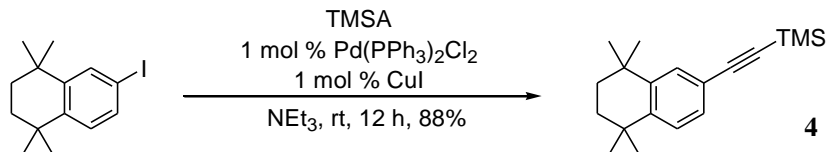


Figure 3.5 GC (TIC) of the Sonogashira reaction of **2** with 2-methyl-3-butyn-2-ol to give **3** after 72 h.



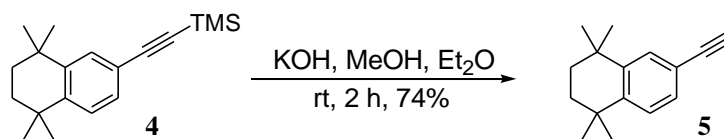
In light of the low activity of **2**, more reactive coupling partners were required. The use of the iodide analogue of **2** (previously detailed in Chapter 2, compound **15**) allowed for the

reaction to be carried out at room temperature, using of 1 mol% Pd(PPh₃)₂Cl₂ and 1 mol % CuI as catalysts, with full conversion to **4** observed after 12 hours (**Equation 3.4**).



Equation 3.4 Mild Sonogashira cross-coupling to give **4**.

TMS-protected alkyne **4** was desilylated by treatment with KOH in Et₂O / MeOH to give **5** (**Equation 3.5**). Deprotection of **3** with KOH in refluxing toluene was sluggish and, in the light of the higher reactivity of TMSA in Sonogashira cross-couplings with bromide **2**, and the more facile deprotection of **4**, the use of **3** was not pursued further.



Equation 3.5 Desilylation of **4** with KOH to give acetylene **5**.

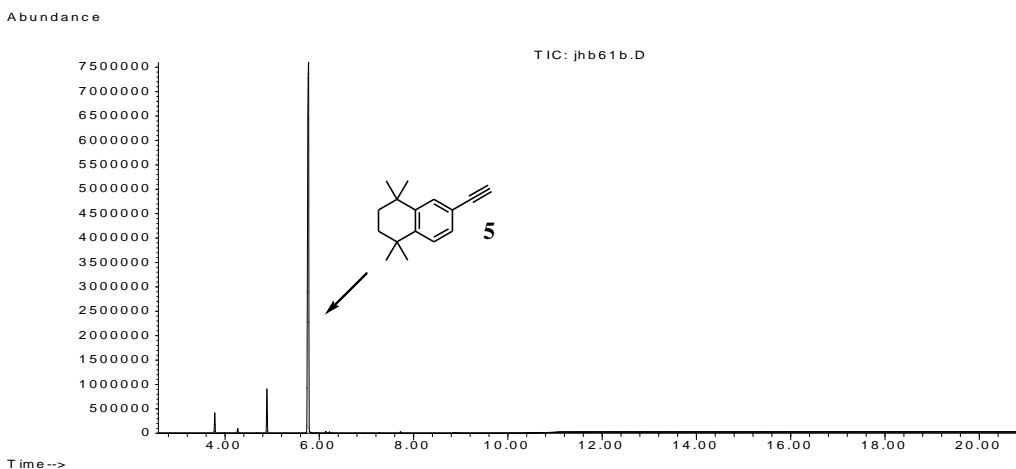


Figure 3.9 GC (TIC) for the desilylation of **4** with KOH to give **5**.

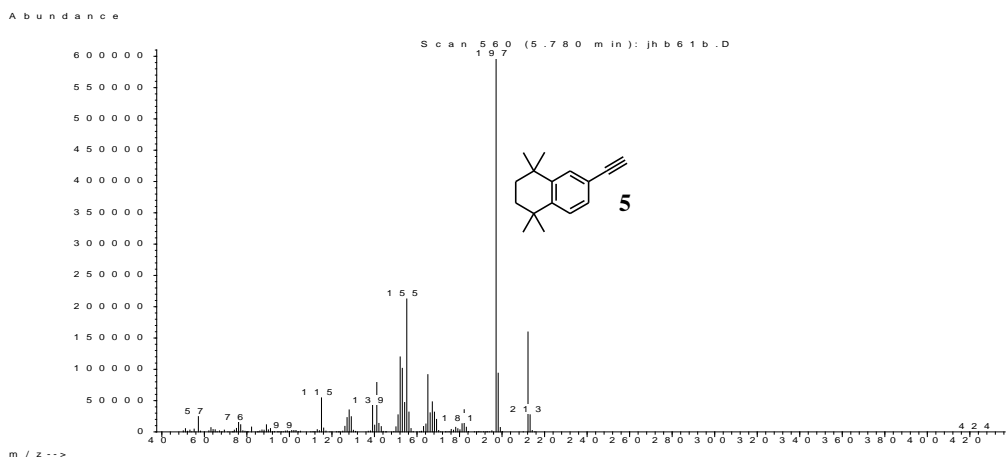


Figure 3.10 MS of **5**.

Monoclinic single crystals of **5** ($P2_1/c$) grew from pure liquid **5** upon standing. The alkyne triple bond distance C(15)-C(16) was found to be 1.1789(16) Å (**Figure 3.11**).

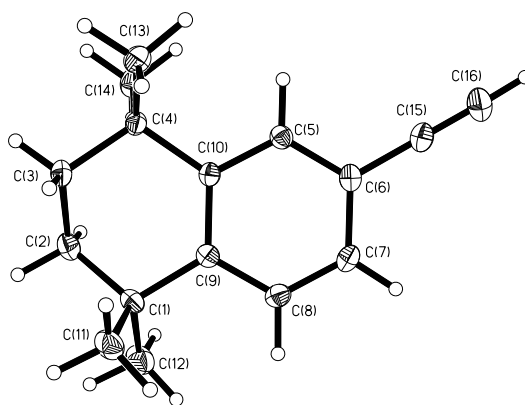
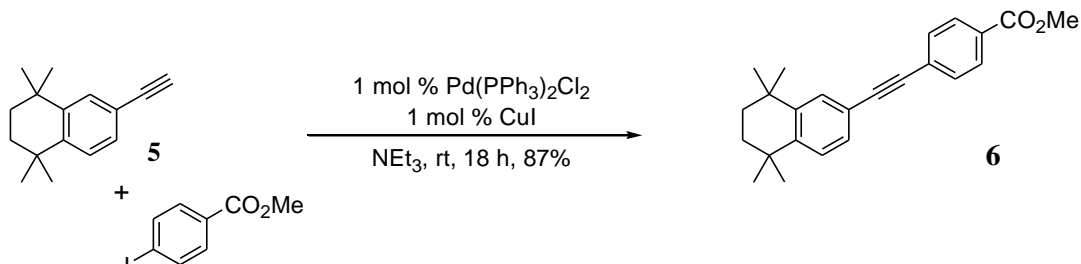


Figure 3.11 Molecular structure of alkyne **5**. Thermal ellipsoids are drawn at the 50% probability level.

Terminal alkyne **5**, was coupled with 4-iodomethylbenzoate with a 1 mol % loading of both $\text{Pd}(\text{PPh}_3)_2\text{Cl}_2$ and CuI in neat NEt_3 at room temperature to give retinoid methyl ester **6** in a high yield (**Equation 3.6**).



Equation 3.6 Sonogashira cross-coupling of **5** with 4-iodomethylbenzoate to give **6**.

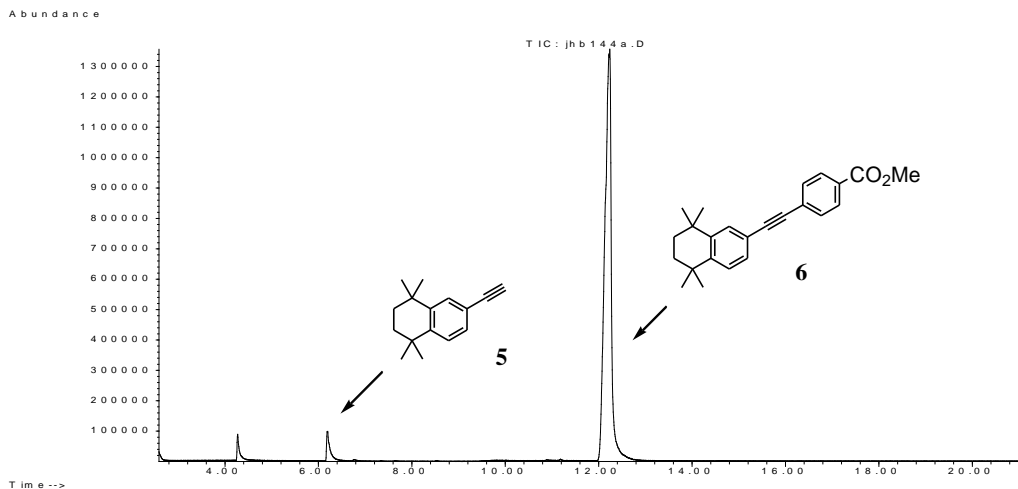


Figure 3.12 GC (TIC) for the Sonogashira cross-coupling of **5** with 4-iodomethylbenzoate to give **6**.

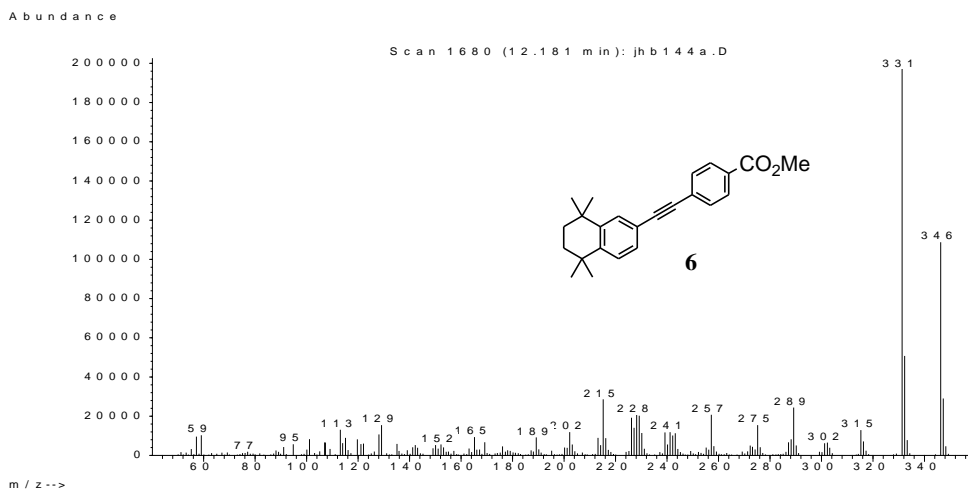


Figure 3.13 MS of **6**.

Triclinic single crystals of *para*-retinoid ester **6** (*P-1*) were grown from a concentrated solution of **6** in MeOH at $-20\text{ }^{\circ}\text{C}$. The interplanar angle between rings *i* and *ii* is 69.3° , while that between ring *ii* and the methoxycarbonyl group is 6.4° . The torsion angle C(7)-C(6)⋯C(17)-C(22) is $66.2(2)^{\circ}$ (**Figure 3.14**).

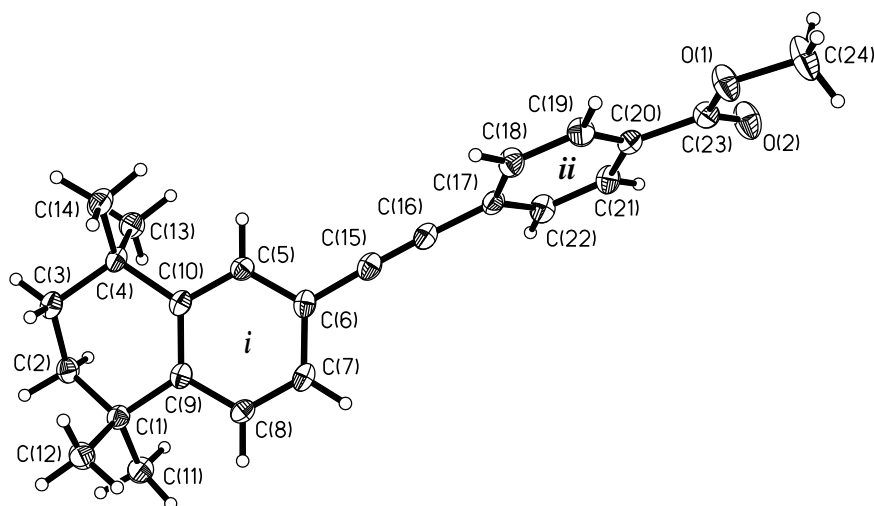
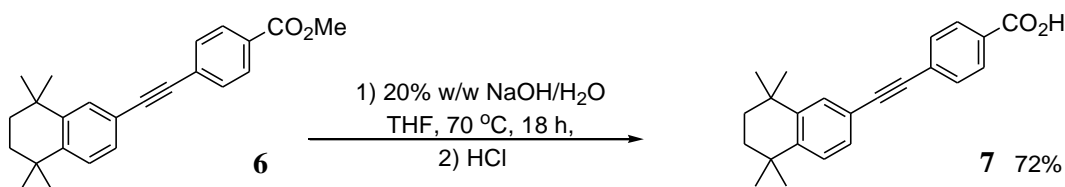


Figure 3.14 Molecular structure of compound **6**. Thermal ellipsoids are drawn at the 50% probability level.^{*304}

Hydrolysis of **6** with concentrated aqueous NaOH in refluxing THF gave the target compound **7** in high yield (**Equation 3.7**) after acidification. The synthesis of **7** directly could be achieved *via* the Sonogashira cross-coupling of **5** with 4-iodobenzoic acid under the same conditions described for the synthesis of **6**. However, yields were lower than for the 2 step process and both the work up and purification of the product proved troublesome.



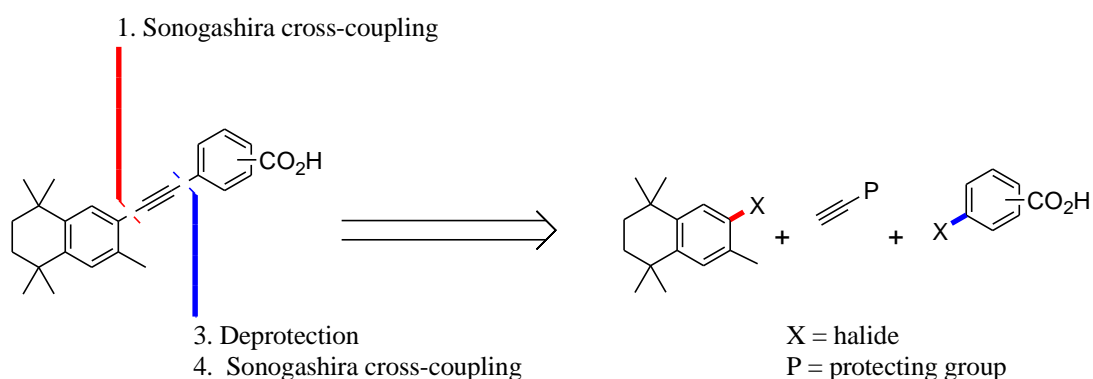
Equation 3.7 Hydrolysis of **6** with aqueous hydroxide to give **7**.

3.2.2 Synthesis of 3-methylated retinoids based on the tolan structure

*The molecular structures of **2**, its iodide analogue, **4**, and the *meta*-analogue of **6** were also determined. Crystals of these compounds were grown by Ms E. B. Cartmell and Dr. J. C. Collings.

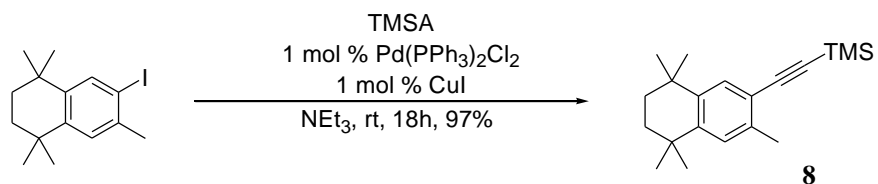
The replacement of the proton in the 3-position of certain arotinoids with larger substituents (i.e., Me) results in substantial changes in the binding affinities for RARs and RXRs and in the toxicity. This effect, often termed the α -methyl effect, is believed to result from the increase in the dihedral angle between the plane of the hydrophobic unit and that of the linker unit due to unfavourable steric interactions between the 3-substituent and the linker unit.³⁰⁵ The adoption of this twisted conformation (more similar to that of 9cRA than to ATRA) results in an increased selectivity for RXR binding over RAR binding and reduced toxicity (which is associated with pathways mediated by RAR activation).³⁰⁶ In addition, the toxicity of retinoids with 3-alkyl substituents may also be reduced by their more facile oxidative metabolism, which predominantly occurs in allylic / benzylic positions in retinoids.³⁰⁷ Thus, by comparing 3-methylated retinoids with linear and non-linear linker units it may be possible to determine the extent of the contributions of conformational and metabolic effects to the change in biological activity observed upon the addition of a 3-methyl group to arotinoids.

A short synthesis of 3-methylated tolan-based arotinoids was devised. Again, this was based upon the Sonogashira cross-coupling of an aryl halide with a monoprotected alkyne, removal of the alkyne protecting group and subsequent Sonogashira reaction of the monosubstituted alkyne with a second aryl halide to give the tolan products (**Scheme 3.2**).



Scheme 3.2 Retrosynthetic analysis for the 3-methylated EC retinoid skeleton *via* Sonogashira cross-couplings.

The desired iodide (detailed in Chapter 2, compound **13**) was synthesised by the iodination of 1,1,4,4,6-pentamethyl-1,2,3,4-tetrahydronaphthalene (chapter 2, compound **9**) with a combination of I_2/HIO_4 in acetic acid. Sonogashira cross-coupling with TMSA with 1 mol % of $Pd(PPh_3)_2Cl_2$ and CuI catalysts gave the desired TMS-protected alkyne **8** in excellent yield.



Equation 3.8 Synthesis of **8** via Sonogashira cross-coupling.

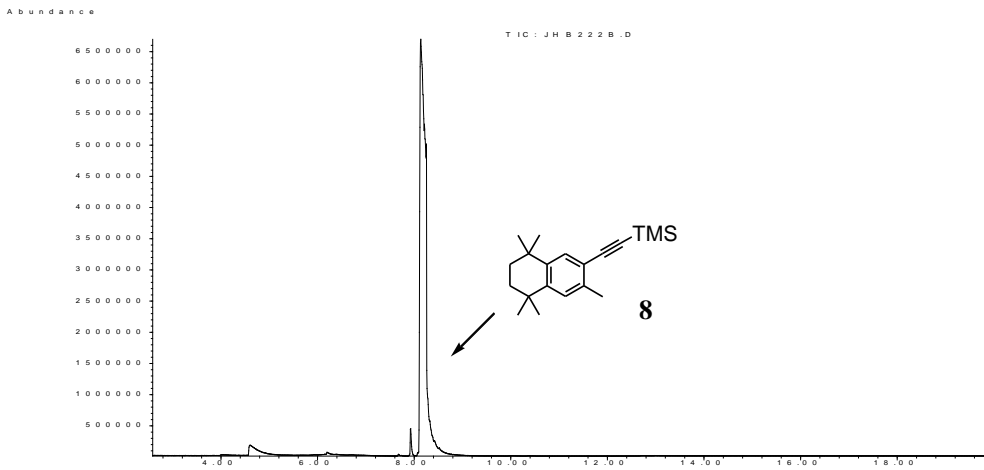


Figure 3.15 GC (TIC) for the synthesis of **8** via Sonogashira cross-coupling.

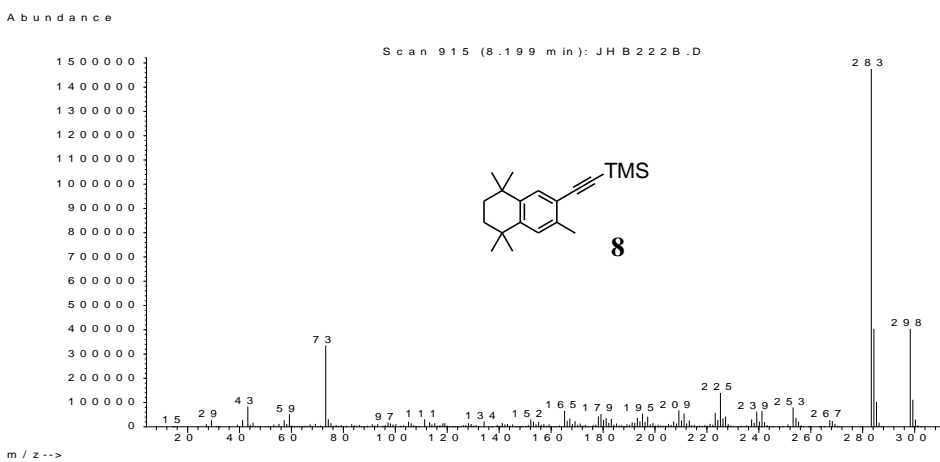
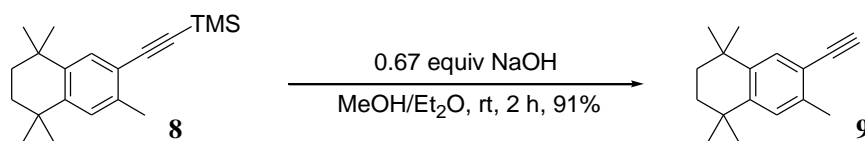


Figure 3.16 MS of **8**.

Desilylation of compound **8** was achieved with NaOH in MeOH / Et₂O to give the terminal alkyne **9**³⁰⁸ in excellent yield.



Equation 3.9 Desilylation of **8** with NaOH to give **9**.

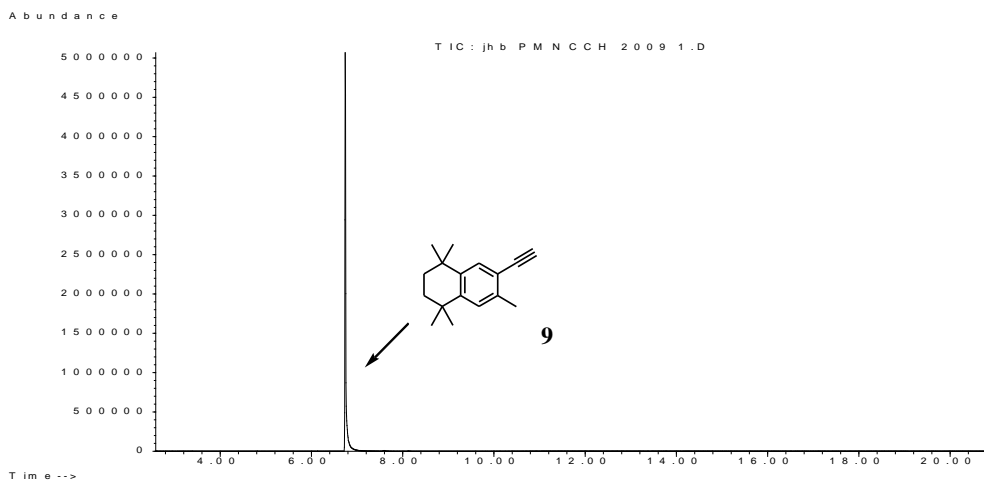


Figure 3.17 GC (TIC) for the desilylation of **8** to give **9** after 2 h.

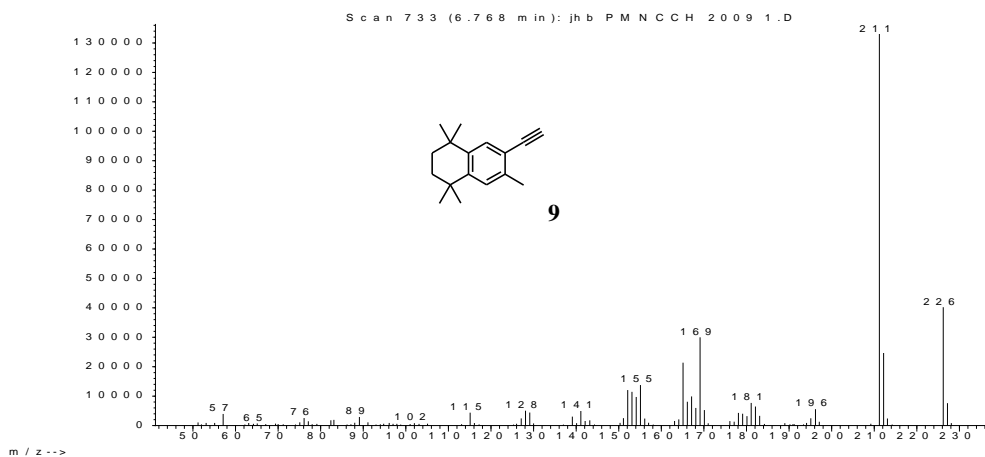
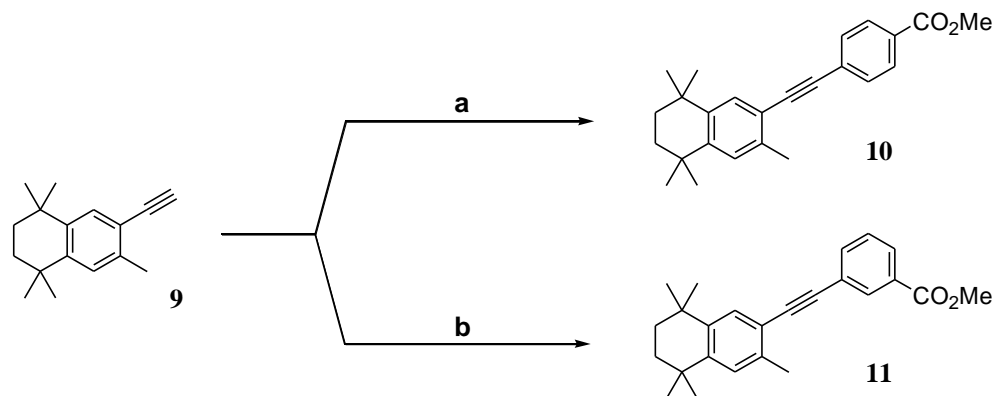


Figure 3.18 MS of **8**.

Terminal alkyne **9** underwent Sonogashira cross-couplings with 3-, and 4-iodomethylbenzoate in the presence of 1 mol % of Pd(PPh₃)₂Cl₂ and CuI catalysts at ambient temperature to give the 3-methylated retinoid esters in good yields.



- a.** *p*-I-C₆H₄-CO₂Me, 1 mol % Pd(PPh₃)₂Cl₂, 1 mol % CuI, NEt₃, rt, 18 h, 77%
b. *m*-I-C₆H₄-CO₂Me, 1 mol % Pd(PPh₃)₂Cl₂, 1 mol % CuI, NEt₃, rt, 18 h, 71%

Equation 3.10 Sonogashira cross-couplings of **9** with iodomethylbenzoates to give **10** and **11**.

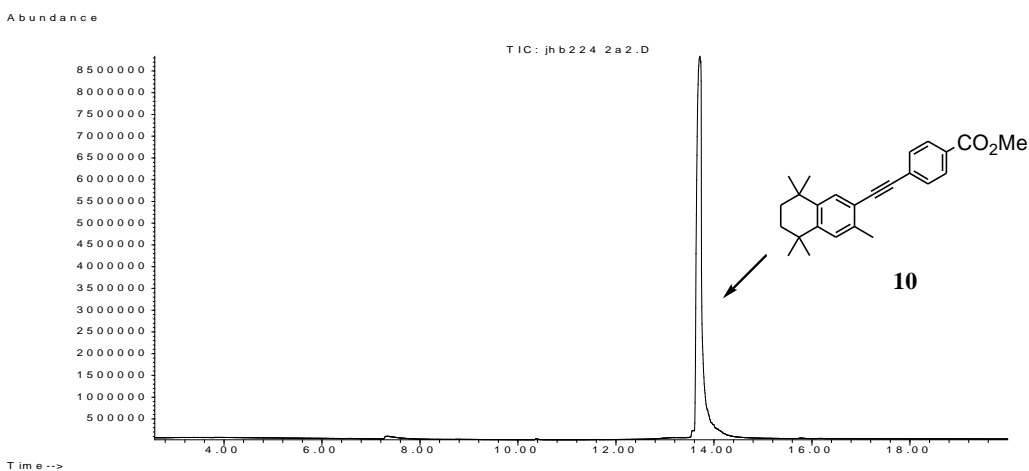


Figure 3.19 GC (TIC) for the synthesis of **10** from **9** and 4-iodomethylbenzoate after 18 h.

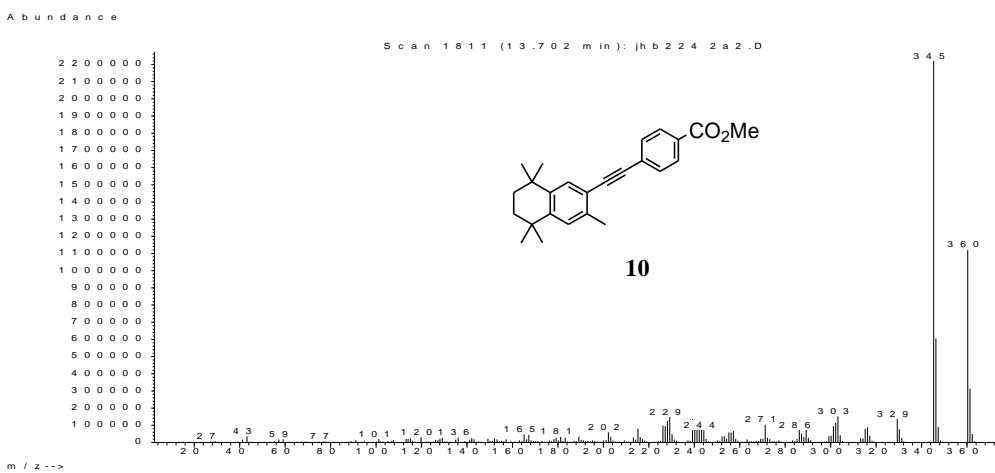


Figure 3.20 MS of **10**.

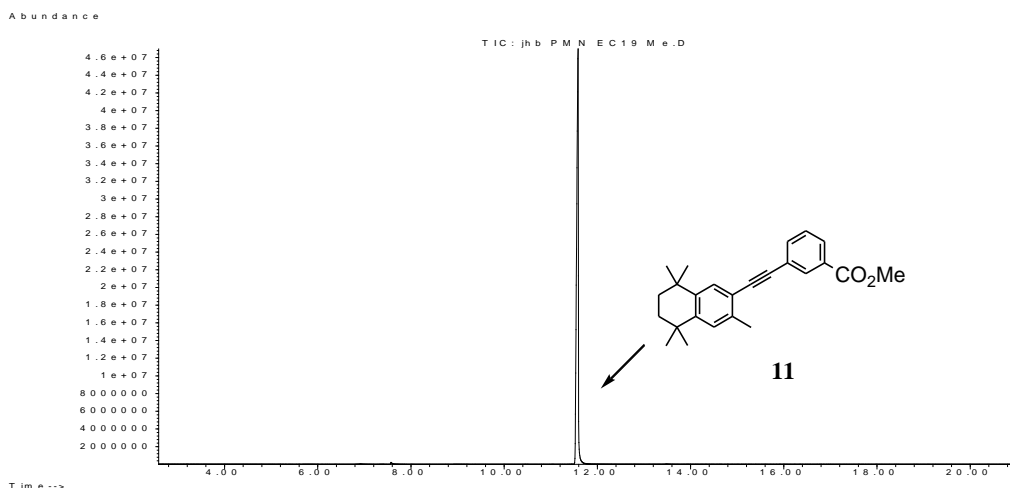


Figure 3.21 GC (TIC) for the synthesis of **11** from **9** and 3-iodomethylbenzoate after 18 h.

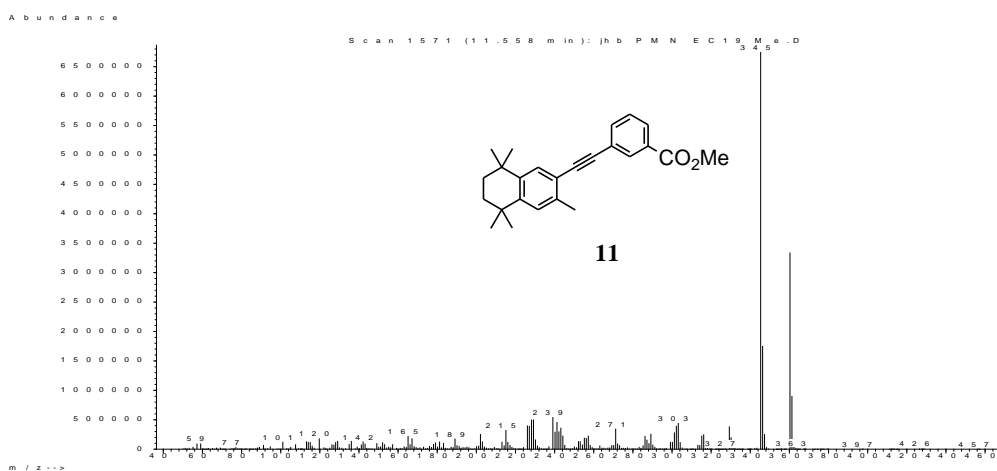


Figure 3.22 MS of **11**.

Orthorhombic single crystals of **10** (*Pccn*) were grown from a concentrated EtOH solution at $-20\text{ }^{\circ}\text{C}$ (**Figure 3.23**), while monoclinic single crystals of **11** (*P2₁/c*) were grown *via* slow evaporation of a concentrated EtOH/Et₂O solution at room temperature (**Figure 3.24**).

For **10**, the interplanar angle between rings *i* and *ii* is 16.3° , and that between ring *ii* and the methoxycarbonyl group is 7.7° . For **11** the interplanar angle between rings *i* and *ii* is 5.3° , and that between ring *ii* and the methoxycarbonyl group is 5.5° .

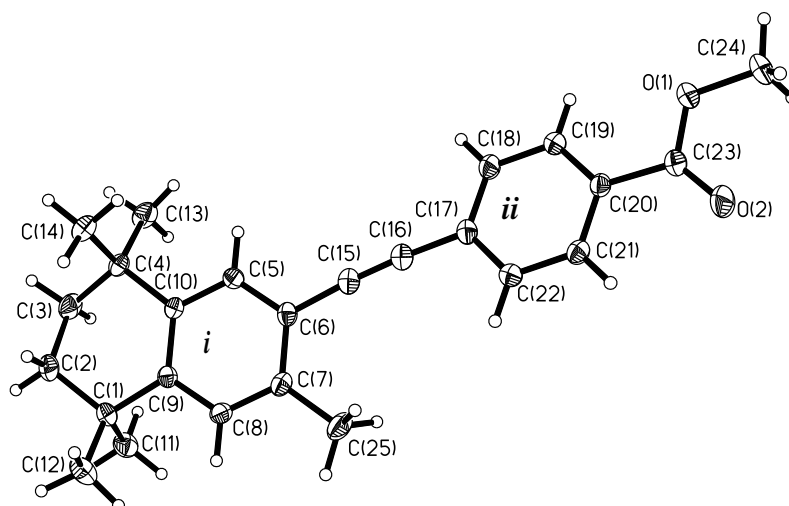


Figure 3.23 Molecular structure of compound **10**. Thermal ellipsoids are drawn at the 50% probability level.

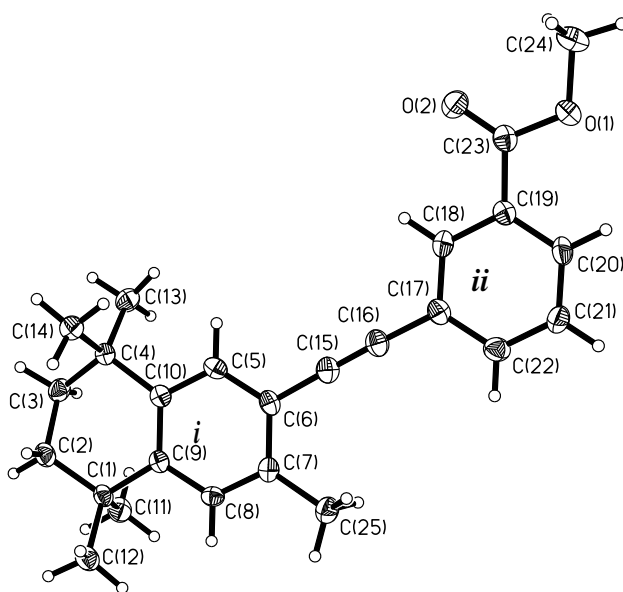
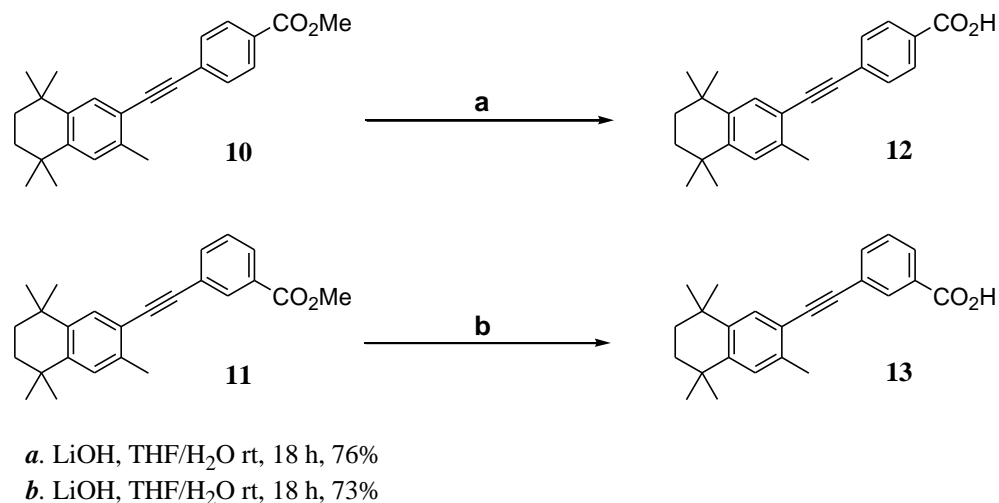


Figure 3.24 Molecular structure of compound **11**. Thermal ellipsoids are drawn at the 50% probability level.

Retinoid methyl esters **10** and **11** were hydrolysed with LiOH at ambient temperature in a mixture of THF and H₂O to give their acid derivatives **12** and **13**, respectively, in good yields (**Equation 3.11**).



Equation 3.11 Hydrolysis of **10** and **11** with LiOH to give **12** and **13**.

3.3 Synthesis of retinoid esters based on the biaryl structure

Biaryl-based arotinoids, such as TTNN,^{309,310} have been shown to possess high activities in a variety of screens for retinoidal activity, such as the TOC (tracheal organ cells) assay. In addition, biaryl moieties can be efficiently constructed by Suzuki-Miyaura cross-couplings making these compounds excellent targets for synthesis using the combined aromatic C-H borylation / cross-coupling approach for retinoid synthesis previously applied to the TTNPB series in Chapter 2.

Building upon the synthesis of 3-methylated and non-methylated 1,1,4,4-tetramethyl 1,2,3,4-tetrahydronaphthalene boronate esters **a**, **b**, **c** and **d** (detailed in Chapter 2, as compounds **6**, **16**, **10a** and **14**, respectively) (**Figure 3.25**) rapid syntheses of a range of biaryl retinoid esters were envisaged utilising Suzuki-Miyaura cross-couplings of these useful building blocks.

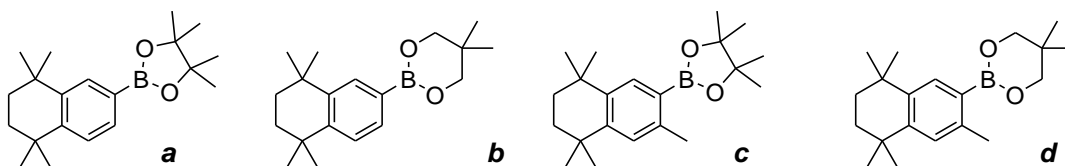
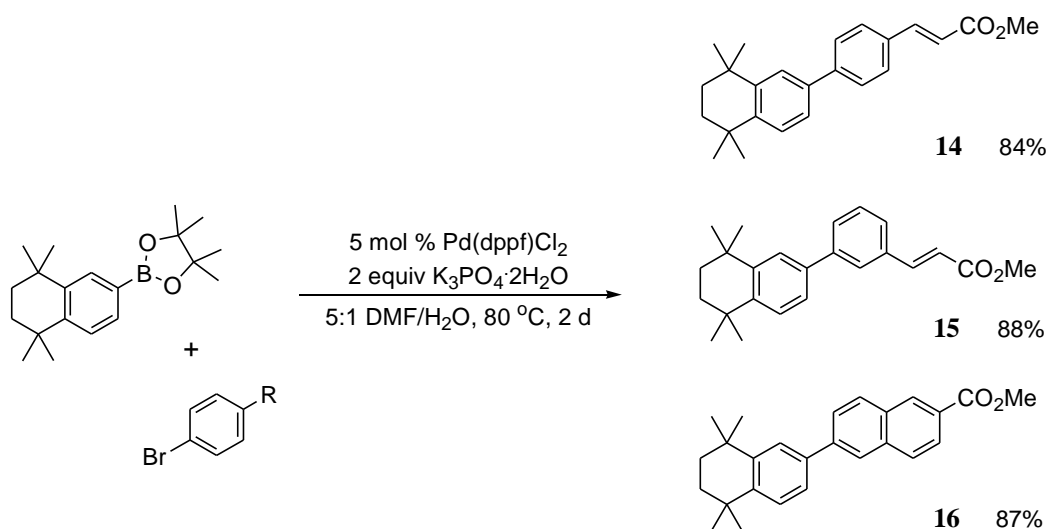


Figure 3.25 Boronate ester building blocks for retinoid synthesis.

For the synthesis of the non-methylated biaryl retinoid esters **14**, **15** and **16**, pinacolboronate ester **a** (Chapter 2, compound **6**) was utilised due to its ease of synthesis (*via* Ir-catalysed C-H borylation with B₂pin₂) and its marginally higher reactivity, compared to its neopentane glycolate ester analogue **b**.

The pinacol boronate ester underwent Suzuki-Miyaura cross-coupling with 3-, and 4-bromo-cinnamic acid methyl esters and 6-bromonaphthalene-2-carboxylic acid methyl ester to give the retinoid esters **14**, **15** and **16**, respectively, in high yields (**Equation 3.12**). The reactions were carried out in the presence of 5 mol % Pd(dppf)Cl₂ catalyst and 2 molar equivalents of K₃PO₄·2H₂O base in a combination of DMF/H₂O at 80 °C. The reactions were heated for 2 days, at which time analysis by *in situ* GC-MS showed all reactions to be complete.



Equation 3.12 Synthesis of biaryl retinoid esters **14**, **15** and **16** *via* Suzuki-Miyaura cross-couplings.

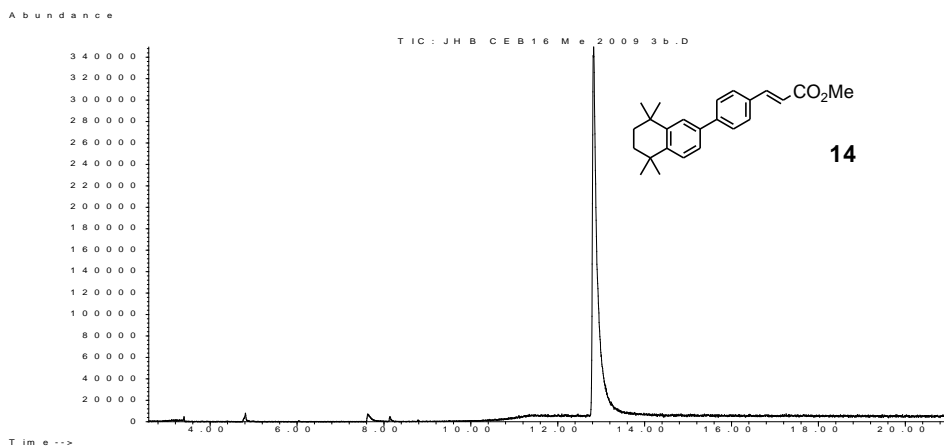


Figure 3.26 GC (TIC) for the synthesis of **14** from boronate ester *a*.

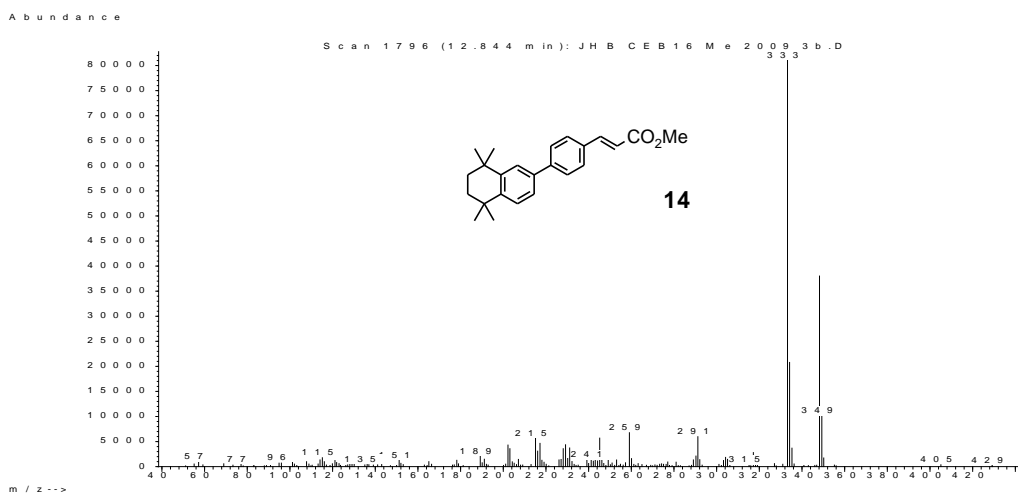


Figure 3.27 MS of **14**.

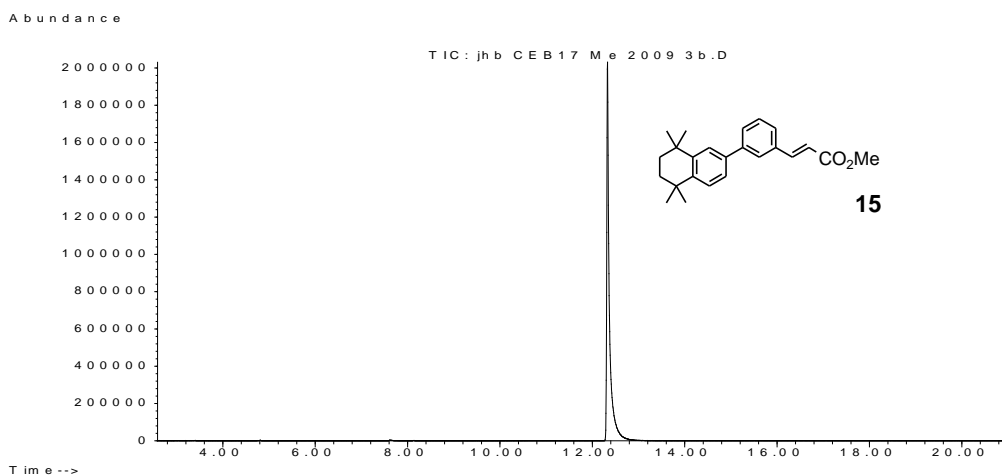


Figure 3.28 GC (TIC) for the synthesis of **15** from boronate ester *a*.

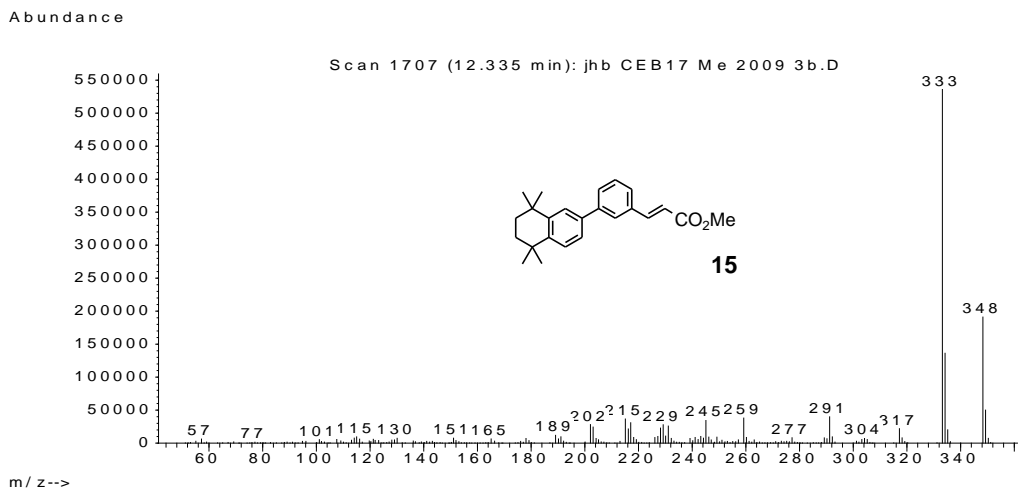


Figure 3.29 MS of 15.

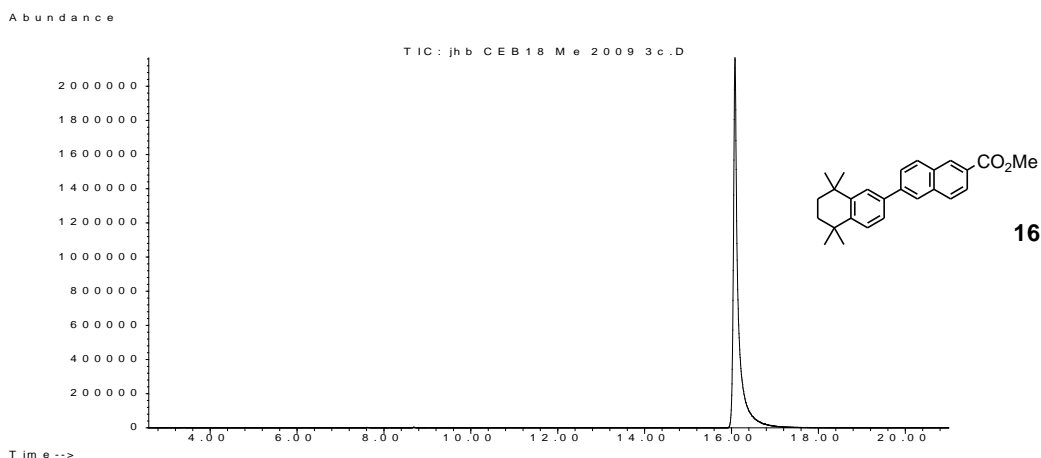


Figure 3.30 GC (TIC) for the synthesis of 16 from boronate ester *a*.

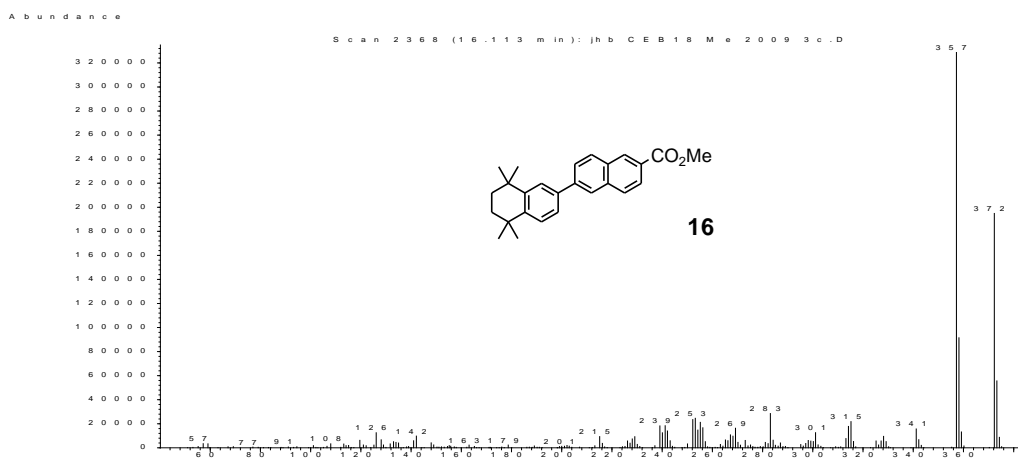
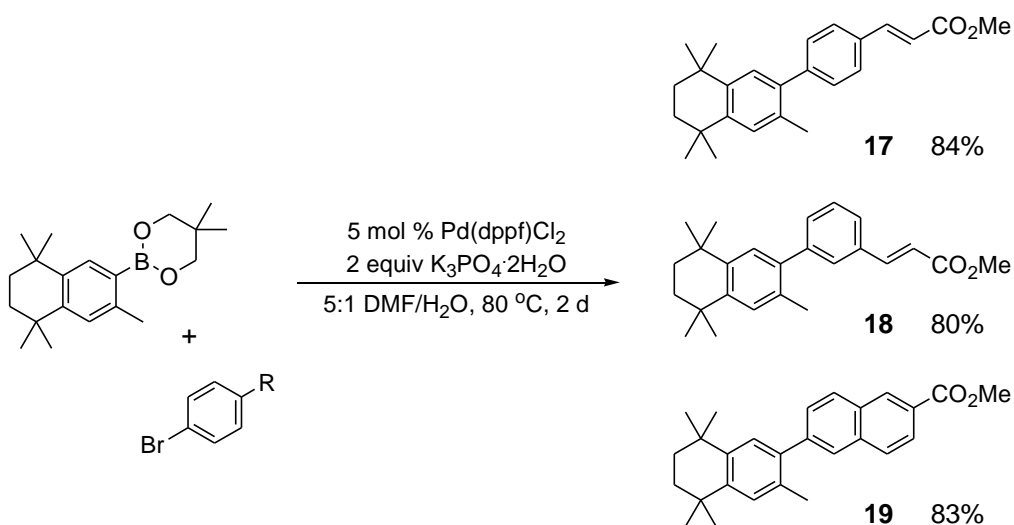


Figure 3.31 MS of 16.

For the synthesis of 3-methylated biaryl retinoid esters, the neopentane glycolato boronate ester *d* was utilised as a precursor. Although compound *d* is marginally less reactive than

its pinacol boronate ester analogue **c**, the synthesis of **d** from the corresponding aryl-iodide *via* Pd-catalysed Miyaura borylation with B₂neop₂ is much more rapid than the corresponding borylation with B₂pin₂ to give **c** (18 hours at 80 °C versus 4 days at 80 °C, respectively), making the synthesis from arene to retinoid ester *via* an iodination / borylation / Suzuki-Miyaura cross-coupling sequence much more rapid (4 days versus 7 days).

Neopentane glycolate boronate ester **d** underwent Suzuki-Miyaura cross-coupling with 3-, and 4-bromo-cinnamic acid methyl esters and 6-bromonaphthalene-2-carboxylic acid methyl ester to give the retinoid esters **17**, **18** and **19**, respectively, in high yields (**Equation 3.13**). The reactions were carried out in the presence of 5 mol % Pd(dppf)Cl₂ catalyst and 2 molar equivalents of K₃PO₄·2H₂O based in a combination of DMF/H₂O at 80 °C. The reactions were heated for 2 days, at which time analysis by *in situ* GC-MS showed all reactions to be complete.



Equation 3.13 Synthesis of biaryl retinoid esters **17**, **18** and **19** *via* Suzuki-Miyaura cross-couplings of **d**.

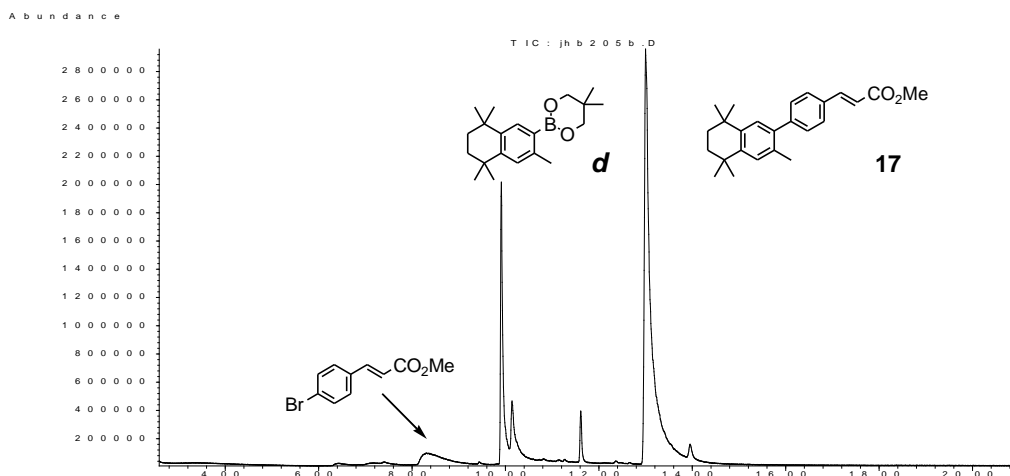


Figure 3.32 GC (TIC) for the synthesis of **17** from boronate ester **d**.

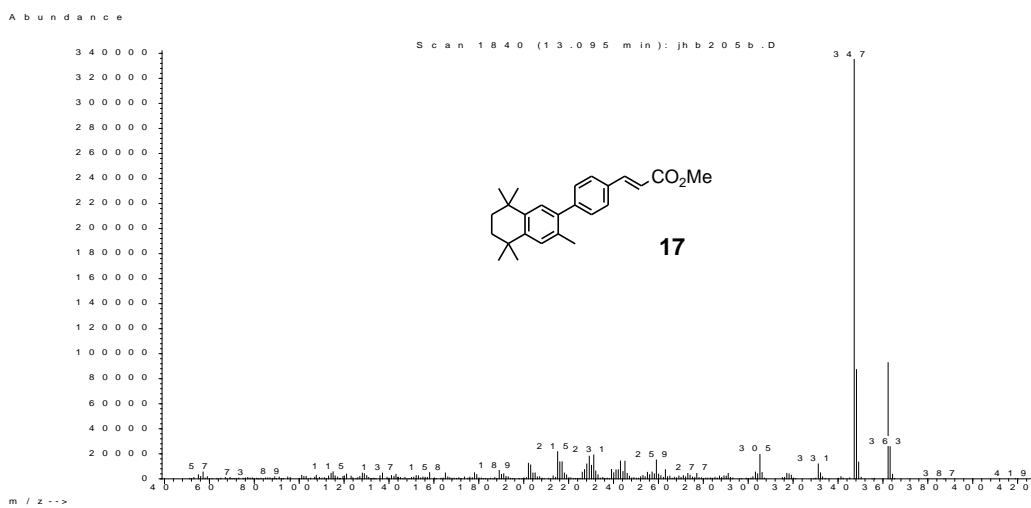


Figure 3.33 MS of **17**.

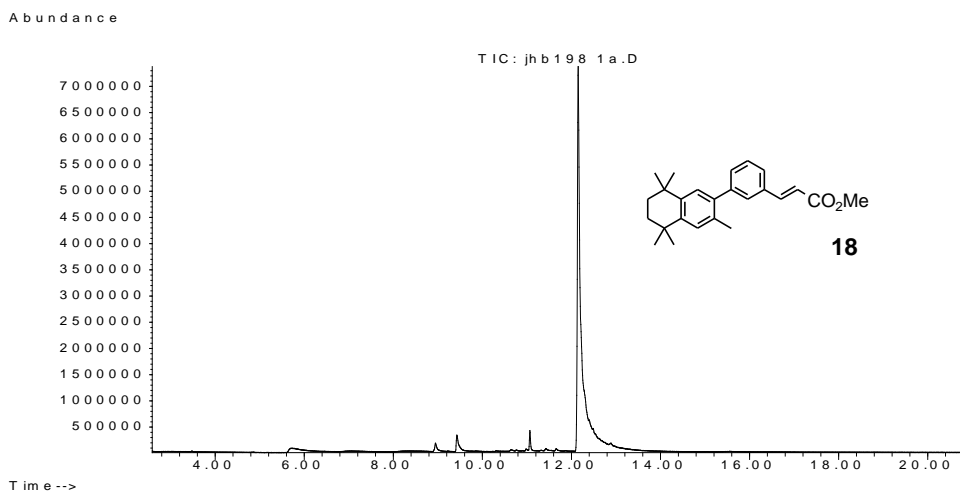


Figure 3.34 GC (TIC) for the synthesis of **18** from boronate ester **d**.

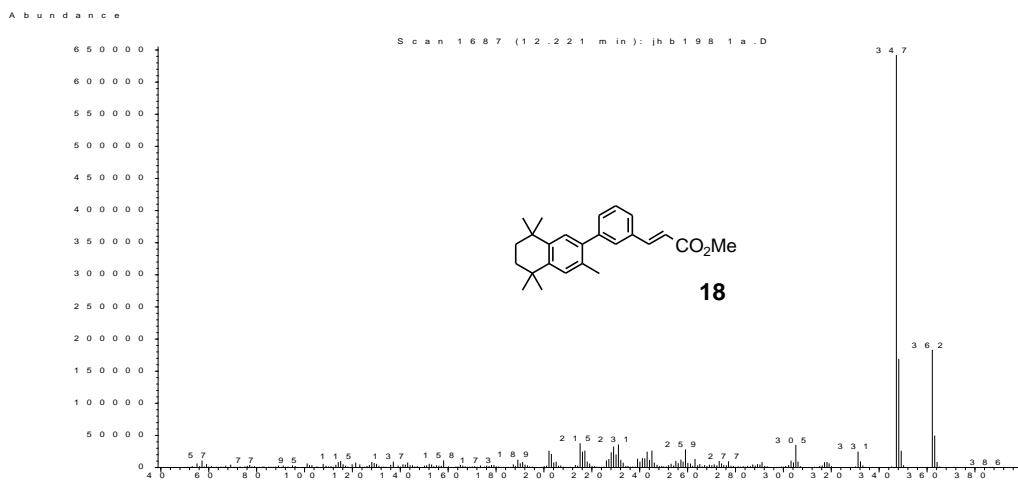


Figure 3.35 MS of **18**.

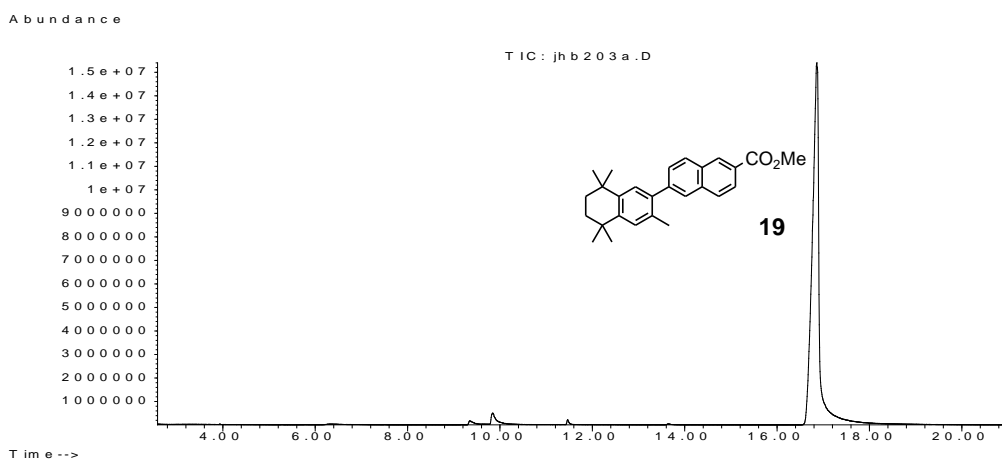


Figure 3.36 GC (TIC) for the synthesis of **19** from boronate ester *d*.

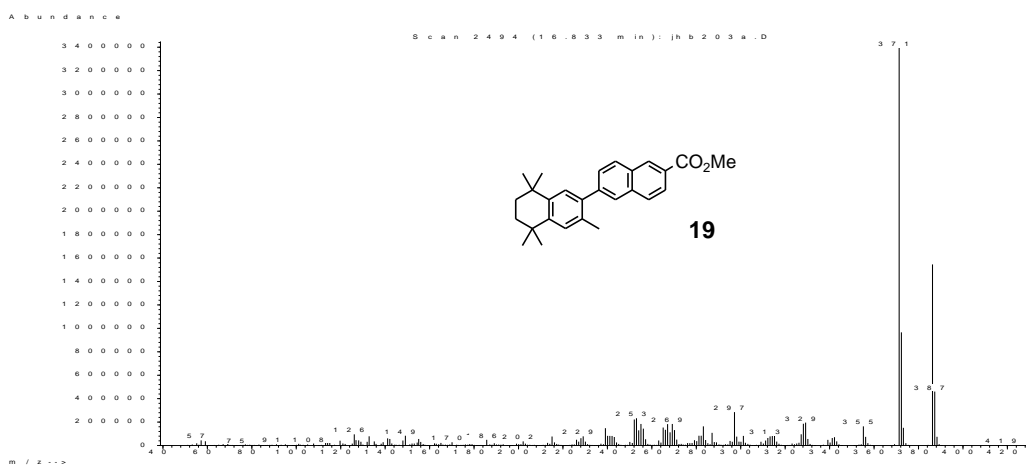
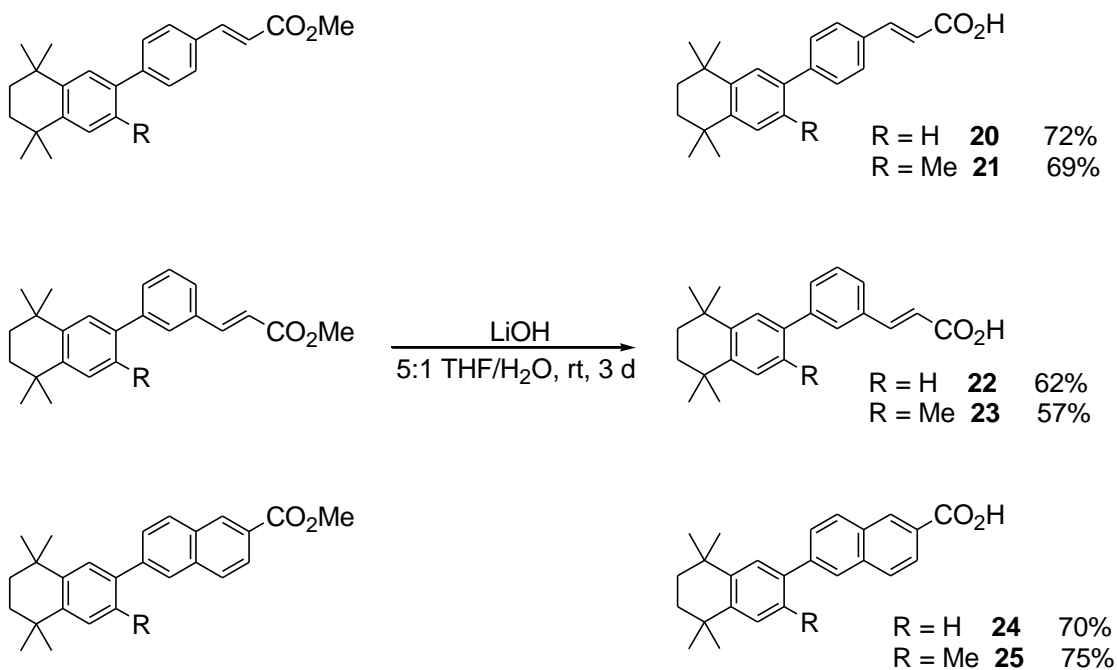


Figure 3.37 MS of **19**.

The biaryl retinoid esters **14** – **19** were hydrolysed with aqueous LiOH at ambient temperature to give their corresponding carboxylic acids in moderate to good yields (**Equation 3.14**).



Equation 3.14 Hydrolysis of biaryl retinoid esters **14** – **19**.

3.4 Conclusions

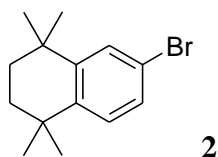
Two series of highly rigid arotinoids have been synthesised *via* combinations of aromatic iodinations and palladium-catalysed C-C and C-B forming reactions, giving the products with good to high yields. Preliminary results³⁰⁴ have shown that compound **7** and its *meta*-analogue are highly effective in inducing the differentiation of the human embryonal carcinoma stem cell line, TERA2.cl.SP12, with **7** leading to the formation of neuronal cells (similar to the effects of ATRA) while its *meta*-analogue led to the formation of ‘plaques’ of epithelial cells showing a marked difference in selectivity between the *para* and *meta* isomers.

In contrast to the stilbene-based arotinoids (TTNPB series) detailed in Chapter 2, the incorporation of *ortho*-methyl groups on the arene ring of the hydrophobic terminus does not result in any conformational change in the alkynyl compounds, as observed by comparisons of the molecular structures and λ_{max} values of compounds differing only by the presence of an *ortho*-methyl group. As a result, these compounds can be used to assess the effects (if any) of increasing the steric bulk of the hydrophobic terminus by incorporation of this *ortho*-methyl group, and further work is currently underway to evaluate the ability of these compounds to induce the differentiation of the human embryonal carcinoma stem cell line, TERA2.cl.SP12.

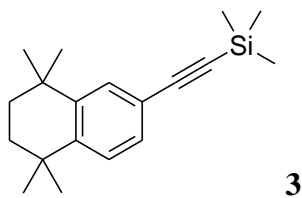
3.5 Experimental

All reactions were carried out under a dry nitrogen atmosphere using standard Schlenk techniques or in an Innovative Technology Inc. System 1 double-length glove box. Glassware was oven dried before transfer into the glove box. Hexane was dried over sodium/benzophenone was distilled under nitrogen. The solvents DMF, and DMSO and H₂O were degassed by 3 freeze-pump-thaw-cycles. B₂pin₂ and B₂neop₂ were kindly supplied as gifts by AllyChem Co. Ltd., Frontier Scientific Inc. and NetChem. Inc. Hydrochloric acid was obtained from Fisher Scientific and all other compounds were obtained from Aldrich Chemical Company, tested for purity by GCMS and used without further purification. NMR spectra were recorded at ambient temperature on Varian Systems 700 (¹H, ¹³C{¹H}) Varian Inova 500 (¹H, ¹³C{¹H}), Varian C500 (¹H, ¹³C{¹H}), Bruker 400 Ultrashield (¹H, ¹³C{¹H}) and Bruker AC200 (¹³C{¹H}) instruments. Proton and carbon spectra were referenced to external SiMe₄ via residual protons in the deuterated solvents or solvent resonance respectively. IR spectra were recorded on a Perkin-Elmer Paragon 500 FT-IR spectrometer. UV-vis and fluorescence measurements were recorded in CHCl₃. UV-vis absorption spectra and extinction coefficients were obtained on a Hewlett-Packard 8453 diode array spectrophotometer using standard 1 cm quartz cells. Fluorescence spectra were recorded on a Horiba Jobin-Yvon Fluoromax-3 spectrophotometer. The spectra of dilute solutions with absorbance maxima of less than 0.1 were recorded using conventional 90 degree geometry. The emission spectra were

fully corrected using the manufacturer's correction curves for the spectral response of emission optical components. Elemental analyses were conducted in the Department of Chemistry at Durham University using an Exeter Analytical Inc. CE-440 Elemental Analyser. GC-MS analyses were performed on an Agilent 6890 Plus GC equipped with a 5973N MSD and an Anatune Focus robotic liquid handling system / autosampler. A fused silica capillary column (10 m or 12 m, cross-linked 5% phenylmethylsilicone) was used, and the oven temperature was ramped from 50 °C to 280 °C at a rate of 20 °C/min. UHP grade helium was used as the carrier gas. The screw-cap autosampler vials used were supplied by Thermoquest Inc. and were fitted with Teflon / silicone / Teflon septa and 0.2 mL micro inserts. HRMS spectra were recorded in the Department of Chemistry at Durham University using a Thermo Finnigan LTQ FT Ultra Hybrid mass spectrometer.



6-Bromo-1,1,4,4-tetramethyl-1,2,3,4-tetrahydronaphthalene (2).³⁰² To a solution of 1,1,4,4-tetramethyl-1,2,3,4-tetrahydro-naphthalene (10.0 g, 53.0 mmol) in DCM (60 mL) at 0 °C under N₂ was added 1.8 eq. of Br₂ (15.58 g, 97.5 mmol). BF₃.Et₂O (8.27 g, 58.3 mmol) in DCM (10 mL) was added dropwise over 2 h. The reaction mixture was diluted with 40/60 EtOAc/hexane (150 mL) and washed with saturated Na₂SO₃ solution (100 mL), saturated NaHCO₃ solution (100 mL), and H₂O (100 mL). The organic layer was dried over MgSO₄, filtered and the solvents were removed *in vacuo* to give a dark brown oil. Kugelrohr distillation (120 °C, 8 x 10⁻³ mbar) gave the product as pale yellow crystals (11.0 g, 78%); mp 43-45 °C; EI-MS *m/z*: 266 (30% M⁺), 251 (100%, M⁺ - Me); ¹H NMR (400.13 MHz, CDCl₃) δ 7.40 (1H, d, *J* = 3 Hz), 7.21 (1H, d, *J* = 3 Hz), 7.18 (1H, s), 1.67 (4H, s), 1.27 (6H, s), 1.26 (6H, s); ¹³C{¹H} NMR (100.13 MHz, CDCl₃) δ 147.63, 144.09, 129.67, 128.88, 128.66, 119.62, 35.11, 35.10, 34.70, 34.30, 31.96 (two peaks overlapped); anal. calcd for C₁₄H₁₉Br: C 62.93; H 7.17; found: C 62.81; H 7.16.



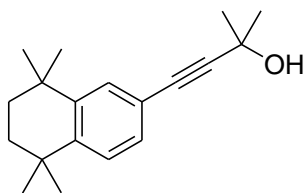
3

Trimethyl-(5,5,8,8-tetramethyl-5,6,7,8-tetrahydronaphthalen-2-ylethynyl)-silane (3).

PdCl₂ (75 mg, 0.43 mmol), Cu(OAc)₂ (77 mg, 0.43 mmol), **1** (1.14 g, 4.30 mmol) and PPh₃ (0.56 g, 2.14 mmol) were placed in a 250 mL Schlenk flask under N₂. Dry, degassed NEt₃ (100 mL) was added *via* cannula and ethynyltrimethylsilane (0.7 mL 5.14 mmol) was added *via* syringe. After 18 h at 70 °C, the NEt₃ was evaporated and the residue was passed through a short silica gel column (hexane as eluent) to give the crude product as a viscous, pale yellow oil after evaporation which slowly solidified to give an off-white solid which was recrystallised from ethanol to give **3** (1.0 g, 81%); mp 51-52 °C; EI-MS *m/z*: 284 (25%, M⁺), 269 (100%, M⁺-Me); ¹H NMR (400.13 MHz, CDCl₃) δ 7.22 (1H, s), 7.02 (2H, s), 1.47 (4H, s), 1.07 (6H, s), 1.07 (6H, s), 0.05 (9H, s); ¹³C{¹H} NMR (100.61 MHz, CDCl₃) δ 145.94, 145.10, 130.45, 129.31, 126.71, 120.31, 106.20, 93.51, 35.23, 35.14, 34.54, 34.39, 31.96, 31.89, 0.31; anal. calcd. for C₁₉H₂₈Si: C 80.21, H 9.92; found: C 80.04, H 9.90.

Synthesis of 3 from 6-iodo-1,1,4,4-tetramethyl-1,2,3,4-tetrahydronaphthalene

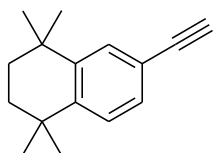
6-Iodo-1,1,4,4-tetramethyl-1,2,3,4-tetrahydronaphthalene (3.14 g, 10.0 mmol), Pd(PPh₃)₂Cl₂ (0.07 g, 0.1 mmol) and CuI (0.02 g, 0.1 mmol) were placed in a 250 mL Schlenk flask under N₂. Dry, degassed NEt₃ (150 mL) was added *via* cannula under N₂ and ethynyltrimethylsilane (1.18 g, 12 mmol) was added *via* syringe. The reaction was stirred under N₂ at room temperature, until analysis by GCMS showed the reaction to be complete (12 h). The NEt₃ solvent was removed *in vacuo* and the residue was passed through a short silica gel column, eluting with hexane. Evaporation of the solvent gave the crude product as a pale yellow oil which slowly solidified to give an off-white solid. Recrystallisation from hot EtOH gave **3** (2.50 g, 88%). All spectroscopic and analytical properties were identical to those reported above.



4

2-Methyl-4-(5,5,8,8-tetramethyl-5,6,7,8-tetrahydronaphthalen-2-yl)-but-3-yn-2-ol

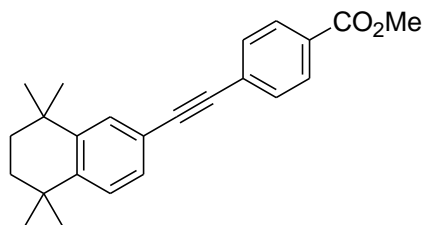
(4). PdCl₂ (0.331 g, 1.87 mmol), Cu(OAc)₂ (0.274 g, 1.87 mmol), **1** (5.0 g, 18.71 mmol) and PPh₃ (2.45 g, 9.35 mmol) were placed in a 500 mL Schlenk flask, and the flask was evacuated and back-filled with N₂ gas (3x). NEt₃ (150 mL) was added *via* cannula, followed by 2-methylbut-3-yn-2-ol (4.72 g, 56.13 mmol). The solution was stirred under N₂ at 70 °C for 3 d. The NEt₃ was evaporated and the residue was passed through a short silica gel column (hexane, then 10% EtOAc/hexane as eluent). The EtOAc/hexane solution was washed with 1M HCl solution (100 mL), dried (MgSO₄) and evaporated to give **4** as an off-white solid (2.25 g, 45%); mp 107–109 °C; EI-MS *m/z*: 236 (90%, M⁺), 205 (100%, OH and Me loss); ¹H NMR (499.76 MHz, CDCl₃) δ 7.36 (1H, s), 7.24 (1H, d, *J* = 8.0 Hz), 7.21 (1H, d, *J* = 8.0 Hz), 2.05 (1H, s), 1.67 (4H, s), 1.62 (6H, s), 1.27 (6H, s), 1.26 (6H, s); ¹³C{¹H} NMR (126 MHz, CDCl₃) δ 145.6, 145.1, 130.1, 128.9, 126.8, 119.8, 92.8, 82.8, 65.8, 35.2, 35.1, 34.5, 34.4, 31.9, 31.9, 31.8; *m/z* (EI) 270 (M⁺); HRMS (ES⁺) calcd. for C₁₉H₂₆ONa ([M + Na]⁺) 293.18759, found 293.18776, and HRMS (ES⁺) calcd. for C₁₉H₂₅ ([M – OH]⁺) 253.19508, found 253.19522.



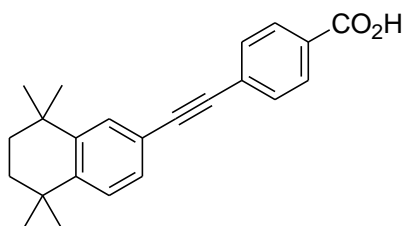
5

6-Ethynyl-1,1,4,4-tetramethyl-1,2,3,4-tetrahydronaphthalene (5). To a solution of **3** (1.42 g, 5 mmol) in MeOH (50 mL) and Et₂O (50 mL), was added NaOH (0.14 g, 3.5 mmol) in H₂O (2 mL). After 4 h, the mixture was extracted with Et₂O (30 mL), washed with H₂O (3 x 30 mL), dried (MgSO₄) and evaporated to give **5** as an oil which slowly solidified to give a white solid (0.78 g, 74%); mp 48–49 °C; IR (KBr disc, cm⁻¹) 2105 (C≡C); ¹H NMR (199.99 MHz, CDCl₃) δ 7.47 (1H, s), 7.27 (2H, s), 3.03 (1H, s), 1.70 (4H, s), 1.29 (6H, s), 1.26 (6H, s); ¹³C{¹H} NMR (100.61 MHz, CDCl₃) δ 146.1, 145.1,

130.5, 129.2, 126.6, 119.1, 84.3, 75.9, 34.9, 34.8, 34.3, 34.2, 31.8, 31.7; m/z (EI-MS): 212 (M^+); anal. calcd. for $C_{16}H_{20}$: C 90.51, H 9.49; found: C 90.27, H 9.57.

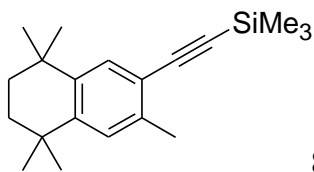


4-(5,5,8,8-Tetramethyl-5,6,7,8-tetrahydronaphthalen-2-ylethynyl)-benzoic acid methyl ester (6). CuI (0.03 g, 0.14 mmol), 4-iodobenzoic acid methyl ester (3.59 g, 13.7 mmol) and Pd(PPh_3) $_2Cl_2$ (0.09 g, 0.14 mmol) were placed in a 500 mL Schlenk flask under N_2 and **5** (3.50 g, 16.48 mmol) was added. Dry, degassed Et_3N (200 mL) was added via cannula and the reaction mixture was stirred under N_2 until GCMS analysis showed the reaction to be complete (18 h). Et_3N was removed *in vacuo* and the remaining crude solid purified *via* passage through a silica plug, eluting with hexane (100 mL), then 10% DCM/hexane. Removal of solvent and drying *in vacuo* gave a crude solid. Recrystallisation from hot EtOH gave the product as a white crystalline solid; (4.13 g, 87%); mp 122 °C; IR (KBr disc, cm^{-1}) 2207 ($C\equiv C$), 1712 ($C=O$); UV-vis ($CHCl_3$) λ_{max} 310 nm (ϵ) 26400 $M^{-1}cm^{-1}$; λ_{em} ($CHCl_3$) 362 nm; m/z (EI-MS) 346 20% M^+ , 331 (100% $M^+ - Me$); 1H NMR (400.13 MHz, $CDCl_3$) δ 8.03 (2H, d, $J = 9.0$ Hz), 7.59 (2H, d, $J = 9.0$ Hz), 7.51 (1H, s), 7.31 (2H, s), 3.94 (3H, s), 1.71 (4H, s), 1.28 (12H, s); $^{13}C\{^1H\}$ NMR (100.61 MHz, $CDCl_3$) δ 166.83, 146.34, 145.41, 131.67, 130.31, 129.69, 129.43, 129.00, 128.61, 126.98, 119.84, 93.30, 87.23, 52.39, 35.16, 35.09, 34.61, 34.45, 31.99, 31.90; anal. calcd. for $C_{24}H_{26}O_2$ C, 83.20; H, 7.56; found: C, 83.03; H, 7.59.



4-(5,5,8,8-Tetramethyl-5,6,7,8-tetrahydronaphthalen-2-ylethynyl)-benzoic acid (7).

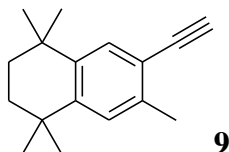
A solution of **6** (0.35 g, 1 mmol) in THF (20 mL) was treated with aqueous 20% NaOH (20 mL). After heating at 70 °C for 20 h, the reaction mixture was diluted with Et₂O (150 mL) and water (150 mL), then 1 M HCl solution was added until mixture reached pH 1. The organic layer was separated, dried (MgSO₄) and evaporated to give an off-white powder, which was recrystallised from MeCN to give the product **7** as a white crystalline solid (0.24 g, 72%); mp 254–256 °C; IR (KBr disc, cm⁻¹) 2205 (C≡C), 1681 (C=O); UV-vis (CHCl₃) λ_{max} 310 nm (ε) 26900 M⁻¹cm⁻¹; λ_{em} (CHCl₃) 365 nm; (ES-MS) *m/z* 377 (20%, MNa₂), 331 (100%, [M-H]⁻); ¹H NMR (400.13 MHz, DMSO-d₆) δ 8.09 (2H, d, *J* = 8.5 Hz), 7.62 (2H, d, *J* = 8.5 Hz), 7.51 (1H, s), 7.31 (2H, s), 1.68 (4H, s), 1.31 (12H, s); ¹³C{¹H} NMR (125.67 MHz, CDCl₃) δ 171.49, 146.46, 145.43, 131.76, 130.35, 130.33, 129.56, 129.02, 128.38, 127.01, 119.69, 93.85, 87.76, 35.10, 35.04, 34.62, 34.46, 31.98, 31.89; HRMS (ES⁻) calcd. for C₂₃H₂₃O₂ 331.16926 [(M - H)⁻], found 331.16949.



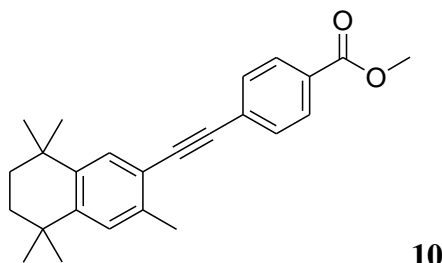
Trimethyl-(3,5,5,8,8-pentamethyl-5,6,7,8-tetrahydronaphthalen-2-ylethynyl)-

silane (8). Pd(PPh₃)₂Cl₂ (0.21 g, 0.31 mmol) CuI (58 mg, 0.31 mmol) and 6-iodo-1,1,4,4,7-pentamethyl-1,2,3,4-tetrahydronaphthalene (10.0 g, 30.5 mmol) were placed in a 1 L Schlenk flask under N₂. Dry, degassed Et₃N (500 mL) was added via cannula and ethynyltrimethylsilane (5.17 mL, 36.6 mmol) was added via syringe. The mixture was stirred under N₂ until GCMS analysis showed the reaction to be complete (18 h). The solvent was removed *in vacuo* and the residue was filtered through a SiO₂ plug eluting with hexane (300 mL). Removal of the solvent *in vacuo* gave a clear oil. Addition of MeOH (5 mL) and cooling gave **8** as analytically pure white crystals (8.82 g, 97%); mp 77-78 °C; IR (KBr disc, cm⁻¹) 2963, 2926, 2860, 2143, 1493, 1457, 1362, 1247; *m/z* (EI-MS) 354 (100%, M⁺ - Me), 339 (25%, M⁺); ¹H NMR (499.80 MHz, CDCl₃) δ 7.37 (1H, s), 7.10, (1H, s), 2.37, (3H, s), 1.65, (4H, s), 1.25 (6H, s), 1.24 (6H, s), 0.25 (9H, s); ¹³C{¹H} NMR (125.67 MHz, CDCl₃) δ 146.02, 142.54, 137.65, 130.58, 127.73, 120.48,

105.02, 97.04, 35.34, 35.32, 34.54, 34.18, 32.12, 32.02, 20.62, 0.50; anal. calcd for C₂₀H₃₀Si: C 80.46, H 10.13; found: C 80.29, H 10.17.

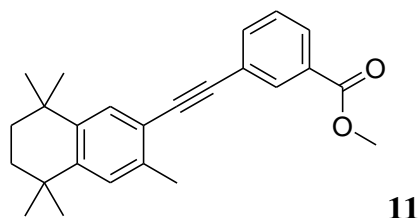


6-Ethynyl-1,1,4,7-pentamethyl-1,2,3,4-tetrahydronaphthalene (9). Compound **8** (6.0 g, 20.1 mmol) and NaOH (0.53 g, 13.4 mmol) were dissolved in a 50/50 mixture of Et₂O and MeOH (100 mL) with 1 mL of H₂O. The mixture was stirred for 2 h at which time GCMS analysis showed the reaction to be complete. H₂O (100 mL) and hexane (100 mL) were added and the product was extracted into the organic layer. The organic layer was dried over MgSO₄, filtered and the solvent removed *in vacuo* to give a white solid. Recrystallisation from MeOH gave **9** as an analytically pure white powder (0.41 mg, 91 %); mp 45-47 °C (lit. 41-43 °C³⁰⁸); IR (KBr disc, cm⁻¹) 2963, 2926, 2861, 2143, 1493, 1458, 1391, 1247; *m/z* (EI-MS) 226 (25%, M⁺), 211 (100%, M⁺ - Me); ¹H NMR (499.80 MHz, CDCl₃) δ 7.42 (1H, s), 7.13 (1H, s), 3.20 (1H, s), 2.40 (3H, s), 1.66 (4H, s) 1.27 (6H, s), 1.26 (6H, s); ¹³C{¹H} NMR (125.67 MHz, CDCl₃) δ 146.32, 142.67, 137.72, 131.161, 127.84, 119.49, 83.38, 79.91, 35.28, 35.27, 34.55, 34.16, 32.12, 32.01, 20.59; anal. calcd for C₁₇H₂₂: C 90.20, H 9.80; found: C 89.95, H 9.80.



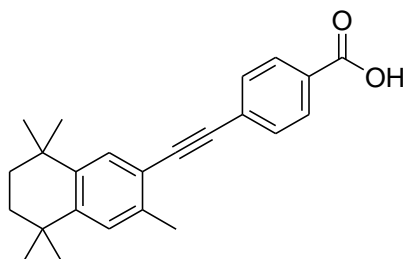
4-(3,5,5,8,8-Pentamethyl-5,6,7,8-tetrahydronaphthalen-2-ylethynyl)-benzoic acid methyl ester (10). Pd(PPh₃)₂Cl₂ (29 mg, 0.042 mmol), CuI (8 mg, 0.004 mmol), 4-iodobenzoic acid methyl ester (1.1 g, 4.2 mmol) and compound **9** (1.0 g, 4.4 mmol) were placed in a 250 mL Schlenk flask under N₂. Dry, degassed Et₃N (100 mL) was added via cannula. The reaction was stirred under N₂ for 3 d. The solvent was removed *in*

vacuo and the residue was filtered through a SiO₂ plug eluting with hexane (200 mL) and then with 50:50 DCM/hexane (200 mL). The DCM/hexane fraction was evaporated *in vacuo* to give a pale brown solid. Recrystallisation from EtOH gave white needles (0.12 g, 77%); mp 135-137; IR (KBr disc, cm⁻¹) 2921, 2857, 1711 (C=O), 1602, 1433, 1287, 1108; UV-vis (CHCl₃) λ_{max} 317 nm (ε) 25700 L mol⁻¹ cm⁻¹; λ_{em} (CHCl₃) 378 nm; *m/z* (EI-MS) 360 (50%, M⁺), 345 (100%, M⁺ - Me); ¹H NMR (499.80 MHz, CDCl₃) δ 8.01 (2H, d, *J* = 8.5 Hz), 7.58 (2H, d, *J* = 8.5 Hz), 7.45 (1H, s), 7.16 (1H, s), 3.93 (3H, s), 2.46 (3H, s), 1.68 (4H, s), 1.29 (6H, s) 1.28 (6H, s); ¹³C{¹H} NMR (125.67 MHz, CDCl₃) δ 166.99, 146.52, 142.89, 137.43, 131.69, 130.63, 129.84, 129.49, 128.94, 127.97, 120.04, 92.36, 91.72, 52.57, 35.29, 34.62, 34.24, 32.16, 32.10 32.02, 20.73; anal. calcd. for C₂₅H₂₈O₂: C 83.29, H 7.83; found: C 82.83, H 7.67.



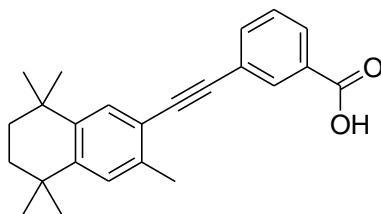
3-(3,5,5,8,8-Pentamethyl-5,6,7,8-tetrahydronaphthalen-2-ylethynyl)-benzoic acid methyl ester (11). Pd(PPh₃)₂Cl₂ (29 mg, 0.042 mmol), CuI (8 mg, 0.0042 mmol), 3-iodobenzoic acid methyl ester (1.1 g, 4.21 mmol) and compound **9** (1.0 g, 4.42 mmol) were placed in a 250 mL Schlenk flask under N₂. Dry, degassed Et₃N (100 mL) was added via cannula. The reaction was stirred under N₂ for 3 d. The solvent was removed *in vacuo* and the residue filtered through a SiO₂ plug eluting with hexane (200 mL) and 50/50 DCM/hexane (200 mL). The DCM/hexane fraction was evaporated *in vacuo* to give a pale brown solid. Recrystallisation from EtOH to gave white needles (0.11 g, 71%); mp 115-117; IR (KBr disc, cm⁻¹) 2956, 2926, 2862, 1725 (C=O), 1439, 1280, 1256; UV-vis (CHCl₃) λ_{max} 290 nm (ε) 22000 L mol⁻¹ cm⁻¹; λ_{em} (CHCl₃) 370 nm; *m/z* (EI-MS) 360 (50%, M⁺), 345 (100%, M⁺ - Me); ¹H NMR (499.80 MHz, CDCl₃) δ 8.04 (1H, s), 7.82 (1H, d, *J* = 7.5 Hz), 7.70 (1H, d, *J* = 7.5 Hz), 7.46 (1H, s), 7.33 (1H, t, *J* = 7.5 Hz) 7.16 (1H, s), 2.46 (3H, s), 3.94 (3H, s), 2.46 (3H, s), 1.68 (4H, s), 1.29 (6H, s) 1.28 (6H, s); ¹³C{¹H} NMR (125.67 MHz, CDCl₃) δ 166.89, 146.23, 142.79, 137.34, 135.97, 132.88, 130.71, 130.57, 129.22, 128.79, 127.91, 124.63, 120.20, 91.33, 90.13,

52.64, 35.31, 34.59, 34.23, 32.17, 32.10, 32.03, 20.76; anal. calcd. for C₂₅H₂₈O₂: C 83.29, H 7.83; found: C 83.03, H 7.36.



12

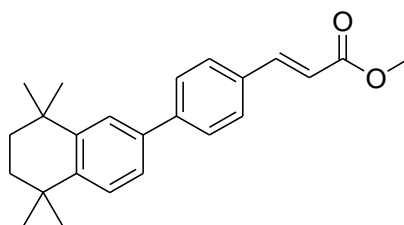
4-(3,5,5,8,8-Pentamethyl-5,6,7,8-tetrahydro-naphthalen-2-ylethynyl)-benzoic acid (12). LiOH·H₂O (17.5 mg, 0.42 mmol) and **10** (0.10 g, 0.28 mmol) were placed in a large screw top vial. THF (5 mL) and H₂O (1 mL) were added and the solution stirred at room temperature until analysis *via* tlc showed the reaction to be complete. Et₂O (30 mL) was added and the mixture washed with dilute HCl_(aq.) (30 mL), and H₂O (2 x 30 mL). The organic layer was dried with MgSO₄, filtered and the solvent removed *in vacuo*. Recrystallisation from MeCN gave the product as a white powder (0.73 mg, 76%); mp 220-222 °C; UV-vis (CHCl₃) λ_{max} 319 nm (ε) 26100 L mol⁻¹ cm⁻¹; λ_{em} (CHCl₃) 381 nm; *m/z* (ES⁺-MS) 692 (2M⁺); ¹H NMR (499.80 MHz, DMSO-d₆) δ 7.96 (2H, d, *J* = 8.0 Hz), 7.65 (2H, d, *J* = 8.0 Hz), 7.45 (1H, s), 7.27 (1H, s), 2.40 (3H, s), 1.62 (4H, s), 1.23 (12H, s); ¹³C{¹H} NMR (125.67 MHz, DMSO-d₆) δ 167.47, 146.68, 142.97, 137.45, 132.03, 130.97, 130.48, 130.28, 128.36, 127.80, 119.67, 92.21, 92.14, 35.14, 35.10, 34.25, 32.17, 32.06, 20.64; anal. calcd. for C₂₄H₂₆O₂: C 83.20, H 7.56; found: C 83.23, H 8.04.



13

3-(3,5,5,8,8-Pentamethyl-5,6,7,8-tetrahydro-naphthalen-2-ylethynyl)-benzoic acid (13). LiOH·H₂O (17.5 mg, 0.42 mmol) and compound **11** (0.10 g, 0.28 mmol) were placed in a large screw top vial. THF (5 mL) and H₂O (1 mL) were added and the solution stirred at room temperature until analysis *via* tlc showed the reaction to be

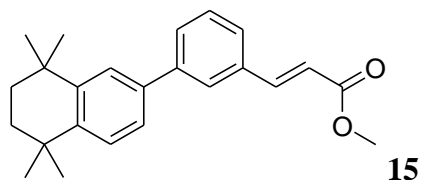
complete. Et₂O (30 mL) was added and the mixture washed with dilute HCl_(aq.) (30 mL), and H₂O (2 x 30 mL). The organic layer was dried with MgSO₄, filtered and the solvent removed *in vacuo*. Recrystallisation from MeCN gave the product as a white powder (71 mg, 73%); mp 206-207 °C; UV-vis (CHCl₃) λ_{max} 290 nm (ε) 23000 L mol⁻¹ cm⁻¹; λ_{em} (CHCl₃) 376 nm; *m/z* (ES⁺-MS) 692 (M⁺); ¹H NMR (499.80 MHz, DMSO-d₆) δ 8.03 (1H, s), 7.93 (1H, d, *J* = 7.5 Hz), 7.76 (1H, d, *J* = 7.5 Hz), 7.54 (1H, t, *J* = 7.5 Hz), 7.44 (1H, s), 7.24 (1H, s), 2.39 (3H, s), 1.60 (4H, s), 1.22 (12H, s); ¹³C{¹H} NMR (125.67 MHz, DMSO-d₆) δ 166.55, 145.69, 136.47, 135.13, 131.37, 129.70, 129.17, 127.54, 123.16, 119.10, 91.04, 89.49, 34.46, 34.42, 33.91, 33.51, 31.44, 19.90; anal. calcd. for C₂₄H₂₆O₂: C 83.20, H 7.56; found: C 83.09, H 8.00.



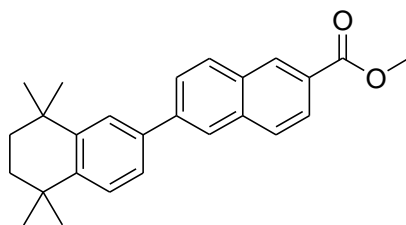
14

3-[4-(5,5,8,8-Tetramethyl-5,6,7,8-tetrahydronaphthalen-2-yl)-phenyl]-acrylic acid methyl ester (14). Pd(dppf)Cl₂ (23 mg, 0.03 mmol), compound **a** (0.20 g, 0.64 mmol), K₃PO₄·2H₂O (0.29 g, 1.16 mmol) and 3-(4-bromo-phenyl)-acrylic acid methyl ester (0.14 g, 0.58 mmol) were placed in a thick walled glass tube fitted with a Young's tap along with DMF (10 mL) and H₂O (2 mL) in a dry, N₂ filled, glovebox. The mixture was heated at 80 °C until GCMS analysis showed the reaction to be complete (2 d). Dilute HCl_(aq.) (2 mL) was added and the mixture was extracted with Et₂O (3 x 10 mL); the organic phase was washed with dilute HCl_(aq.) (3 x 10 mL), dried over MgSO₄ and concentrated *in vacuo*. The mixture was filtered through a silica plug, eluting with hexane and then 10% DCM/hexane, and the solvent was removed *in vacuo*. Recrystallisation from hot EtOH gave the product as a white fluffy powder (180 mg, 84%); mp 167-169 °C; IR (KBr disc, cm⁻¹) 2956, 2922, 2857, 1711 (C=O), 1638, 1313, 1193, 1171; UV-vis (CHCl₃) λ_{max} 307 nm (ε) 28400 L mol⁻¹ cm⁻¹; λ_{em} (CHCl₃) 396 nm; *m/z* (EI-MS) 333 (100%, M⁺ - Me), 348 (20%, M⁺); ¹H NMR (499.80 MHz, CDCl₃) δ 7.75 (1H, d, *J* = 16.0 Hz), 7.60 (2H, d, *J* = 9.0 Hz), 7.58 (2H, d, *J* = 9.0 Hz), 7.53 (1H, d, *J* = 2.0 Hz), 7.40 (1H, d, *J* = 9.0 Hz), 7.37 (1H, dd, *J* = 9.0, 2.0 Hz), 6.46 (1H, d, *J* = 16.0 Hz), 3.82 (3H,

s), 1.72 (4H, s), 1.34 (6H, s), 1.32 (6H, s); $^{13}\text{C}\{^1\text{H}\}$ NMR (125.67 MHz, CDCl_3) δ 167.70, 145.59, 144.96, 144.71, 143.60, 137.42, 133.07, 128.65, 127.59, 127.31, 125.35, 124.46, 117.44, 51.85, 35.24, 35.13, 34.58, 34.35, 32.06, 32.08; HRMS (ES^+) calcd. for $\text{C}_{24}\text{H}_{29}\text{O}_2$ ($[\text{M} + \text{H}]^+$) 349.21621, found 349.21628.

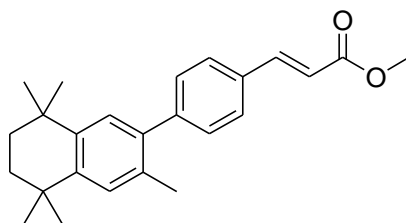


3-[3-(5,5,8,8-Tetramethyl-5,6,7,8-tetrahydronaphthalen-2-yl)-phenyl]-acrylic acid methyl ester (15). Pd(dppf) Cl_2 (23 mg, 0.028 mmol), compound **a** (0.20 g, 0.64 mmol), $\text{K}_3\text{PO}_4 \cdot 2\text{H}_2\text{O}$ (0.29 g, 1.16 mmol) and 3-(3-bromo-phenyl)-acrylic acid methyl ester (0.14 g, 0.58 mmol) were placed in a thick walled glass tube fitted with a Young's tap along with DMF (10 mL) and H_2O (2 mL) in a dry, N_2 filled, glovebox. The mixture was heated at 80 °C until GCMS analysis showed the reaction to be complete (2 d). Dilute $\text{HCl}_{(\text{aq.})}$ (2 mL) was added and the mixture was extracted with Et_2O (3 x 10 mL); the organic phase was washed with dilute $\text{HCl}_{(\text{aq.})}$ (3 x 10 mL), dried over MgSO_4 and concentrated *in vacuo*. The mixture was filtered through a silica plug, eluting with hexane and then 10% DCM/hexane, and the solvent was removed *in vacuo*. Recrystallisation from hot EtOH gave the product as a white fluffy powder (0.178 g, 88%); mp 163-165 °C; IR (KBr disc, cm^{-1}) 2956, 2921, 2856, 1709 (C=O), 1637, 1313, 1170; UV-vis (CHCl_3) λ_{max} 268 nm (ϵ) 14400 $\text{L mol}^{-1} \text{cm}^{-1}$; λ_{em} (CHCl_3) 396 nm; m/z (EI-MS) 333 (100%, $\text{M}^+ - \text{Me}$), 348 (20%, M^+); ^1H NMR (499.80 MHz, CDCl_3) δ 7.78 (1H, d, $J = 16.0$ Hz), 7.70 (1H, s), 7.59 (1H, d, $J = 8.0$ Hz), 7.51 (2H, m), 7.45 (1H, t, $J = 8.0$ Hz), 7.40 (1H, d, $J = 8.0$ Hz), 7.37 (1H, dd, $J = 8.0, 2.0$ Hz), 6.47 (1H, d, $J = 16.0$ Hz), 3.82 (3H, s), 1.72 (4H, s), 1.34 (6H, s), 1.32 (6H, s); $^{13}\text{C}\{^1\text{H}\}$ NMR (125.67 MHz, CDCl_3) δ 167.61, 145.58, 145.13, 144.71, 142.44, 137.79, 134.86, 129.35, 129.24, 127.29, 127.05, 126.54, 125.40, 124.55, 118.08, 51.90, 35.24, 35.14, 34.57, 34.31, 32.07, 32.00; HRMS (ES^+) calcd. for $\text{C}_{24}\text{H}_{28}\text{O}_2\text{Na}$ ($[\text{M} + \text{Na}]^+$) 371.19815, found 371.19816.



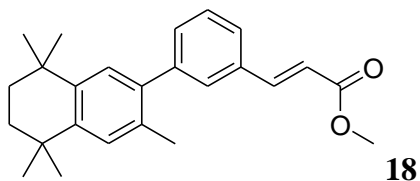
16

5',5',8',8'-Tetramethyl-5',6',7',8'-tetrahydro[2,2']binaphthalenyl-6-carboxylic acid methyl ester (16). Pd(dppf)Cl₂ (23 mg, 0.028 mmol), compound *a* (0.20 g, 0.64 mmol), K₃PO₄·2H₂O (0.29 g, 1.16 mmol) and 2-bromo-naphthalene-6-carboxylic acid methyl ester (0.15 g, 0.58 mmol) were placed in a thick walled glass tube fitted with a Young's tap along with DMF (10 mL) and H₂O (2 mL) in a dry, N₂ filled, glovebox. The mixture was heated at 80 °C until GCMS analysis showed the reaction to be complete (2 d). Dilute HCl (aq.) (2 mL) was added and the mixture was extracted with Et₂O (3 x 10 mL); the organic phase was washed with dilute HCl(aq.) (3 x 10 mL), dried over MgSO₄ and concentrated *in vacuo*. The mixture was filtered through a silica plug, eluting with hexane and then 10% DCM/hexane, and the solvent was removed *in vacuo*. Recrystallisation from hot EtOH gave the product as a white fluffy powder (0.196 g, 87%); mp 169-170; IR (KBr disc, cm⁻¹) 2955, 2922, 2857, 1706 (C=O), 1476, 1293, 1222, 1094; UV-vis (CHCl₃) λ_{max} 266 nm (ε) 34500 L mol⁻¹ cm⁻¹; λ_{em} (CHCl₃) 378 nm; *m/z* (EI-MS) 347 (100%, M⁺ - Me), 372 (20%, M⁺); ¹H NMR (699.73 MHz, CDCl₃) δ 8.63 (1H, s), 8.08 (1H, dd, *J* = 9.0, 2.0 Hz), 8.04 (1H, s), 8.01 (1H, d, *J* = 9.0 Hz), 7.94 (1H, d, *J* = 9.0 Hz), 7.80 (1H, dd, *J* = 9.0, 2.0 Hz), 7.65 (1H, d, *J* = 2.0 Hz), 7.49 (1H, dd, *J* = 9.0, 2.0 Hz), 7.44 (1H, d, *J* = 9.0 Hz), 3.99 (3H, s), 1.75 (4H, s), 1.38 (6H, s), 1.35 (6H, s); ¹³C{¹H} NMR δ 167.44, 145.68, 145.93, 141.48, 137.83, 136.00, 131.63, 130.98, 129.87, 128.46, 127.39, 127.26, 126.70, 125.79, 125.74, 125.38, 124.89, 52.39, 35.29, 35.17, 34.63, 34.37, 32.11, 32.01; HRMS (ES⁺) calcd. for C₂₆H₂₈O₂Na, ([M + Na]⁺) 395.19815, found 395.19813.



17

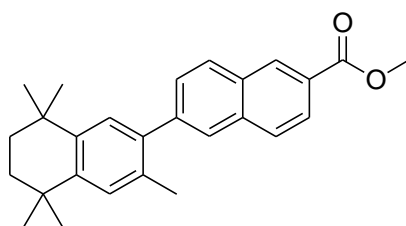
3-[4-(3,5,5,8,8-Pentamethyl-5,6,7,8-tetrahydronaphthalen-2-yl)-phenyl]-acrylic acid methyl ester (17). Pd(dppf)Cl₂ (23 mg, 0.028 mmol), compound *d* (0.20 g, 0.64 mmol), K₃PO₄·2H₂O (0.29 g, 1.16 mmol) and 4-(3-bromo-phenyl)-acrylic acid methyl ester (0.14 g, 0.58 mmol) were placed in a thick walled glass tube fitted with a Young's tap along with degassed DMF (10 mL) and H₂O (2 mL) in a dry, N₂ filled, glovebox. The mixture was heated at 80 °C until GCMS analysis showed the reaction to be complete (2 d). Dilute HCl_(aq.) (2 mL) was added and the mixture was extracted with Et₂O (3 x 10 mL). The organic phase was washed with dilute HCl_(aq.) (3 x 10 mL), dried over MgSO₄ and concentrated *in vacuo*. The mixture was filtered through a silica plug with hexane and then 10% DCM/hexane and the solvent was removed *in vacuo*. Recrystallisation from hot EtOH gave the product as a fluffy, white powder (0.17 g, 80%); mp 152-153; IR (KBr disc, cm⁻¹) 2965, 2922, 2856, 1714 (C=O), 1634, 1491, 1314, 1169; UV-vis (CHCl₃) λ_{max} 307 nm (ε) 29600 L mol⁻¹ cm⁻¹; λ_{em} (CHCl₃) 400 nm; *m/z* (EI-MS) 362 (20%, M⁺), 347 (100%, M⁺ - Me); ¹H NMR (499.80 MHz, CDCl₃) δ 7.74 (1H, d, *J* = 16.0 Hz), 7.57 (2H, d, *J* = 9.0 Hz), 7.37 (2H, d, *J* = 9.0 Hz), 7.19 (1H, s), 7.16 (1H, s), 6.47 (1H, d, *J* = 16.0 Hz), 3.83 (3H, s), 2.26 (3H, s), 1.71 (4H, s), 1.33 (6H, s), 1.29 (6H, s); ¹³C{¹H} NMR (125.67 MHz, CDCl₃) δ 167.71, 142.83, 144.60, 144.56, 142.77, 138.40, 132.78, 132.29, 130.07, 128.63, 127.99, 127.95, 117.55, 51.89, 35.27, 35.26, 34.16, 34.13, 32.04, 32.01, 20.36; HRMS (ES⁺) calcd. for C₂₅H₃₁O₂ ([M + H]⁺) 363.23186, found 363.23189.



18

3-[3-(3,5,5,8,8-Pentamethyl-5,6,7,8-tetrahydronaphthalen-2-yl)-phenyl]-acrylic acid methyl ester (18). Pd(dppf)Cl₂ (23 mg, 0.028 mmol), compound *d* (0.20 g, 0.64 mmol),

K₃PO₄·2H₂O (0.29 g, 1.16 mmol) and 3-(3-bromo-phenyl)-acrylic acid methyl ester (0.14 g, 0.54 mmol) were placed in a thick walled glass tube fitted with a Young's tap along with degassed DMF (10 mL) and H₂O (2 mL) in a dry, N₂ filled, glovebox. The mixture was heated at 80 °C until GCMS analysis showed the reaction to be complete (2 d). Dilute HCl_(aq.) (2 mL) was added and the mixture was extracted with Et₂O (3 x 10 mL). The organic phase was washed with dilute HCl_(aq.) (3 x 10 mL), dried over MgSO₄ and concentrated *in vacuo*. The mixture was filtered through a silica plug with hexane and then 10% DCM/hexane and the solvent was removed *in vacuo*. Recrystallisation from hot EtOH gave the product as a fluffy, white powder (0.17 g, 83%); mp 121-122; IR (KBr disc, cm⁻¹) 2953, 2924, 2857, 1714 (C=O), 1639, 145, 1322, 1170; UV-vis (CHCl₃) λ_{max} 267 nm (ε) 25600 L mol⁻¹ cm⁻¹; λ_{em} (CHCl₃) 378 nm; *m/z* (EI-MS) 362 (20%, M⁺), 347 (100%, M⁺ - Me); ¹H NMR (399.60 MHz, CDCl₃) δ 7.74 (1H, d, *J* = 16.0 Hz), 7.49, (2H, m), 4.40 (2H, ov m), 7.21 (1H, s), 7.16 (1H, s), 6.47 (1H, d, *J* = 16.0 Hz), 3.82 (3H, s), 2.24 (3H, s), 1.72 (4H, s), 1.34 (6H, s), 1.29 (6H, s); ¹³C{¹H} NMR (50.29 MHz, CDCl₃) δ 167.82, 145.22, 144.69, 143.34, 142.97, 138.09, 134.56, 132.49, 131.69, 129.39, 128.02, 128.76, 128.19, 126.59, 118.28, 52.04, 35.54, 35.53, 34.36, 34.33, 32.26, 32.23, 20.47; HRMS (ES⁺) calcd. for C₂₅H₃₀O₂Na ([M + Na]⁺) 385.21434, found 385.21492.

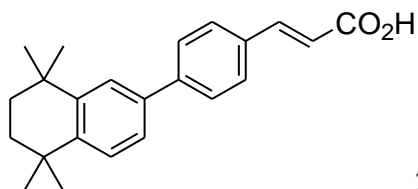


19

3',5',5',8',8'-Tetramethyl-5',6',7',8'-tetrahydro[2,2']binaphthalenyl-6-carboxylic acid methyl ester (19). Pd(dppf)Cl₂ (23 mg, 0.28 mmol), compound **d** (0.20 g, 0.64 mmol), K₃PO₄·2H₂O (0.29 g, 1.16 mmol) and 6-bromo-naphthalene-2-carboxylic acid methyl ester (0.15 g, 0.58 mmol) were placed in a thick walled glass tube fitted with a Young's tap along with degassed DMF (10 mL) and H₂O (2 mL) in a dry, N₂ filled, glovebox. The mixture was heated at 80 °C until GCMS analysis showed the reaction to be complete (2 d). Dilute HCl_(aq.) (2 mL) was added and the mixture was extracted with Et₂O (3 x 10 mL). The organic phase was washed with dilute HCl_(aq.) (3 x 10 mL), dried

over MgSO₄ and concentrated *in vacuo*. The mixture was filtered through a silica plug with hexane and then 10% DCM/hexane and the solvent was removed *in vacuo*. Recrystallisation from hot EtOH gave the product as a fluffy, white powder (0.19 g, 84%); mp 162-163 °C; IR (KBr disc, cm⁻¹) 2954, 2918, 2853, 1709 (C=O), 1436, 1295, 1128, 1096; UV-vis (CHCl₃) λ_{max} 302 nm (ε) 16200 L mol⁻¹ cm⁻¹; λ_{em} (CHCl₃) 369 nm; *m/z* (EI-MS) 386 (20%, M⁺), 372 (100%, M⁺ - Me); ¹H NMR (499.80 MHz, CDCl₃) δ 8.64 (1H, s), 8.08 (1H, dd, *J* = 9.0, 2.0 Hz), 7.98 (1H, d, *J* = 9.0 Hz), 7.89 (1H, d, *J* = 9.0 Hz), 7.82 (1H, s), 7.56 (1H, dd, *J* = 9.0, 2.0 Hz), 7.25 (1H, s), 7.24 (1H, s), 4.00 (3H, s), 2.29, (3H, s), 1.73 (4H, s), 1.35 (6H, s), 1.31 (6H, s); ¹³C{¹H} NMR (125.67 MHz, CDCl₃) δ 167.49, 144.58, 142.59, 142.53, 138.74, 135.60, 132.51, 131.35, 131.00, 129.01, 128.97, 128.62, 128.36, 128.28, 128.83, 127.32, 125.63, 52.40, 35.30, 35.29, 34.19, 34.17, 32.18, 32.14, 20.41; HRMS (ES⁺) calcd. for C₂₇H₃₁O₂ ([M + H]⁺) 387.23186, found 387.23155.

General procedure for the hydrolysis of retinoid esters 14 – 19 with LiOH. To a large, screw top vial equipped with a stirred bar was added a solution of the retinoid methyl ester in 5:1 THF/H₂O (6 mL) and LiOH monohydrate (3.0 equiv. w.r.t, retinoid ester). The mixture was stirred at room temperature until analysis *via* tlc showed the reaction to be complete (3 days). Et₂O (30 mL) was added and the mixture was washed with dilute HCl_(aq.) (30 mL), and H₂O (2 x 30 mL). The organic layer was dried with MgSO₄, filtered and the solvent was removed *in vacuo*. Recrystallisation from MeCN gave the products as white powders.

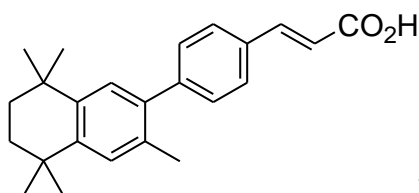


20

3-[4-(5,5,8,8-Tetramethyl-5,6,7,8-tetrahydro-naphthalen-2-yl)-phenyl]-acrylic acid (20).

The reaction was performed on a 0.18 mmol scale.

(43 mg, 72%); mp 275-277 °C; IR (KBr disc, cm^{-1}) 2953, 2920, 1675, 1626, 1420, 1310, 1181, 1107; m/z (ES^-) 333 ($[\text{M} - \text{H}]^-$); ^1H NMR (400.13 MHz, DMSO-d_6) δ 7.56 (5H, ov, m), 7.46 (1H, s), 7.31 (2H, ov, s), 6.38 (1H, d, $J = 16.0$ Hz), 1.64 (4H, s), 1.27 (6H, s), 1.24 (6H, s); $^{13}\text{C}\{^1\text{H}\}$ NMR (100.67 MHz, DMSO-d_6) δ 166.92, 144.00, 143.33, 142.50, 141.49, 135.63, 131.81, 127.28, 125.89, 123.53, 122.86, 117.47 two aromatic/vinylic carbon resonances are overlapped, 33.70, 33.58, 33.02, 32.80, 30.64, 30.54; anal. calcd. for $\text{C}_{23}\text{H}_{26}\text{O}_2$: C 82.60, H 7.84; found: C 81.97, H 8.02.

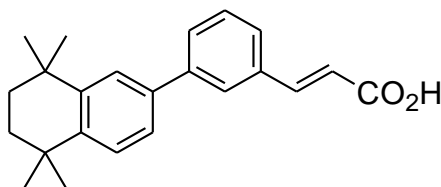


21

3-[4-(3,5,5,8,8-Pentamethyl-5,6,7,8-tetrahydro-naphthalen-2-yl)-phenyl]-acrylic acid (21).

The reaction was performed on a 0.28 mmol scale.

(66 mg, 69%); mp 235-238 °C; m/z (ES^-) 347 ($[\text{M} - \text{H}]^-$); ^1H NMR (400.13 MHz, DMSO-d_6) δ 7.70 (2H, d, $J = 8.0$ Hz), 7.60 (1H, d, $J = 16.0$ Hz), 7.35 (2H, d, $J = 8.0$ Hz), 7.20 (1H, s), 7.09 (1H, s), 6.54 (2H, d, $J = 16.0$ Hz), 2.17 (3H, s), 1.63 (4H, s), 1.25 (6H, s), 1.22 (6H, s); $^{13}\text{C}\{^1\text{H}\}$ NMR (100.67 MHz, DMSO-d_6) δ 168.48, 150.38, 149.63, 144.15, 142.47, 138.36, 136.57, 134.78, 132.06, 130.02, 128.72, 128.43, 127.66, 35.28 (two carbon environments), 34.22, 34.16, 32.21 (two carbon environments), 20.50; anal. calcd. for $\text{C}_{24}\text{H}_{28}\text{O}_2$: C 82.72, H 8.10; found: C 82.41, H 8.36.



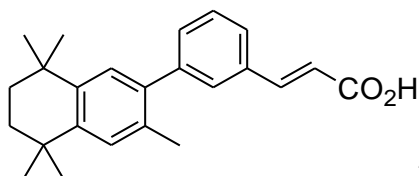
22

3-[3-(5,5,8,8-Tetramethyl-5,6,7,8-tetrahydro-naphthalen-2-yl)-phenyl]-acrylic acid (22).

The reaction was performed on a 0.12 mmol scale.

(24 mg, 62%); mp 207-208 °C; m/z (ES^-) 333 ($[\text{M} - \text{H}]^-$); ^1H NMR (400.13 MHz, DMSO-d_6) δ 12.20 (1H, br), 7.73 (1H, s), 7.66 (1H, d $J = 16.0$ Hz), 7.54 (1H, tr $J = 7.5$

Hz), 7.49 (2H, m), 7.41 (1H, tr, $J = 7.5$ Hz), 7.33 (2H, ov, s), 6.49 (1H, d $J = 16.0$ Hz), 1.66 (4H, s), 1.29 (6H, s), 1.25 (6H, s); $^{13}\text{C}\{^1\text{H}\}$ NMR 100.61 MHz, DMSO- d_6) δ 166.30, 143.52, 142.59, 142.49, 140.07, 135.48, 133.34, 127.76, 126.90, 125.47, 125.03, 124.76, 123.25, 122.67, 117.94, 33.37, 33.22, 32.66, 32.38, 30.28, 30.20; anal. calcd. for $\text{C}_{23}\text{H}_{26}\text{O}_2$: C 82.60, H 7.84; found: C 81.97, H 8.02.

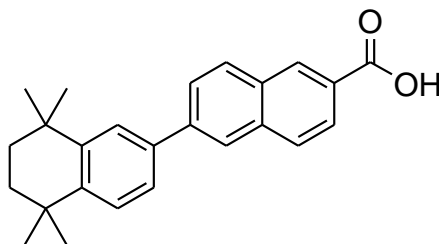


23

3-[3-(3,5,5,8,8-Pentamethyl-5,6,7,8-tetrahydro-naphthalen-2-yl)-phenyl]-acrylic acid (23).

The reaction was performed on a 0.21 mmol scale.

(42 mg, 57%); mp 170-172 °C; m/z (ES^-) 347 ($[\text{M} - \text{H}]^-$); ^1H NMR (400.13 MHz, DMSO- d_6) δ 7.58 (3H, ov, m), 7.44 (1H, t, $J = 8.0$ Hz), 7.33 (1H, d, $J = 8.0$ Hz), 7.20 (1H, s), 7.09 (1H, s), 6.56 (1H, d, $J = 16.0$ Hz), 2.16 (3H, s), 1.65 (4H, s), 1.25 (6H, s), 1.24 (6H, s); $^{13}\text{C}\{^1\text{H}\}$ NMR (100.67 MHz, DMSO- d_6) δ 168.85, 144.23, 142.85, 142.63, 138.68, 134.96, 132.34, 131.45, 129.40, 128.83, 127.98, 126.79, 125.66, 125.11 two aromatic/vinylic carbon resonances are overlapped, 35.38, 35.34, 34.29, 34.25, 32.30 (two carbon environments), 20.56; anal. calcd. for $\text{C}_{24}\text{H}_{28}\text{O}_2$: C 82.72, H 8.10; found: C 82.83, H 7.67.



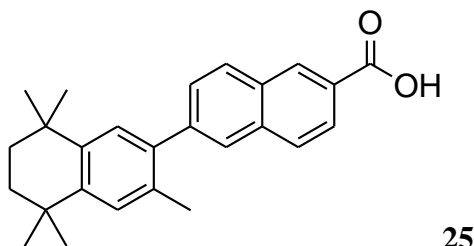
24

5',5',8',8'-Tetramethyl-5',6',7',8'-tetrahydro[2,2']binaphthalenyl-6-carboxylic acid (24).

The reaction was performed on a 0.13 mmol scale.

(33 mg, 70%); m/z (ES^-) 357 ($[\text{M} - \text{H}]^-$); mp 280-282 °C (lit. 287.5-288.5 °C); ^1H NMR (499.76 MHz, DMSO- d_6) δ 13.06 (1H, br, s), 8.62 (1H, s), 8.26 (1H, s), 8.18 (1H, d, $J =$

9.0 Hz), 8.08 (1H, d, $J = 9.0$ Hz), 7.99 (1H, d, $J = 9.0$ Hz), 7.91 (1H, d, $J = 9.0$ Hz), 7.74 (1H, s), 7.56 (1H, d, $J = 8.0$ Hz), 7.46 (1H, d, $J = 8.0$ Hz), 1.69 (4H, s), 1.34 (6H, s), 1.29 (6H, s); $^{13}\text{C}\{^1\text{H}\}$ NMR (126.67 MHz, DMSO- d_6) δ 167.50, 145.13, 144.34, 140.14, 136.78, 135.40, 131.23, 130.30, 129.89, 128.51, 127.87, 127.24, 126.12, 125.56, 125.08, 124.72, 124.51, 34.74, 34.55, 34.17, 33.91, 31.69, 31.60; anal. calcd. for $\text{C}_{25}\text{H}_{26}\text{O}_2$: C 83.76, H 7.31; found: C 83.32, H 7.09.



3',5',5',8',8'-Tetramethyl-5',6',7',8'-tetrahydro[2,2']binaphthalenyl-6-carboxylic acid (25).

The reaction was performed on a 0.08 mmol scale.

(22 mg, 75%); mp 260-263 °C (lit.³¹⁰ 263-265 °C); m/z (ES^-) 371 ($[\text{M} - \text{H}]^-$); ^1H NMR (400 MHz, DMSO- d_6) δ 8.64 (1H, s), 8.14 (1H, d, $J = 9.0$ Hz), 8.04 (1H, d, $J = 9.0$ Hz), 7.99 (1H, d, $J = 9.0$ Hz), 7.92 (1H, s), 7.59 (1H, d, $J = 9.0$ Hz), 7.24 (1H, s), 7.19 (1H, s), 2.20 (3H, s), 1.63 (4H, s), 1.27 (6H, s), 1.24 (6H, s); $^{13}\text{C}\{^1\text{H}\}$ NMR (125.67 MHz, DMSO- d_6) δ 167.56, 143.80, 142.06, 141.61, 138.19, 134.95, 131.87, 130.92, 128.95, 128.60, 128.29, 127.89, 127.57, 127.30, 125.46, two aromatic peaks are believed to be overlapped, 34.71, 34.70, 33.68, 33.62, 31.65 two carbon resonances overlapped, 19.97; anal. calcd. for $\text{C}_{26}\text{H}_{28}\text{O}_2$: C 83.83, H 7.58; found: C 83.39, H, 7.55.

References for Chapter 3

²⁹⁵ (a) Christie, V. B.; Marder, T. B.; Whiting, A.; Przyborski, S. A. *Mini-Rev. Med. Chem.* **2008**, *8*, 601-608; (b) Maden, M. *Nat. Rev. Neurosci.* **2007**, *8*, 755-765.

²⁹⁶ (a) Murayama, A.; Suzuki, T.; Matsui, M. *J. Nutr. Sci. Vitaminol.* **1997**, *43*, 167-176; (b) Bempong, D. K.; Honigberg, I. L.; Meltzer, M. N. *J. Pharm. Biomed. Anal.* **1995**, *13*, 285-291; (c) Suzuki, T.; Rao Kunchala, S.; Matsui, M.; Murayama, A. *J. Nutr. Sci.*

Vitaminol. **1998**, *43*, 729-736; (d) Kunchala, S. R.; Suzuki T.; Murayama, A. *Ind. J. Biochem. Biophys.* **2000**, *37*, 71-76.

²⁹⁷ (a) Han, G. Y.; Chang, B. S.; Connor, M. J.; Sidell, N. *Differentiation* **1995**, *59*, 61-69; (b) Lansink, M.; van Bennekum, A. M.; Blaner, W. S.; Kooistra, T. *Eur. J. Biochem.* **1997**, *247*, 596-604; (c) Han, H.; Kwon, J.; Park, M.; Park, S.; Cho, S. K.; Rho, Y.; Kim, J.; Sin H.; Um, S. *Bioorg. Med. Chem.* **2003**, *11*, 3839-3845.

²⁹⁸ Alvarez, R.; Vega, M. J.; Kammerer, S.; Rossin, A.; Germain, P.; Gronemeyer H.; de Lera, A. R. *Bioorg. Med. Chem. Lett.* **2004**, *14*, 6117-6122.

²⁹⁹ (a) Mavilio, F.; Simeone, A.; Boncinelli, E.; Andrews, P. W. *Differentiation* **1988**, *37*, 73-70; (b) Simeone, A.; Acampora, D.; Arcioni, L.; Andrews, P. W.; Boncinelli, E.; Mavilio, F. *Nature* **1990**, *346*, 763-766.

³⁰⁰ (a) Venepally, P.; Reddy L. G.; Sani, B. P. *Arch. Biochem. Biophys.* **1997**, *343*, 234-248; (b) Curley, R. W.; Fowble, J. W. *Photochem. Photobiol.* **1988**, *47*, 831-835.

³⁰¹ Sonogashira, K.; Tohda, Y.; Hagihara, N. *Tetrahedron Lett.* **1975**, *50*, 4467-4470

³⁰² Garipova, G.; Gautier, A.; Piettre, S. R. *Tetrahedron* **2005**, *61*, 4755-4759.

³⁰³ Vuligonda, V.; Thacher, S. M.; Chandraratna, R. A. S. *J. Med. Chem.* **2001**, *44*, 2298-2303.

³⁰⁴ Christie, V. B.; Barnard, J. H.; Batsanov, A. S.; Bridgens, C. E.; Cartmell, E. B.; Collings, J. C.; Maltman, D. J., Redfern, C. P. F.; Marder, T. B.; Pryzborski, S.; Whiting, A. *Org. Biomol. Chem.*, **2008**, *6*, 3497-3507.

³⁰⁵ (a) Strickland, S.; Breitman, T. R.; Frickel, F.; Nürrenbach, A.; Hädicke, E.; Sporn, M. B. *Cancer Res.* **1983**, *43*, 5268-5272; (b) Boehm, M. F.; McClurg, M. R.; Pathirana, C.; Mangelsdorf, D.; White, S. K.; Hebert, J.; Winn, D.; Goldman, M. E.; Heyman, R. A. *J. Med. Chem.* **1994**, *37*, 408-414; (c) Boehm, M. F.; Zhang, L.; Badea, B. A.; White, S. K.; Mais, D. E.; Berger, E.; Suto, C. M.; Goldman, M. E.; Heyman, R. A. *J. Med. Chem.* **1994**, *37*, 2930-2941; (d) Beard, R. L.; Gil, D. W.; Marler, D. K.; Henry, E.; Colon, D. F.; Gillett, S. J.; Arefieg, T.; Breen, T. S.; Krauss, H.; Davies, P. J. A.; Chandraratna, R. A. S. *Bioorg. Med. Chem. Lett.* **1994**, *4*, 1447-1452; (e) Totpal, K.; Chaturvedi, M. M.; LaPushin, R.; Aggarwal, B. B. *Blood* **1995**, *85*, 3547-3555; (f) Islam, T. C.; Skarin, T.; Sumitran, S.; Toftgård, R. *Br. J. Dermatol.* **2000**, *143*, 709-719; (g) Gambone, C. J.;

Hutcheson, J. M.; Gabriel, J. L.; Beard, R. L.; Chandraratna, R. A. S.; Soprano, K. J.; Soprano, D. R. *Mol. Pharmacol.* **2002**, *61*, 334-342.

³⁰⁶ Love, J. D.; Gooch, J. T.; Benko, S.; Li, C.; Nagy, L.; Chatterjee, V. K. K.; Evans, R. M.; Schwabe, J. W. R. *J. Biol. Chem.* **2002**, *277*, 11385-11391.

¹ Roberts, A. B.; Nichols, M. D.; Newton, D. L.; Sporn, m. B. *J. Biol. Chem.* **1979**, *254*, 6296-6303.

³⁰⁷ Beard, R. L.; Chanraratna, R. A. S.; Colon, D. F.; Gillett, S. J.; Henry, E.; Marler, D. K.; Song, T.; Denys, L.; Garst, M. E.; Arefeig, T.; Klein, E.; Gil, D. W.; Wheeler, L.; Kochar, D. M.; Davies, P. D. *J. Med. Chem.* **1995**, *38*, 2820-2829.

³⁰⁸ Dawson, M. I.; Chan, R. L. S.; Derdzinski, K.; Hobbs, P. D.; Chao, W. R.; Schiff, L. J. *J. Med. Chem.* **1983**, *26*, 1653-1656.

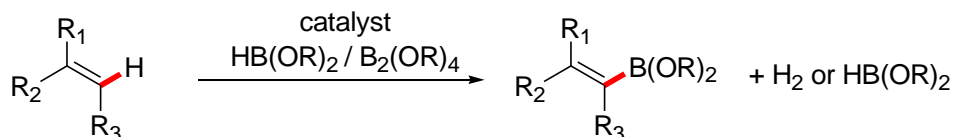
³⁰⁹ Dawson, M. I.; Hobbs, P. D.; Derdzinski, K. A.; Chao, W.-R.; Frenking, G.; Loew, G. H.; Jetten, A. M.; Napoli, J. L.; Williams, J. B.; Sani, B. P.; Wille, J. J. Jr.; Schiff, L. J. *J. Med. Chem.* **1989**, *32*, 1504-1517.

³¹⁰ Dawson, M. I.; Hobbs, P. D.; Derdzinski, K. A.; Chao, W.-R.; Frenking, G.; Loew, G. H.; Jetten, A. M.; Napoli, J. L.; Williams, J. B.; Sani, B. P.; Wille, J. J. Jr.; Schiff, L. J. *J. Med. Chem.* **1989**, *32*, 1504-1517.

Mild and selective formation of vinylboronate esters *via* the Rh-catalysed dehydrogenative borylation of alkenes

4.1 Introduction

Vinyl boronate esters (VBEs)³¹¹ are useful intermediates in organic chemistry, having been employed as precursors to aldehydes and vinyl halides, and can undergo transition metal-catalysed additions to a range of electrophiles. VBEs can be synthesised by a variety of methods including: (a) lithiation of vinyl halides and subsequent trapping with trialkylborates,³¹² (b) palladium-catalysed borylation of vinyl halides,³¹³ (c) transmetallation of vinyl metal reagents,³¹⁴ (d) hydrozirconation of 1-borylalkynes,³¹⁵ (e) cross-metathesis of terminal alkenes with pinacolvinylboronate,³¹⁶ (f) hydrogenation of 1-borylalkynes,³¹⁷ (g) transfer of a boryl group between two alkenes,³¹⁸ (h) hydroboration of alkynes,³¹⁹ and (i) transition metal-catalysed diboration of alkynes with diboron reagents.³²⁰ However, the majority of these methods involve the preactivation of the vinyl group (a-f) or are unsuitable for the synthesis of β,β -disubstituted vinylboronates (h-i). Thus, the dehydrogenative borylation of alkenes³²¹ (**Scheme 4.1**), in which a vinyl C-H bond is replaced by a C-B bond, is an attractive alternative to these methods as it does not require the preactivation of the substrate, and is suitable for the synthesis of VBEs from β,β -disubstituted alkenes.



Scheme 4.1 Catalytic dehydrogenative borylation of alkenes.

The formation of VBE products has been observed as a side reaction in rhodium-catalysed diborations^{321a} and hydroborations of alkenes.^{321b,c} Combinations of phosphine free Rh(I)^{321d-g} catalysts and boranes have been shown to give 1:1 mixtures of VBEs and hydrogenation products while Ru catalysts^{321g,n,o} (not phosphine free) give

mixtures of VBEs and products resulting from hydroboration and hydrogenation. Significant amounts of VBE products were observed in the Rh(PPh₃)₃Cl-catalysed reactions of 1,1-disubstituted alkenes and catecholborane.^{321b,c} In the majority of cases it has been demonstrated, or is believed, that the reaction occurs through 1,2-insertion of the alkene substrate, followed by β-hydride elimination to give the VBE product.^{321a-t} Alternatively, VBE formation can occur by the direct oxidative addition of a vinylic C-H bond, followed by C-B reductive elimination.^{321u,v} For the majority of dehydrogenative borylation reactions, the concomitant hydrogenation and/or hydroboration of the substrate leads to the formation of unwanted by-products and remains a major obstacle to the realisation of effective dehydrogenative borylations of unactivated alkenes. In 2003, it was reported that *trans*-[Rh(PPh₃)₂(CO)Cl] (**1**) catalyses the dehydrogenative borylation of a range of vinylarenes,^{321k,l} to give *E*-VBEs with high levels of chemo-, and stereoselectivity and a dehydrogenative borylation reaction catalysed by **1** has recently been utilised as a key step in the stereoselective synthesis of TTNPB retinoids.³²² However, dehydrogenative borylations involving **1** require temperatures of 80 °C and prolonged reaction times in order to give acceptable conversions. Also, the nature of the catalytic cycle and active species were not determined for reactions involving **1**. Thus, in order to realize an efficient synthesis of VBEs from unactivated alkenes, there is a need for catalysts which are stable and display high activities under mild conditions. In addition, elucidation of the catalytic cycle would give information on the factors determining the activity of the catalysts and allow for the future development of more efficient catalysts for this reaction.

4.2 Results and discussion

Although reactions of rhodium(I) phosphine complexes with boranes and diboron reagents have been studied extensively,³²³ the Rh-boryl complex postulated to be the active catalyst in reactions involving **1** has not been identified. Whereas *trans*-[Ir(PPh₃)₂(CO)Cl] oxidatively adds HBcat (cat = 1,2-O₂C₆H₄),³²⁴ no reaction was observed between the rhodium analogue **1** and either B₂pin₂ or B₂cat₂.^{323d}

In light of the acceleration, in the presence of basic additives, of the transmetallation of diboron, and organoboron reagents to transition metal centers^{325,326,327,328,329} the borylation of 2-phenylpropene with B₂pin₂ catalysed by **1** in the presence of oxygen containing bases (1.1 equiv w.r.t, Rh) was investigated (**Table 4.1**). Reactions were performed in 3:1 C₆D₆/CD₃CN, a solvent combination which was previously shown to be especially effective for **1**-catalysed dehydrogenative borylations.^{321k,l}

Table 4.1 Dehydrogenative borylations of 2-phenylpropene with B₂pin₂ in the presence of bases

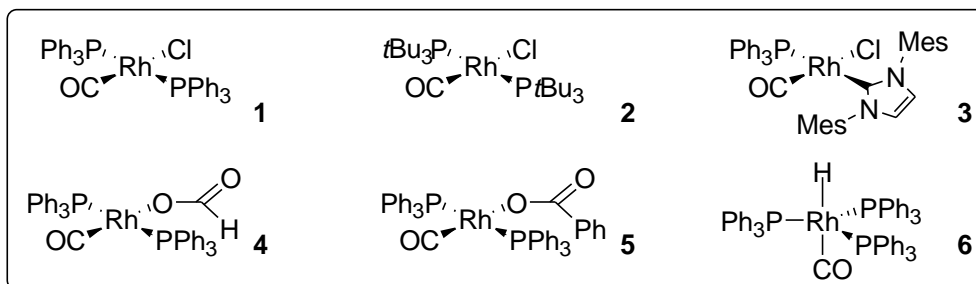
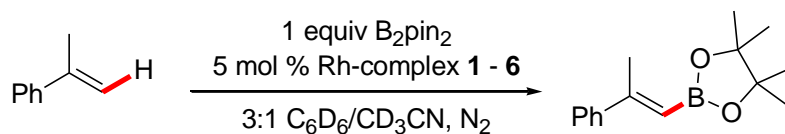
Entry	base	temp °C	conversion % ^a
1	none	20	5
2	none	45	43
3	KO(<i>t</i>)Bu	45	65
4	KOAc	45	43
5	KOH	45	77
6	KOH	20	28

Reactions were analysed after 18 h by *in situ* ¹H NMR and GC-MS. ^aConversions were determined by comparison of the integrals of the resonances of the vinylic protons of 2-phenylpropene and the *E*-VBE product by ¹H NMR. Product identities and conversions were confirmed by GC-MS analysis.

Reactions performed in the presence of KOH and KO(*t*)Bu showed enhanced activity (w.r.t, **1** alone), with KOH found to be the most effective. In addition, the reaction with **1** and 5.5 mol % KOH gave 28% conversion to the VBE product after 18 h at room temperature, whereas the use of **1** without additional base showed very low activity (ca. 1 turnover). Reasoning that the additive reacts with **1** to form a Rh-OR species *in situ*, although other pathways are possible,^{329c,330} a range of Rh(I) complexes bearing different anionic and neutral ligands (**Table 4.2**) were screened as catalyst precursors for the

dehydrogenative borylation of 2-phenylpropene with B₂pin₂ in a 3:1 mixture of C₆D₆/CD₃CN.^{321k,1} The activity of **6**, the well known hydroformylation catalyst,³³¹ was also examined.

Table 4.2 Rh-catalysed dehydrogenative borylations of 2-phenylpropene with B₂pin₂ after 18h.



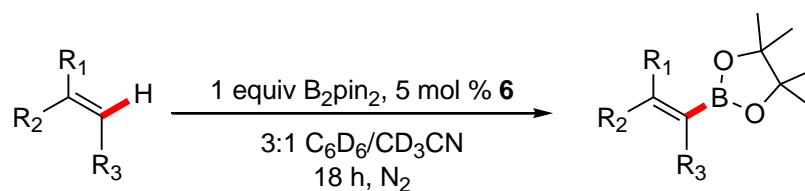
entry	Rh-complex	temp °C	conversion % ^a
1	1	20	5
2	1	45	43
3	1	80	71
4	2	20	8
5	2	45	23
6	2	80	89
7	3^b	20	1
8	3^b	45	12
9	3^b	80	36
10	4	20	11
11	4	45	57
12	4	80	88
13	5	20	10
14	5	45	51
14	5	80	84
16	6	20	32

17	6	45	48
18	6	80	87

Reactions were analysed after 18 hours by *in situ* ^1H NMR and GC-MS. ^aConversions were determined by comparison of the integrals of the vinylic protons signals of 2-phenylpropene and the *E*-VBE products by ^1H NMR. ^bConversion determined by comparison of the integrals of 2-phenylpropene, B_2pin_2 and VBE product peaks in the GC (TIC) trace.

All of the Rh(I) complexes examined catalysed the dehydrogenative borylation reaction, with VBE products formed with high selectivity. At 80 °C, the complexes **1**, **2**, **4**, **5** and **6** gave similar results, within experimental error. At lower temperatures, the effect of exchanging chloride for hydride or oxy-anions was more pronounced, with complexes **4**, **5**, and **6** exhibiting increased catalytic activity in comparison to Rh-Cl complexes **1**, **2** and **3**, suggesting that the ease of the initial transmetallation ($\text{Rh-X} + \text{B-B} \rightarrow \text{Rh-B} + \text{B-X}$) process may be important for high catalytic activity by increasing the rate of catalyst initiation.

The activity of **6** was further examined (**Table 4.3**) for a range of substrates including monosubstituted alkenes (Entries 1-4), 1,1-disubstituted alkenes (Entries 5-8) and cyclic alkenes (Entries 9-12). Monosubstituted substrates were borylated at 45 °C in order to reduce the formation of products resulting from further borylation of the VBE products, a process which yields saturated or unsaturated bis-boronates or even tris-boronates,^{320a,320k,320l,332} while the less reactive 1,1-, and 1,2-disubstituted alkenes were borylated at 80 °C.

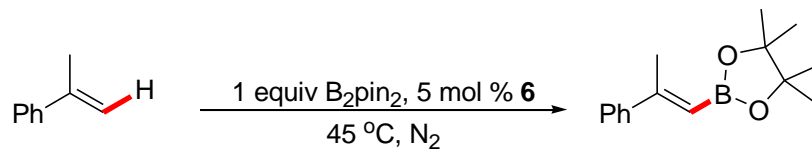
Table 4.3 Dehydrogenative borylation of alkenes with B₂pin₂ catalysed by **6**

Entry	substrate	temp °C	Yield %	Isolated VBE product	HB % ^a	VBE % ^a	VBBE % ^a
1		45	31		10	53	36
2		45	28		27	60	13
3		45	n.d.	-	35	11	51
4		45	n.d.	-	6	26	18
5		80	85 ^b		0	84	0
6		80	92 ^b		trace	73	0
7		80	73		trace	>98	0
8		80	89 ^b		0	84	0
9		80	n.d.	-	0	trace	0
10		80	n.d.	-	0	trace	0
11		80	n.d.		trace	30	0

Reactions were carried out with 5 mol % **6** and 1 equiv of B₂pin₂ in 3:1 C₆D₆/CD₃CN at 45 °C or 80 °C, and analysed by *in situ* ¹H NMR and GC-MS after 18 hours. ^a% conversion to each product type at 18 h. HB = hydroboration. VBBE = vinyl-bis-boronate ester. For entries 1, 2 and 7, isolated yields are for the VBE product after 18 h reaction. ^bFor 5, 6 and 8, isolated yields are for the VBE product after 42 h reaction, i.e. when the reaction is complete, rather than after 18 h. n.d. = not determined.

Borylations of styrene and 4-vinylanisole (entries 1 and 2) were found to be rapid, with full consumption of both the alkene and B₂pin₂ observed after 18 hours. VBE products were formed with moderate selectivities, along with significant amounts of vinyl bis-boronate ester (VBBE) products, resulting from the further dehydrogenative borylation of the VBE products. The borylation of 1-octene led to full consumption of the substrate after 18 h giving a complex mixture of hydroboration, VBE and VBBE products (due to double bond migration in either, or both, the substrate or products), with VBBEs being the major product type. 4-Allylanisole gave a single VBE product along with a mixture of isomeric hydroboration and VBBE products. In contrast, reactions of 1,1-disubstituted alkenes were more selective, giving VBEs and only trace amounts of hydroboration products. This high degree of chemo-, and stereoselectivity is in contrast to Heck reactions of 1,1-disubstituted alkenes³³³ such as 2-phenylpropene which typically give mixtures of allylic and vinylic products with poor *E/Z* selectivities. In both cases, borylation of 1,1-dialkyl-substituted alkenes (entries 6 and 7) led to the selective formation of the exocyclic VBE product, over the endocyclic allylboronate ester. For indene, previously found to be extremely unreactive,^{321k,l} 30% conversion to the synthetically useful 2-borylated product **7g** (*vide infra*) was observed after 18 h. This compares to 19% conversion after 148 h using **1** as a catalyst precursor.^{321l} In the reactions of cyclohexene and cyclooctene, only trace amounts of VBE products were observed after 18 h. The low reactivity of cyclic substrates^{321m} may result from the difficulty of achieving planarity between the β-hydride and rhodium moieties leading to an unfavourable β-hydride elimination process or the poor binding of cyclohexene and cyclooctene to rhodium.

The use of 3:1 toluene/MeCN or C₆D₆/CD₃CN was previously found to be highly effective at minimizing side product formation in the dehydrogenative borylation of 4-vinyl anisole with **1**, however, MeCN retards the rate of the reaction.^{321k} In light of the high selectivities exhibited in the borylations of 1,1-disubstituted substrates, the borylation of 2-phenylpropene with B₂pin₂ and 5 mol % **6** at 45 °C in different solvents (**Table 4.4**) was examined.

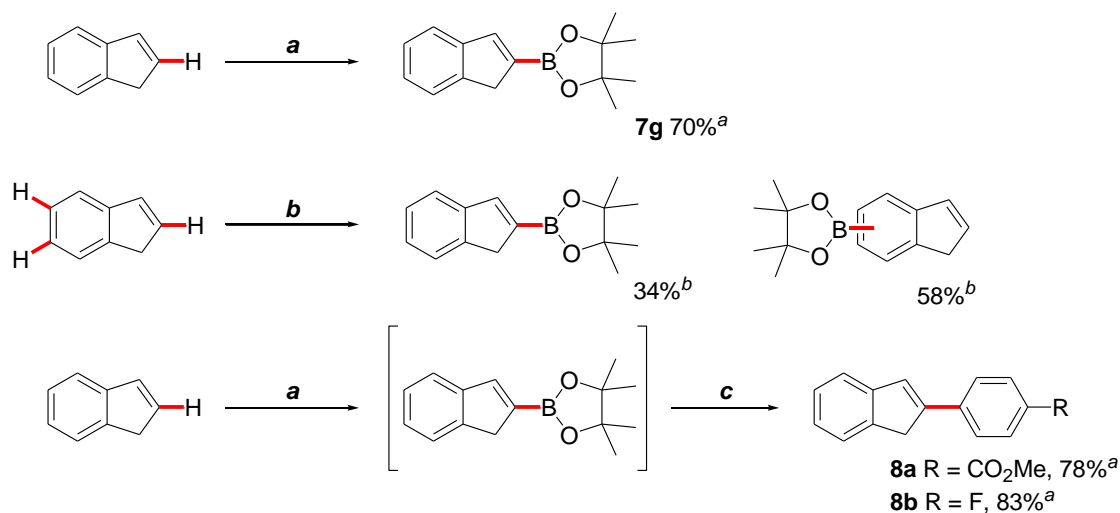
Table 4.4 Dehydrogenative borylation of 2-phenylpropene in different solvents

entry	solvent	% VBE at 4 h
1	Hexane	57
2	Toluene	61
3	Benzene	57
4	MTBE	70
5	THF	15
6	3:1 benzene/MeCN	22

Reactions were carried out with 5 mol % **6** and 1 equiv of B_2pin_2 at 45 °C, and analysed periodically by 1H NMR and GC-MS. % conversions were determined by comparisons of the integrals of NMR resonances corresponding to 2-phenylpropene and the *E*-VBE product. Product identities and conversions were confirmed by comparison with the substrate and VBE peaks in the GC/MS (TIC) trace.

Reactions performed in non-coordinating solvents showed increased rate w.r.t, the use of 3:1 C_6D_6/CD_3CN . MTBE (Me-O-(*t*)Bu) was found to be the most effective solvent followed by hexane, toluene and benzene. In contrast to MBTE, reactions performed in the more strongly coordinating ether, THF, showed the lowest activity.

It has recently shown that MTBE is an excellent solvent for a one-pot, single solvent process involving Ir-catalysed arene or heteroarene C-H borylation^{334,335} followed by Suzuki-Miyaura cross-coupling. The high activity displayed by **6** in MTBE led us to explore a one-pot, single solvent dehydrogenative borylation/Suzuki-Miyaura cross-coupling sequence for the direct functionalisation of indene. 2-Arylindenes are highly desirable products due to their use as ligands in organometallic chemistry, especially in the Zr-catalysed polymerization of propene,³³⁶ but current methods for their synthesis are limited by side reactions related to the high basicity of the arylmetal reagents used,³³⁷ the need for preactivation of the 2-position,³³⁸ or a lack of selectivity for 2-functionalisation.³³⁹



a. 1 equiv B₂pin₂, 5 mol % **6**, MTBE, 80 °C, 42 h

b. 1 equiv B₂pin₂, 1.5 mol % [Ir(OMe)COD]₂, 3 mol % dtbpy MTBE, 45 °C, 18 h

c. 0.85 equiv *p*-I-C₆H₄-R, 3 mol % Pd(dppf)Cl₂·DCM, 2 equiv. K₃PO₄·2H₂O, H₂O (20% v/v), 80 °C

a Isolated yields; *b* Conversions by ¹H NMR spectroscopy

Equation 4.1 Borylation of indene and synthesis of 2-arylindenes *via* one-pot, single solvent C-H borylation/Suzuki-Miyaura cross-coupling.

Ir-catalysed borylation³³⁵ with 1.5 mol % [Ir(μ-OMe)COD]₂ / 3 mol % 4,4'-di-*tert*-2,2'-bipyridine as catalyst was investigated, and found to give a mixture of products resulting from vinylic C-H borylation at the 2-position and aromatic C-H borylation at the 5- and 6-positions. In contrast, borylation of indene with 5 mol % **6** and B₂pin₂ in MTBE at 80 °C led to full conversion to **7g** after 42 h. After addition of Ar-I, Pd(dppf)Cl₂·CH₂Cl₂, K₃PO₄·2H₂O and H₂O to the completed Rh-catalysed reactions, heating (80 °C) gave the 2-arylidene products in good yields (**Equation 4.1**) offering an efficient alternative route to these products.

4.3 Investigations into the mechanism of the dehydrogenative borylation reaction

Borylations of 2-phenylpropene with 1 equivalent of B_2pin_2 and 20 mol % of **4** or **6** as the catalyst precursor were performed in 3:1 C_6D_6/CD_3CN at 20 °C and analysed by *in situ* 1H , $^{31}P\{^1H\}$ and ^{11}B NMR spectroscopy after 6 hours.

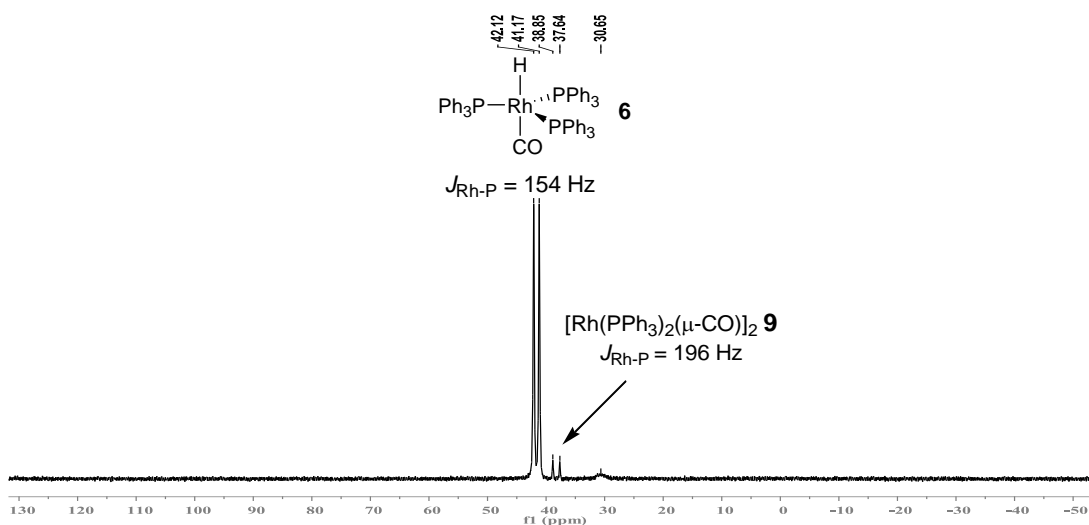


Figure 4.1 162 MHz $^{31}P\{^1H\}$ NMR spectrum of the borylation of 2-phenylpropene with 20 mol % of **6** in 3:1 C_6D_6/CD_3CN after 6 h at 20 °C.

For the use of **6** as the catalyst precursor, *in situ* $^{31}P\{^1H\}$ NMR spectroscopy showed **6** to be the main phosphine containing species present (Figure 1), along with a doublet at 37.8 ppm ($J_{Rh-P} = 196$ Hz) corresponding to the known dimer $[Rh(\mu-CO)(PPh_3)_2]_2$ **9**^{340,341} and a small, broad peak at 30.5 ppm.

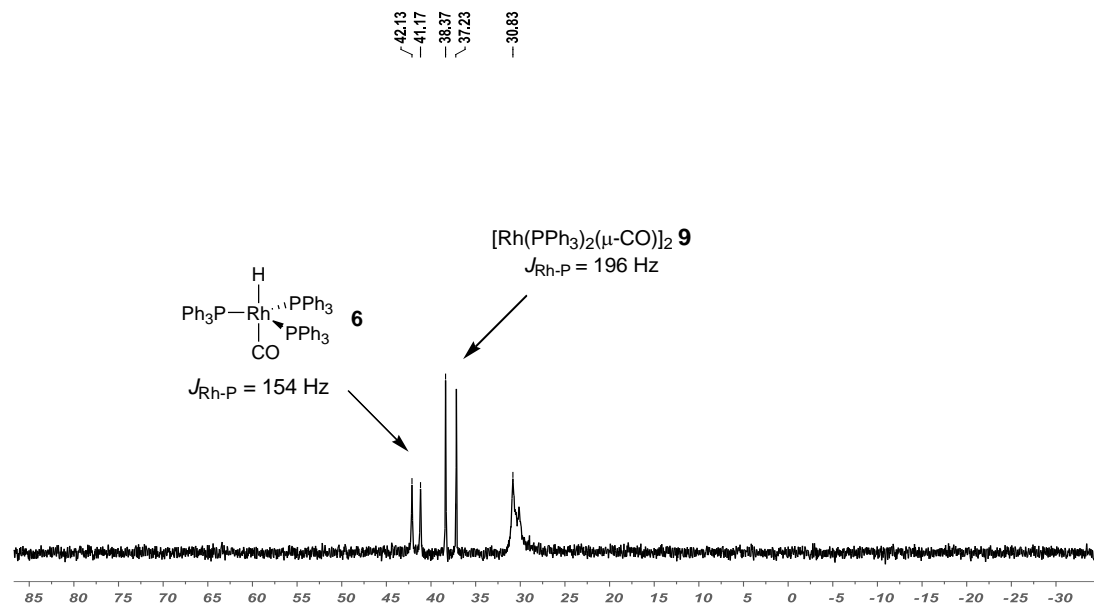


Figure 4.2 162 MHz $^{31}\text{P}\{^1\text{H}\}$ NMR spectrum of the borylation of 2-phenylpropene with 20 mol % of **4** in 3:1 $\text{C}_6\text{D}_6/\text{CD}_3\text{CN}$ after 6 h at 20 °C.

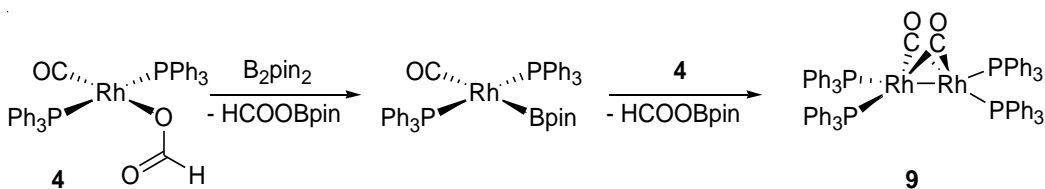
In contrast, *in situ* $^{31}\text{P}\{^1\text{H}\}$ NMR spectra of the same reaction with **4** instead of **6** did not display the doublet corresponding to **4**. Peaks corresponding to **6** and **9** were observed, as well as a broad peak at 31.5 ppm (**Figure 4.2**). Although **6** can be synthesised from **4** in the presence of PPh_3 ,³⁴² solutions of **4** in $\text{C}_6\text{D}_6/\text{MeCN}$ showed no formation of **6** after 18 hours at room temperature, suggesting that **6** is formed from **4** *via* a process involving B_2pin_2 and 2-phenylpropene.

Reactions of **4** and **6** with stoichiometric amounts of B_2pin_2 in 3:1 $\text{C}_6\text{D}_6/\text{CD}_3\text{CN}$ at 20 °C resulted in the formation of HCOO-Bpin and HBpin , respectively, as observed by ^{11}B NMR spectroscopy, suggesting that transmetallation had occurred. It is possible that HBpin and HCOO-Bpin are formed *via* oxidative addition of the B-B bond, followed by rapid reductive elimination; however, the lack of reactivity displayed by **1** under the same conditions (*vide supra*) suggests otherwise. It should be noted that no ^{11}B NMR signal corresponding to any Rh-boryl species was observed in the ^{11}B NMR spectra. Marder, Norman *et al.* have reported that they were unable to observe a resonance for the boryl group of $[\text{Rh}(\text{dppe})_2(\text{Bcat})]$ in the ^{11}B NMR spectrum, presumably because it is extremely broad.^{323d} *In situ* $^{31}\text{P}\{^1\text{H}\}$ NMR spectra of the reaction of **4** or **6** with B_2pin_2

did not reveal any resonances which could be attributed to the expected Rh(I) monoboryl complex *trans*-[Rh(PPh₃)₂(CO)Bpin]. Instead, a new ³¹P signal at 37.8 ppm (*J*_{Rh-P} = 196 Hz) was observed, corresponding to [Rh(μ-CO)(PPh₃)₂]₂ **9** (Scheme 4.2) and its intensity was found to increase with time.

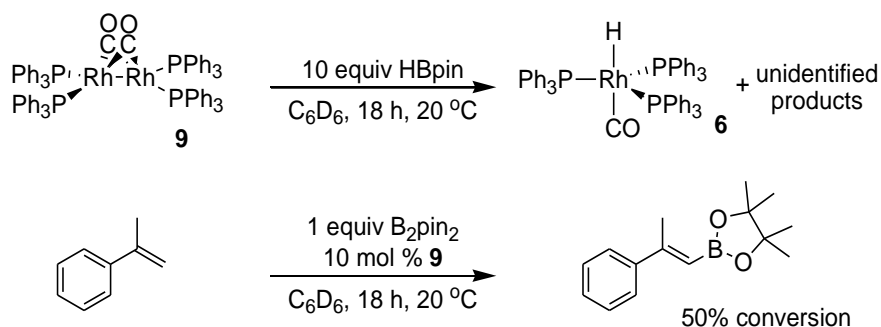
To investigate whether the rhodium boryl complex was consumed *via* reaction with the arene solvent, solutions of **4** and **6** with 10 equivalents of B₂pin₂ were stirred in benzene at room temperature and were then analysed by ³¹P{¹H} NMR spectroscopy and *in situ* GC-MS. Reactions of **6** were found to contain small amounts of **9** as well as residual **6** as the major phosphorus-containing species, while reactions of **4** resulted in its complete consumption within 4 hours, with **9** being the major phosphorus-containing species observed by ³¹P{¹H} NMR spectroscopy. Analysis of the reaction mixtures by *in situ* GC-MS showed the formation of substoichiometric amounts of C₆H₅-Bpin. However, performing the reactions in C₆D₆ did not lead to the formation of C₆D₅-Bpin, nor did analogous reactions in toluene give tolyl-Bpin. Instead C₆H₅-Bpin was formed in all cases, indicating that the source of the C₆H₅ fragment is not the solvent, but most likely the PPh₃ ligands which may be undergoing P-C bond cleavage. However, due to the small amounts of arylboronate ester products observed, any further mechanistic speculation is unwarranted at present.

As borylation of the solvent was not observed, it is proposed that the rhodium boryl species, in the absence of substrate, is consumed by reaction with unreacted **4** or **6** to yield additional HCOO-Bpin or HBpin, respectively, and **9** (Scheme 4.2). Such bimolecular reductive elimination processes have been previously observed in the reaction of *trans*-[Rh(PPh₃)₂(CO)(*p*-C₆H₄Me)] with **6** to give toluene and **9**.³⁴⁰



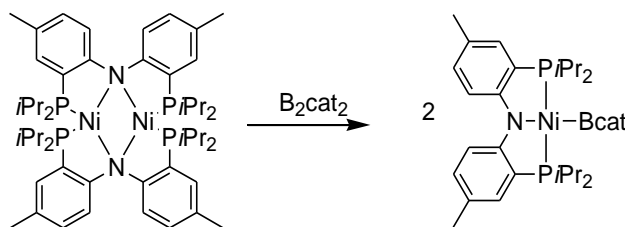
Scheme 4.2 Proposed formation of **9** from **4**.

As previously noted, **9** and **6** are observed by $^{31}\text{P}\{^1\text{H}\}$ NMR in borylations of 2-phenylpropene with B_2pin_2 using **4**, **5** and **6** as catalyst precursors. For reactions with **4** and **5**, these catalyst precursors are not observed by *in situ* $^{31}\text{P}\{^1\text{H}\}$ NMR during the reaction. However, for reactions with **6**, **6** is observed as the major species. In order to assess whether **6** or **9** might be the catalytically active species, a solution of **9** was prepared by reacting **4** with 10 equivalents of B_2pin_2 in C_6D_6 at room temperature. Full consumption of the starting material was observed after 4 hours. Addition of HBpin (10 equiv) and stirring for 18 h at 20 °C generated the rhodium hydride complex **6**, along with an unidentified product (a broad peak at 30.5 ppm). Addition of 2-phenylpropene (10 equiv) to a solution of **9** and B_2pin_2 led to the formation of the VBE product with 50% conversion after 18 hours at 20 °C. Analysis by *in situ* ^{11}B NMR spectroscopy showed that HBpin had been formed, while the $^{31}\text{P}\{^1\text{H}\}$ NMR spectrum of the reaction mixture showed the presence of **6**, as well as **9**. This suggests that **9** is not an inactive side product of catalyst breakdown, but is able to react with B_2pin_2 and HBpin to give species capable of catalysing the dehydrogenative borylation of alkenes.



Scheme 4.3 Reactions of **9**.

Compound **9** has been reported to undergo bimetallic oxidative addition of H_2 in the presence of excess PPh_3 to give 2 equivalents of $\text{HRh}(\text{PPh}_3)_3\text{CO}$ **6**, to undergo oxidative cleavage in the presence of I_2 ³⁴³ and to mediate the reductive coupling of alkyl halides to give *trans*- $[\text{Rh}(\text{PPh}_3)_2(\text{CO})\text{X}]$ and the dialkyl coupling products.³⁴⁴ In addition, the bimetallic oxidative addition of B_2cat_2 to an isoelectronic bimetallic Ni^{I} complex has recently been reported by Mindiola and coworkers (**Scheme 4.4**).³⁴⁵

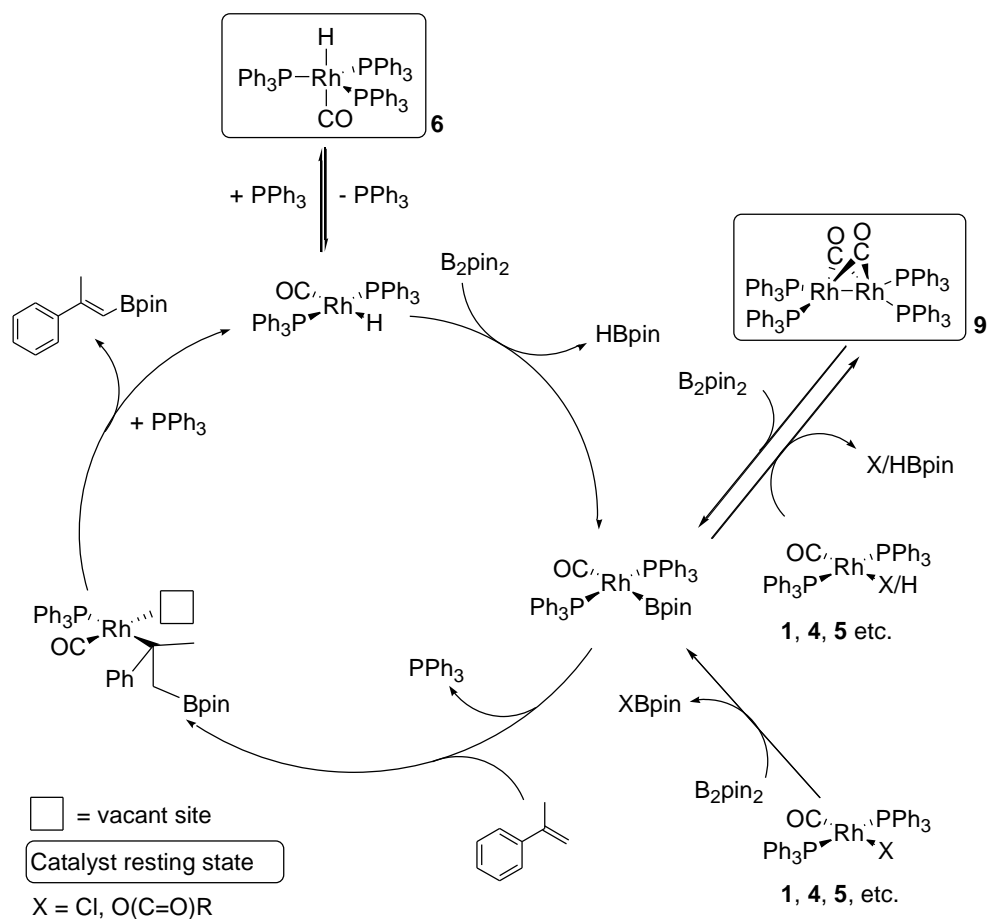


Scheme 4.4 Bimetallic oxidative addition of B_2cat_2 to a dimeric Ni^I complex.

Analysis of a control experiment (in which the borylation of 2-phenylpropene with B_2pin_2 in C_6D_6 at 20 °C was catalysed by 10 mol % **6**) by *in situ* GC-MS and $^{31}P\{^1H\}$ NMR spectroscopy showed **6** to be the major phosphine containing species present after 18 hours, with small amounts of **9** observed. Both the conversions and product selectivities for the reactions catalysed by 10 mol % **6** and 5 mol % **9** are similar, suggesting that both **6** and **9** give rise to the same catalytically active species.

Based on the above observations, a catalytic cycle is proposed for the dehydrogenative borylation of alkenes catalysed by $Rh(PPh_3)_n(CO)X$ catalyst precursors (**Scheme 4.5**).

Transmetallation of *trans*- $[Rh(PPh_3)_2(CO)X]$ with B_2pin_2 would give the Rh(I) boryl complex *trans*- $[Rh(PPh_3)_2(CO)Bpin]$. This is much more efficient when $X = OR$ or $O(C=O)R$ than when $X = Cl$, as is established for other metal centres.³²⁵⁻³²⁹ The same rhodium compound could also be formed from $HRh(PPh_3)_3CO$ *via* the initial dissociation of PPh_3 and subsequent reaction with B_2pin_2 , forming $HBpin$ as the byproduct. Reaction of *trans*- $[Rh(PPh_3)_2(CO)Bpin]$ with *trans*- $[Rh(PPh_3)_2(CO)X]$ or *trans*- $[Rh(PPh_3)_2(CO)H]$ would give $XBpin$ or $HBpin$, respectively, along with $[Rh(\mu-CO)(PPh_3)_2]_2$ **9**. Dissociation of PPh_3 from *trans*- $[Rh(PPh_3)_2(CO)Bpin]$, followed by binding and 1,2 insertion of the alkene substrate into the rhodium-boron bond would give a coordinatively unsaturated tertiary alkyl-rhodium complex. Subsequent diastereoselective β -hydride elimination^{321o} and coordination of PPh_3 would release the VBE product and regenerate $[Rh(PPh_3)_2(CO)H]$, completing the catalytic cycle. In contrast to $Rh(PPh_3)_3Cl$ -catalysed additions of $HB(OR)_2/B_2(OR)_2$ to alkenes and alkynes,^{321a,346} the proposed catalytic cycle does not involve oxidative addition of $HB(OR)_2/B_2(OR)_2$ to Rh(I), due to the strongly electron-withdrawing effects of the carbonyl ligand.



Scheme 4.5 Proposed catalytic cycle for the $\text{Rh}(\text{PPh}_3)_n(\text{CO})\text{X}/\text{H}$ -catalysed dehydrogenative borylation of alkenes with B_2pin_2 .

4.4 Conclusions

The use of the commercially available hydroformylation catalyst $\text{HRh}(\text{PPh}_3)_3\text{CO}$ **6** allows for the mild, stereoselective C-H borylation of alkenes to give (*E*)-VBE products in one step and has been utilised in the one-pot synthesis of 2-arylindenes from the parent hydrocarbon. This represents the first catalytic dehydrogenative borylation of unactivated alkenes which proceeds under mild conditions without the formation of large amounts of unwanted hydrogenation and hydroboration products. Combined multinuclear NMR and GC-MS studies of stoichiometric and catalytic reactions have identified two viable

catalyst resting states. A catalytic cycle is proposed, in which the active rhodium-boryl complex is formed *via* transmetallation of rhodium hydride or carboxylate with the diboron reagent rather than oxidative addition of the B-B bond and subsequent reductive elimination of B-X. Further applications of this reaction are under investigation.

4.5 Experimental

All reactions were carried out under a dry nitrogen atmosphere using standard Schlenk techniques or in an Innovative Technology Inc. System 1 double-length glove box. Glassware was oven dried before transfer into the glove box. Hexane was dried over sodium / benzophenone and acetonitrile and benzene were dried over CaH₂ and both were distilled under nitrogen. The solvents H₂O and anhydrous MTBE were degassed by 3 freeze-pump-thaw-cycles. Toluene was dried and deoxygenated by passage through columns of activated alumina and BASF-R311 catalyst under Ar pressure using a locally modified version of the Innovative Technology Inc. SPS-400 solvent purification system. THF was dried by passage through columns of activated alumina under Ar pressure using the same system and then degassed by 3 freeze-pump-thaw-cycles. *Trans*-[Rh(PPh₃)₂(CO)Cl] **1**,³⁴⁷ *trans*-[Rh(*Pt*-Bu₃)₂(CO)Cl] **2**,³⁴⁸ *trans*-[Rh(PPh₃)₂(CO)OOCH] **4**,³⁴⁹ HRh(PPh₃)₃CO **6**,³⁵⁰ were synthesised by literature procedures. *Trans*-[Rh(PPh₃)(iMes)(CO)Cl]³⁵¹ **3** was a gift from Prof Antonio M. Echavarren, Fundació Privada Institut Català D'investigació Química (ICIQ). B₂pin₂ was supplied as a gift by AllyChem Co. Ltd., Frontier Scientific Inc. and NetChem Inc. Hydrochloric acid was obtained from Fisher Scientific and all other compounds were obtained from Aldrich Chemical Company, tested for purity by ¹H NMR and GC-MS, degassed and used without further purification. NMR spectra were recorded at ambient temperature on Varian Inova 500 (¹H, ¹³C{¹H}), Varian C500 (¹H, ¹³C{¹H}, ³¹P{¹H}, ¹⁹F), Bruker 400 Ultrashield (¹H, ¹³C{¹H}, ¹¹B and ¹¹B{¹H}) instruments. Proton and carbon spectra were referenced to external SiMe₄ *via* residual protons in the deuterated solvents or solvent resonances, respectively. ¹¹B NMR spectra were referenced to external BF₃·OEt₃. Elemental analyses were conducted in the Department of Chemistry at Durham University using an Exeter Analytical Inc. CE-440 Elemental Analyser. GC-MS

analyses were performed on an Agilent 6890 Plus GC equipped with a 5973N MSD and an Anatune Focus robotic liquid handling system / autosampler. A fused silica capillary column (10 m or 12 m, cross-linked 5% phenylmethylsilicone) was used, and the oven temperature was ramped from 50 °C to 280 °C at a rate of 20 °C/min. UHP grade helium was used as the carrier gas. The screw-cap autosampler vials used were supplied by Thermoquest Inc. and were fitted with Teflon / silicone / Teflon septa and 0.2 mL micro inserts.

Unless otherwise specified the vinylboronate ester products were synthesised *via* the following methods.

Method A: synthesis of VBEs *via* Rh-catalysed dehydrogenative borylation. In dry, N₂-filled glovebox, a solution of alkene, B₂pin₂ (1.0 equiv) and HRh(PPh₃)₃CO **6** (5 mol %) in 3:1 C₆D₆/CD₃CN was added to a thick-walled glass tube which was then sealed. The mixture was heated at the appropriate temperature and monitored by *in situ* ¹H NMR and GC-MS. Reactions were performed on a 0.2 mmol scale in 1 mL of solvent or on a 0.4 mmol scale in 2 mL of solvent. Unless otherwise specified, the products were purified in the following manner. The solvent was removed *in vacuo* and the residue was dissolved in 3:2 hexanes/CH₂Cl₂ and passed through a silica plug. The solvent was removed *in vacuo* to give a crude product that was purified *via* silica gel chromatography (hexanes to 1:1 CH₂Cl₂/hexanes, gradient elution).

Method B: synthesis of VBEs *via* Ir-catalysed dehydrogenative borylation. In dry, N₂-filled glovebox, alkene (0.5 mmol) was added to a premixed solution of [Ir(OMe)COD]₂ (1.5 mol %, 5.0 mg, 7.5 μmol), dtbpy (3 mol %, 4.0 mg, 1.5 μmol mol) and B₂pin₂ (1.0 equiv 127 mg, 0.5 mmol) in MTBE (1.2 mL). Additional MTBE (1 mL) was added, and the solution was transferred to a thick-walled glass tube which was then sealed. The mixture was heated at the appropriate temperature and monitored by *in situ* ¹H NMR and GC-MS. The solvent was removed *in vacuo* and the residue was dissolved in 3:2 hexanes/CH₂Cl₂ and passed through a silica plug. The solvent was removed *in*

vacuo to give a crude product that was purified *via* silica gel chromatography (hexanes to 1:1 CH₂Cl₂/hexanes, gradient elution).

Synthesis of 4,4,5,5-tetramethyl-2-styryl-[1,3,2]dioxaborolane^{316b, 321g} (7a) *via* method A (0.2 mmol scale). The reaction with styrene was heated at 45 °C and found to be complete within 18 h. Chromatographic purification gave a clear oil (15 mg, 31%); ¹H NMR (400.13 MHz, CDCl₃) δ 7.50 (m, 2H), 7.40 (d, *J* = 16.0 Hz, 1H), 7.27 (m, 3H), 6.10 (d, *J* = 16.0 Hz, 1H), 1.24 (s, 12H); ¹³C{¹H} NMR (100.59 MHz, CDCl₃) δ 149.65, 137.64, 129.02, 128.71, 127.20, 83.49, 24.97 (the resonance for the carbon attached to the boron atom was not observed); ¹¹B NMR (128.38 MHz, CDCl₃) δ 30.13 (s, br); *m/z* (EI-MS) 230 (M⁺, 80%), 215 ([M – Me]⁺, 40%), 130 ([M – MeC(O)CMe₃]⁺, 100%).

Synthesis of 2-[2-(4-methoxy-phenyl)-vinyl]-4,4,5,5-tetramethyl-[1,3,2]dioxaborolane^{321g} (7b) *via* method A (0.2 mmol scale). The reaction with 4-vinyl anisole was heated at 45 °C and found to be complete within 18 h. Chromatographic purification gave a clear oil (15 mg, 28%); ¹H NMR (400.13 MHz, CDCl₃) δ 7.43 (d, *J* = 8.0 Hz, 2H), 7.36 (d, *J* = 16.0 Hz, 1H), 7.86 (d, *J* = 8.0 Hz, 2H), 6.04 (d, *J* = 16.0 Hz 1H), 3.82 (s, 3H), 1.30 (s, 12H); ¹³C{¹H} NMR (100.59 MHz, CDCl₃) δ 160.43, 149.18, 130.55, 126.59, 114.10, 83.33, 55.40, 26.95 (the resonance for the carbon attached to the boron atom was not observed); ¹¹B NMR (128.38 MHz, CDCl₃) δ 30.34 (s, br); *m/z* (EI-MS) 260 (M⁺, 100%), 245 ([M – Me]⁺, 15%), 160 ([M - MeC(O)CMe₃]⁺, 70%).

Synthesis of 4,4,5,5-tetramethyl-2-(2-phenyl-propenyl)-[1,3,2]dioxaborolane³²¹ⁱ (7c) *via* method A (0.2 mmol scale). The reaction with 2-phenyl propene was heated at 80 °C and found to be complete within 42 h. Chromatographic purification gave a clear oil (42 mg, 85 %); ¹H NMR (400.13 MHz, CDCl₃) δ 7.49 (m, 2H), 7.28 (m, 3H), 5.76 (s, 1H), 2.41 (s, 3H), 1.32 (s, 12H); ¹³C{¹H} NMR (100.59 MHz, CDCl₃) δ 157.93, 143.93, 128.28, 128.06, 125.95, 83.08, 25.04, 20.24 (the resonance for the carbon attached to the boron atom was not observed); ¹¹B NMR (128.38 MHz, CDCl₃) δ 30.15 (s, br); *m/z* (EI-MS) 244 (M⁺, 90%), 229 ([M – Me]⁺, 25%), 144 ([M - MeC(O)CMe₃]⁺, 100%, HRMS for C₁₅H₂₁BO₂ calcd: 244.1749, found: 244.1752.

Synthesis of 2-(2,2-diphenyl-vinyl)-4,4,5,5-tetramethyl-[1,3,2]dioxaborolane^{321i, 352} (**7d**) *via method A (0.2 mmol scale)*. The reaction with 2,2-diphenylethene was heated at 80 °C and found to be complete within 42 h. Chromatographic purification gave a clear oil (55 mg, 89%); ¹H NMR (400.13 MHz, CDCl₃) δ 7.33 (m, 4H), 7.28 (m, 6H), 6.00 (s, 1H), 1.16 (s, 12H); ¹³C{¹H} NMR (100.59 MHz, CDCl₃) δ 159.91, 143.22, 141.98, 129.97, 128.16, 128.122, 127.74, 127.67, 83.28, 24.75 (the resonance for the carbon attached to the boron atom was not observed); ¹¹B NMR (128.38 MHz, CDCl₃) δ 30.20 (s, br); *m/z* (EI-MS) 306 (M⁺, 50 %), 291 ([M – Me]⁺, 10%), 190 ([Ph₂CCHB]⁺, 100%).

Synthesis of 2-cyclohexylidenemethyl-4,4,5,5-tetramethyl-[1,3,2]dioxaborolane^{316b, 321i} (**7e**) *via method A (0.2 mmol scale)*. The reaction with methylene cyclohexane was performed at 80 °C and was found to be complete within 42 h. Chromatographic purification gave a clear oil (41 mg, 92%); ¹H NMR (400.13 MHz, CDCl₃) δ 5.00 (s, 1H), 2.50 (m, 2H) 2.18 (m, 2H) 1.57 (m, 6H), 1.24 (s, 12H); ¹³C{¹H} NMR (100.59 MHz, CDCl₃) δ 167.03, 82.65, 40.23, 33.34, 28.83, 28.59, 26.57, 24.96 (the resonance for the carbon attached to the boron atom was not observed); ¹¹B NMR (128.38 MHz, CDCl₃) δ 29.79 (s, br); *m/z* (EI-MS) 222 (M⁺, 10 %), 207 ([M - Me]⁺, 15%), 165 ([M - OCM₂]⁺) (100%), HRMS for C₁₃H₂₃¹⁰BO₂ calcd: 222.1906, found: 222.1899.

Synthesis of 2-cyclopentylidenemethyl-4,4,5,5-tetramethyl-[1,3,2]dioxaborolane^{316g, 321i} (**7f**) *via method A (0.2 mmol scale)*. The reaction with methylene cyclopentane was performed at 80 °C and was found to be complete within 42 h. Chromatographic purification gave a clear oil (30 mg, 73%) containing trace amounts of three isomeric products (**7f2-4**) and the hydroboration product (**7f5**), as determined by GC-MS; ¹H NMR (400 MHz, CDCl₃) δ 5.27 (t, *J* = 4.0 Hz, 1H), 2.52 (t, *J* = 7.0 Hz, 2H), 2.36 (t, *J* = 7.0 Hz, 2H), 1.73 – 1.59 (m, 4H), 1.25 (s, 12H); ¹³C{¹H} NMR (100.59 MHz, CDCl₃) δ 172.09, 82.68, 37.17, 33.43, 26.97, 26.03, 25.05 (the resonance for the carbon attached to the boron atom was not observed); ¹¹B NMR (128.38 MHz, CDCl₃) δ 29.74 (s, br); *m/z* (EI-MS) 208 (M⁺, 10 %), 193 ([M - Me]⁺, 15%), 151 ([M - OCM₂]⁺) (100%).

Synthesis of 2-(1H-inden-2-yl)-4,4,5,5-tetramethyl-[1,3,2]dioxaborolane ^{32011, 337} (**7g**) *via a modification of method A (0.4 mmol scale)*. The reaction with indene was performed in MTBE (2 mL) at 80 °C and was found to be complete within 42 h. Chromatographic purification gave an off-white solid (67 mg, 70%); mp 67–69 °C (lit²⁸ 73–74 °C); ¹H NMR (400.13 MHz, CDCl₃) δ 7.85 (d, *J* = 7.5 Hz, 1H), 7.47 (d, *J* = 7.5 Hz, 1H), 7.27 (m overlapped, 2H), 7.21 (t, *J* = 7.5 Hz, 1H), 3.47 (s, 2H), 1.36 (s, 12H); ¹³C{¹H} NMR (100.59 MHz, CDCl₃) δ 149.14, 146.93, 143.95, 126.32, 124.40, 123.54, 122.87, 83.64, 40.75, 25.05 (the resonance for the carbon attached to the boron atom was not observed); ¹¹B NMR (128.38 MHz, CDCl₃) δ 29.47 (s, br); *m/z* (EI-MS) 242 (M⁺, 80%), 227 ([M – Me]⁺, 20%), 142 ([indenyl-B-O]⁺, 100%).

Synthesis of 2-(4-fluoro-phenyl)-1H-indene³⁵³ (**8a**) (0.4 mmol scale). The synthesis of **7g** was performed as above. Once the consumption of the starting materials had been confirmed by GC-MS analysis, the reaction vessel was transferred to a dry, N₂ filled glovebox and opened. 4-Fluoro-1-iodobenzene (75 mg, 0.34 mmol, 0.85 equiv w.r.t, **7g**), Pd(dppf)Cl₂·CH₂Cl₂ (10 mg, 0.012 mmol), K₃PO₄·2H₂O (198 mg, 0.8 mmol) and degassed H₂O (0.5 mL) were added, the vessel was sealed and heated at 80 °C until analysis by *in situ* GC-MS showed the reaction to be complete (3 h). The reaction mixture was diluted in CH₂Cl₂ (20 mL) and washed with H₂O (3 x 20 mL), the organic layer was dried (MgSO₄), filtered and the solvent removed *in vacuo* to give a crude product that was purified by silica gel chromatography (hexanes to 1:1 CH₂Cl₂/hexanes, gradient elution) to give the product as a off-white solid (59 mg, 83% w.r.t, aryl iodide); mp 155–156 °C; ¹H NMR (400 MHz, CDCl₃) δ 7.64 – 7.56 (m, 2H), 7.47 (d, *J* = 7.5 Hz, 1H), 7.40 (d, *J* = 7.5 Hz, 1H), 7.28 (t, *J* = 7.5 Hz, 1H), 7.19 (td, *J* = 7.5, 1.0 Hz, 1H), 7.16 (s, 1H), 7.11 – 7.03 (m, 2H), 3.77 (s, 2H); ¹³C NMR (101 MHz, CDCl₃) δ 163.69, 161.23, 145.45, 143.12, 132.47, 132.43, 127.39, 127.31, 126.84, 126.43, 126.41, 124.94, 123.80, 121.11, 115.87, 115.65, 77.48, 77.16, 76.84, 39.30; ¹⁹F NMR (376 MHz, CDCl₃) δ -114.77 to -114.81 (m); *m/z* (EI-MS) 210 (M⁺, 100%), 191 ([M – F]⁺, 10%).

Synthesis of 4-(1H-inden-2-yl)-benzoic acid methyl ester (8b) (0.4 mmol scale). The synthesis of **7g** was performed as above. Once the consumption of the starting materials

had been confirmed by GC-MS analysis, the reaction vessel was transferred to a dry, N₂ filled glovebox and opened. 4-Iodomethylbenzoate (89 mg, 0.34 mmol, 0.85 equiv w.r.t, **7g**), Pd(dppf)Cl₂·CH₂Cl₂ (10 mg, 0.012 mmol), K₃PO₄·2H₂O (198 mg, 0.8 mmol) and degassed H₂O (0.5 mL) were added, the vessel was sealed and heated at 80 °C until analysis by *in situ* GC-MS showed the reaction to be complete (3 h). The reaction mixture was diluted in CH₂Cl₂ (20 mL) and washed with H₂O (3 x 20 mL), the organic layer was dried (MgSO₄), filtered and the solvent removed *in vacuo* to give a crude product that was purified by silica gel chromatography (hexanes to 1:1 CH₂Cl₂/hexanes, gradient elution) to give the product as a white solid (66 mg, 78% w.r.t, aryl iodide); mp 191-192 °C; IR (solid) 2357, 2327, 2060, 1952, 1711 ($\nu_{C=O}$), 1425, 1275, 1175, 1098; ¹H NMR (400.13 MHz, CDCl₃) δ 8.04 (d, J = 9.0 Hz, 2H), 7.69 (d, J = 9.0 Hz, 2H), 7.50 (d, J = 7.5 Hz, 1H), 7.44 (d, J = 7.5 Hz, 1H), 7.36 (s, 1H), 7.30 (t, J = 7.5 Hz, 1H), 7.23 (dt, J = 7.5, 1.0 Hz, 1H), 3.93 (s, 3H), 3.82 (s, 2H); ¹³C{¹H} NMR (100.59 MHz, CDCl₃) δ 167.00, 145.30, 145.04, 143.52, 140.43, 130.18, 129.19, 128.90, 126.95, 125.61, 125.53, 123.94, 121.64, 52.22, 39.10; m/z (EI-MS) 250 (M⁺, 100%), 219 ([M⁺ - MeO], 35%); HRMS for C₁₇H₁₈O₂ calcd: 251.1072, found: 251.1066.

Formation of [Rh(PPh₃)₂(μ -CO)]₂ **9 from *trans*-[Rh(PPh₃)₂(CO)OOCH] **4** and B₂pin₂.** *Trans*-[Rh(PPh₃)₂(CO)OOCH] **4** (40 mg, 0.057 mmol) and B₂pin₂ (145 mg, 0.57 mmol) were dissolved in C₆D₆ (1 mL). A colour change from yellow to dark red was observed within 5 minutes. Analysis by ³¹P{¹H} NMR spectroscopy after four hours showed the complete consumption of **4** and the formation of **9** (δ 37.75, dd, J_{Rh-P} = 196 Hz, $J_{Rh-Rh-P}$ = 12 Hz) along with a broad doublet (δ 30.5 ppm, J_{Rh-P} = 120 Hz). Analysis of the reaction at 18 hours showed no additional change in the ³¹P{¹H} NMR spectrum.

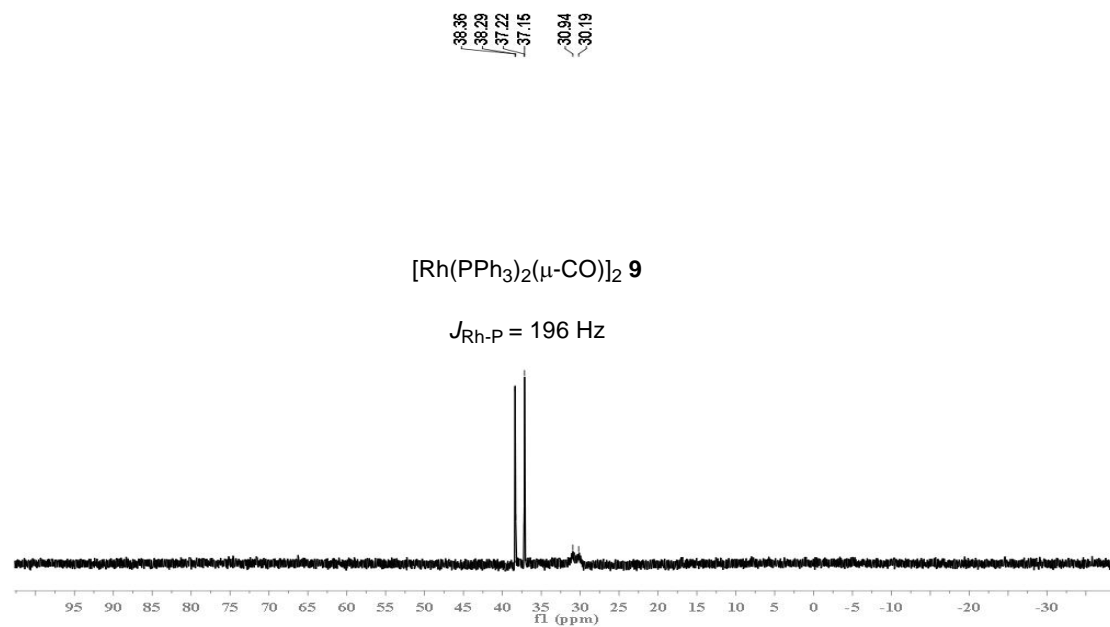


Figure 4.3 162 MHz $^{31}\text{P}\{^1\text{H}\}$ NMR spectrum of the reaction of **4** and B_2pin_2 (10 equiv) in C_6D_6 after 4 h at 20 °C.

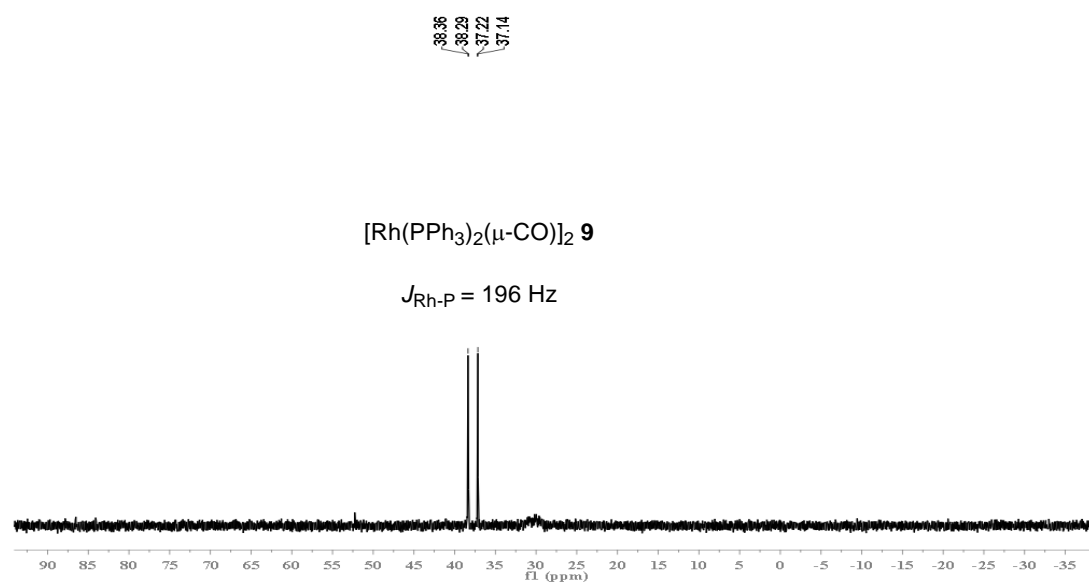


Figure 4.4 162 MHz $^{31}\text{P}\{^1\text{H}\}$ NMR spectrum of the reaction of **4** and B_2pin_2 (10 equiv) in C_6D_6 after 18 h at 20 °C.

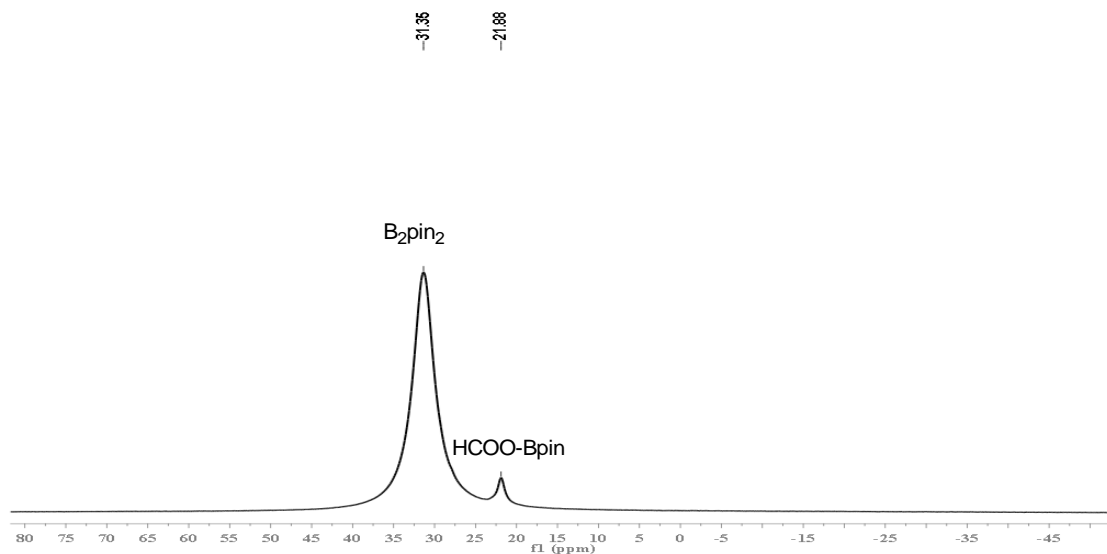


Figure 4.5 128 MHz ^{11}B NMR spectrum of the reaction of **4** and B_2pin_2 (10 equiv.) in C_6D_6 after 18 h at 20 °C.

Formation of $[\text{Rh}(\text{PPh}_3)_2(\mu\text{-CO})]_2$ **9 from $\text{HRh}(\text{PPh}_3)_3\text{CO}$ **6** and B_2pin_2 .** $\text{HRh}(\text{PPh}_3)_3\text{CO}$ **6** (26 mg, 0.03 mmol) and B_2pin_2 (73 mg, 0.29 mmol) were dissolved in C_6D_6 (0.5 mL). A slow colour change from yellow to dark orange was observed within ~1 hour. The mixture was analysed after 18 h at 20 °C by $^{31}\text{P}\{^1\text{H}\}$ NMR spectroscopy, showing partial consumption of **6** and the formation of **9** (δ 37.75, d, $J_{\text{Rh-P}} = 196$ Hz). Analysis by ^{11}B NMR spectroscopy showed the formation of HBpin (δ 28.1, d, $J_{\text{H-B}} = 173$ Hz).

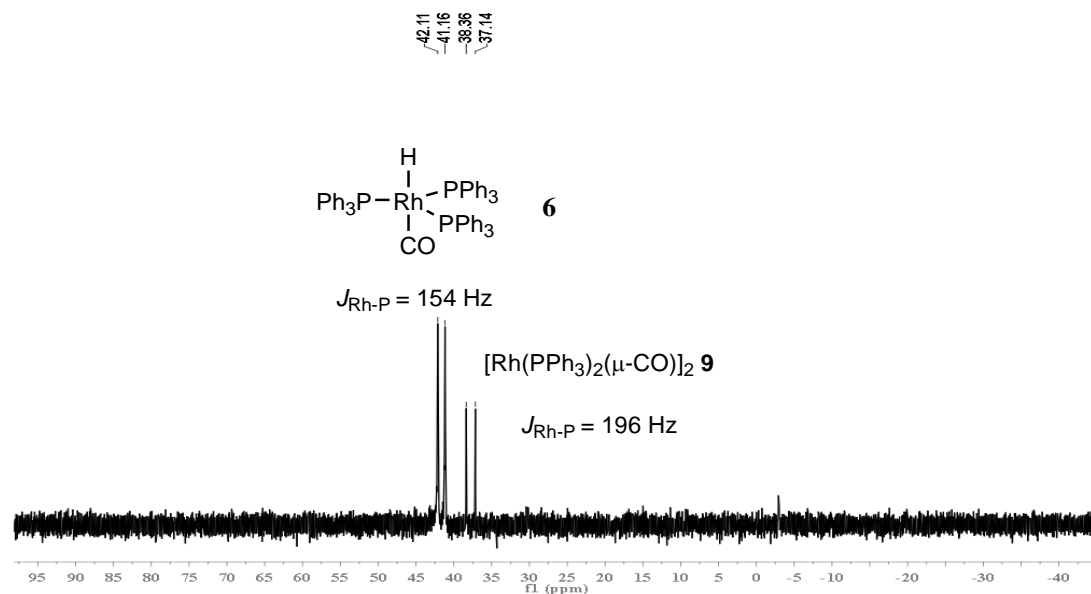


Figure 4.6 162 MHz $^{31}\text{P}\{^1\text{H}\}$ NMR spectrum of the reaction of **6** and B_2pin_2 (10 equiv.) in C_6D_6 after 18 h at 20 °C.

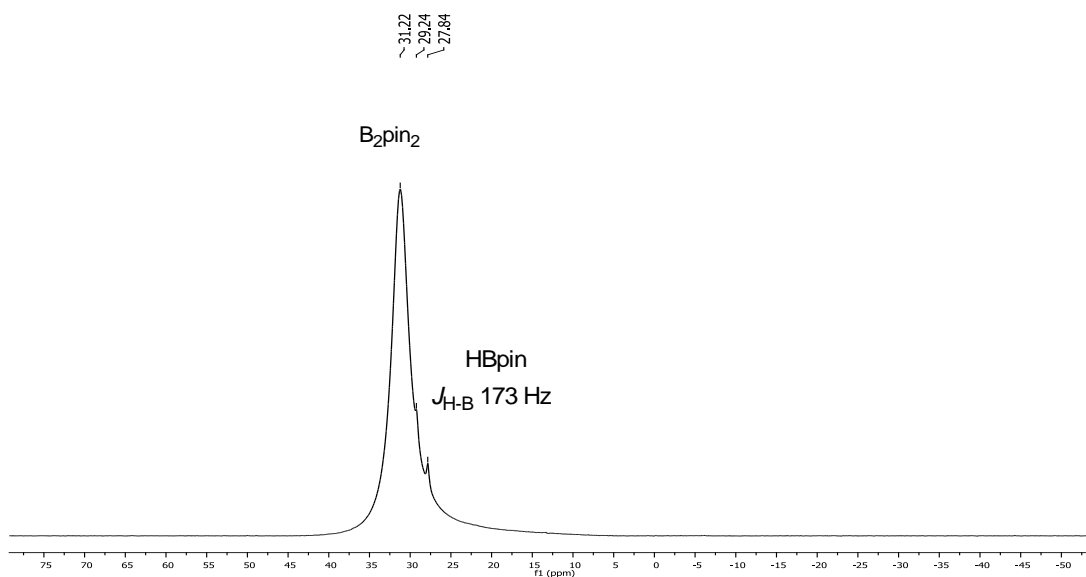


Figure 4.7 128 MHz ^{11}B NMR spectrum of the reaction of **6** and B_2pin_2 (10 equiv.) in C_6D_6 after 18 h at 20 °C.

Reaction of 9 with pinacolborane (HBpin). *Trans*- $[\text{Rh}(\text{PPh}_3)_2(\text{CO})\text{OOCH}]$ **4** (40 mg, 0.057 mmol) and B_2pin_2 (145 mg, 0.57 mmol) were dissolved in C_6D_6 (1 mL), the solution was left for 18 h at 20 °C, at which time analysis by $^{31}\text{P}\{^1\text{H}\}$ NMR spectroscopy showed the complete conversion of **4** into **9**. Pinacolborane (82 μL , 0.57 mmol) was

added. After 18 hours at 20 °C, the mixture was analysed by $^{31}\text{P}\{^1\text{H}\}$ and ^{11}B NMR spectroscopy.

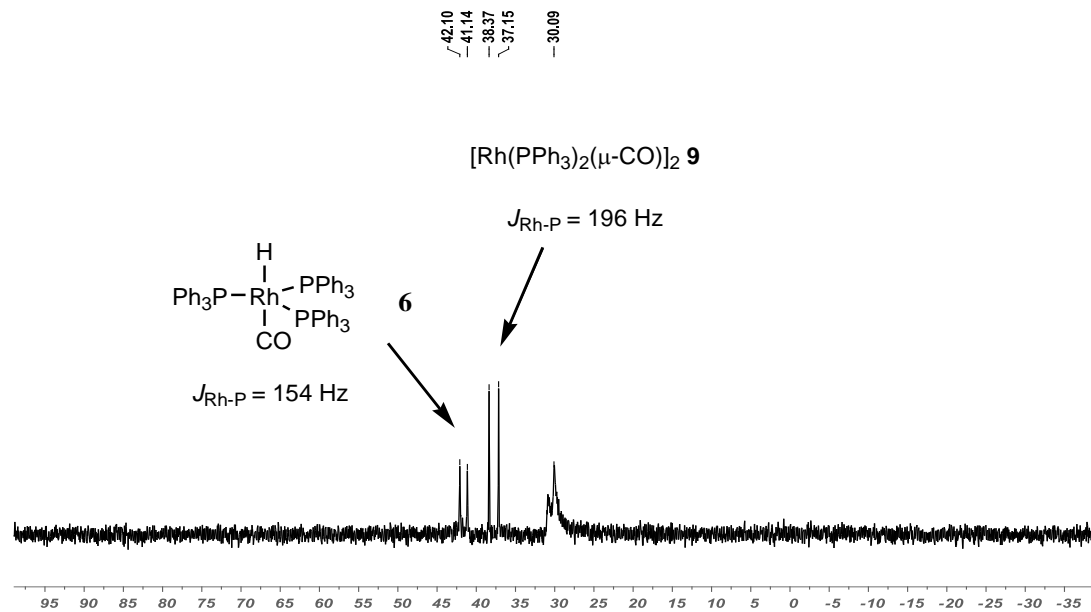


Figure 4.8 162 MHz $^{31}\text{P}\{^1\text{H}\}$ NMR spectrum of the reaction of HBpin with **9** and B₂pin₂ in C₆D₆ after 18 h at 20 °C.

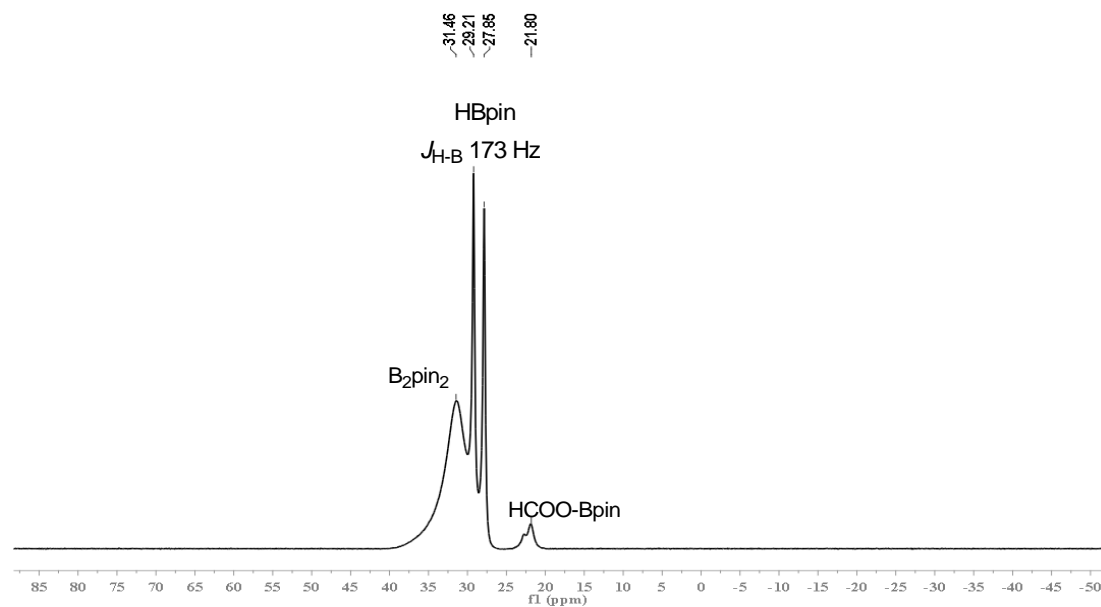


Figure 4.9 128 MHz ^{11}B NMR spectrum of the reaction of HBpin with **9** and B₂pin₂ in C₆D₆ after 18 h at 20 °C.

Dehydrogenative borylation of 2-phenylpropene in the presence of 5 mol % 9. *Trans*-[Rh(PPh₃)₂(CO)OOCH] **4** (40 mg, 0.057 mmol) and B₂pin₂ (145 mg, 0.57 mmol) were dissolved in C₆D₆ (1 mL), the solution was left for 18 h at 20 °C, at which time analysis by ³¹P{¹H} NMR spectroscopy showed the complete conversion of **4** into **9**. 2-phenylpropene (60 μL, 0.57 mmol) was added. After 18 hours at 20 °C, the mixture was analysed by ³¹P{¹H} and ¹¹B NMR spectroscopy and by GC-MS and the reaction was found to be 50% complete by GC-MS.

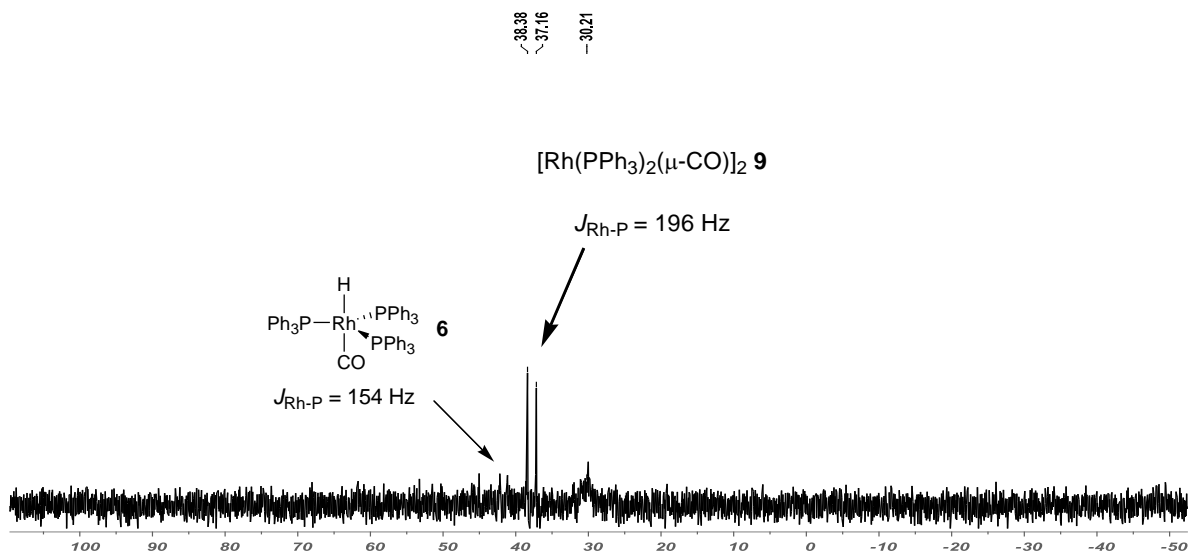


Figure 4.10 162 MHz ³¹P{¹H} NMR spectrum of the reaction of 2-phenylpropene with **9** and B₂pin₂ in C₆D₆ after 18 h at 20 °C.

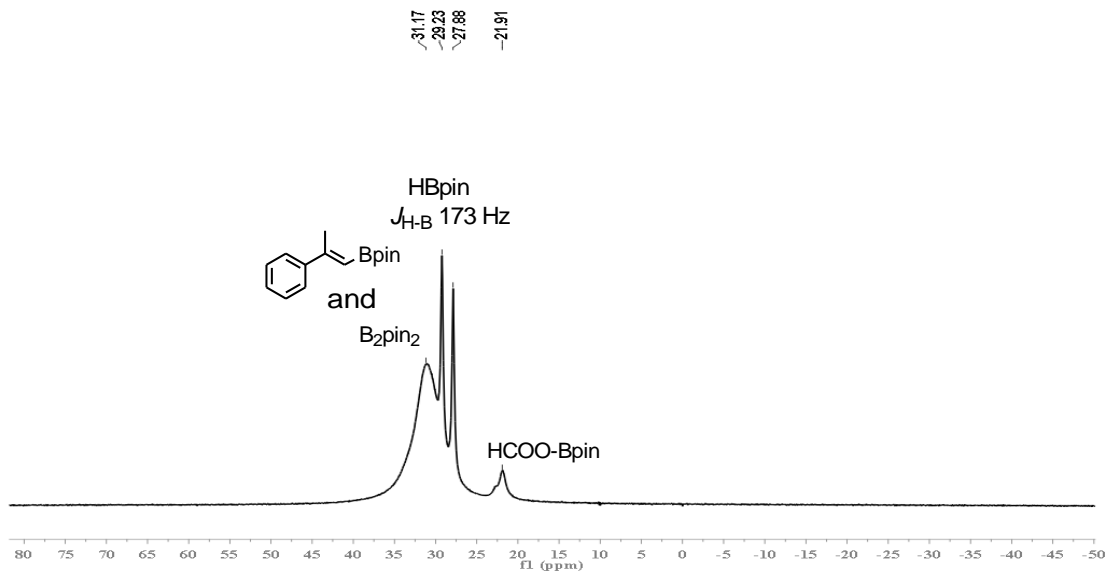


Figure 4.11 128 MHz ^{11}B NMR spectrum of the reaction of 2-phenylpropene with **9** and B₂pin₂ in C₆D₆ after 18 h at 20 °C.

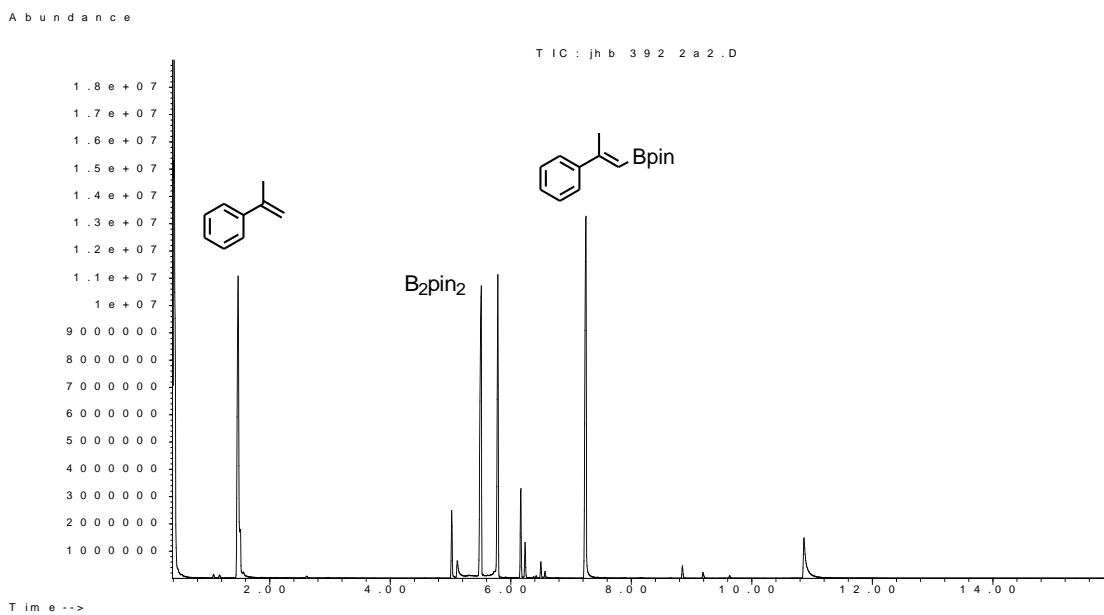


Figure 4.12 GC (TIC) of the reaction of 2-phenylpropene with **9** and B₂pin₂ in C₆D₆ after 18 h at 20 °C.

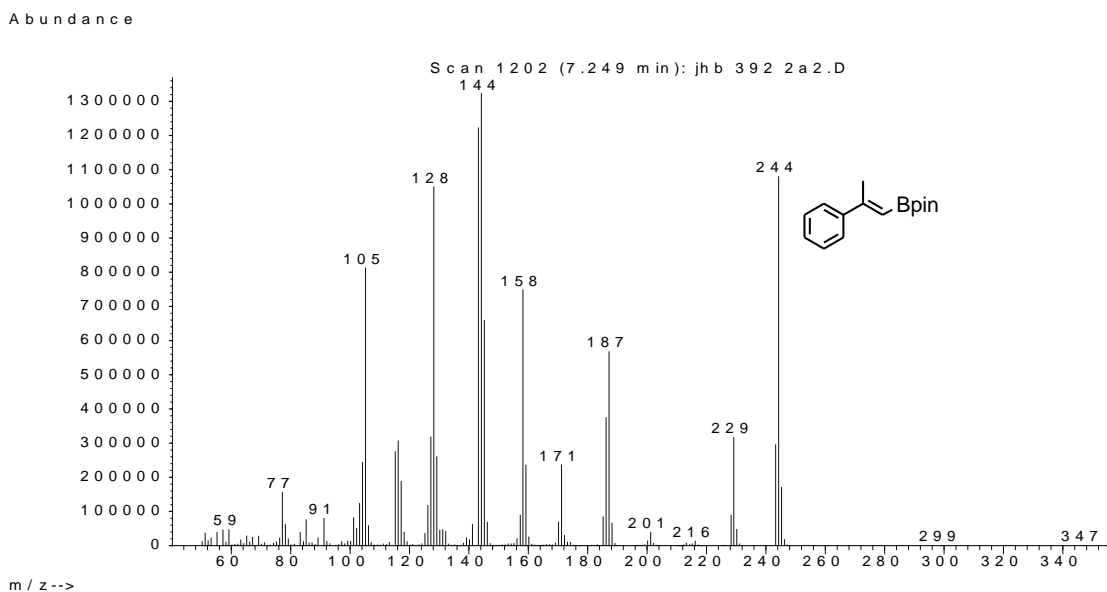


Figure 4.13 EI-MS of the peak at 7.3 minutes for the reaction of 2-phenylpropene with **9** and B₂pin₂ in C₆D₆ after 18 h at 20 °C.

The reaction was analysed further by ³¹P{¹H} and ¹¹B NMR spectroscopy after the borylation reaction was complete, as determined by *in situ* ¹H NMR spectroscopy (3 d). The broad peak at 30.5 ppm was now the major phosphorus-containing species present in solution, suggesting that in the absence of substrate catalyst breakdown occurs.

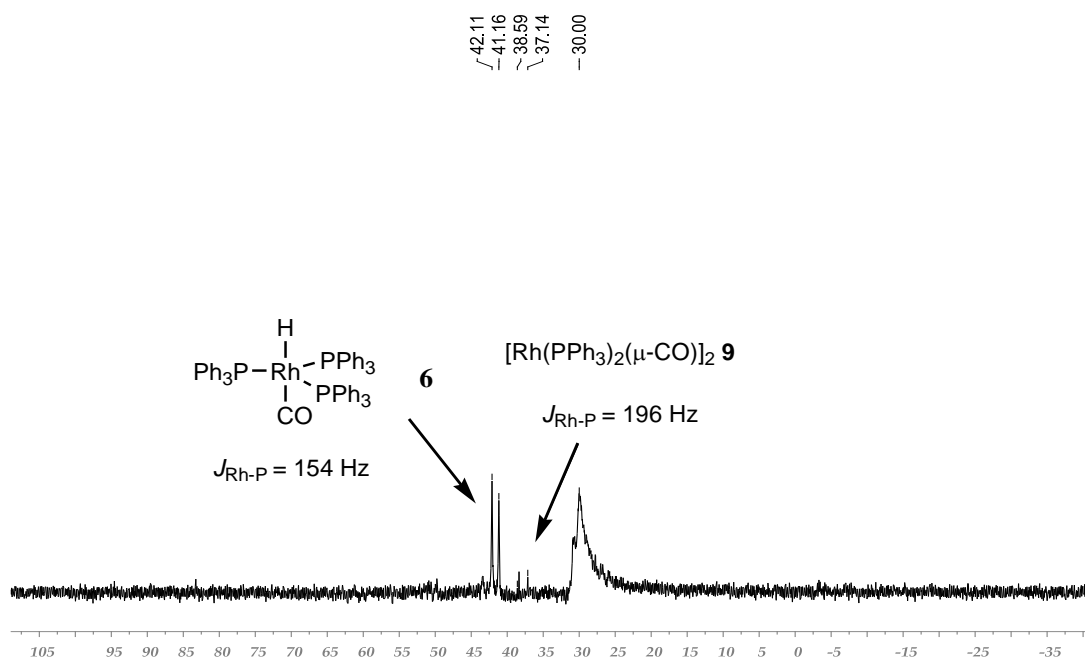


Figure 4.14 162 MHz $^{31}\text{P}\{^1\text{H}\}$ NMR spectrum of the reaction of 2-phenylpropene with **9** and B_2pin_2 in C_6D_6 after 3 d at 20 °C.

Dehydrogenative borylation of 2-phenylpropene in the presence of 10 mol % 6. A solution of $\text{HRh}(\text{PPh}_3)_3\text{CO}$ **6** (26 mg, 0.029 mmol) and B_2pin_2 (70 mg, 0.29 mmol) and 2-phenylpropene (30 μL , 0.29 mmol) in C_6D_6 (0.5 mL) was prepared. After 18 hours at 20 °C, the mixture was analysed by $^{31}\text{P}\{^1\text{H}\}$ and ^{11}B NMR spectroscopy and by GC-MS and the reaction was found to be 65% complete by GC-MS.

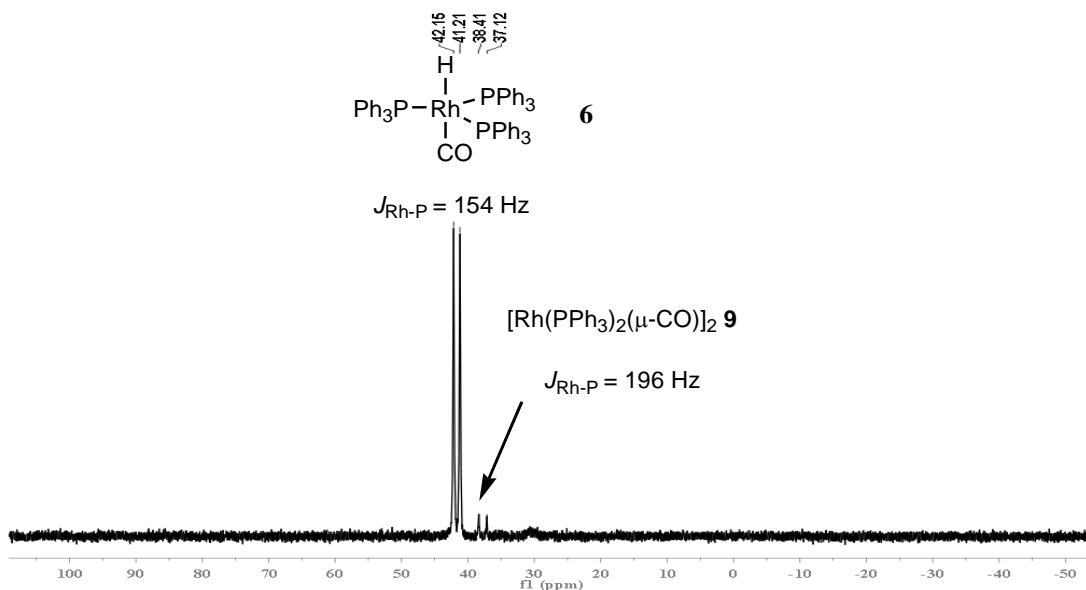


Figure 4.15 162 MHz $^{31}\text{P}\{^1\text{H}\}$ NMR spectrum of the reaction of 2-phenylpropene with **6** and B_2pin_2 in C_6D_6 after 18 h at 20 °C.

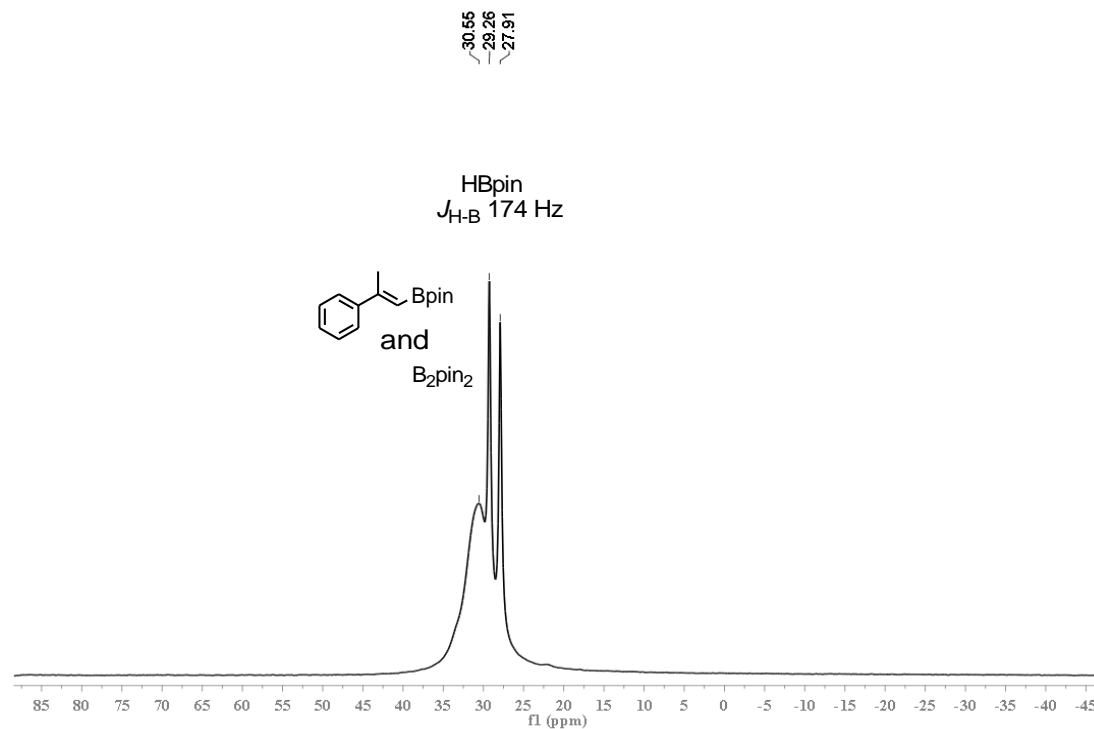


Figure 4.16 128 MHz ^{11}B NMR spectrum of the reaction of 2-phenylpropene with **6** and B_2pin_2 in C_6D_6 after 18 h at 20 °C.

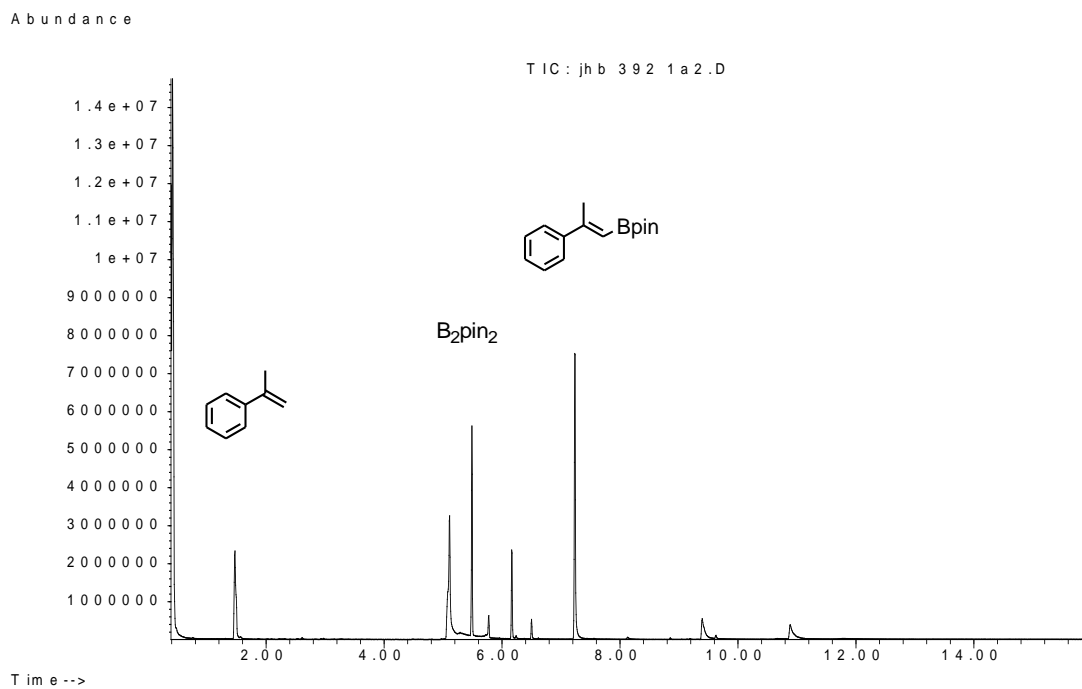


Figure 4.17 GC (TIC) of the reaction of 2-phenylpropene with **6** and B_2pin_2 in C_6D_6 after 18 h at 20 °C.

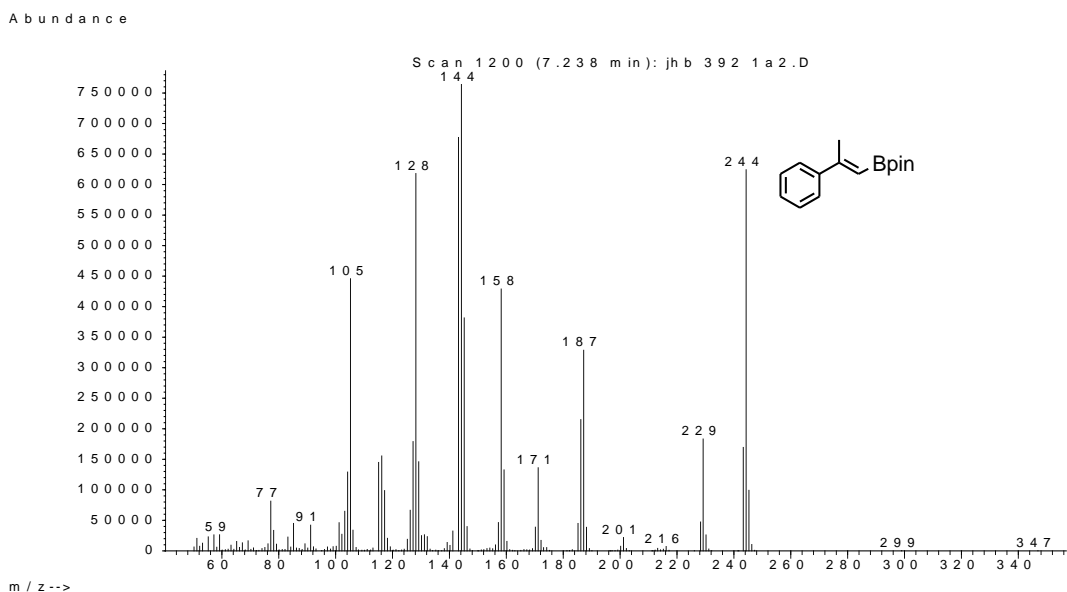


Figure 4.18 EI-MS of the peak at 7.3 minutes for the reaction of 2-phenylpropene with **6** and B₂pin₂ in C₆D₆ after 18 h at 20 °C.

Synthesis of *trans*-[Rh(PPh₃)₂(CO)O₂CPh] **5 and related data.** The compound was synthesised by the method of Robinson *et al.*³⁵⁴ In a dry, N₂ filled glovebox HRh(PPh₃)₃CO (200 mg, 0.21 mmol) and benzoic acid (500 mg, 4.1 mmol) were added to a thick walled glass tube fitted with a Young's tap. Degassed ethanol (10 mL) was added, the vessel was sealed and heated under reflux for 30 mins. The mixture was cooled and the precipitate was filtered under N₂. The crude solid was recrystallised from EtOH/DCM at -20 °C and dried *in vacuo* to give the product as a bright yellow solid; yield 107 mg, 62%; ¹H NMR (400 MHz, C₆D₆) δ 7.95 (m, 14H), 7.00 (m, 21H); ³¹P{¹H} NMR (162 MHz, C₆D₆) δ 32.91 (d, *J*_{Rh-P} = 136 Hz); IR (solid) 1958 (ν_{CO}), 1816 (ν_{asym}OCO), 1352 (ν_{sym}OCO); elemental anal. Calcd for C₄₄H₃₅O₃P₂Rh·CH₃OH: C, 66.84; H, 4.86, found C, 65.71; H, 4.47.

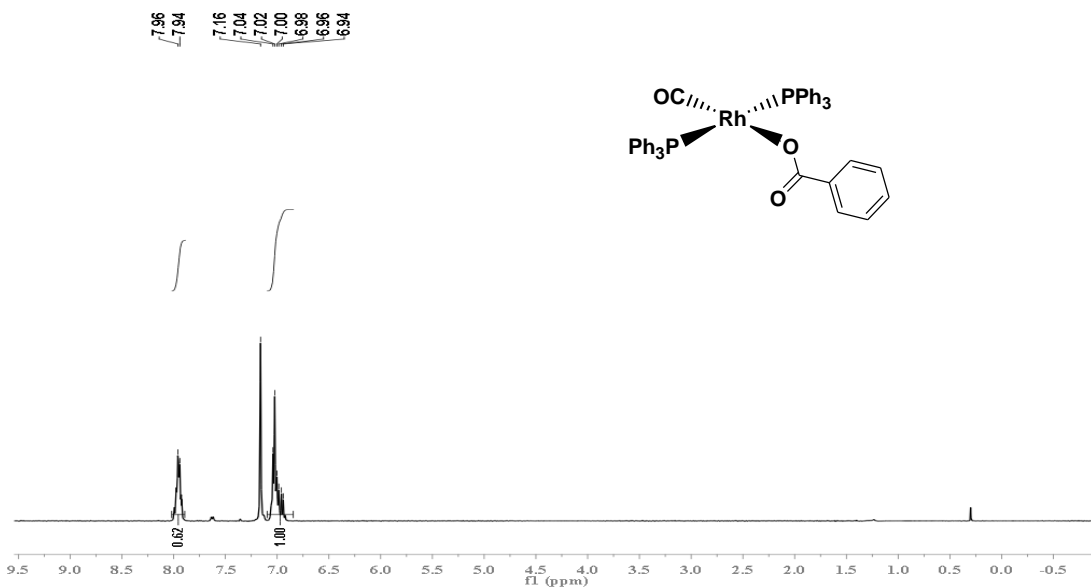


Figure 4.19 400 MHz ^1H NMR spectrum of compound **5** in C_6D_6 .

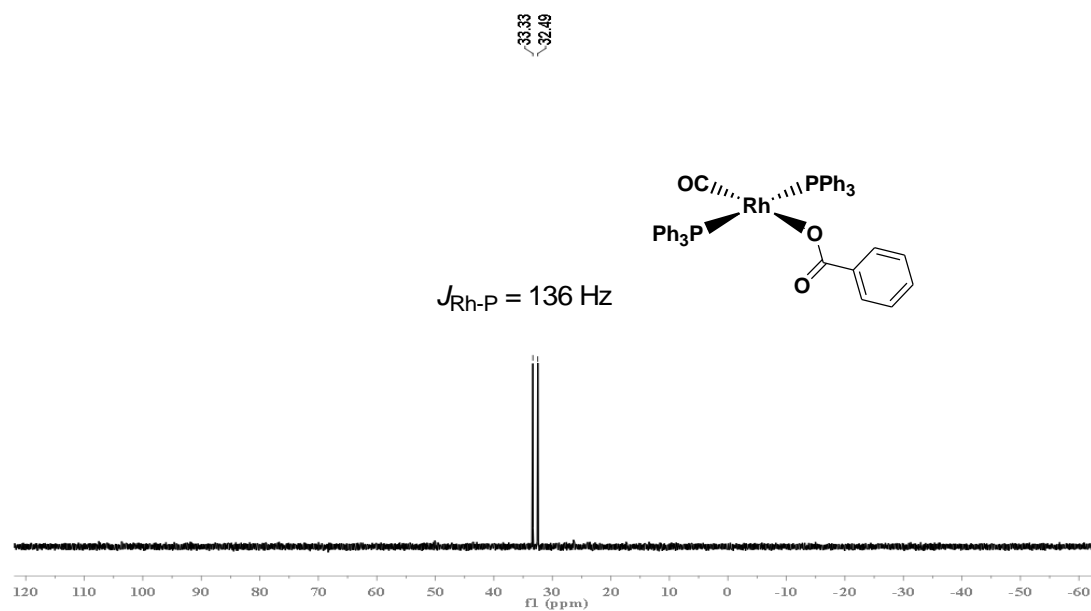


Figure 4.20 162 MHz $^{31}\text{P}\{^1\text{H}\}$ NMR spectrum of compound **5** in C_6D_6 .

Triclinic single crystals ($P\bar{1}$) of compound **5** were grown from a solution in a 1:1 mixture of MeOH/DCM at $-20\text{ }^\circ\text{C}$. Compound **5** was characterised by a single-crystal X-ray structure determination.³⁵⁵

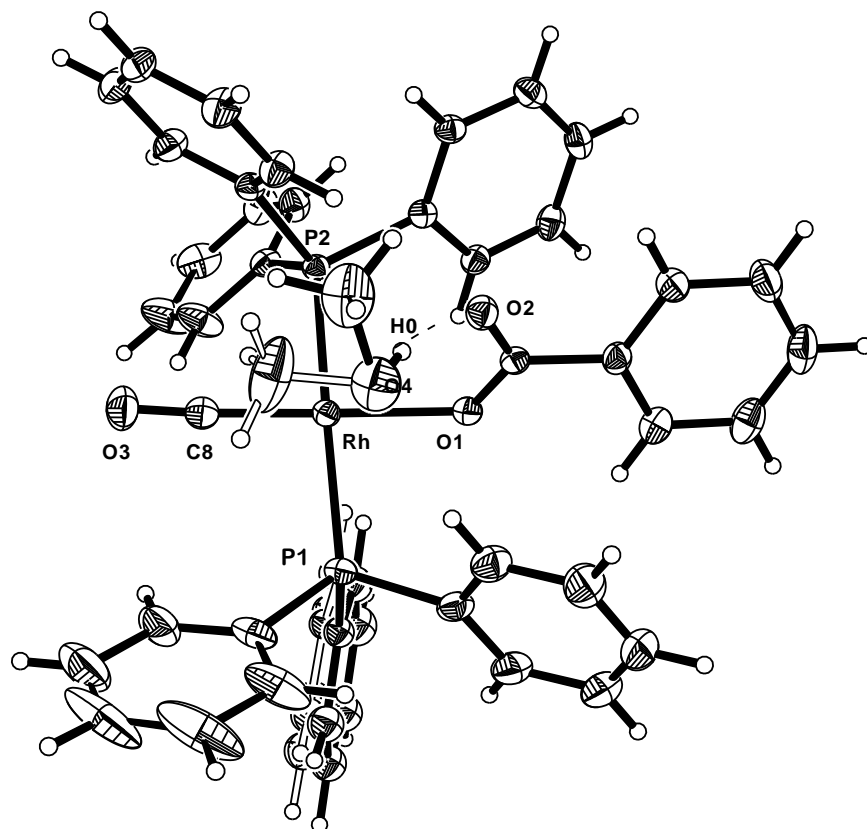


Figure 4.21 X-ray molecular structure of *trans*-[Rh(PPh₃)₂(CO)(O₂CPh)]·MeOH (**5**), showing thermal ellipsoids at the 50% probability level and the disorder of the methanol molecule and the PPh₃ phenyl ring.

The rhodium atom adopts a square-planar coordination geometry with a slight tetrahedral distortion. The benzoate ligand is monodentate, the un-coordinated oxygen atom accepting a hydrogen bond from the disordered methanol molecule of crystallization. The carboxylate plane is inclined by 68° to the mean coordination plane of Rh and by 19° to the adjacent phenyl ring. Bond distances (Å) and angles (°): Rh–P(1) 2.3377(6), Rh–P(2) 2.3216(6), Rh–O(1) 2.066(1), Rh–C(8) 1.808(2), O(1)–C(7) 1.284(2), O(2)–C(7) 1.245(2), P(1)–Rh–P(2) 170.26(2), O(1)–Rh–C(8) 176.93(6), Rh–O(1)–C(7) 117.9(1). Bond distances are similar to those in *trans*-[Rh(PPh₃)₂(CO)(O₂CR)] analogues, where R = H (compound **4**),³⁴⁴ Me³⁵⁶ and CF₃.³⁵⁷

References for Chapter 4

Synthesis of vinyl boronate esters

- ³¹⁰ *Boronic Acids*; Hall, D. G., Ed.; Wiley-VCH: Weinheim, Germany, 2005
- ³¹¹ Brown, H. C.; Bhat, N. G. *Tetrahedron Lett.* **1988**, *29*, 21-24.
- ³¹² Takagi, J.; Takahashi, K.; Ishiyama, T.; Miyaura, N. *J. Am. Chem. Soc.* **2002**, *124*, 8001-8006.
- ³¹³ Cole, T. E.; Quintanilla, R.; Rodewald, S. *Organometallics* **1991**, *10*, 3777-3781.
- ³¹⁴ Deloux, L.; Skrzypczak-Jankun, E.; Cheesman, B. V.; Srebnik, M.; Sabat, M., *J. Am. Chem. Soc.* **1994**, *116*, 10302-10303.
- ³¹⁵ (a) Blackwell, H. E.; O'Leary, D. J.; Chatterjee, A. K.; Washenfelder, R. A.; Busmann, D. A.; Grubbs, R. H. *J. Am. Chem. Soc.* **2000**, *122*, 58-71; (b) Morrill, C.; Grubbs, R. H. *J. Org. Chem.* **2003**, *68*, 6031-6034; (c) Morrill, C.; Funk, T. W.; Grubbs, R. H. *Tetrahedron Lett.* **2004**, *45*, 7733-7736; (d) Funk, T. W.; Efskind, J.; Grubbs, R. H. *Org. Lett.* **2005**, *7*, 187-190; (e) Jankowska, M.; Pietraszuk, C.; Marciniak, B.; Zaidlewicz, M. *Synlett* **2006**, 1695.
- ³¹⁶ Srebnik, M.; Bhat, N. G.; Brown, H. C. *Tetrahedron Lett.* **1988**, *29*, 2635-2938.
- ³¹⁷ Marciniak, B.; Jankowska, M.; Pietraszuk, C. *Chem. Commun.* **2005**, 663-665.
- ³¹⁸ (a) Brown, H. C.; Gupta, S. K. *J. Am. Chem. Soc.* **1974**, *97*, 5249-5255; (b) Lee, J.-E.; Kwon, J.; Yun, J. *Chem. Commun.* **2008**, 33-734.
- ³¹⁹ (a) Ishiyama, T.; Matsuda, N.; Miyaura, N.; Suzuki, A. *J. Am. Chem. Soc.* **1993**, *115*, 11018-11019; (b) Ishiyama, T.; Matsuda, N.; Murata, M.; Ozawa, F.; Suzuki, A.; Miyaura, N. *Organometallics* **1996**, *15*, 713-720; (c) Ishiyama, T., Miyaura, N. *J. Organomet. Chem.* **2000**, *611*, 392-402; (d) Miyaura, N. *Bull. Chem. Soc. Jpn.* **2008**, *81*, 1535-1553; (e) Ishiyama, T., Miyaura, N. *Chem. Rev.* **2004**, *3*, 271-280; (f) Lesley, G.; Nguyen, P.; Taylor, N. J.; Marder, T. B.; Scott, A. J.; Clegg, W.; Norman, N. C. *Organometallics* **1996**, *15*, 5137-5154; (g) Thomas, R. Ll.; Souza, F. E. S.; Marder, T. B., *Dalton Trans.* **2001**, 1650-1656; (h) Marder, T. B.; Norman, N. C. *Top. Catal.* **1998**, *5*, 63-73; (i) Iverson, C. N.; Smith, M. R. III *Organometallics* **1996**, *15*, 5155-5165; (j) Smith, M. R. III *Prog. Inorg. Chem.* **1999**, *48*, 505-567; (k) Abu Ali, H.; El Aziz Al Qunter, A.; Goldberg, I.; Srebnik, M. *Organometallics* **2002**, *21*, 4433-4539; (l) Dembitsky, V. M.; Abu Ali, H.; Srebnik, M. *Appl. Organomet. Chem.* **2003**, *17*, 327-

345; (m) Dembitsky, V. M.; Abu Ali, H.; Srebnik, M. *Adv. Organomet. Chem.* **2004**, *51*, 193-250.

³²⁰ **Dehydrogenative alkene borylation**

Rhodium (a) Baker, R. T.; Nguyen, P.; Marder, T. B.; Westcott, S. A. *Angew. Chem. Int. Ed.* **1995**, *34*, 1336-1338; (b) Westcott, S. A.; Marder, T. B.; Baker, R. T. *Organometallics* **1993**, *12*, 975-979; (c) **Burgess**, K.; van der Donk, W. A.; Westcott, S. A.; **Marder**, T. B.; Baker, R. T.; Calabrese, J. C. **J. Am. Chem. Soc.** **1992**, *114*, 9350-9359; (d) Brown, J. M.; Lloyd-Jones, G. C., *Chem. Commun.* **1992**, 710-712; (e) Brown, J. M.; Lloyd-Jones, G. C., *J. Am. Chem. Soc.* **1994**, *116*, 866-878; (f) Murata, M.; Watanabe, S.; Masuda, Y. *Tetrahedron Lett.* **1999**, *40*, 2585-2588; (g) Murata, M.; Kawakita, K.; Asana, T.; Watanabe, S.; Masuda, Y. *Bull. Chem. Soc. Jpn.* **2002**, *75*, 825-829; (h) Vogels, C. M.; Hayes, P. G.; Shaver, M. P.; Westcott, S. A. *Chem. Commun.* **2000**, 51-52; (i) Geier, S. J.; Chapman, E. E.; McIsaac, D. I.; Vogels, C. M.; Decken, A.; Westcott, S. A. *Inorg. Chem. Commun.* **2006**, *9*, 788-791; (j) Garon, C. N.; McIsaac, D. I.; Vogels, C. M.; Decken, A.; Williams, I. D.; Kleeburg, C.; Marder, T. B.; Westcott, S. A. *Dalton Trans.* **2009**, 1624-1631; (k) Coapes, R. B.; Souza, F. E. S.; Thomas, R. L.; Hall, J. J.; Marder, T. B. *Chem. Commun.* **2003**, 614-615; (l) Mkhaliid, I. A. I.; Coapes, R. B.; Edes, S. N.; Coventry, D. N.; Souza, F. E. S.; Thomas, R. L.; Hall, J. J.; Bi, S.-W.; Lin, Z.; Marder, T. B. *Dalton Trans.* **2008**, 1055-1064; (m) Kondoh, A.; Jamison, T. F. *Chem. Commun.* **2010**, *46*, 907-909; **Ruthenium** (n) Montiel-Parma, V.; Lumbierres, M.; Donnadiou, B.; Sabo-Etienne, S.; Chaudret, B. *J. Am. Chem. Soc.* **2002**, *124*, 5624-5625; (o) Caballero, A.; Sabo-Etienne, S. *Organometallics* **2007**, *26*, 1191-1195; **Iridium** (p) Olsson, V. J.; Szabó, K. J. *Angew. Chem. Int. Ed.* **2007**, *46*, 6891-6893; (i) Olsson, V. J.; Szabó, K. J. *Org. Lett.* **2008**, *10*, 3129-3131; (q) Olsson, V. J.; Szabó, K. J. *J. Org. Chem.* **2009**, *74*, 7715-7723; **Titanium** (r) Motry, D. H.; Smith, M. R. III *J. Am. Chem. Soc.* **1995**, *117*, 6615-6616; (s) Motry, D. H.; Brazil, A. G.; Smith, M. R. III *J. Am. Chem. Soc.* **1997**, *119*, 2743-2744; **Platinum** (t) Ohmura, T.; Takasaki, Y.; Furukawa, H.; Suginome, M. *Angew. Chem. Int. Ed.* **2009**, *48*, 2372-2375; **Direct C-H oxidative addition with Iridium** (u) Kikuchi, T.; Takagi, J.; Ishiyama, T.; Miyaura, N. *Chem. Lett.*

2008, 37, 664-665; (v) Kikuchi, T.; Takagi, J.; Isou, H.; Ishiyama, T.; Miyaura, N. *Chem. Asian J.* **2008**, 3, 2082-2090.

³²¹ Barnard, J. H.; Mkhaliid, I. A. I.; Bridgens, C. E.; Batsanov, A. S.; Howard, J. A. K.; Przyborski, S. A.; Whiting, A.; Marder T. B. in preparation

³²² (a) Irvine, G. J.; Lesley, M. J. G.; Marder, T. B.; Norman, N. C.; Rice, C. R.; Robins, E. G.; Roper, W. R.; Whittell, G. R.; Wright, L. J. *Chem. Rev.* **1998**, 98, 2685-2722; (b) Nguyen, P.; Lesley, G.; Taylor, N. J.; Marder, T. B.; Pickett, N. L.; Clegg, W.; Elsegood, M. R. J.; Norman, N. C. *Inorg. Chem.* **1994**, 33, 4623-4624; (c) Marder, T. B.; Norman, N. C.; Rice, C. R.; Robins, E. G. *Chem. Commun.* **1997**, 53-54; (d) Clegg, W.; Lawlor, F. J.; Marder, T. B.; Nguyen, P.; Norman, N. C.; Orpen, A. G.; Quayle, M. J.; Rice, C. R.; Robins, E. G.; Scott, A. J.; Souza, F. E. S.; Stringer, G.; Whittell, G. R. *J. Chem. Soc., Dalton Trans.* **1998**, 301-310; (e) Dai, C.; Stringer, G.; Marder, T. B.; Scott, A. J.; Clegg, W.; Norman, N. C. *Inorg. Chem.* **1997**, 36, 272-273; (f) Câmpian, M. V.; Harris, J. L.; Jasim, N.; Perutz, R. N.; Marder, T. B.; Whitwood, A. C. *Organometallics* **2006**, 25, 5093-5104.

³²³ Westcott, S. A.; Marder, T. B.; Baker, R. T.; Calabrese, J. C. *Can. J. Chem.* **1993**, 73, 930-936.

³²⁴ (a) Hayashi, T.; Takahashi, M.; Tanaka, Y.; Ogasawara, M. *J. Am. Chem. Soc.* **2002**, 124, 5052-5058; (b) Shiomi, T.; Adachi, T.; Toribatake, K.; Zhou, L.; Nishiyama, H. *Chem. Commun.* **2009**, 5987-5989.

³²⁵ (a) Ishiyama, T.; Murata, M.; Miyaura, N. *J. Org. Chem.* **1995**, 60, 7508-7510; (b) Takagi, J.; Takahashi, K.; Ishiyama, T.; Miyaura, N. *J. Am. Chem. Soc.* **2002**, 124, 8001-8006; (c) Miyaura, N. *J. Organomet. Chem.* **2002**, 653, 54-57; (d) Sunimoto, M.; Iwane, N.; Takahama, T.; Sakaki, S. *J. Am. Chem. Soc.* **2004**, 126, 10457-10471.

³²⁶ (a) Miyaura, N.; Suzuki, A. *Chem. Rev.* **1995**, 95, 2457-2483; (b) Braga, A. A. C.; Morgon, N. H.; Ujaque, G.; Maseras, F. *J. Am. Chem. Soc.* **2005**, 127, 9298-9307.

³²⁷ (a) Ishiyama, T.; Takagi, J.; Hartwig, J.F.; Miyaura N. *Angew. Chem. Int. Ed.* **2002**, 41, 3056-3058; (b) Tamura, H.; Yamazaki, H.; Sato, H.; Sakaki, S. *J. Am. Chem. Soc.* **2003**, 125, 16114-16126.

³²⁸ (a) Mun, S.; Lee, J.-E.; Yun, J. *Org. Lett.*, **2006**, 8, 4887-4889; (b) Zhu, W.; Ma, D. *Org. Lett.* **2006**, 8, 261-263; (c) Kleeburg, C.; Dang, L.; Lin, Z.; Marder, T. B. *Angew.*

Chem. Int. Ed. **2009**, *48*, 5350-5354; (d) Zhao, H. T.; Lin, Z. Y.; Marder, T. B. *J. Am. Chem. Soc.* **2006**, *128*, 15637-15643; (e) Zhao, H. T.; Lin, Z. Y.; Marder, T. B. *J. Am. Chem. Soc.* **2008**, *30* 5586-5594; (f) Dang, I.; Lin, Z. Y.; Marder, T. B. *Organometallics* **2008**, *27*, 4443-4454; (g) Dang, I.; Lin, Z. Y.; Marder, T. B. *Chem. Commun.* **2009**, 3987-3995.

³²⁹ For the formation of reactive adducts from B₂pin₂ and nucleophilic species see; (a) Lee, K.-S.; Zhugralin, A. R.; Hoveyda, A. H. *J. Am. Chem. Soc.* **2009**, *131*, 7253-7255; (b) Gao, M.; Thorpe, S. B.; Santos, W. S. *Org. Lett.* *11*, 3478-3481.

For the formation of Lewis base adducts of B₂cat₂, see: (c) Nguyen, P.; Dai, C.; Taylor, N. J.; Power, W. P.; Marder, T. B. Pickett, N. L.; Norman, N. C. *Inorg. Chem.* **1995**, *34*, 4290-4291; (d) Clegg, W.; Dai, C.; Lawlor, F. J.; Marder, T. B.; Nguyen, P.; Norman, N. C.; Pickett, N. L.; Power, W. P.; Scott, A. J.; *J. Chem. Soc., Dalton Trans.* **1997**, 839-846; (e) Dai, C.; Johnson, S. M.; Lawlor, F. J.; Lightfoot, P.; Marder, T. B.; Norman, N. C.; Orpen, A. G.; Pickett, N. L.; Quayle, M. J.; Rice, C. R. *Polyhedron*, **1998**, *17*, 4139-4143.

³³⁰ Evans, D.; Osborn, J. A.; Wilkinson, G. **1968**, *33*, 3133-3142.

³³¹ Nguyen, P.; Coapes, R. B.; Woodward, A. D.; Taylor, N. J.; Burke, J. M.; Howard, J. A. K.; Marder, T. B. *J. Organomet. Chem.* **2002**, *652*, 77-85.

³³² Beller, M.; Riermeier, T. H. *Eur. J. Inorg. Chem.* **1998**, 29-35.

³³³ (a) Harrisson, P.; Morris, J.; Steel, P. G.; Marder, T. B. *Synlett* **2009**, 147-150; (b) Harrisson, P.; Morris, J.; Steel, P. G.; Marder, T. B. *Org. Lett.* **2009**, *11*, 3586-3589.

³³⁴ For a comprehensive review see Mkhaliid, I. A. I.; Murphy, J. M.; Barnard, J. H.; Marder, T. B.; Hartwig, J. F. *Chem. Rev.* **2010**, *110*, 890-931.

³³⁵ Coates, G. W.; Waymouth, R. M.; *Science* **1995**, *267*, 217-219.

³³⁶ Lee, G. Y.; Xue, M.; Kang, M. S.; Kwon, O. C.; Yoon, J.-S.; Lee, Y.-S.; Kim, H. S.; Lee, H. J.; Lee, I.-M. *J. Organomet. Chem.* **1998**, *558*, 11-18.

³³⁷ Lee, D.-W.; Yun, D. *Bull. Korean Chem. Soc.* **2004**, *25*, 29-30.

³³⁸ Nifantev, I. E.; Sitnikov, A. A.; Andriukhova, N. V.; Laishevtsev, I. P.; Luzikov, Y. N. *Tetrahedron Lett.* **2002**, *43*, 3213-3215.

³³⁹ Evans, D.; Yagupsky, G.; Wilkinson, G. *J. Chem. Soc. A* **1968**, 2660-2665.

³⁴⁰ Krug, C.; Hartwig, J. F. *J. Am. Chem. Soc.* **2002**, *124*, 1674-1679

- ³⁴¹ Varshavsky, Y. S.; Cherkasova, T. G.; Podkorytov, I. S. *Inorg. Chem. Commun.* **2004**, 7, 489-491.
- ³⁴² Booth, B. L.; Casey, G. C.; Haszeldene, R. N. *J. Organomet. Chem.* **1982**, 224, 197–205.
- ³⁴³ Singh, P.; Dammann, C. B.; Hodgson, D. J. *Inorg. Chem.* **1973**, 12, 1335-1339.
- ³⁴⁴ Adhikari, D.; Mossin, S.; Basuli, F.; Dible, B. R.; Chipara, M.; Fan, H.; Huffman, J. C.; Meyer, K.; Mindiola, D. J. *Inorg. Chem.* **2008**, 47, 10479-10490.
- ³⁴⁵ (a) Marder, T. B.; Norman, N. C. *Topics in Catalysis* **1998**, 5, 63-73; (b) Burgess K.; Ohlmeyer, M. J. *Chem. Rev.* **1991**, 91, 1179-1191; (c) Beletskaya, I.; Pelter, A. *Tetrahedron* **1997**, 53, 4957-5026; (d) Fu, G. C.; Evans, D. A.; Muci, A. R. in *Advances in Catalytic Processes*, Doyle, M. P. Eds. JAI, Greenwich, CT, **1995**, 95-121; (e) Burgess, K.; van der Donk, W. A. in *Encyclopedia of Inorganic Chemistry*; King, R. B., Ed.; John Wiley & Sons: Chichester, England, 1994; Vol. 3, 1420.
- ³⁴⁶ (a) Evans, D.; Osborn, J. A.; Wilkinson, G. *Inorg. Synth.* **1966**, 8, 215; (b) McLeverly, J. A.; Wilkinson, G. *Inorg. Synth.* **1968**, 11, 99.
- ³⁴⁷ Harlow, R. L.; Westcott, S. A.; Thorn, D. L.; Baker, R. T. *Inorg. Chem.* **1992**, 31, 323-326.
- ³⁴⁸ Grushin, V. V.; Kuznetsov, V. F.; Bensimon, C.; Alper, H. *Organometallics* **1995**, 14, 3927–3932.
- ³⁴⁹ Varshavsky, Y. S.; Cherkasova, T. G.; Podkorytov, I. S. *Inorg. Chem. Commun.* **2004**, 7, 489-491.
- ³⁵⁰ (a) Chen, A. C.; Allen, D. P.; Crudden, C. M.; Wang, R.; Decken, A. *Can. J. Chem.* **2005**, 83, 943-957; (b) Chen, A. C.; Ren, L.; Decken, A.; Crudden, C. M. *Organometallics* **2000**, 19, 3459-3461.
- ³⁵¹ Itami, K.; Tonogaki, K.; Ohashi, Y.; Yoshida, J.-i. *Org. Lett.* **2004**, 6, 4093-4096.
- ³⁵² Deng, R.; Sun, L.; Li, Z. *Org. Lett.* **2007**, 9, 5207–5210.
- ³⁵³ Robinson, S. D.; Uttley, M. F. *J. Chem. Soc. Dalton Trans.* **1973**, 1912-1920.
- ³⁵⁴ 5-MeOH, C₄₄H₃₅O₃P₂Rh·CH₄O, *M_r* = 808.61, yellow blade (0.52×0.17×0.05 mm), triclinic, space group P $\bar{1}$ (No. 2), *a* = 9.461(1), *b* = 11.420(1), *c* = 19.433(3) Å, α = 78.08(1), β = 86.09(1), γ = 66.78(1)°, *V* = 1887.9(4) Å³, *Z* = 2, *d*_{calcd} = 1.422 g cm⁻³, μ =

0.58 mm⁻¹, $T = 120$ K, Bruker SMART 6000 CCD area detector, 24309 reflections (10972 unique), $R1=0.031$ [$I > 2\sigma(I)$], $wR2 = 0.080$.

³⁵⁵ Varshavsky, Yu. S.; Cherkasova, T. G.; Podkorytov, I. S.; Korlyukov, A. A.; Khrustalev, V. N.; Nikol'skii, A. B. *Russ. J. Coord. Chem.* **2005**, *31*, 121-131.

³⁵⁶ Sokol, V. I.; Gol'dshleger, N. F.; Porai-Koshits, M. A. *Koord. Khim.* **1993**, *19*, 47-53.

Future work

5.1 Future work relating to Chapter 2

Although the synthesis of the TTNPB series of retinoid was successfully completed, possibilities for improving the work exist. In particular, the Pd-catalysed borylation reactions of aryl iodides with B_2pin_2 or B_2neop_2 could be coupled with subsequent Suzuki-Miyaura cross-couplings to give the cross coupled products directly from the aryl iodides in two-step, one-pot procedures. In addition, work in Chapter 4 has demonstrated that Rh-catalysed dehydrogenative borylations of alkenes can be performed in MTBE and followed by Suzuki-Miyaura cross-couplings to give the cross-coupled products in a one-pot procedure. Applying this to the synthesis of the TTNPB retinoids would allow for the syntheses to be carried out in two one-pot procedures from the parent arene or aryl iodide.

5.2 Future work relating to Chapter 3

Similarly, the syntheses of biaryl-based retinoid esters could be performed by one-pot borylation/Suzuki-Miyaura cross-coupling sequences, while the tolan-based retinoid esters could possibly be synthesised in a one-pot sequence consisting of a Sonogashira reaction between aryl iodides and TMSA, *in situ* desilylation of the protected alkyne products and addition of a second aryl halide and subsequent Sonogashira cross-coupling to give the retinoid ester products.

5.3 Future work relating to Chapter 4

Chapter 4 details the development of second generation catalysts for the synthesis of vinyl boronate esters (VBEs) from unactivated alkenes. In this work it is established that

the anionic ligand in the rhodium complex is lost in the catalyst initiation step and that catalyst initiation is rapid when the anionic ligand is OR or H. The low activity exhibited by *trans*-[Rh(PPh₃)(iMes)(CO)Cl] compared to *trans*-[Rh(PPh₃)₂(CO)Cl] shows that catalytic activity can be altered by changing the dative ligand. Thus, to further improve catalytic activity a range of HRh(PR₃)₃(CO) complexes should be screened to assess the effects of phosphine structure on catalytic activity.

In addition a catalytic system that gave VBEs as the sole products from styrenes and other mono-substituted terminal olefins would be desirable as the current system, though highly active and selective for the borylation 1,1-disubstituted alkenes and indene, is poorly selective for VBE formation from styrenes.



















































\bar{i}